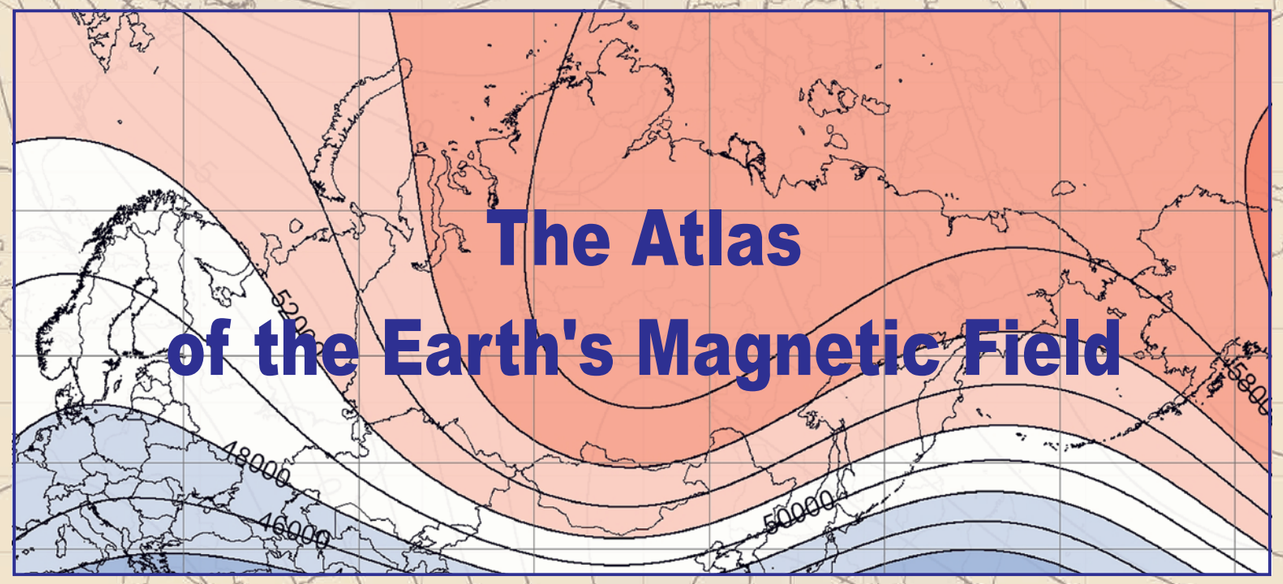

The Atlas of the Earth's Magnetic Field

Editors:
A. Gvishiani, A. Frolov, V. Lapshin

Moscow, 2013

RUSSIAN ACADEMY OF SCIENCES
DIVISION OF EARTH SCIENCES
GEOPHYSICAL CENTER

ROSHYDROMET
E. K. FEDOROV INSTITUTE
OF APPLIED GEOPHYSICS

The Atlas
of the Earth's Magnetic Field

Moscow, 2013

Editors:
Academician *A. Gvishiani*,
PhD *A. Frolov*,
Professor *V. Lapshin*

Soloviev, A., A. Khokhlov, E. Jalkovsky, A. Berezko, A. Lebedev, E. Kharin, I. Shestopalov, M. Mandea, V. Kuznetsov, T. Bondar, J. Mabie, M. Nisilevich, V. Nechitailenko, A. Rybkina, O. Pyatygina, A. Shibaeva (2013), *The Atlas of the Earth's Magnetic Field* (Eds.: A. Gvishiani, A. Frolov, V. Lapshin). Publ. GC RAS, Moscow, 361 pp, doi:10.2205/2013BS011_Atlas_MPZ.

The Atlas of the Earth's Magnetic Field represents a unified set of physical, geographic, thematic, and historical materials for a detailed study of the geomagnetic field from 1500 to 2010. The Atlas is intended for a wide range of scientists, teachers, students and experts in applied areas relating to the geosciences, including geologists and geophysicists studying geomagnetism. The Atlas is a unique cartographic product that contains comprehensive and scientifically grounded characteristics of geomagnetic phenomenon, and contains the results of historical and modern studies of the Earth's magnetic field.

ISBN 978-5-904509-13-2
DOI: 10.2205/2013BS011_Atlas_MPZ
URL: http://ebooks.wdcb.ru/2013/2013BS011/Atlas_MPZ_eng.pdf

© Geophysical Center of the Russian Academy of Sciences, 2013
© Fedorov Institute of Applied Geophysics ROSHYDROMET, 2013

Publishing group of GC RAS: E. Kedrov, O. Aleksanova, E. Firsova.

The version of record of this book was prepared in PDF format by the Laboratory of electronic publishing of the Geophysical Center RAS in the LaTeX publishing system using a specially designed template atlase.sty.

Contents

Preface 6

Chapter 1. Present-day maps of the Earth's magnetic field 7

- 1.1 Maps of MGMF for 1900–2010 7
- 1.2 Maps of MGMF for 1500–1900 7
- 1.3 Maps of MGMF secular variation for 1902–2007 9
- 1.4 Maps of non-dipole magnetic field of the Earth for 1900–2010 10
- 1.5 Maps of movement of magnetic poles 11
- 1.6 Map of magnetic field anomalies 12
- 1.7 Maps of distribution of magnetic field variations during the global magnetic storm of 20–25 January 2005 13

Chapter 2. Historical charts of the Earth's magnetic field 15

- 2.1 World chart of 1603 with the first appearance of the geomagnetic equator 15
- 2.2 The first world chart of magnetic declination of 1701 (1-st and 2-nd editions) 15
- 2.3 World chart of magnetic declination for 1744 16
- 2.4 World chart of magnetic declination of 1760 16
- 2.5 The first world chart of lines of equal magnetic inclination values of 1768 16
- 2.6 World charts of isogons according to Euler's theory (1819), isoclines and isogons (1830) 16
- 2.7 World charts of isogons (1841), magnetic meridians and parallels (1840) and isodynamics of magnetic intensity (1837–1939) 17
- 2.8 Comparison of 1837–1841 charts with analogous maps obtained from the *gufm1* model in 2010 18
  - 2.8.1 Declination maps 18
  - 2.8.2 Inclination maps 18
  - 2.8.3 Total intensity maps 18
- 2.9 Charts of the Earth's magnetic field features of 1840 18
- 2.10 Charts of isogons for 1787 and 1840, isoclines for 1780 and 1840, magnetic declination and inclination (65–90°N) as computed by Gauss' theory, and isodynamic lines for 1840 (1856) 19
- 2.11 World charts of isogons for 1858, and isoclines and isodynamics of magnetic intensity (1862) 19

Chapter 3. Auxiliary maps 21

- 3.1 Map of the INTERMAGNET network of observatories 21
- 3.2 Map of IGY observatories from 1957 to 1959 21
- 3.3 Global networks of ground-based geomagnetic observatories from 1813–2005 22

References 23

Annex 1. Present-day maps of the Earth's magnetic field 25

Annex 2. Historical charts of the Earth's magnetic field 311

Annex 3. Auxiliary maps 349

Preface

Global study of the Earth's magnetic field presents one of the fundamental problems of geophysics. Understanding of the magnetic field is essential for studying the structure of Earth's core, mantle, crust, lithosphere, hydrosphere and atmosphere. At the same time, this knowledge is an integral part of addressing important challenges in navigation, including the operation of satellites and aircraft. Study of the Earth's magnetic field has important implications in economic development and national security, including impacts on biological systems, and monitoring and prediction of the consequences of industrial processes.

These tasks are particularly important for studying the effects of the geomagnetic field on automatic pilot systems and aircraft crew members. Radar interference can also be caused by spatial and temporal field anomalies. Studying the dynamics of the Earth's magnetic field allows quick assessment and prediction of its behavior during magnetic storms caused by solar flares, improving the operational decision-making process related to the functioning of technological and biological systems.

Global modeling of the Earth's magnetic field is one of the principal domains of geophysical research. Indeed, the geopotential field, along with data obtained from analysis of seismic waves, provides the most comprehensive source of information about the structure and composition of our planet, as well as the evolutionary processes that go on. Spatial and temporal models of the magnetic field provide additional information that is indispensable for navigation, geodesy, and the study of ocean circulation and sea level variation.

This Atlas of the Earth's Magnetic Field covering the years 1500–2010 is the result of a joint collaborative project between the Russian Academy of Sciences (RAS) and the Federal Service for Hydrometeorology and Environmental Monitoring of Russia (ROSHYDROMET).

The authors of this project developed a new technology for digital mapping of the Geomagnetic Field (GMF). A resulting series of digital charts of the GMF were developed, including peculiar characteristics of the mapped phenomenon. Among them are the charts of the Main Geomagnetic Field (MGMF), GMF anomalies, spatial characteristics, cyclic variation, and other features.

Thematic digital charts of the MGMF components relate to different geomagnetic epochs according to results of historical and instrumental observations. They provide an effective way of presenting and exploring the MGMF and its evolution over time. The charts can be issued as individual cartographic works, and in the form of special collections. An example of the latter is the present Atlas of the Earth's Magnetic Field.

The authors applied professional tools for creating the GMF digital charts, including ArcGIS for creating maps in raster and vector formats. With the help of this software, digital charts of the MGMF components, secular variations of the MGMF, isolines, and the non-dipole component of the MGMF were transformed into separate raster images. State borders as of 2010 are represented in the charts given in Sections 1.1–1.4.

This Atlas also contains historical charts beginning with the world map of 1603, which includes the geomagnetic equator, shown for the first time by Guillaume Le Nautonier. It continues through the series of charts constructed by F. A. Garnier in 1862, that demonstrate historical and scientific points of view in contrast with those seen in modern charts.

To understand the history and the process of collection of geomagnetic data, we have included additional maps in this Atlas, showing the growth dynamics of terrestrial observation networks since 1813.

Scale, projection, symbols and legend were chosen according to the requirements found in "General Editorial Guide for Publishing Charts of the Earth's Magnetic Field" [*Report*, 2009]. The developed methods of editing, quality control and publishing digital charts abide by these guidelines.

Due to the vastness of the material, this Atlas is designed for a wide range of users from different scientific and applied areas of knowledge. This Atlas is a true original and unparalleled cartographic product having the most comprehensive and scientifically accurate parameters of the GMF for the period from 1500 to 2010. This Atlas demonstrates the breadth of scientific achievements in the field of geomagnetism.

This Atlas was created under the direction of *A. Gvishiani*, Academician of RAS (Geophysical Center RAS), *A. Frolov*, Head of ROSHYDROMET, *V. Lapshin*, Professor (Academician E. Fedorov Institute of Applied Geophysics of ROSHYDROMET).

The authors:

A. Soloviev, A. Khokhlov, E. Jalkovsky, A. Berezko, A. Lebedev, E. Kharin, I. Shestopalov, M. Nisilevich, V. Nechitailenko, A. Rybkina, O. Pyatygina, A. Shibaeva

Geophysical Center of the Russian Academy of Sciences.

V. Kuznetsov, T. Bondar

N. Pushkov Institute of Terrestrial Magnetism, Ionosphere and Radio Wave Propagation, Russian Academy of Sciences.

M. Mandea

Centre National d'Etudes Spatiales, France.

J. Mabie

US NOAA National Geophysical Data Center.

The authors express their deepest gratitude to the colleagues, who made their valuable contribution at different stages of this project:

J.-L. Le Mouël, Institut de Physique du Globe de Paris,
A. Jackson, Eidgenössische Technische Hochschule Zürich,
S. Maus, US NOAA National Geophysical Data Center,
M. Korte, Deutsches GeoForschungs Zentrum Potsdam,
J. Love, United States Geological Survey,
K. Mikhalchenko, Scientific Geoinformation Center RAS,
Task Group "Earth and Space Science Data Interoperability", ICSU CODATA,
M. Kaufman, Mark Kaufman Charity Foundation,
V. Pyatygin, E. Kedrov, O. Aleksanova, E. Firsova, Geophysical Center RAS.

A. Gvishiani, A. Frolov, V. Lapshin
August 2013, Moscow

Chapter 1. Present-Day Maps of the Earth's Magnetic Field

1.1 Maps of MGMF for 1900–2010

Historical observations of the Earth's magnetic field demonstrate varying levels of quality in regions of practical interest, such as data collected along sea routes by missions of opportunity [*Jackson et al.*, 2000]. Geomagnetic observatories that collect high precision data are few in numbers and don't have a good spatial distribution. Presently, the largest global network of observatories is the International Real-time Magnetic Observatory Network (INTERMAGNET) [http://www.intermagnet.org], which consists of nearly 120 observatories. Since the beginning of the space age, representation of geomagnetic field (GMF) data has changed drastically as it became possible to project field measurements onto the Earth's surface to provide high density coverage of the geoid [http://www-app2.gfz-potsdam.de/pb1/op/champ/].

The basic procedure of interpolation for mapping spatial and temporal variations in the GMF is essentially the same as was introduced by Karl Friedrich Gauss one hundred and fifty years ago. Field potential data collected over a particular time interval is decomposed using spherical harmonics projected on the spheroid, and then interpolated. Decomposition coefficients are obtained using least squares, where accuracy is essentially dependent on the spatial distribution of points on the sphere. Modern space-based observations with high spatial resolution, allow for high precision computation of these coefficients. Decomposition of the Main Geomagnetic Field (MGMF) allows for high precision mapping of a vector field at any point on the Earth's surface. The International Geomagnetic Reference Field (IGRF), by the International Association of Geomagnetism and Aeronomy (IAGA), and the corresponding IGRF coefficients have been developed using this method [http://www.ngdc.noaa.gov/IAGA/vmod/igrf.html]. The IGRF model makes it possible to compute characteristics of the MGMF from 1900 to 2010 in 5 year intervals. Continuous field measurements by INTERMAGNET observatories allow for regular improvements in the accuracy of the IGRF model.

The IGRF data were used as a basis for constructing maps of the MGMF components for the period 1900–2010. The MGMF components were calculated at nodes of the geographical grid with a 0.2 degree spatial resolution, in 5 year time steps. Coefficients of the IGRF, to the tenth power, were used for the calculations. At each node of the grid, the calculated values were modulus and six components of the MGMF vector: declination, inclination, three axial projections, and projection onto a plane tangential to the geoid at sea level.

The obtained matrices are used to compute digital maps of isolines of the corresponding components of the MGMF, using linear interpolation. 1 μT (microtesla) isodynams were used for the Eastern component and 2 μT for the Northern, vertical, horizontal components, and modulus of the vector. Isogonic and isoclinic lines are computed at intervals of 5 degrees. Isodynamic lines of total intensity, Northward, Eastward, vertical and horizontal components, isogonic lines of declination and isoclinic lines of inclination were plotted with continuous lines.

The Miller cylindrical projection with the scale $1 : 120,000,000$ was used for global mapping of the modeled MGMF components in this Atlas. Boundaries are shown on the digital cartographic background. Auxiliary elements in the maps include title, frame, geographical background, meridians, parallels, and geographic and magnetic equators. Elements outside the frames include the legend and symbols.

The final step of the preparation was automated generation of the maps. Corresponding calculated components of the MGMF are shown on the maps as isolines, related to three neighboring magnetic epochs (for example, 1900, 1905, 1910; 1910, 1915, 1920, etc.), which are mutually superimposed. Each subsequent map overlaps the previous map by one epoch. The resulting 77 maps had been constructed for the period 1900–2010 (Figure 1.1 – Figure 1.7).

1.2 Maps of MGMF for 1500–1900

Determination of the historic magnetic field of the Earth for the period from 1500 to 1900 was met with some difficulties. As a result, the coefficients of corresponding models have been the subject of debate within the scientific community. There are three primary reasons for this:

1. Observational points are irregularly distributed, and during the historic periods of the 16–18th centuries, observations were mainly carried out along shipping routes.
2. Observational data itself contains errors resulting from inadequate instrument quality.
3. Early observations of the magnetic field were made using direction, and not magnitude of the field vector.

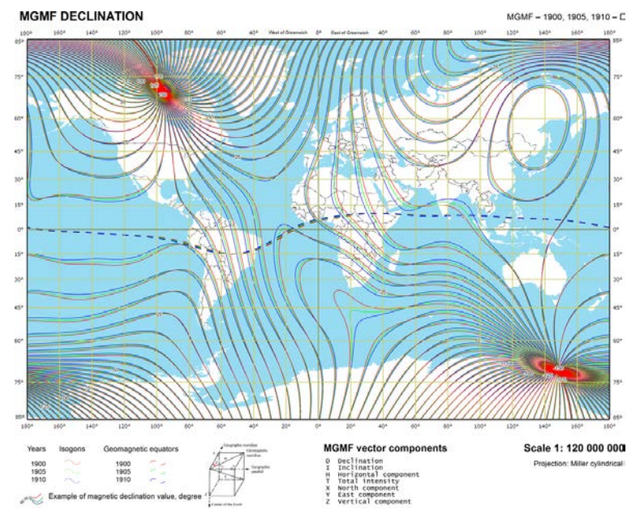

Figure 1.1. Maps of the MGMF declination for 1900–2010. **Enlarge.**

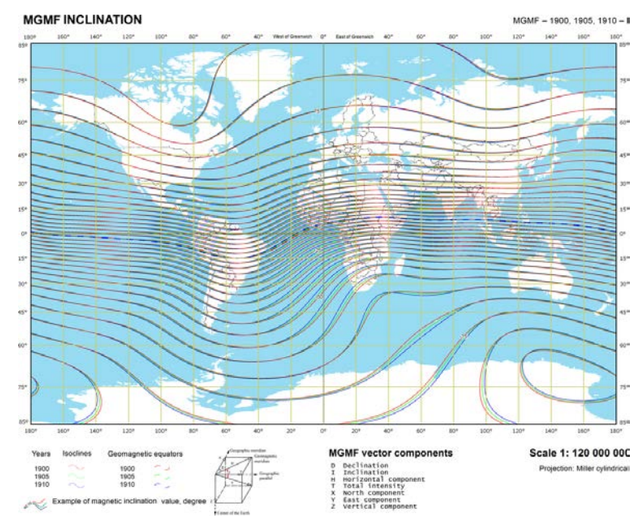

Figure 1.2. Maps of the MGMF inclination for 1900–2010. **Enlarge.**

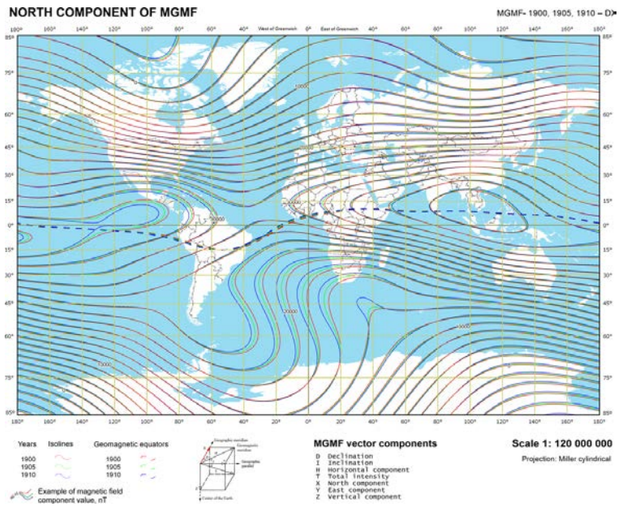

Figure 1.3. Maps of the Northern component of the MGMF for 1900–2010. **Enlarge.**

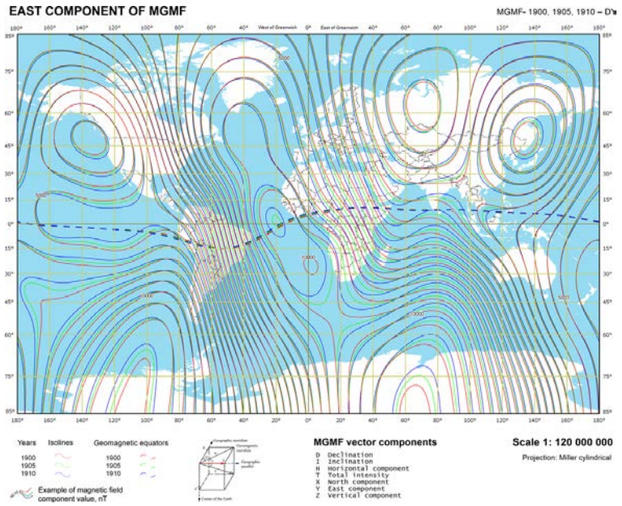

Figure 1.4. Maps of the Eastern component of the MGMF for 1900–2010. **Enlarge.**

Uncertainty in the magnitude of the field vector has recently been reduced by applying modern theories on the total field, applied to different time intervals during the period. This application has been generally accepted [*Hulot et al.*, 1997]. A research team consisting of A. Jonkers, A. Jackson, and A. Murrey [*Jonkers et al.*, 2003] conducted a robust investigation aimed at quality control and systematization of all observations obtained between 1510 and 1930. Models for this period were constructed using the results of this work. Several modern models allow reconstruction of a field for a given period. In development of this Atlas, we used only those which are most widely accepted among the scientific community [*Jackson et al.*, 2000; *Korte et al.*, 2009]. Differences between values of the modeled magnetic vector between the various models of historic MGMF are not significant, but the accuracy of each such model remains an open question.

In practice, computational methods used for determination of the above coefficients are far more accurate than the observational data itself. Thus, errors in the calculations have a negligibly small effect on model accuracy.

When creating maps of the MGMF components for the period of 1600–1900, we used data obtained by the *gufm*1 model, presented by the Great Britain Geological Survey [*Jackson et al.*, 2000]. The data consists of values of the Gauss coefficients of decomposition up to the 14-th degree. This is needed for computation of the

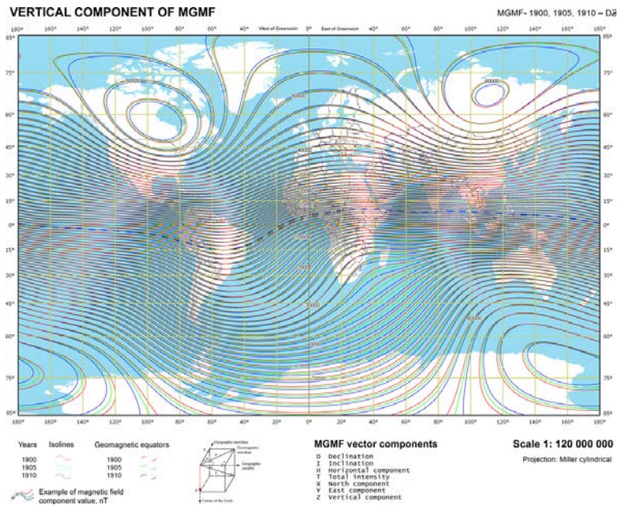

Figure 1.5. Maps of the vertical component of the MGMF for 1900–2010. **Enlarge.**

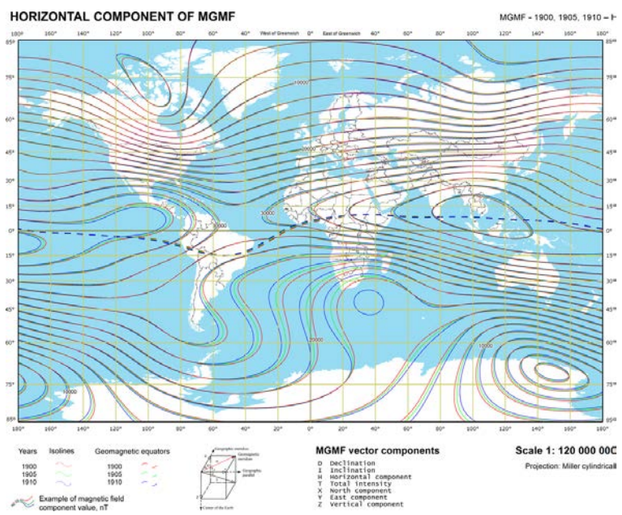

Figure 1.6. Maps of the horizontal component of the MGMF for 1900–2010. **Enlarge.**

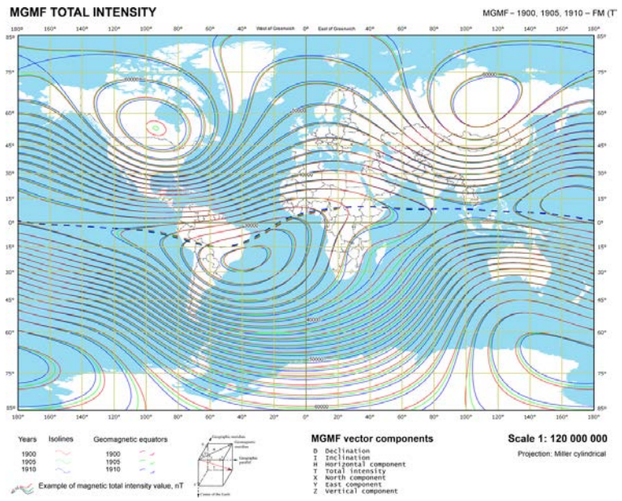

Figure 1.7. Maps of total intensity of the MGMF for 1900–2010. **Enlarge.**

MGMF parameters from 1590–1990 with a one year interval. The coefficients were calculated using all available geomagnetic measurements beginning in 1510.

Maps of the MGMF components for the period of 1500–1600 were constructed using data obtained by the CALS3K.3 model, and were presented by the German Center for Geosciences (GFZ) in Potsdam, Germany [*Korte et al.*, 2009]. These Gauss coefficients of decomposition up to the tenth degree, are calculated using paleomagnetic data, including data extracted from sedimentary rock.

The MGMF components were calculated at nodes of the geographical grid with a 0.2 degree interval in latitude and longitude. Coefficients of the MGMF decomposition up to the sixth degree were used in the calculations. For the periods 1500–1600 and 1600–1900, the time interval is 25 years. The modulus of the vector and the following six components of the MGMF: declination, inclination, three axial projections, and projection onto a plane tangential to the geoid, were calculated for each grid node at sea level.

Applying linear interpolation to the obtained matrices, isoline charts of the corresponding components of the MGMF were generated. Intervals between computed isodynamic lines were equal to 1 μT for the Eastern component and 2 μT for the Northern, vertical, horizontal components, and modulus of the vector. The interval between calculated isogonic and isoclinic lines is equal to 5 degrees. All the isodynamic, isogonic and isoclinic lines were plotted as continuous lines.

Miller projection maps were generated in the same manner described in Section 1.1. An automated routine produced the final product with corresponding components of the MGMF shown as isolines, related to the three neighboring epochs. The resulting 56 maps were constructed for the period of 1500–1900 (Figure 1.8 – Figure 1.14).

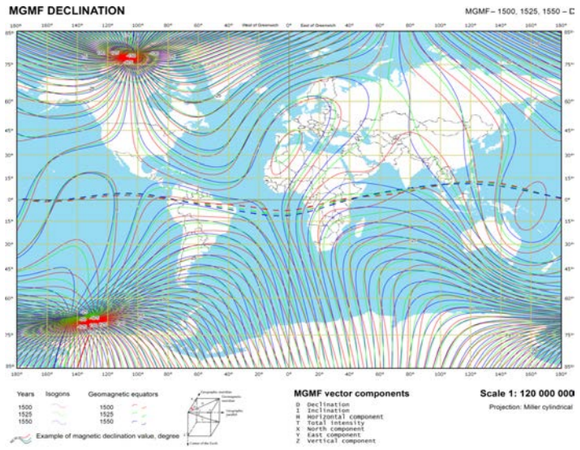

Figure 1.8. Maps of the MGMF declination for years 1500–1900. **Enlarge.**

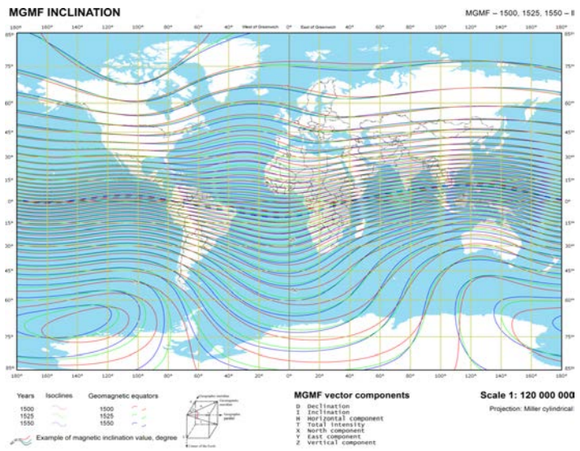

Figure 1.9. Maps of the MGMF inclination for years 1500–1900. **Enlarge.**

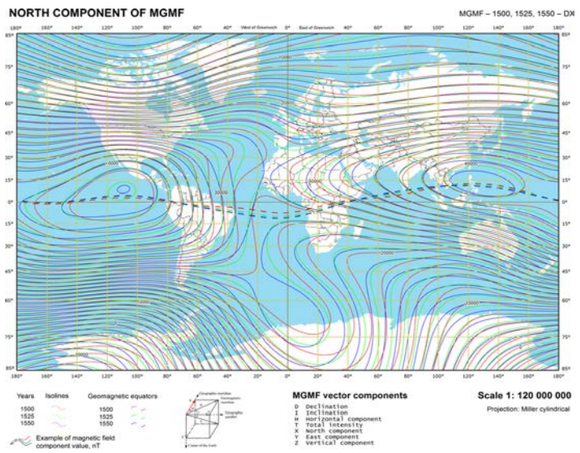

Figure 1.10. Maps of the Northern component of the MGMF for years 1500–1900. **Enlarge.**

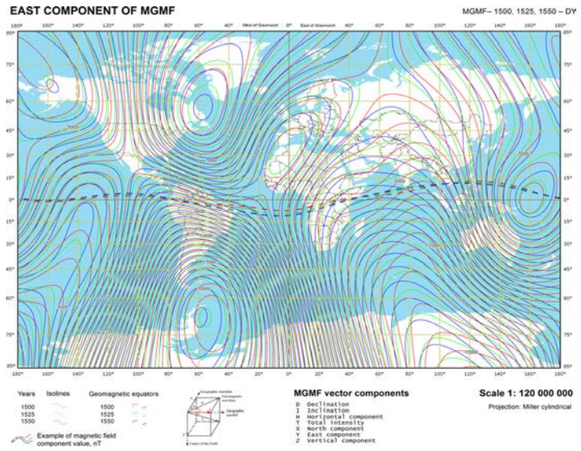

Figure 1.11. Maps of the Eastern component of the MGMF for years 1500–1900. **Enlarge.**

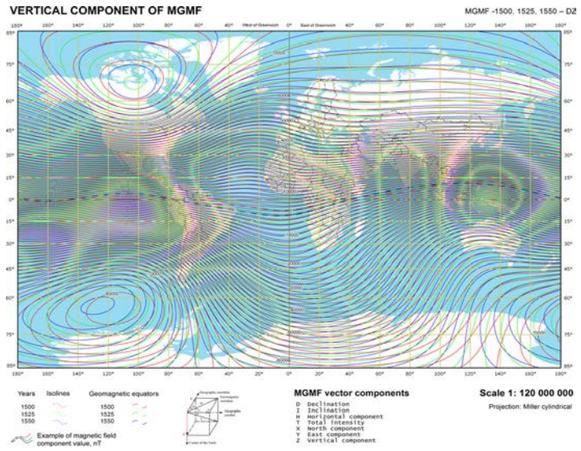

Figure 1.12. Maps of the vertical component of the MGMF for years 1500–1900. **Enlarge.**

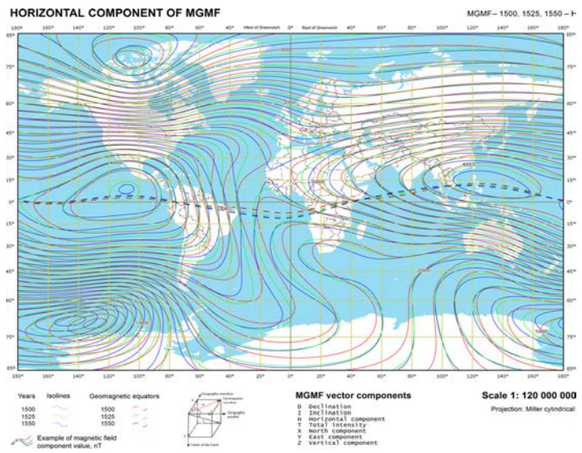

Figure 1.13. Maps of the horizontal component of the MGMF for years 1500–1900. **Enlarge.**

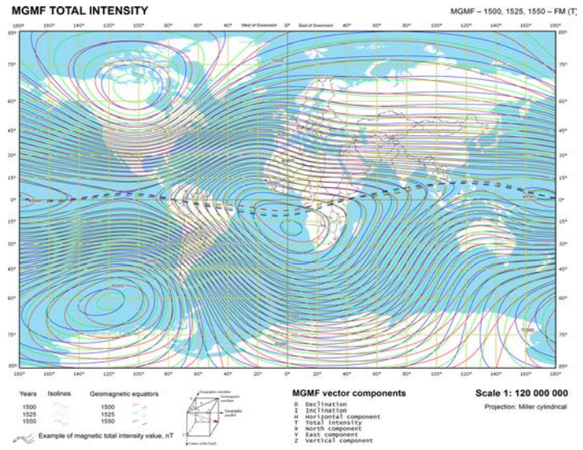

Figure 1.14. Maps of total intensity of the MGMF for years 1500–1900. **Enlarge.**

1.3 Maps of MGMF Secular Variation for 1902–2007

Magnetic field variations occur over periods that range from tenths of a second to hundreds of years. Rapid fluctuations are associated with space weather and solar activity, while long term variations are caused by processes that occur in the Earth's interior. The slowest MGMF variations that have been observed using historic records and paleomagnetic investigations demonstrate that the field strength and its components change over time.

Different types of magnetic variations are distinguished: secular, annual, diurnal, magnetic storms, pulsations, etc. Secular magnetic field variations occur over periods of tens to hundreds of years, and result in significant changes of mean annual elements of terrestrial magnetism. These secular variations were first observed in 1634 when Henry Gellibrand compared observations of magnetic declination in London with earlier data.

The change in an element of the magnetic field (secular variation) is defined as the difference in the values of the element between epochs, divided by the number of years between the epochs (Figure 1.15 – Figure 1.17). Secular variations are calculated from generalized data of global magnetic surveys over the previous five years [http://www.ngdc.noaa.gov/IAGA/vmod/igrf.html]. The results of this study have revealed variations on the order of 500 years, 2000 years, 5000 years and longer.

The nature of secular variations change from one geographic region to another, where the Earth's surface can be divided into regions that are characterized by their nature. Mean annual values of magnetic elements measured at observatories, coupled with results of magnetic surveys, show the geomagnetic field is slowly changing. These variations are plotted onto maps as isolines by the magnitude of annual variations for given periods. Regions where the field varies quickly tend to be characterized by oval shaped isopores. Isopores are shown to vary over periods of one or two decades, and tend to drift westward.

A slow rotation of the field is also seen to occur about a fixed direction. For instance, observations at the London observatory

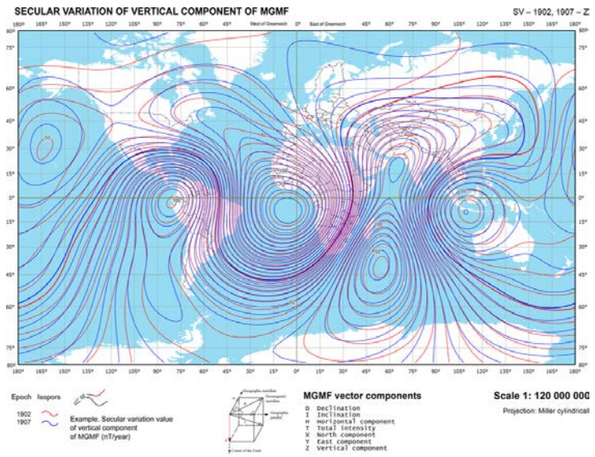

Figure 1.15. Maps of secular variations in the vertical component of the MGMF for 1902–2007. **Enlarge.**

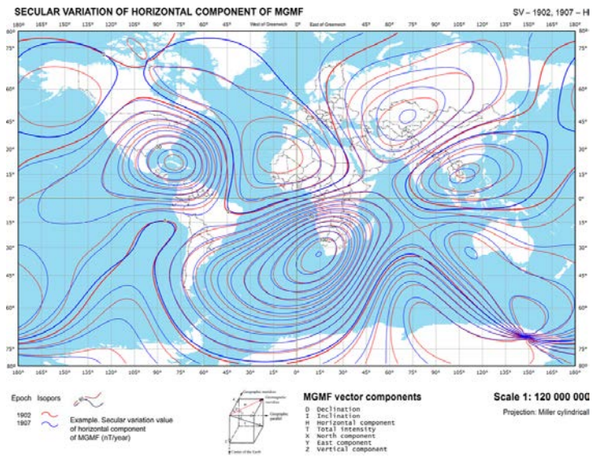

Figure 1.16. Maps of secular variations in the horizontal component of the MGMF for 1902–2007. **Enlarge.**

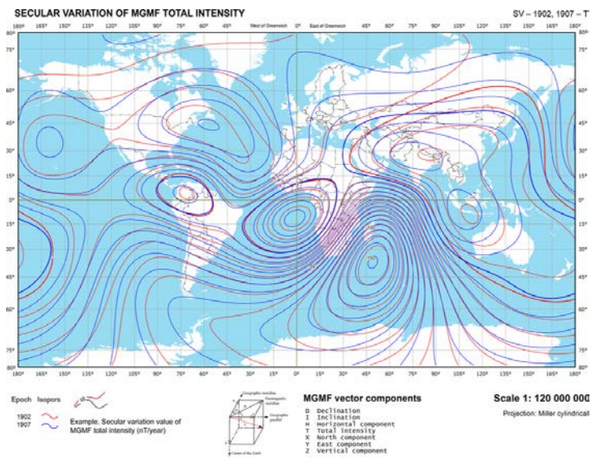

Figure 1.17. Maps of secular variations in total intensity of the MGMF for 1902–2007. **Enlarge.**

indicate that over the past 400 years the magnetic field has rotated nearly 270 degrees.

Maximum variations are shown to occur at several zones that move across the Earth's surface. For example, during 1942, variations in Indonesia reached +130 nT, while a +110 nT variation was observed south of the Caspian Sea. Initiation of secular variations is understood to be caused by processes occurring in the Earth's core, and at the core-mantle boundary.

1.4 Maps of Non-Dipole Magnetic Field of the Earth for 1900–2010

To the first order, the Earth's main magnetic field can be approximated as a magnetic dipole. Magnetic anomalies at the Earth's surface must be isolated from the observed field in order to define the principal (main) magnetic field. Determination of the main magnetic field is a complicated problem that can be solved in different ways. The most common method to compute the main field is the method of averaging. Arithmetically subtracting the dipole field gives values of the remainder, which represents the anomalous and non-dipole components of the main field. Using previously applied terminology, we refer to this as a field of global anomalies.

The observed magnetic field H can be presented as a geometric sum of the dipole field H_0, the non-dipole component H_T, the field of anomalies H_a, and a field of magnetic variations H_e, so that:

$$H = H_0 + H_T + H_a + H_e$$

where the sum $H_0 + H_T$ is the Earth main field. The non-dipole component of the main field is obtained by subtraction of the dipole field from the principal geomagnetic field. The mean intensity of the non-dipole component is approximately 10,000 nT (where the average total intensity is around 45,000 nT). Hence, the contribution of the non-dipole component is essential, but represents only a small fraction of the mean magnetic energy at the Earth's surface. It is of interest to examine what the non-dipole portion of the field is physically. On the Earth's surface, the field diverges from the pure dipole model, most notably over six geographical regions. One of these regions is East Asia where the East-Asian continental anomaly is observed to be the most intensive and right in its form.

For the year 2000, the non-dipole field is lower in the Pacific area than the Atlantic or Asian regions. Major non-dipole contributions are in the Central and South Atlantic, where the total field seems anomalously low, and beneath Australia and Eastern Asia, where it is on average rather high. Analysis of the geomagnetic secular variation, the rate of change with time, in the total and non-dipole parts of the field for the year 2000 shows that the non-dipole field is increasing in some regions and decreasing in others, with the largest rates of change in the Atlantic and Asian regions. At present, the secular variation in the geomagnetic field is predominantly in the non-dipole part of the field [*Constable*, 2007].

We have reason to assume that fields H_T and H_0 are generated from the same sources located within the core, so that division of the main field into the components H_T and H_0 is merely a formality.

It follows from the Gauss theory that farther from the Earth's surface, the influence of the non-dipole component is reduced. This is why at distances ranging from around 5 to 30–40 Earth radii, where the magnetic field still can be observed, it should be completely dipole; the field strength diminishes inversely with the cube of the distance from the center of the Earth. At large distances, satellite based observations of the field show the dipole character is lost due to disturbances in the interplanetary medium such as variations in the solar wind and interplanetary shock waves.

Features of the spatial structure and temporal dynamics of the main field during the 20-th century have been analyzed [*Simonyan, Golovkov*, 2009]. Variations resulting from the global dissipation of the dipole component of the geomagnetic field are distinguished from regional variations described using non-dipole spatial harmonics from a series expansion of spherical harmonics. The components of the non-dipole part of the Earth's main magnetic field were determined by zeroing the decomposition coefficients of the first degree g10, g11 and h11 according to the IGRF model (Figure 1.18 – Figure 1.24).

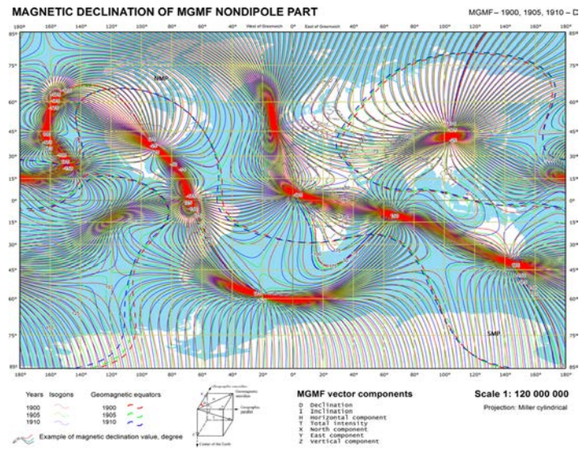

Figure 1.18. Maps of magnetic declination of the MGMF non-dipole part for years 1900–2010. **Enlarge.**

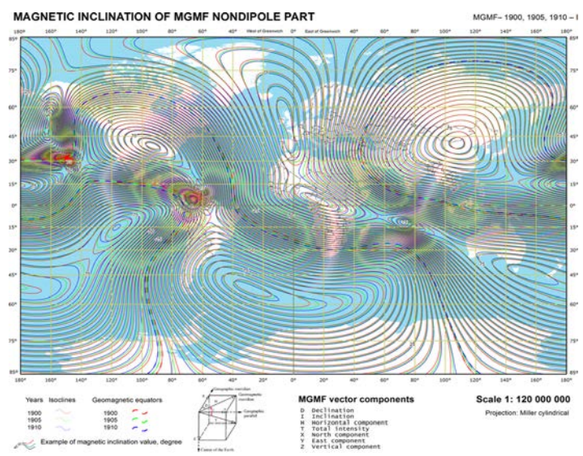

Figure 1.19. Maps of magnetic inclination of the MGMF non-dipole part for years 1900–2010. **Enlarge.**

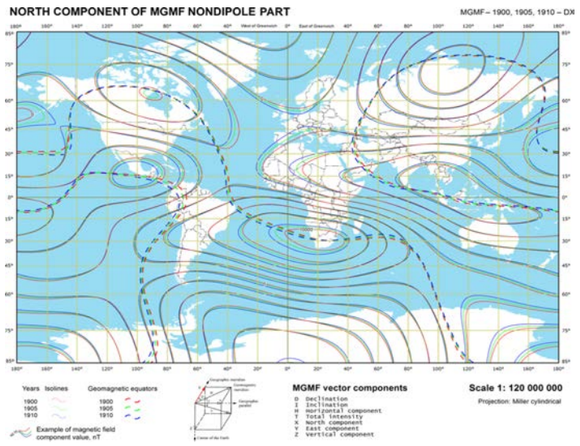

Figure 1.20. Maps of Northward component of the MGMF non-dipole part for years 1900–2010. **Enlarge.**

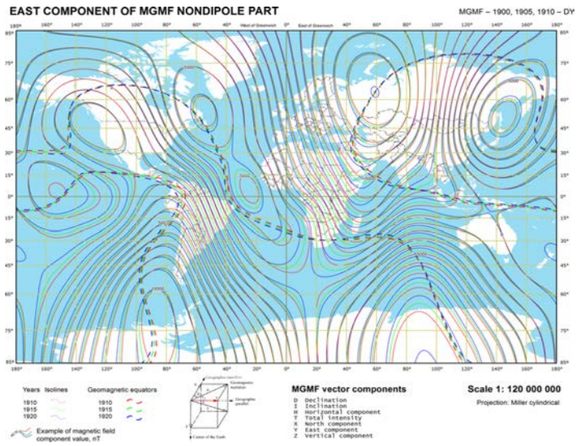

Figure 1.21. Maps of Eastward component of the MGMF non-dipole part for years 1900–2010. **Enlarge.**

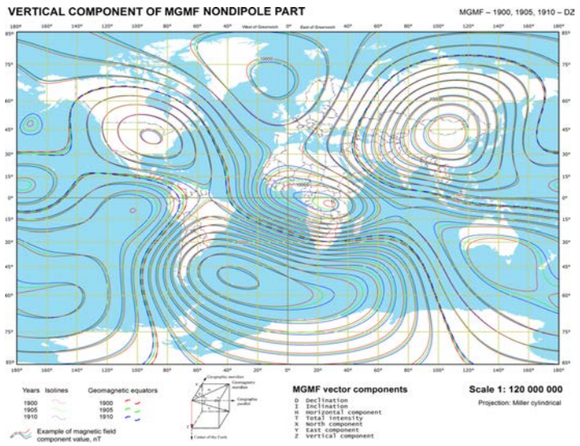

Figure 1.22. Maps of vertical component of the MGMF non-dipole part for years 1900–2010. **Enlarge.**

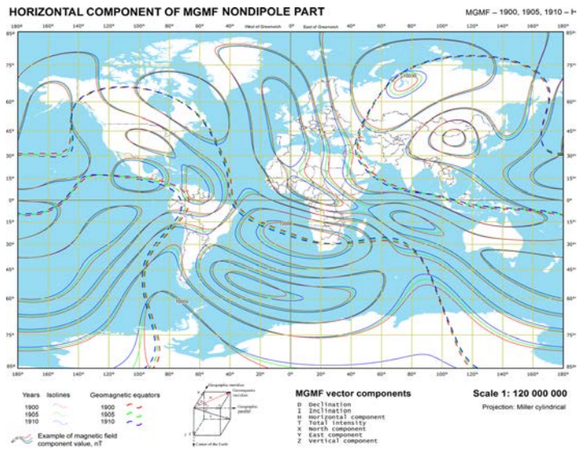

Figure 1.23. Maps of horizontal component of the MGMF non-dipole part for years 1900–2010. **Enlarge.**

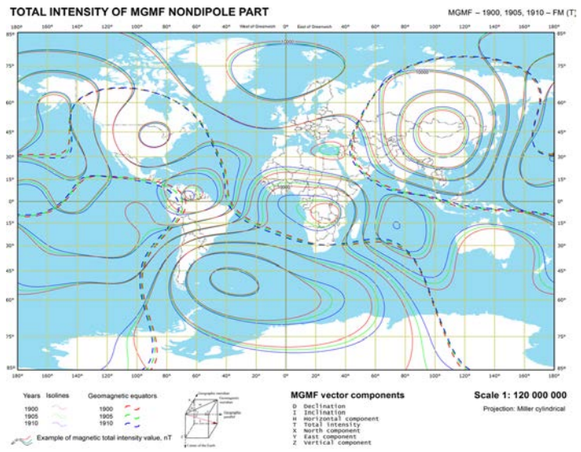

Figure 1.24. Maps of total intensity of the MGMF non-dipole part for years 1900–2010. **Enlarge.**

1.5 Maps of Movement of Magnetic Poles

The generic term "magnetic poles of the Earth" is sometimes used with differing meaning depending on the type of analysis used to define them (see [*Fraser-Smith*, 1987]). In the following, we are interested in the magnetic dip poles, to which we will simply refer to as "magnetic poles". The magnetic pole positions are defined as the location where the direction of the field vector is perpendicular to the surface. The "modeled" magnetic dip poles are determined using ground and satellite data (Figure 1.25, Figure 1.26). These models are the International Geomagnetic Reference Field/ Definitive Geomagnetic Reference Field (IGRF/DGRF) [*Mandea and Macmillan*, 2000] or Oersted Initial Field Model (OIFM) [*Olsen et al.*, 2000]. The "true" magnetic pole locations are obtained through a ground magnetic survey of a relevant polar region (Figure 1.27, Figure 1.28).

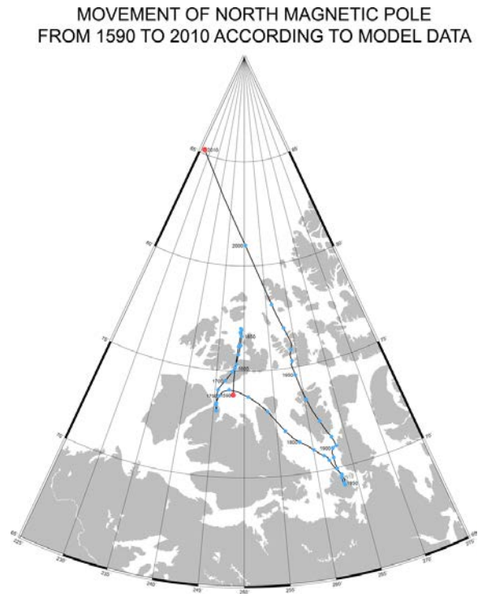

Figure 1.25. Map of displacement of the Northern magnetic pole for the period from 1590 to 2010. [http://www.ngdc.noaa.gov/geomag/] using model data: 1590–1940 – model [*Jackson et al.,* 2000], 1950–2010 – model [http://www.ngdc.noaa.gov /IAGA/vmod/igrf.html]. **Enlarge.**

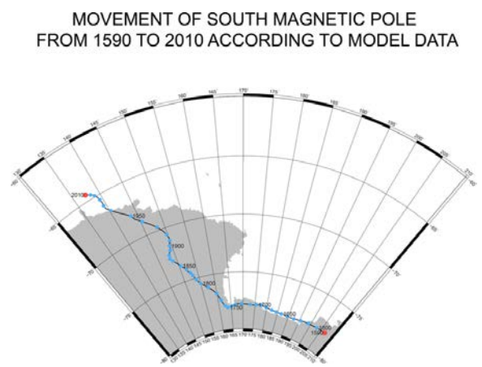

Figure 1.26. Map of displacement of the Southern magnetic pole for the period from 1590 to 2010. [http://www.ngdc.noaa.gov/geomag/] using model data: 1590–1940 – model [*Jackson et al.,* 2000], 1950–2010 – model [http://www.ngdc.noaa.gov/ IAGA/vmod/igrf.html]. **Enlarge.**

Because the dipole field is dominant, the Earth's field only exhibits two magnetic poles that are located near the geographic poles. Paleomagnetic studies (e.g. [*Carlut et al.,* 2000]) demonstrate that when the geomagnetic field is averaged over a long period of time (hundreds of thousands of years), it is consistent with a pure axial dipole (i.e. the magnetic poles coincide with the geographic ones). On shorter time scales, the precise positions of these poles vary with time around these equilibrium positions.

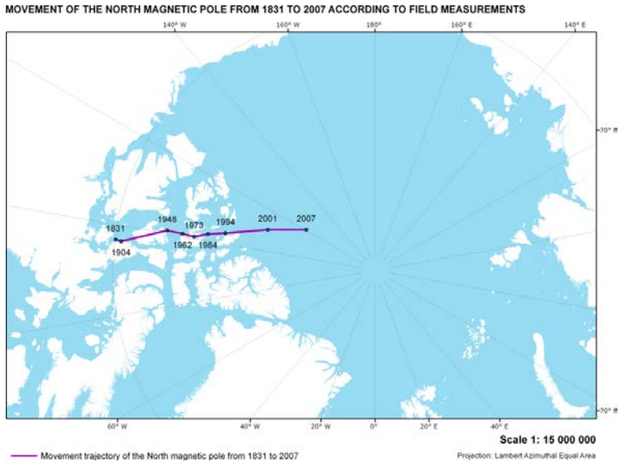

Figure 1.27. Map of displacement of the Northern magnetic pole for the period from 1831 to 2007 using field measurements. **Enlarge.**

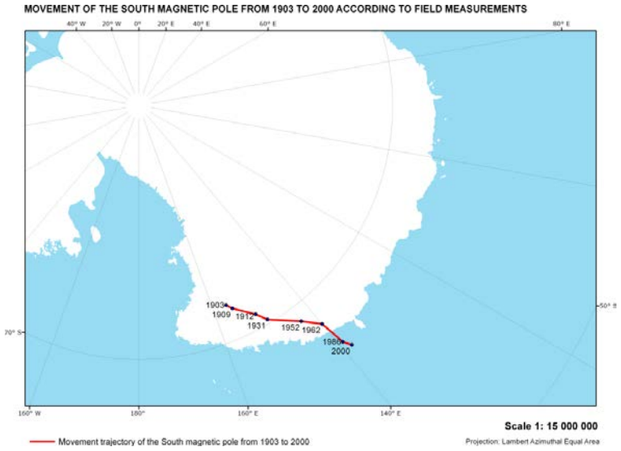

Figure 1.28. Map of displacement of the Southern magnetic pole for the period from 1903 to 2000 using field measurements. **Enlarge.**

Surprisingly, the migration rate of the North Magnetic Pole (NMP) has more than doubled over the last 30 years, reaching around 40 km/year in 2001. This is the fastest migration rate yet observed since the beginning of the 20th century, and has been given much attention in recent research [*Newitt et al.*, 2002]. Combined with weakening of the Earth's magnetic field strength over the past century, concerns have been raised of the possibility of an approaching polarity reversal [*Hulot et al.,* 2002]. Nevertheless, such an imminent reversal remains hypothetical; the Earth's dipole reverses direction only a few times over a million year period.

Seemingly random movements on the km scale occur almost daily as the poles wander in a roughly elliptical path about their average position. Frequently they can be 100 km away from this average position, depending on magnetic disturbances in the Ionosphere and Magnetosphere. Additionally, the magnetic poles seem to also have had a general north–north-western drift over the past century. Near the pole, a compass will behave erratically and eventually become unstable as the horizontal component of the field approaches zero.

The first attempts to locate the magnetic poles came in the form of 19-th century expeditions. The NMP was first located by Sir John Ross, in 1831, at Cape Adelaide on the west coast of the Boothia Peninsula. During this expedition, he measured a dip of 89°59'. The next attempt to reach the NMP came some 70 years later, by Roald Amundsen. The following observations were made by Paul Serson and Jack Clark in 1947, and thereafter by scientists from the Geological Survey of Canada. The most recent position of the NMP was obtained from measurements made by a Canadian-French team [*Newitt et al.*, 2002]. During this expedition, the direction of the magnetic field was measured using a declinometer-inclinometer magnetometer consisting of a single-axis fluxgate sensor, mounted on a non-magnetic theodolite. The theodolite was also used for making observations of the Sun, which was needed to determine the direction of true North. A proton magnetometer provided the total field intensity.

Measurements of the position of the South Magnetic Pole (SMP) were also made during the 19th century, although not all of these observations are accurate. D. Mawson made the first real determination of the SMP position in 1909. There have since been expeditions from many countries to precisely locate the SMP. The most recent measurements are described in [*Barton*, 2002; *Mandea and Dormy*, 2003].

1.6 Map of Magnetic Field Anomalies

Maps of magnetic anomalies allow better insight into the structure of the Earth's surface and crust. They are widely used in geophysics, such as for mineral resource surveys, illustrations of plate tectonics, the interaction between the crust and mantle, and other elements of geodynamics. Additionally, observed structure and magnetic field values, including maps of magnetic anomalies, can be correlated with processes responsible for the formation of the ocean floor, subduction of crustal plates, formation of the continental crust, and volcanicity.

Data on magnetic anomalies collected over a half of century, provide global coverage. However, complications arising from secular changes in the main field along with variations in data quality and coverage, makes creation of a global magnetic network a complicated problem. The World Digital Magnetic Anomaly Map (WDMAM) is an example of an attempt to integrate all available ground based, aeromagnetic and satellite data on the magnetic anomalies.

IAGA and the Commission for the Geological Map of the World (CGMW) solicited candidate maps based on a general pool of the data sets. The WDMAM map (Figure 1.29) published in 2007, is based on the MF5 model [*Maus et al.,* 2007]. After a detailed analysis of the presented materials, the EMAG3 model was chosen. This model had been proposed by the USA National Geophysical Data Center (NGDC) of the National Oceanic and Atmospheric Administration (NOAA).

The digital WDMAM map is presented in the form of a gridded data set with a resolution of 3 arc minutes over the entire surface of the Earth. The data were compiled from the results of magnetic measurements made from satellites, ground based instruments, oceangoing vessels, and aircraft. Using this data, values of the intensity of magnetic anomalies are determined at a height of 5 km above sea level.

The new EMAG2 model was released in February 2009 after two years of work done by an international group of scientists. Compared to the previous version of the EMAG3 model, resolution had been improved from three to two arc-minutes. This version also included data obtained from observation networks and surveys of the land and ocean surfaces. In addition, the quality of interpolation between different ocean routes has been improved using a model of the oceanic crust age by means of directional construction of network and extrapolation.

The EMAG2 model was developed as a result of collaboration between more than one hundred data providers across the world. The organizations that provided data of satellite, marine, air, and ground magnetic measurements are enumerated on the following web-page [http://geomag.org/models/EMAG2/acknowledgments.html]. It should be noted that the WDMAM map is the officially accepted work, improved with the use of the MF5 model (Figure 1.29a and Figure 1.29b).

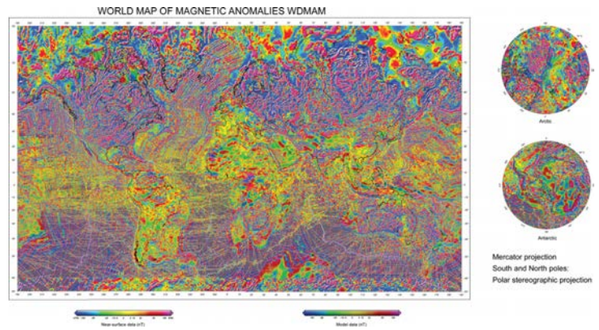

Figure 1.29a. World map of magnetic anomalies WDMAM. **Enlarge.**

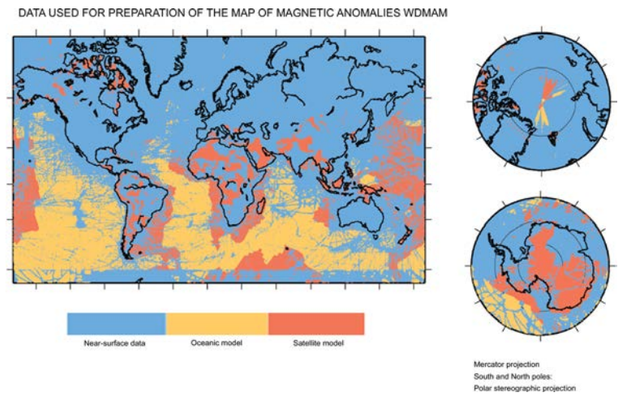

Figure 1.29b. Data used in the construction of the map WDMAM. **Enlarge.**

1.7 Maps of Distribution of Magnetic Field Variations During the Global Magnetic Storm of 20–25 January 2005

The global magnetic storm of 20–25 January 2005 was caused by a series of solar flares from 16–20 January 2005. A flare that occurred of 20 January 2005 was accompanied by a radiation storm with a spectral range from the optical to hard x-ray, and a coronal mass ejection into the interplanetary space. Earth based neutron monitors registered a wide energetic range of particles, including relativistic ones. This was one of the most energetic solar events since the beginning of the cosmic rays registration in 1942.

To study features of the geomagnetic field during this storm we used observations of the magnetic components X and Z obtained from approximately 120 INTERMAGNET observatories, and data from six stations located along the magnetic meridian 210 of the Kyushu University (Japan) and AARI (Arctic and Antarctic Research Institute, Russia).

The storm onset was recorded by observatories located in the morning and day-time sectors of the globe. The peak value of the magnetic field disturbance was observed at these stations of 21 January at 18:38 UTC. Minimal values were observed at Irkutsk and Novosibirsk located in the evening and nighttime sectors of 21 January at 20:56 UTC.

Based on the analysis performed, the following tables were prepared, and storm time maps of the X and Z components of the GMF were constructed:

1. The epoch of the first extreme of the disturbance (21 January at 18:38 UTC; Figure 1.30 and Figure 1.31);

2. The epoch when the extreme was observed in the eastern hemisphere, determined from data taken at the Irkutsk observatory (21 January at 20:56 UTC; Figure 1.32 and Figure 1.33);

3. The peak values of the magnetic field during the storm for all observatories (Figure 1.34 and Figure 1.35).

The onset of a disturbance in the geomagnetic field during the storm coincides with changes in the intensity of the inter-planetary magnetic field and the speed and density of the solar wind. The onset of a magnetic disturbance during the storm was observed in the Western hemisphere on morning and day-time sectors. In the Eastern hemisphere, minimum negative field values were observed approximately two hours later than in the Western hemisphere. It was noticed that the onset time of the disturbance depended on geographical location. There were several regions where the vertical component of the magnetic field was positive, while others had negative values. A gradual alternation of the values in these regions was observed along with an east-west asymmetry in the amplitudes of the magnetic variations.

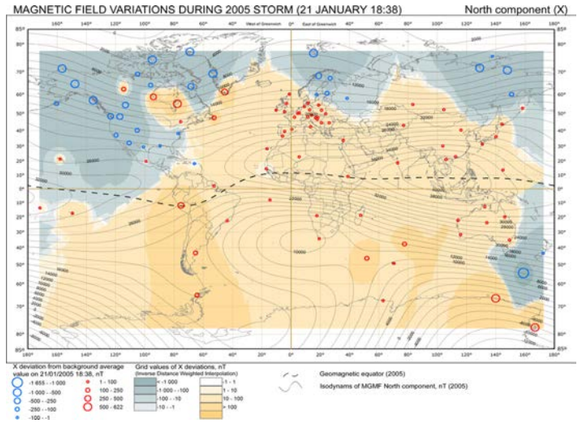

Figure 1.30. Map of the Northward component of geomagnetic field variations during the 2005 storm. **Enlarge.**

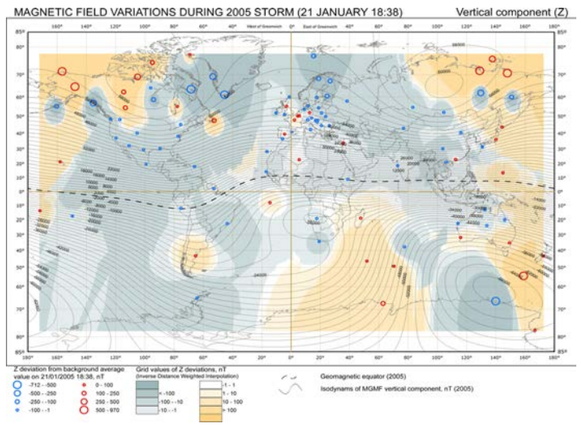

Figure 1.31. Map of the vertical component of geomagnetic field variations during the 2005 storm. **Enlarge.**

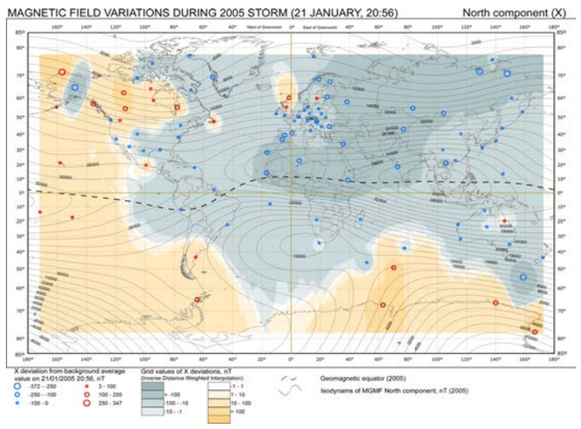

Figure 1.32. Map of the Northward component of geomagnetic field variations during the 2005 storm. **Enlarge.**

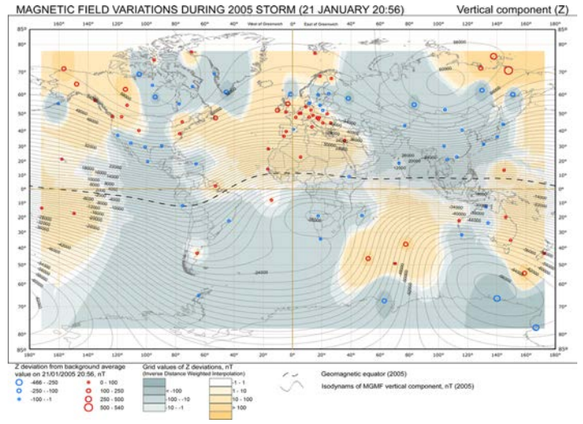

Figure 1.33. Map of the vertical component of geomagnetic field variations during the 2005 storm. **Enlarge.**

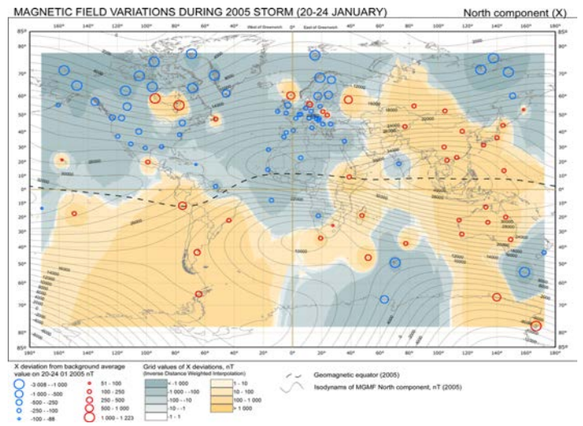

Figure 1.34. Map of the Northward component of geomagnetic field variations during the 2005 storm. **Enlarge.**

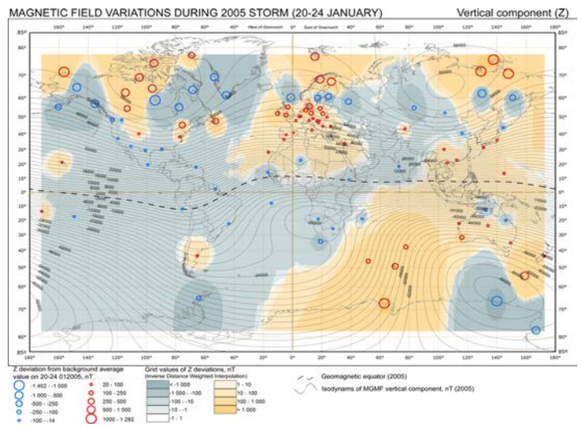

Figure 1.35. Map of the vertical component of geomagnetic field variations during the 2005 storm. **Enlarge.**

Chapter 2. Historical Charts of the Earth's Magnetic Field

2.1 World Chart of 1603 With the First Appearance of the Geomagnetic Equator

G. Le Nautonier noted that the magnetic declination was close to zero on the merdian near the Canary Islands, where the values were positive to the east and negative to the west. Using a remarkable geometrical technique, he was able to introduce the geomagnetic dipole, where approximations of latitude could be made from the value of magnetic declination. He made measurements in Novaya Zemlya that demonstrated very large D variations (which Gilbert was aware of, but refused to consider a priori). Nautonier made the bold proposition that all measurements can be explained by an offset grid of magnetic meridians and parallels (Figure 2.1), where the zero magnetic meridian is co-located with the Canary Islands geographic meridian and that the magnetic axis is tilted by 22.5°. [*Mandea, Mayaud*, 2004] explain how this figure was arrived at, from a set of four widely separated observations and delicate geometrical constructions projected onto a sphere.

Assuming the South magnetic pole was located on the 0° meridian, and the North magnetic pole was on the 180° meridian, he expressed the magnetic equator as a sinusoid, and even more remarkably, the local maximum of D at the 90° magnetic meridian (the shape of which can be quickly calculated with a modern computer, but required astute graphical constructions in the time when Le Nautonier did his work). From this, Le Nautonier derived his tabulated values. Although the location of the poles computed by Le Nautonier contained significant errors (mainly due to lack of observations in Northern Canada, the Pacific, and the Arctic), his model accounted reasonably well for a large number of observations, and from a modern perspective, was conceptually superior to Gilbert's, in which the magnetic and rotational axes had to coincide.

Using this model and applying spherical constructions, Le Nautonier derived magnetic variation, declination and inclination across the globe. The theory he put forward was mathematically complete, and his geometrical analysis was correct. In principle, although not in practice, this would allow navigators, using a known value of latitude (e.g., through an observation of Polaris) and magnetic declination (e.g., by taking bearings on a rising astronomical body), to find longitude by referencing his tables [*Courtillot, Le Mouël*, 2007].

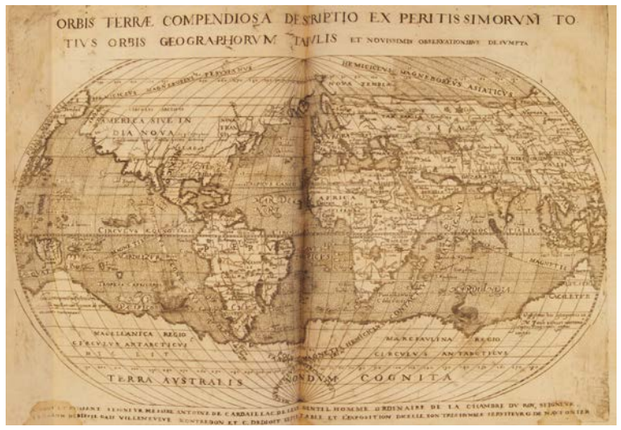

Figure 2.1. The global map of 1603 with the first plot of the geomagnetic equator [*Le Nautonier,* 1603] (Sainte-Genevieve Library in Paris, France). **Enlarge.**

2.2 The First World Chart of Magnetic Declination of 1701 (1-st and 2-nd Editions)

During the eighteenth century, significant progress was made in the fields of electricity and magnetism. Edmund Halley's work as the leader of the first global magnetic survey (1698–1700) on the Paramore resulted in the well-known charts (1701 for the chart of the Atlantic and 1701–1702 for the chart of the world) of lines of equal values of declination (isogons, then known as "Halleyan lines"), which remain classics (Figure 2.2, Figure 2.3). These isogons follow and vindicate some of Le Nautonier's ideas, but are based on a larger number of observations and are consequently, far more detailed. Halley's mapping of geomagnetism phenomenon of the world arose from his study of the journals of several explorers. The Pacific Ocean was not included, Halley said, due to lack of reliable data over the basin.

The first edition of Halley's world chart was published in France in 1701 (Figure 2.2). Although he is best known for determining the periodicity of the comet which bears his name, Halley was also an accomplished surveyor and cartographer. In 1702, he created a map of Britain's coastlines, which charted the tides. On Halley's world map, California is shown as an island, Australia is only partially mapped, and New Zealand is not shown at all. The Eastern coast of Australia and Polynesia are not outlined.

Although the second edition is undated (Figure 2.3), the English corrected edition of Halley's world chart, now exceedingly difficult to find, is generally believed to have been published in 1702 [*Whitfield*, 1996]. Guillaume Delisle compiled very large amounts of data and criticized the Halley charts in 1710, finding many errors and inconsistencies [*Jonkers*, 2000]. Still, many more charts were published in the following decades which confirmed the importance and value of the concept [*Courtillot, Le Mouël*, 2007].

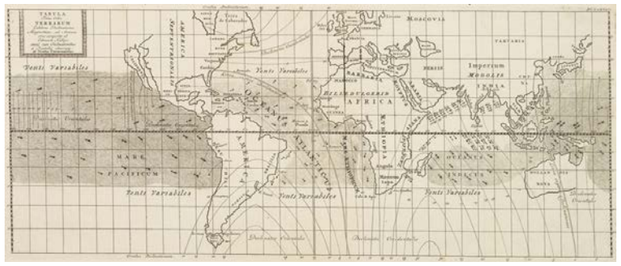

Figure 2.2. The first global map (1-st edition) of isogons of magnetic declination constructed by E. Halley in 1701 [*Halley,* 1701] (Paulus Swaen old Maps and Prints, USA). **Enlarge.**

Figure 2.3. The first global map (2-nd edition) of isogons of magnetic declination constructed by E. Halley in 1702 [*Halley, Mortier,* 1702] (Martayan Lan Fine Antique Maps, New York, USA). **Enlarge.**

2.3 World Chart of Magnetic Declination for 1744

In 1747, Emanuel Bowen plotted a new and accurate chart of the world, drawn with isogons (Figure 2.4). It was created using authentic surveys, assisted by the highest quality maps and charts available, and regulated by astronomical observations. The map describes lines that show the movement of the magnetic needle, according to observations made by several experienced navigators around the year 1744. It also includes notes on the lines of magnetic declination, and dates of European discoveries.

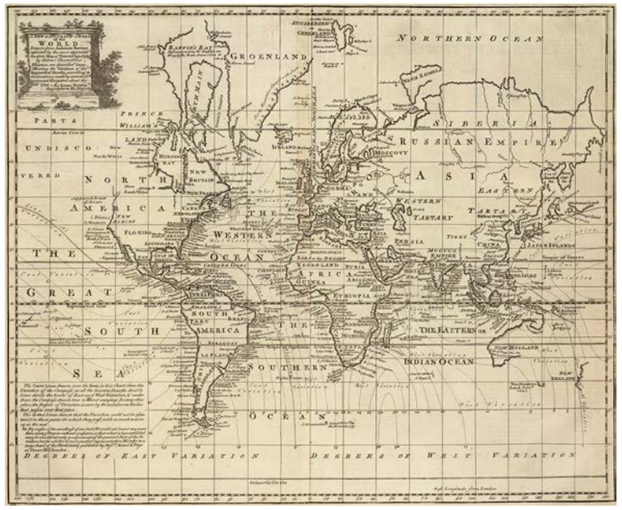

Figure 2.4. E. Bowen's global map of isogons of magnetic declination of 1744, including dates of European discoveries constructed in 1747 [*Bowen,* 1752] (David Rumsey Map Collection, www.davidrumsey.com, USA; Images copyright © 2000 by Cartography Associates). **Enlarge.**

2.4 World Chart of Magnetic Declination of 1760

The 1744 global map of isogons (Figure 2.5) represents two hemispheres. Deviations of the compass needle from true North are shown, illustrated with some explanations in Latin. This map had been constructed by N. F. Sauerbrey. L. Euler (Basel, 1707 – Saint Petersburg, 1783; cartographer, physician, and mathematician) included the map in the "Atlas of Geophysics" published by him between 1753 and 1760 for the Prussian Royal Academy of Sciences and Literature in Berlin.

2.5 The First World Chart of Lines of Equal Magnetic Inclination Values of 1768

Around 1720, William Whiston (1667–1752) prepared the first inclination chart for southeastern England and the coast of Normandy in the hope that because secular variation of dip was slower

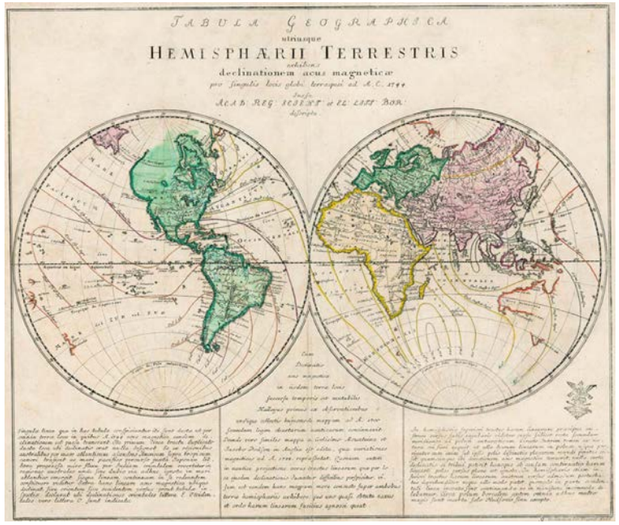

Figure 2.5. N. F. Sauerbrey's global map of isogons of magnetic declination for 1744, constructed in 1760 [*Sauerbrey,* 1760] (Philographikon Gallery (Germany), http://www.philographikon.com/). **Enlarge.**

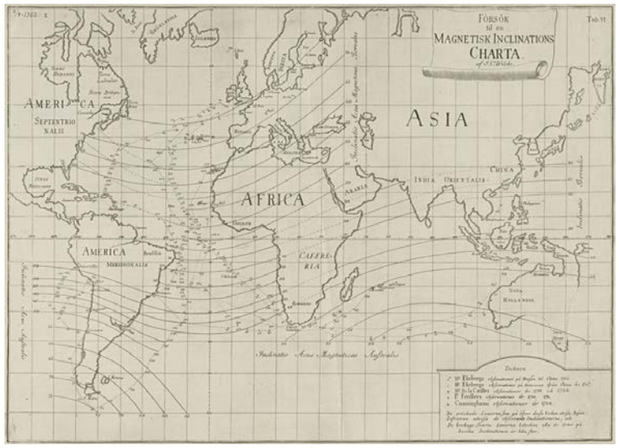

Figure 2.6. The first global map of isoclines of magnetic inclination published by J. C. Wilcke in 1768 [*Wilcke,* 1768] (National Library of Sweden). **Enlarge.**

they would provide a better way to determine longitude (still the same pursuit). The first world chart of lines of equal values of inclination (isoclines, which were then called parallels of inclination, Figure 2.6) was published by Swedish physicist Johan Carl Wilcke (1732–1796) in 1768 in Stockholm [*Courtillot, Le Mouël,* 2007; *Wilcke,* 1768] The map is based on inclinations observed on board of Swedish Eastindiamen [*Jonkers,* 2007].

2.6 World Charts of Isogons According to Euler's Theory (1819), Isoclines and Isogons (1830)

Christopher Hansteen (1784–1873) from Norway, is remembered by the solid Earth geophysicists community for his statement: "The mathematicians of Europe since the times of Kepler and Newton have all turned their eyes to the heavens, to follow the planets in their finest motions and mutual perturbations: it is now to be wished that for a time they would turn their gaze downward toward the Earth's center, where also there are marvels to be seen; the Earth speaks of its internal movements through the silent voice of the magnetic needle".

A theory on a multiplicity of magnetic poles was proposed in the early 19-th century. In 1819, C. Hansteen published a manuscript called "Studies of the Earth's Magnetism" in which he summarized the data collected up to this time, and made an effort to develop a mathematical model that could explain this data. It could be seen from his model that just one pair of poles was not sufficient, and at least one more pair was needed. In addition to a pair of first order poles, located in the north of Canada, and in the eastern area of the Antarctic continent, he introduced two more poles: one in Siberia, and the second in the south-east part of the Pacific (Figure 2.7).

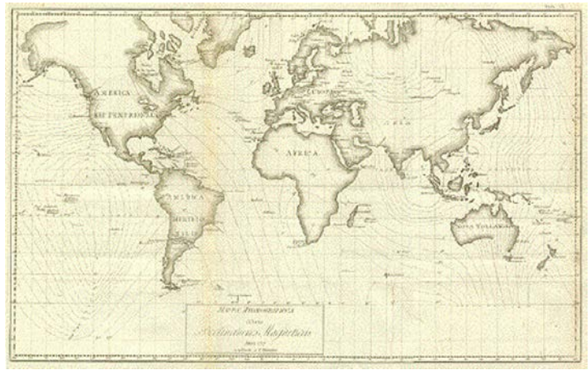

Figure 2.7. Global map of isogons of magnetic declination according to Euler's theory, published by C. Hansteen in 1819 [*Hansteen,* 1819] (Philographikon Gallery (Germany), http://www.philographikon.com/). **Enlarge.**

A Norwegian expedition under the leadership of Hansteen operated in Siberia in the years 1828–1830, traveling to the Baikal Sea and crossing the border into China [*Hansteen,* 1859]. One measured the numerical values of the total magnetic field strength, the inclination (Figure 2.8), and the declination (Figure 2.9). Hansteen found no evidence of a magnetic pole in Siberia. To him, this was an enormous disappointment. Nevertheless, in a letter to H. C. Ørsted of 21 June 1841, he proudly relates the written statement of Gauss, that to a large extent, it was the measurements of Hansteen, that had made Gauss devote himself to the study of magnetism [*Hansteen,* 2007].

The first global isodynamic charts for horizontal intensity (H)

and total intensity (F) were published in 1825–1826 by Christopher Hansteen [*Hansteen*, 1895]. The units used in this work were those introduced by von Humboldt [*Chapman, Bartels*, 1940]. More complete charts were subsequently published by Heinrich Berghaus, Duperrey and Edward Sabine in 1837.

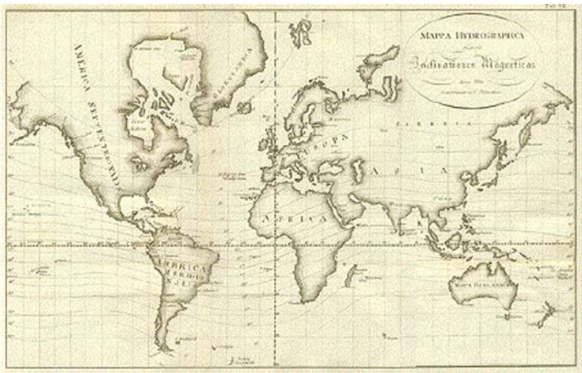

Figure 2.8. Global map of isoclines of magnetic inclination of 1780, published by C. Hansteen in 1830 [*Hansteen,* 1830a] (Philographikon Gallery (Germany), http://www.philographikon.com/). **Enlarge.**

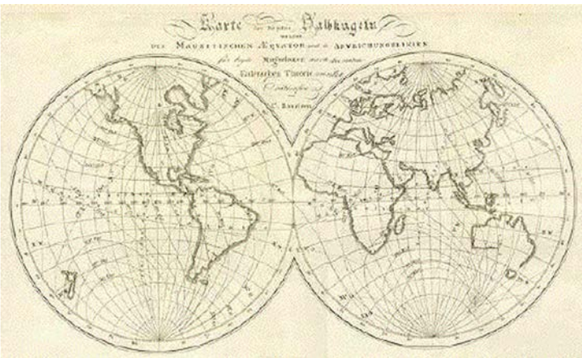

Figure 2.9. Global map of isogons of magnetic declination of 1787, published by C. Hansteen in 1830 [*Hansteen,* 1830b] (Philographikon Gallery (Germany), http://www.philographikon.com/). **Enlarge.**

2.7 World Charts of Isogons (1841), Magnetic Meridians and Parallels (1840) and Isodynamics of Magnetic Intensity (1837–1939)

During his expeditions in the Americas and Europe, Alexander Von Humboldt recorded and reported on magnetic measurements of declination, inclination and field intensity. During the first decades of the 19th century, more efforts to measure these three magnetic field components has resulted in a large number of observations, all of which have been mapped on a global scale. These measurements were taken over nearly the same period, varying from one component to another, but all were made prior to 1839. Alexander Von Humboldt asked Heinrich Berghaus to compile the illustrations for all observations of nature and natural phenomena in an Atlas [*Berghaus*, 1849] accompanying the Kosmos. It became possible to obtain magnetic global charts by interpolating available measurements, and characterize the magnetic vector at any point on the Earth's surface. This was worked on by Gauss [*Gauss*, 1839], who represented the magnetic field as a derivative of the gradient of a potential function. Maps describing both the direction and relative intensity of the field, (i.e. all that was known about the total magnetic field vector at that time) are shown (Figure 2.10–Figure 2.12). In contrast to Gauss, Von Humboldt was not a mathematical analyst, but he had the ability to organize large amount of data, chart the spatial geomagnetic field variations, and to provide useful conclusions about changes in the field. For example, his observations using the total intensity map (Figure 2.12) allowed him to discover the increase in the total field intensity with latitude. Only because of the large volume of data, this statement was generally accepted [*Mandea et al.*, 2010].

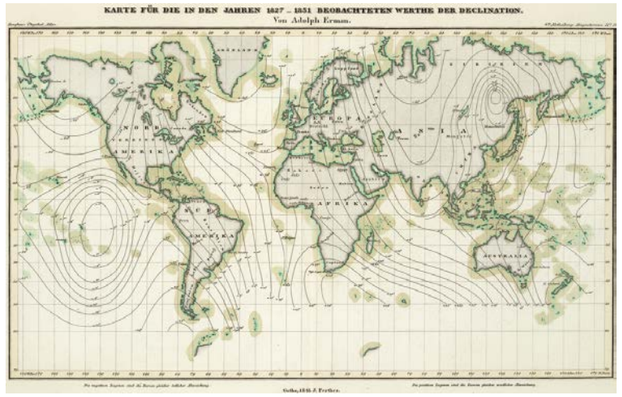

Figure 2.10. Global map of isogons of magnetic declination from measurements between 1827–1831, constructed by H. Berghaus in 1841 [*Berghaus,* 1849] (David Rumsey Map Collection www.davidrumsey.com, USA; Images copyright © 2000 by Cartography Associates). **Enlarge.**

It should be noted that the first global maps of relative magnetic intensity were constructed by C. Hansteen in 1825 (isodynams of horizontal intensity) and in 1826 (isodynams of total intensity) [*Hansteen*, 1895]. Here, one can find a more detailed map of isodynams of total intensity in relative units that had been constructed by Berghaus in 1837 and 1839, on the basis of observations made from 1790–1830 (Figure 2.12a, Figure 2.12b). Data sources and collection periods are shown at the bottom of the map:

1. De Rossel, 1790–1793;
2. A. v. Humboldt, 1799–1805;
3. Sabine, 1818–1819, 1823;
4. Hansteen, 1820–1830;
5. Duperrey, 1822–1825;
6. Keilhau and Boeck, 1826;
7. Keilhau, 1827;
8. Litke, 1826–1828;
9. King, 1826–1829;
10. Due, 1828–1830;
11. Erman, 1828–1830;
12. Kupffer, 1829.

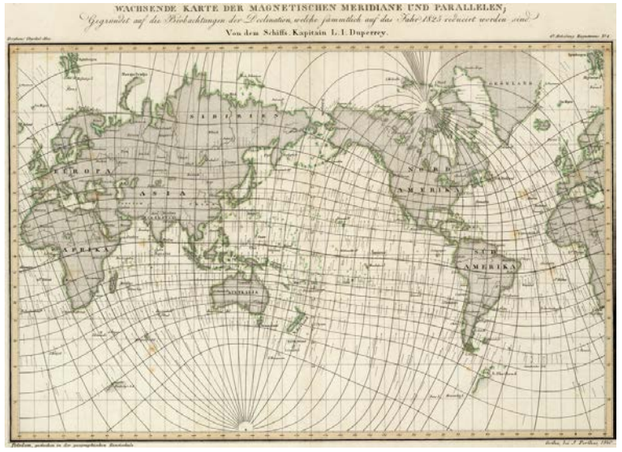

Figure 2.11a. Global map of magnetic meridians and parallels from measurements in 1825, constructed by Berghaus in 1840 [*Berghaus,* 1849] (David Rumsey Map Collection www.davidrumsey.com, USA; Images copyright © 2000 by Cartography Associates). **Enlarge.**

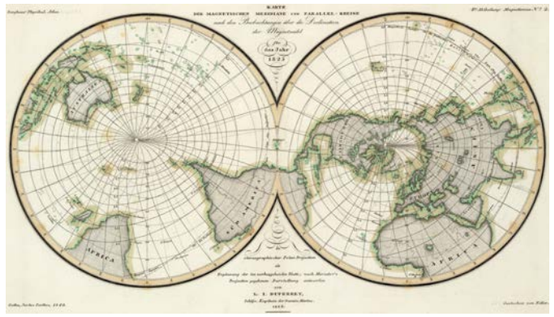

Figure 2.11b. Global map of magnetic meridians and parallels from measurements in the polar zones in 1825, constructed by Berghaus in 1840 [*Berghaus,* 1849] (David Rumsey Map Collection www.davidrumsey.com, USA; Images copyright © 2000 by Cartography Associates). **Enlarge.**

On the three maps the epochs range from 1827–1831 for declination (Figure 2.10), and 1790–1830 for intensity (Figure 2.12). For inclination (Figure 2.11), the header indicates all values have been reduced to 1825.

The quality of these maps, published about two centuries ago, was analyzed by comparison to similar maps, reconstructed using the *gufm*1 model in 2010 [*Mandea et al.*, 2010].

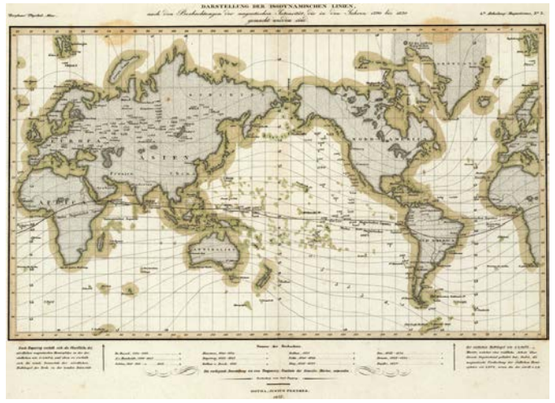

Figure 2.12a. Global map of isodynams of magnetic intensity using measurements from 1790–1830, constructed by Berghaus in 1837 [*Berghaus,* 1849] (David Rumsey Map Collection www.davidrumsey.com, USA; Images copyright © 2000 by Cartography Associates). **Enlarge.**

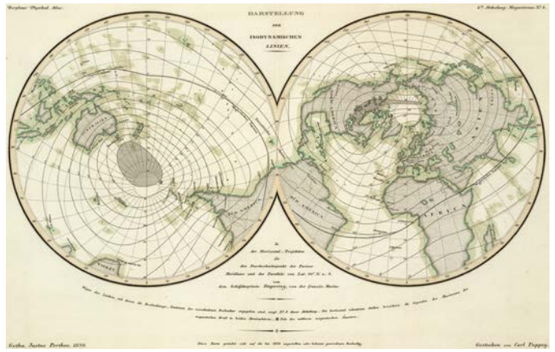

Figure 2.12b. Global map of isodynams of magnetic intensity using measurements in the polar zone from 1790–1830, constructed by Berghaus in 1839 [*Berghaus,* 1849] (David Rumsey Map Collection www.davidrumsey.com, USA; Images copyright © 2000 by Cartography Associates). **Enlarge.**

2.8 Comparison of 1837–1841 Charts With Analogous Maps Obtained From the *gufm*1 Model in 2010

2.8.1 Declination maps

The first observation is linked to the agonic lines, where declination has no curvature. Between the Berghaus declination map (Figure 2.10), and the one we computed from the *gufm*1 model (Figure 2.13) there are three distinct agonic lines; one circling a region over the Sea of Japan, another crossing European Russia, India and Australia, and the third one running from the North magnetic pole to the South magnetic pole over the western part of North and South America. At the bottom of Berghaus' map, the legend states, "Die negativen Isogonen sind die Kurven gleicher

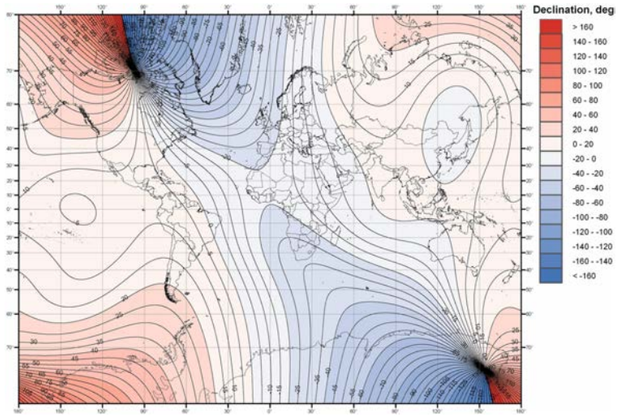

Figure 2.13. Global map of isogons for 1830, constructed using the *gufm*1 model [*Mandea et al.*, 2010]. **Enlarge.**

ostlicher Abweichung", which translates as "The negative isogonal curves correspond to eastern deviation and The positive isogonal curves correspond to western deviation". Indeed, the isoline values on Berghaus' map are shown with the opposite sign compared to the modern convention (Figure 2.13). For example, in both maps the values of declination over the Atlantic basin and the African continent reach comparable values with modulus near 20°, but with opposite signs. It seems that Von Humboldt or Berhaus chose to express the magnetic variations in the western declination using positive values and the eastern declination using negative values. It can be seen from Berghaus' map that few regions are characterized by measurements of higher precision, e.g. "22°,5" in the Northwest region of Africa.

2.8.2 Inclination maps

Figure 2.11 indicates "magnetic parallels", which we consider to be a representation of magnetic inclination. Berghaus' map (Figure 2.11a) together with the one we computed from the *gufm*1 model (Figure 2.14) show the existence of the magnetic equator with comparable detail. Berghaus' map very nicely demonstrates the "knee" in the zero curve in the South American region. Moreover, in both maps it is possible to see how well the Northern and Southern magnetic regions are delimited.

2.8.3 Total intensity maps

Comparing the maps of total intensity (Figure 2.12 and Figure 2.15). makes it possible to appreciate the quality of Berghaus' map, that was created at a time when measurements of this field component were not completely understood. Berghaus' map shows isolines expressed in "Humboldt units" (Hu). Both maps indicate the existence of the South Atlantic Anomaly, the area where the magnetic field intensity has its minimum values; the anomaly of 0.9 Hu, which equals to 31,446.9 nT, shown on Figure 2.12a covers nearly the same area as the 32,000 nT anomaly shown in Figure 2.15. Another remarkable feature present in Berghaus' map and in the one built using the *gufm*1 model is the two lobes of maxima over Canada and Siberia. Both maps show these maxima in the

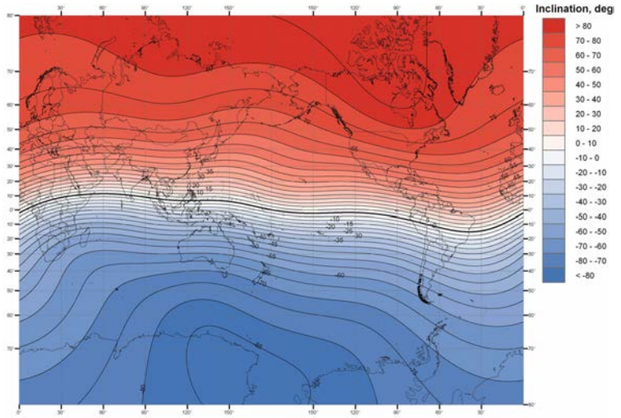

Figure 2.14. Global map of isoclines of 1830, constructed by the *gufm*1 model. The bold line represents the magnetic equator [*Mandea et al.*, 2010]. **Enlarge.**

same regions. The South magnetic pole is indicated by the maxima situated in Antarctica.

The worldwide geomagnetic observations made by Von Humboldt (via the British Colonial Observatories, the Gottingen Magnetic Union, and the Russian chain of observatories) have been valuable ingredients in mapping the Earth's magnetic field. Comparison of Von Humboldt's pioneering efforts on charting declination, inclination and total intensity with similar maps obtained from more complete datasets and well-developed models, is a testament to the quality of his work [*Mandea et al.*, 2010].

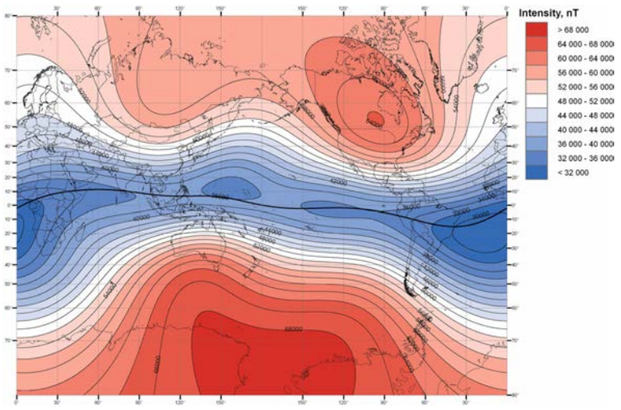

Figure 2.15. Global map of total intensity for 1830, constructed by the *gufm*1 model. The magnetic equator is shown as a bold line [*Mandea et al.*, 2010]. **Enlarge.**

2.9 Charts of the Earth's Magnetic Field Features of 1840

Johann Carl Friedrich Gauss, a German mathematician, astronomer and physicist, is recognized as one of greatest scientists of all times. He is connected to much of the fundamental research

in nearly all basic branches of mathematics: algebra, differential and non-Euclidean geometry, numerical analysis, theory of functions of complex variables, probability theory, as well as astronomy, geodesy and mechanics.

Since 1831, Gauss' main interests were in physics. Progression of Gauss' scientific interests in the field of terrestrial magnetism can be seen in his regular correspondence with astronomers Olbers, Schumacher, Encke, and Gerling, over a long period of time. Gauss had not only created the method of absolute determination of intensity but he also improved the accuracy of magnetic measurements by attaching a mirror to a suspended magnet and measuring a deviation angle of the magnet through a tube, using a scale installed at a distance of several meters from the magnet and mirror. Gauss was the first who used this accurate and convenient method of measuring angles of turns that known as the Kohlrausch method.

In addition to his works on the techniques of making magnetic field measurements, Gauss developed a mathematical theory of terrestrial magnetism. His work "General Theory of Terrestrial Magnetism" was published in 1839 in the annals "Results of Observations of the Magnetic Union for 1838". In this book he made an assumption that the Earth's magnetic field has a potential that depends on geographic location.

In 1840, Gauss and Weber published the "Atlas of Terrestrial Magnetism" [*Gauss, Weber,* 1840]. This Atlas contained global maps of the distribution of magnetic potential, the density of the fictitious "magnetic liquid" on a surface, and maps of declination, inclination, horizontal intensity, and total intensity of the geomagnetic field (Figure 2.16), complete with explanations of each map. In development of his theory of terrestrial magnetism, Gauss used some known theorems as well as introducing new ones related to the properties of the potential function.

2.10 Charts of Isogons for 1787 and 1840, Isoclines for 1780 and 1840, Magnetic Declination and Inclination (65–90°N) as Computed by Gauss' Theory, and Isodynamic Lines for 1840 (1856)

Sabine's campaign for global magnetic surveys (Figure 2.17) is regarded by historians of science as the first scientific endeavor requiring substantial government support, both financial and in kind in the form of naval ships and army logistics. It is known as the Magnetic Crusade and is described in detail by [*Cawood*, 1979].

Sabine was almost fanatical in his collection and archiving of observations, which he believed to be the essential foundation of the advancement of knowledge. His main scientific legacy is his review of all magnetic observations made from about 1818 until 1876, when his scientific activity ceased. The compilation is thorough and accurate, and is published in fifteen contributions to the "Philosophical Transactions of the Royal Society". His compilation forms the major part of modern models of the geomagnetic field for the first half of the 19-th century [*Bloxham*, 1986; *Bloxham et al.*, 1989; *Jackson et al.*, 2000]; so carefully was it constructed that

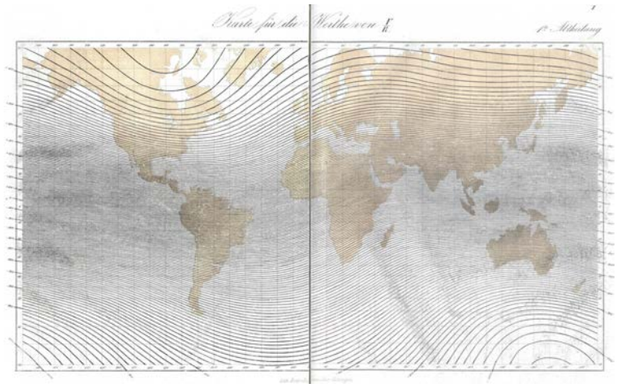

Figure 2.16. Global maps of GMF characteristics, published by C. F. Gauss in 1840 [*Gauss, Weber,* 1840]. **Enlarge.**

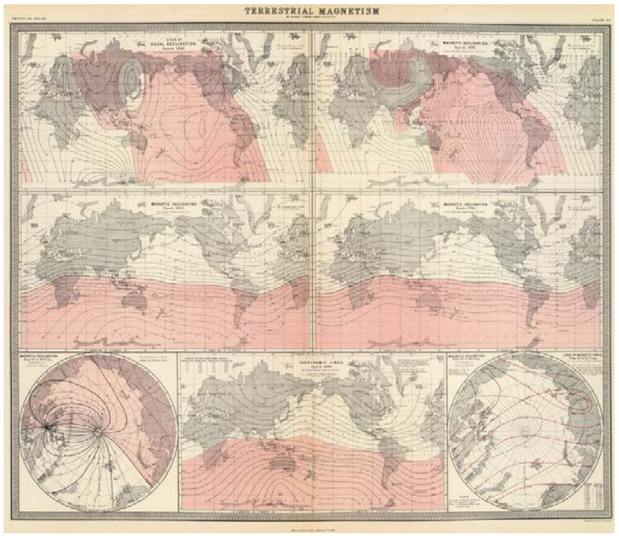

Figure 2.17. Terrestrial magnetism: isogons of magnetic declination (1840); isoclines of magnetic inclination (1840); isogons of magnetic declination (1787); isoclines of magnetic inclination (1780); magnetic declination (65–90°N), calculated by the Gauss method; isodymanic lines of magnetic intensity (1840); magnetic inclination (65–90°N), calculated by the Gauss method; magnetic intensity (65–90°N) (David Rumsey Map Collection, www.davidrumsey.com, USA; Images copyright © 2000 by Cartography Associates). The maps were constructed by E. Sabine in 1856 [*Sabine,* 1856]. Global map of isoclinic lines for 1780 and the map of isogons for 1787 were constructed on the basis of materials published by Hansteen in 1830 [*Hansteen,* 1830a, 1830b]. **Enlarge.**

it could be used virtually unedited in a modern inversion. Sabine's work was not restricted to data compilation, and by careful statistical analysis he demonstrated a relationship between sunspots and magnetic storms, thus heralding the start of a completely new discipline of solar-terrestrial physics [*Gubbins*, 2007].

2.11 World Charts of Isogons for 1858, and Isoclines and Isodynamics of Magnetic Intensity (1862)

In 1862, the World Atlas had been published containing three full-color maps of the geomagnetic field characteristics on a single sheet (Figure 2.18). The maps were given the title "System of Terrestrial Magnetism", authored by F. A. Garnier. The scale for the isogons is presented in the main map, and was approximately 1 : 70,000,000, with the zero meridian running through Paris. Contents of the maps are given below:

1. Declination is shown as an image of isogons running through points of equal declination of a magnetic needle for 1858;
2. Inclination is shown as an image of isoclinic lines indicating the degree of vertical slope of a magnetic needle as it moves away from the equator in each hemisphere;
3. Intensity is shown as an image of isodynams related to the northern and southern hemispheres. They demonstrate increasing magnetic field strength moving off a line of minimal intensity near the equator.

An insertion with partial map of Antarctica and the South magnetic pole is given at the bottom of the main map.

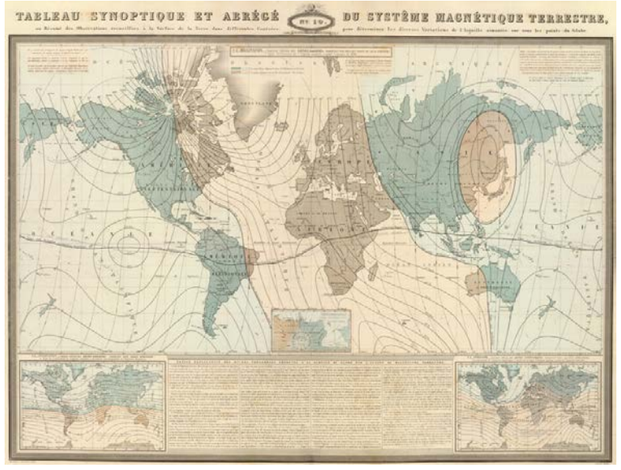

Figure 2.18. Three world maps: isogons of magnetic declination for 1858, isoclinic lines of magnetic inclination, and isodynams of magnetic strength, constructed by F. A. Garnier in 1862 [*Garnier,* 1862] (David Rumsey Map Collection, www.davidrumsey.com, USA; Images copyright © 2000 by Cartography Associates). **Enlarge.**

Chapter 3. Auxiliary Maps

3.1 Map of the INTERMAGNET Network of Observatories

The international network of ground observatories, INTERMAGNET, provides the most precise and operational information about the Earth magnetic field [*Kerridge*, 2001] (Figure 3.1). This network of observatories, that carries out regular observations of the geomagnetic field, was established in 1987. INTERMAGNET functions under the aegis of the International Association of Geomagnetism and Aeronomy (IAGA) [http://www.iugg.org/IAGA/]. For the first time, a robust network of continually operating and permanent observatories were registered under a single entity [*Kerridge*, 2001]. Previous organization of world geophysical observations were all temporary. Thus, many geophysical observatories that were created under the framework of the International Geophysical Year (IGY) near the end of 1950's [*Chapman*, 1959], operated for only 2–3 years. The basic purpose of the INTERMAGNET network is to guarantee performance of observations as well as collection, archiving, distribution, and scientific analysis of data in an operational environment. The global INTERMAGNET network has been continually expanding, and currently includes approximately 120 observatories [http://www.intermagnet.org/] (Figure 3.1).

Most observatory operations are financed by national governments. Some of them are supported by universities, and a few are owned and operated by private interests [*Love*, 2008]. Most geomagnetic observations are transmitted from the observatories to five data centers within 72 hours of collection. The data centers are located in the cities of Edinburgh (Great Britain), Golden (Colorado State, USA), Kyoto (Japan), Ottawa (Canada), and Paris (France) [*St-Louis*, 2008]. In 2012, the Russian segment of INTERMAGNET consisted of six observatories including the settlements of Borok (BOX) [*Chulliat, Anisimov*, 2008] and Arti (ARS), and the cities of Irkutsk (IRT), Novosibirsk (NVS), Magadan (MGD), and Yakutsk (YAK). Recording of data on the geomagnetic field is done in the form of a time series. Observatories are located across the entire globe, and each of them is equipped with instruments needed for digital recording of absolute values of the three components and the modulus of the vector of the geomagnetic field at the corresponding location [*Jankowski, Sucksdorff*, 1996; *Turner et al.*, 2007]. This equipment includes:

1. Fluxgate magnetometer on non-magnetic theodolite (declinometer/inclinometer) for measuring absolute values of magnetic declination and inclination;
2. Scalar proton magnetometer for measuring the absolute value of the geomagnetic field intensity;
3. Vector fluxgate magnetometer (variometer) for measuring geomagnetic field variations;
4. System of continuous collection and recording (a complex of hardware and software) of data coming from the vector and scalar magnetometers.

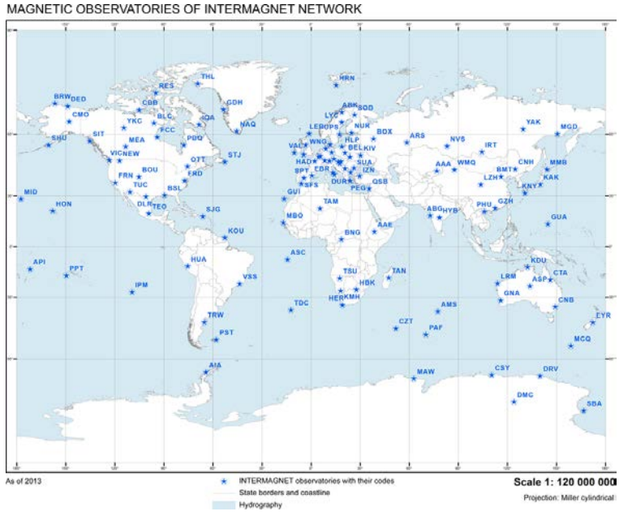

Figure 3.1. Map of geomagnetic observatories of the INTERMAGNET network in 2012. **Enlarge.**

3.2 Map of IGY Observatories From 1957 to 1959

2007 marks 125 years since start of the First International Polar Year (1-st IPY, 1882–1883), 75 years since the beginning of the Second International Polar Year (2-nd IPY, 1932–1933), and 50 years since the International Geophysical Year (IGY, 1957–1959). These international efforts resulted in many extremely important discoveries in the field of geomagnetism and aeronomy. The Third International Polar Year (IPY) was organized and took place from 2007–2008 [http://www.ipy.org/]. International observations conducted during the 3-rd IPY are regarded as a continuation of scientific programs of the two previous IPY's. It was already clear by the 19-th century, that investigation of global processes required large scale international collaboration between geophysicists from around the world. In January 1875, Austrian scientist K. Weyprecht declared: "The North polar area should be surrounded by a ring of stations where simultaneous observations could be carried out over a single year with identical instruments and techniques. And in doing so, most attention should be given to geophysics. There is almost no branch of natural and physical-geophysical sciences which would not be seriously interested in the very thorough investigations of polar regions. It is evident with respect to terrestrial magnetism and polar auroras since the magnetic poles are located at high latitudes". Twelve countries participated in the 1-st IPY where 15 stations were organized. There were already 44 countries and 100 stations participating by the Second IPY.

These campaigns, as well as a world-wide growing observational network demonstrated that a specifically global approach provides a promising opportunity for real progress in the prediction of weather, environmental analysis for radio communications, high altitude aviation, studies of geomagnetic field and other magnetic disturbances, defining of the Earth's oblate spheroid, exploitation of the world ocean resources, and many other practical applications. The idea to organize a new polar year had been quickly adapted into a plan for an International Geophysical Year (IGY). An IGY would allow collaboration of observations not only from polar regions, but also monitoring of physical processes in the tropics and mid-latitudes (i.e. to turn the entire globe into a laboratory). This idea was supported by the International Council of Scientific Unions (ICSU), [http://www.icsu.org/], and its branches, including the International Union of Geodesy and Geophysics (IUGG), [http://www.iugg.org/], the International Astronomical Union (IAU), [http://www.iau.org/], the World Meteorological Organization (WMO), [http://www.wmo.int/], and the International Union of Radio Science (URSI), [http://www.ursi.org/]. About eighty thousand scientists from 67 countries worked under the framework of the IGY. For example, the USSR used 557 stations and observatories to carry out observations across all sections of the IGY Program. These observations were performed in accor-

dance with the coordinated methodology agreed to by participating countries and international organizations. Below we present more detailed information about the works in geomagnetism.

About 110 geomagnetic observatories had operated prior to IGY. To support the IGY, many new observatories and stations were developed. In total, for the year 1957, the World Data Centers contain data from more than 200 observatories and stations (Figure 3.2).

In the USSR, observations of the Earth magnetic field were carried out at 32 stations. The basic goals of these investigations were: study of geomagnetic disturbances (i.e. magnetic storms and sub-storms), short term periodic geomagnetic variations, and study of the interaction of the geomagnetic field with the oceans.

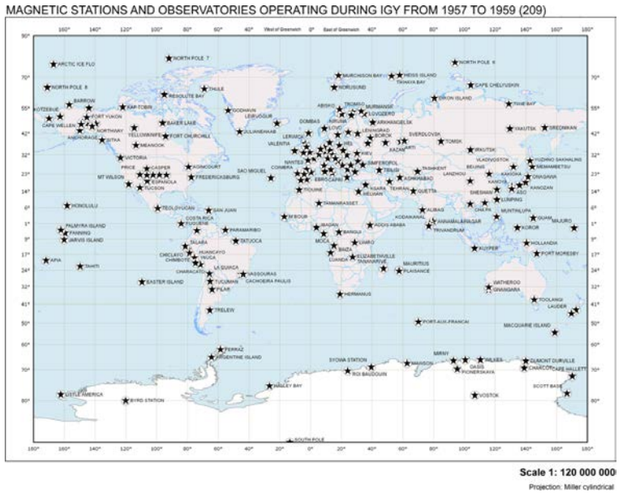

Figure 3.2. Map of geomagnetic stations and observatories in operation during IGY in 1957–1959 [*Allen et al.,* 1985]. **Enlarge.**

Geomagnetic stations were equipped with supplementary variometers, having different sensitivities and additional control instrumentation, including quartz magnetometers. At about 15 stations that were co-located with Ionospheric sounding radars (Ionosonde), magnetometers were made to produce visual records. This made it possible for these stations to operationally identify the onset of geomagnetic disturbances and provide near real time warnings of the disturbances. At high latitudes, stations on the shore of the Arctic Ocean and the isles of the Soviet drifting stations "North Pole 6, 7, and 8" carried out the IGY program on geomagnetic observations. Scientific station "North Pole 6" was constructed in the spring of 1956 by the Arctic and Antarctic Research Institute (ROSHYDROMET) on an ice-floe north of Wrangel Island. Over a period of 41 months, the station drifted a distance of 8750 km. The station "North Pole 7" began operation at the end of April of 1957 on pack ice in the Arctic Ocean to the north-east of Wrangel Island. The station "North Pole 8" was constructed in April of 1959, and was also north-east of Wrangel Island. Over a year, this station drifted a distance of 2700 km.

For registration of short-period geomagnetic oscillations (SGO) the specially designed magnetic-flux meter devices were used for the first time in the USSR. This observation method allowed registration of periods ranging from tenths of a second to several minutes with a high enough sensitivity and thus opened the era of SGO studies. This helped to better understand plasma and oscillation processes in the magnetosphere and interplanetary medium. The following six stations were equipped with magnetic-flux meter devices: Lovozero, Borok, Tbilisi, Simferopol, Petropavlovsk-Kamchatsky, and Mirny.

A large volume of geomagnetic observations was collected from the Soviet non-magnetic schooner "Zarya" that was built for study of the geomagnetic field. Over two and a half of years, Zarya covered a distance of about 100,000 km. The schooner crossed the Atlantic ocean at different latitudes six times, and the Indian Ocean five times. Previously unknown magnetic anomalies were discovered, which was important for both science and navigation. Before the IGY, observational information on oceanic magnetic fields was rather irregular and incomplete. Geomagnetic observations were also carried out on the Antarctic continent at Soviet stations Mirny, Vostok, Pionerskaya, and Komsomolskaya.

A new system of World Data Centers (WDC) had been created for collection and long-term preservation of environmental data [http://www.icsu-wds.org/]. This system proved to be extremely efficient because it could guarantee not only long-term storage that maintained the data quality, but provided free and open access to the data. This system has been maintained and expanded upon since IGY.

International scientific cooperation established during IGY yielded striking results for both science and practical applications. As a result, many new problems were raised, and the search for answers to these problems has yielded even more progress in geophysics and its practical applications.

3.3 Global Networks of Ground-Based Geomagnetic Observatories From 1813–2005

Ground based observations of the geomagnetic field began in the 19-th century, during which time, the first magnetic stations began operation. This section discusses the dynamics of an increasing network of geomagnetic observatories from 1813 to 2005, as well as the main stages of its growth. The data archive of historical observations is presented in the form of mean annual values of the geomagnetic field parameters, which are served by the Internet site "Space Physics Interactive Data Resource" [http://spidr.ngdc.noaa.gov/].

International scientific campaigns such as the first International Polar Year in 1882/1883, the second International Polar Year in 1932/1933, and the International Geophysical Year in 1957/1958 encouraged the opening of many observatories around the world. Geomagnetism is an interdisciplinary science. As a result, observatories are operated by a wide variety of institutes with interests ranging from geology, cartography, geophysics (including seismology and earthquake prediction), meteorology and solar terrestrial physics, and astronomy [*Macmillan*, 2007].

Figure 3.3 presents maps of stations and observatories in operation during the following time periods: 1813–1837, 1843–1872, 1877–1901, 1903–1922, 1923–1947, 1948–1957, 1959–1968, 1969–1988, 1989–1999 and 2000–2005. The selected intervals were chosen as the most representative in terms of the growth dynamics of the global network of geomagnetic observations from 1813 to 2005.

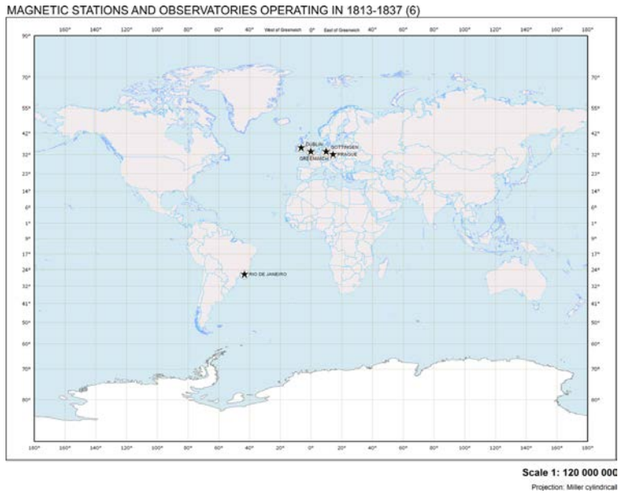

Figure 3.3. Map of geomagnetic stations and observatories operating during different time intervals from 1813 until 2005. **Enlarge.**

References

Allen, J. H., et al. (1985), Combined international catalog of geomagnetic data, *Volume 92 of Report UAG*, U.S. Dept. of Commerce, NOAA, National Environmental Satellite, Data, and Information Service, NGDC, 291.

Barton, C. (2002), Survey tracks current position of South magnetic pole, *EOS, 83*, 27, 291.

Berghaus, H. (1849), *Berghaus' Physikalischer Atlas (1837–1848)*, 1st edition, Gotha, Justus Perthes.

Bloxham, J. (1986), Models of the magnetic field at the core-mantle boundary, *J. Geophys. Res., 91*, 13954–13966.

Bloxham, J., D. Gubbins, A. Jackson (1989), Geomagnetic secular variation, *Philosophical Transactions of the Royal Society of London, 329*, 415–502.

Bowen, E. (1752), *A Complete Atlas or Distinct Views of the Known World*, London.

Carlut, J., V. Courtillot, G. Hulot (2000), Over how much time should the geomagnetic field be averaged to obtain the mean paleomagnetic field? *Terra Nova, 11*, 5, 239–243.

Cawood, J. (1979), *The Magnetic Crusade: science and politics in early Victorian Britain*, Isis, 70, 493–519.

Chapman, S. (1959), *IGY: Year of Discovery: The Story of the International Geophysical Year*, USA, University of Michigan Press.

Chapman, S., J. Bartels (1940), *Geomagnetism,* Oxford Univ. Press, New York, 1049.

Chulliat, A., S. Anisimov (2008), The Borok INTERMAGNET magnetic observatory, *Russ. J. Earth. Sci.*, 10, ES3003. doi:10.2205/2007ES000238.

Constable, C. (2007), Nondipole field, in *Encyclopedia of Geomagnetism and Paleomagnetism*, edited by D. Gubbins and E. Herrero-Bervera, Earth Science Series, Springer, The Netherlands, 1054, ISBN: 978-1-4020-3992-8.

Courtillot, V., J.-L. Le Mouël (2007), The study of Earth's magnetism (1269–1950): A foundation by Peregrinus and subsequent development of geomagnetism and paleomagnetism, *Rev. Geophys., 45*, RG3008, doi:10.1029/2006RG000198.

Fraser-Smith, A. C. (1987), Centered and eccentric geomagnetic dipoles and their poles, 1600–1985, *Rev. Geophys., 25*, 1–16.

Garnier, F. A. (1862), *Atlas spheroidal et universel de geographie*, Paris.

Gauss, C. F. (1839), Allgemeine Theorie des Erdmagnetismus, in: *Resultate aus den Beobachtungendes Magnetischen Vereins im Jahre 1838*, C. F. Gauss and W. Weber (Eds.), 146–148, Leipzig, Germany.

Gauss, C. F., W. E. Weber (1840), *Atlas Des Erdmagnetismus: Nach Den Elementen Der Theorie Entworfen*, Leipzig, Weidmann'sche Buchhandlung.

Gubbins, D. (2007), Sabine, Edward (1788–1883), in *Encyclopedia of Geomagnetism and Paleomagnetism*, edited by D. Gubbins and E. Herrero-Bervera, Earth Science Series, Springer, The Netherlands, 1054, ISBN: 978-1-4020-3992-8.

Halley, E. (1701), *Tabula Totius Orbis Terrarum Exhibens Declinationes Magneticas, ad Annum 1700 composita ab Edmundo Halleyo simul cum Inclinationibus a Poundio observatis et Ventis Universalibus*, Paris.

Halley, E., P. Mortier (1702), *Carte Generale De Toutes Les Costes Du Monde Avec Un Indice Des Variations Magnetiques Selon Les Observations Faites En L'Annee 1700 Par Edm. Halley*, Amsterdam.

Hansteen, C. (1819), *Karte der beyden Halbkugeln welche den Magnetischen Equator und die Abweichingslinien für beyde Magnetaxen nach der ersten Eulerschen Theorie vorstellt entworfen, von C. Hansteen.*

Hansteen, C. (1830a), *Mappa Hydrographica Sistens Inclinationes Magneticas, Anni 1780 constructa a C. Hansteen.*

Hansteen, C. (1830b), *Mappa Hydrographica Sistens Declinationes Magneticas, Anni 1787 constructa a C. Hansteen.*

Hansteen, C. (1859), *Reiseerindringer, Chr. Tonsbergs Forlag, Christiania.*

Hansteen, C. (1895), Die ättest en Karten der Isogonen, Isoclinen, Isodynamen, *Nature, 51*, 509, doi:10.1038/051509b0.

Hansteen, J. M. (2007), Hansteen, Christopher (1784–1873), in *Encyclopedia of Geomagnetism and Paleomagnetism*, edited by D. Gubbins and E. Herrero-Bervera, Earth Science Series, Springer, The Netherlands, 1054, ISBN: 978-1-4020-3992-8.

Hulot, G., C. Eymin, B. Langlais, M. Mandea, N. Olsen (2002), Small-scale structure of the geodynamo inferred from Oersted and Magsat satellite data, *Nature, 416*, 620–623.

Hulot, G., A. Khokhlov, J.-L. LeMouël (1997), Uniqueness of mainly dipolar magnetic fields recovered from directional data, *Geophys. J. Int., 129*, 347–354.

Jackson, A., A. R. T. Jonkers, M. R. Walker (2000), Four centuries of geomagnetic secular variation from historical records, *Philosophical Transactions of the Royal Society of London, 358*, 957–990.

Jankowski, J., C. Sucksdorff (1996), *Guide for Magnetic Measurements and Observatory*, IAGA publication, Practice, Warsaw, 235.

Jonkers, A. R. T. (2000), *North by Northwest*, 2 vols., Cuvillier, Gottingen, Germany, 1002.

Jonkers, A. R. T., A. Jackson, A. Murray (2003), Four centuries of geomagnetic data from historical records, *Reviews of Geophysics, 41*, 2, 1006.

Jonkers, A. R. T. (2007), Geomagnetism, History of, in *Encyclopedia of Geomagnetism and Paleomagnetism,* edited by D. Gubbins and E. Herrero-Bervera, Earth Science Series, Springer, The Netherlands, 1054, ISBN: 978-1-4020-3992-8.

Kerridge, D. (2001), Intermagnet: worldwide near-real-time geomagnetic observatory data, *Proceedings of the Workshop on Space Weather*, ESTEC.

Korte, M., F. Donadini, C. Constable (2009), Geomagnetic Field for 0–3 ka, Part II: A new Series of Time-Varying Global Models, *Geochem., Geophys. Geosys.*, 10, Q06008, doi:10.1029/2008GC002297.

Le Nautonier, G. (1603), *Mecometrie de l'Eyment: C'est a dire la maniere de mesurer les longitudes par le moyen de l'eyment (avec Priuilege du Roy, Fontaine Bleau, le quinziesme jour d'octobre 1601)*, France.

Love, J. J. (2008), Magnetic monitoring of Earth and space, *Physics Today*, 61, 31–37.

Macmillan, S. (2007), Observatories, Overview, in *Encyclopedia of Geomagnetism and Paleomagnetism*, edited by D. Gubbins and E. Herrero-Bervera, Earth Science Series, Springer, The Netherlands, 1054, ISBN: 978-1-4020-3992-8.

Mandea, M., E. Dormy (2003), Asymmetric behavior of magnetic dip poles, *Earth Planets Space, 55*, 3, 153–157.

Mandea, M., M. Korte, A. Soloviev, A. Gvishiani (2010), Alexander von Humboldt's charts of the Earth's magnetic field: an assessment based on modern models, *Hist. Geo Space. Sci., 1*, 63–76, doi:10.5194/hgss-1-63-2010.

Mandea, M., S. Macmillan (2000), International geomagnetic reference fieldthe eighth generation, *Earth Planets Space, 52*, 1119–1124.

Mandea, M., P.-N. Mayaud (2004), Guillaume le Nautonier, un precurseur dans l'histoire du geomagnetisme, *Rev. Hist. Sci., 57*, 161–174.

Maus, S., T. Sazonova, K. Hemant, J. D. Fairhead, and D. Ravat (2007), National Geophysical Data Center candidate for the World Digital Magnetic Anomaly Map, *Geochem. Geophys. Geosyst., 8*, Q06017, doi:10.1029/2007GC001643.

Newitt, L. R., M. Mandea, L. A. McKee, J.-J. Orgeval (2002), Recent acceleration of the North Magnetic Pole linked to magnetic jerks, *EOS, 83*, 381–388.

Olsen, N., et al. (2000), Oersted Initial Field Model (OIFM), *Geophys. Res. Lett., 27*, 22, 3607–3610.

Report (2009), Creation of maps for magnetic epochs 1940–2005, *Interim report on the research project "Development of the Atlas of the Earth's Magnetic Field", Stage 2,*, IAG, Moscow.

Sabine, E. (1856), Terrestrial Magnetism, *Johnston A. K., The Physical Atlas of Natural Phenomena*, Edinburgh, William Blackwood and Sons.

Sauerbrey, N. F. (1760), *Tabula Geographica utriusque Hemisphaerii Terrestris exhibens declinationem acus magneticae pro singulis locis globi terraquei ad A.C. 1744*, Prussian Academy of Sciences, Germany.

Simonyan A. O., V. P. Golovkov (2009), Spatial features of the manifestation of the geomagnetic field westward drift, *Geomagn. Aeron., 49*, 6, 805–812.

St-Louis, B. (2008), *INTERMAGNET Technical Reference Manual*, Version 4.4.

Turner, G. M., J. L. Rasson, C. V. Reeves (2007), Observation and measurement techniques Treatise on Geophysics, Vol. 5, *Geomagnetism*, Ed. M. Kono, 93–146.

Whitfield, P. (1996), *Charting of the Oceans*, Pomegranate Artbooks, 102–105.

Wilcke, J., C. Försök (1768), *Til en magnetisk inclinations charta (Kartografiskt material), Skala* 1 : 70000000.

Annex 1. Present-Day Maps of the Earth's Magnetic Field

MGMF DECLINATION

MGMF – 1900, 1905, 1910 – D

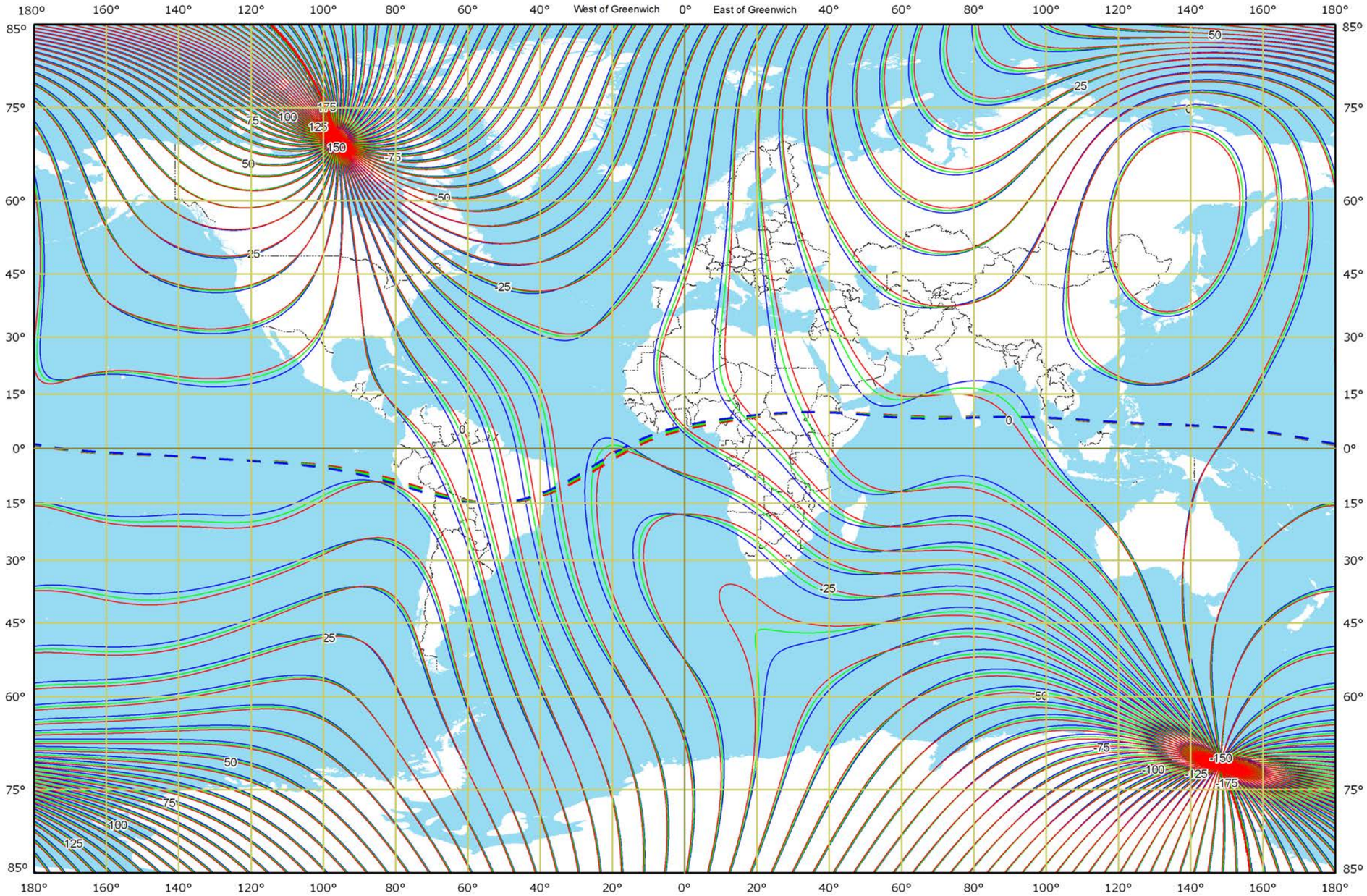

Years	Isogons	Geomagnetic equators
1900		1900
1905		1905
1910		1910

Example of magnetic declination value, degree

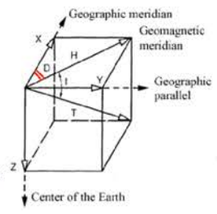

MGMF vector components

D Declination
I Inclination
H Horizontal component
T Total intensity
X North component
Y East component
Z Vertical component

Scale 1: 120 000 000

Projection: Miller cylindrical

MGMF DECLINATION

MGMF – 1910, 1915, 1920 – D

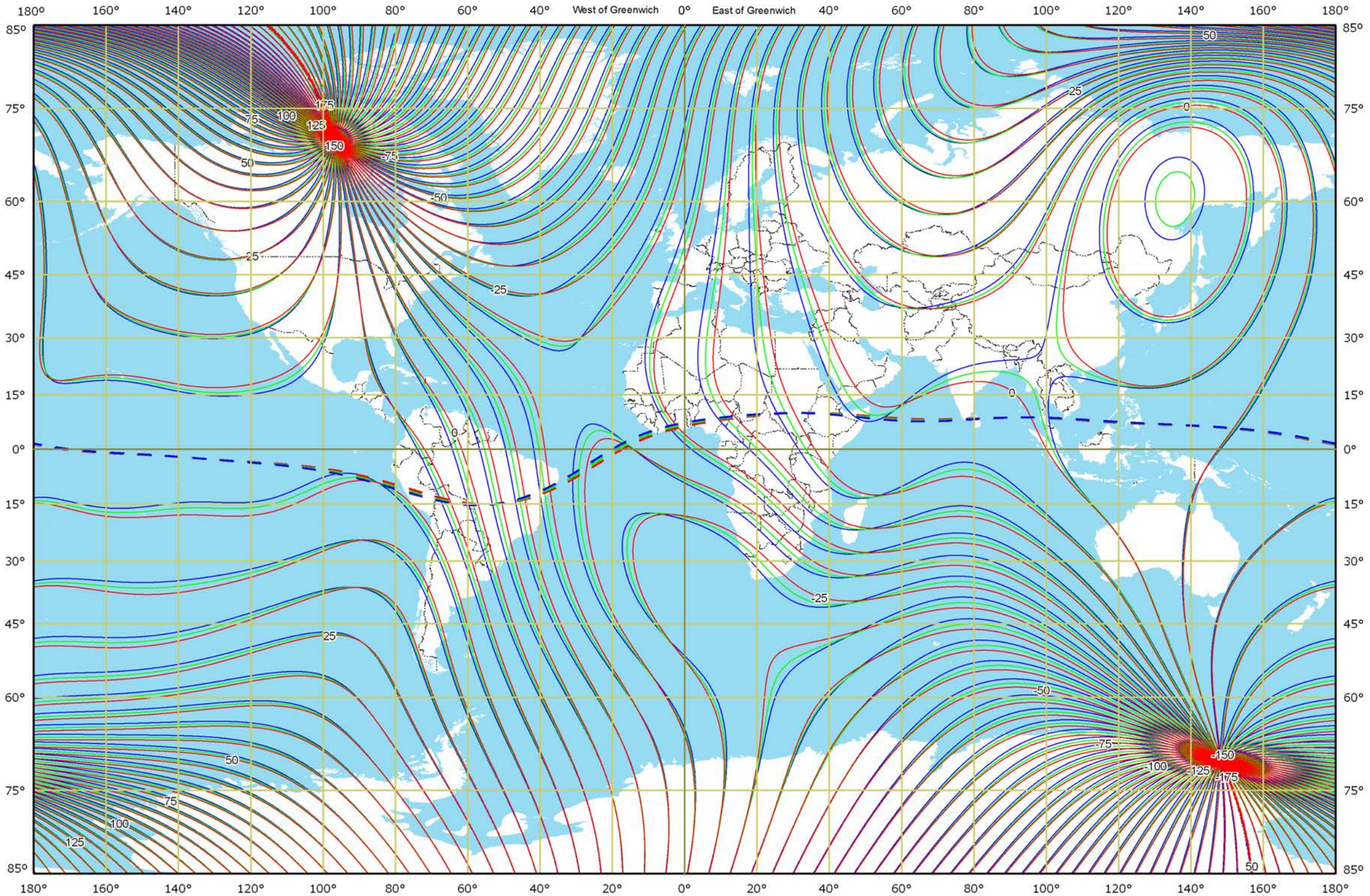

Years	Isogons	Geomagnetic equators
1910		1910
1915		1915
1920		1920

Example of magnetic declination value, degree

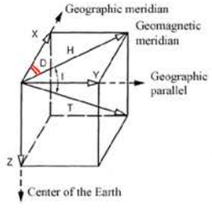

MGMF vector components

D Declination
I Inclination
H Horizontal component
T Total intensity
X North component
Y East component
Z Vertical component

Scale 1: 120 000 000

Projection: Miller cylindrical

MGMF DECLINATION

MGMF– 1920, 1925, 1930 – D

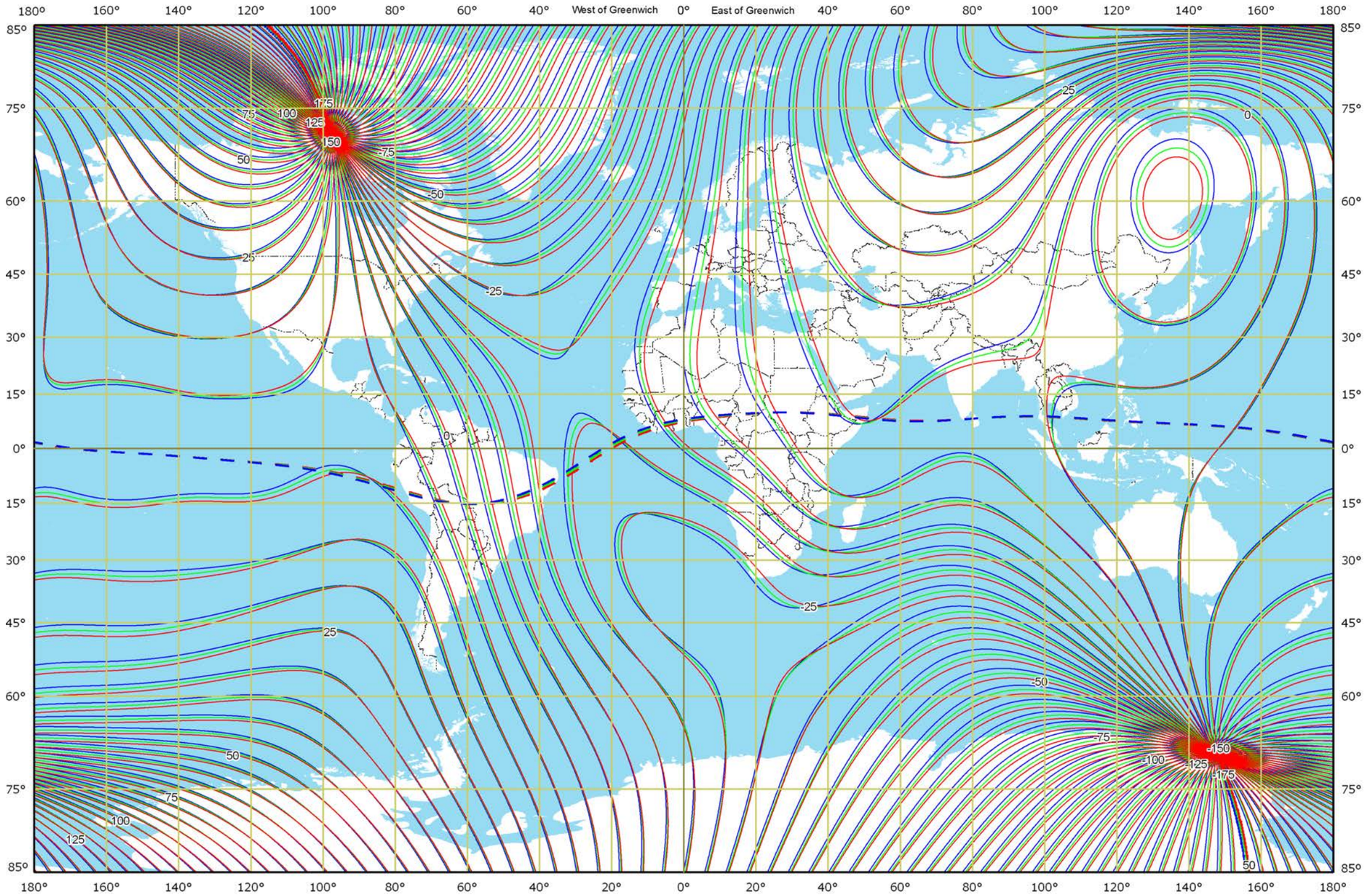

Years	Isogons	Geomagnetic equators
1920		1920
1925		1925
1930		1930

Example of magnetic declination value, degree

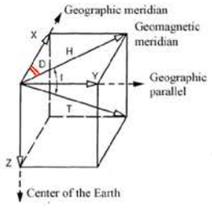

MGMF vector components

D Declination
I Inclination
H Horizontal component
T Total intensity
X North component
Y East component
Z Vertical component

Scale 1: 120 000 000

Projection: Miller cylindrical

MGMF DECLINATION

MGMF – 1930, 1935, 1940 – D

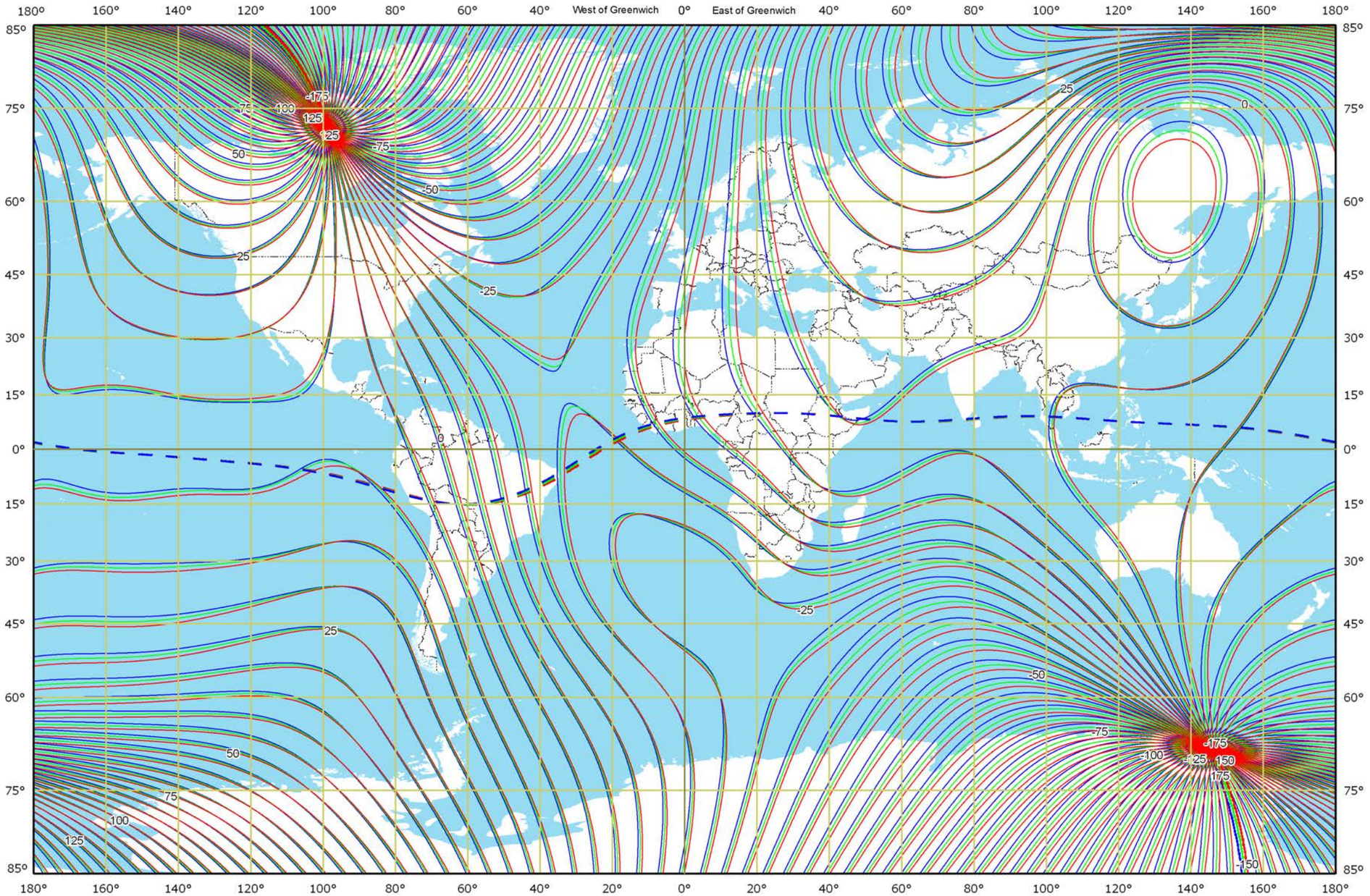

Years	Isogons	Geomagnetic equators
1930		1930
1935		1935
1940		1940

Example of magnetic declination value, degree

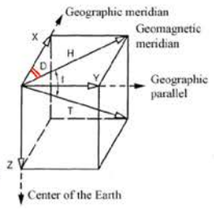

MGMF vector components

D Declination
I Inclination
H Horizontal component
T Total intensity
X North component
Y East component
Z Vertical component

Scale 1: 120 000 000

Projection: Miller cylindrical

MGMF DECLINATION

MGMF – 1940, 1945, 1950 – D

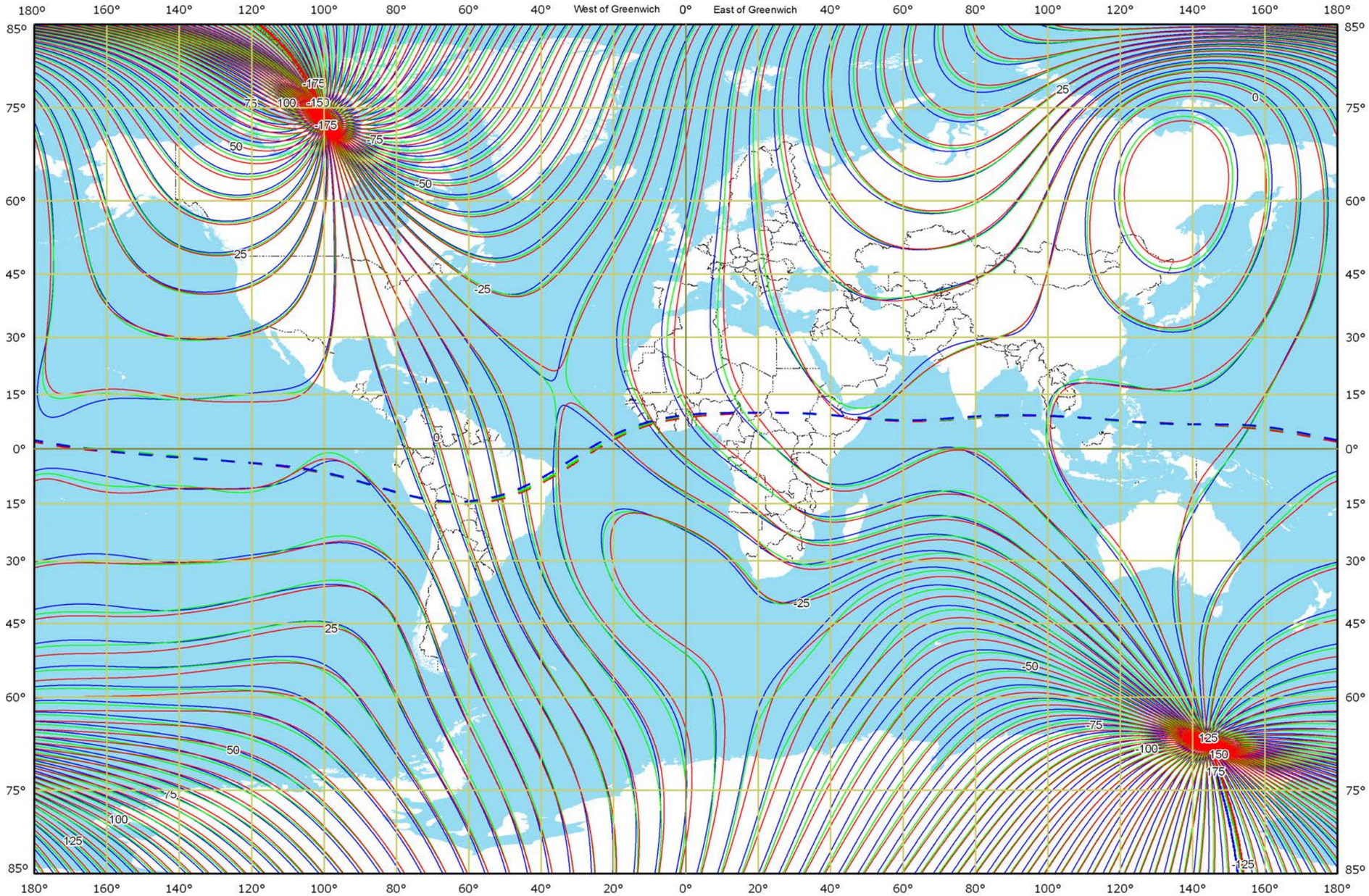

Years	Isogons	Geomagnetic equators
1940		1940
1945		1945
1950		1950

Example of magnetic declination value, degree

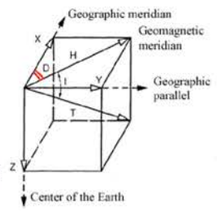

MGMF vector components

D Declination
I Inclination
H Horizontal component
T Total intensity
X North component
Y East component
Z Vertical component

Scale 1: 120 000 000

Projection: Miller cylindrical

MGMF DECLINATION

MGMF – 1950, 1955, 1960 – D

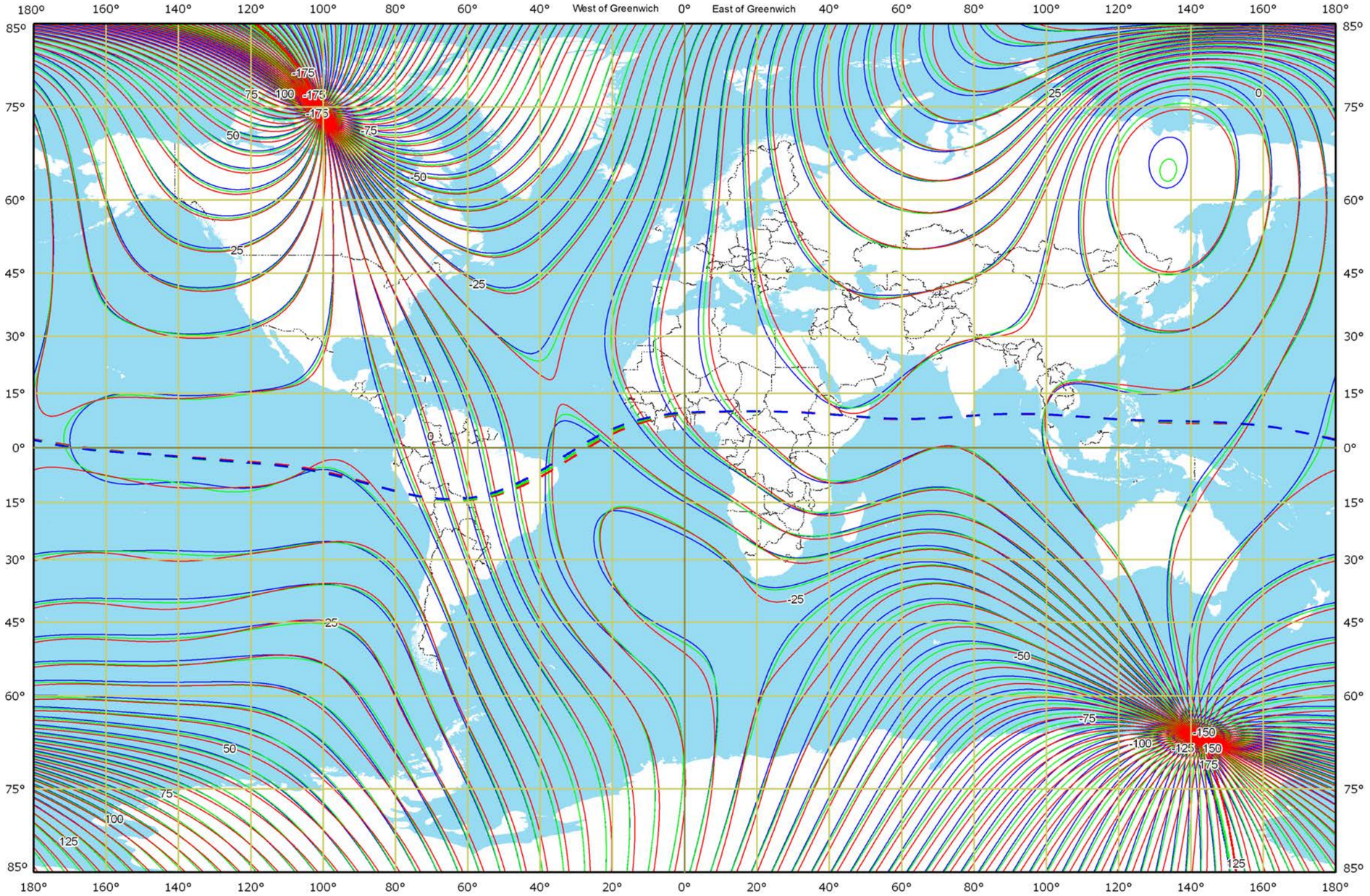

Years	Isogons	Geomagnetic equators
1950		1950
1955		1955
1960		1960

Example of magnetic declination value, degree

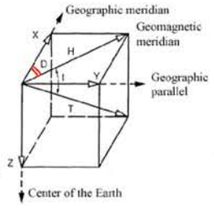

MGMF vector components

D Declination
I Inclination
H Horizontal component
T Total intensity
X North component
Y East component
Z Vertical component

Scale 1: 120 000 000

Projection: Miller cylindrical

MGMF DECLINATION

MGMF– 1960, 1965, 1970 – D

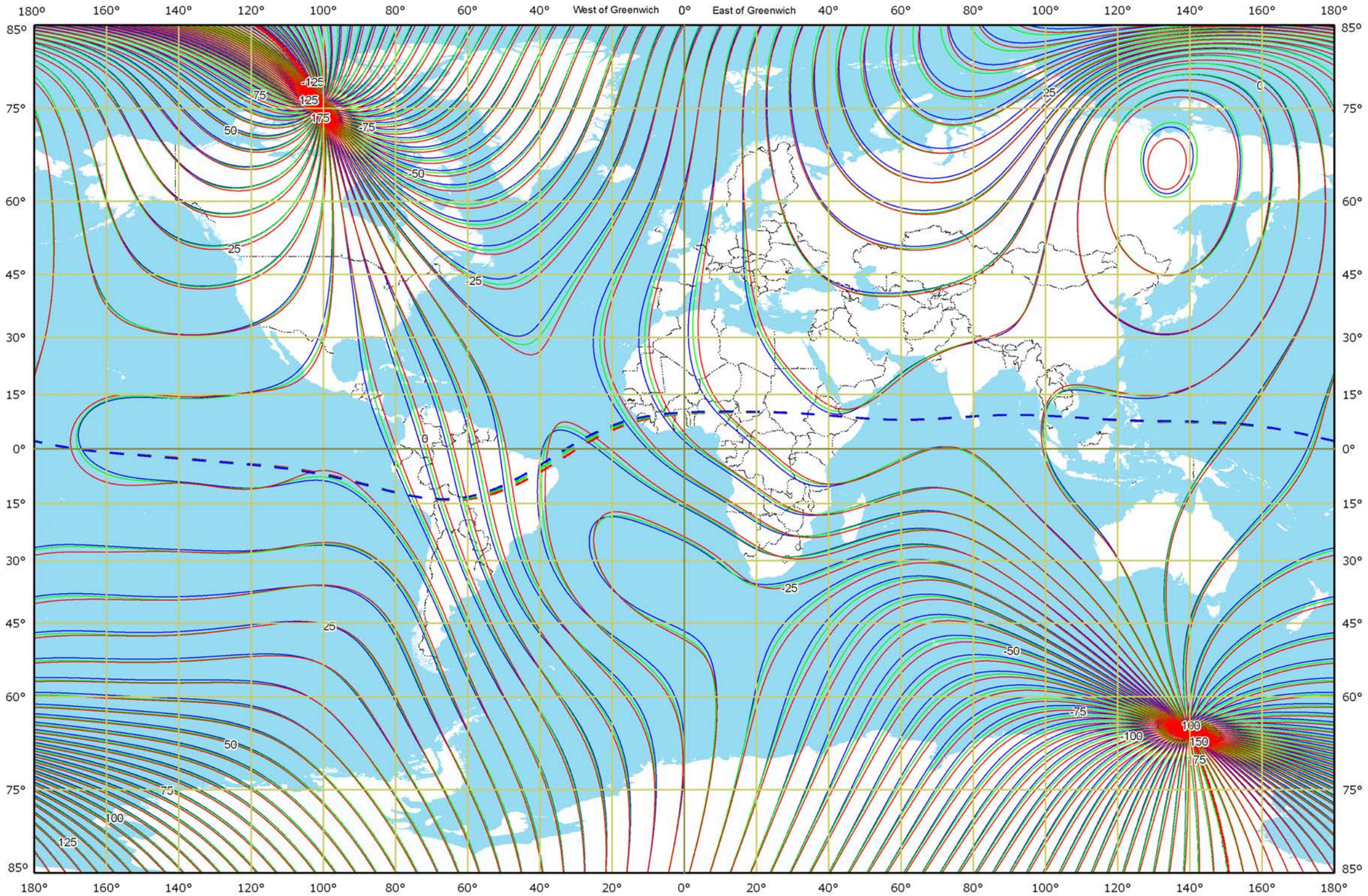

Years	Isogons	Geomagnetic equators
1960		1960
1965		1965
1970		1970

Example of magnetic declination value, degree

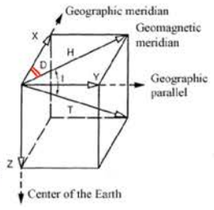

MGMF vector components

D Declination
I Inclination
H Horizontal component
T Total intensity
X North component
Y East component
Z Vertical component

Scale 1: 120 000 000

Projection: Miller cylindrical

MGMF DECLINATION

MGMF – 1970, 1975, 1980 – D

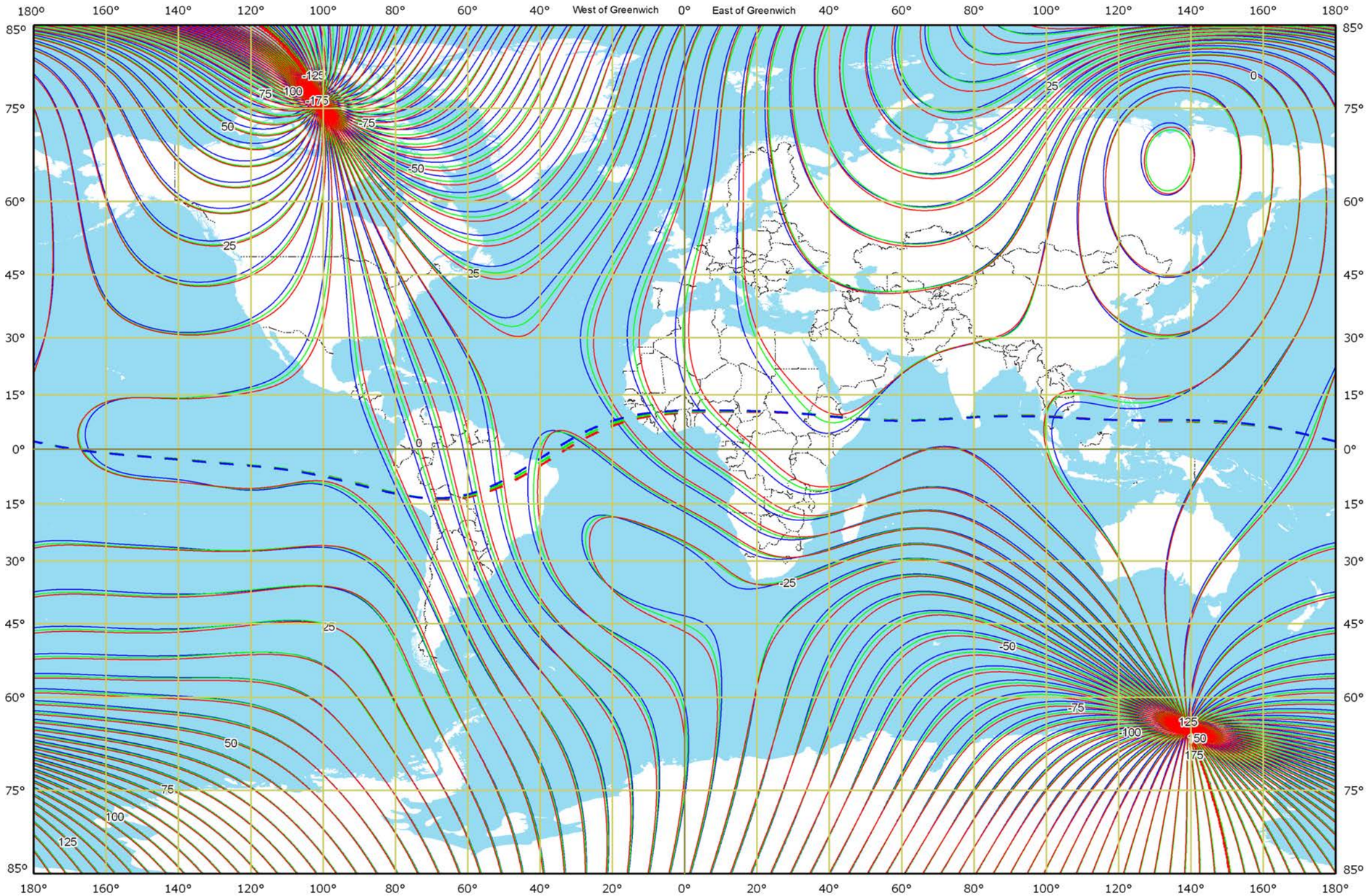

Years	Isogons	Geomagnetic equators
1970		1970
1975		1975
1980		1980

Example of magnetic declination value, degree

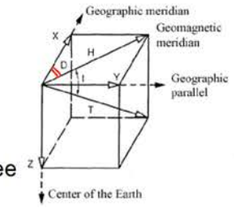

MGMF vector components

D Declination
I Inclination
H Horizontal component
T Total intensity
X North component
Y East component
Z Vertical component

Scale 1: 120 000 000

Projection: Miller cylindrical

MGMF DECLINATION

MGMF – 1980, 1985, 1990 – D

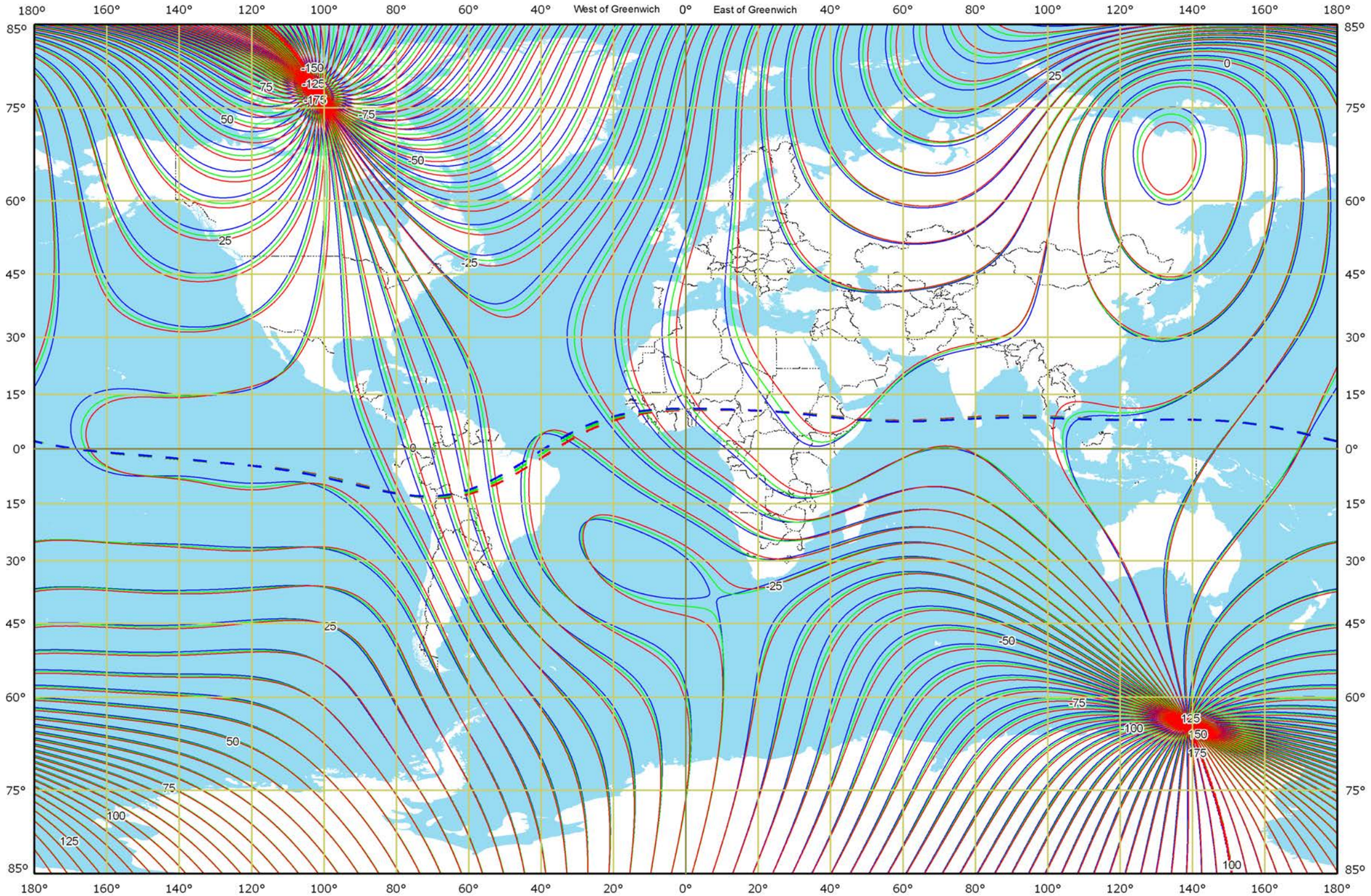

Years	Isogons	Geomagnetic equators
1980		1980
1985		1985
1990		1990

Example of magnetic declination value, degree

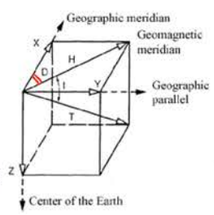

MGMF vector components

D Declination
I Inclination
H Horizontal component
T Total intensity
X North component
Y East component
Z Vertical component

Scale 1: 120 000 000

Projection: Miller cylindrical

MGMF DECLINATION

MGMF - 1990, 1995, 2000 – D

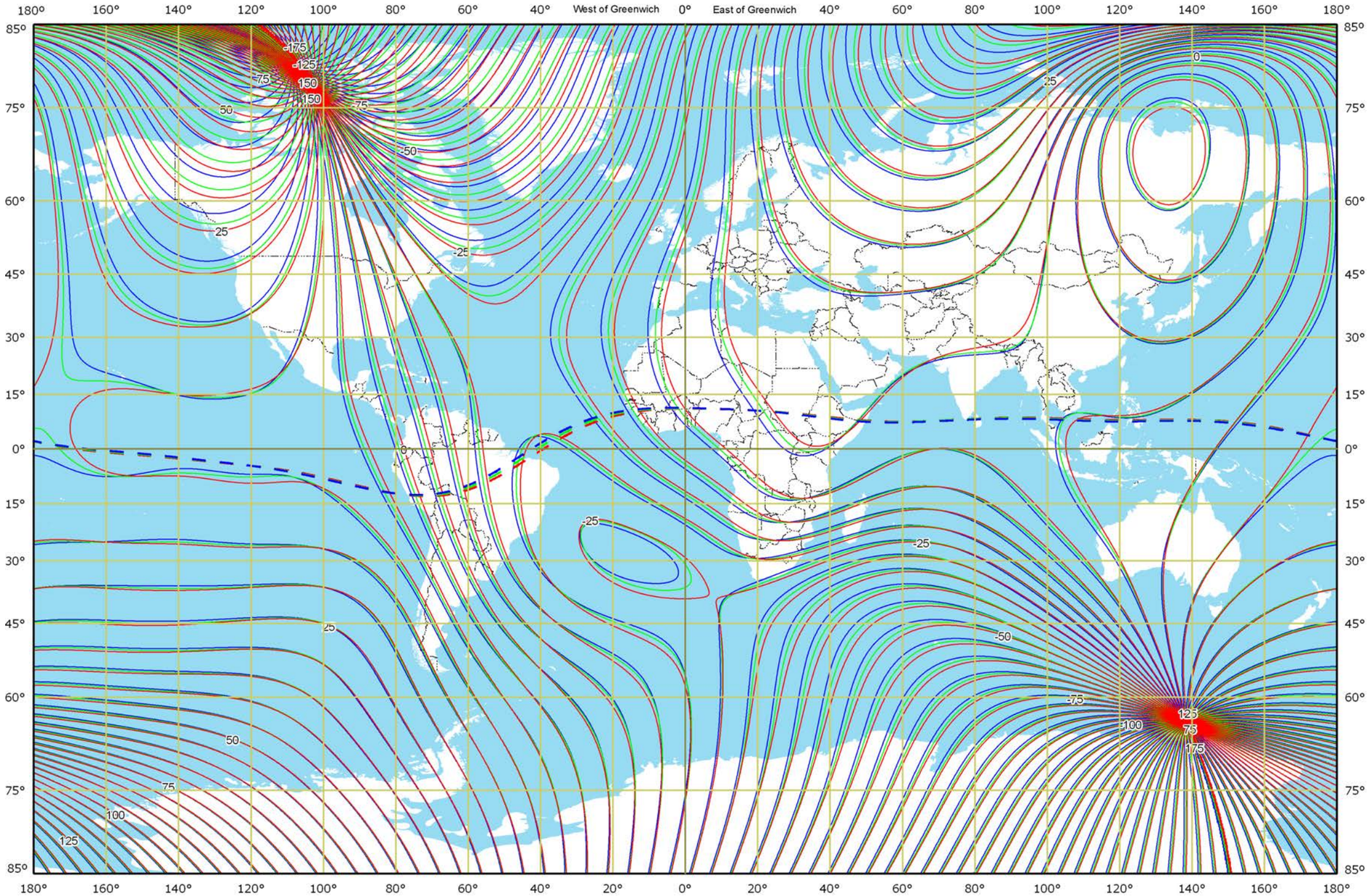

Years	Isogons	Geomagnetic equators
1990		1990
1995		1995
2000		2000

Example of magnetic declination value, degree

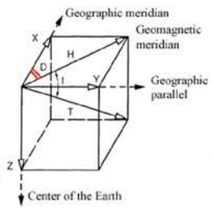

MGMF vector components

D Declination
I Inclination
H Horizontal component
T Total intensity
X North component
Y East component
Z Vertical component

Scale 1: 120 000 000

Projection: Miller cylindrical

MGMF DECLINATION

MGMF –2000, 2005, 2010 – D

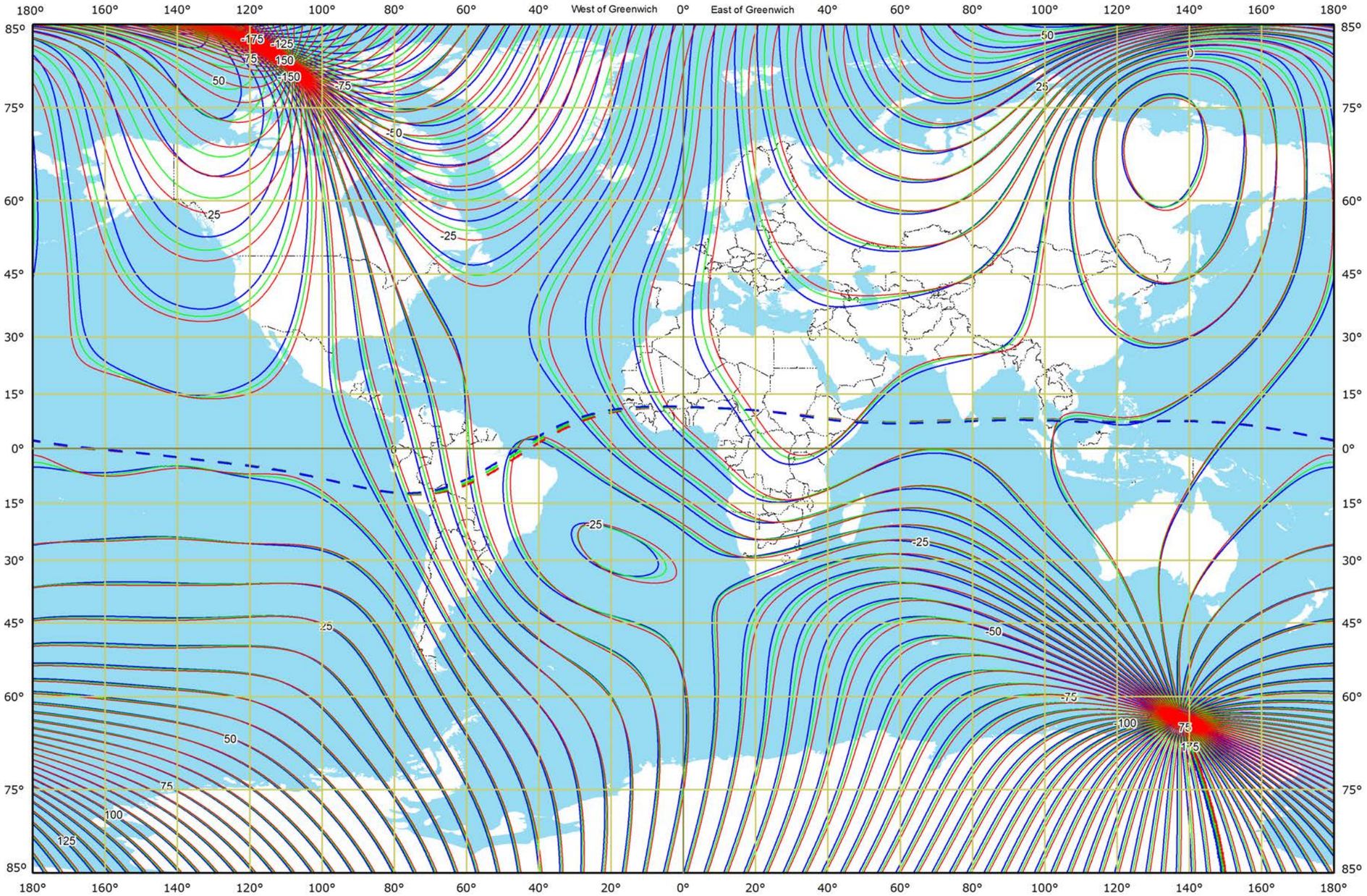

Years	Isogons	Geomagnetic equators
2000		2000
2005		2005
2010		2010

Example of magnetic declination value, degree

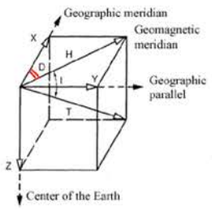

MGMF vector components

D Declination
I Inclination
H Horizontal component
T Total intensity
X North component
Y East component
Z Vertical component

Scale 1: 120 000 000

Projection: Miller cylindrical

MGMF INCLINATION

MGMF – 1900, 1905, 1910 – I

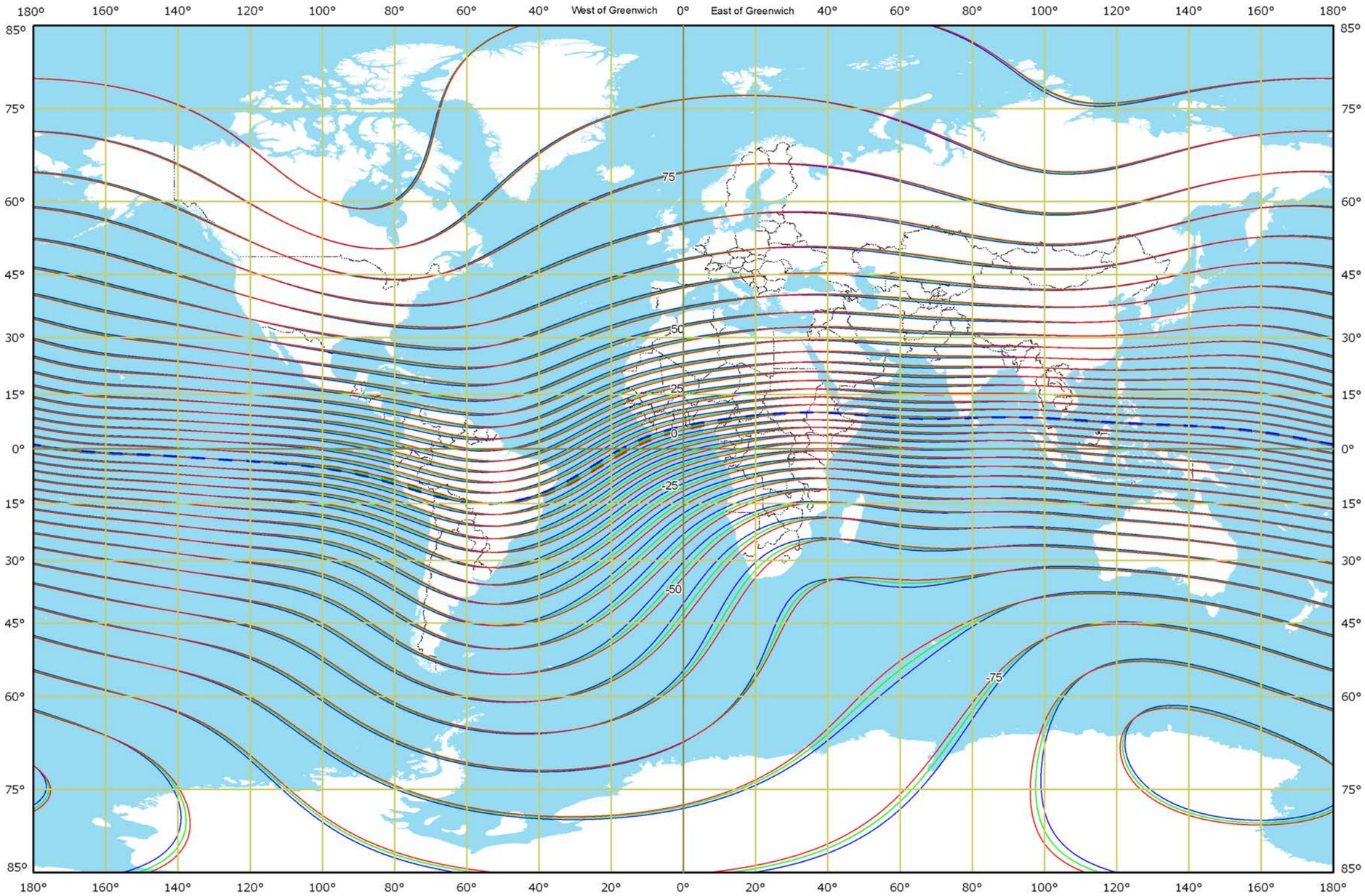

Years	Isoclines	Geomagnetic equators
1900		1900
1905		1905
1910		1910

Example of magnetic inclination value, degree

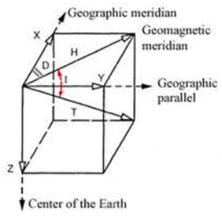

MGMF vector components

D Declination
I Inclination
H Horizontal component
T Total intensity
X North component
Y East component
Z Vertical component

Scale 1: 120 000 000

Projection: Miller cylindrical

MGMF INCLINATION

MGMF – 1910, 1915, 1920 – I

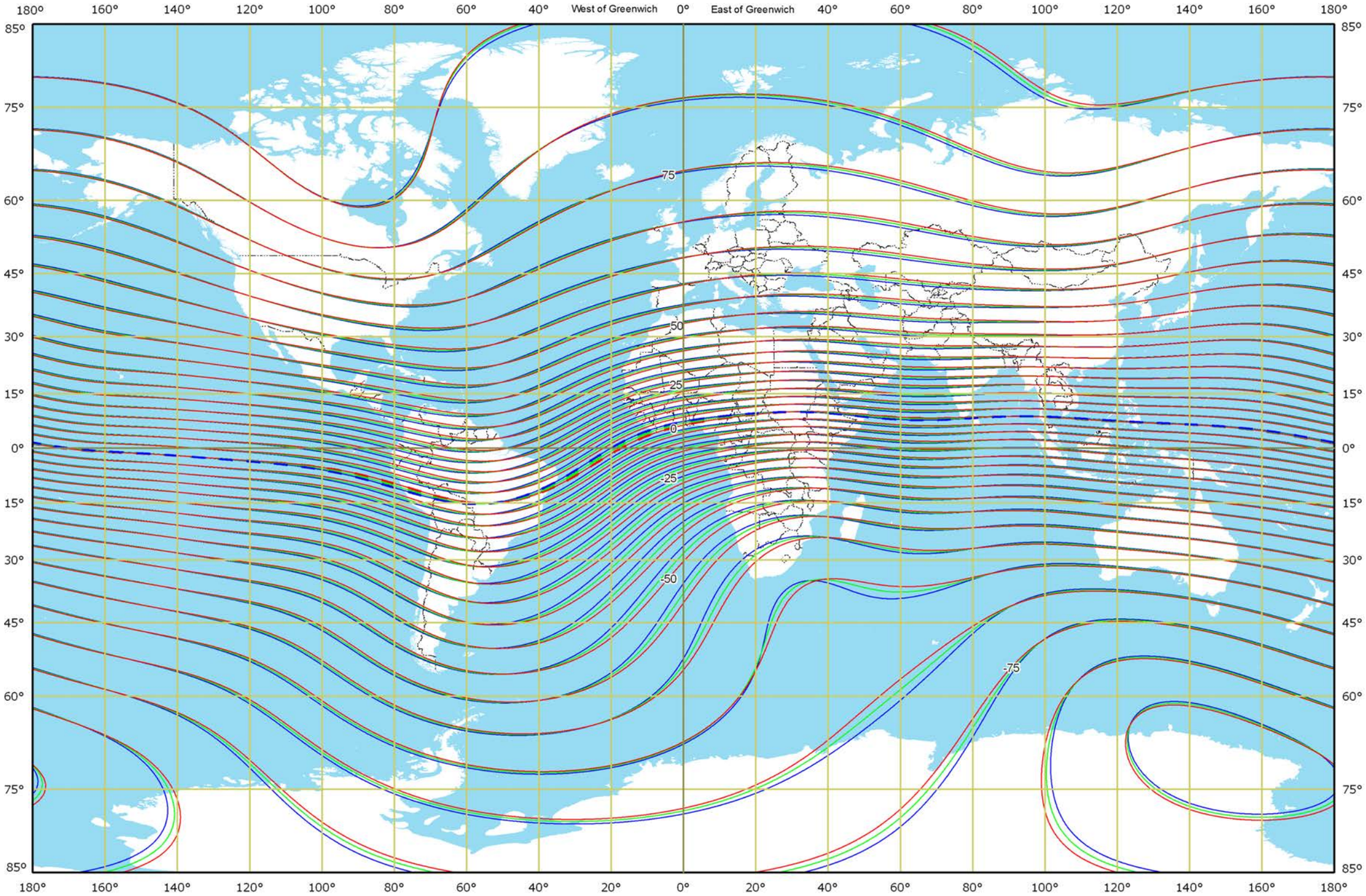

Years	Isoclines	Geomagnetic equators
1910		1910
1915		1915
1920		1920

Example of magnetic inclination value, degree

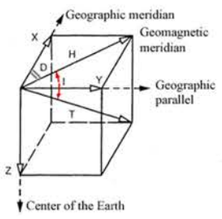

MGMF vector components

D Declination
I Inclination
H Horizontal component
T Total intensity
X North component
Y East component
Z Vertical component

Scale 1: 120 000 000

Projection: Miller cylindrical

MGMF INCLINATION

MGMF – 1920, 1925, 1930 – I

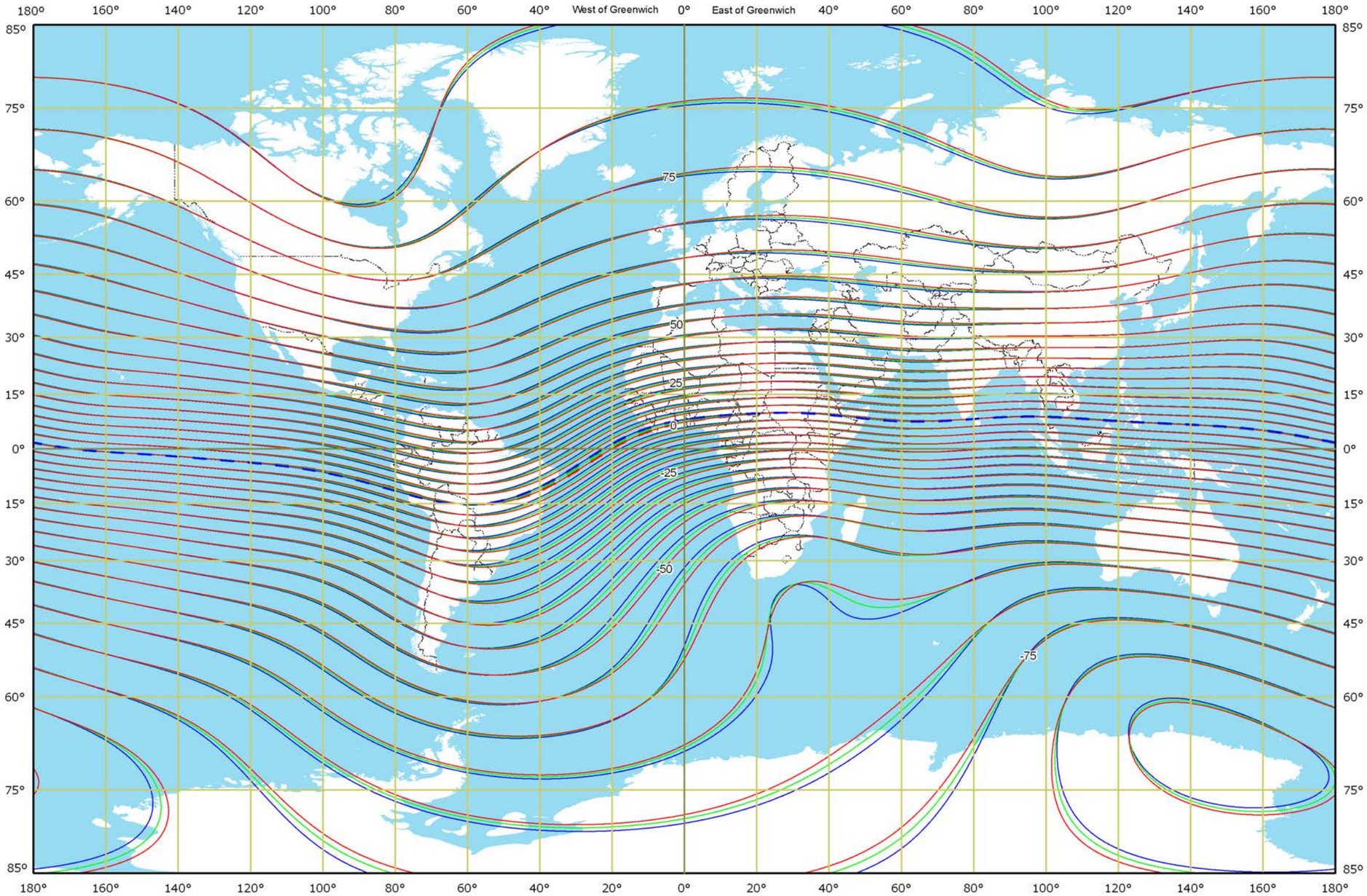

Years	Isoclines	Geomagnetic equators
1920		1920
1925		1925
1930		1930

Example of magnetic inclination value, degree

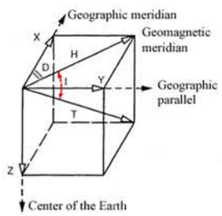

MGMF vector components

D Declination
I Inclination
H Horizontal component
T Total intensity
X North component
Y East component
Z Vertical component

Scale 1: 120 000 000

Projection: Miller cylindrical

MGMF INCLINATION

MGMF – 1930, 1935, 1940 – I

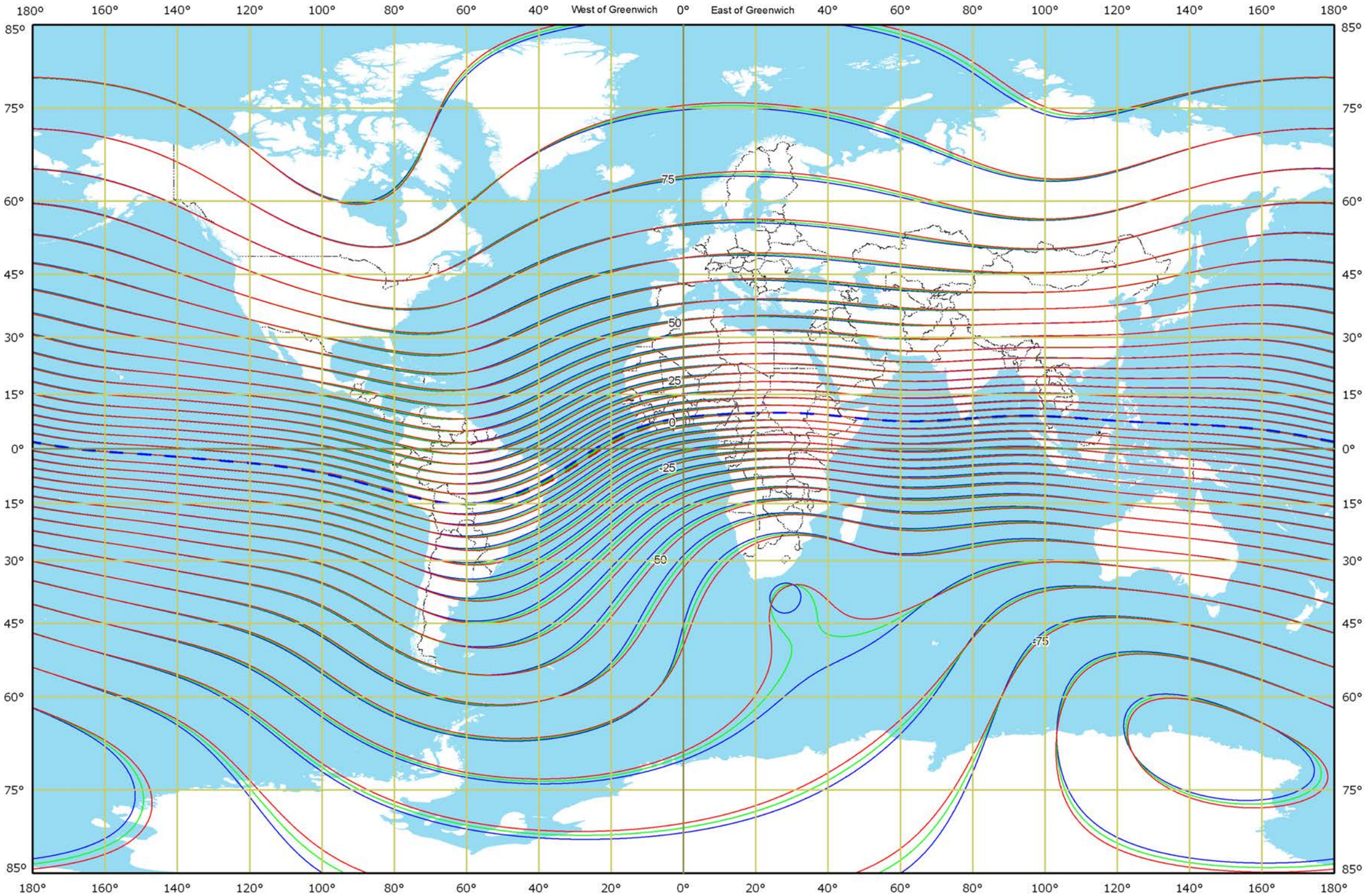

Years	Isoclines	Geomagnetic equators
1930		1930
1935		1935
1940		1940

Example of magnetic inclination value, degree

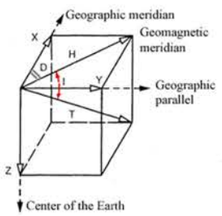

MGMF vector components

D Declination
I Inclination
H Horizontal component
T Total intensity
X North component
Y East component
Z Vertical component

Scale 1: 120 000 000

Projection: Miller cylindrical

MGMF INCLINATION

MGMF – 1940, 1945, 1950 – I

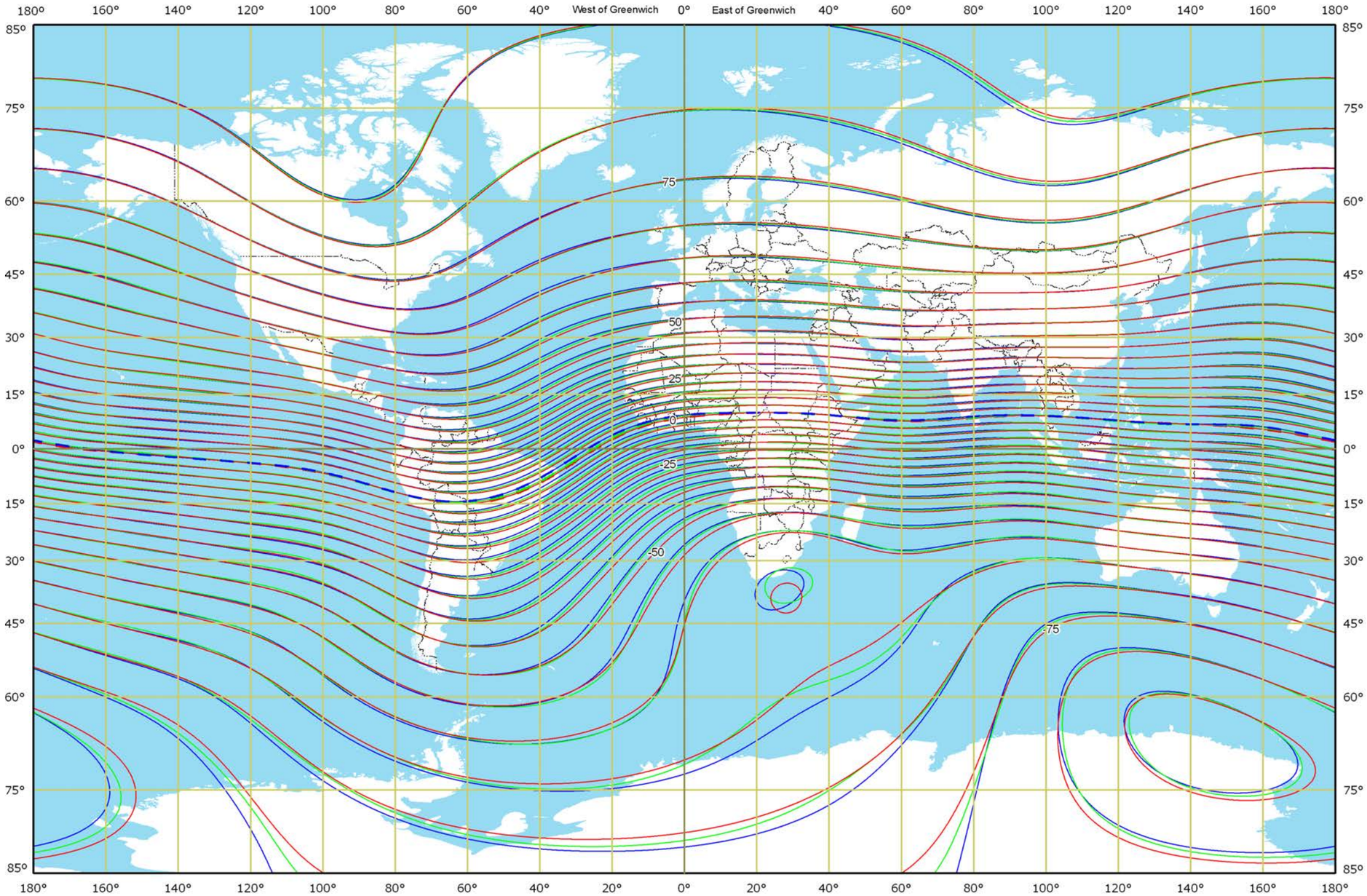

Years	Isoclines	Geomagnetic equators
1940		1940
1945		1945
1950		1950

Example of magnetic inclination value, degree

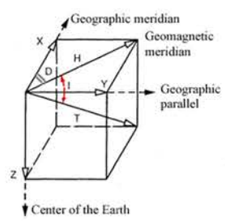

MGMF vector components

D Declination
I Inclination
H Horizontal component
T Total intensity
X North component
Y East component
Z Vertical component

Scale 1: 120 000 000

Projection: Miller cylindrical

MGMF INCLINATION

MGMF – 1950, 1955, 1960 – I

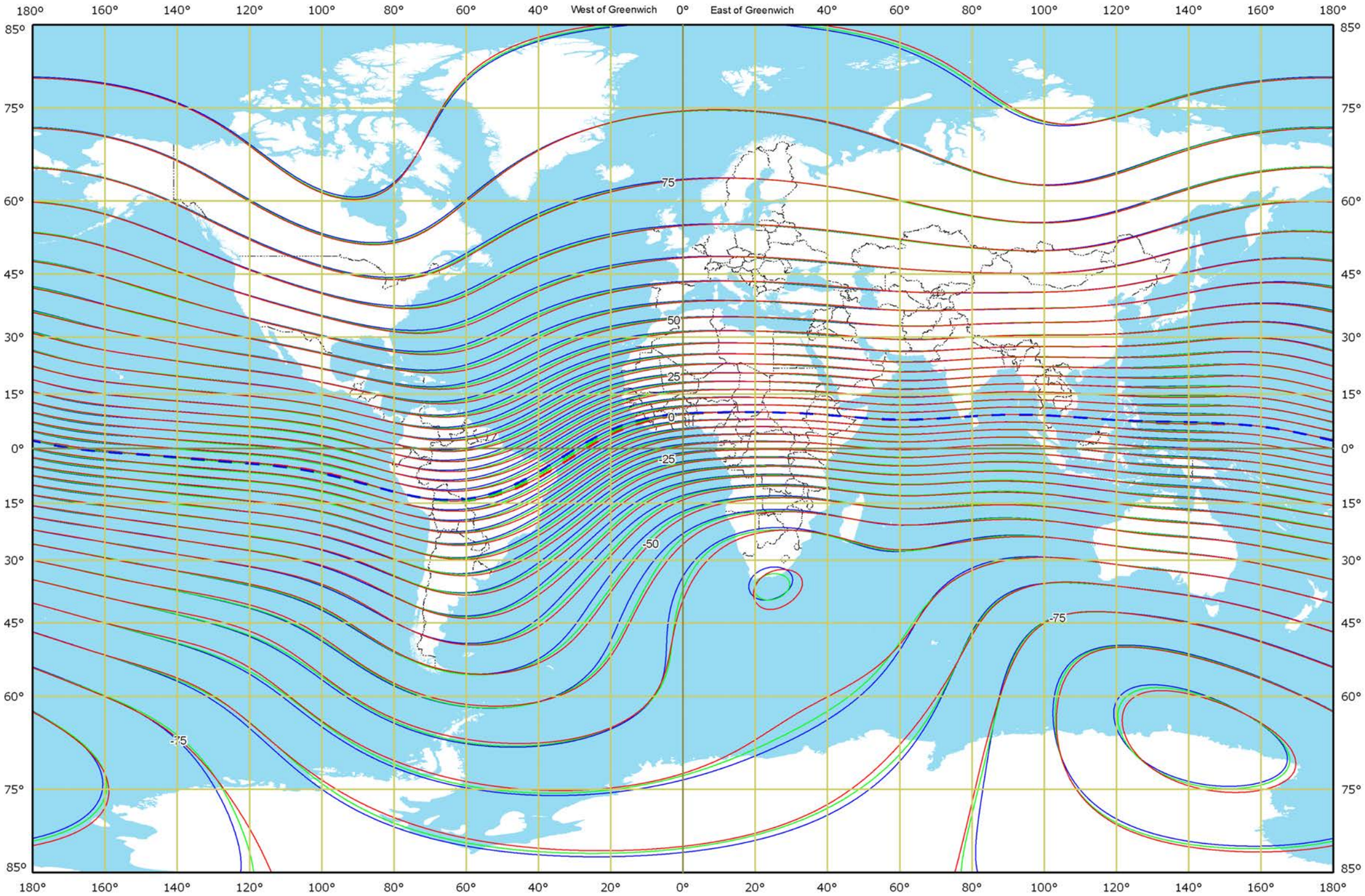

Years	Isoclines	Geomagnetic equators
1950		1950
1955		1955
1960		1960

Example of magnetic inclination value, degree

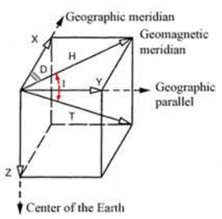

MGMF vector components

D Declination
I Inclination
H Horizontal component
T Total intensity
X North component
Y East component
Z Vertical component

Scale 1: 120 000 000

Projection: Miller cylindrical

MGMF INCLINATION

MGMF – 1960, 1965, 1970 – I

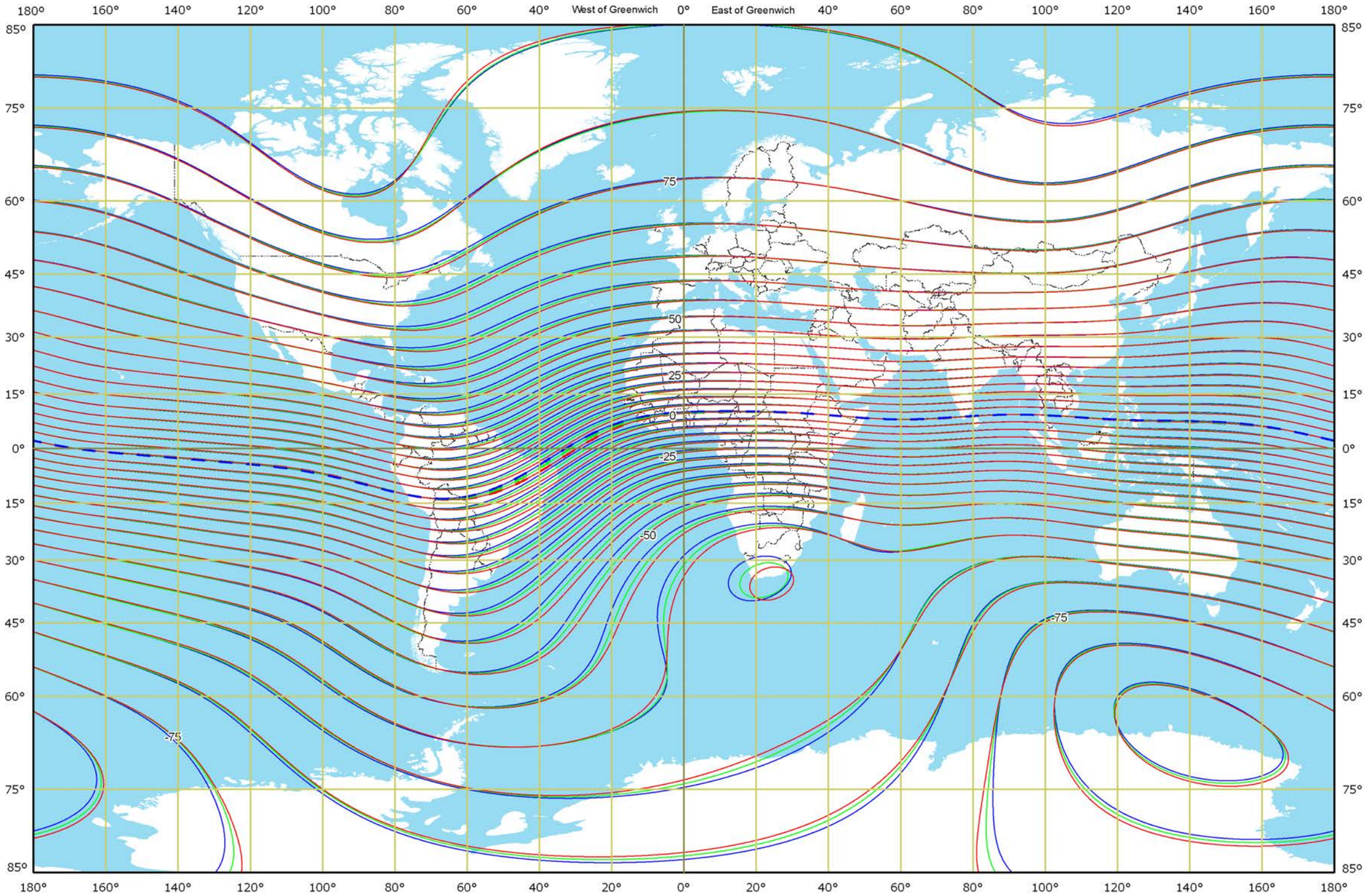

Years	Isoclines	Geomagnetic equators
1960		1960
1965		1965
1970		1970

Example of magnetic inclination value, degree

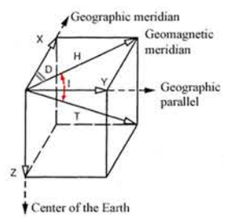

MGMF vector components

D Declination
I Inclination
H Horizontal component
T Total intensity
X North component
Y East component
Z Vertical component

Scale 1: 120 000 000

Projection: Miller cylindrical

MGMF INCLINATION

MGMF – 1970, 1975, 1980 – I

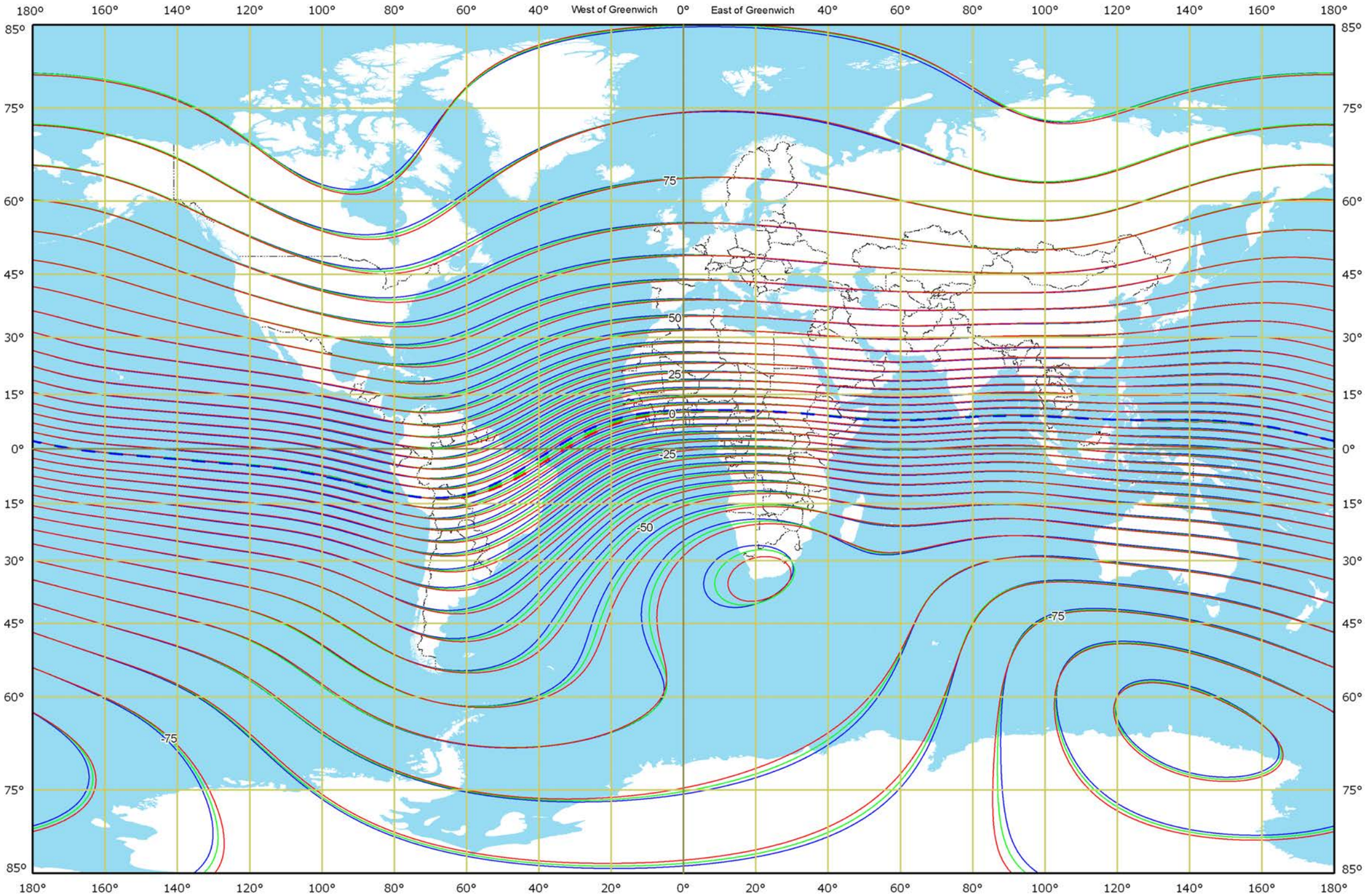

Years | Isoclines | Geomagnetic equators

1970 | 1970
1975 | 1975
1980 | 1980

Example of magnetic inclination value, degree

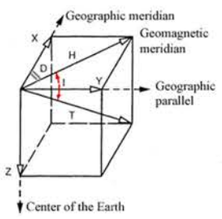

MGMF vector components

D Declination
I Inclination
H Horizontal component
T Total intensity
X North component
Y East component
Z Vertical component

Scale 1: 120 000 000

Projection: Miller cylindrical

MGMF INCLINATION

MGMF – 1980, 1985, 1990 – I

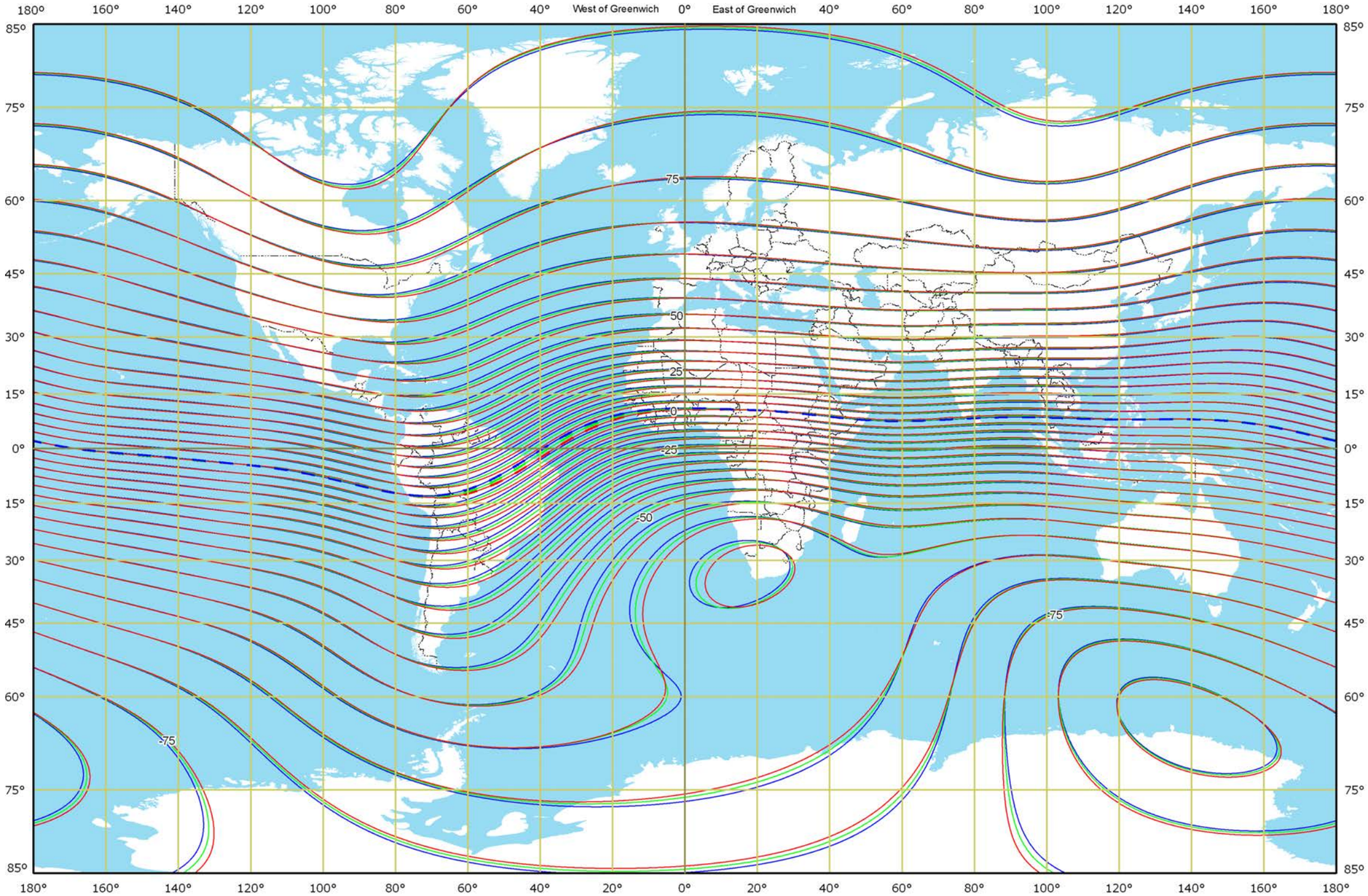

Years	Isoclines	Geomagnetic equators
1980		1980
1985		1985
1990		1990

Example of magnetic inclination value, degree

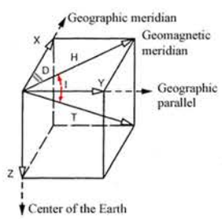

MGMF vector components

D Declination
I Inclination
H Horizontal component
T Total intensity
X North component
Y East component
Z Vertical component

Scale 1: 120 000 000

Projection: Miller cylindrical

MGMF INCLINATION

MGMF – 1990, 1995, 2000 – I

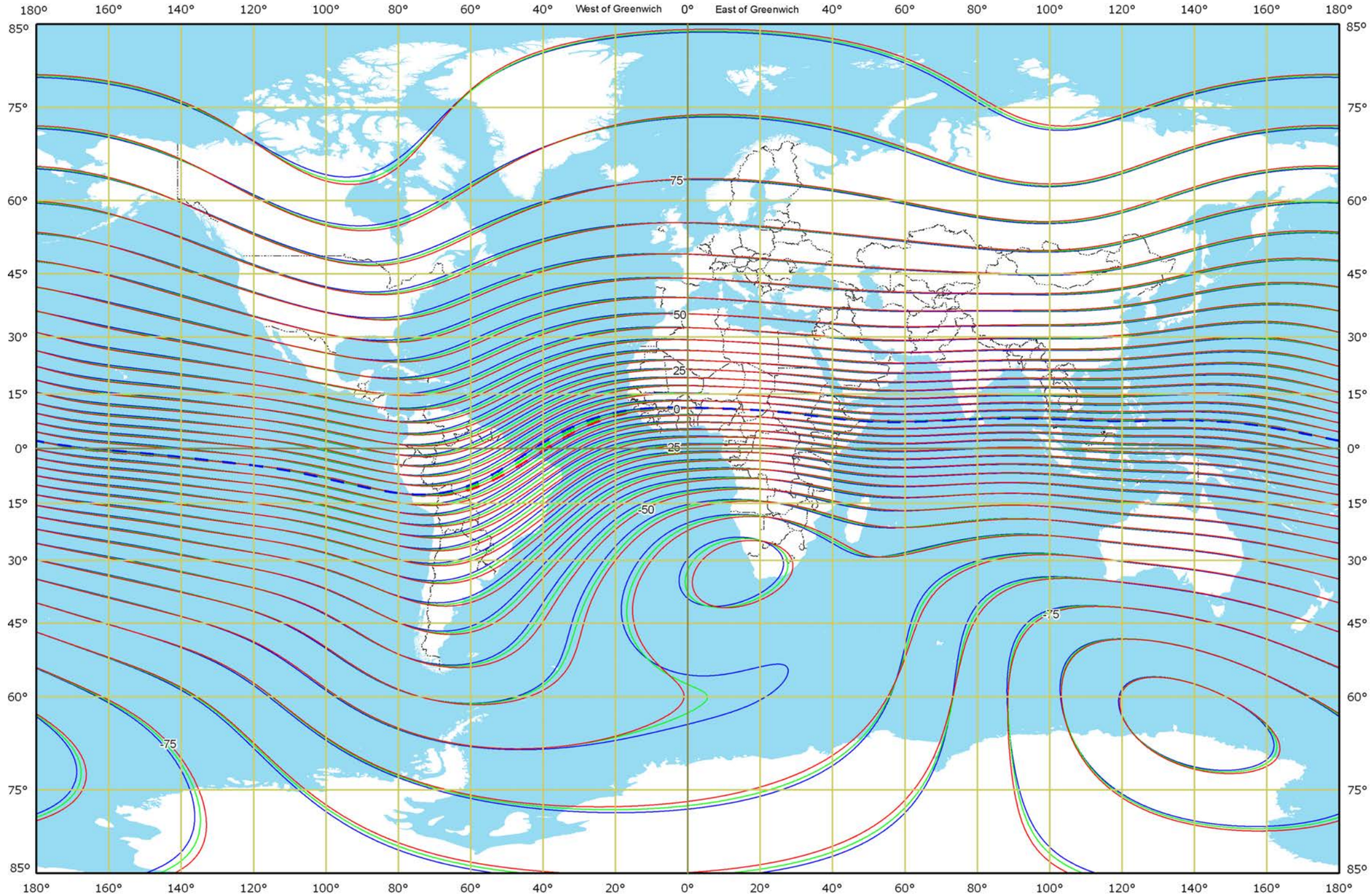

Years	Isoclines	Geomagnetic equators
1990		1990
1995		1995
2000		2000

Example of magnetic inclination value, degree

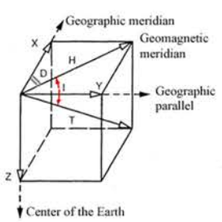

MGMF vector components

D Declination
I Inclination
H Horizontal component
T Total intensity
X North component
Y East component
Z Vertical component

Scale 1: 120 000 000

Projection: Miller cylindrical

MGMF INCLINATION

MGMF – 2000, 2005, 2010 – I

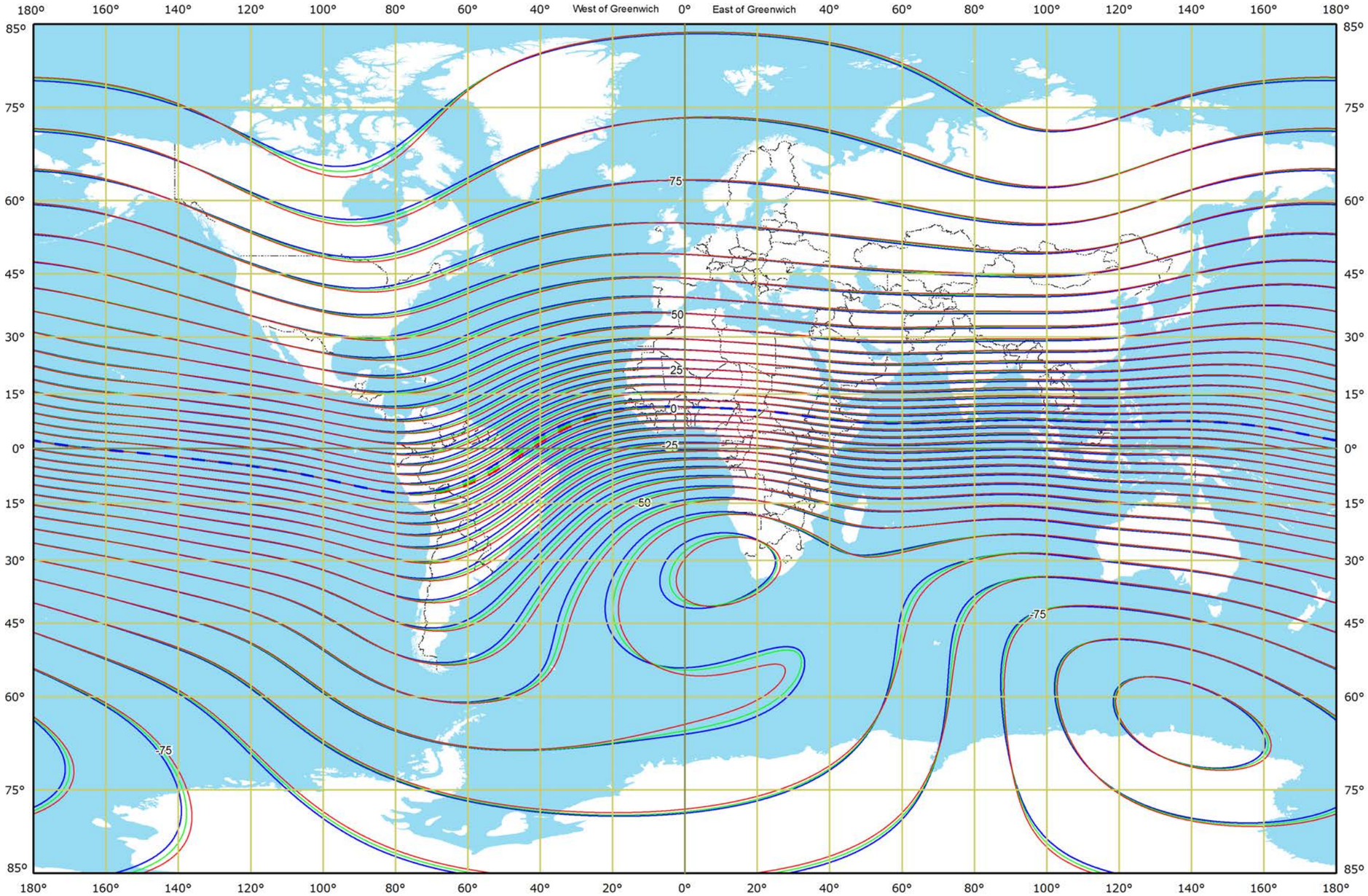

Years	Isoclines	Geomagnetic equators
2000		2000
2005		2005
2010		2010

Example of magnetic inclination value, degree

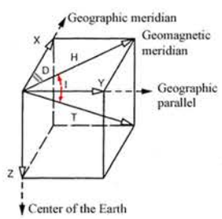

MGMF vector components

D Declination
I Inclination
H Horizontal component
T Total intensity
X North component
Y East component
Z Vertical component

Scale 1: 120 000 000

Projection: Miller cylindrical

NORTH COMPONENT OF MGMF

MGMF- 1900, 1905, 1910 – DX

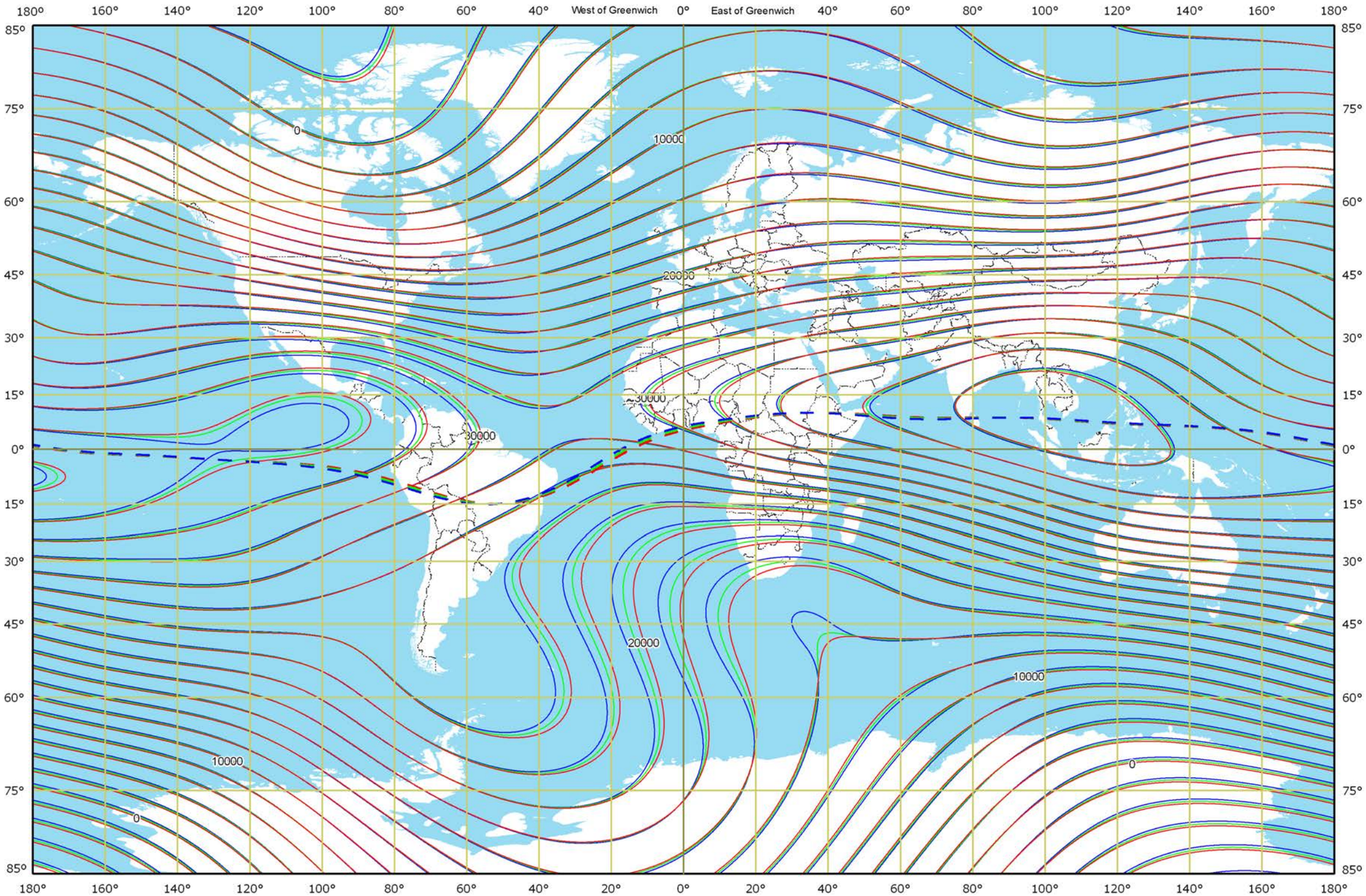

Years	Isolines	Geomagnetic equators
1900		1900
1905		1905
1910		1910

Example of magnetic field component value, nT

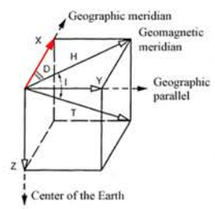

MGMF vector components

D Declination
I Inclination
H Horizontal component
T Total intensity
X North component
Y East component
Z Vertical component

Scale 1: 120 000 000

Projection: Miller cylindrical

NORTH COMPONENT OF MGMF

MGMF- 1910, 1915, 1920 – DX

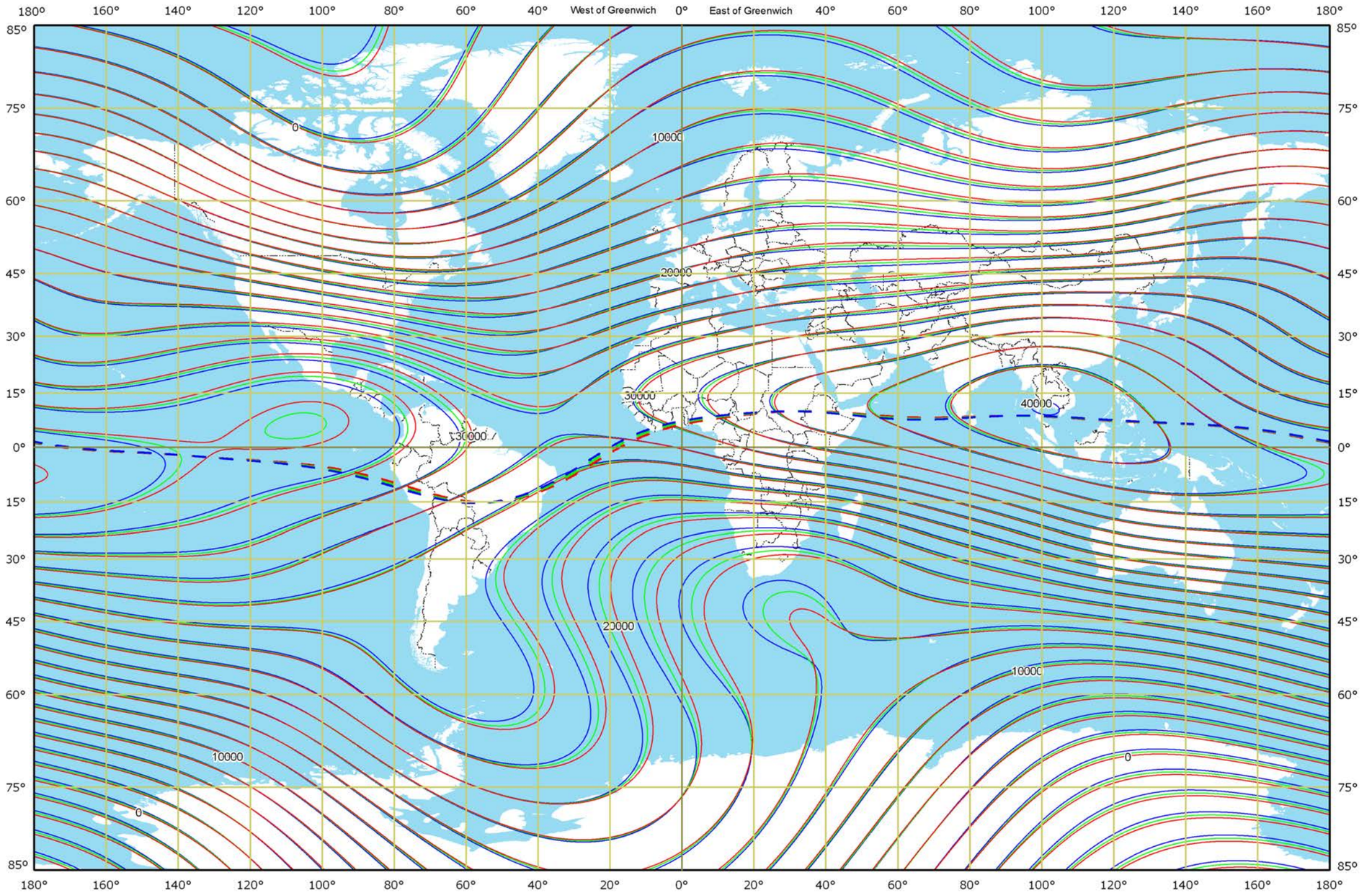

Years	Isolines	Geomagnetic equators
1910		1910
1915		1915
1920		1920

Example of magnetic field component value, nT

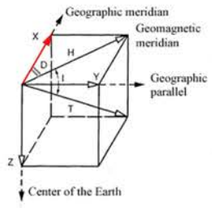

MGMF vector components

D Declination
I Inclination
H Horizontal component
T Total intensity
X North component
Y East component
Z Vertical component

Scale 1: 120 000 000

Projection: Miller cylindrical

NORTH COMPONENT OF MGMF

MGMF- 1920, 1925, 1930 – DX

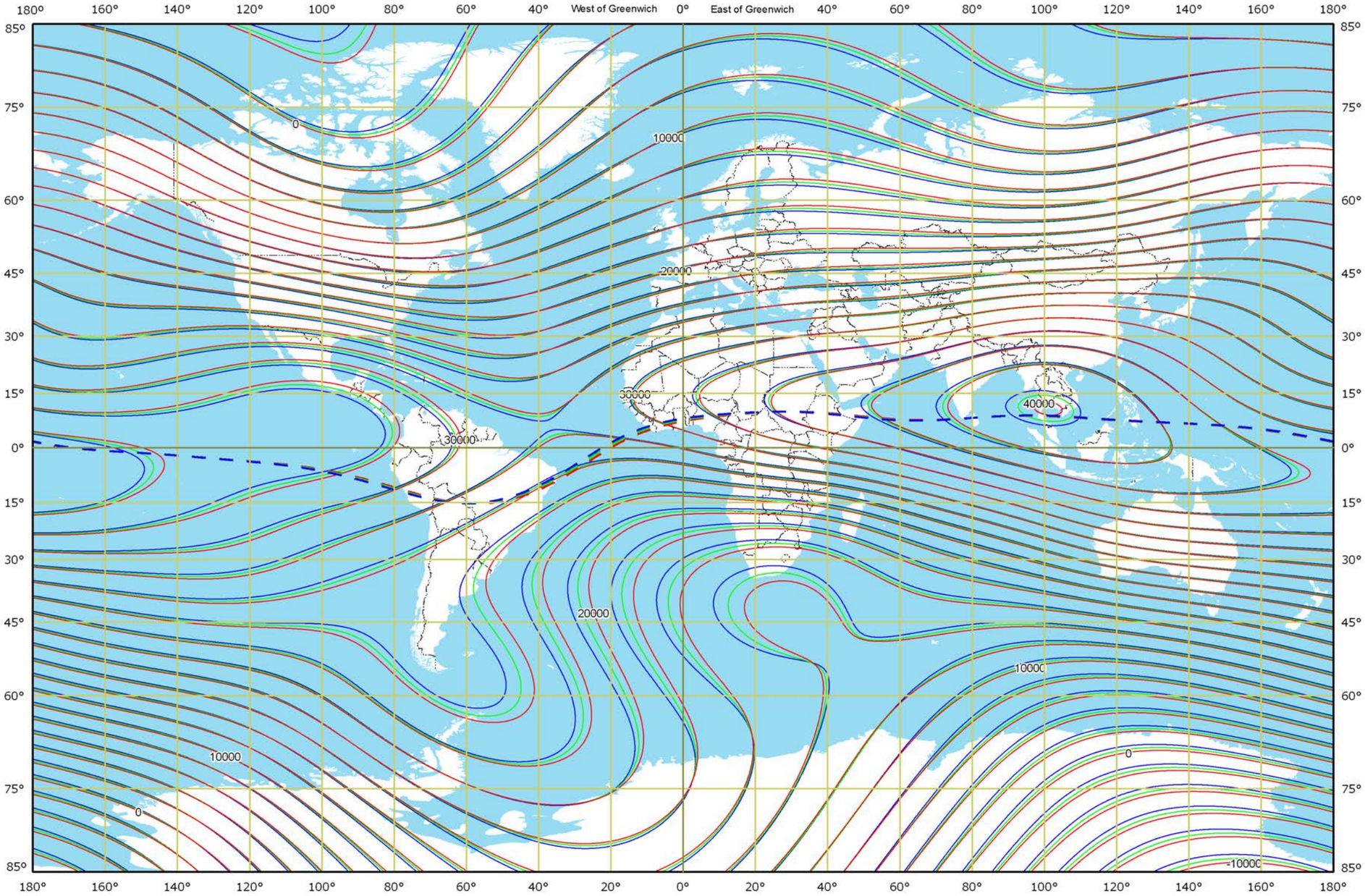

Years	Isolines	Geomagnetic equators
1920		1920
1925		1925
1930		1930

Example of magnetic field component value, nT

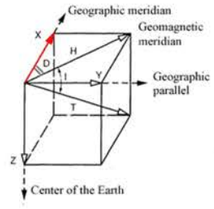

MGMF vector components

D Declination
I Inclination
H Horizontal component
T Total intensity
X North component
Y East component
Z Vertical component

Scale 1: 120 000 000

Projection: Miller cylindrical

NORTH COMPONENT OF MGMF

MGMF- 1930, 1935, 1940 – DX

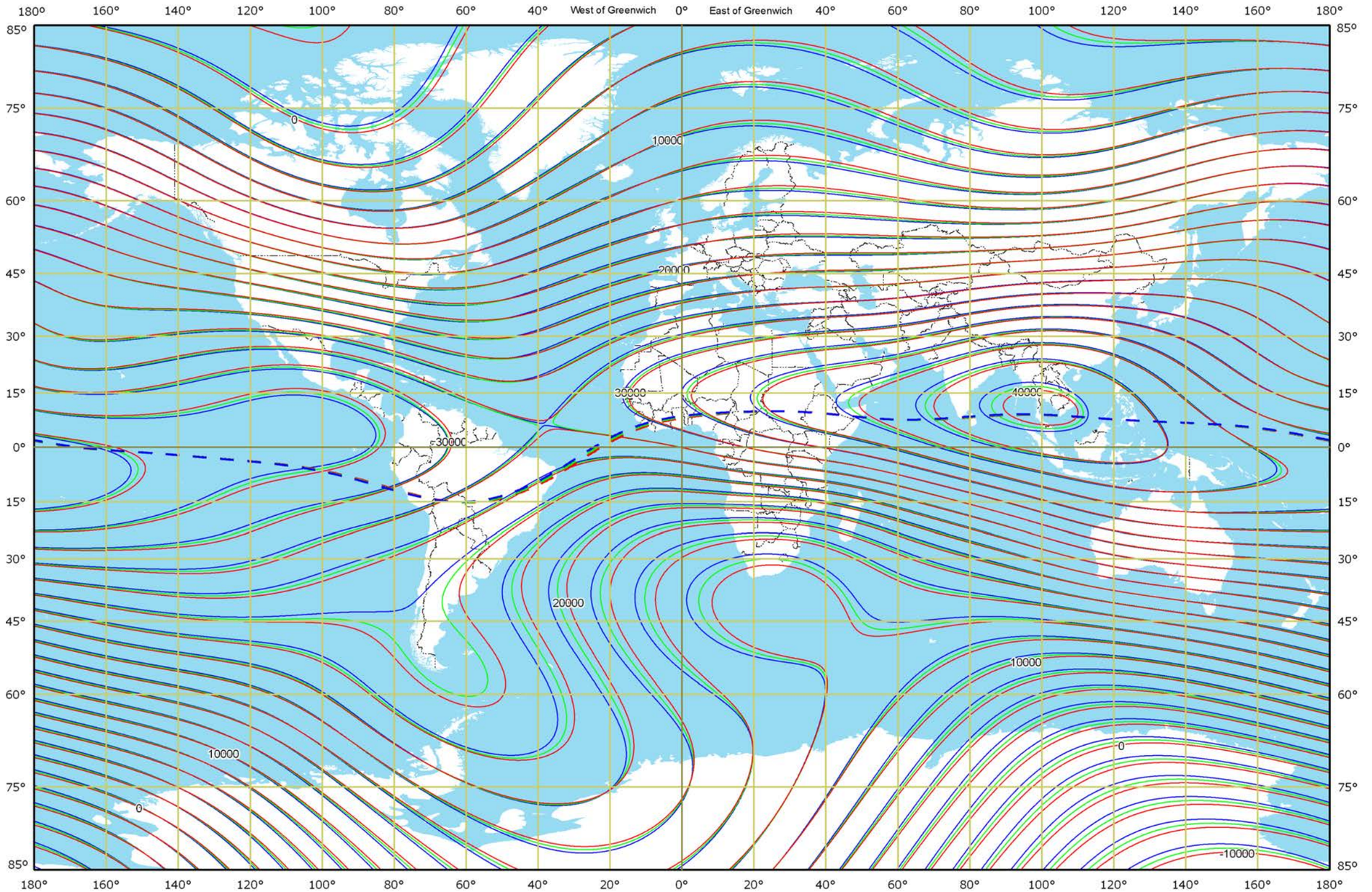

Years	Isolines	Geomagnetic equators
1930		1930
1935		1935
1940		1940

Example of magnetic field component value, nT

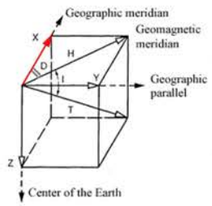

MGMF vector components

D Declination
I Inclination
H Horizontal component
T Total intensity
X North component
Y East component
Z Vertical component

Scale 1: 120 000 000

Projection: Miller cylindrical

NORTH COMPONENT OF MGMF

MGMF- 1940, 1945, 1950 – DX

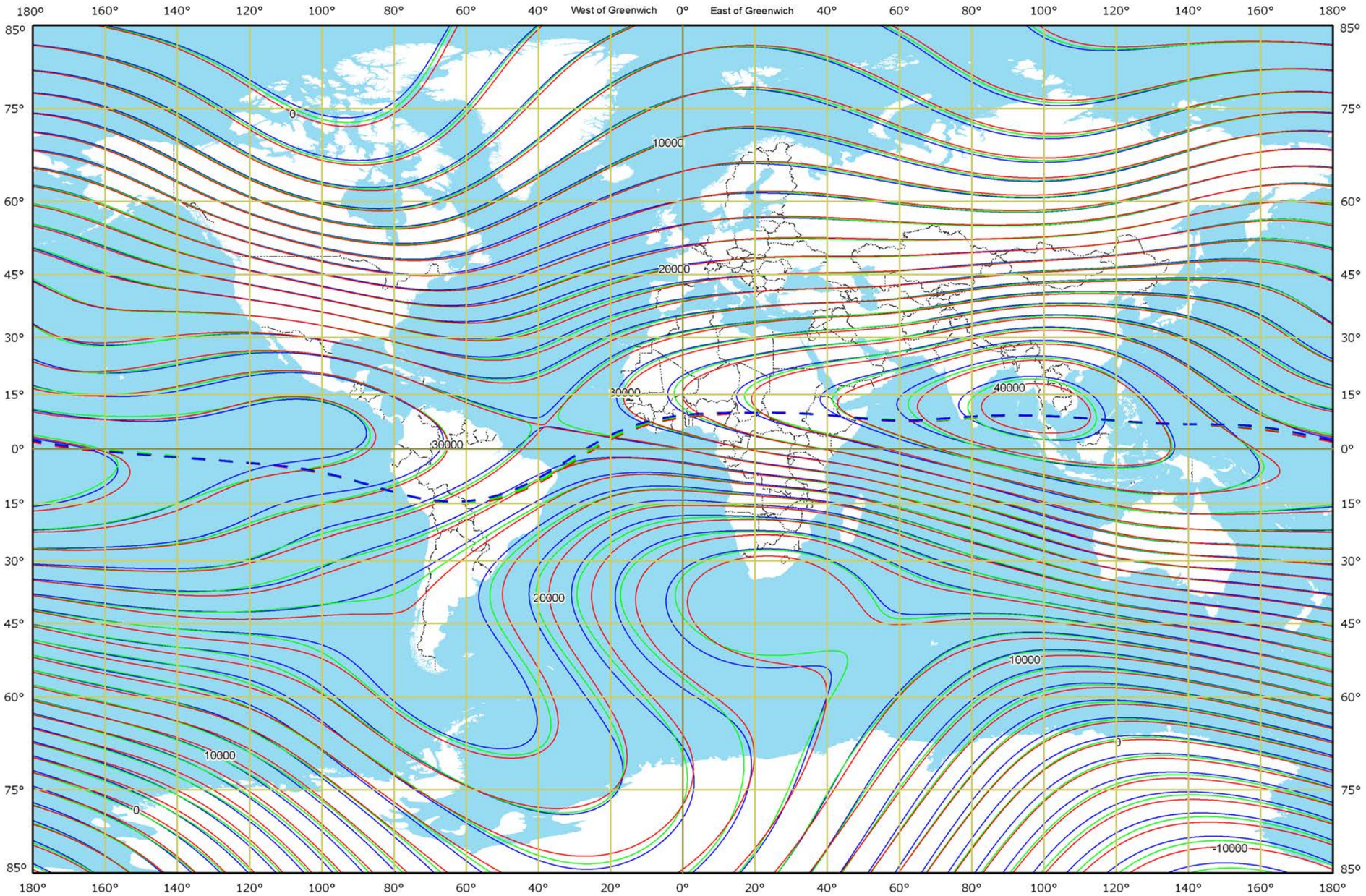

Years	Isolines	Geomagnetic equators
1940		1940
1945		1945
1950		1950

Example of magnetic field component value, nT

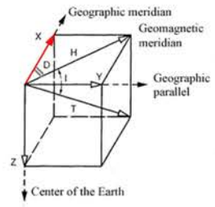

MGMF vector components

D Declination
I Inclination
H Horizontal component
T Total intensity
X North component
Y East component
Z Vertical component

Scale 1: 120 000 000

Projection: Miller cylindrical

NORTH COMPONENT OF MGMF

MGMF- 1950, 1955, 1960 – DX

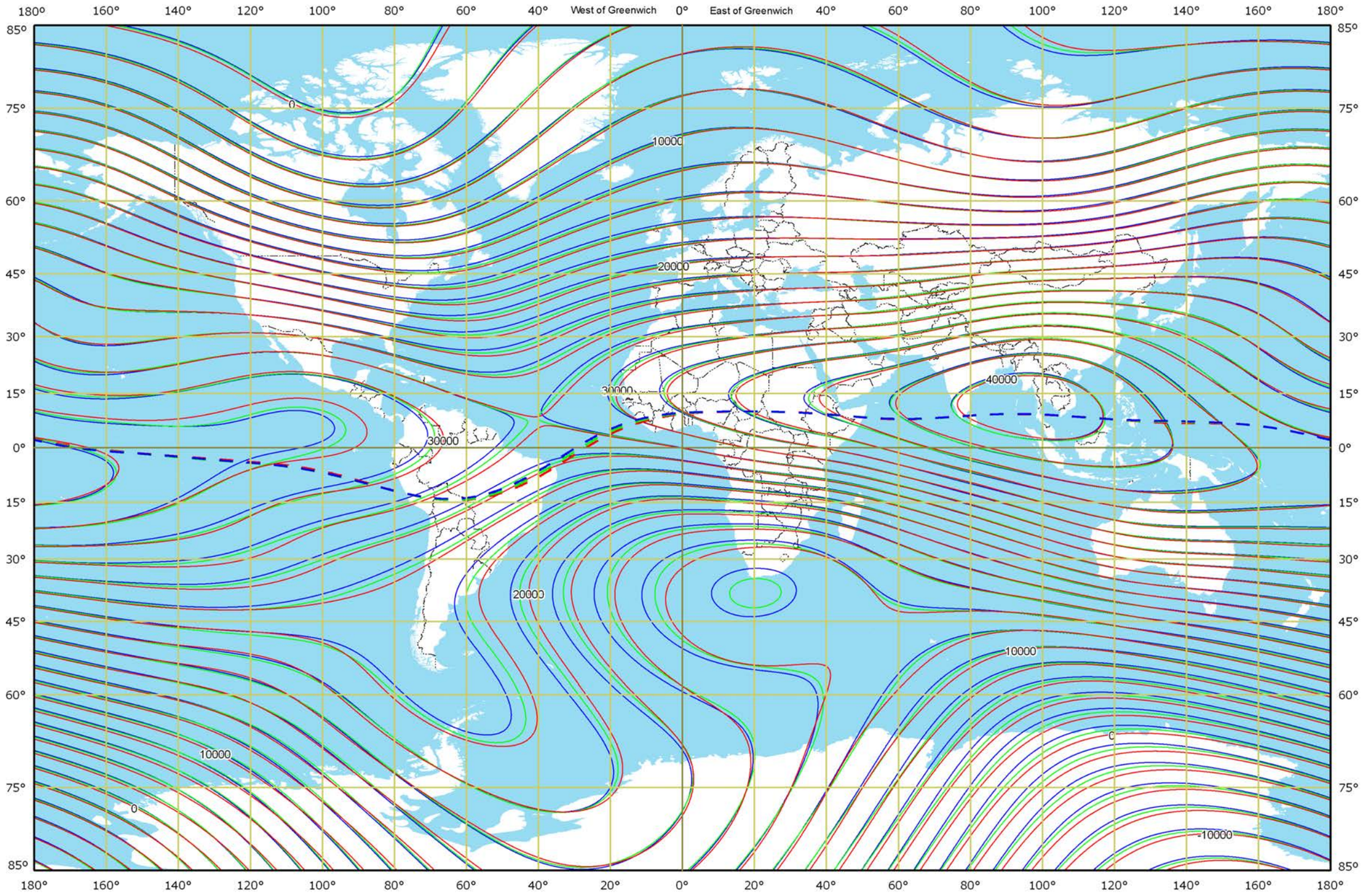

Years	Isolines	Geomagnetic equators
1950		1950
1955		1955
1960		1960

Example of magnetic field component value, nT

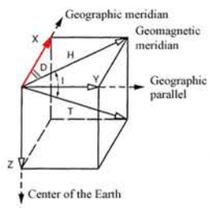

MGMF vector components

D Declination
I Inclination
H Horizontal component
T Total intensity
X North component
Y East component
Z Vertical component

Scale 1: 120 000 000

Projection: Miller cylindrical

NORTH COMPONENT OF MGMF

MGMF- 1960, 1965, 1970 – DX

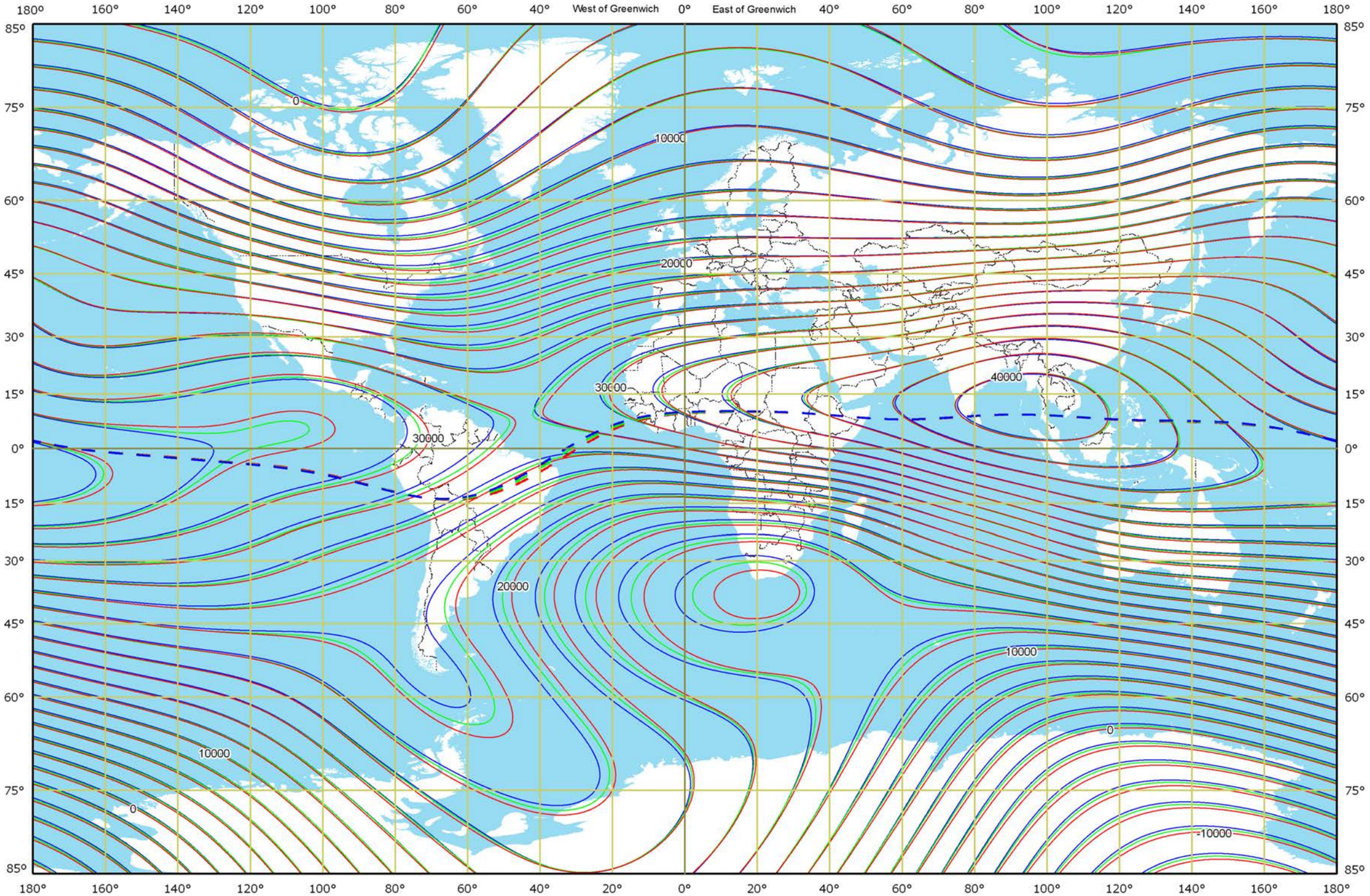

Years	Isolines	Geomagnetic equators
1960		1960
1965		1965
1970		1970

Example of magnetic field component value, nT

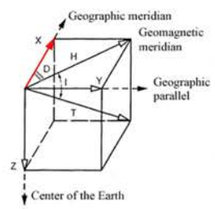

MGMF vector components

D Declination
I Inclination
H Horizontal component
T Total intensity
X North component
Y East component
Z Vertical component

Scale 1: 120 000 000

Projection: Miller cylindrical

NORTH COMPONENT OF MGMF

MGMF- 1970, 1975, 1980 – DX

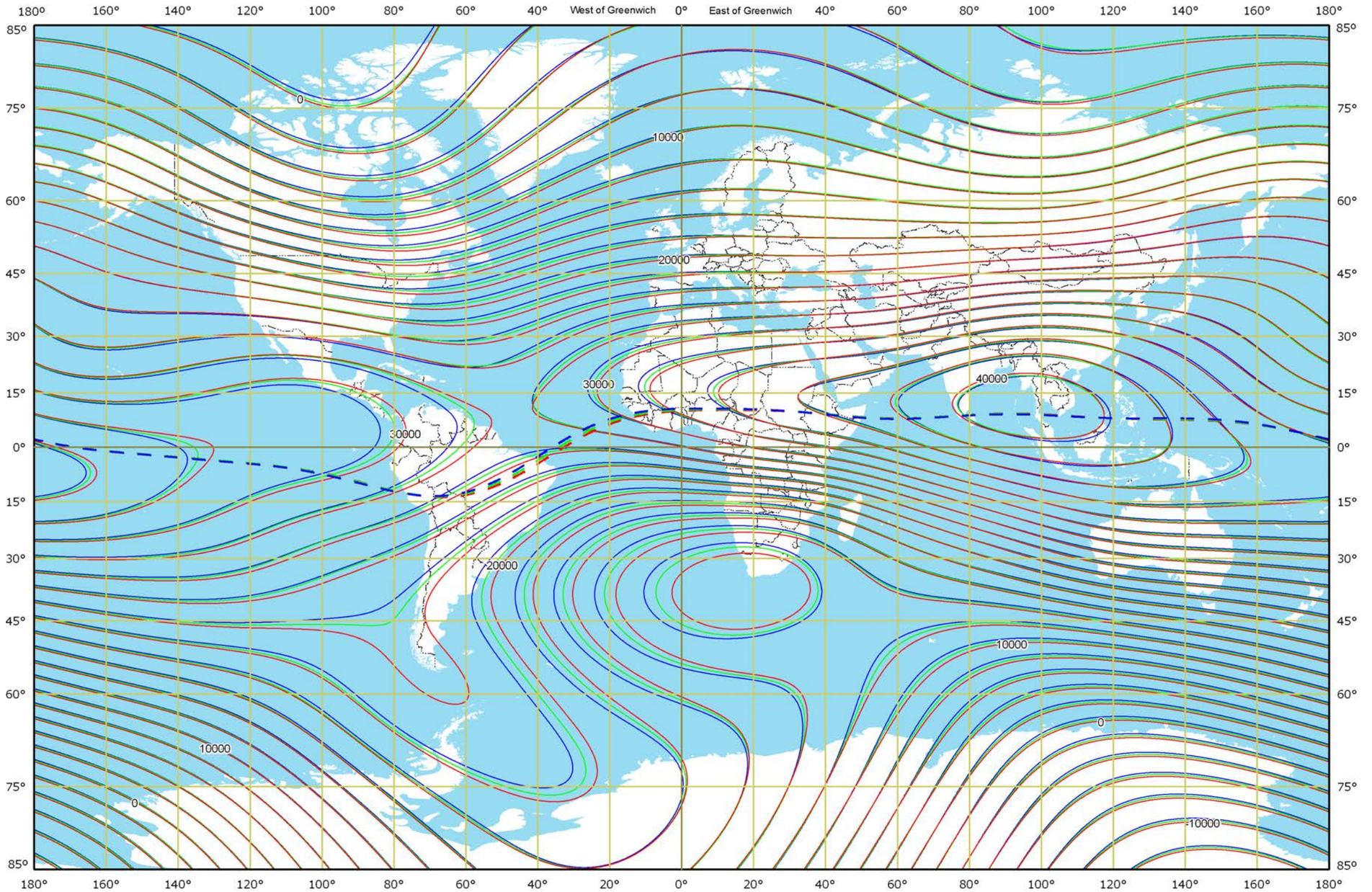

Years	Isolines	Geomagnetic equators
1970		1970
1975		1975
1980		1980

Example of magnetic field component value, nT

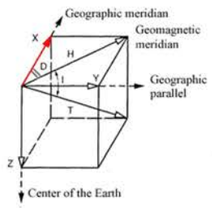

MGMF vector components

D Declination
I Inclination
H Horizontal component
T Total intensity
X North component
Y East component
Z Vertical component

Scale 1: 120 000 000

Projection: Miller cylindrical

NORTH COMPONENT OF MGMF

MGMF- 1980, 1985, 1990 – DX

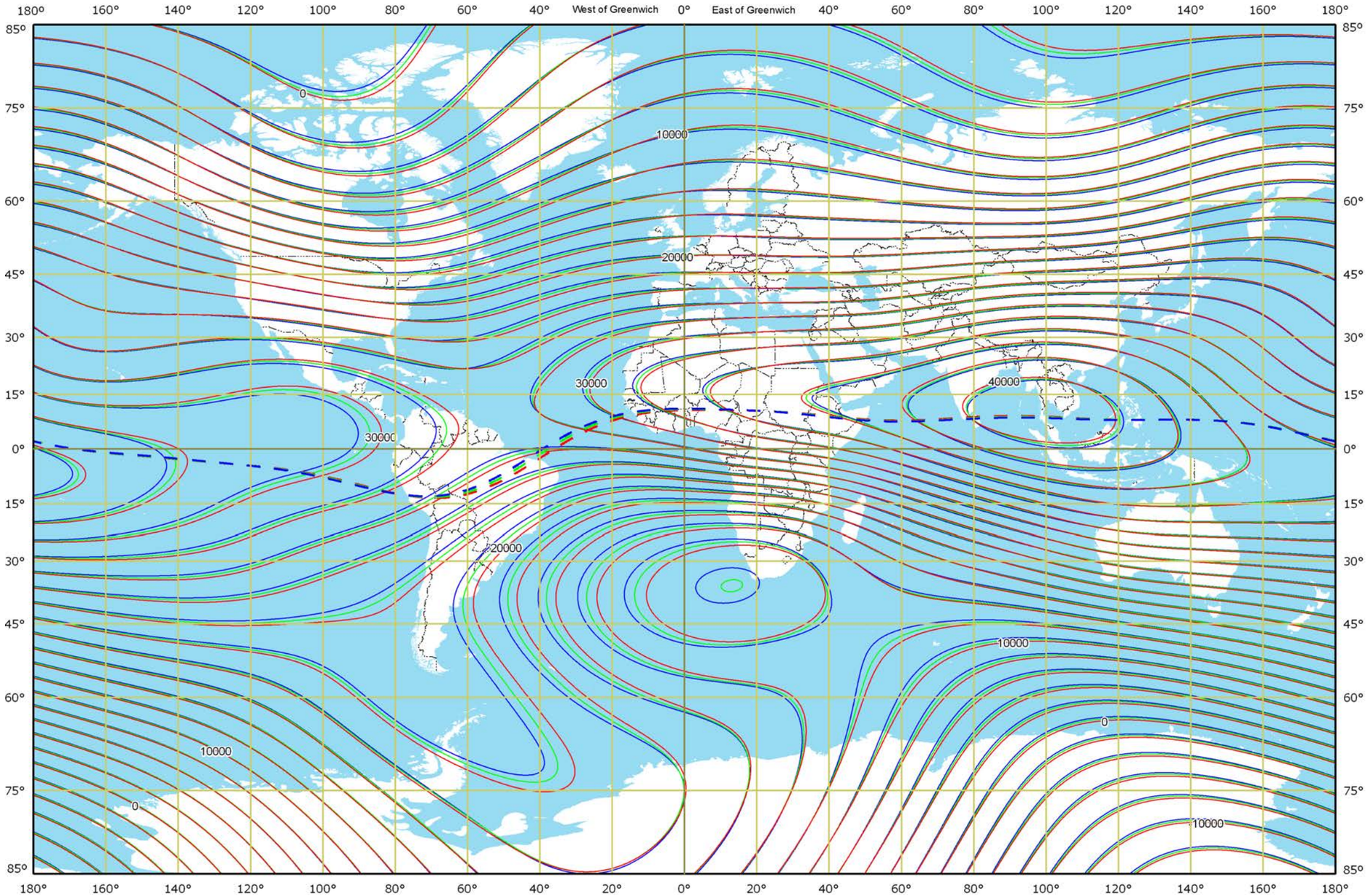

Years	Isolines	Geomagnetic equators
1980		1980
1985		1985
1990		1990

Example of magnetic field component value, nT

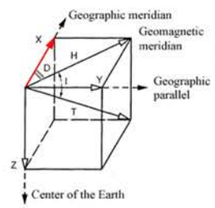

MGMF vector components

D Declination
I Inclination
H Horizontal component
T Total intensity
X North component
Y East component
Z Vertical component

Scale 1: 120 000 000

Projection: Miller cylindrical

NORTH COMPONENT OF MGMF

MGMF- 1990, 1995, 2000 – DX

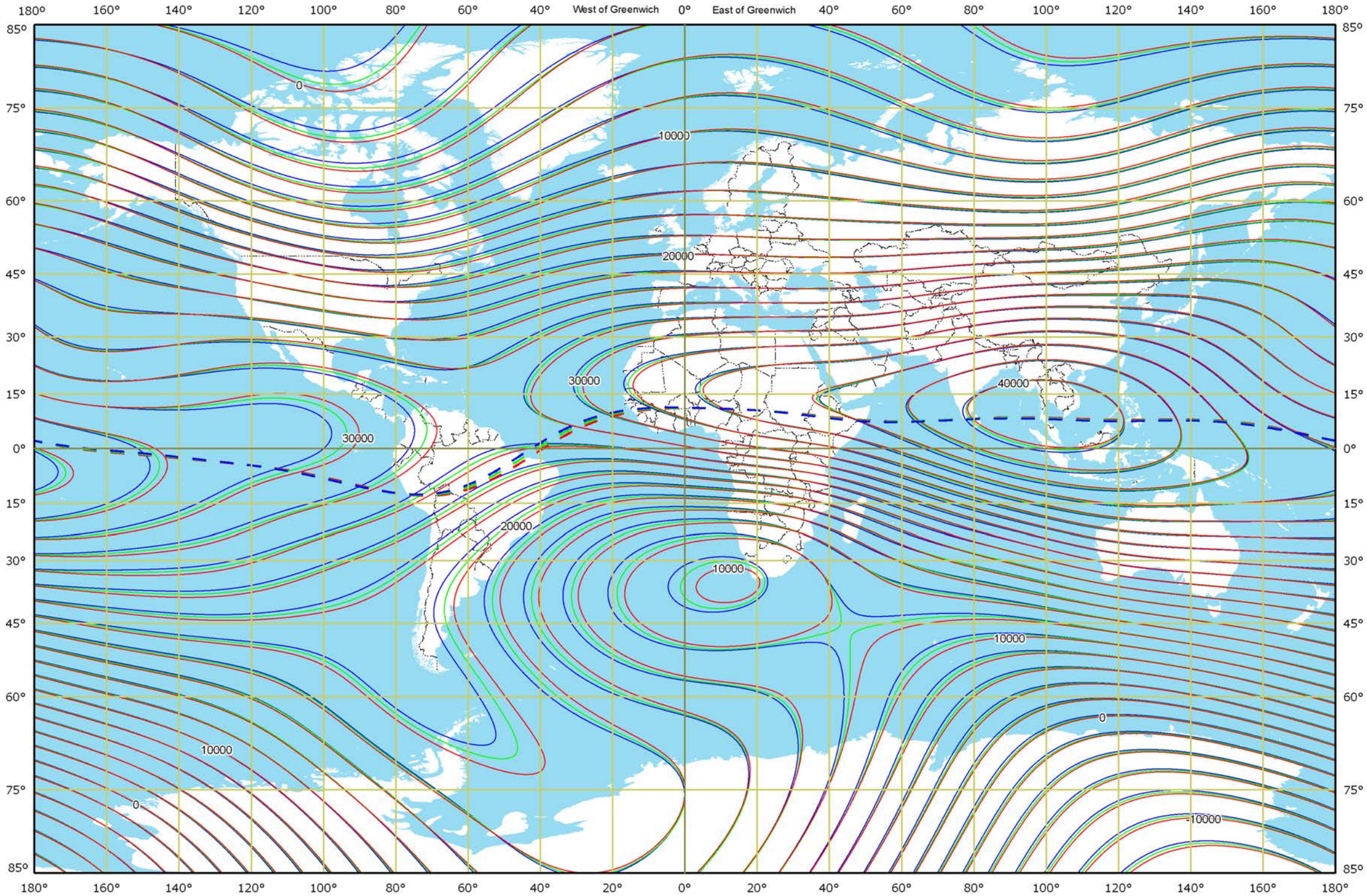

Years	Isolines	Geomagnetic equators
1990		1990
1995		1995
2000		2000

Example of magnetic field component value, nT

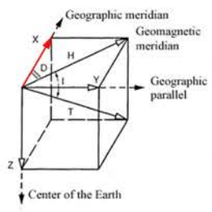

MGMF vector components

D Declination
I Inclination
H Horizontal component
T Total intensity
X North component
Y East component
Z Vertical component

Scale 1: 120 000 000

Projection: Miller cylindrical

NORTH COMPONENT OF MGMF

MGMF– 2000, 2005, 2010 – DX

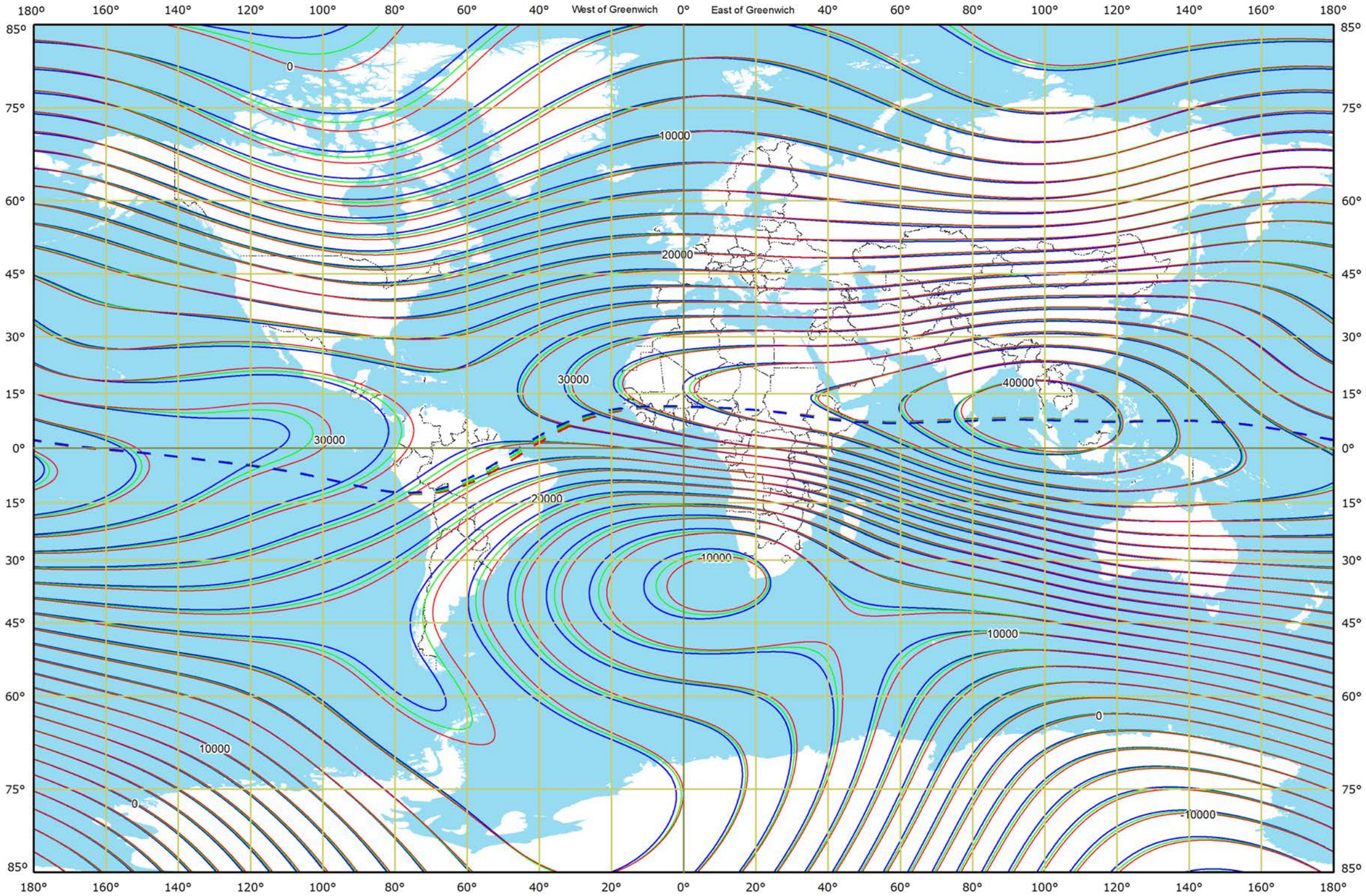

Years	Isolines	Geomagnetic equators
2000		2000
2005		2005
2010		2010

Example of magnetic field component value, nT

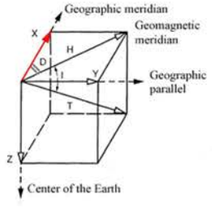

MGMF vector components

D Declination
I Inclination
H Horizontal component
T Total intensity
X North component
Y East component
Z Vertical component

Scale 1: 120 000 000

Projection: Miller cylindrical

EAST COMPONENT OF MGMF

MGMF- 1900, 1905, 1910 – DY

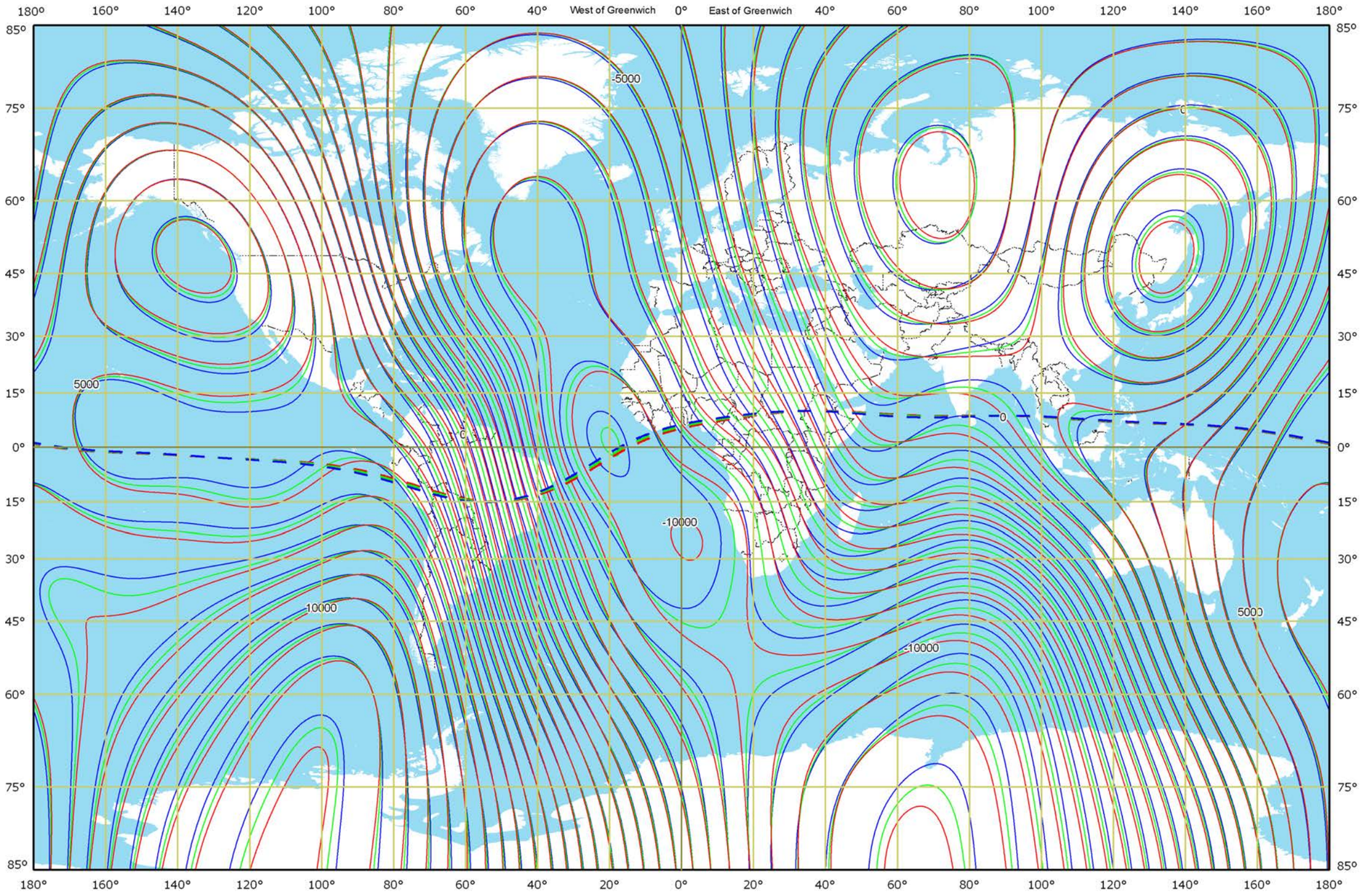

Years	Isolines	Geomagnetic equators
1900		1900
1905		1905
1910		1910

Example of magnetic field component value, nT

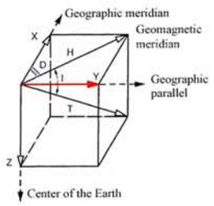

MGMF vector components

D Declination
I Inclination
H Horizontal component
T Total intensity
X North component
Y East component
Z Vertical component

Scale 1: 120 000 000

Projection: Miller cylindrical

EAST COMPONENT OF MGMF

MGMF- 1910, 1915, 1920 – DY

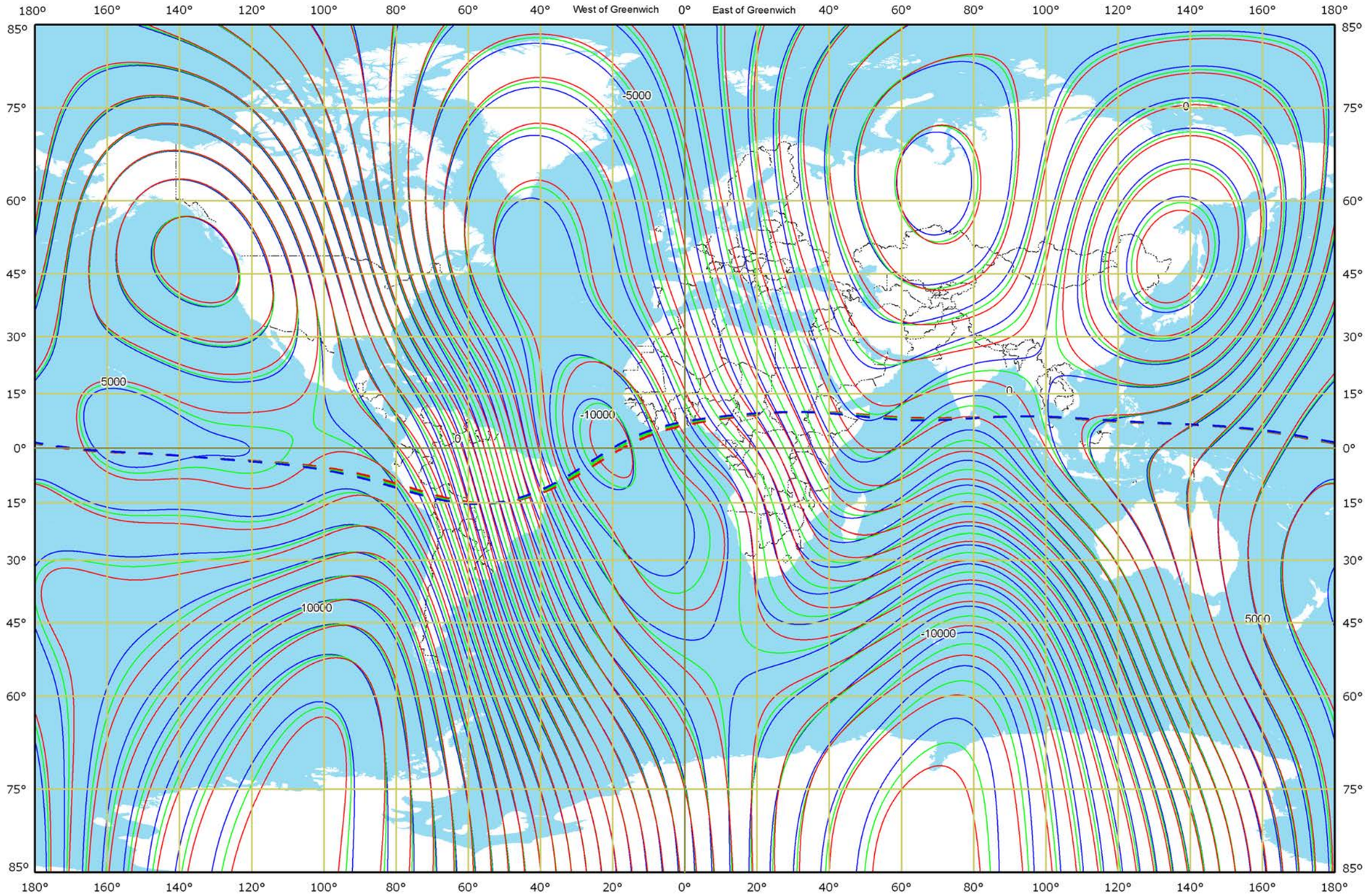

Years	Isolines	Geomagnetic equators
1910		1910
1915		1915
1920		1920

Example of magnetic field component value, nT

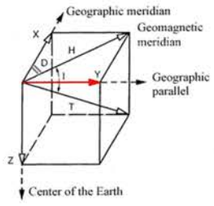

MGMF vector components

D Declination
I Inclination
H Horizontal component
T Total intensity
X North component
Y East component
Z Vertical component

Scale 1: 120 000 000

Projection: Miller cylindrical

EAST COMPONENT OF MGMF

MGMF- 1920, 1925, 1930 – DY

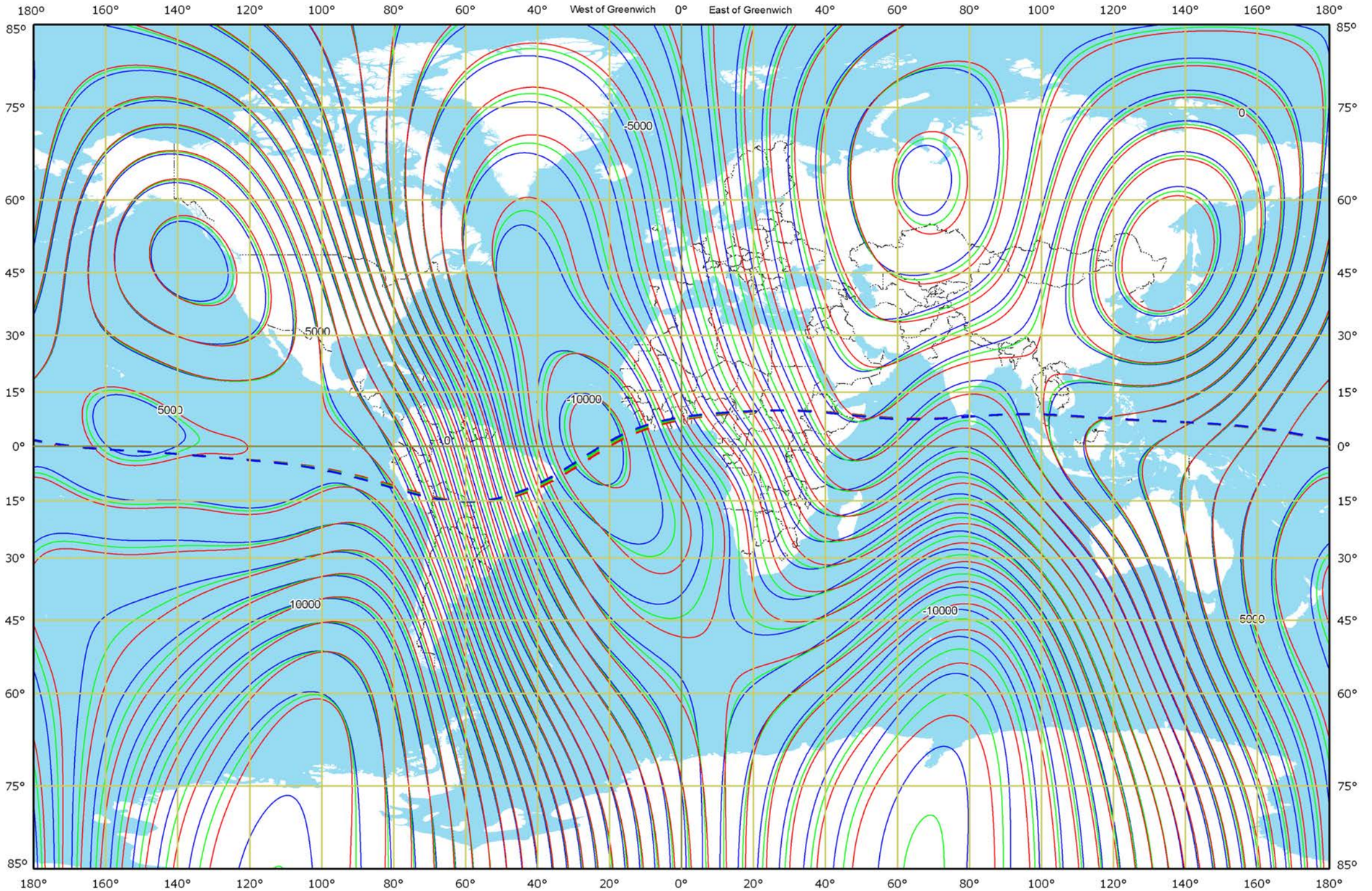

Years	Isolines	Geomagnetic equators
1920		1920
1925		1925
1930		1930

Example of magnetic field component value, nT

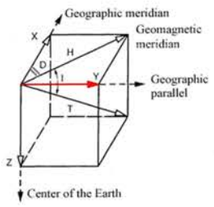

MGMF vector components

D Declination
I Inclination
H Horizontal component
T Total intensity
X North component
Y East component
Z Vertical component

Scale 1: 120 000 000

Projection: Miller cylindrical

EAST COMPONENT OF MGMF

MGMF- 1930, 1935, 1940 – DY

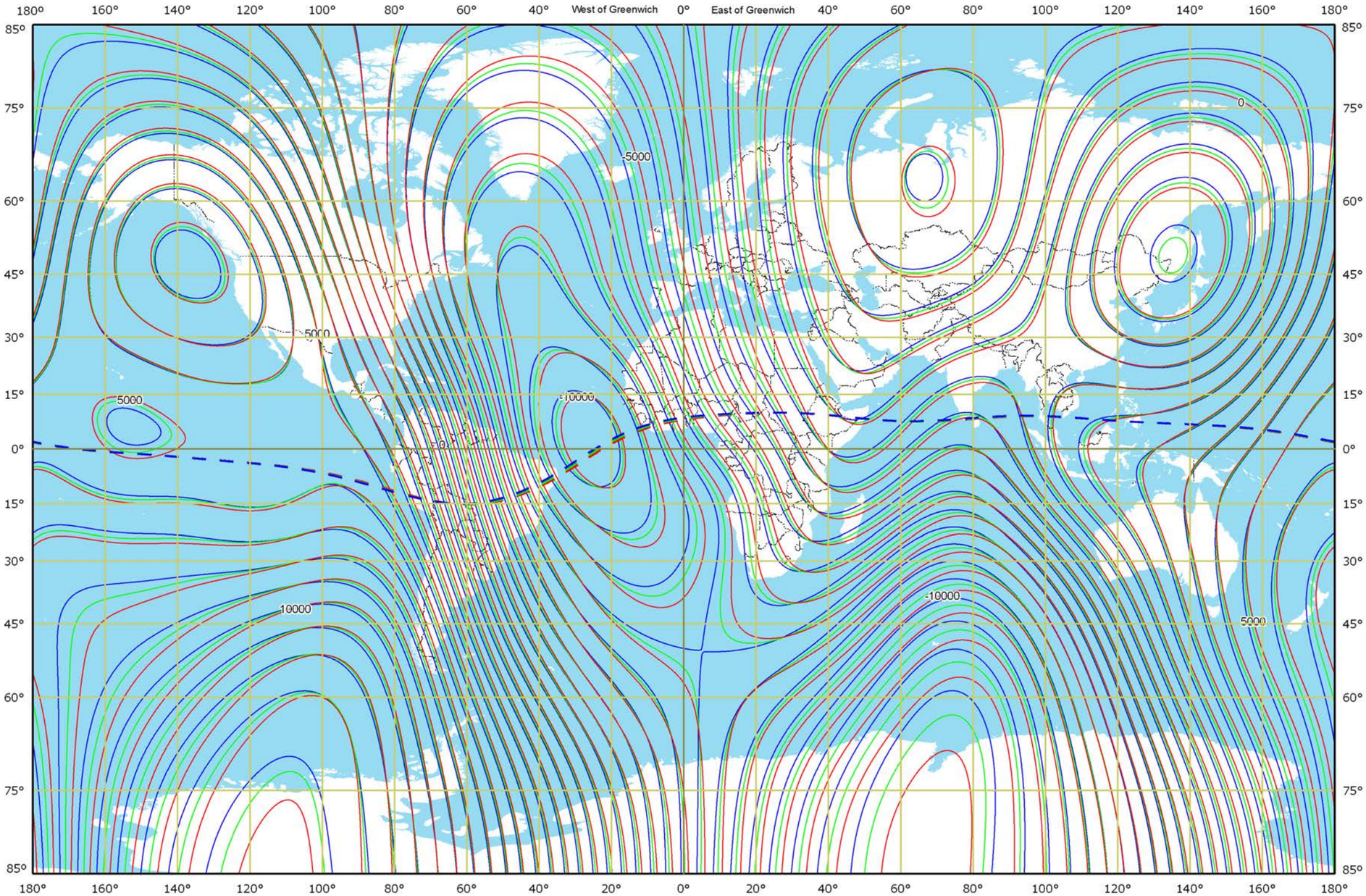

Years	Isolines	Geomagnetic equators
1930		1930
1935		1935
1940		1940

Example of magnetic field component value, nT

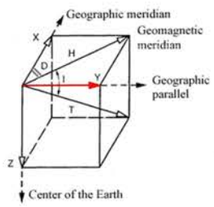

MGMF vector components

D Declination
I Inclination
H Horizontal component
T Total intensity
X North component
Y East component
Z Vertical component

Scale 1: 120 000 000

Projection: Miller cylindrical

EAST COMPONENT OF MGMF

MGMF- 1940, 1945, 1950 – DY

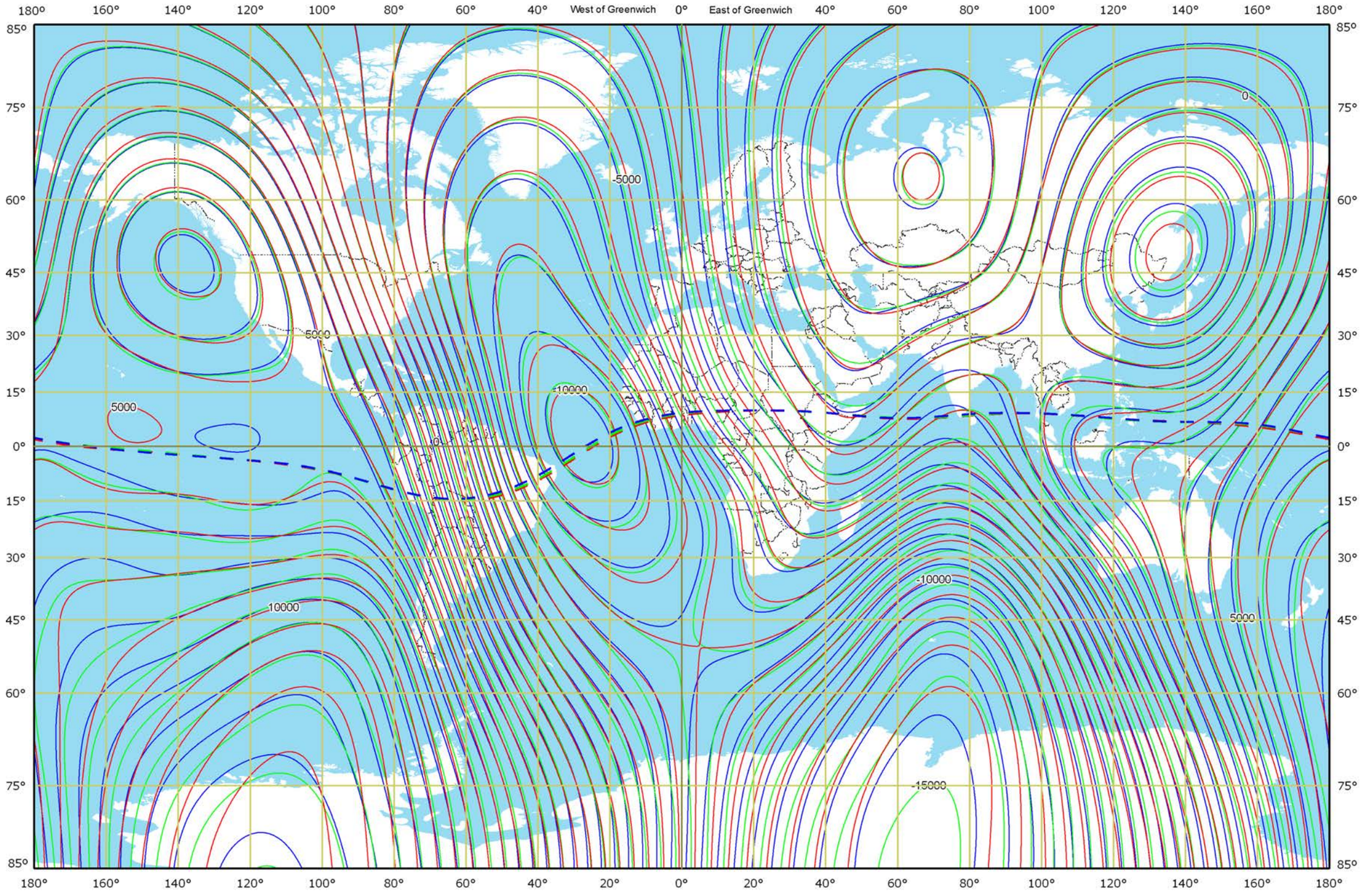

Years	Isolines	Geomagnetic equators
1940		1940
1945		1945
1950		1950

Example of magnetic field component value, nT

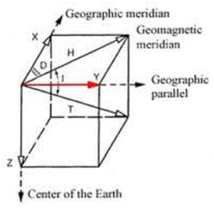

MGMF vector components

D Declination
I Inclination
H Horizontal component
T Total intensity
X North component
Y East component
Z Vertical component

Scale 1: 120 000 000

Projection: Miller cylindrical

EAST COMPONENT OF MGMF

MGMF- 1950, 1955, 1960 – DY

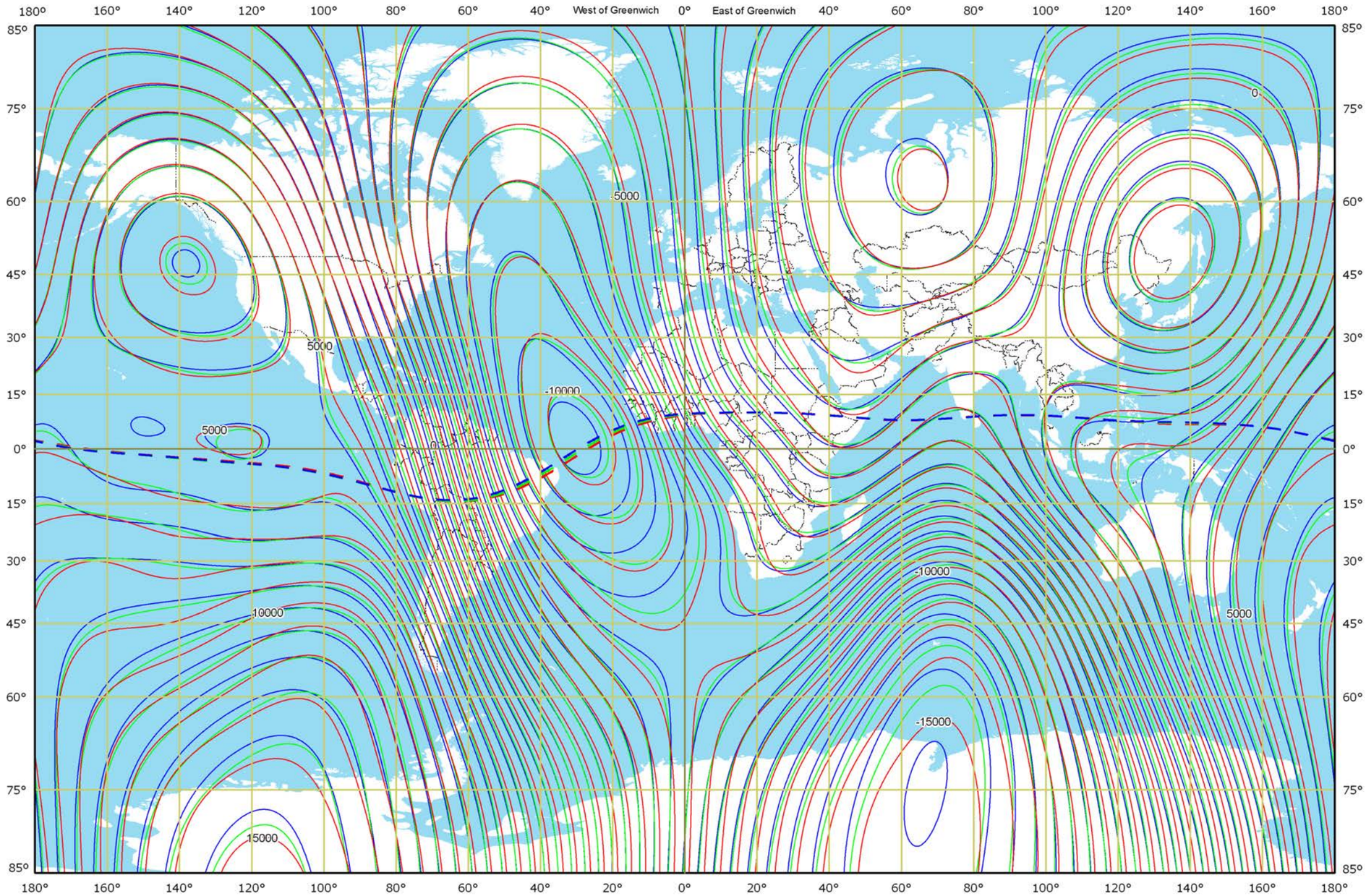

Years	Isolines	Geomagnetic equators
1950		1950
1955		1955
1960		1960

Example of magnetic field component value, nT

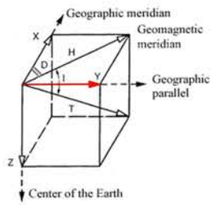

MGMF vector components

D Declination
I Inclination
H Horizontal component
T Total intensity
X North component
Y East component
Z Vertical component

Scale 1: 120 000 000

Projection: Miller cylindrical

EAST COMPONENT OF MGMF

MGMF- 1960, 1965, 1970 – DY

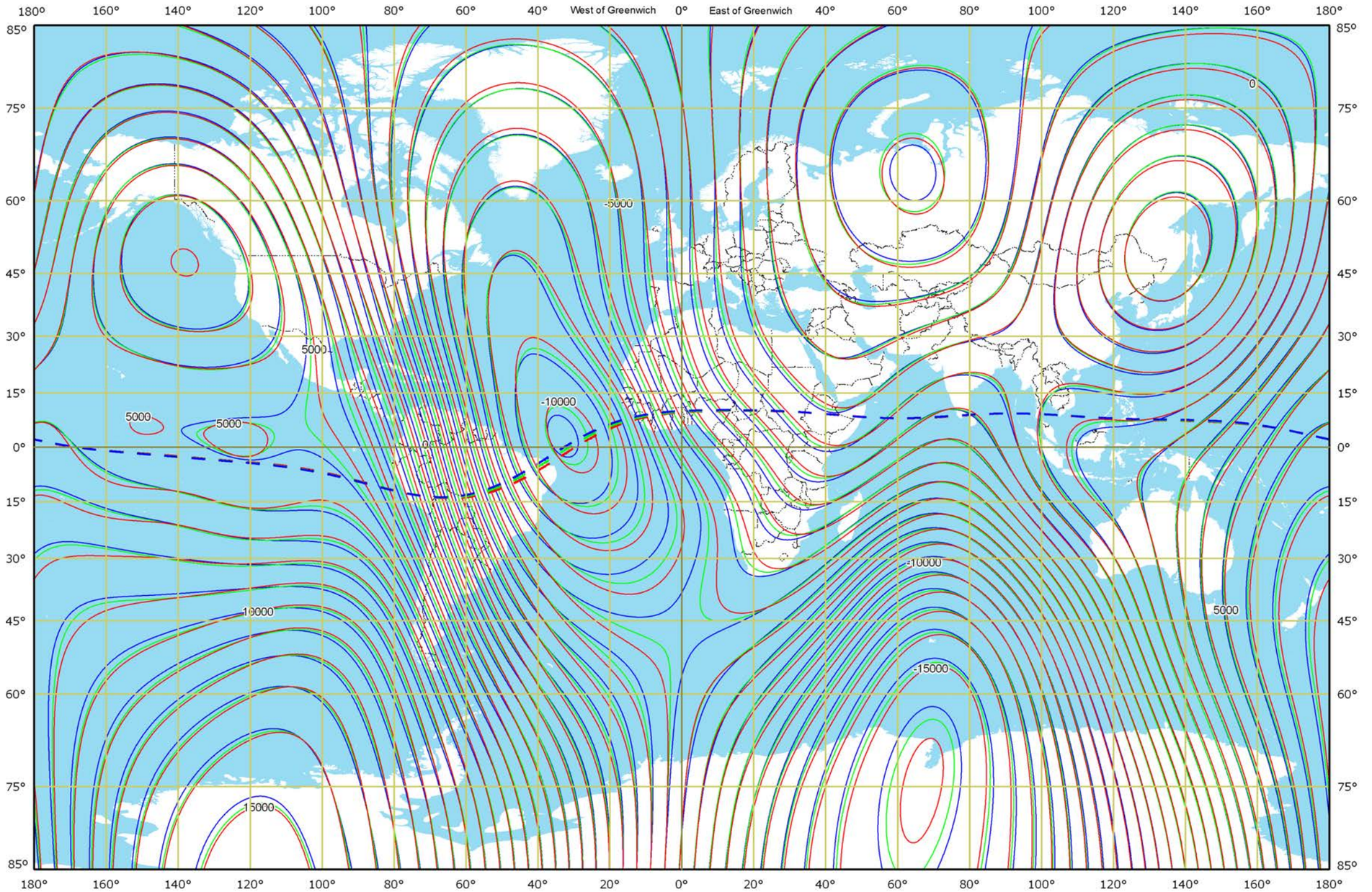

Years	Isolines	Geomagnetic equators
1960		1960
1965		1965
1970		1970

Example of magnetic field component value, nT

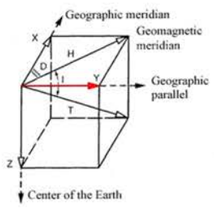

MGMF vector components

D Declination
I Inclination
H Horizontal component
T Total intensity
X North component
Y East component
Z Vertical component

Scale 1: 120 000 000

Projection: Miller cylindrical

EAST COMPONENT OF MGMF

MGMF- 1970, 1975, 1980 – DY

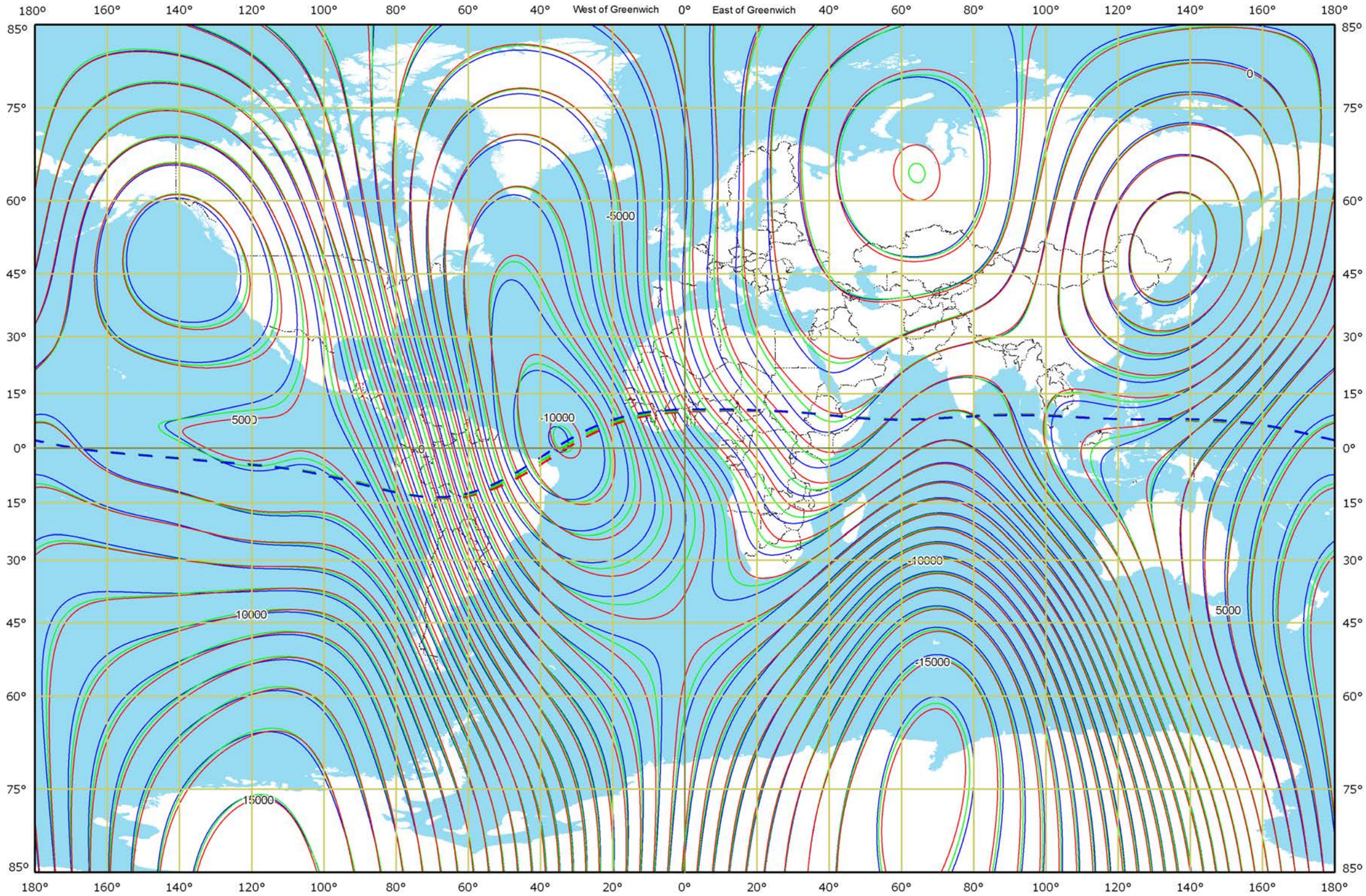

Years	Isolines	Geomagnetic equators
1970		1970
1975		1975
1980		1980

Example of magnetic field component value, nT

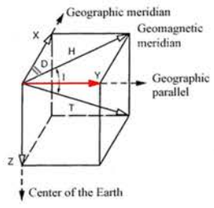

MGMF vector components

D Declination
I Inclination
H Horizontal component
T Total intensity
X North component
Y East component
Z Vertical component

Scale 1: 120 000 000

Projection: Miller cylindrical

EAST COMPONENT OF MGMF

MGMF- 1980, 1985, 1990 – DY

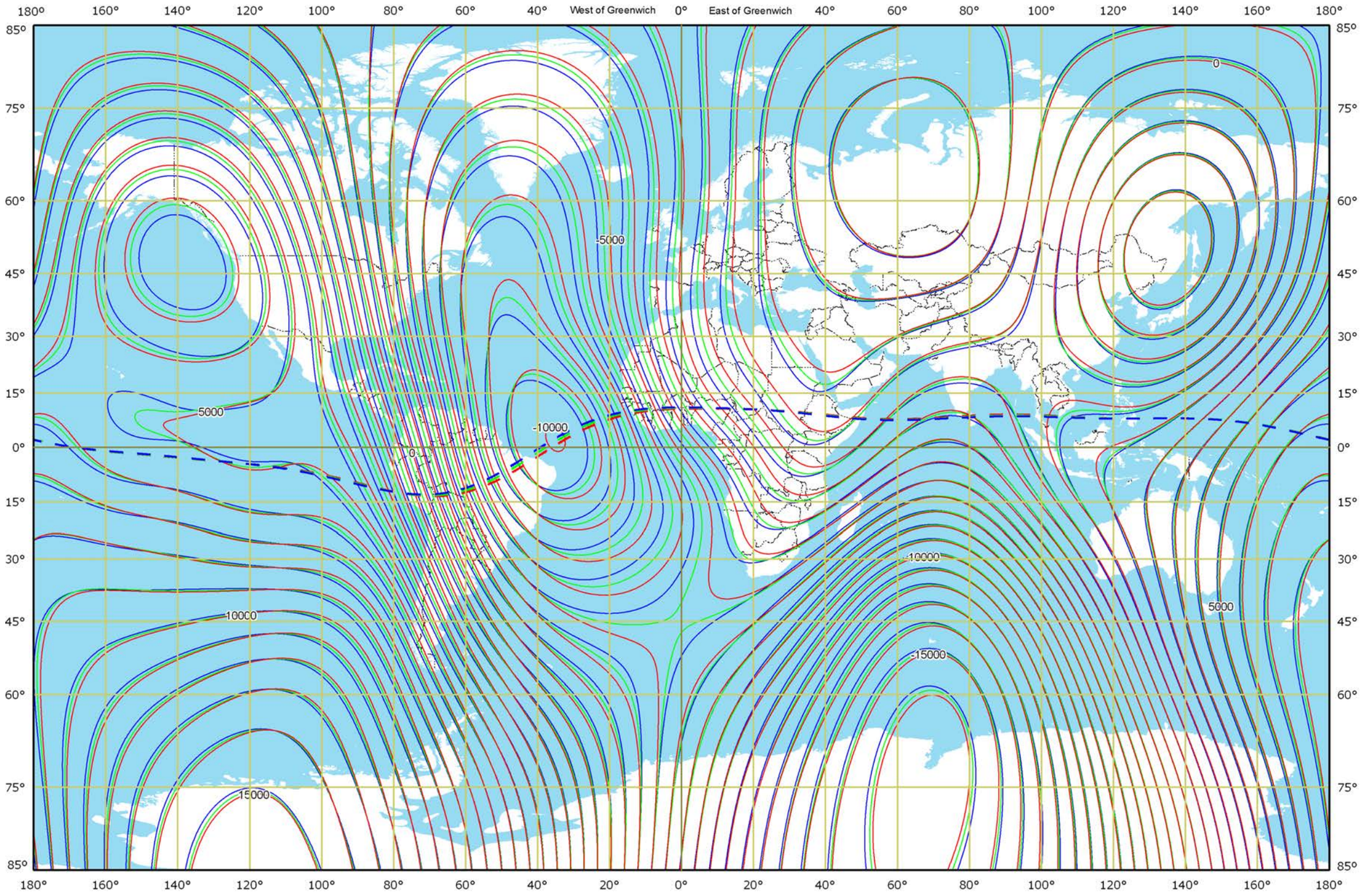

Years	Isolines	Geomagnetic equators
1980		1980
1985		1985
1990		1990

Example of magnetic field component value, nT

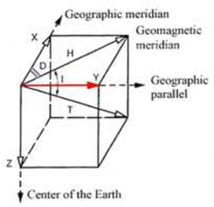

MGMF vector components

D Declination
I Inclination
H Horizontal component
T Total intensity
X North component
Y East component
Z Vertical component

Scale 1: 120 000 000

Projection: Miller cylindrical

EAST COMPONENT OF MGMF

MGMF- 1990, 1995, 2000 – DY

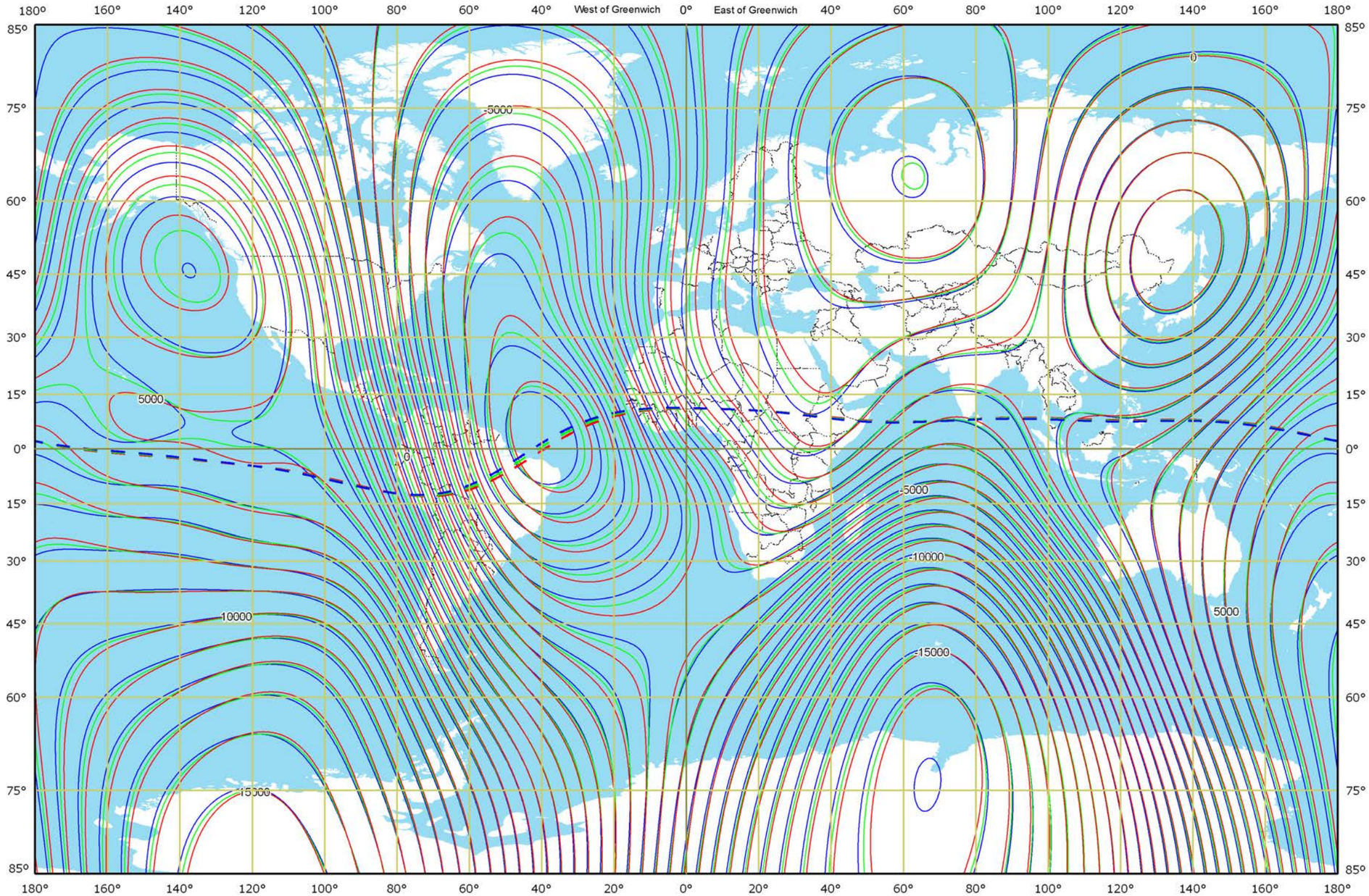

Years	Isolines	Geomagnetic equators
1990		1990
1995		1995
2000		2000

Example of magnetic field component value, nT

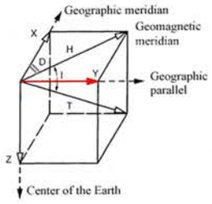

MGMF vector components

D Declination
I Inclination
H Horizontal component
T Total intensity
X North component
Y East component
Z Vertical component

Scale 1: 120 000 000

Projection: Miller cylindrical

EAST COMPONENT OF MGMF

MGMF- 2000, 2005, 2010 – DY

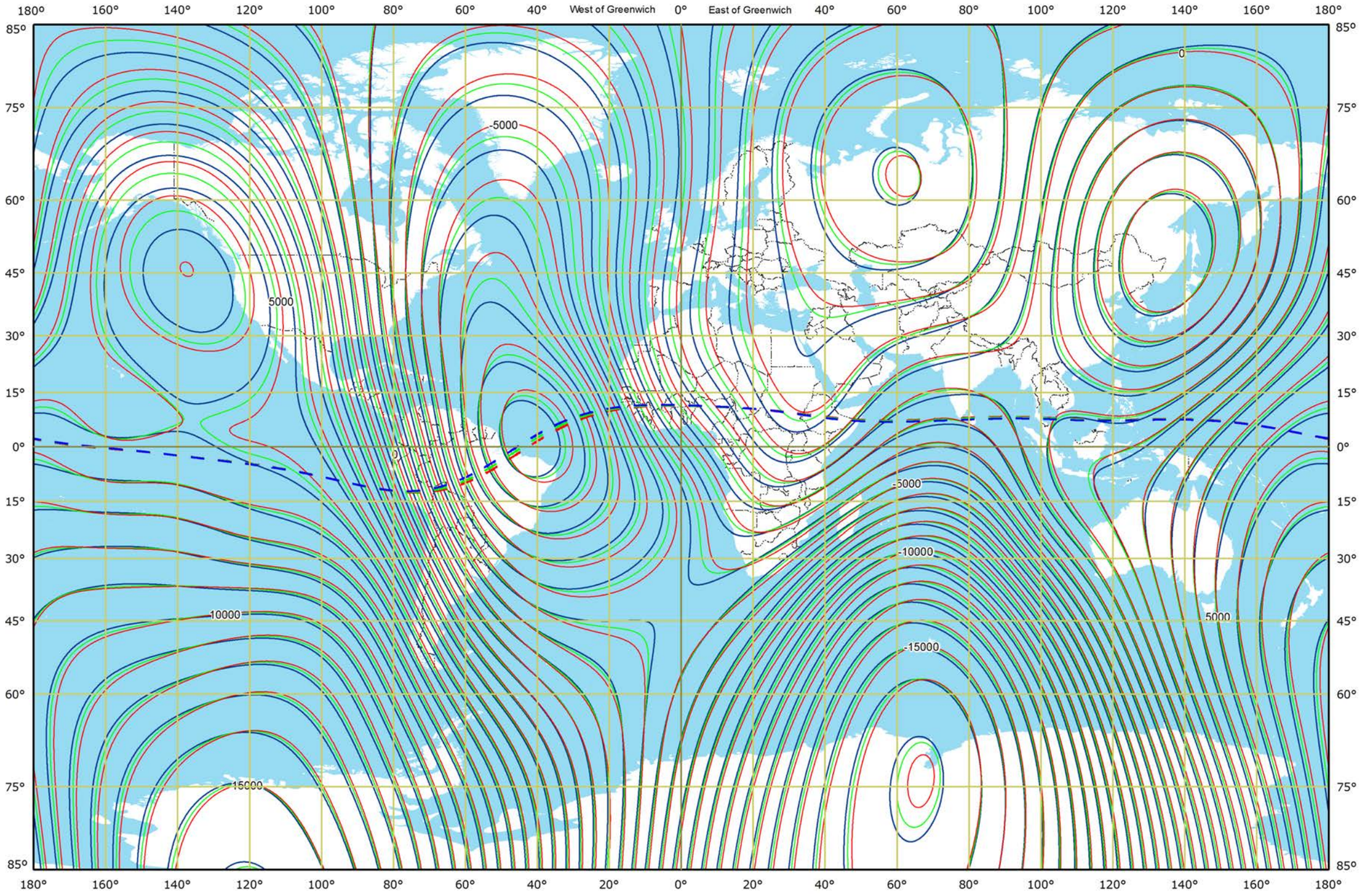

Years	Isolines	Geomagnetic equators
2000		2000
2005		2005
2010		2010

Example of magnetic field component value, nT

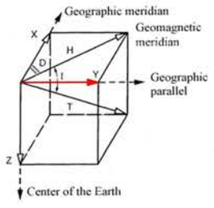

MGMF vector components

D Declination
I Inclination
H Horizontal component
T Total intensity
X North component
Y East component
Z Vertical component

Scale 1: 120 000 000

Projection: Miller cylindrical

VERTICAL COMPONENT OF MGMF

MGMF- 1900, 1905, 1910 – DZ

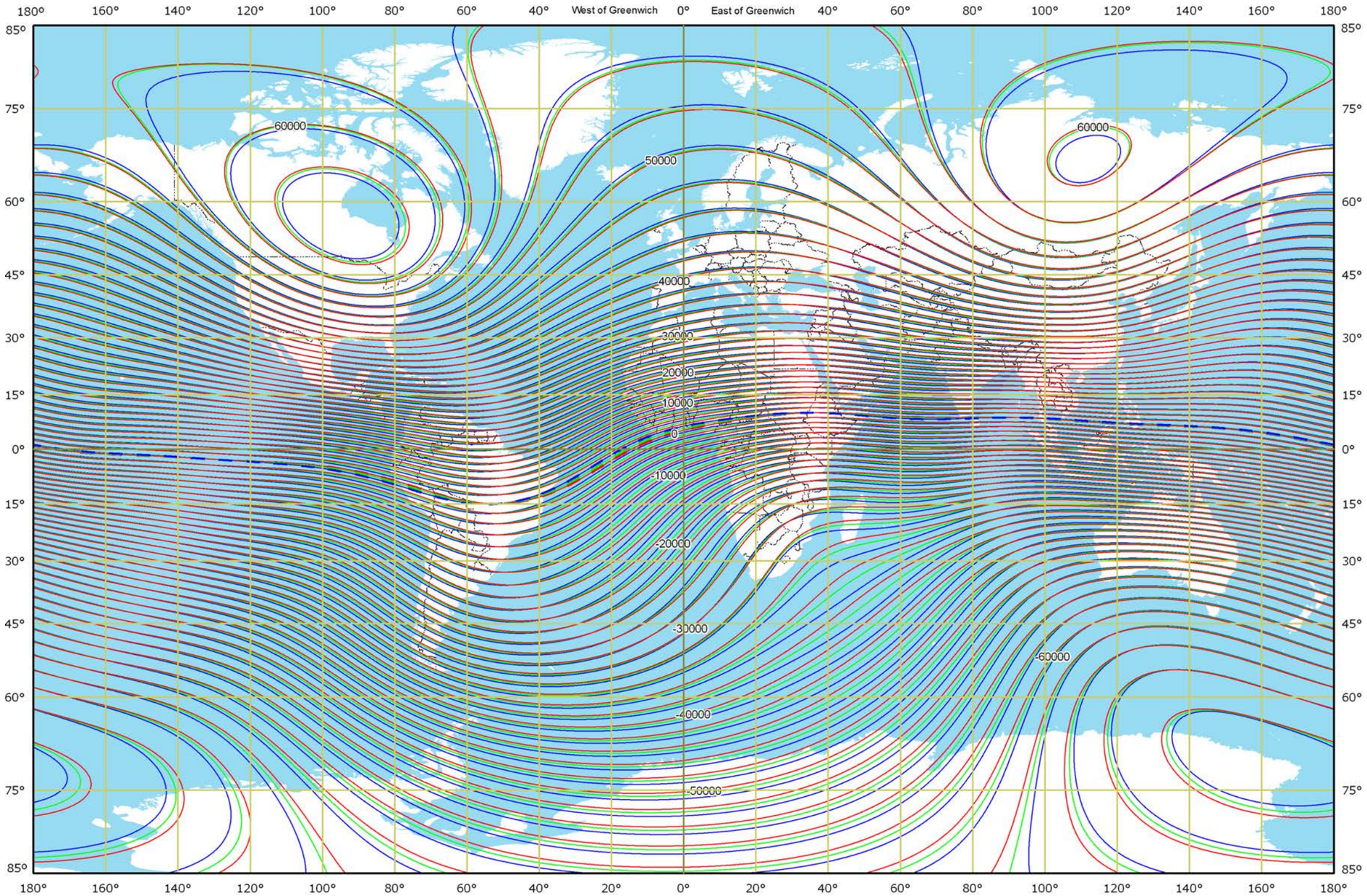

Years	Isolines	Geomagnetic equators
1900		1900
1905		1905
1910		1910

Example of magnetic field component value, nT

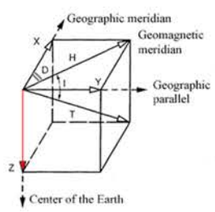

MGMF vector components

D Declination
I Inclination
H Horizontal component
T Total intensity
X North component
Y East component
Z Vertical component

Scale 1: 120 000 000

Projection: Miller cylindrical

VERTICAL COMPONENT OF MGMF

MGMF- 1910, 1915, 1920 – DZ

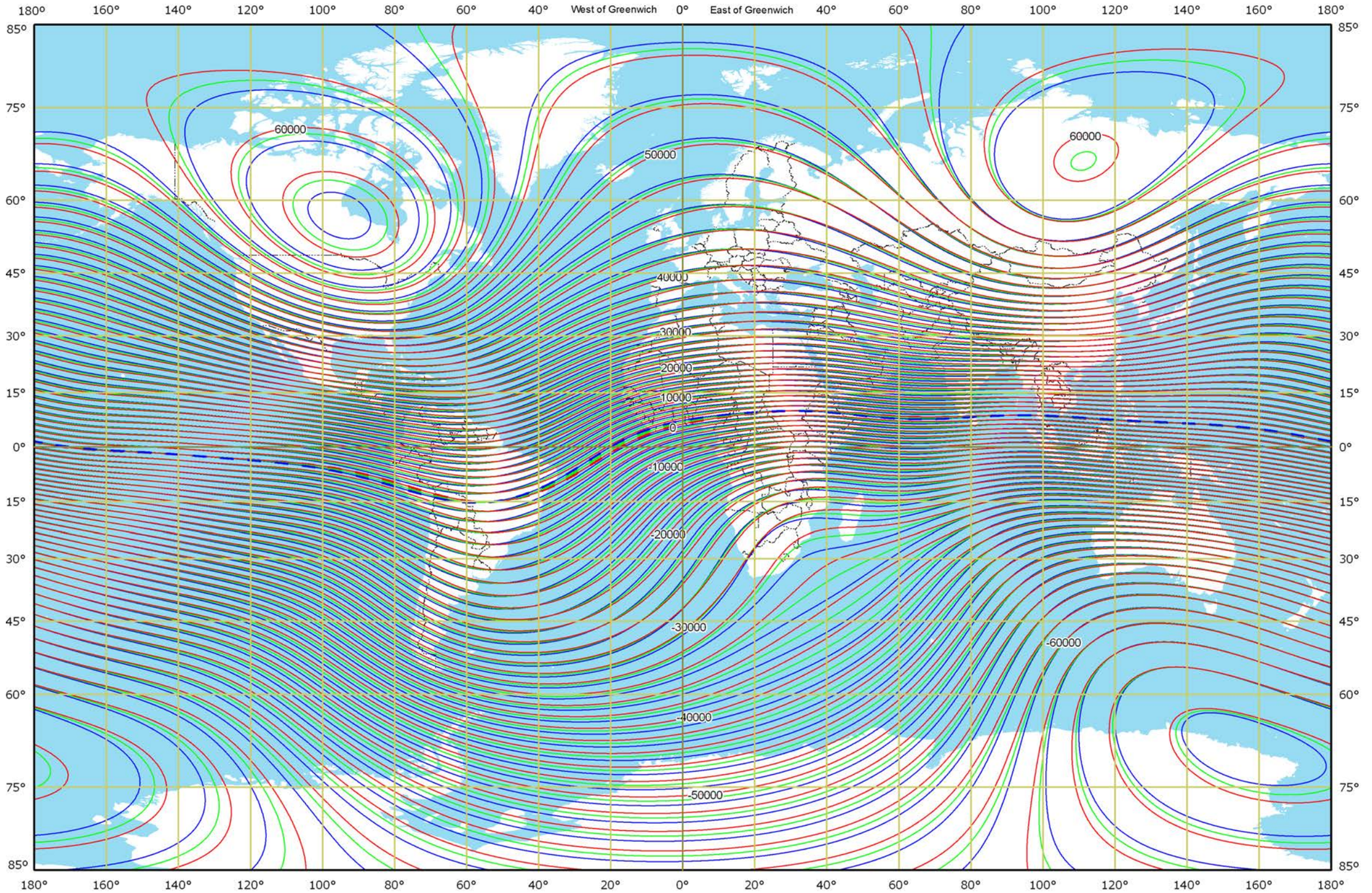

Years	Isolines	Geomagnetic equators
1910		1910
1915		1915
1920		1920

Example of magnetic field component value, nT

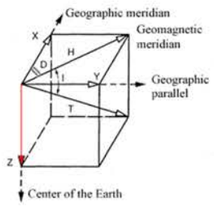

MGMF vector components

D Declination
I Inclination
H Horizontal component
T Total intensity
X North component
Y East component
Z Vertical component

Scale 1: 120 000 000

Projection: Miller cylindrical

VERTICAL COMPONENT OF MGMF

MGMF- 1920, 1925, 1930 – DZ

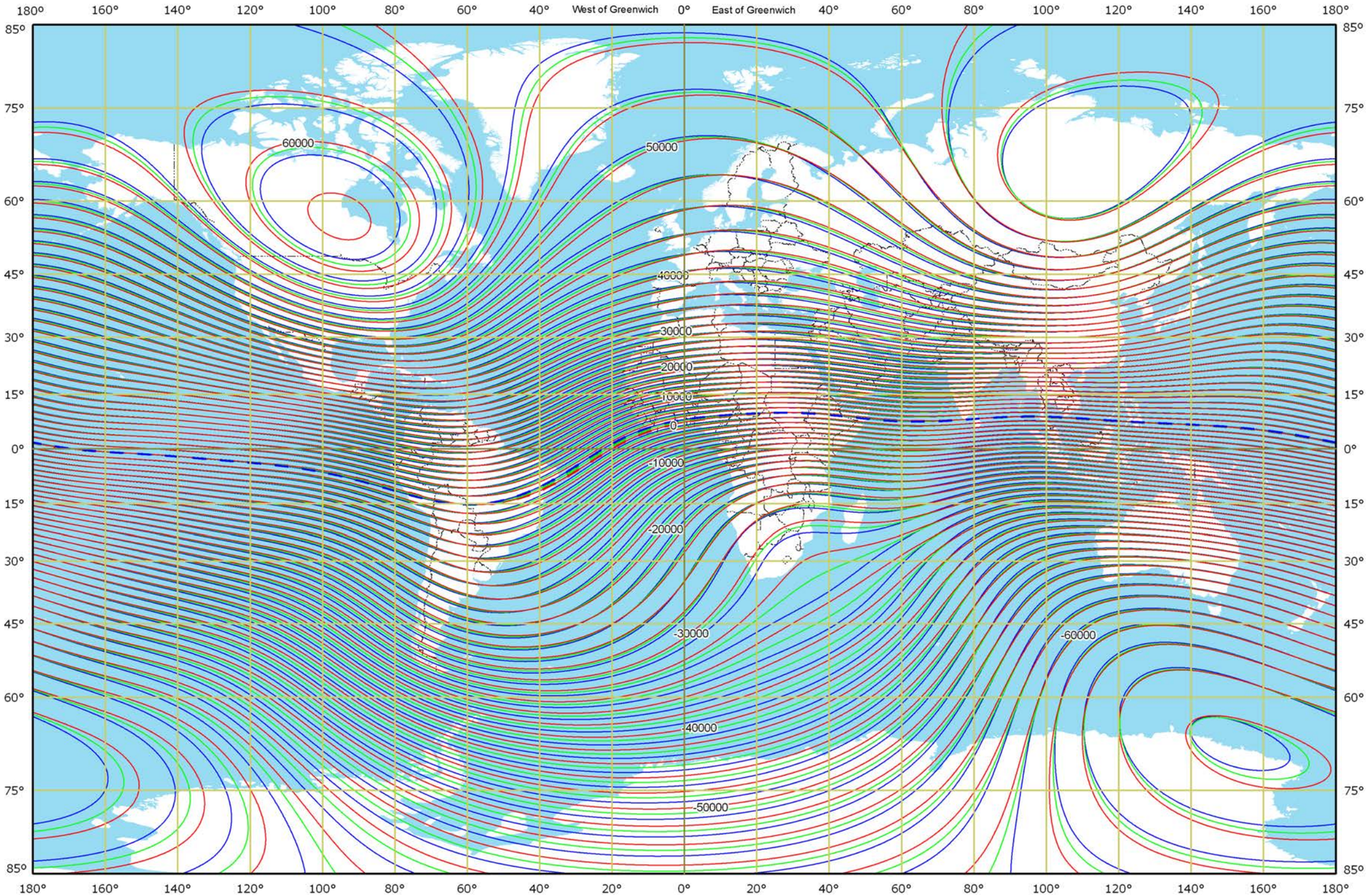

Years	Isolines	Geomagnetic equators
1920		1920
1925		1925
1930		1930

Example of magnetic field component value, nT

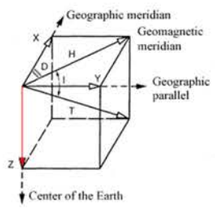

MGMF vector components

D Declination
I Inclination
H Horizontal component
T Total intensity
X North component
Y East component
Z Vertical component

Scale 1: 120 000 000

Projection: Miller cylindrical

VERTICAL COMPONENT OF MGMF

MGMF- 1930, 1935, 1940 – DZ

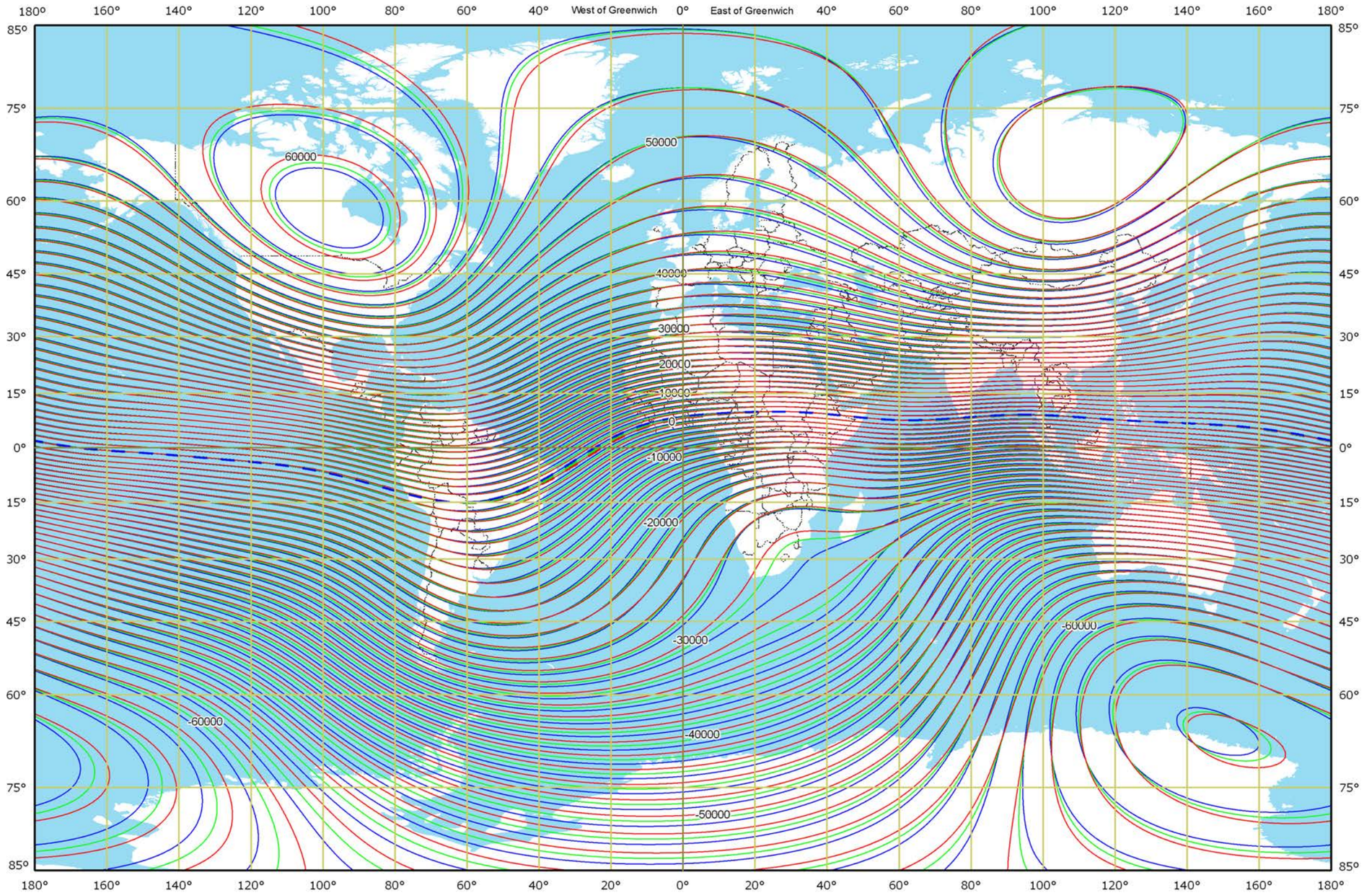

Years	Isolines	Geomagnetic equators
1930		1930
1935		1935
1940		1940

Example of magnetic field component value, nT

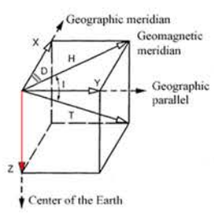

MGMF vector components

D Declination
I Inclination
H Horizontal component
T Total intensity
X North component
Y East component
Z Vertical component

Scale 1: 120 000 000

Projection: Miller cylindrical

VERTICAL COMPONENT OF MGMF

MGMF- 1940, 1945, 1950 – DZ

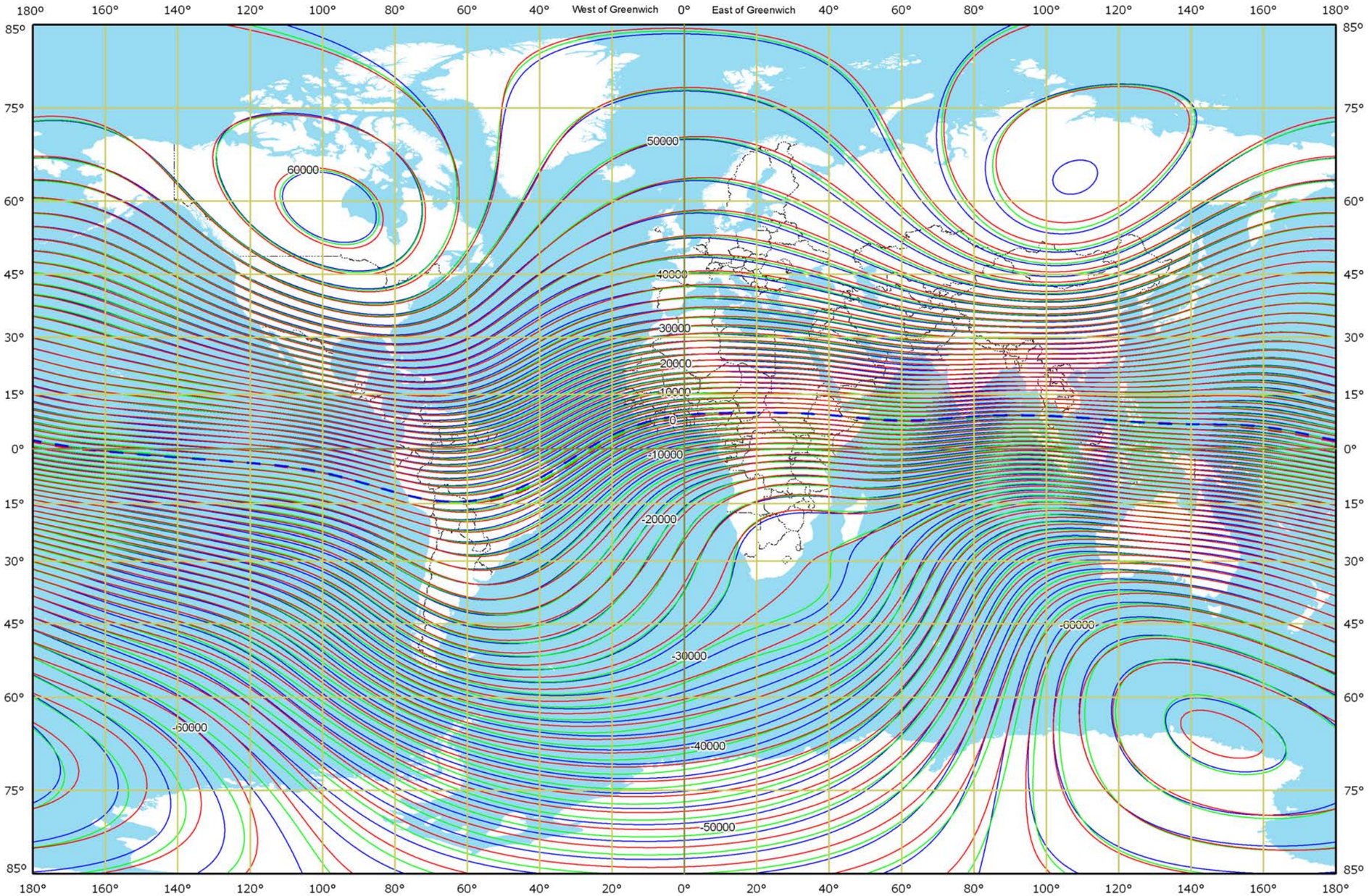

Years	Isolines	Geomagnetic equators
1940		1940
1945		1945
1950		1950

Example of magnetic field component value, nT

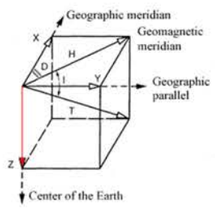

MGMF vector components

D Declination
I Inclination
H Horizontal component
T Total intensity
X North component
Y East component
Z Vertical component

Scale 1: 120 000 000

Projection: Miller cylindrical

VERTICAL COMPONENT OF MGMF

MGMF- 1950, 1955, 1960 – DZ

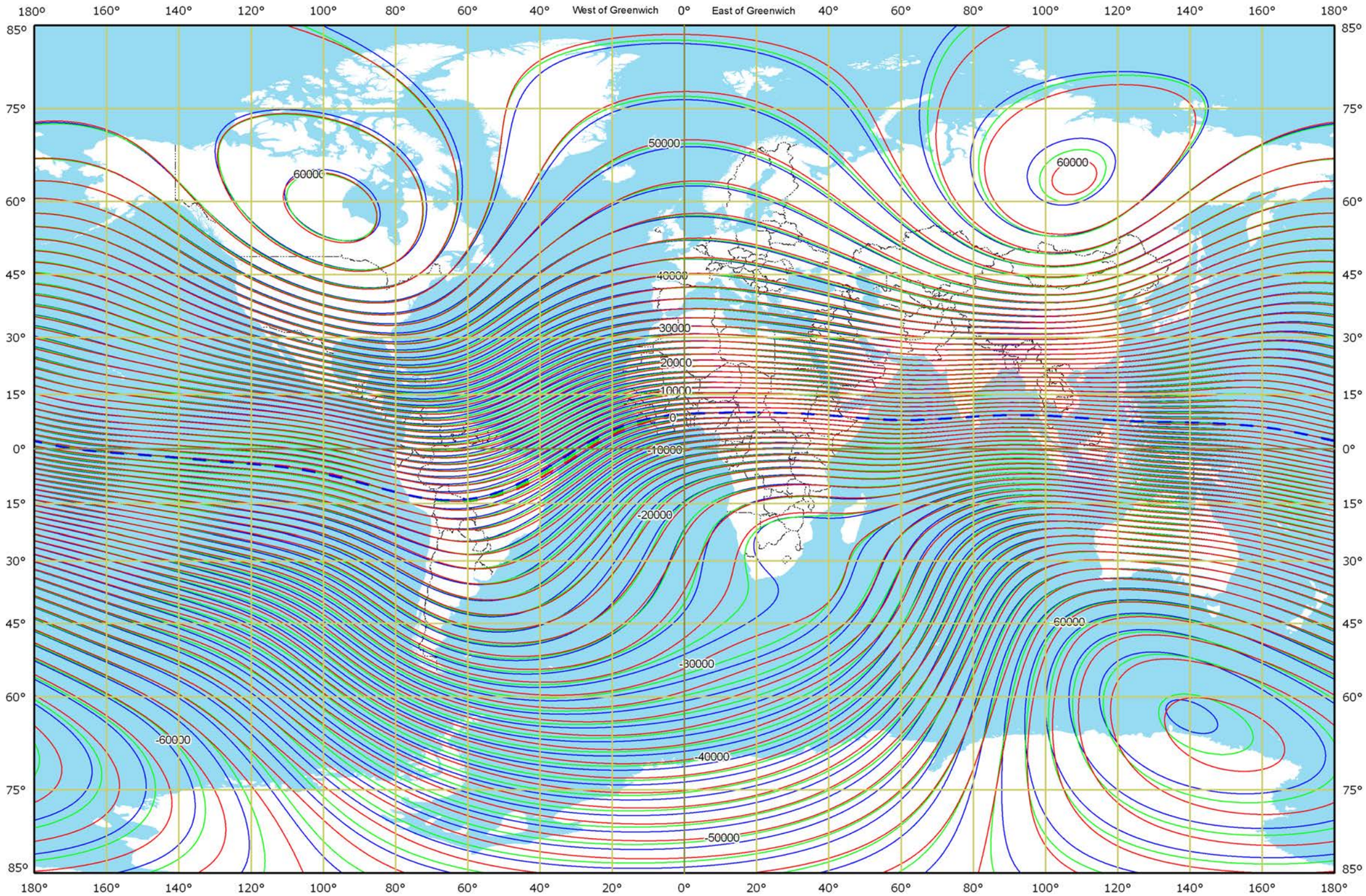

Years	Isolines	Geomagnetic equators
1950		1950
1955		1955
1960		1960

Example of magnetic field component value, nT

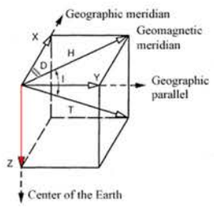

MGMF vector components

D Declination
I Inclination
H Horizontal component
T Total intensity
X North component
Y East component
Z Vertical component

Scale 1: 120 000 000

Projection: Miller cylindrical

VERTICAL COMPONENT OF MGMF

MGMF- 1960, 1965, 1970 – DZ

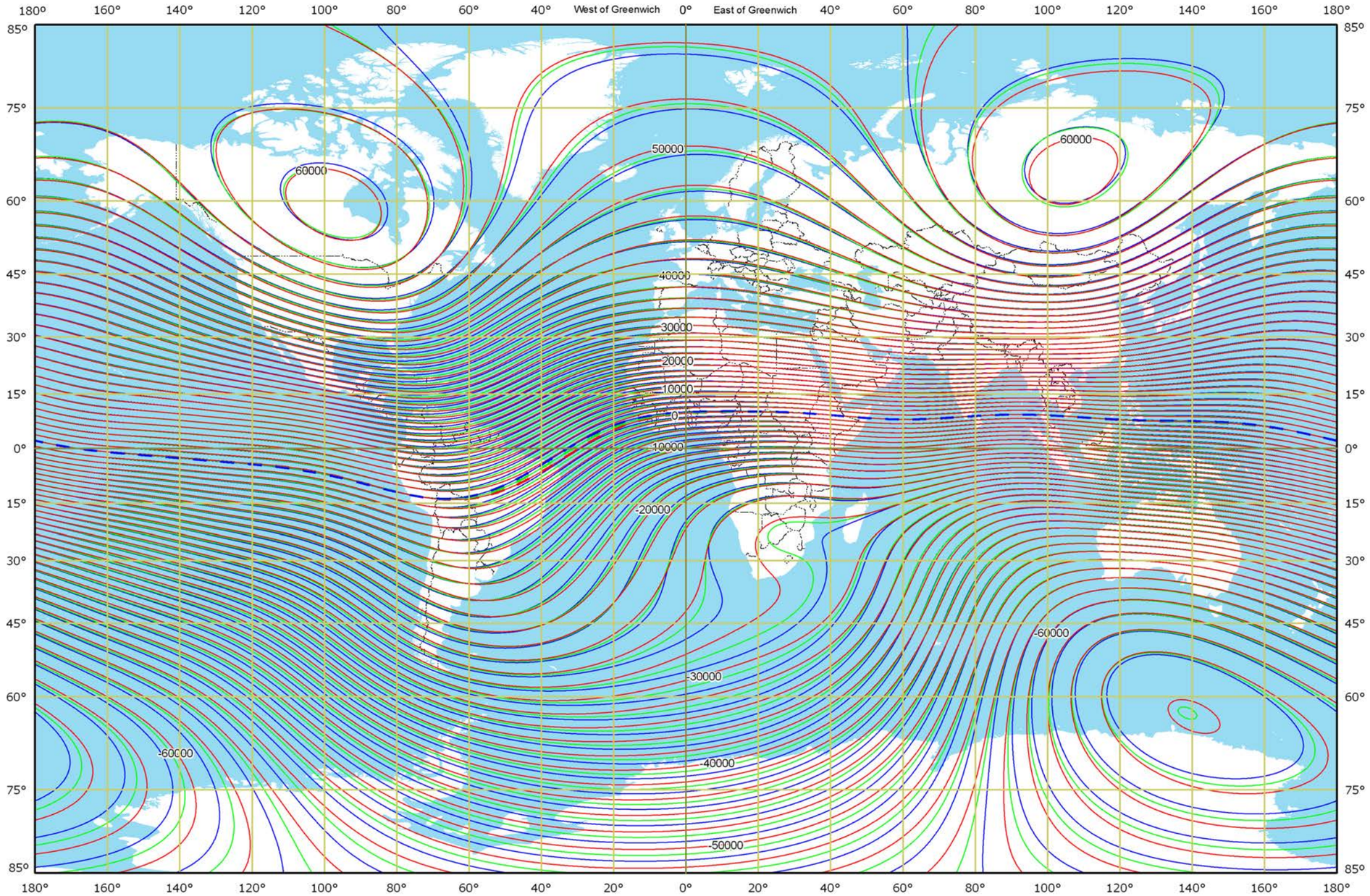

Years	Isolines	Geomagnetic equators
1960		1960
1965		1965
1970		1970

Example of magnetic field component value, nT

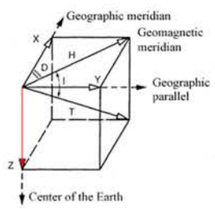

MGMF vector components

D Declination
I Inclination
H Horizontal component
T Total intensity
X North component
Y East component
Z Vertical component

Scale 1: 120 000 000

Projection: Miller cylindrical

VERTICAL COMPONENT OF MGMF

MGMF- 1970, 1975, 1980 – DZ

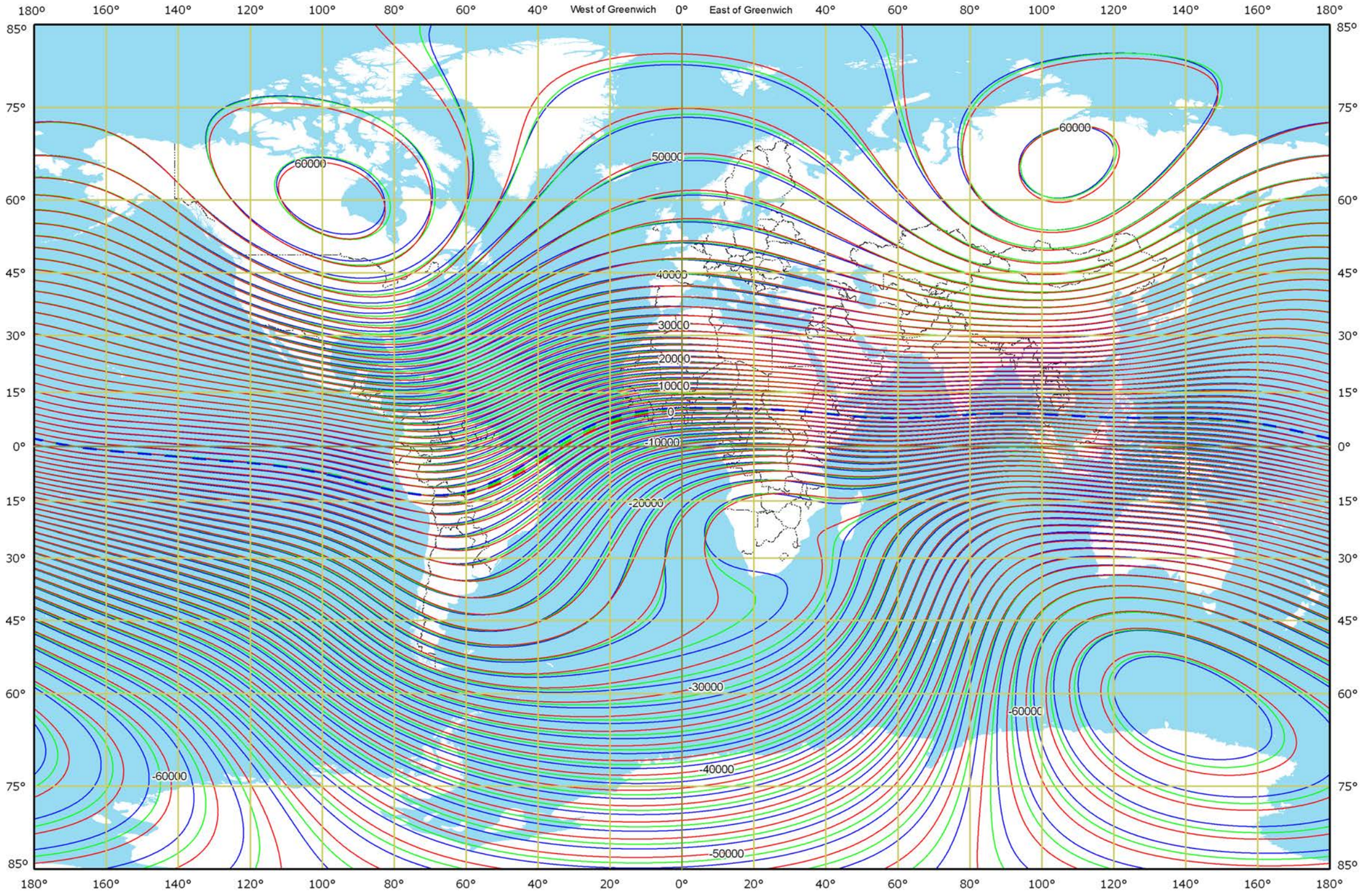

Years	Isolines	Geomagnetic equators
1970		1970
1975		1975
1980		1980

Example of magnetic field component value, nT

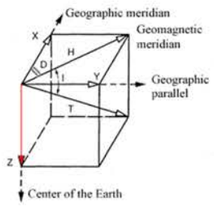

MGMF vector components

D Declination
I Inclination
H Horizontal component
T Total intensity
X North component
Y East component
Z Vertical component

Scale 1: 120 000 000

Projection: Miller cylindrical

VERTICAL COMPONENT OF MGMF

MGMF- 1980, 1985, 1990 – DZ

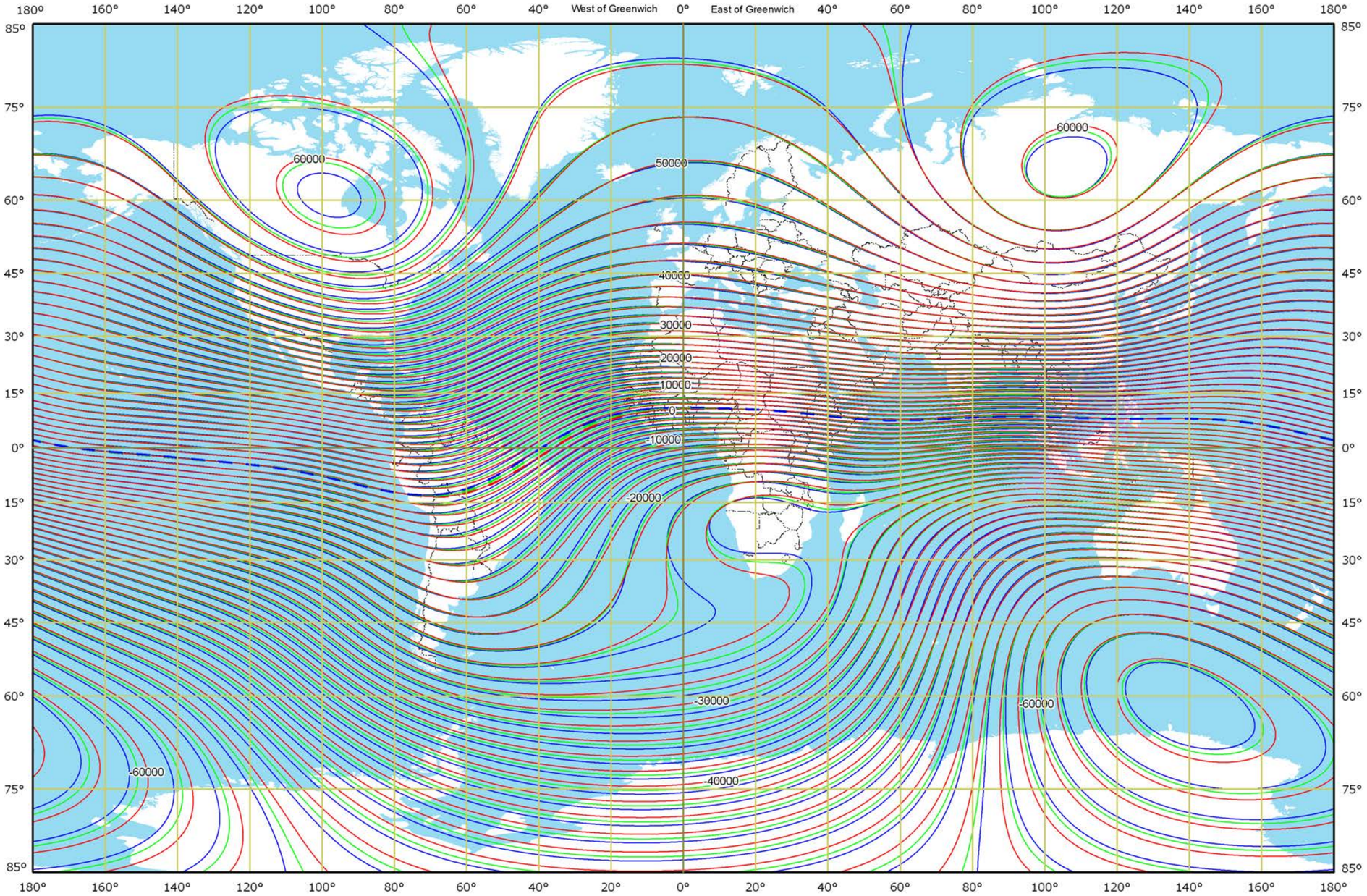

Years	Isolines	Geomagnetic equators
1980		1980
1985		1985
1990		1990

Example of magnetic field component value, nT

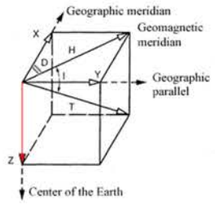

MGMF vector components

D Declination
I Inclination
H Horizontal component
T Total intensity
X North component
Y East component
Z Vertical component

Scale 1: 120 000 000

Projection: Miller cylindrical

VERTICAL COMPONENT OF MGMF

MGMF- 1990, 1995, 2000 – DZ

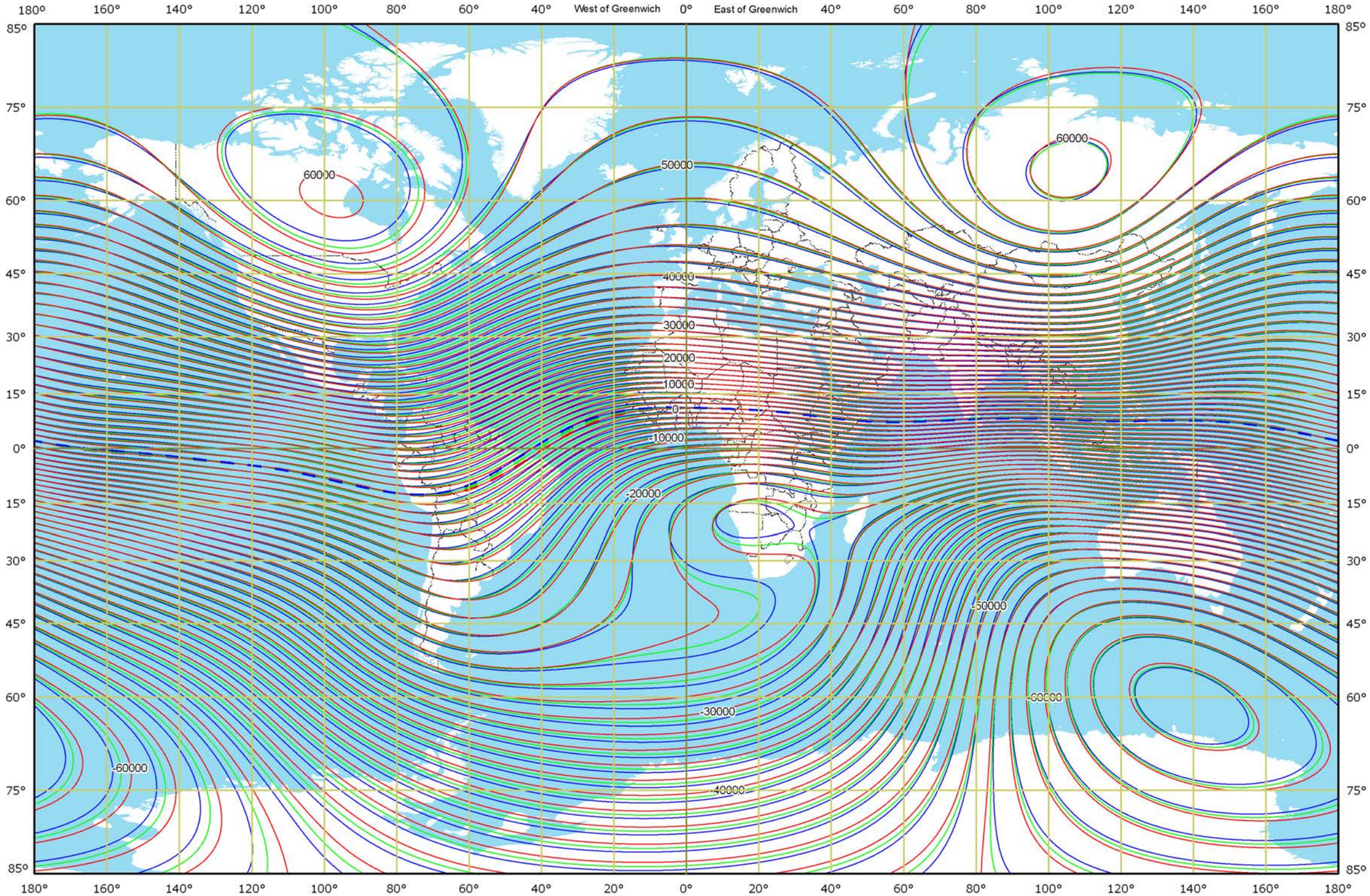

Years	Isolines	Geomagnetic equators
1990		1990
1995		1995
2000		2000

Example of magnetic field component value, nT

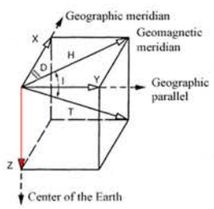

MGMF vector components

D Declination
I Inclination
H Horizontal component
T Total intensity
X North component
Y East component
Z Vertical component

Scale 1: 120 000 000

Projection: Miller cylindrical

VERTICAL COMPONENT OF MGMF

MGMF– 2000, 2005, 2010 – DZ

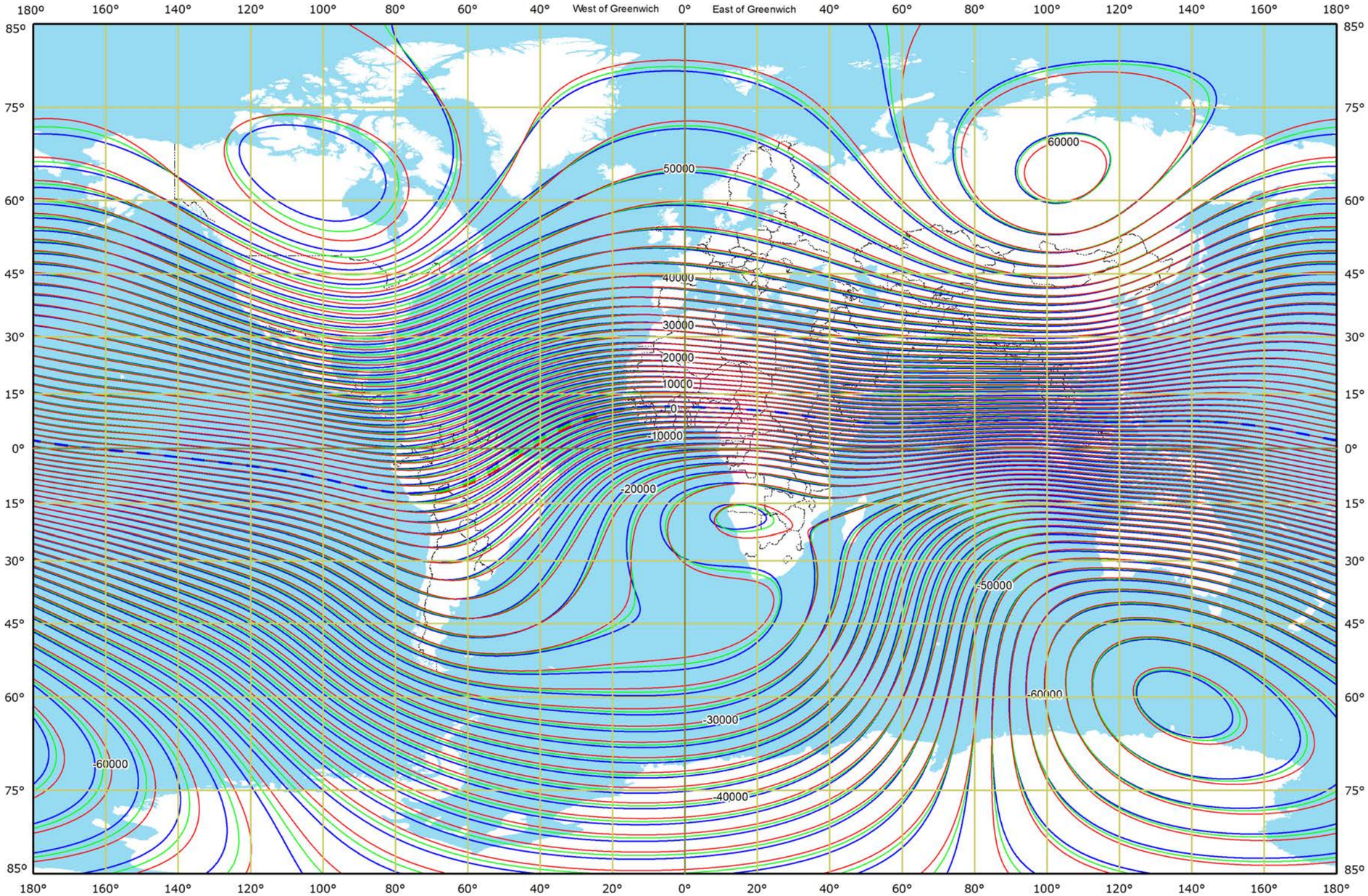

Years	Isolines	Geomagnetic equators
2000		2000
2005		2005
2010		2010

Example of magnetic field component value, nT

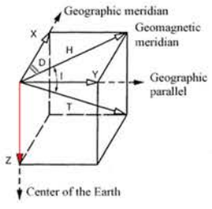

MGMF vector components

D Declination
I Inclination
H Horizontal component
T Total intensity
X North component
Y East component
Z Vertical component

Scale 1: 120 000 000

Projection: Miller cylindrical

HORIZONTAL COMPONENT OF MGMF

MGMF - 1900, 1905, 1910 – H

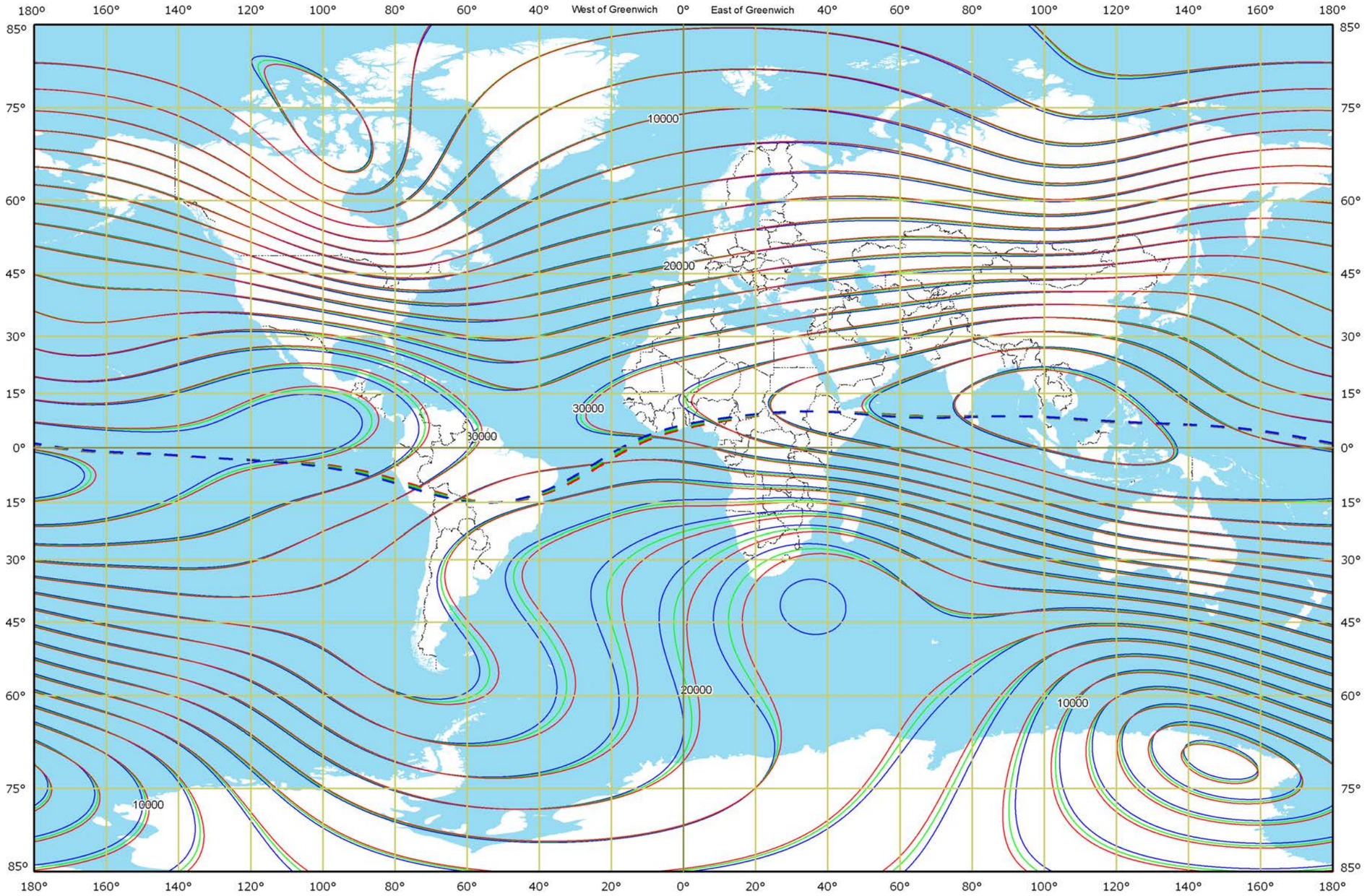

Years	Isolines	Geomagnetic equators
1900		1900
1905		1905
1910		1910

Example of magnetic field component value, nT

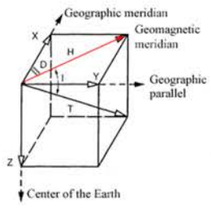

MGMF vector components

D Declination
I Inclination
H Horizontal component
T Total intensity
X North component
Y East component
Z Vertical component

Scale 1: 120 000 000

Projection: Miller cylindrical

HORIZONTAL COMPONENT OF MGMF

MGMF– 1910, 1915, 1920 – H

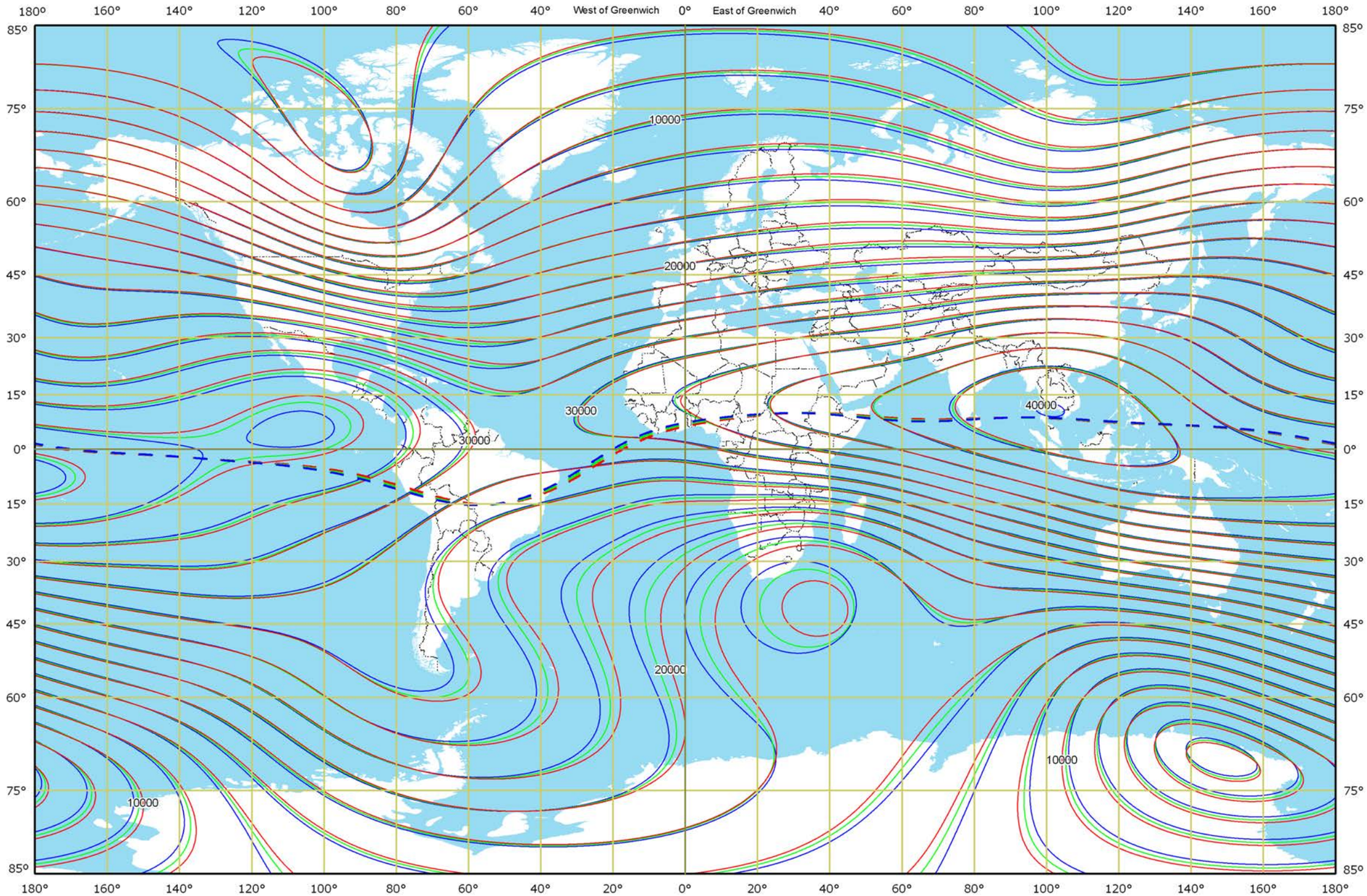

Years	Isolines	Geomagnetic equators
1910		1910
1915		1915
1920		1920

Example of magnetic field component value, nT

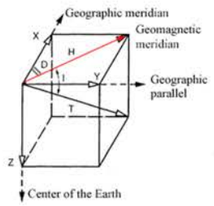

MGMF vector components

D Declination
I Inclination
H Horizontal component
T Total intensity
X North component
Y East component
Z Vertical component

Scale 1: 120 000 000

Projection: Miller cylindrical

HORIZONTAL COMPONENT OF MGMF

MGMF – 1920, 1925, 1930 – H

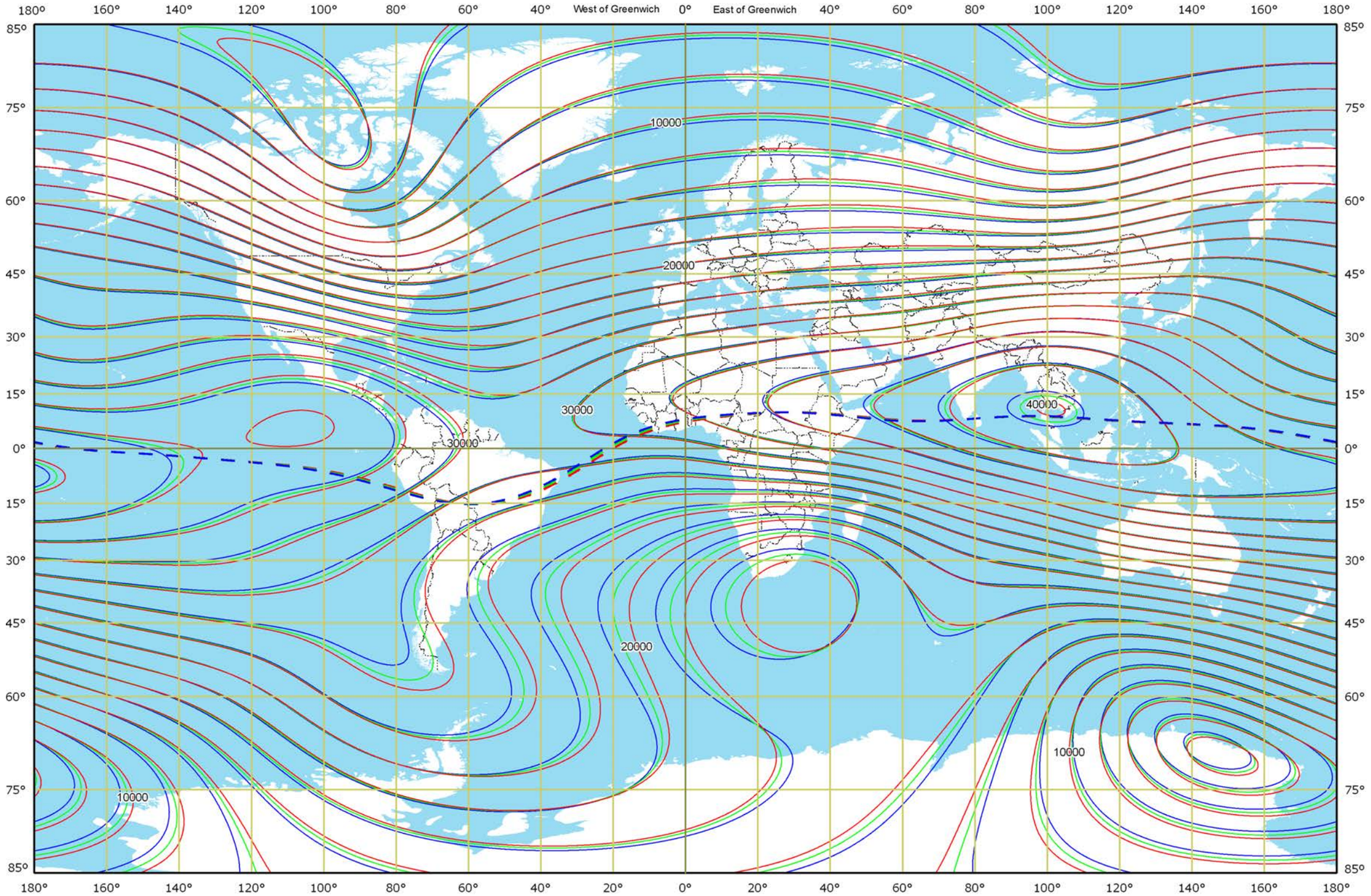

Years	Isolines	Geomagnetic equators
1920		1920
1925		1925
1930		1930

Example of magnetic field component value, nT

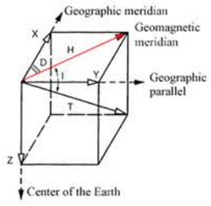

MGMF vector components

D Declination
I Inclination
H Horizontal component
T Total intensity
X North component
Y East component
Z Vertical component

Scale 1: 120 000 000

Projection: Miller cylindrical

HORIZONTAL COMPONENT OF MGMF

MGMF – 1930, 1935, 1940 – H

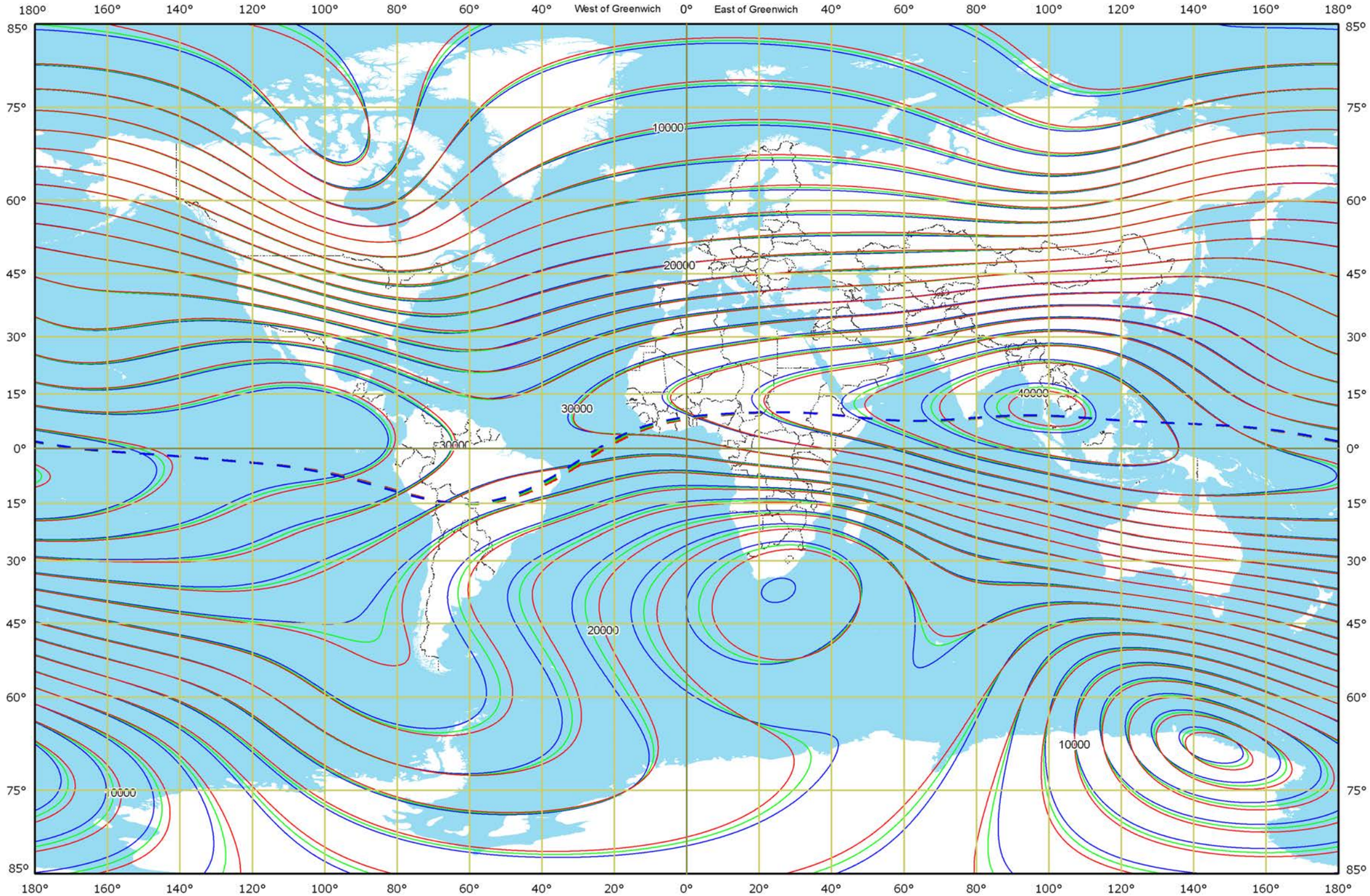

Years	Isolines	Geomagnetic equators
1930		1930
1935		1935
1940		1940

Example of magnetic field component value, nT

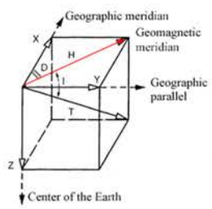

MGMF vector components

D Declination
I Inclination
H Horizontal component
T Total intensity
X North component
Y East component
Z Vertical component

Scale 1: 120 000 000

Projection: Miller cylindrical

HORIZONTAL COMPONENT OF MGMF

MGMF – 1940, 1945, 1950 – H

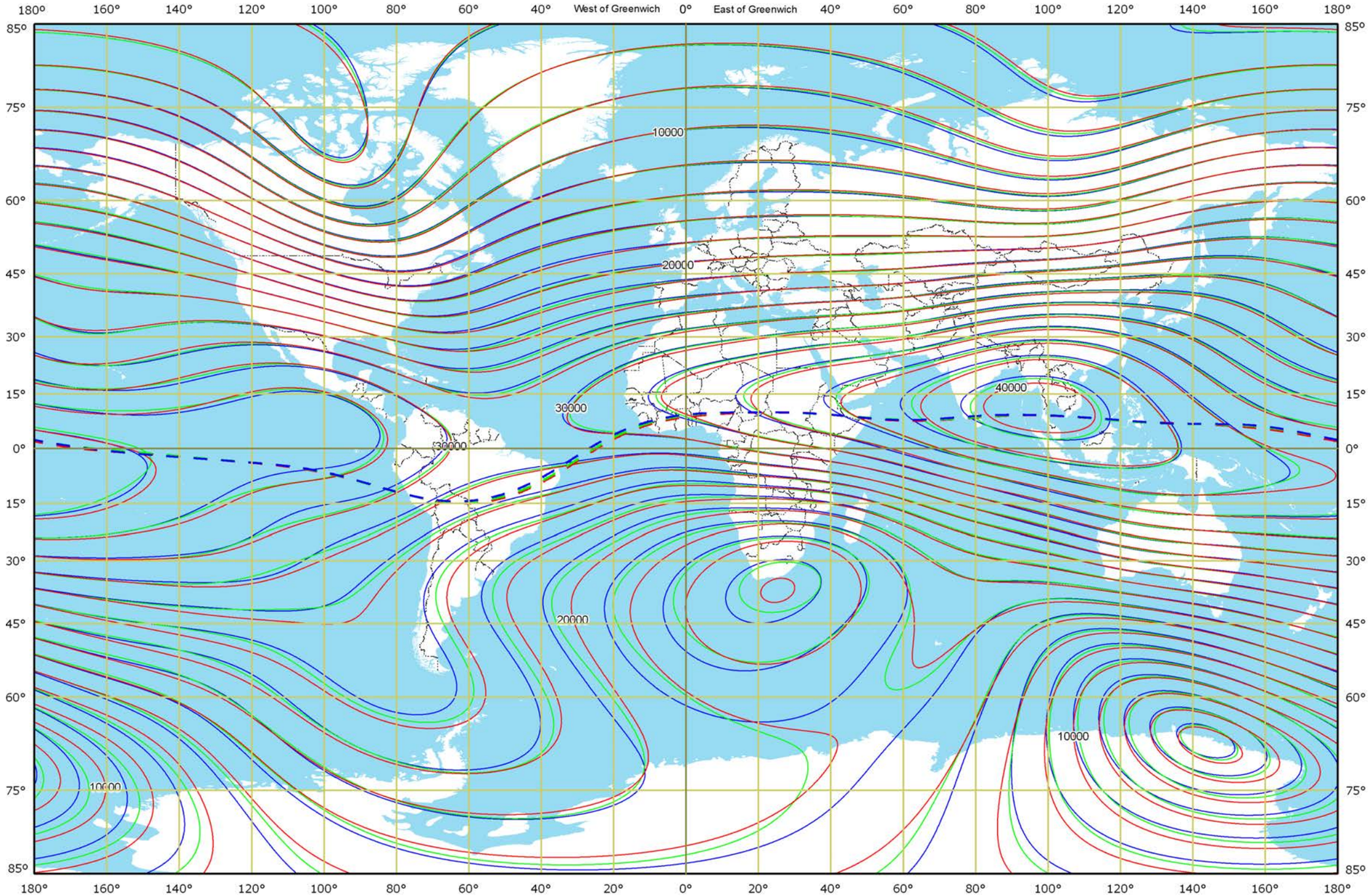

Years	Isolines	Geomagnetic equators
1940		1940
1945		1945
1950		1950

Example of magnetic field component value, nT

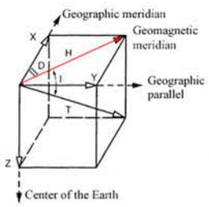

MGMF vector components

D Declination
I Inclination
H Horizontal component
T Total intensity
X North component
Y East component
Z Vertical component

Scale 1: 120 000 000

Projection: Miller cylindrical

HORIZONTAL COMPONENT OF MGMF

MGMF – 1950, 1955, 1960 – H

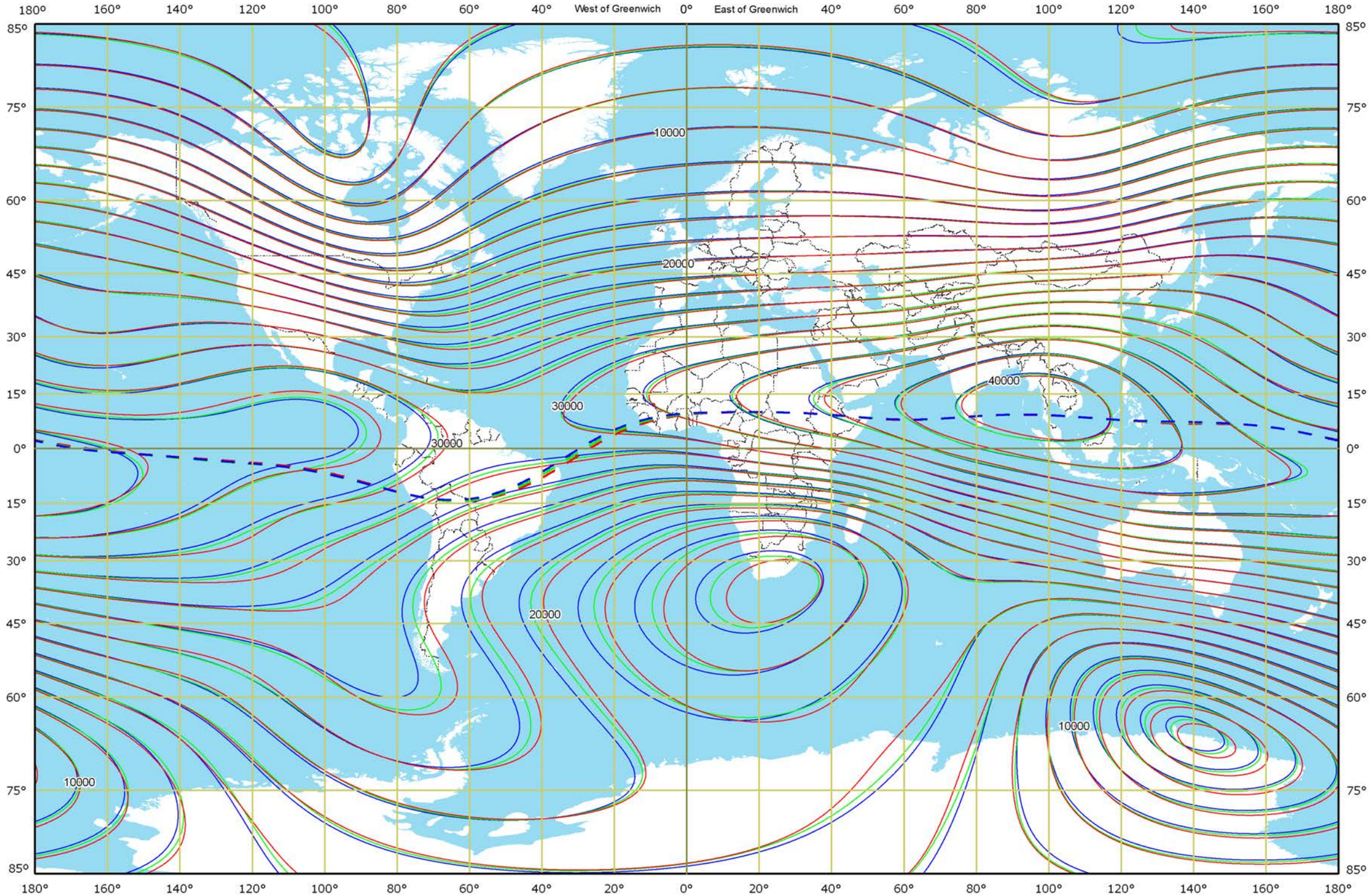

Years	Isolines	Geomagnetic equators
1950		1950
1955		1955
1960		1960

Example of magnetic field component value, nT

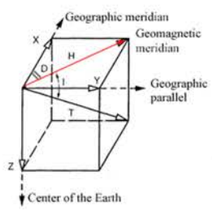

MGMF vector components

D Declination
I Inclination
H Horizontal component
T Total intensity
X North component
Y East component
Z Vertical component

Scale 1: 120 000 000

Projection: Miller cylindrical

HORIZONTAL COMPONENT OF MGMF

MGMF – 1960, 1965, 1970 – H

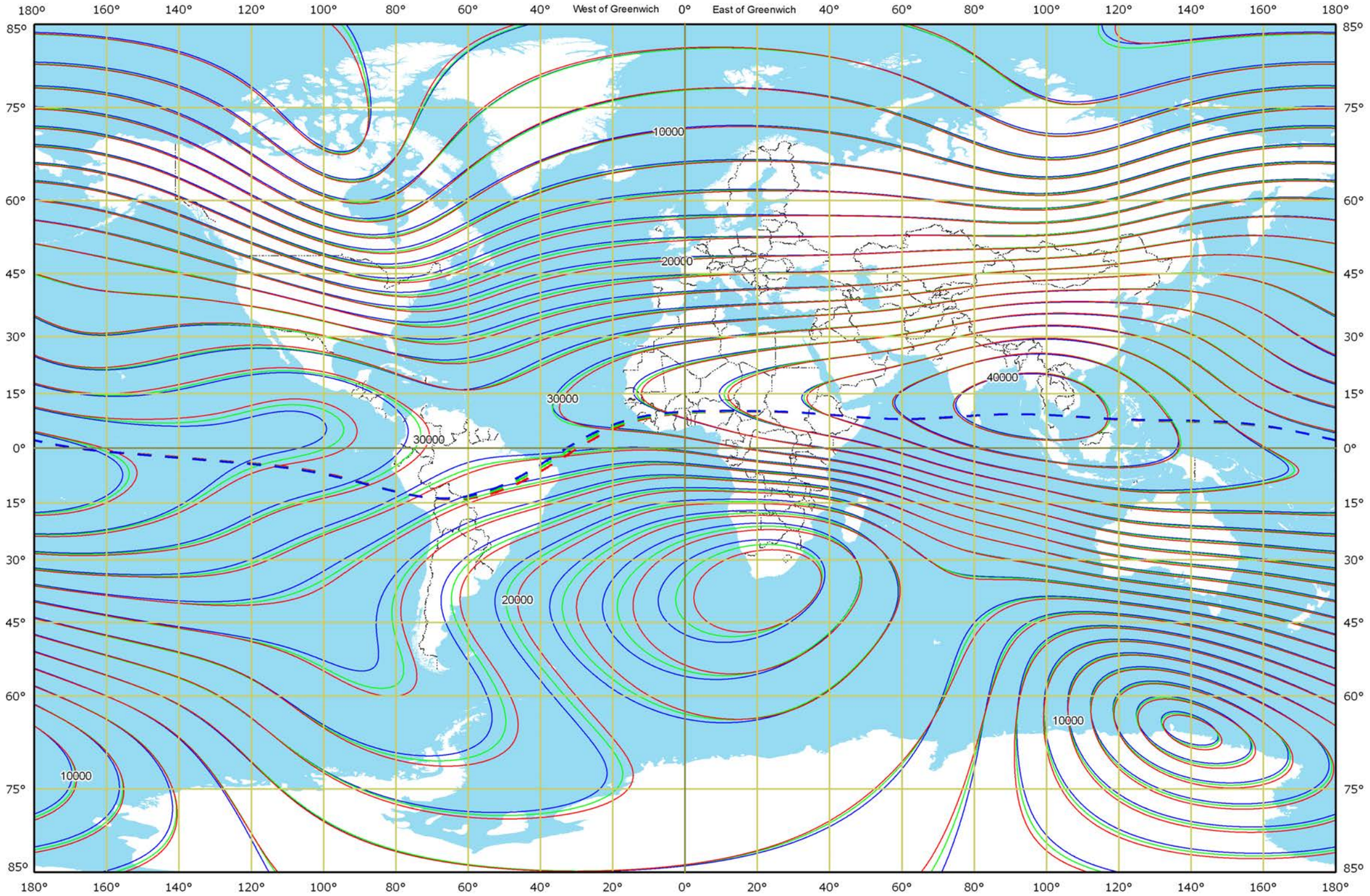

Years	Isolines	Geomagnetic equators
1960		1960
1965		1965
1970		1970

Example of magnetic field component value, nT

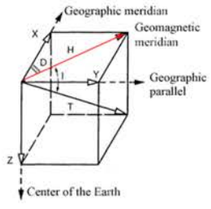

MGMF vector components

D Declination
I Inclination
H Horizontal component
T Total intensity
X North component
Y East component
Z Vertical component

Scale 1: 120 000 000

Projection: Miller cylindrical

HORIZONTAL COMPONENT OF MGMF

MGMF – 1970, 1975, 1980 – H

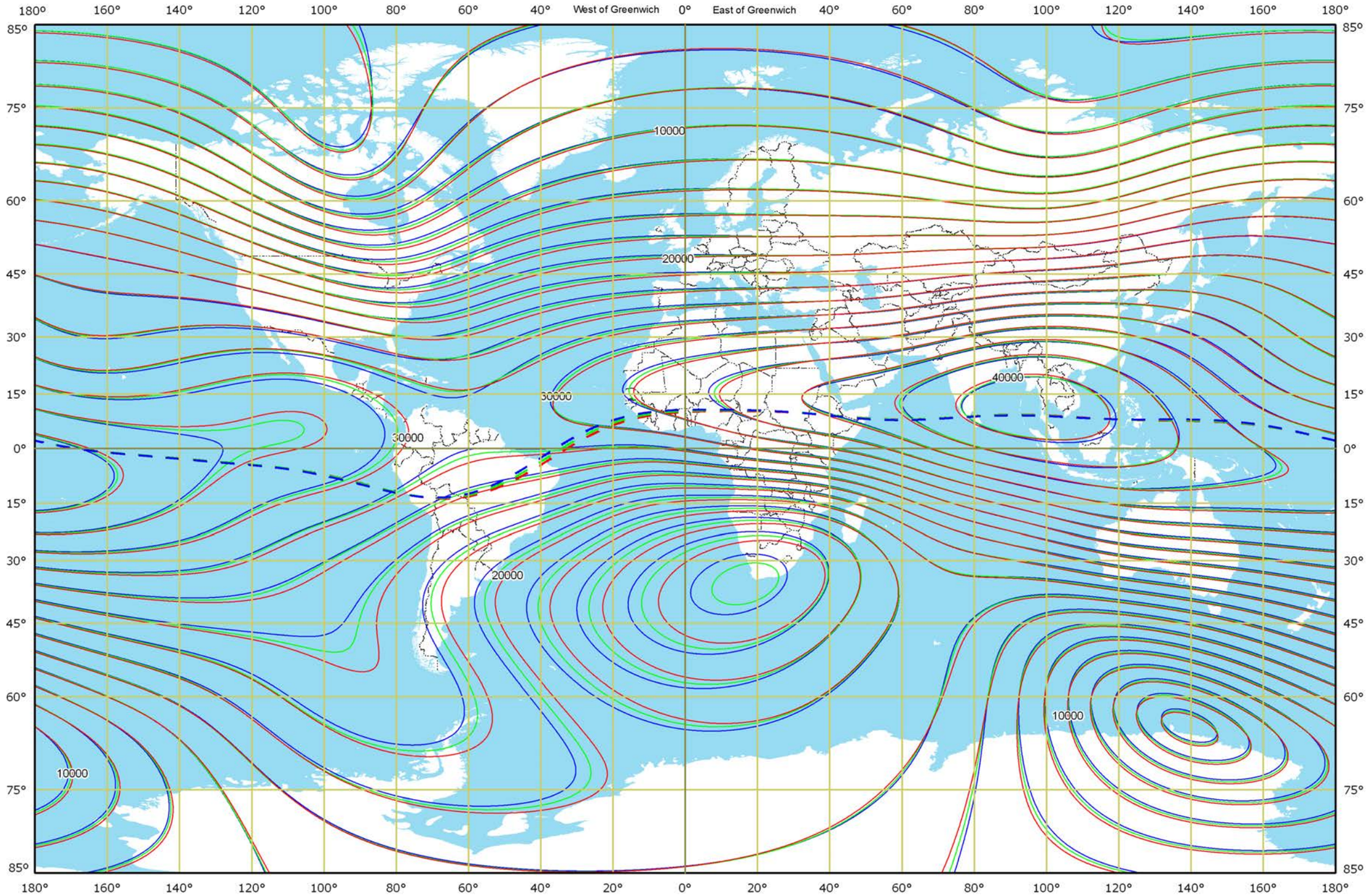

Years	Isolines	Geomagnetic equators
1970		1970
1975		1975
1980		1980

Example of magnetic field component value, nT

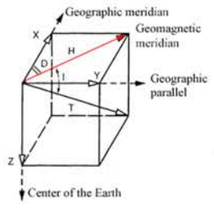

MGMF vector components

D Declination
I Inclination
H Horizontal component
T Total intensity
X North component
Y East component
Z Vertical component

Scale 1: 120 000 000

Projection: Miller cylindrical

HORIZONTAL COMPONENT OF MGMF

MGMF – 1980, 1985, 1990 – H

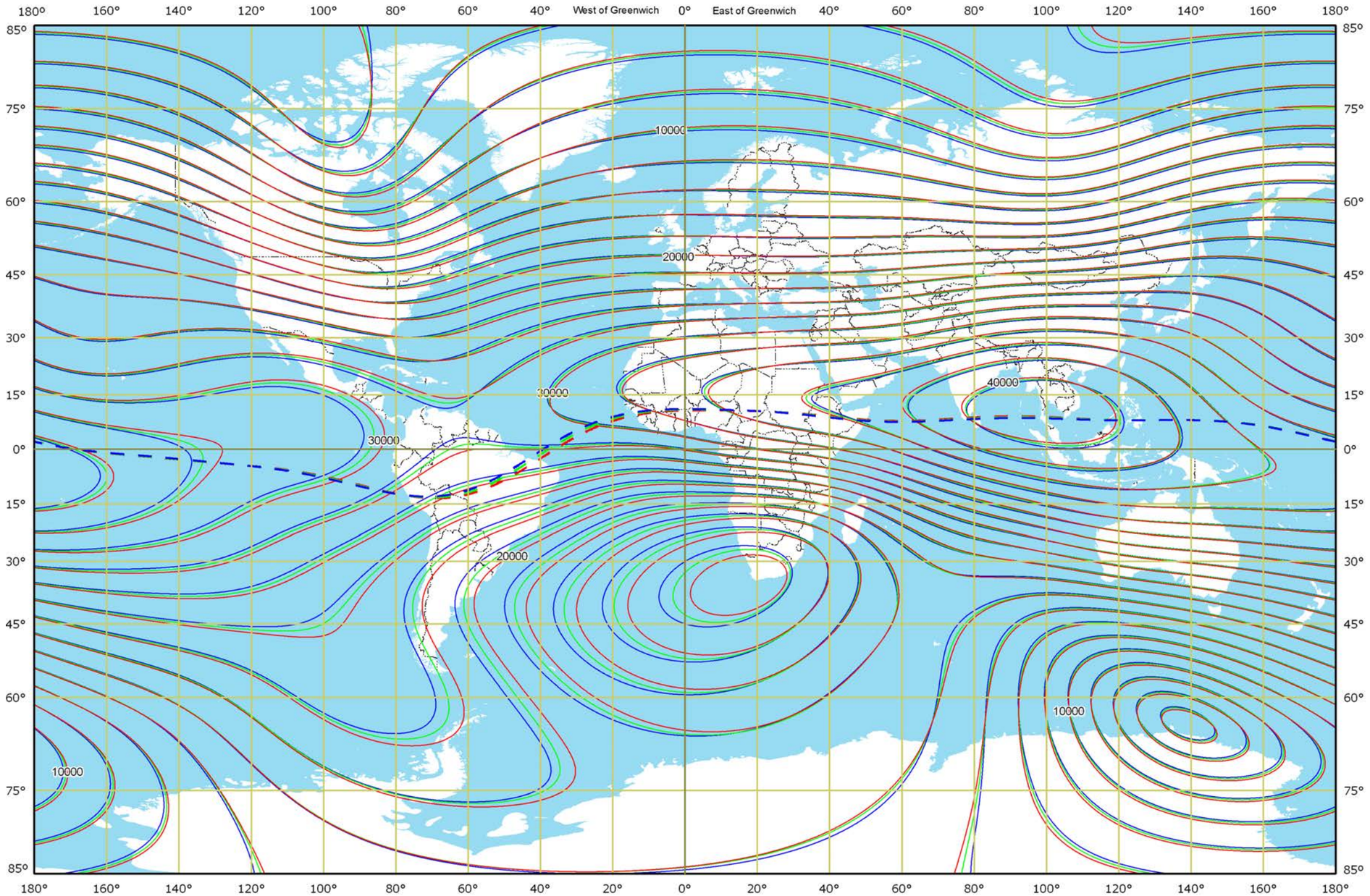

Years	Isolines	Geomagnetic equators
1980		1980
1985		1985
1990		1990

Example of magnetic field component value, nT

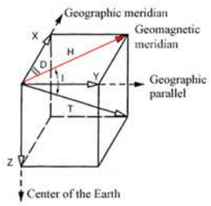

MGMF vector components

D Declination
I Inclination
H Horizontal component
T Total intensity
X North component
Y East component
Z Vertical component

Scale 1: 120 000 000

Projection: Miller cylindrical

HORIZONTAL COMPONENT OF MGMF

MGMF– 1990, 1995, 2000 – H

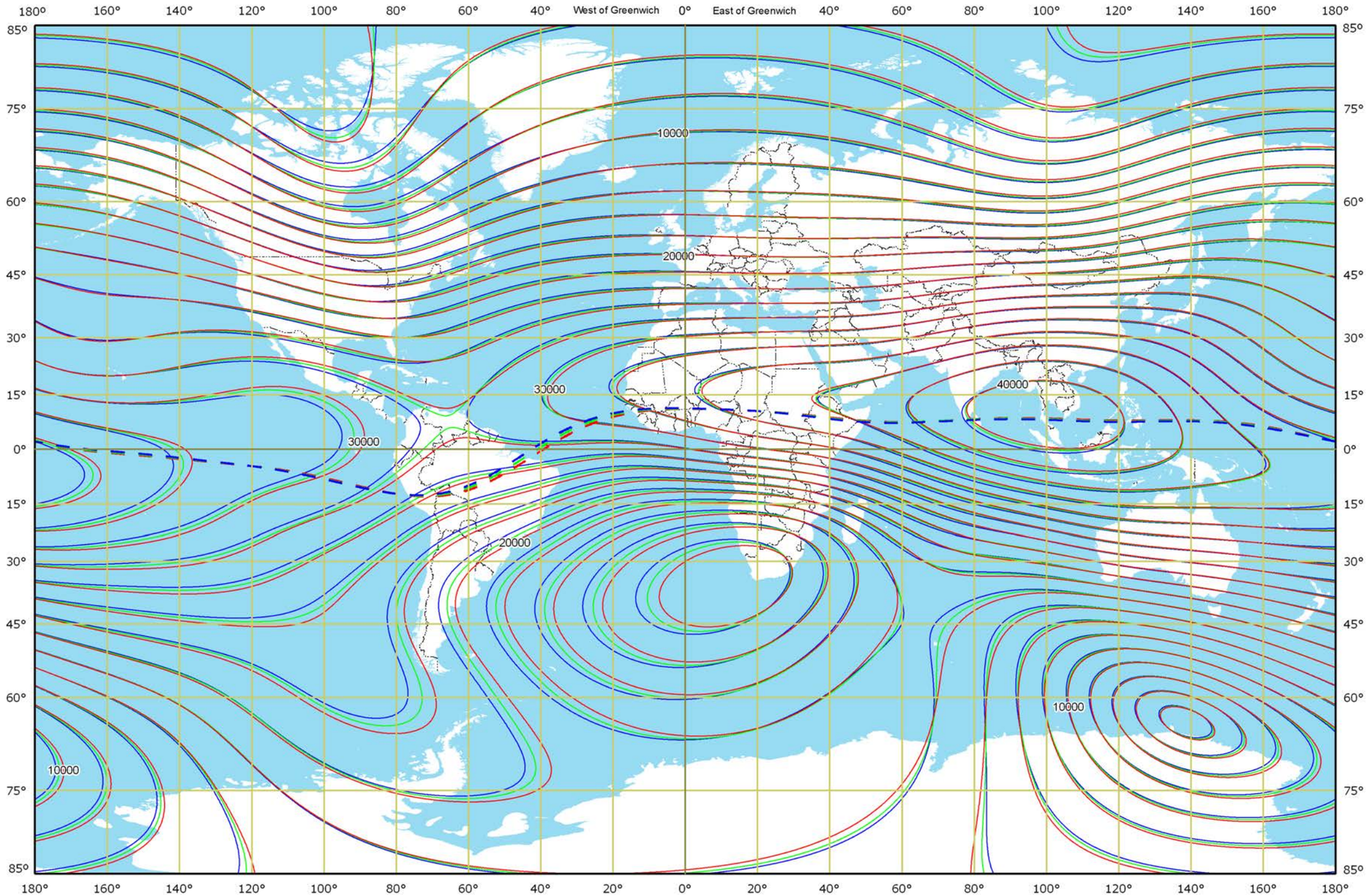

Years	Isolines	Geomagnetic equators
1990		1990
1995		1995
2000		2000

Example of magnetic field component value, nT

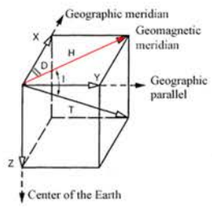

MGMF vector components

D Declination
I Inclination
H Horizontal component
T Total intensity
X North component
Y East component
Z Vertical component

Scale 1: 120 000 000

Projection: Miller cylindrical

HORIZONTAL COMPONENT OF MGMF

MGMF – 2000, 2005, 2010 – H

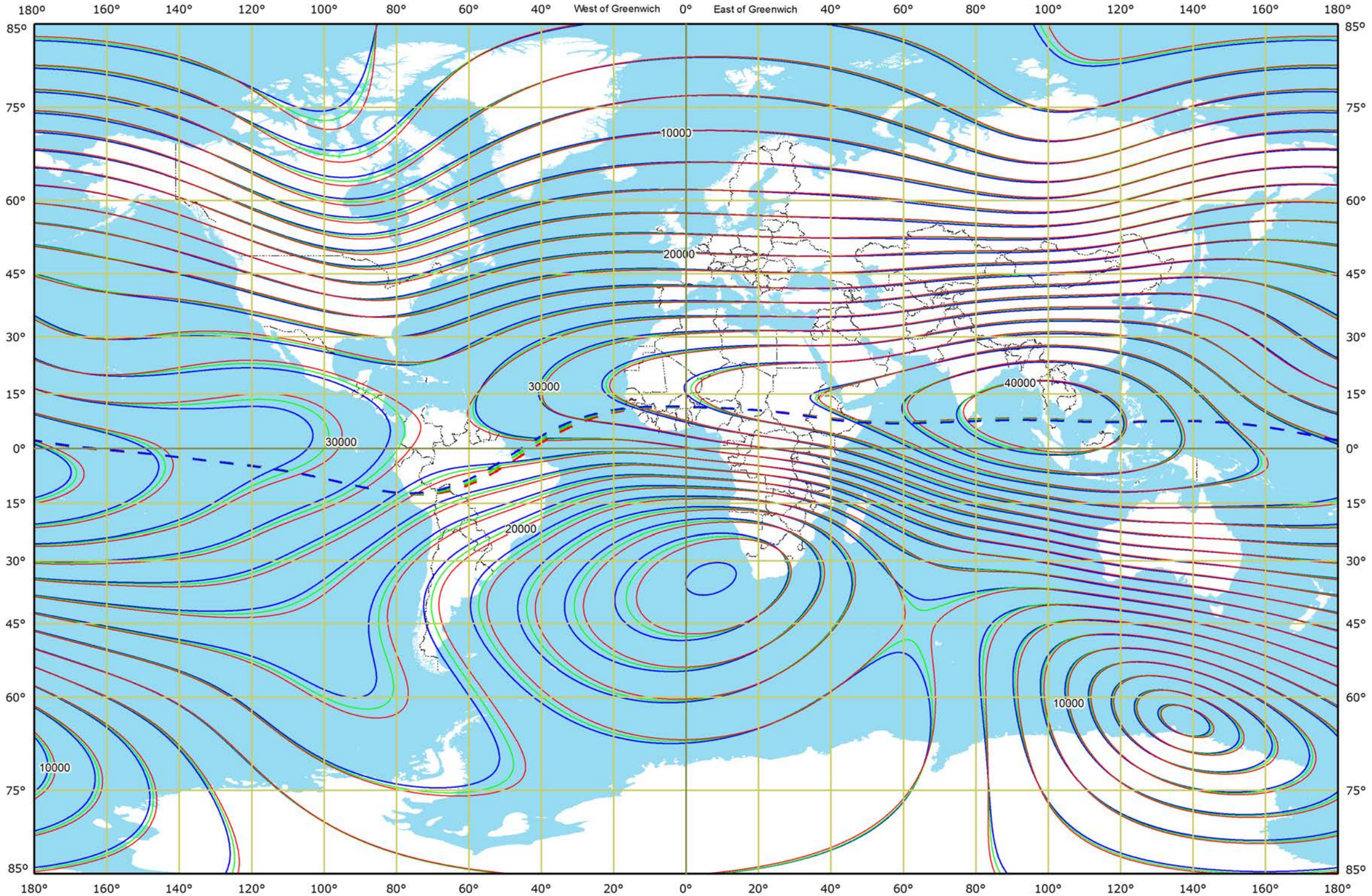

Years	Isolines	Geomagnetic equators
2000		2000
2005		2005
2010		2010

Example of magnetic field component value, nT

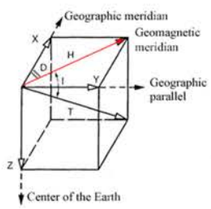

MGMF vector components

D Declination
I Inclination
H Horizontal component
T Total intensity
X North component
Y East component
Z Vertical component

Scale 1: 120 000 000

Projection: Miller cylindrical

MGMF TOTAL INTENSITY

MGMF – 1900, 1905, 1910 – FM (T)

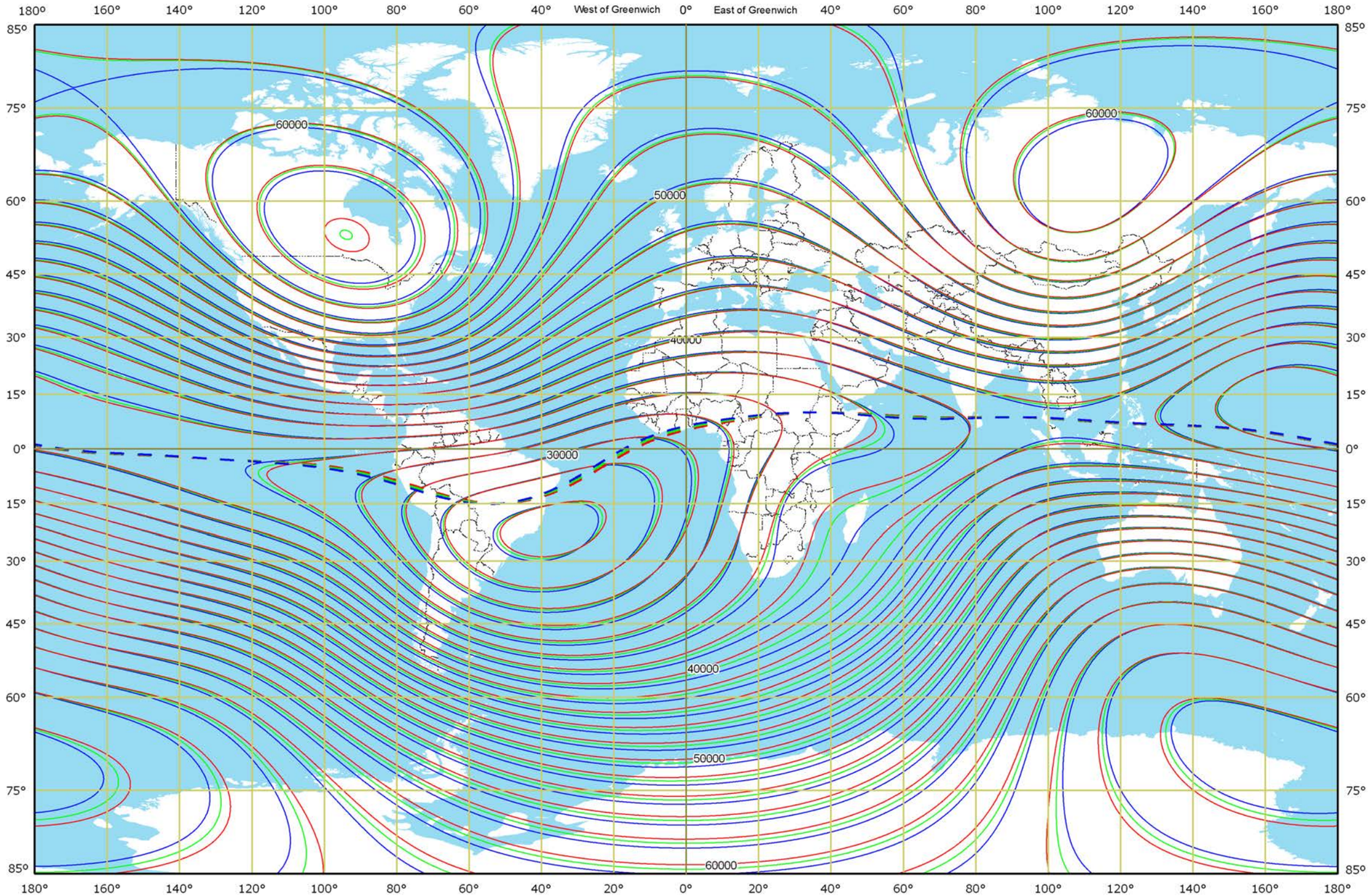

Years	Isolines	Geomagnetic equators
1900		1900
1905		1905
1910		1910

Example of magnetic total intensity value, nT

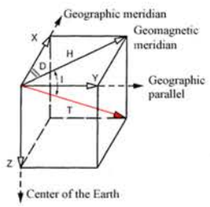

MGMF vector components

D Declination
I Inclination
H Horizontal component
T Total intensity
X North component
Y East component
Z Vertical component

Scale 1: 120 000 000

Projection: Miller cylindrical

MGMF TOTAL INTENSITY

MGMF– 1910, 1915, 1920 – FM (T)

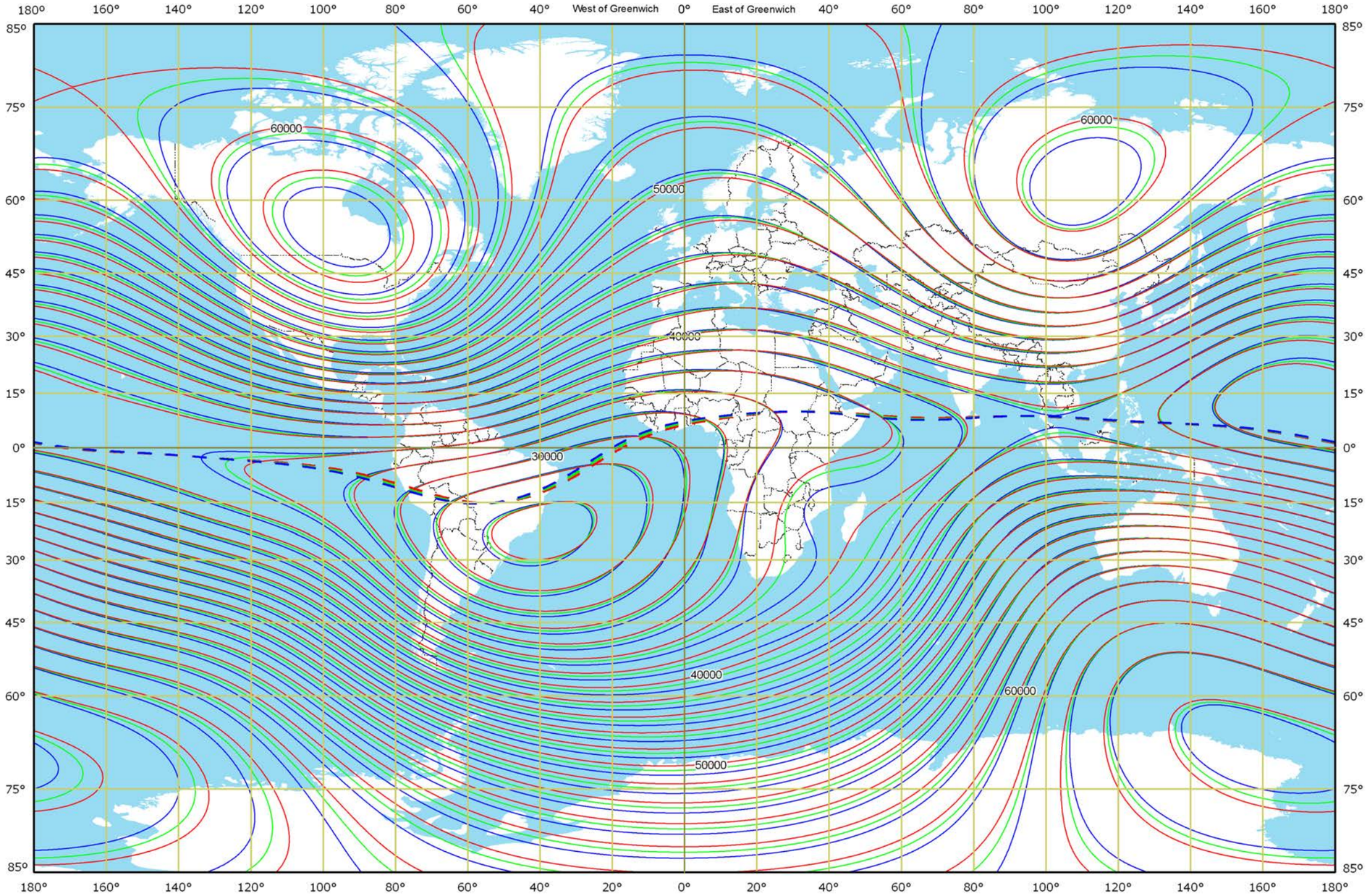

Years	Isolines	Geomagnetic equators
1910		1910
1915		1915
1920		1920

Example of magnetic total intensity value, nT

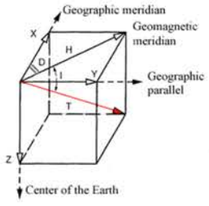

MGMF vector components

D Declination
I Inclination
H Horizontal component
T Total intensity
X North component
Y East component
Z Vertical component

Scale 1: 120 000 000

Projection: Miller cylindrical

MGMF TOTAL INTENSITY

MGMF– 1920, 1925, 1930 – FM (T)

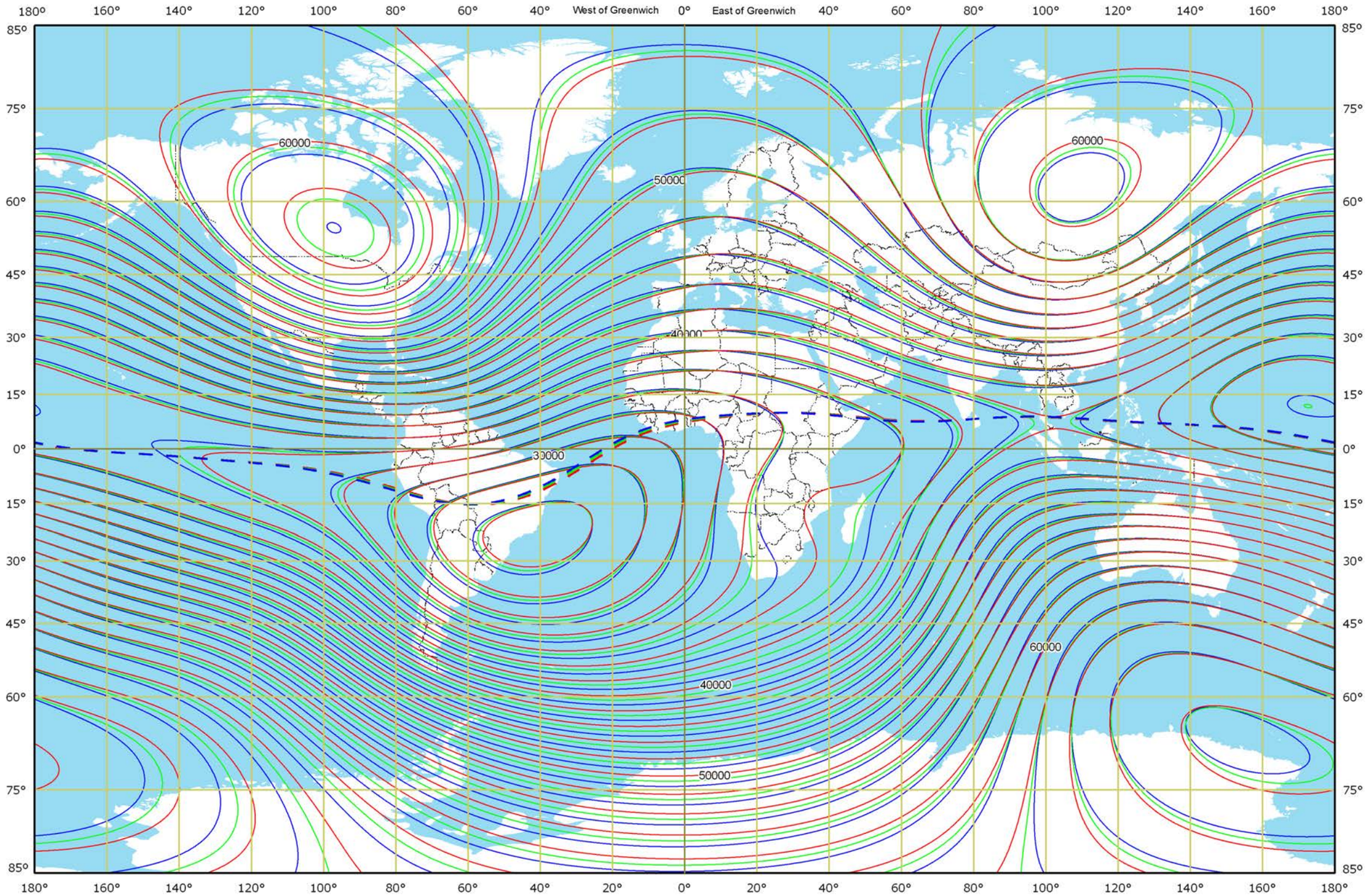

Years	Isolines	Geomagnetic equators
1920		1920
1925		1925
1930		1930

Example of magnetic total intensity value, nT

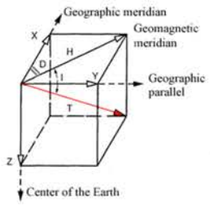

MGMF vector components

D Declination
I Inclination
H Horizontal component
T Total intensity
X North component
Y East component
Z Vertical component

Scale 1: 120 000 000

Projection: Miller cylindrical

MGMF TOTAL INTENSITY

MGMF– 1930, 1935, 1940 – FM (T)

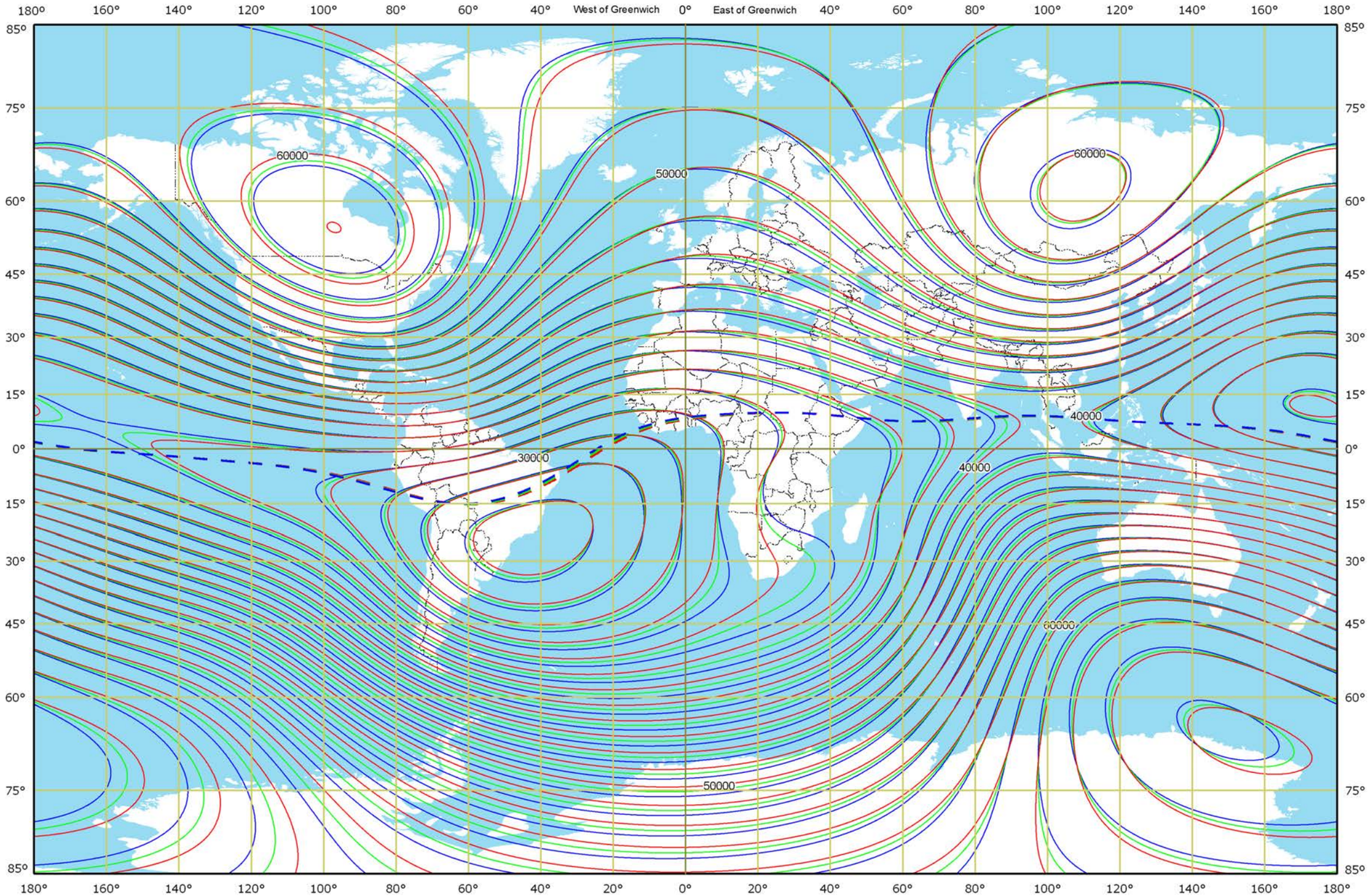

Years	Isolines	Geomagnetic equators
1930		1930
1935		1935
1940		1940

Example of magnetic total intensity value, nT

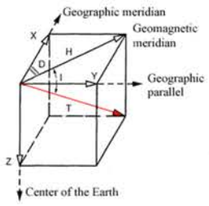

MGMF vector components

D Declination
I Inclination
H Horizontal component
T Total intensity
X North component
Y East component
Z Vertical component

Scale 1: 120 000 000

Projection: Miller cylindrical

MGMF TOTAL INTENSITY

MGMF– 1940, 1945, 1950 – FM (T)

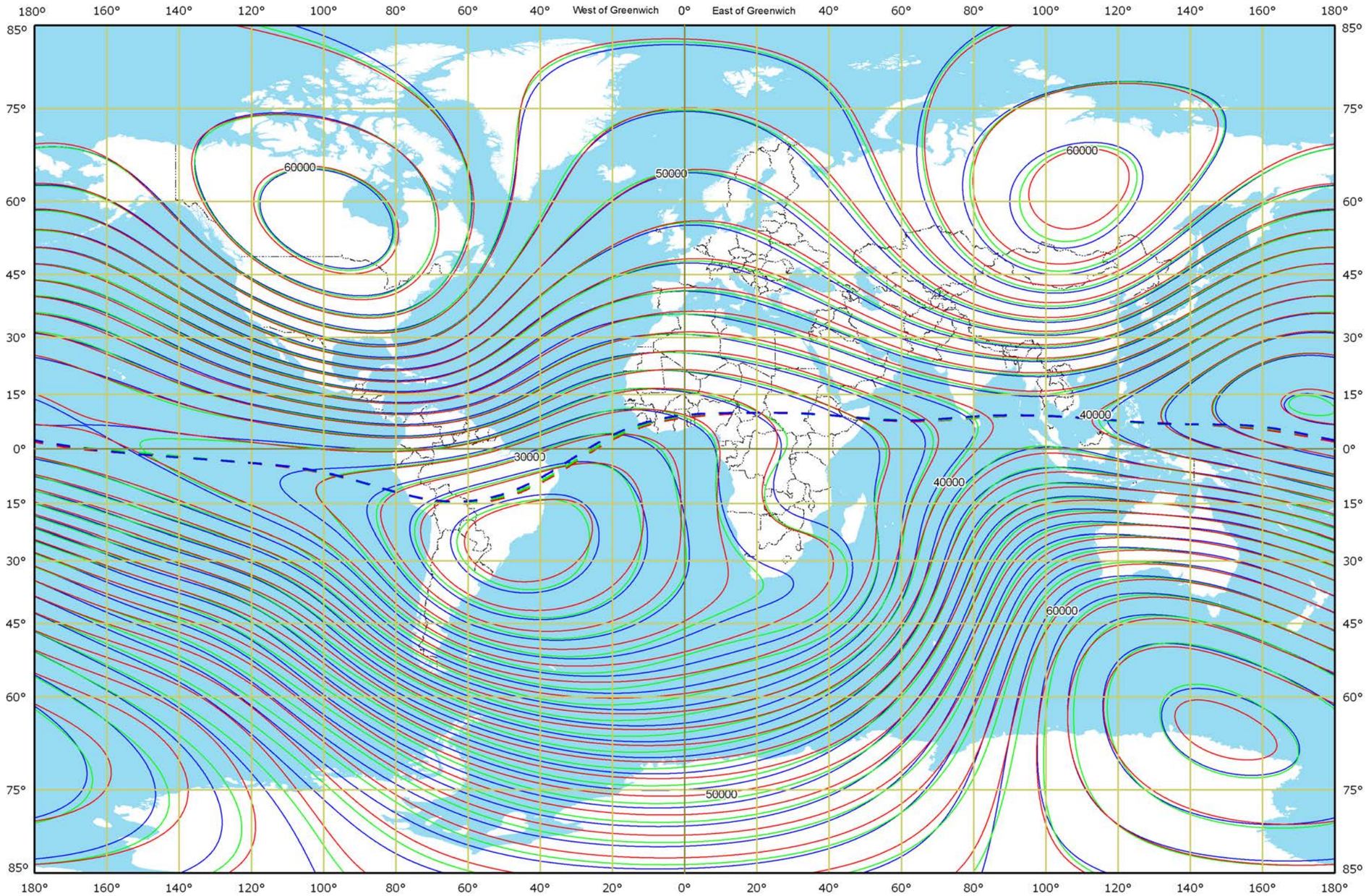

Years	Isolines	Geomagnetic equators
1940		1940
1945		1945
1950		1950

Example of magnetic total intensity value, nT

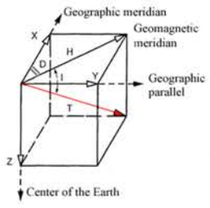

MGMF vector components

D Declination
I Inclination
H Horizontal component
T Total intensity
X North component
Y East component
Z Vertical component

Scale 1: 120 000 000

Projection: Miller cylindrical

MGMF TOTAL INTENSITY

MGMF– 1950, 1955, 1960 – FM (T)

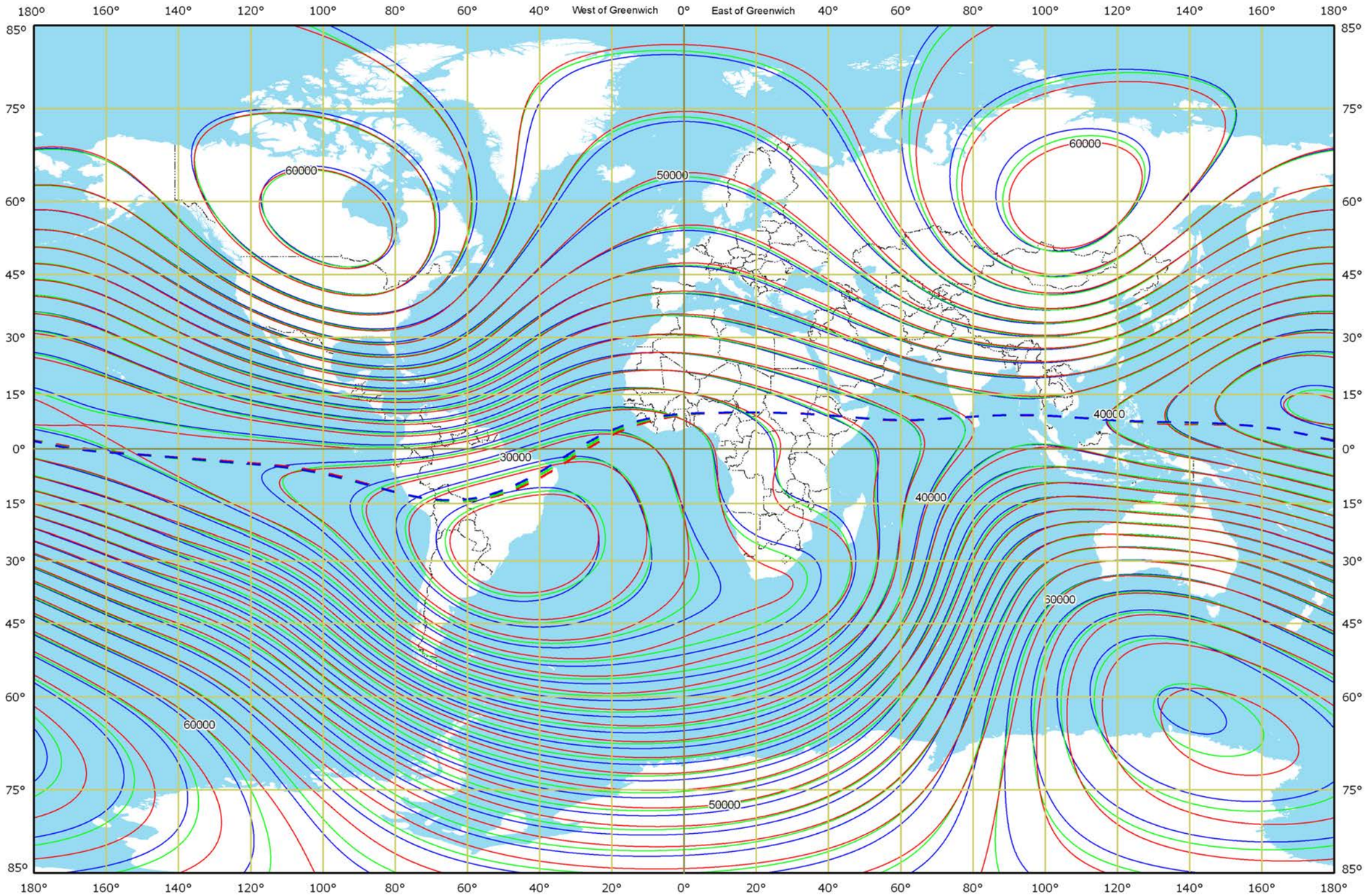

Years	Isolines	Geomagnetic equators
1950		1950
1955		1955
1960		1960

Example of magnetic total intensity value, nT

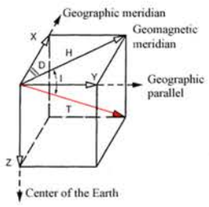

MGMF vector components

D Declination
I Inclination
H Horizontal component
T Total intensity
X North component
Y East component
Z Vertical component

Scale 1: 120 000 000

Projection: Miller cylindrical

MGMF TOTAL INTENSITY

MGMF– 1960, 1965, 1970 – FM (T)

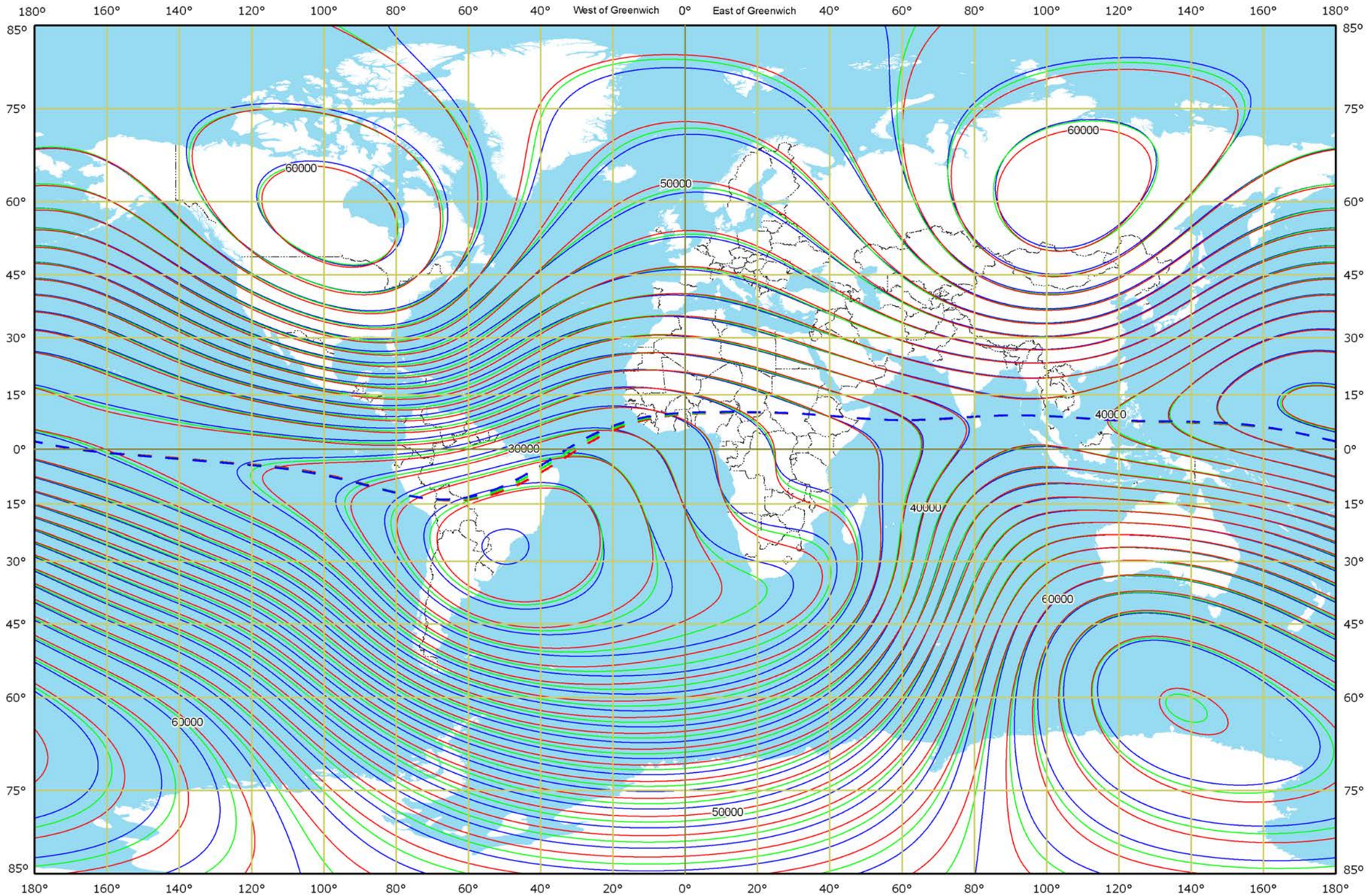

Years	Isolines	Geomagnetic equators
1960		1960
1965		1965
1970		1970

Example of magnetic total intensity value, nT

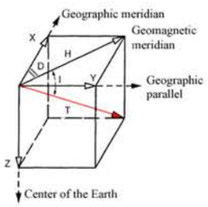

MGMF vector components

D Declination
I Inclination
H Horizontal component
T Total intensity
X North component
Y East component
Z Vertical component

Scale 1: 120 000 000

Projection: Miller cylindrical

MGMF TOTAL INTENSITY

MGMF– 1970, 1975, 1980 – FM (T)

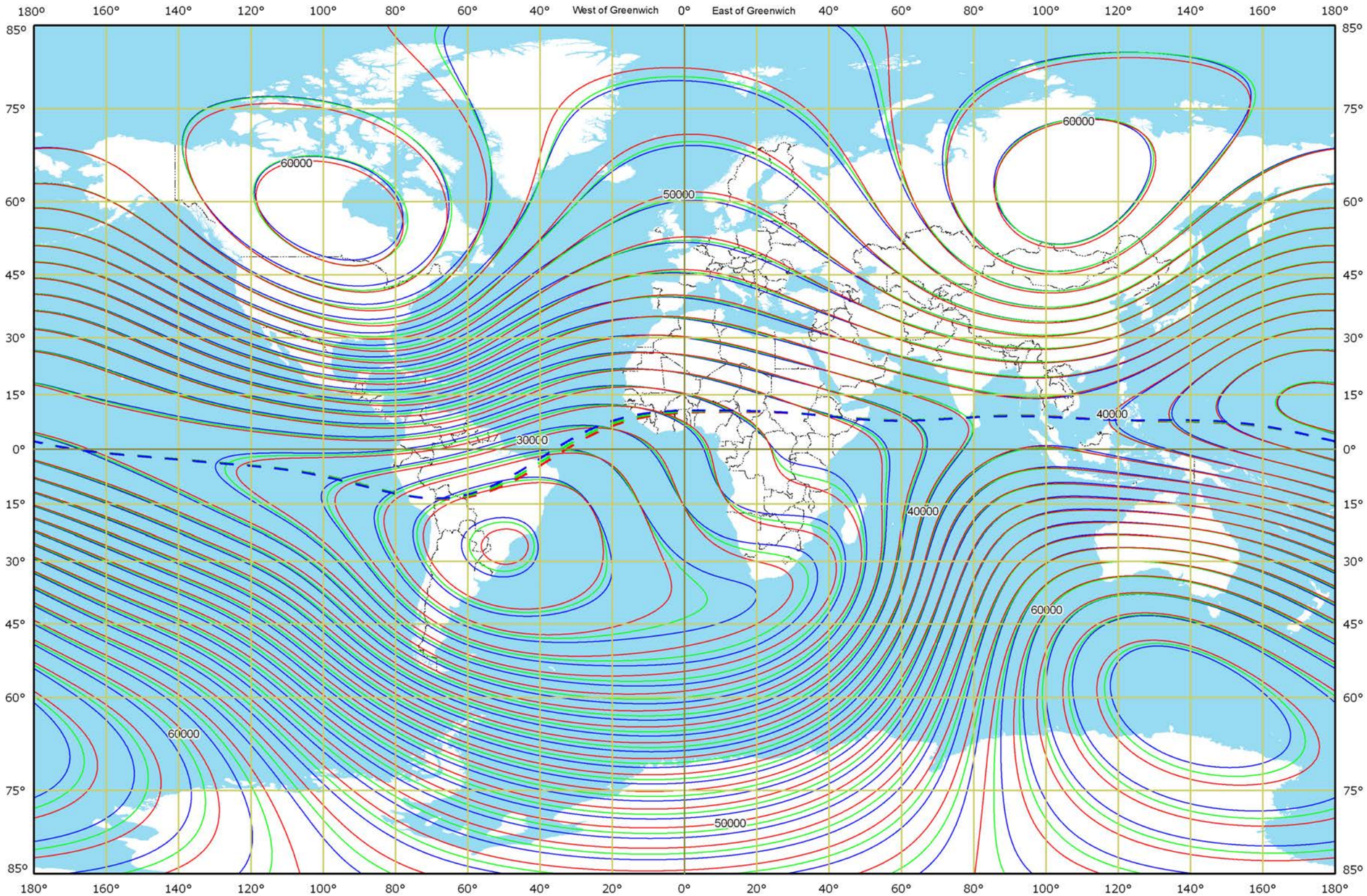

Years	Isolines	Geomagnetic equators
1970		1970
1975		1975
1980		1980

Example of magnetic total intensity value, nT

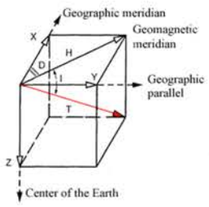

MGMF vector components

D Declination
I Inclination
H Horizontal component
T Total intensity
X North component
Y East component
Z Vertical component

Scale 1: 120 000 000

Projection: Miller cylindrical

MGMF TOTAL INTENSITY

MGMF– 1980, 1985, 1990 – FM (T)

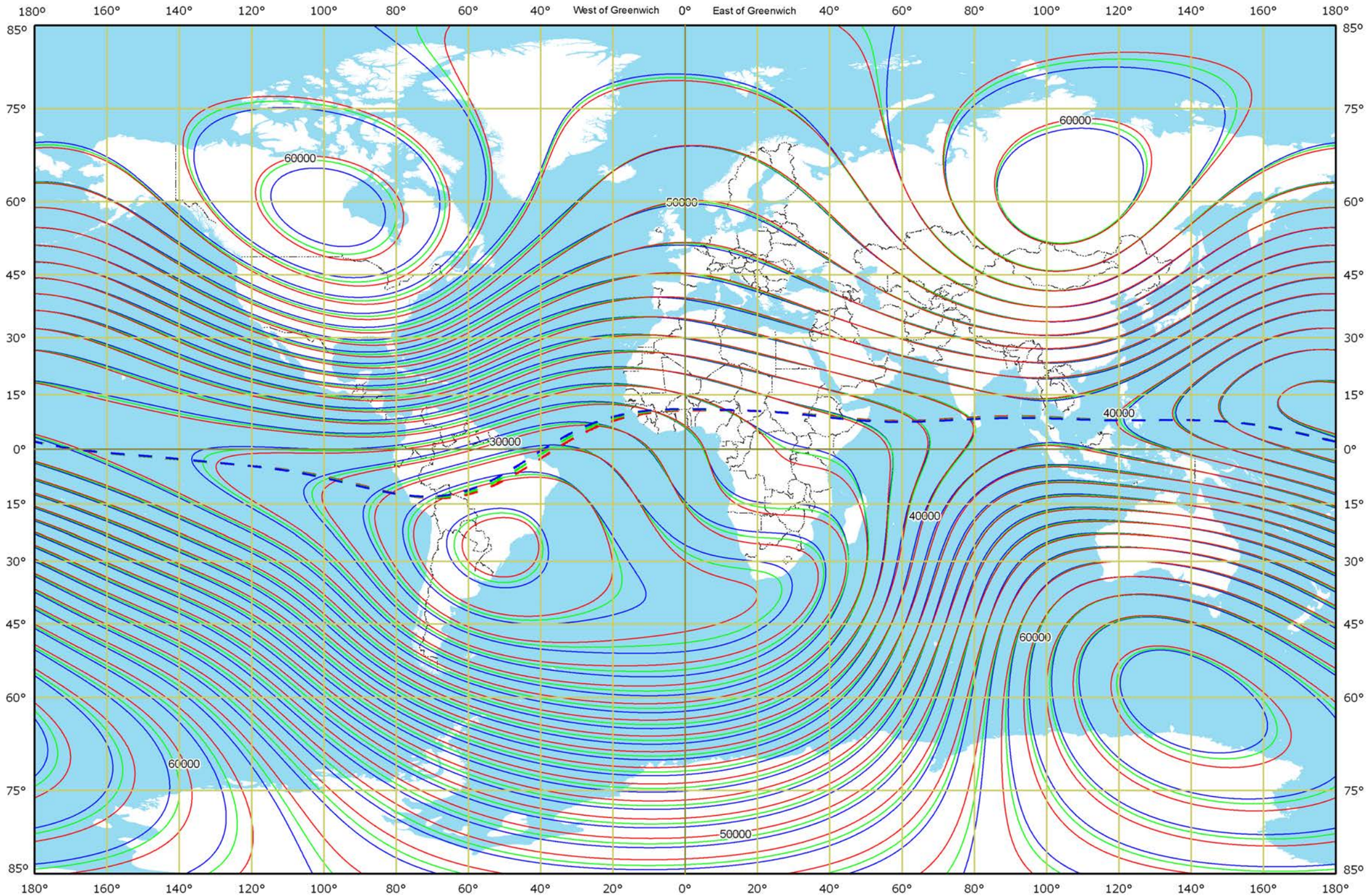

Years	Isolines	Geomagnetic equators
1980		1980
1985		1985
1990		1990

Example of magnetic total intensity value, nT

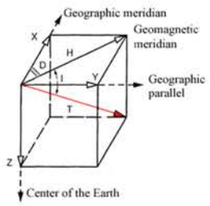

MGMF vector components

D Declination
I Inclination
H Horizontal component
T Total intensity
X North component
Y East component
Z Vertical component

Scale 1: 120 000 000

Projection: Miller cylindrical

MGMF TOTAL INTENSITY

MGMF– 1990, 1995, 2000 – FM (T)

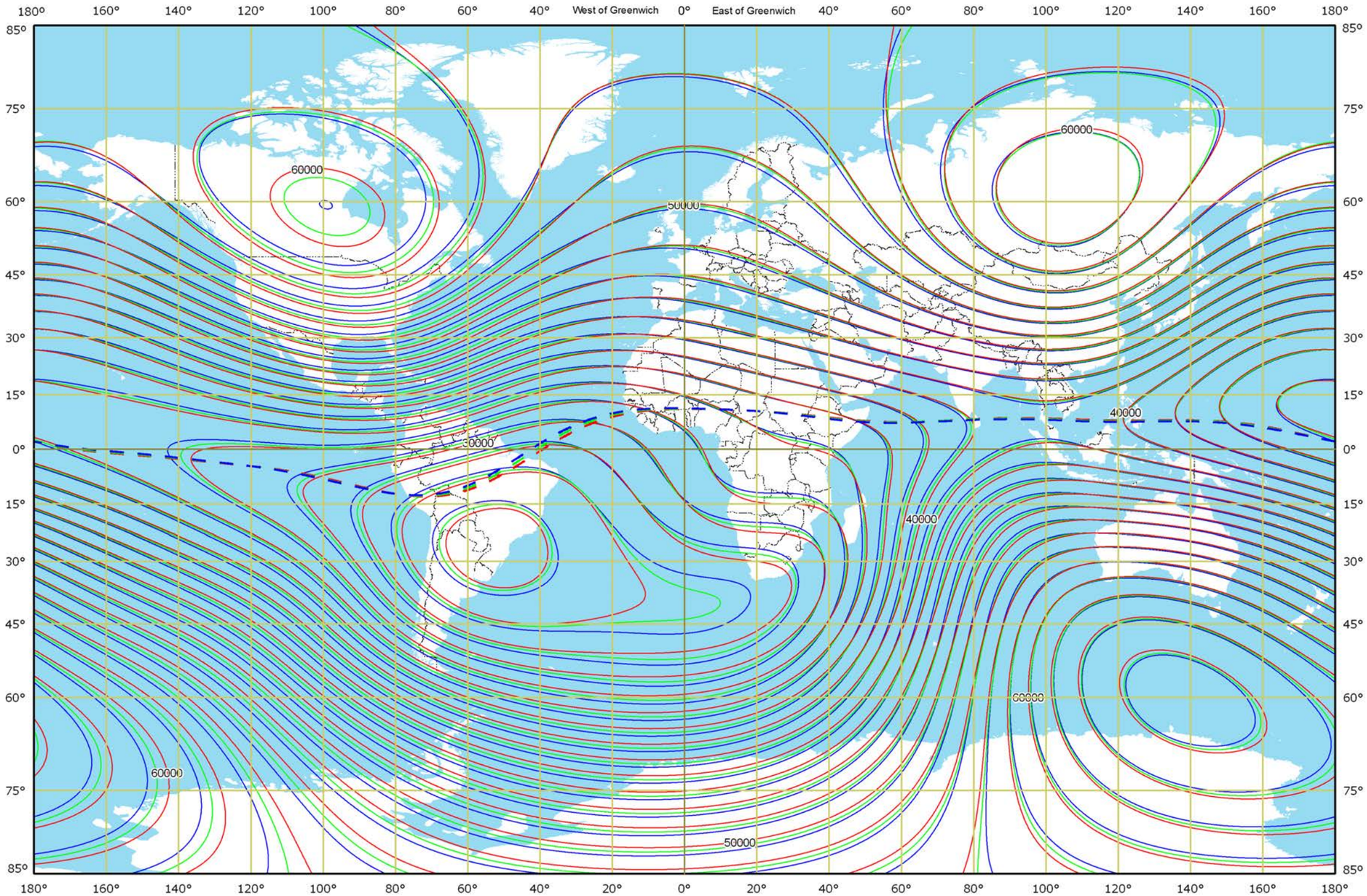

Years	Isolines	Geomagnetic equators
1990		1990
1995		1995
2000		2000

Example of magnetic total intensity value, nT

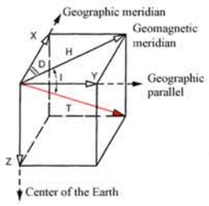

MGMF vector components

D Declination
I Inclination
H Horizontal component
T Total intensity
X North component
Y East component
Z Vertical component

Scale 1: 120 000 000

Projection: Miller cylindrical

MGMF TOTAL INTENSITY

MGMF – 2000, 2005, 2010 – FM (T)

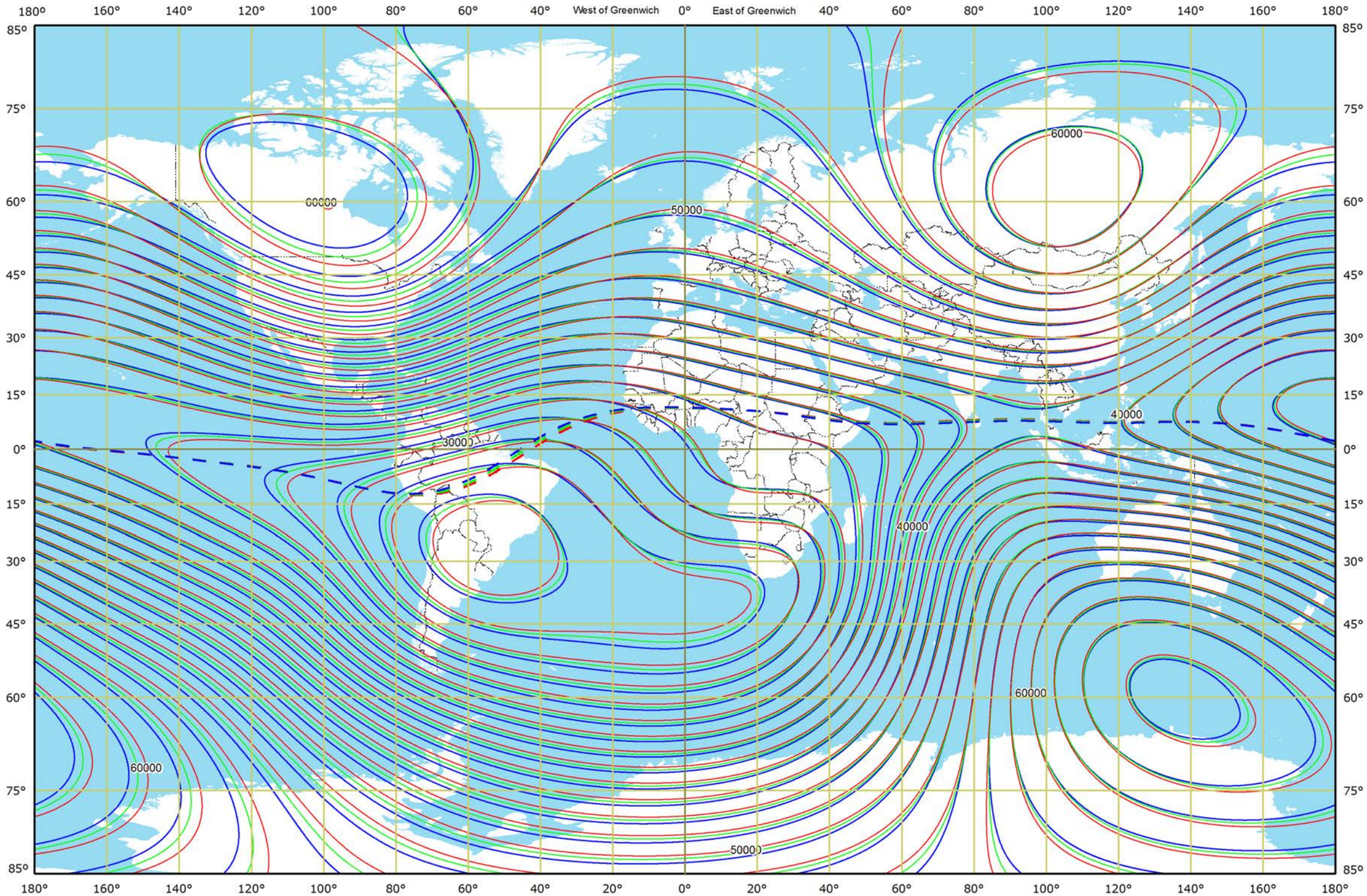

Years	Isolines	Geomagnetic equators
2000		2000
2005		2005
2010		2010

Example of magnetic total intensity value, nT

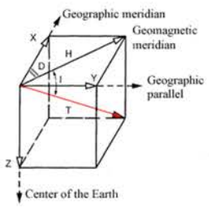

MGMF vector components

D Declination
I Inclination
H Horizontal component
T Total intensity
X North component
Y East component
Z Vertical component

Scale 1: 120 000 000

Projection: Miller cylindrical

MGMF DECLINATION

MGMF – 1500, 1525, 1550 – D

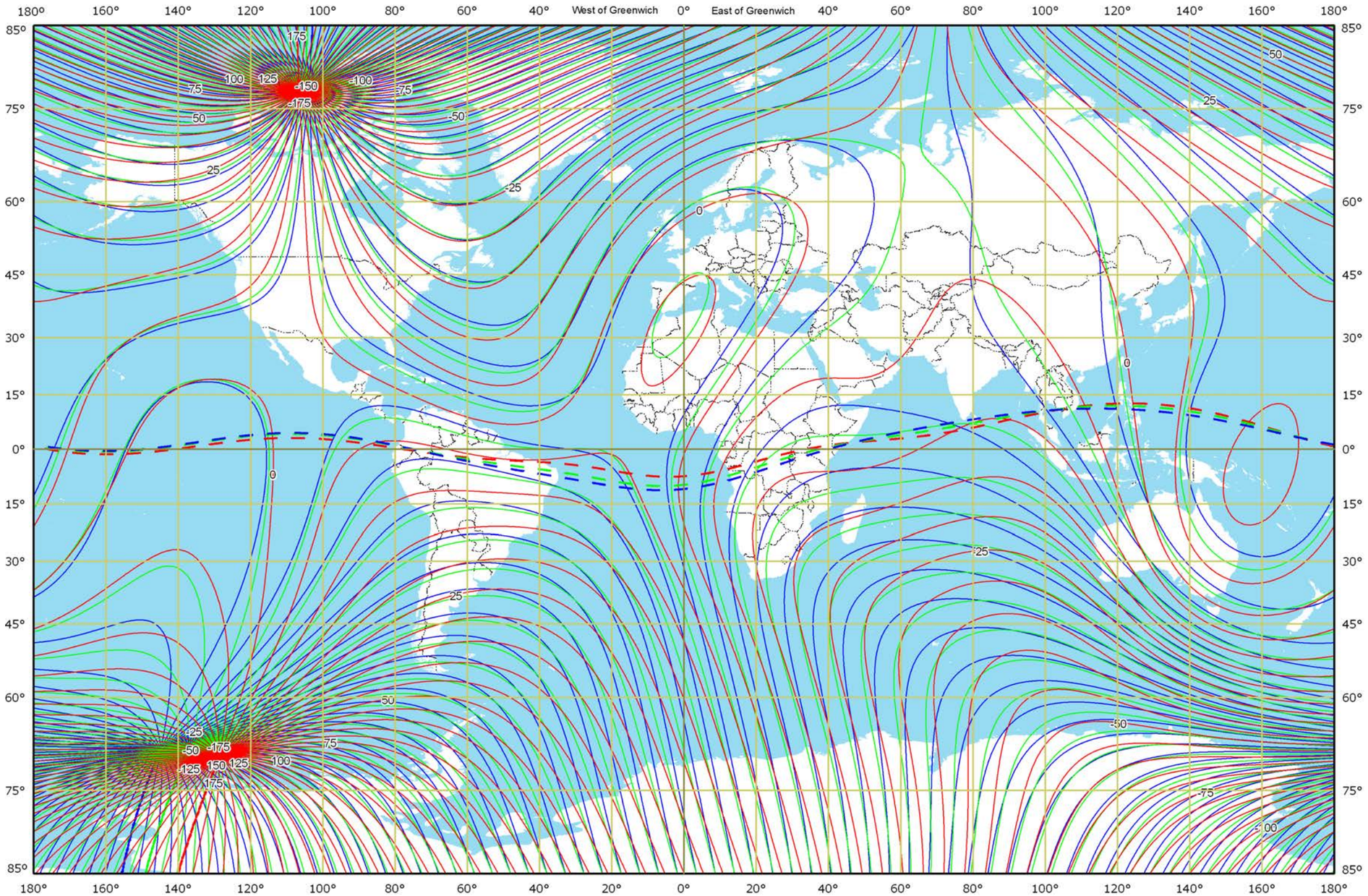

Years	Isogons	Geomagnetic equators
1500		1500
1525		1525
1550		1550

Example of magnetic declination value, degree

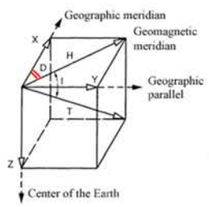

MGMF vector components

D Declination
I Inclination
H Horizontal component
T Total intensity
X North component
Y East component
Z Vertical component

Scale 1: 120 000 000

Projection: Miller cylindrical

MGMF DECLINATION

MGMF – 1550, 1575, 1600 – D

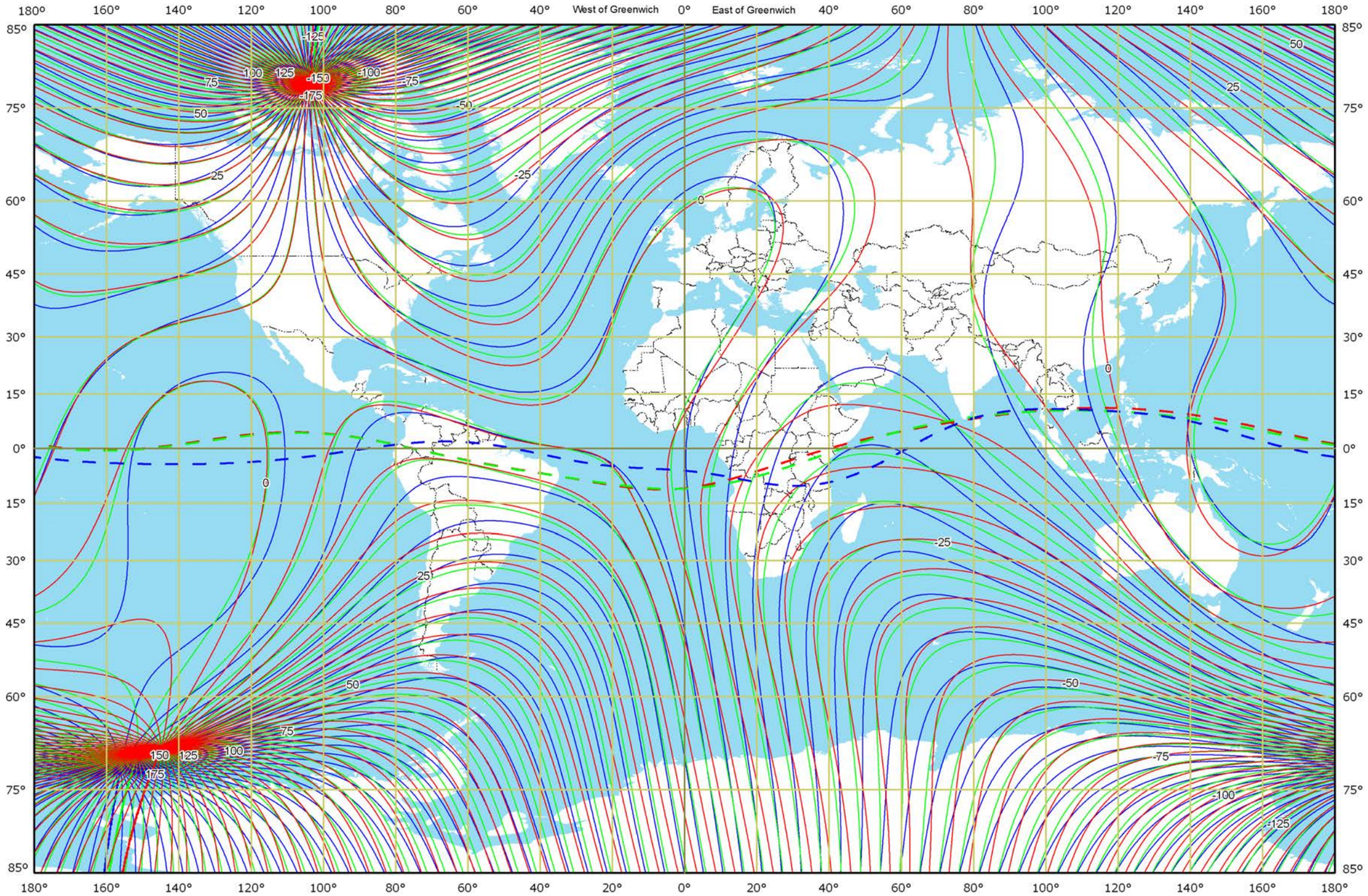

Years	Isogons	Geomagnetic equators
1550		1550
1575		1575
1600		1600

Example of magnetic declination value, degree

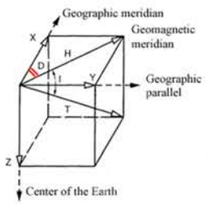

MGMF vector components

D Declination
I Inclination
H Horizontal component
T Total intensity
X North component
Y East component
Z Vertical component

Scale 1: 120 000 000

Projection: Miller cylindrical

MGMF DECLINATION

MGMF – 1600, 1625, 1650 – D

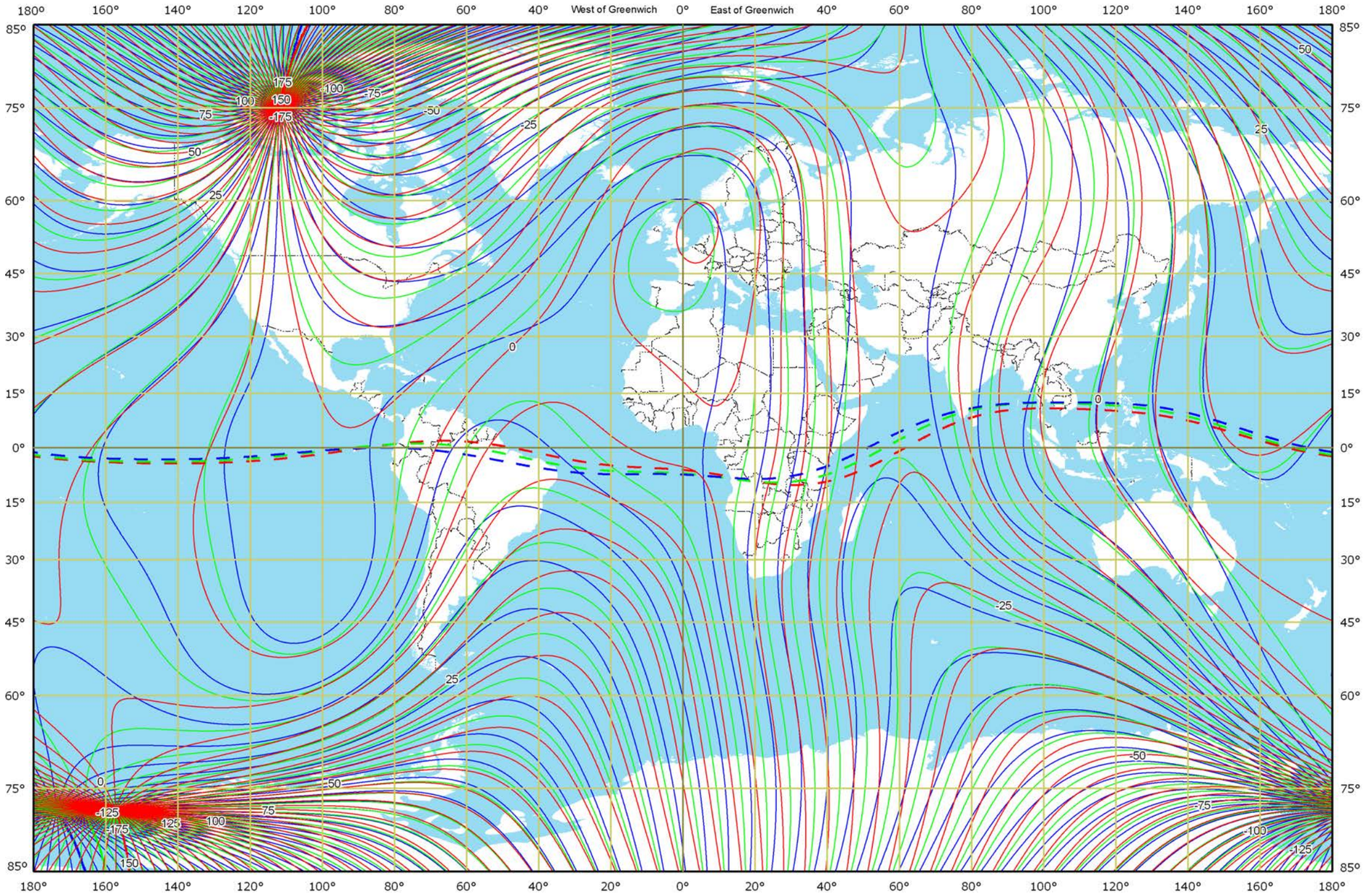

Years	Isogons	Geomagnetic equators
1600		1600
1625		1625
1650		1650

Example of magnetic declination value, degree

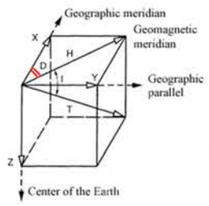

MGMF vector components

D Declination
I Inclination
H Horizontal component
T Total intensity
X North component
Y East component
Z Vertical component

Scale 1: 120 000 000

Projection: Miller cylindrical

MGMF DECLINATION

MGMF – 1650, 1675, 1700 – D

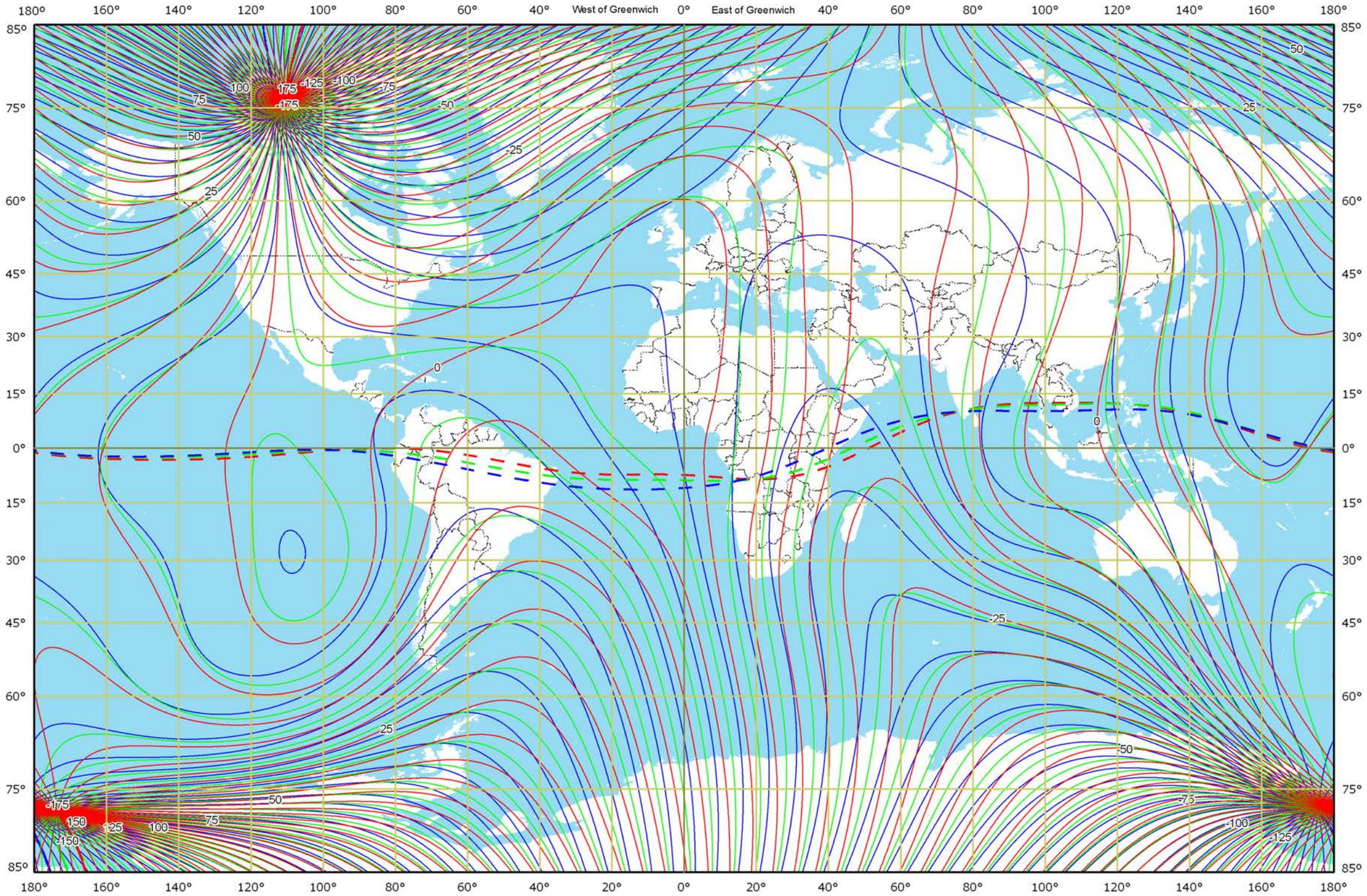

Years	Isogons	Geomagnetic equators
1650		1650
1675		1675
1700		1700

Example of magnetic declination value, degree

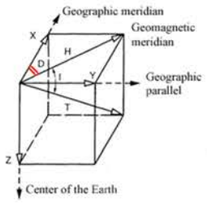

MGMF vector components

D Declination
I Inclination
H Horizontal component
T Total intensity
X North component
Y East component
Z Vertical component

Scale 1: 120 000 000

Projection: Miller cylindrical

MGMF DECLINATION

MGMF – 1700, 1725, 1750 – D

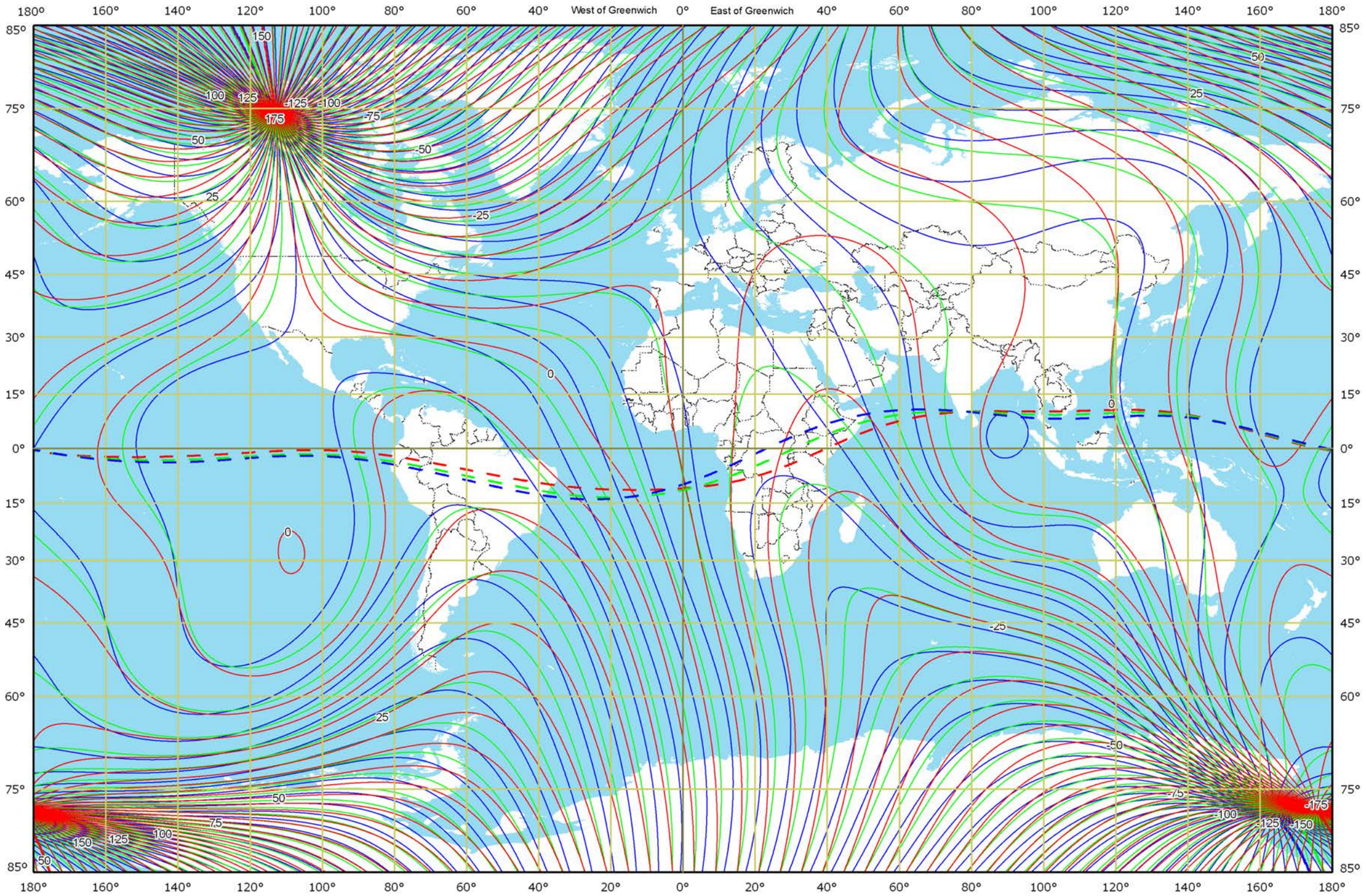

Years	Isogons	Geomagnetic equators
1700		1700
1725		1725
1750		1750

Example of magnetic declination value, degree

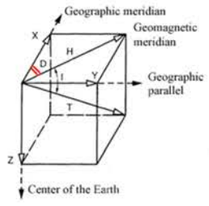

MGMF vector components

D Declination
I Inclination
H Horizontal component
T Total intensity
X North component
Y East component
Z Vertical component

Scale 1: 120 000 000

Projection: Miller cylindrical

MGMF DECLINATION

MGMF – 1750, 1775, 1800 – D

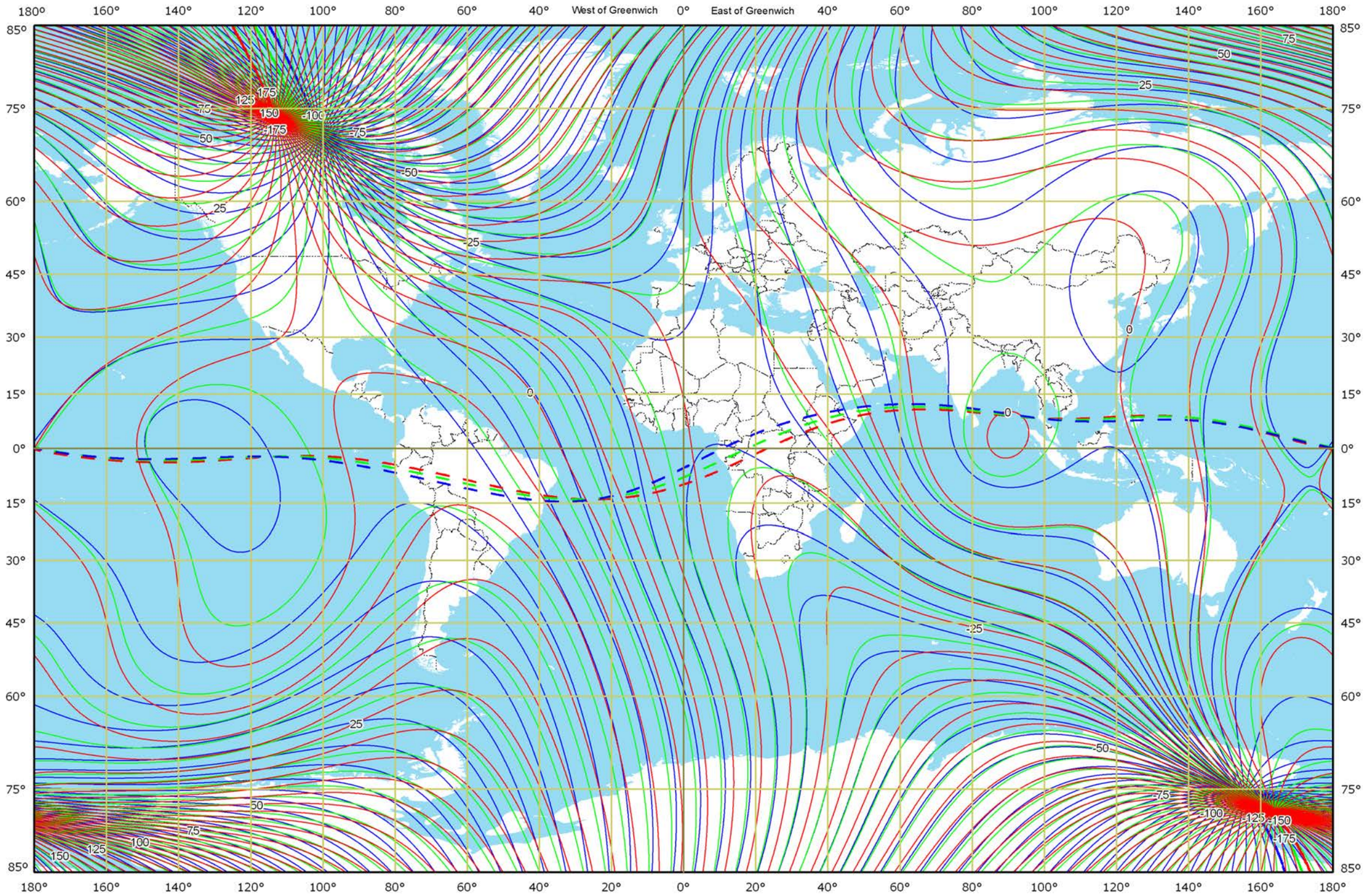

Years	Isogons	Geomagnetic equators
1750		1750
1775		1775
1800		1800

Example of magnetic declination value, degree

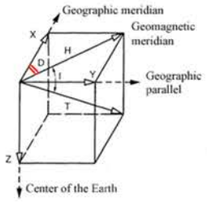

MGMF vector components

D Declination
I Inclination
H Horizontal component
T Total intensity
X North component
Y East component
Z Vertical component

Scale 1: 120 000 000

Projection: Miller cylindrical

MGMF DECLINATION

MGMF – 1800, 1825, 1850 – D

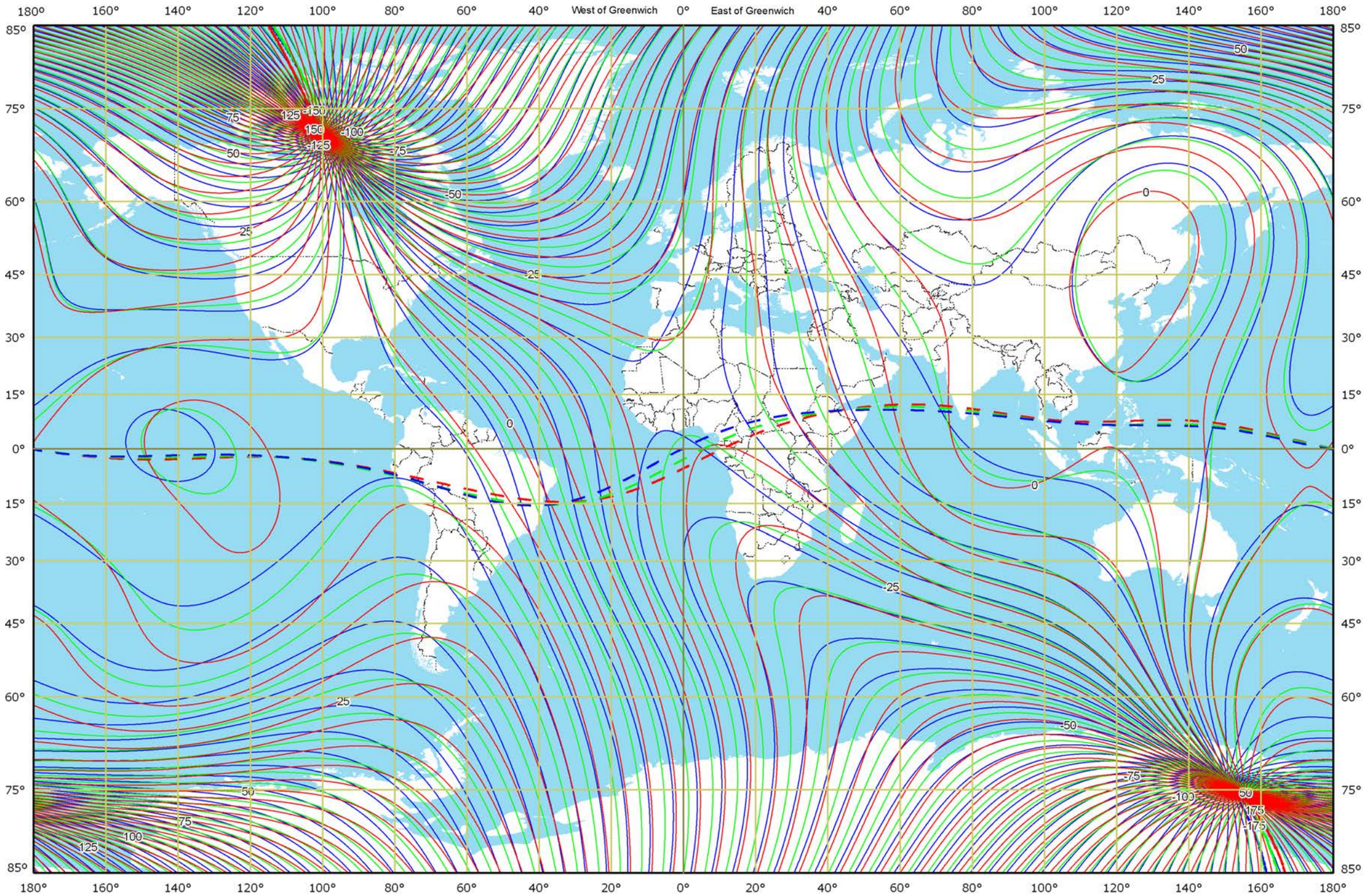

Years	Isogons	Geomagnetic equators
1800		1800
1825		1825
1850		1850

Example of magnetic declination value, degree

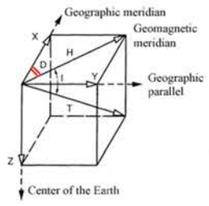

MGMF vector components

D Declination
I Inclination
H Horizontal component
T Total intensity
X North component
Y East component
Z Vertical component

Scale 1: 120 000 000

Projection: Miller cylindrical

MGMF DECLINATION

MGMF – 1850, 1875, 1900 – D

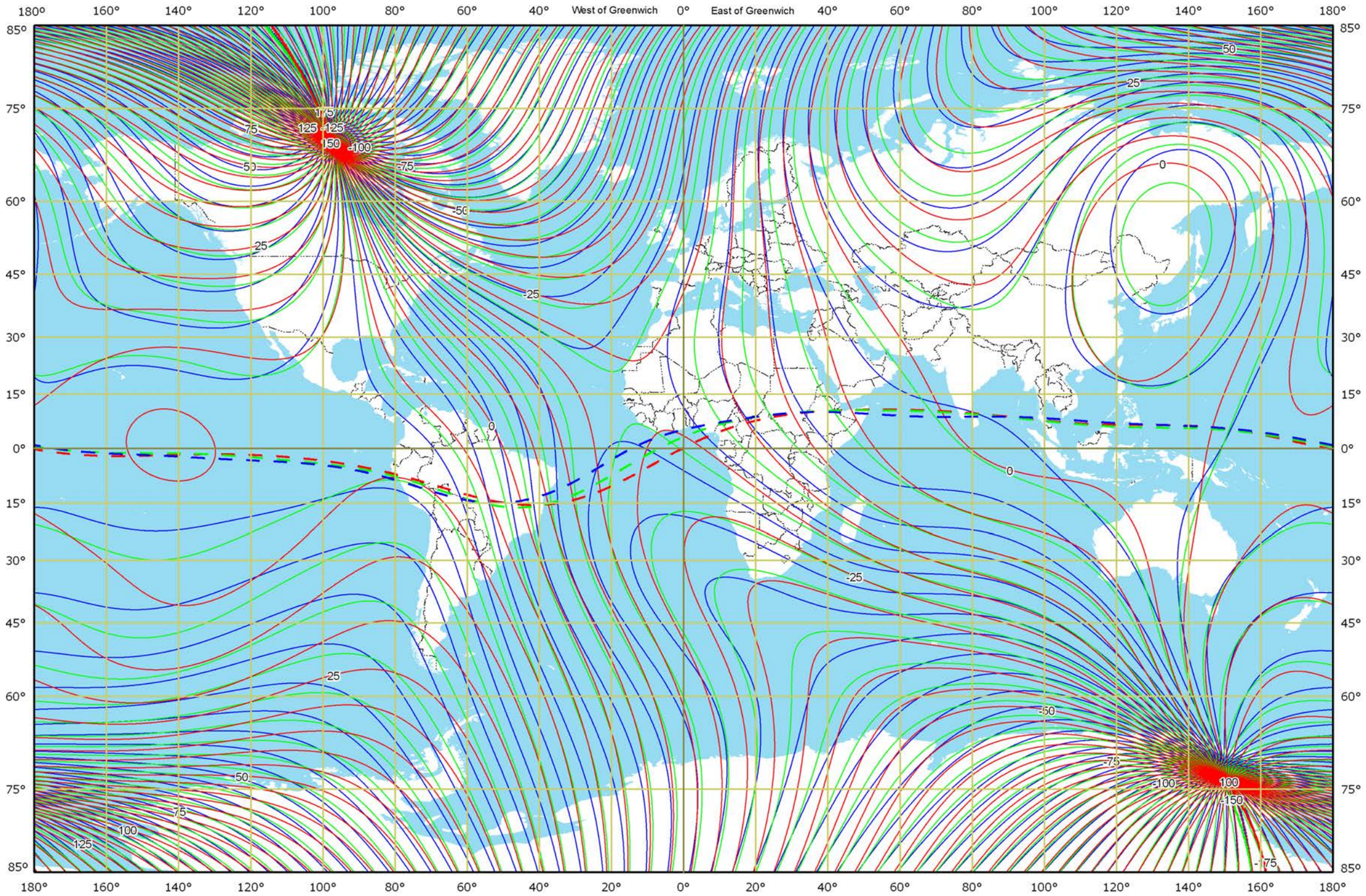

Years	Isogons	Geomagnetic equators
1850		1850
1875		1875
1900		1900

Example of magnetic declination value, degree

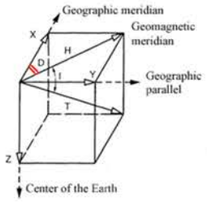

MGMF vector components

D Declination
I Inclination
H Horizontal component
T Total intensity
X North component
Y East component
Z Vertical component

Scale 1: 120 000 000

Projection: Miller cylindrical

MGMF INCLINATION

MGMF – 1500, 1525, 1550 – I

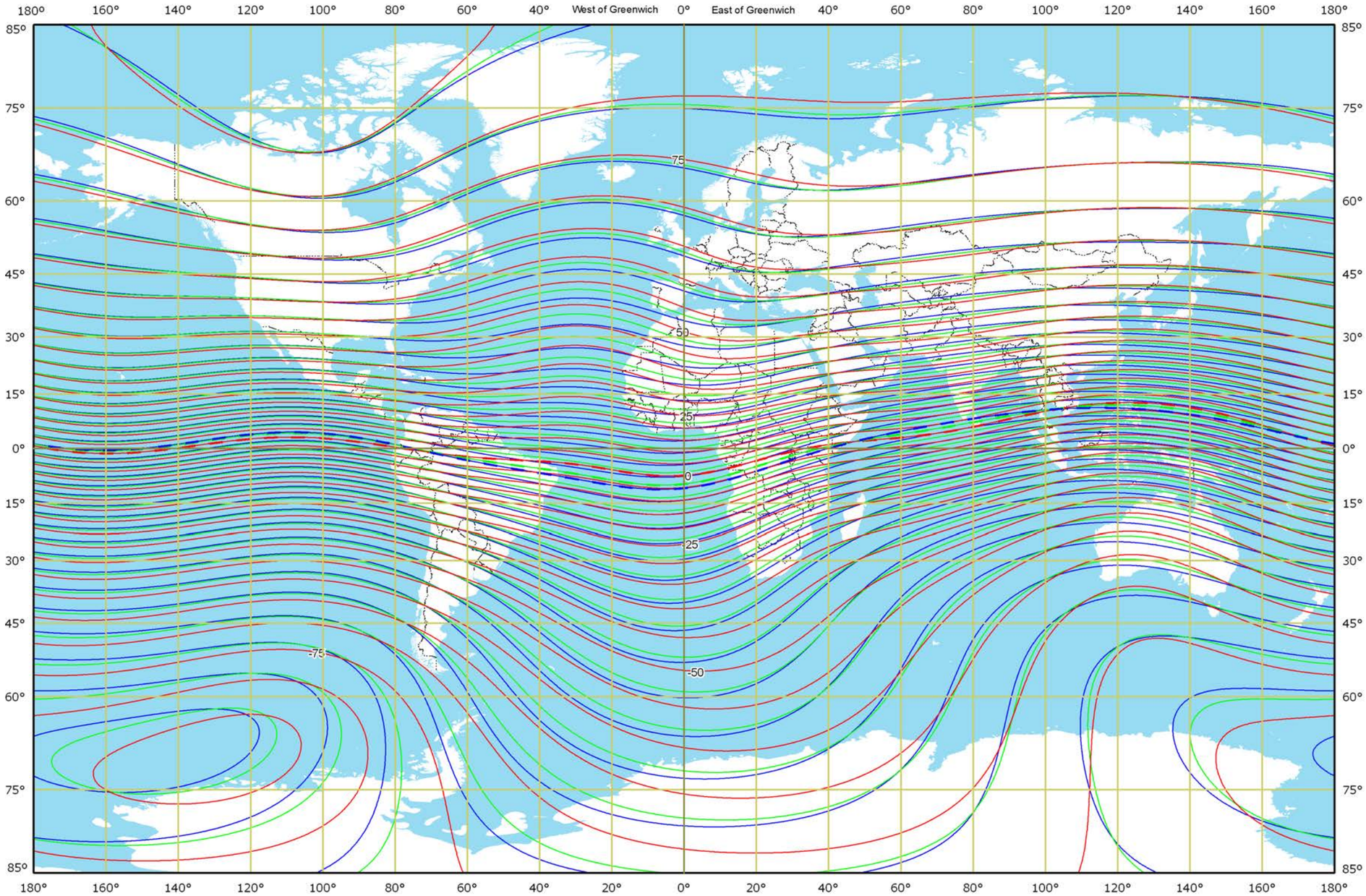

Years	Isoclines	Geomagnetic equators
1500		1500
1525		1525
1550		1550

Example of magnetic inclination value, degree

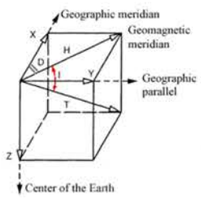

MGMF vector components

D Declination
I Inclination
H Horizontal component
T Total intensity
X North component
Y East component
Z Vertical component

Scale 1: 120 000 000

Projection: Miller cylindrical

MGMF INCLINATION

MGMF – 1550, 1575, 1600 – I

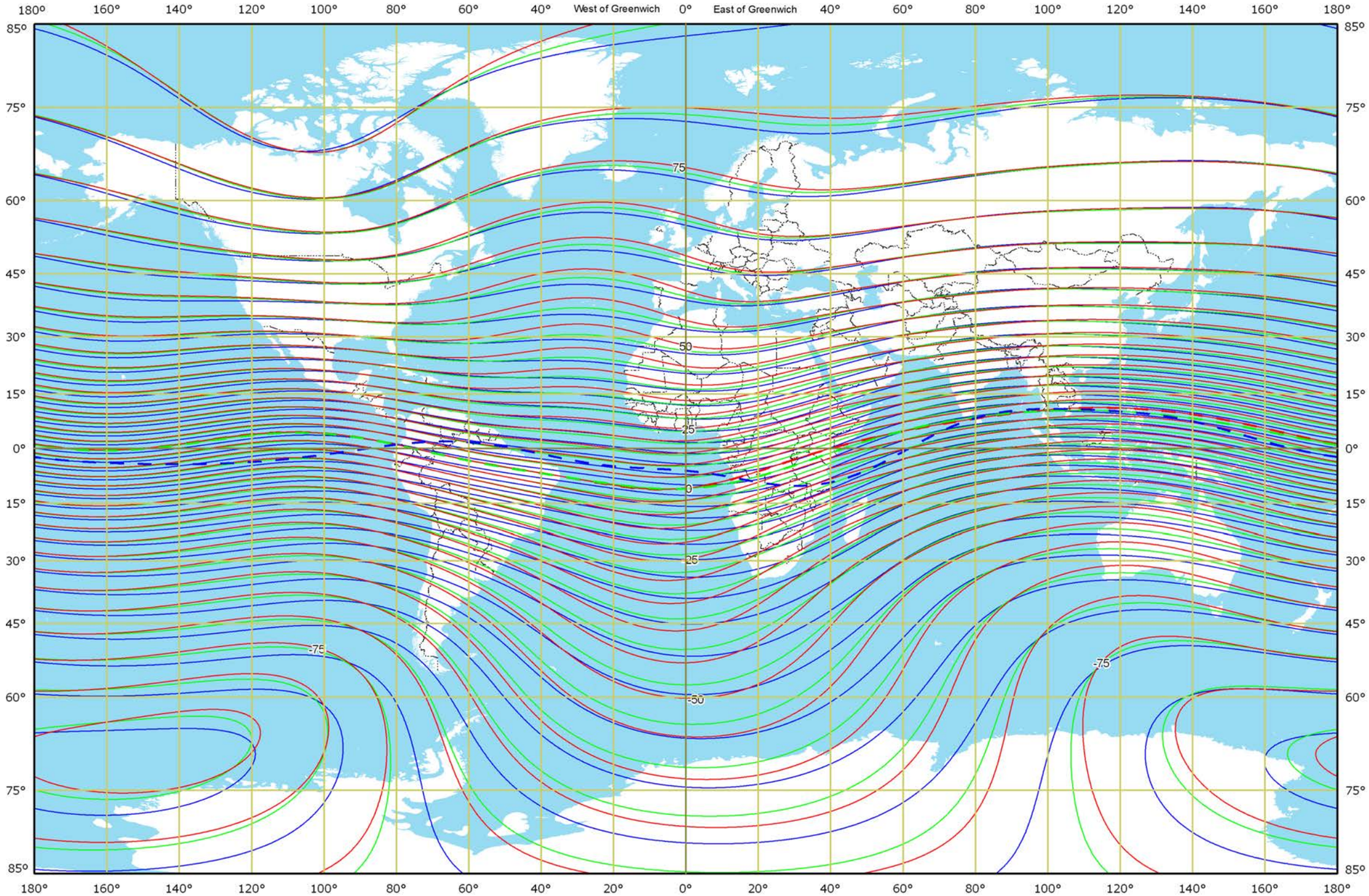

Years	Isoclines	Geomagnetic equators
1550		1550
1575		1575
1600		1600

Example of magnetic inclination value, degree

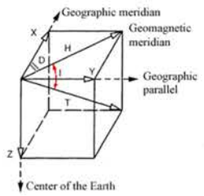

MGMF vector components

D Declination
I Inclination
H Horizontal component
T Total intensity
X North component
Y East component
Z Vertical component

Scale 1: 120 000 000

Projection: Miller cylindrical

MGMF INCLINATION

MGMF – 1600, 1625, 1650 – I

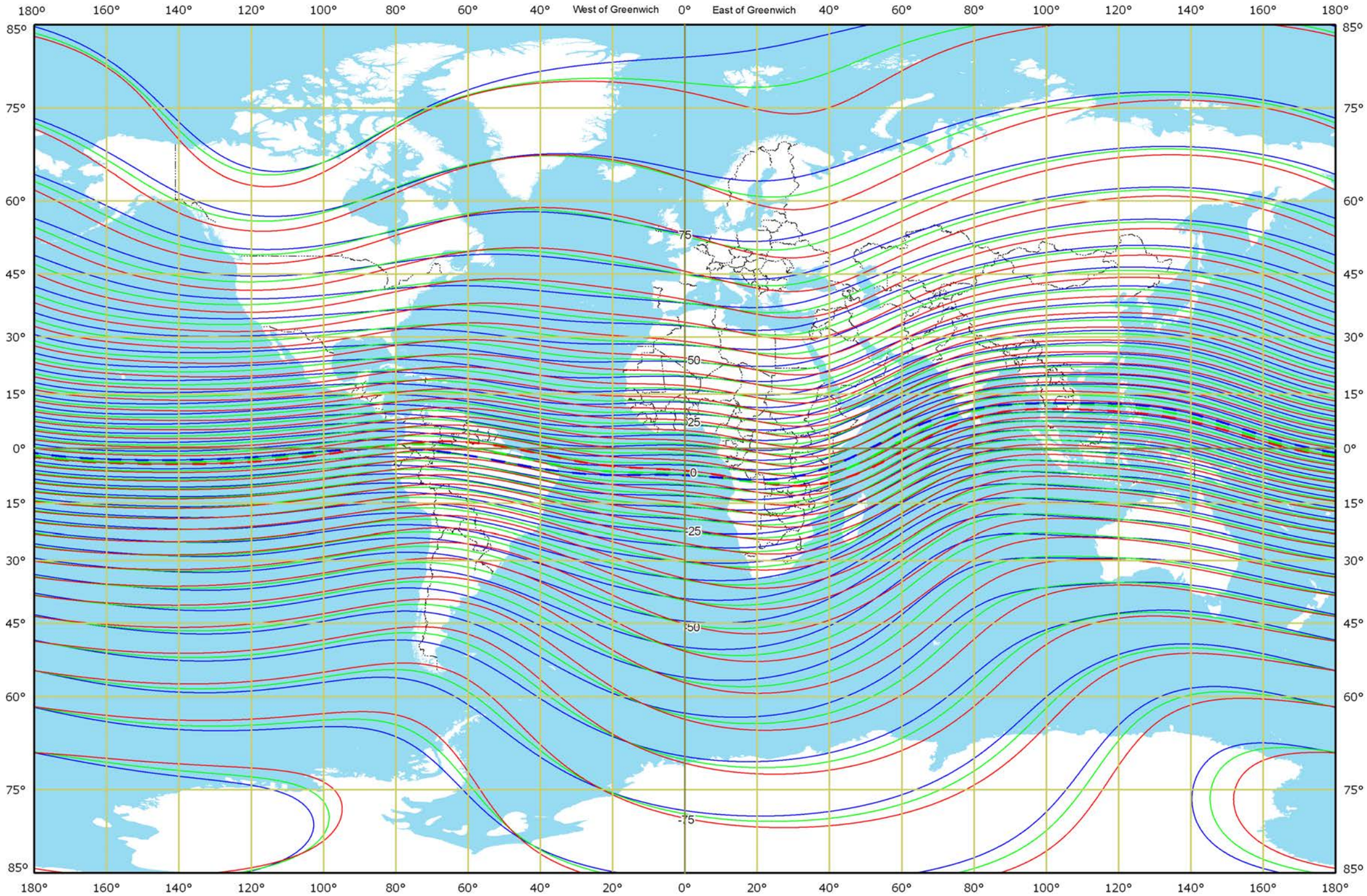

Years	Isoclines	Geomagnetic equators
1600		1600
1625		1625
1650		1650

Example of magnetic inclination value, degree

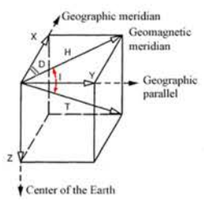

MGMF vector components

D Declination
I Inclination
H Horizontal component
T Total intensity
X North component
Y East component
Z Vertical component

Scale 1: 120 000 000

Projection: Miller cylindrical

MGMF INCLINATION

MGMF – 1650, 1675, 1700 – I

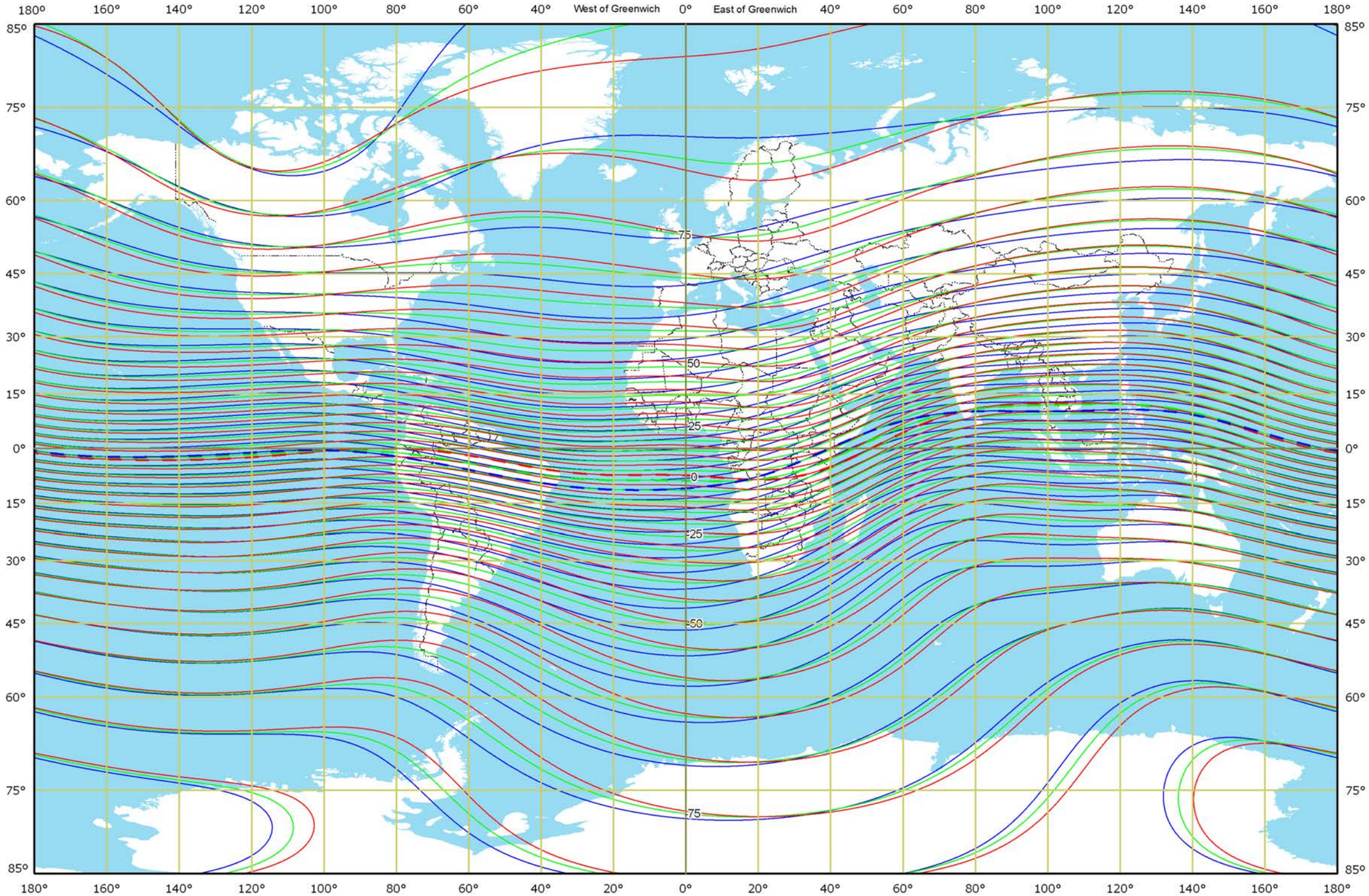

Years	Isoclines	Geomagnetic equators
1650		1650
1675		1675
1700		1700

Example of magnetic inclination value, degree

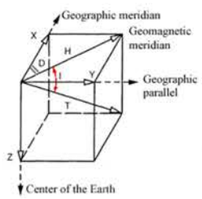

MGMF vector components

D Declination
I Inclination
H Horizontal component
T Total intensity
X North component
Y East component
Z Vertical component

Scale 1: 120 000 000

Projection: Miller cylindrical

MGMF INCLINATION

MGMF – 1700, 1725, 1750 – I

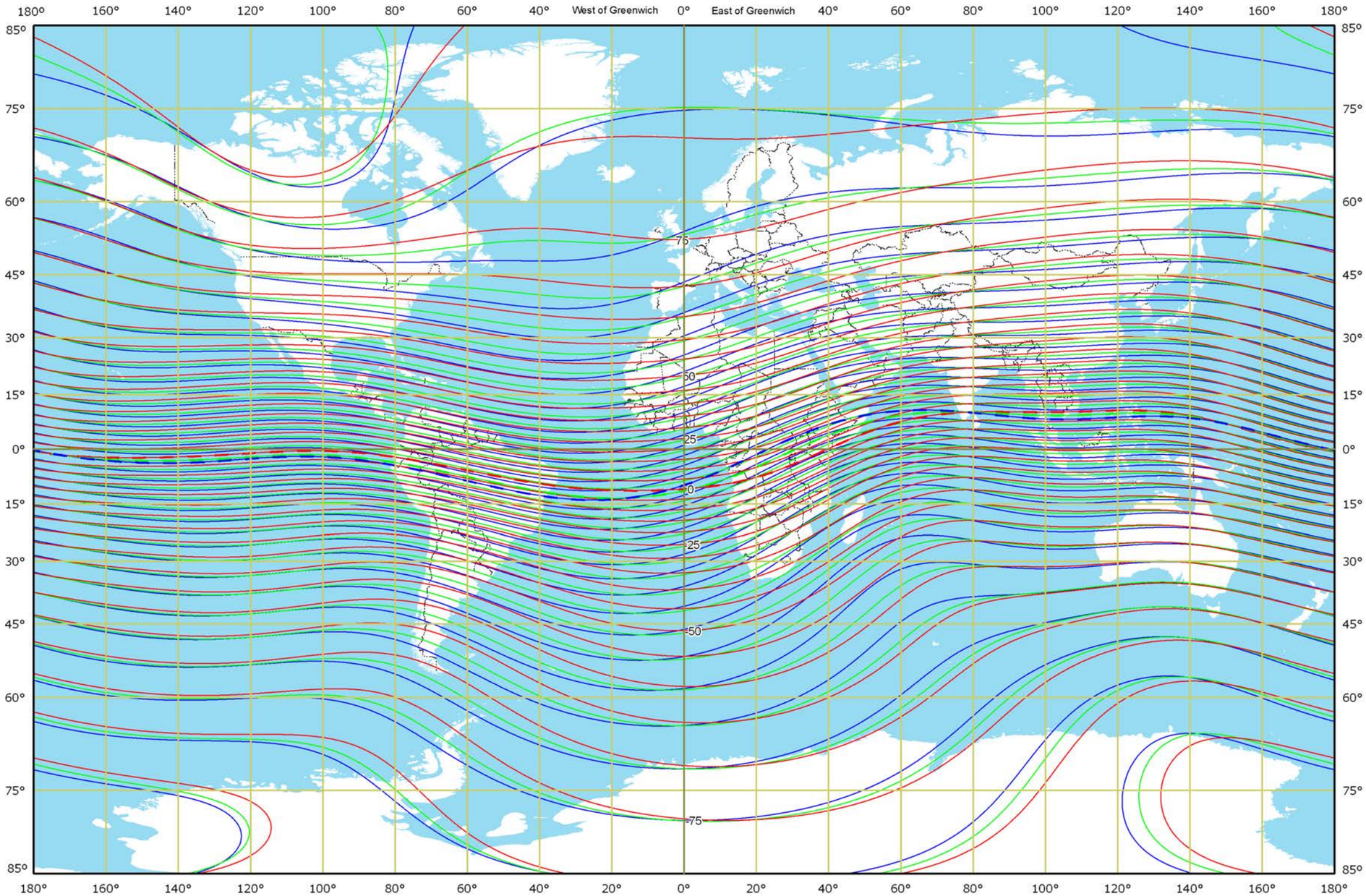

Years	Isoclines	Geomagnetic equators
1700		1700
1725		1725
1750		1750

Example of magnetic inclination value, degree

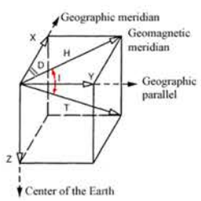

MGMF vector components

D Declination
I Inclination
H Horizontal component
T Total intensity
X North component
Y East component
Z Vertical component

Scale 1: 120 000 000

Projection: Miller cylindrical

MGMF INCLINATION

MGMF – 1750, 1775, 1800 – I

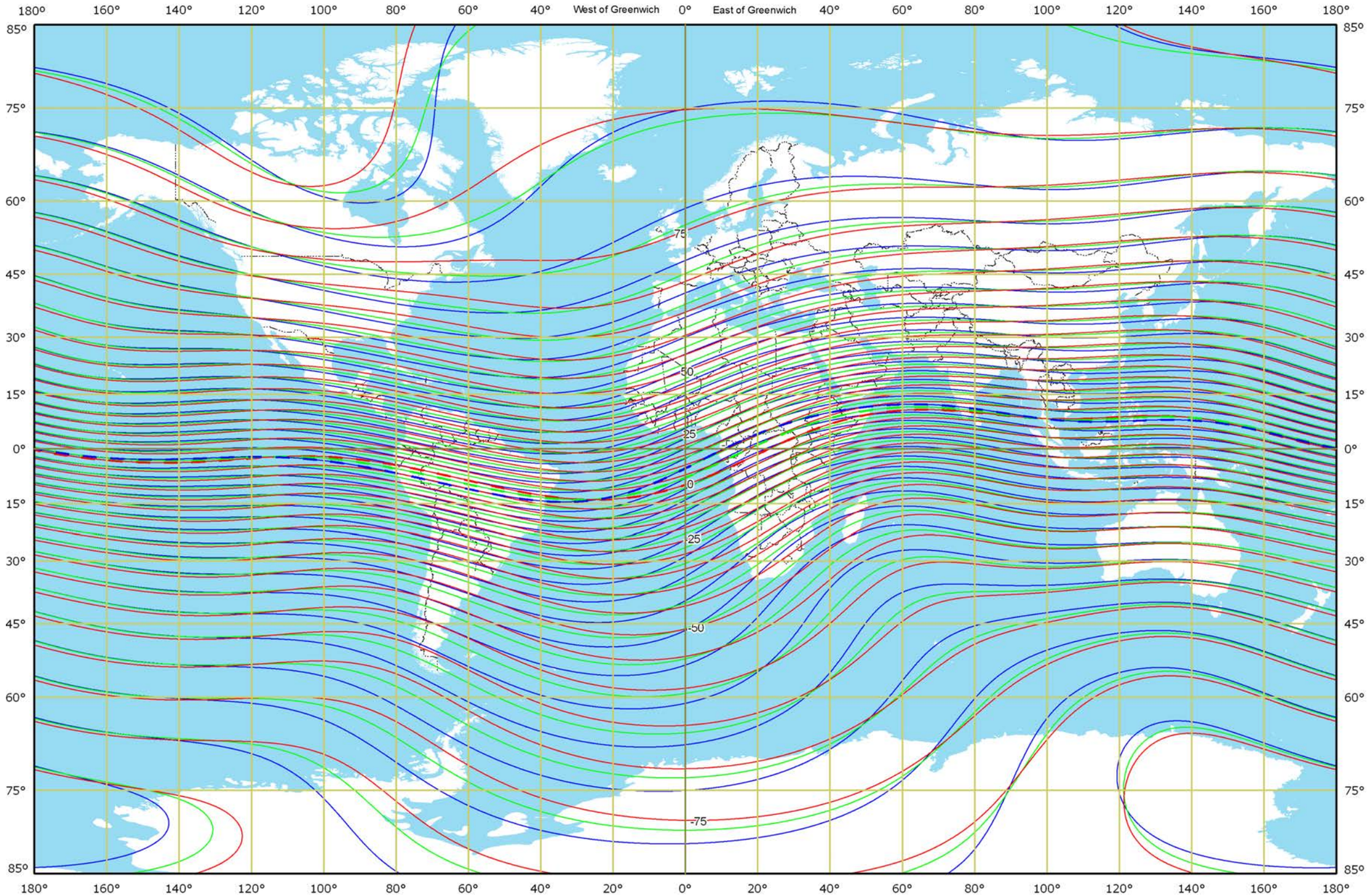

Years	Isoclines	Geomagnetic equators
1750		1750
1775		1775
1800		1800

Example of magnetic inclination value, degree

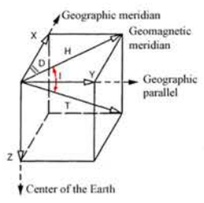

MGMF vector components

D Declination
I Inclination
H Horizontal component
T Total intensity
X North component
Y East component
Z Vertical component

Scale 1: 120 000 000

Projection: Miller cylindrical

MGMF INCLINATION

MGMF – 1800, 1825, 1850 – I

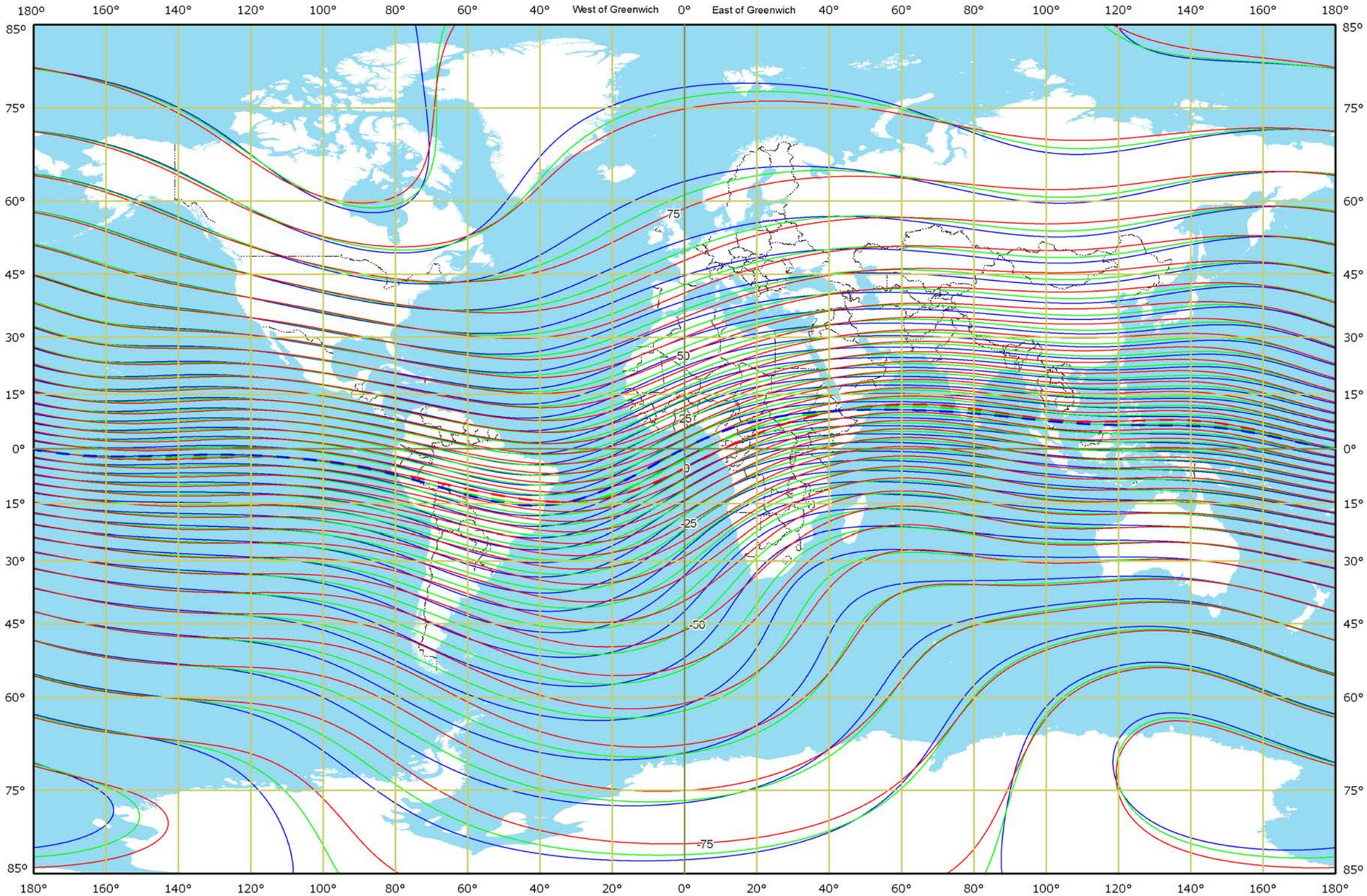

Years	Isoclines	Geomagnetic equators
1800		1800
1825		1825
1850		1850

Example of magnetic inclination value, degree

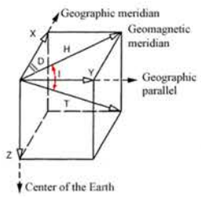

MGMF vector components

D Declination
I Inclination
H Horizontal component
T Total intensity
X North component
Y East component
Z Vertical component

Scale 1: 120 000 000

Projection: Miller cylindrical

MGMF INCLINATION

MGMF – 1850, 1875, 1900 – I

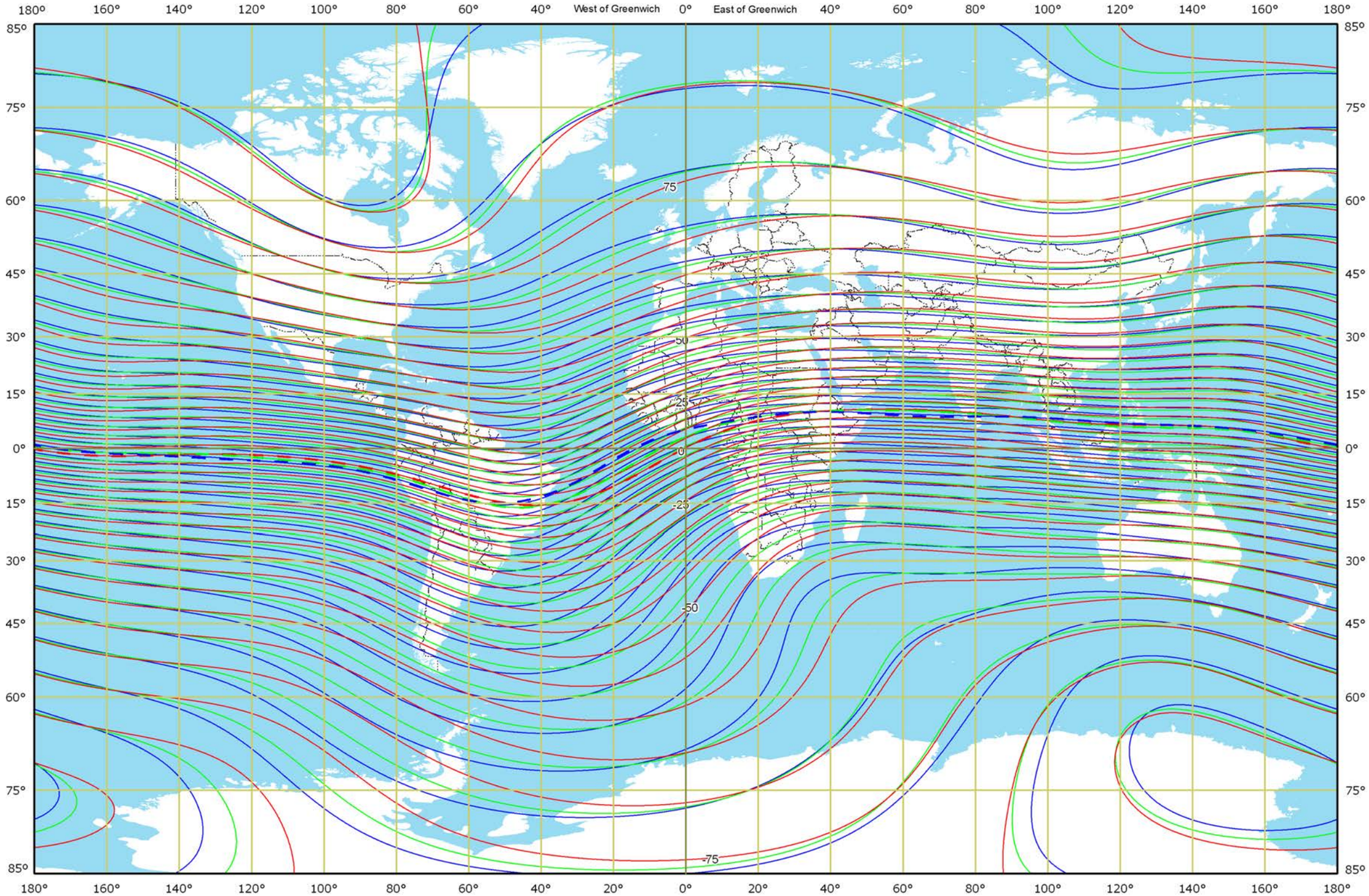

Years	Isoclines	Geomagnetic equators
1850		1850
1875		1875
1900		1900

Example of magnetic inclination value, degree

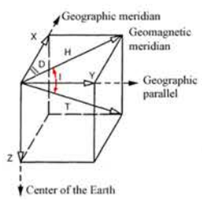

MGMF vector components

D Declination
I Inclination
H Horizontal component
T Total intensity
X North component
Y East component
Z Vertical component

Scale 1: 120 000 000

Projection: Miller cylindrical

NORTH COMPONENT OF MGMF

MGMF – 1500, 1525, 1550 – DX

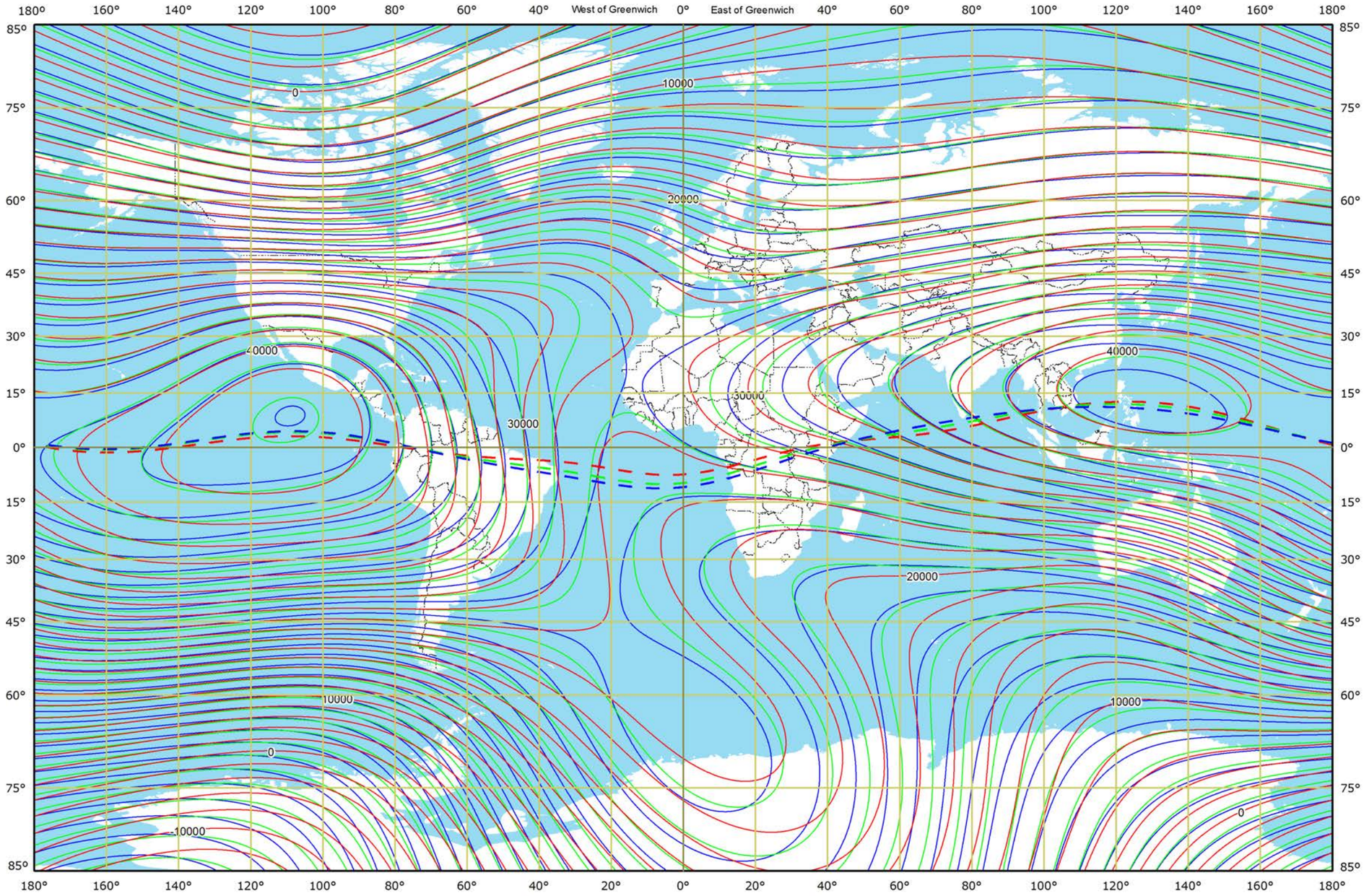

Years	Isolines	Geomagnetic equators
1500		1500
1525		1525
1550		1550

Example of magnetic field component value, nT

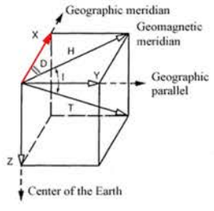

MGMF vector components

D Declination
I Inclination
H Horizontal component
T Total intensity
X North component
Y East component
Z Vertical component

Scale 1: 120 000 000

Projection: Miller cylindrical

NORTH COMPONENT OF MGMF

MGMF – 1550, 1575, 1600 – DX

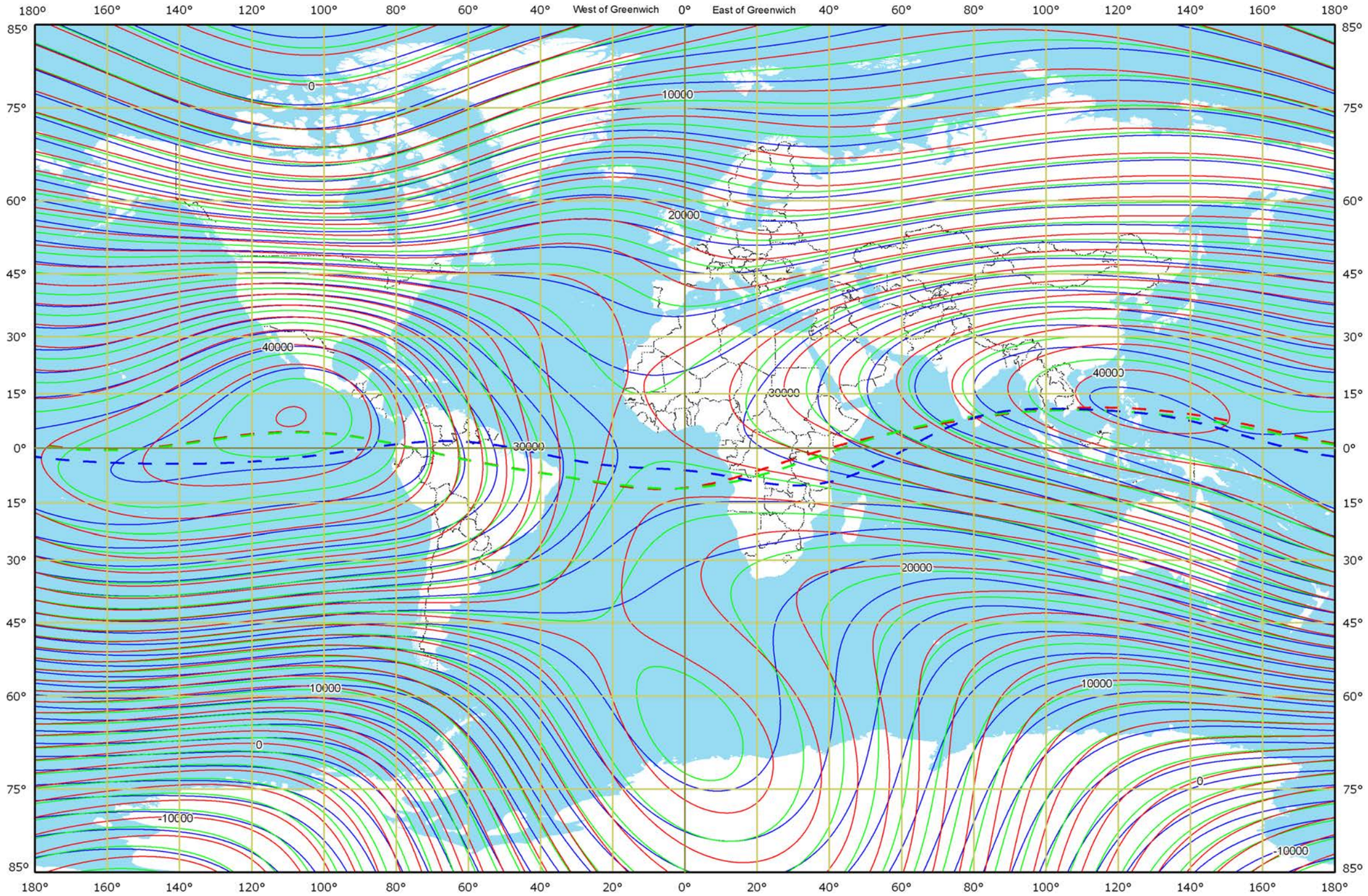

Years	Isolines	Geomagnetic equators
1550		1550
1575		1575
1600		1600

Example of magnetic field component value, nT

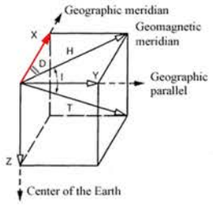

MGMF vector components

D Declination
I Inclination
H Horizontal component
T Total intensity
X North component
Y East component
Z Vertical component

Scale 1: 120 000 000

Projection: Miller cylindrical

NORTH COMPONENT OF MGMF

MGMF – 1600, 1625, 1650 – DX

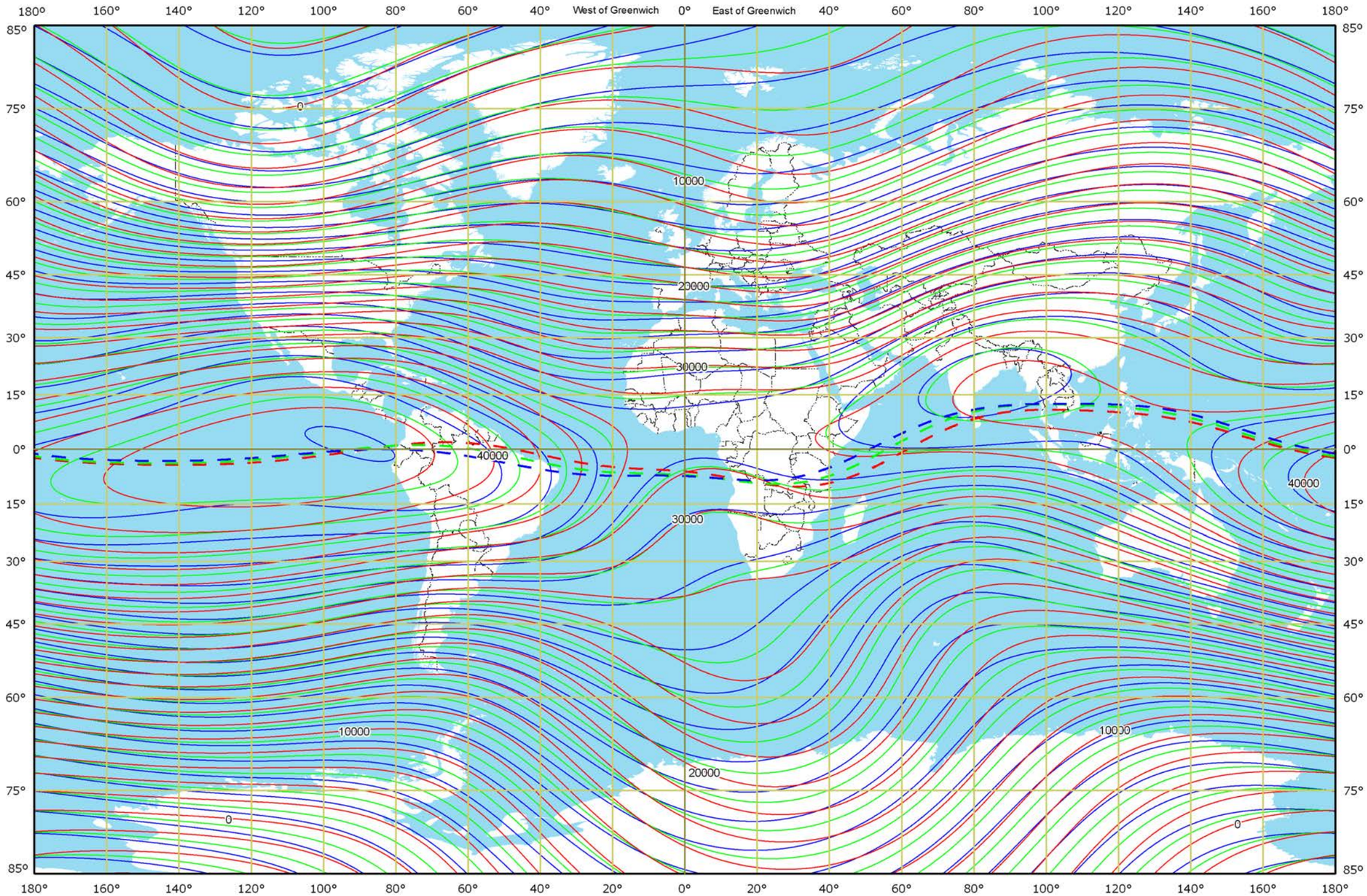

Years	Isolines	Geomagnetic equators
1600		1600
1625		1625
1650		1650

Example of magnetic field component value, nT

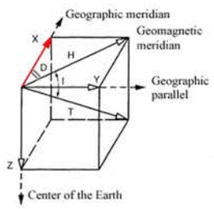

MGMF vector components

D Declination
I Inclination
H Horizontal component
T Total intensity
X North component
Y East component
Z Vertical component

Scale 1: 120 000 000

Projection: Miller cylindrical

NORTH COMPONENT OF MGMF

MGMF – 1650, 1675, 1700 – DX

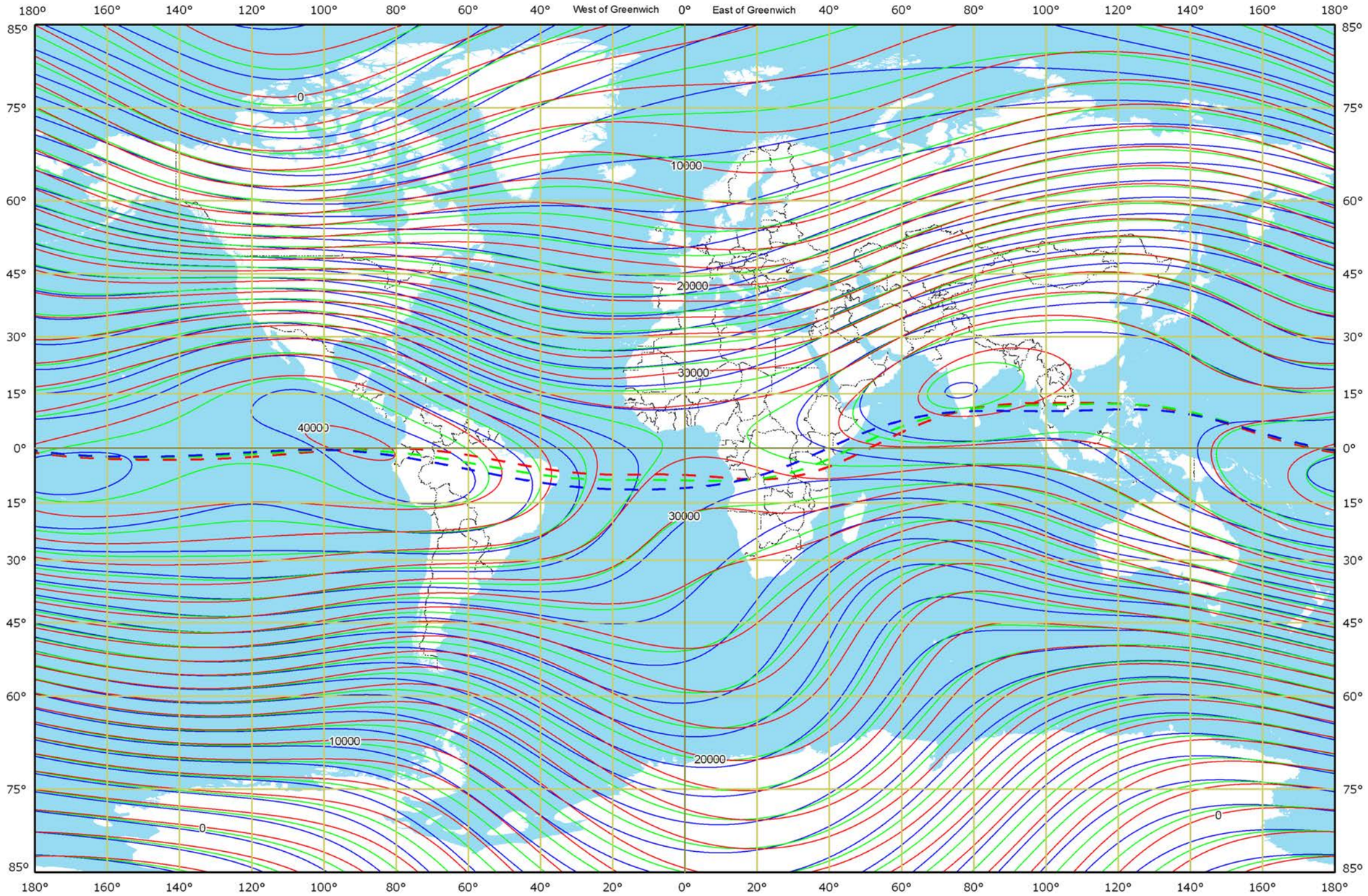

Years	Isolines	Geomagnetic equators
1650		1650
1675		1675
1700		1700

Example of magnetic field component value, nT

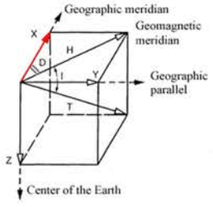

MGMF vector components

D Declination
I Inclination
H Horizontal component
T Total intensity
X North component
Y East component
Z Vertical component

Scale 1: 120 000 000

Projection: Miller cylindrical

NORTH COMPONENT OF MGMF

MGMF – 1700, 1725, 1750 – DX

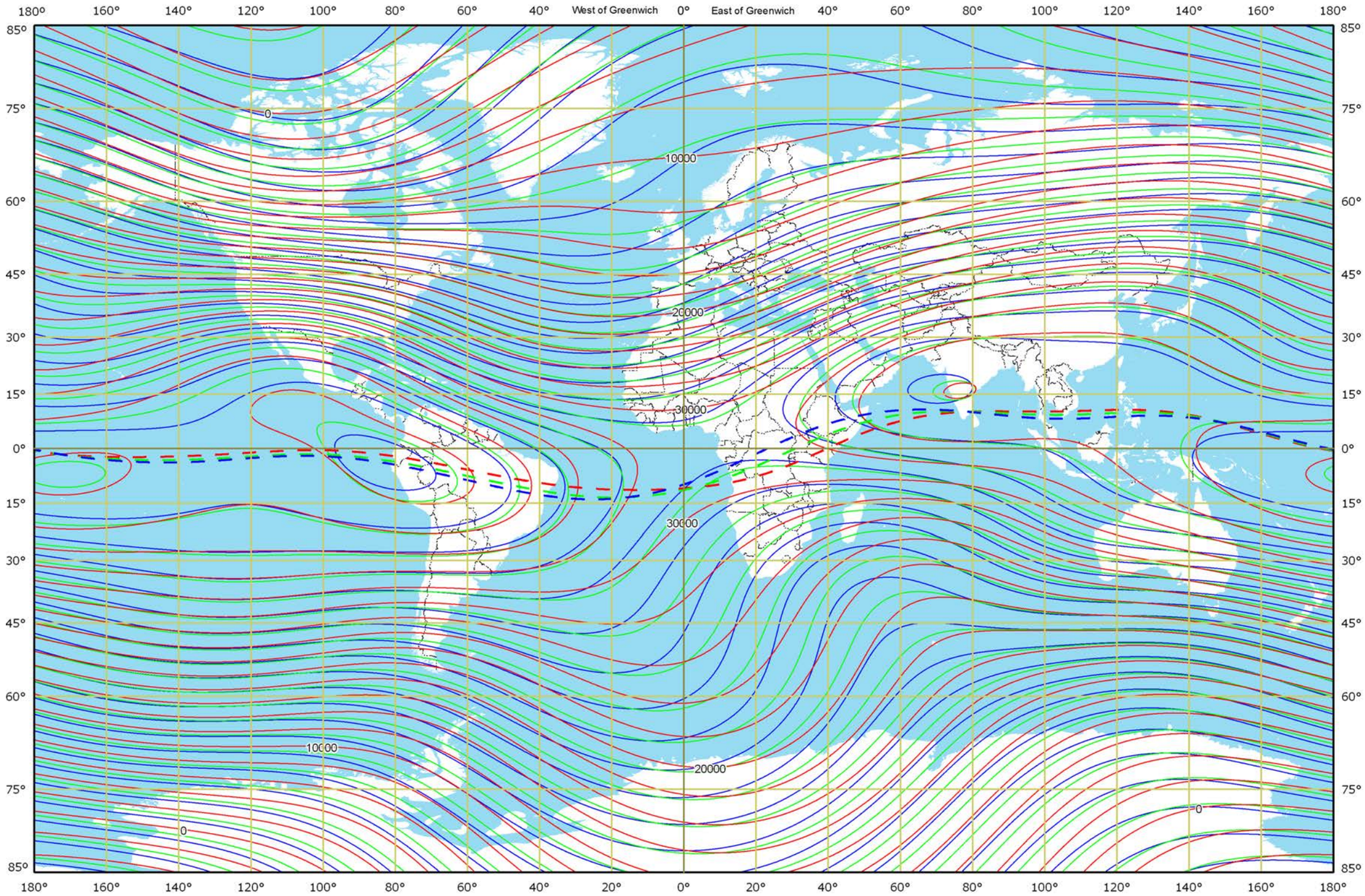

Years	Isolines	Geomagnetic equators
1700		1700
1725		1725
1750		1750

Example of magnetic field component value, nT

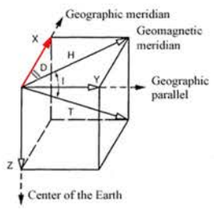

MGMF vector components

D Declination
I Inclination
H Horizontal component
T Total intensity
X North component
Y East component
Z Vertical component

Scale 1: 120 000 000

Projection: Miller cylindrical

NORTH COMPONENT OF MGMF

MGMF – 1750, 1775, 1800 – DX

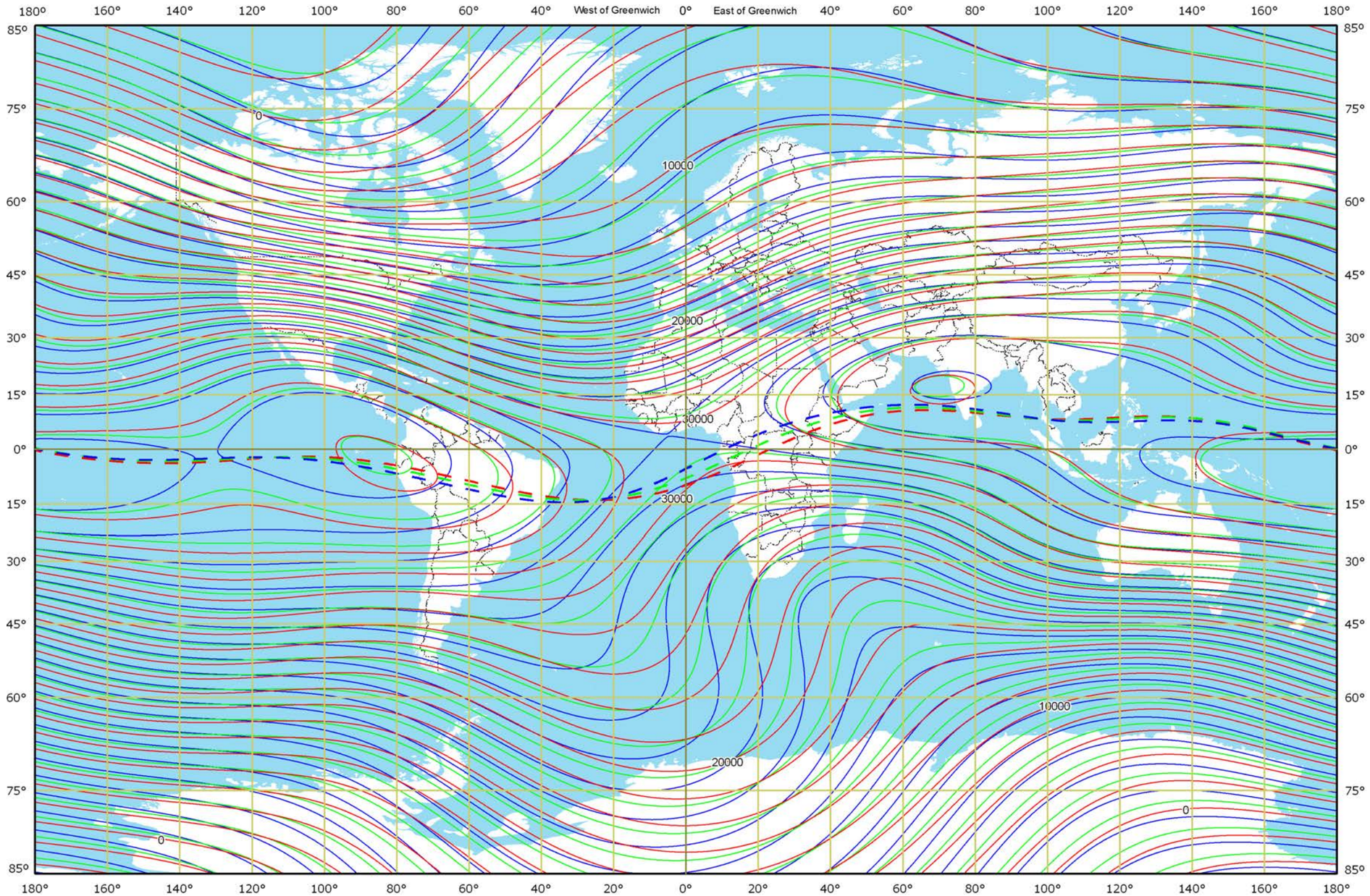

Years	Isolines	Geomagnetic equators
1750		1750
1775		1775
1800		1800

Example of magnetic field component value, nT

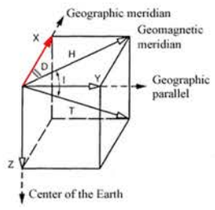

MGMF vector components

D Declination
I Inclination
H Horizontal component
T Total intensity
X North component
Y East component
Z Vertical component

Scale 1: 120 000 000

Projection: Miller cylindrical

NORTH COMPONENT OF MGMF

MGMF – 1800, 1825, 1850 – DX

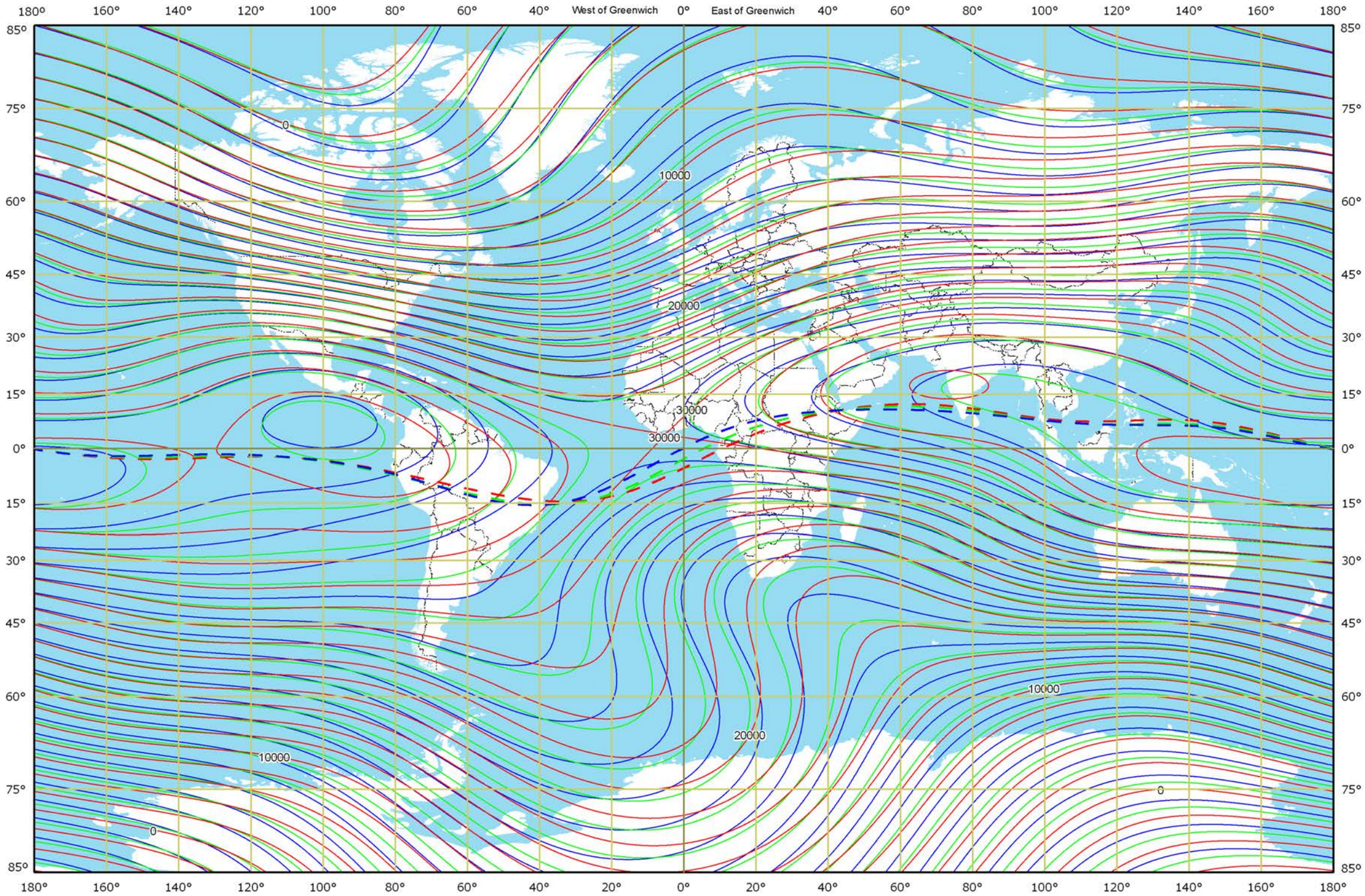

Years	Isolines	Geomagnetic equators
1800		1800
1825		1825
1850		1850

Example of magnetic field component value, nT

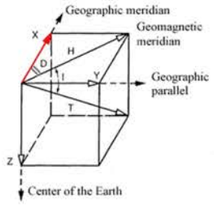

MGMF vector components

D Declination
I Inclination
H Horizontal component
T Total intensity
X North component
Y East component
Z Vertical component

Scale 1: 120 000 000

Projection: Miller cylindrical

NORTH COMPONENT OF MGMF

MGMF – 1850, 1875, 1900 – DX

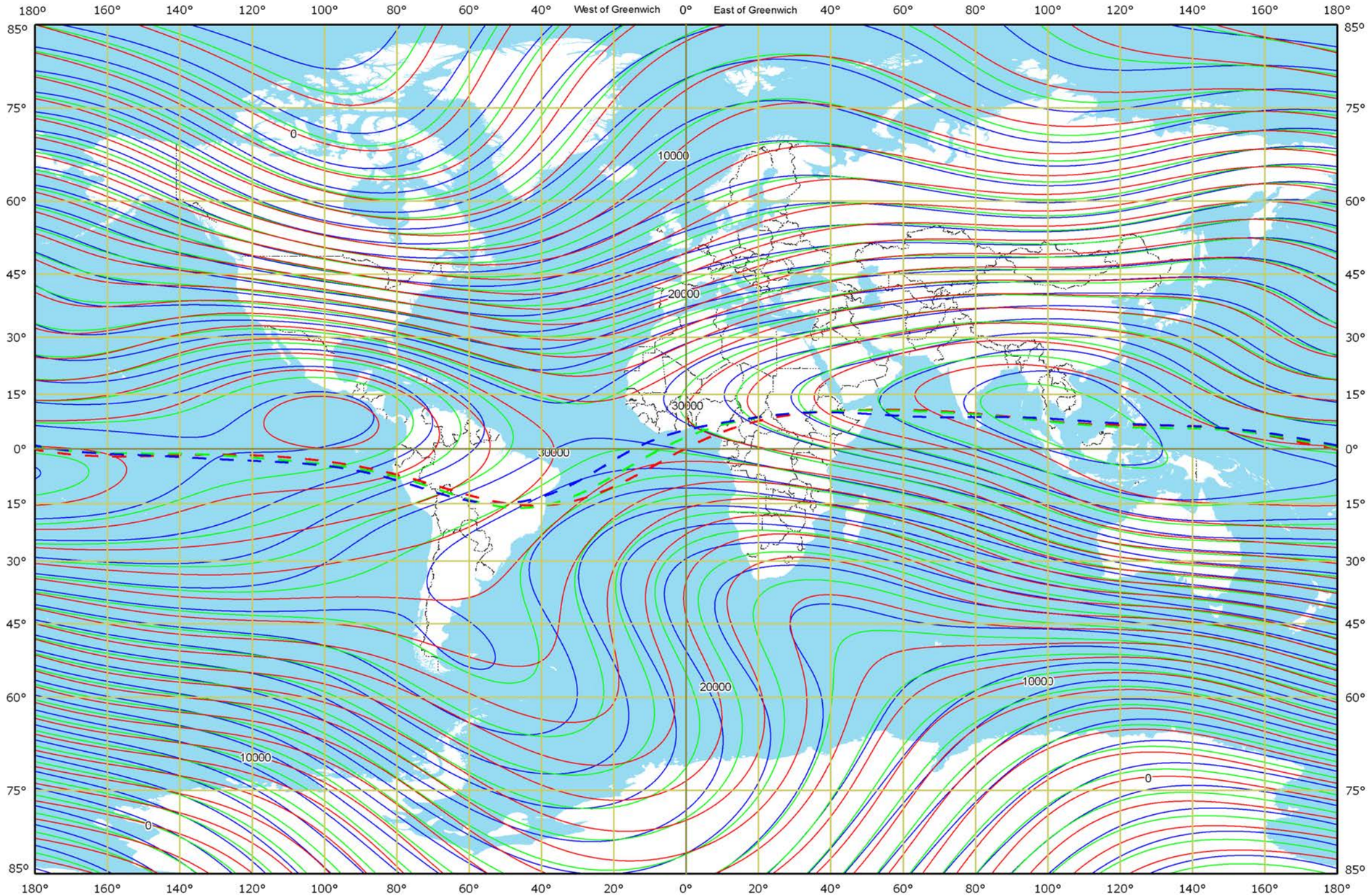

Years	Isolines	Geomagnetic equators
1850		1850
1875		1875
1900		1900

Example of magnetic field component value, nT

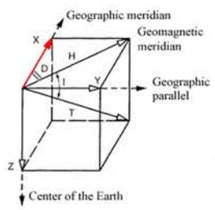

MGMF vector components

D Declination
I Inclination
H Horizontal component
T Total intensity
X North component
Y East component
Z Vertical component

Scale 1: 120 000 000

Projection: Miller cylindrical

EAST COMPONENT OF MGMF

MGMF– 1500, 1525, 1550 – DY

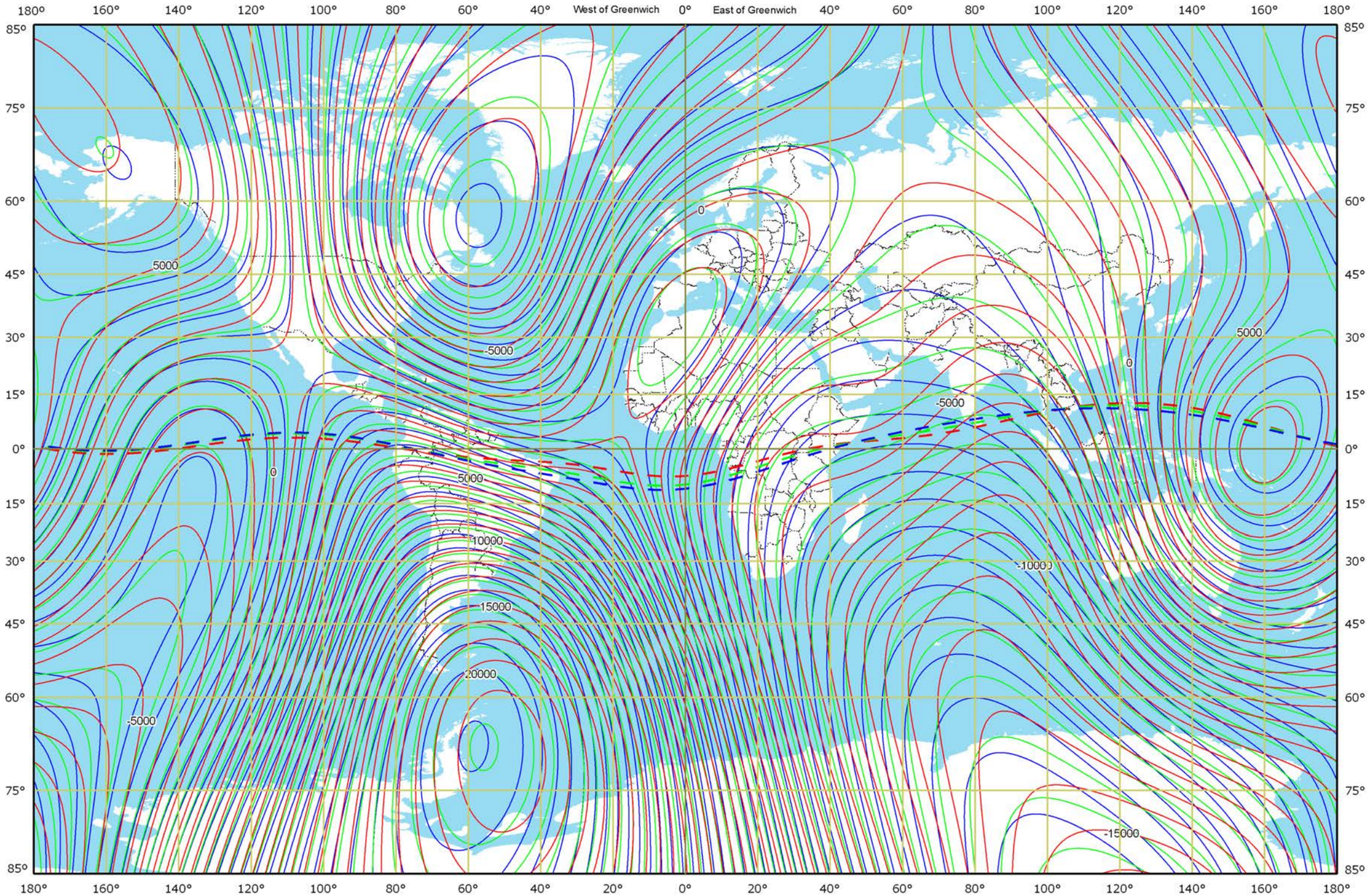

Years	Isolines	Geomagnetic equators
1500		1500
1525		1525
1550		1550

Example of magnetic field component value, nT

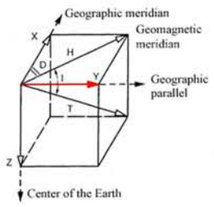

MGMF vector components

D Declination
I Inclination
H Horizontal component
T Total intensity
X North component
Y East component
Z Vertical component

Scale 1: 120 000 000

Projection: Miller cylindrical

EAST COMPONENT OF MGMF

MGMF– 1550, 1575, 1600 – DY

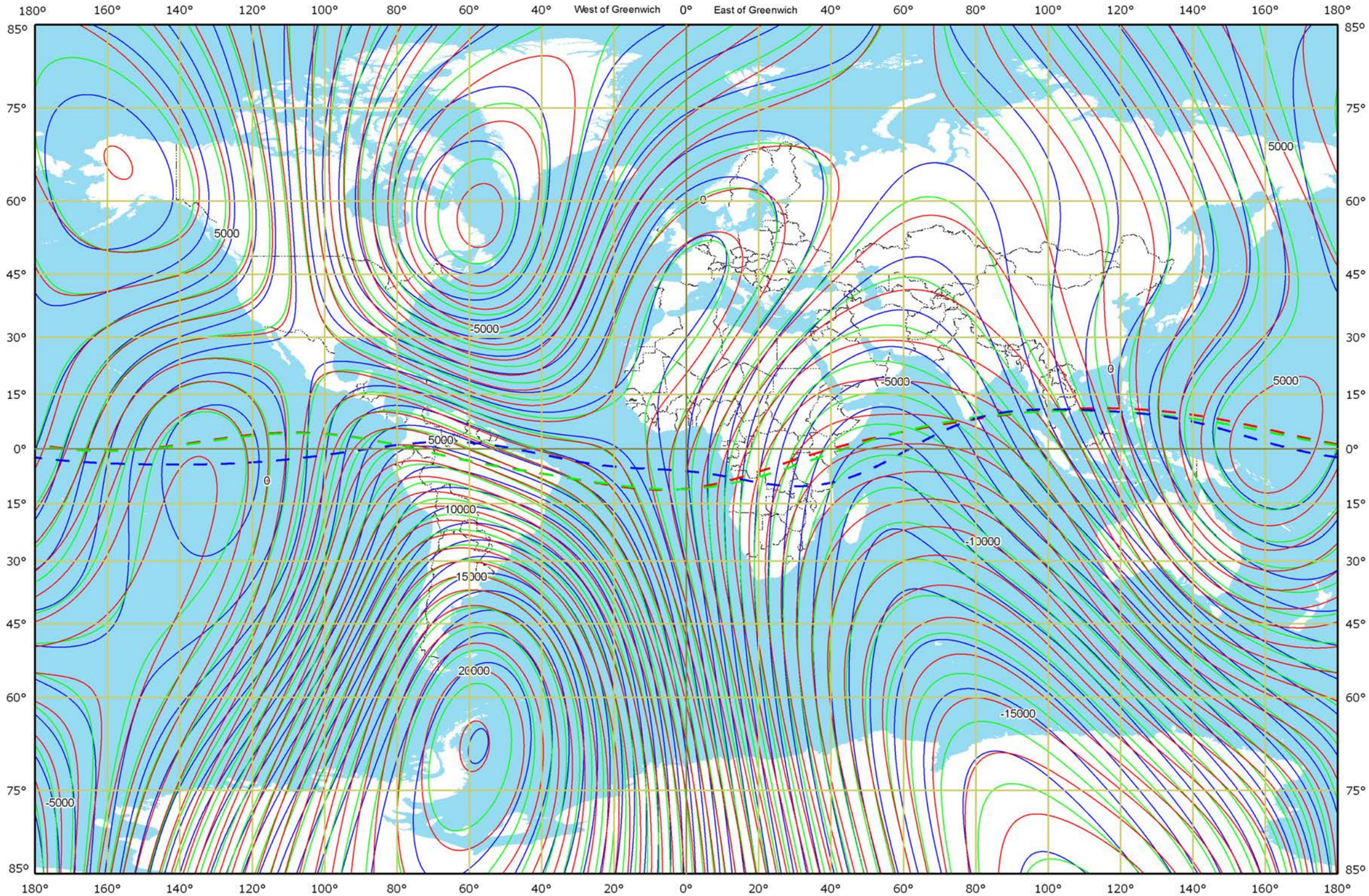

Years	Isolines	Geomagnetic equators
1550		1550
1575		1575
1600		1600

Example of magnetic field component value, nT

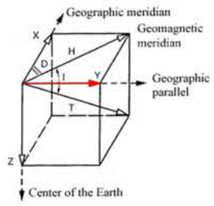

MGMF vector components

D Declination
I Inclination
H Horizontal component
T Total intensity
X North component
Y East component
Z Vertical component

Scale 1: 120 000 000

Projection: Miller cylindrical

EAST COMPONENT OF MGMF

MGMF– 1600, 1625, 1650 – DY

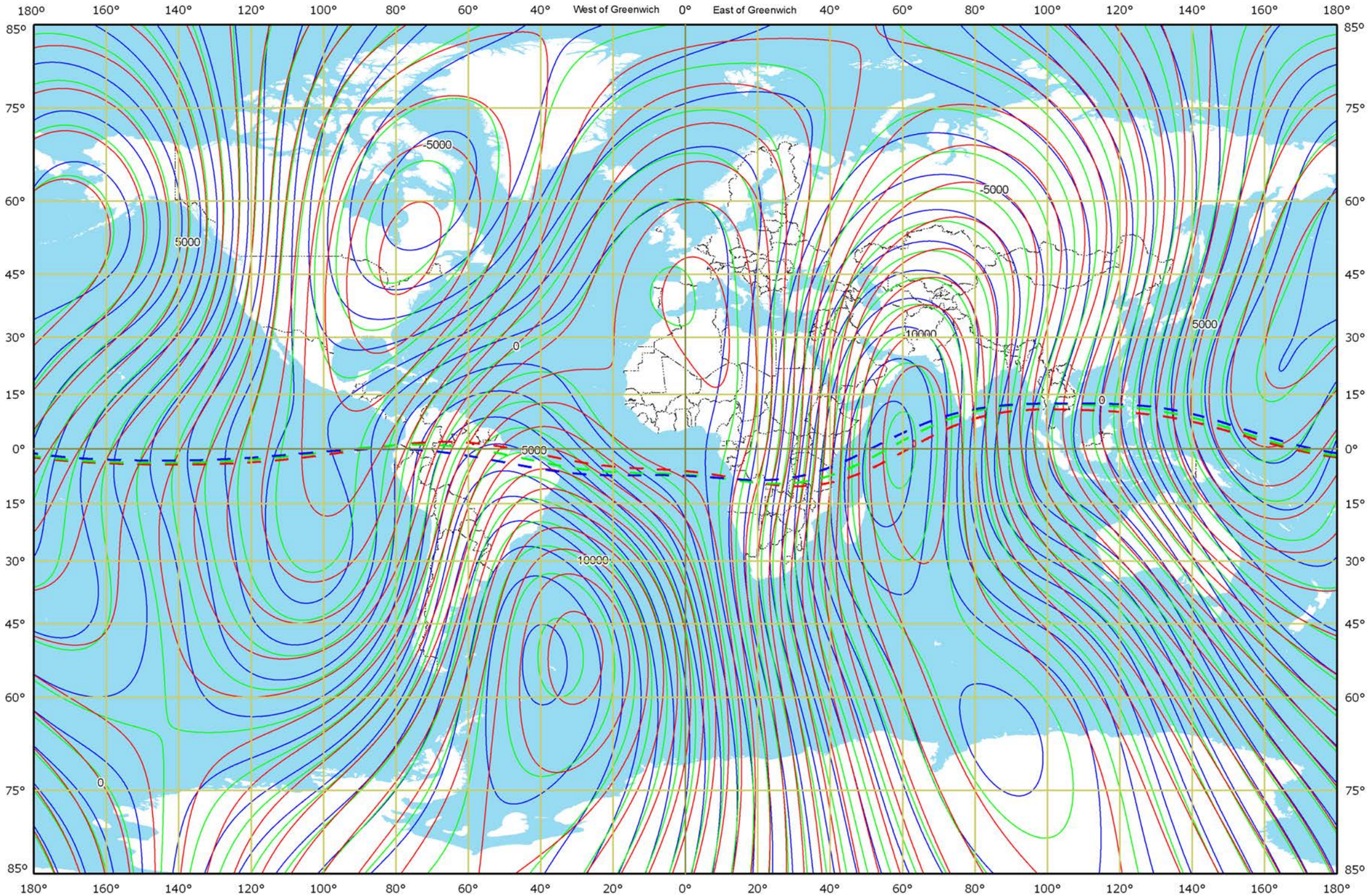

Years	Isolines	Geomagnetic equators
1600		1600
1625		1625
1650		1650

Example of magnetic field component value, nT

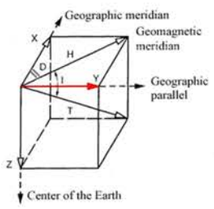

MGMF vector components

D Declination
I Inclination
H Horizontal component
T Total intensity
X North component
Y East component
Z Vertical component

Scale 1: 120 000 000

Projection: Miller cylindrical

EAST COMPONENT OF MGMF

MGMF– 1650, 1675, 1700 – DY

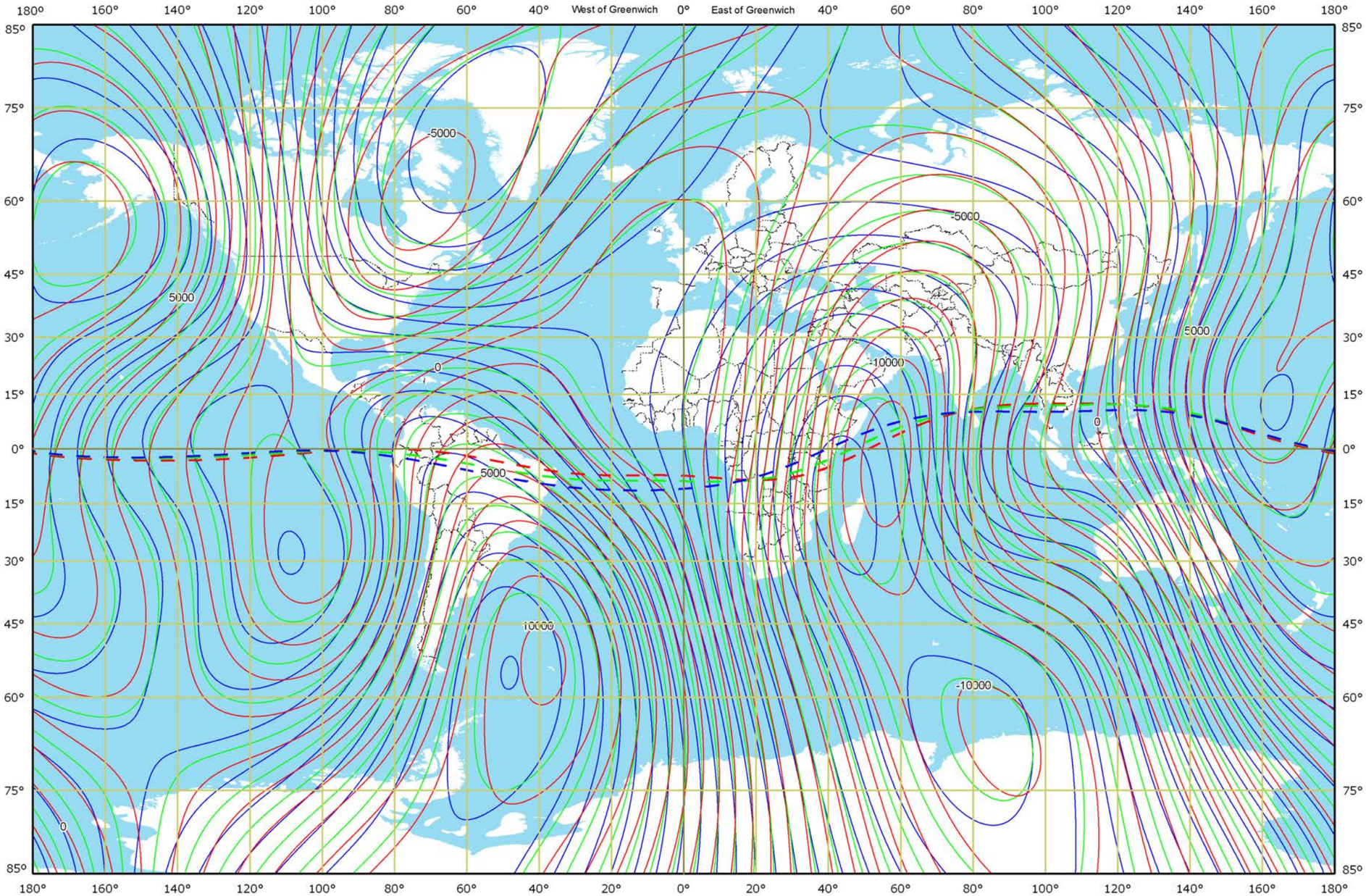

Years	Isolines	Geomagnetic equators
1650		1650
1675		1675
1700		1700

Example of magnetic field component value, nT

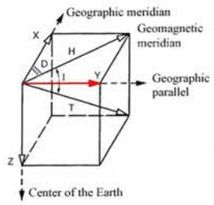

MGMF vector components

D Declination
I Inclination
H Horizontal component
T Total intensity
X North component
Y East component
Z Vertical component

Scale 1: 120 000 000

Projection: Miller cylindrical

EAST COMPONENT OF MGMF

MGMF– 1700, 1725, 1750 – DY

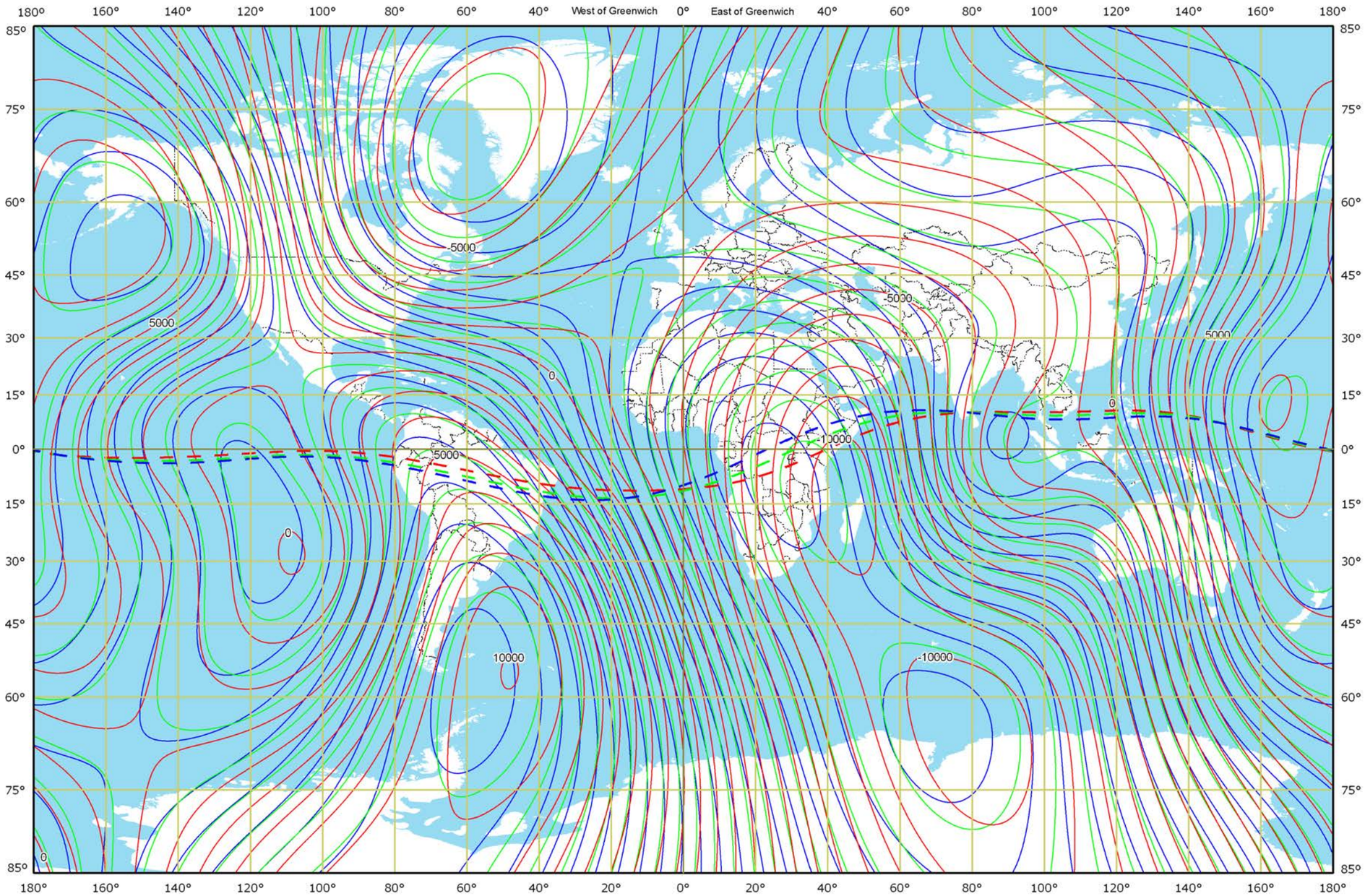

Years	Isolines	Geomagnetic equators
1700		1700
1725		1725
1750		1750

Example of magnetic field component value, nT

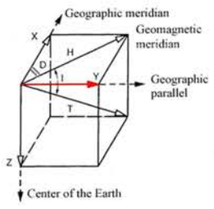

MGMF vector components

D Declination
I Inclination
H Horizontal component
T Total intensity
X North component
Y East component
Z Vertical component

Scale 1: 120 000 000

Projection: Miller cylindrical

EAST COMPONENT OF MGMF

MGMF– 1750, 1775, 1800 – DY

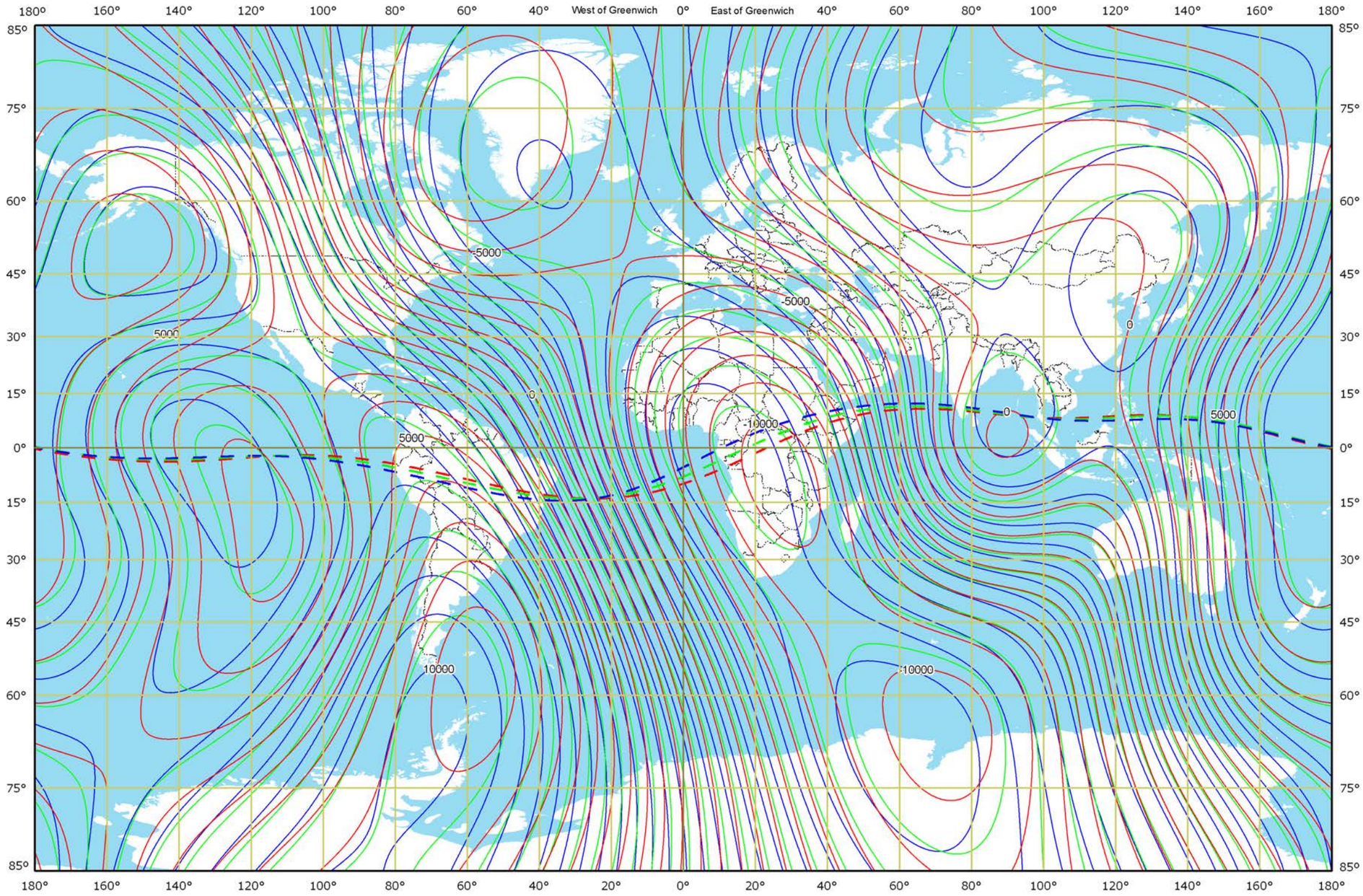

Years	Isolines	Geomagnetic equators
1750		1750
1775		1775
1800		1800

Example of magnetic field component value, nT

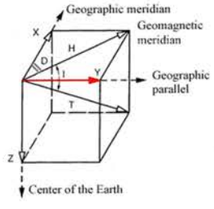

MGMF vector components

D Declination
I Inclination
H Horizontal component
T Total intensity
X North component
Y East component
Z Vertical component

Scale 1: 120 000 000

Projection: Miller cylindrical

EAST COMPONENT OF MGMF

MGMF – 1800, 1825, 1850 – DY

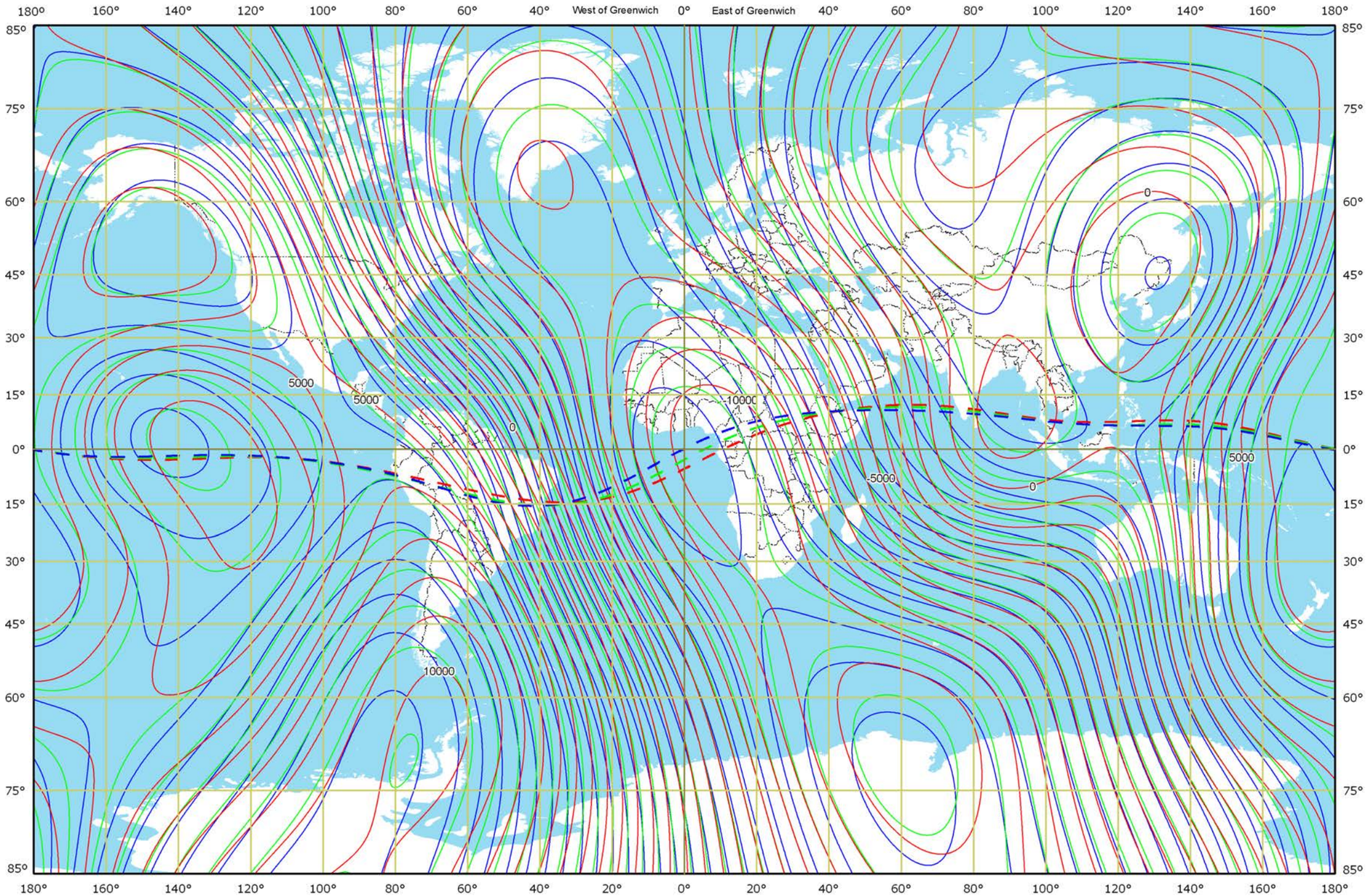

Years	Isolines	Geomagnetic equators
1800		1800
1825		1825
1850		1850

Example of magnetic field component value, nT

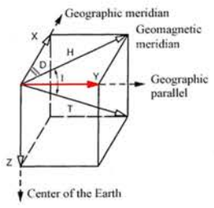

MGMF vector components

D Declination
I Inclination
H Horizontal component
T Total intensity
X North component
Y East component
Z Vertical component

Scale 1: 120 000 000

Projection: Miller cylindrical

EAST COMPONENT OF MGMF

MGMF– 1850, 1875, 1900 – DY

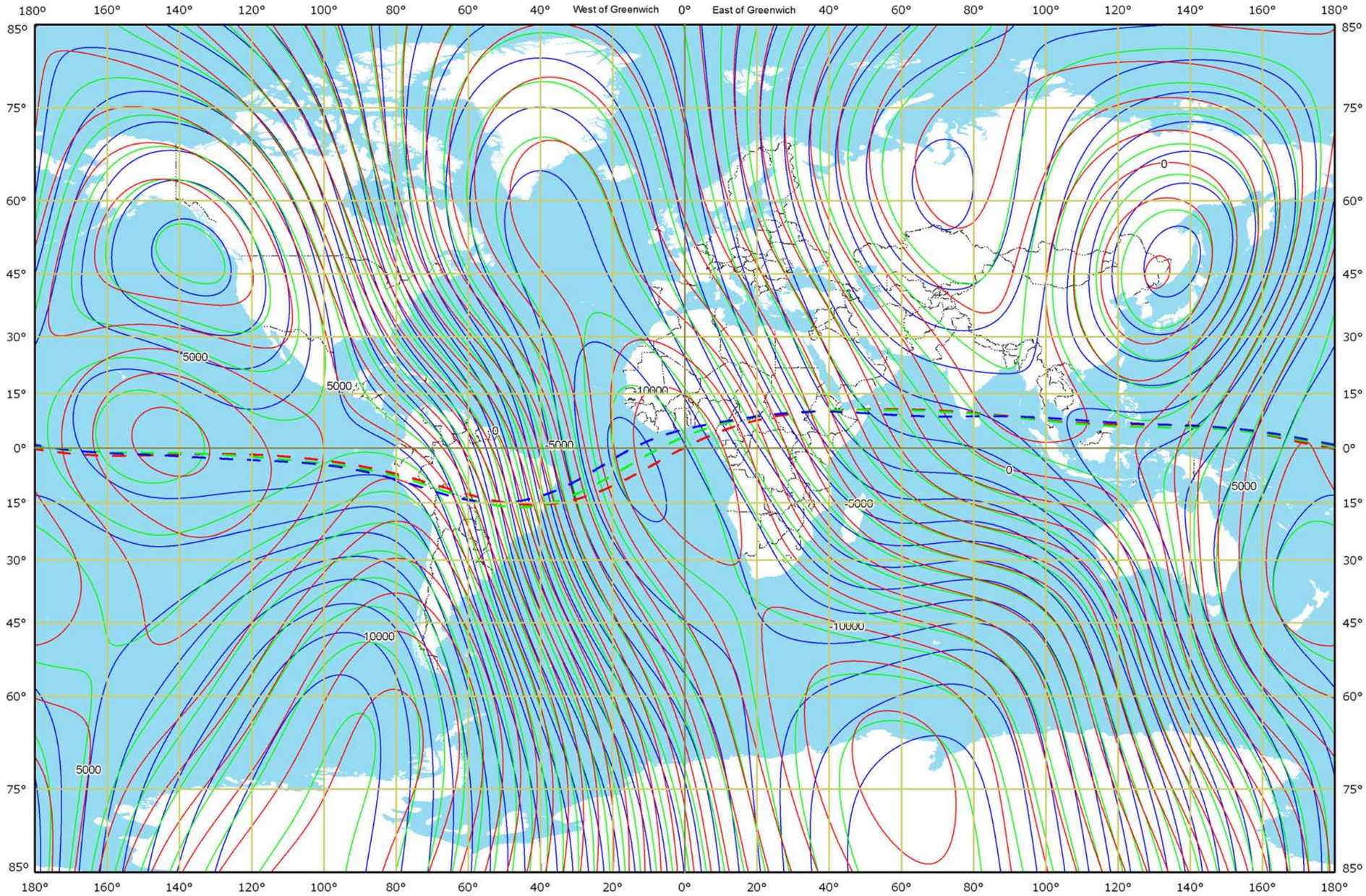

Years	Isolines	Geomagnetic equators
1850		1850
1875		1875
1900		1900

Example of magnetic field component value, nT

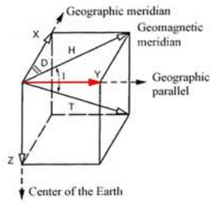

MGMF vector components

D Declination
I Inclination
H Horizontal component
T Total intensity
X North component
Y East component
Z Vertical component

Scale 1: 120 000 000

Projection: Miller cylindrical

VERTICAL COMPONENT OF MGMF

MGMF -1500, 1525, 1550 – DZ

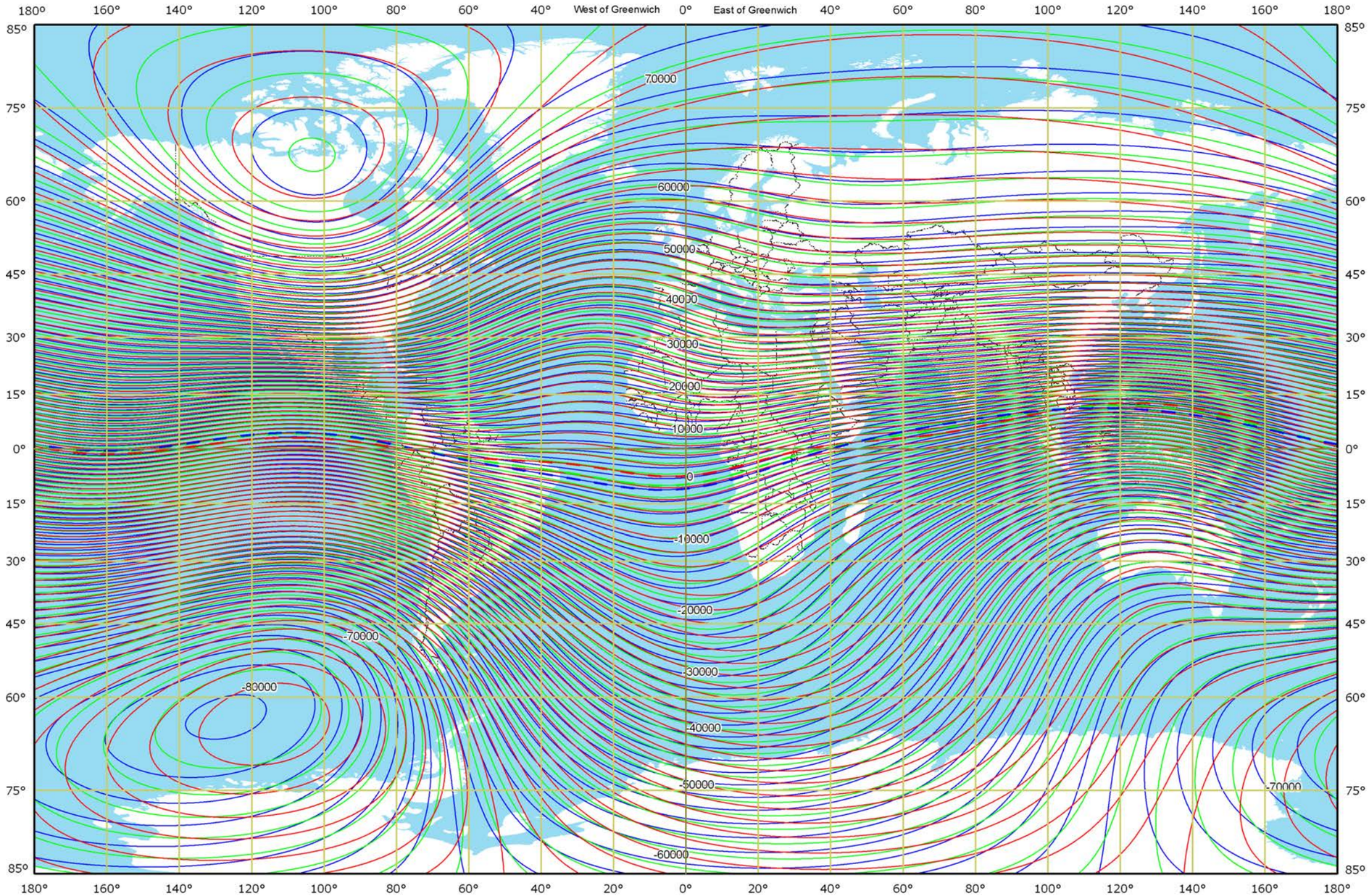

Years	Isolines	Geomagnetic equators
1500		1500
1525		1525
1550		1550

Example of magnetic field component value, nT

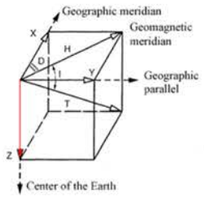

MGMF vector components

D Declination
I Inclination
H Horizontal component
T Total intensity
X North component
Y East component
Z Vertical component

Scale 1: 120 000 000

Projection: Miller cylindrical

VERTICAL COMPONENT OF MGMF

MGMF- 1550, 1575, 1600 – DZ

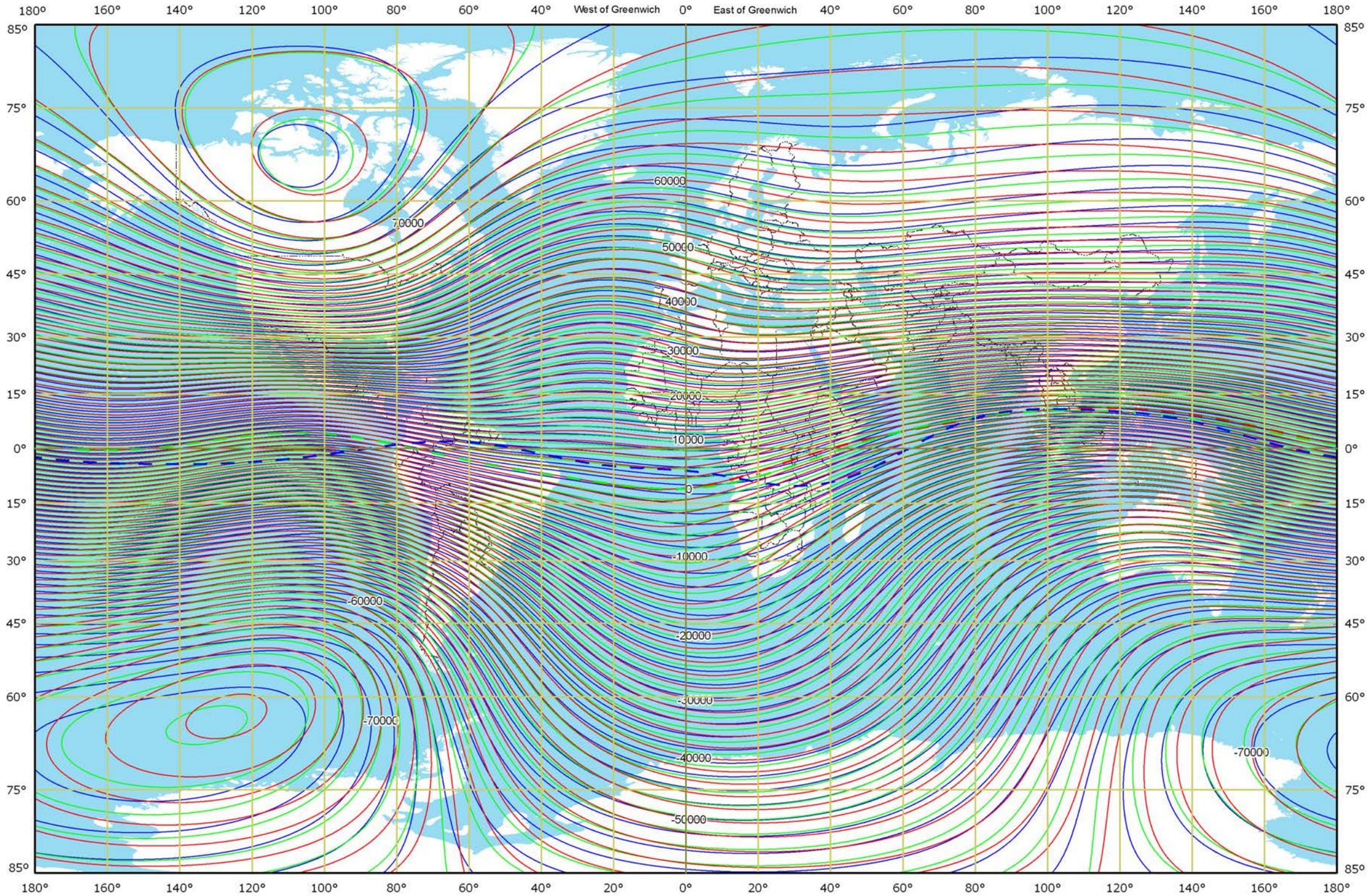

Years	Isolines	Geomagnetic equators
1550		1550
1575		1575
1600		1600

Example of magnetic field component value, nT

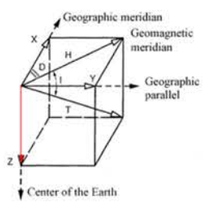

MGMF vector components

D Declination
I Inclination
H Horizontal component
T Total intensity
X North component
Y East component
Z Vertical component

Scale 1: 120 000 000

Projection: Miller cylindrical

VERTICAL COMPONENT OF MGMF

MGMF- 1600, 1625, 1650 – DZ

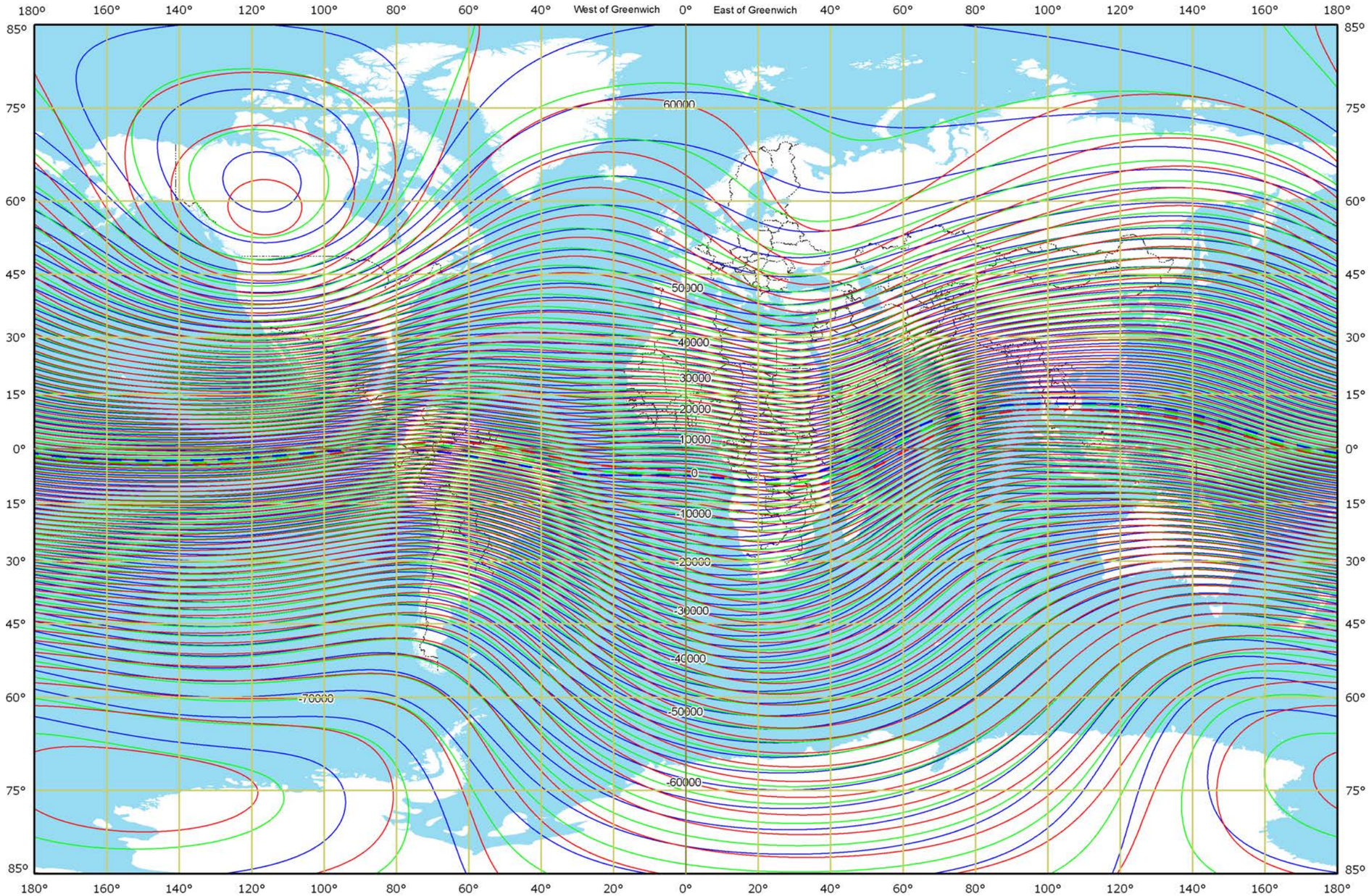

Years	Isolines	Geomagnetic equators
1600		1600
1625		1625
1650		1650

Example of magnetic field component value, nT

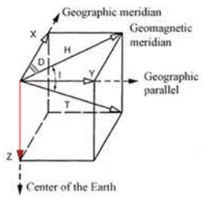

MGMF vector components

D Declination
I Inclination
H Horizontal component
T Total intensity
X North component
Y East component
Z Vertical component

Scale 1: 120 000 000

Projection: Miller cylindrical

VERTICAL COMPONENT OF MGMF

MGMF- 1650, 1675, 1700 – DZ

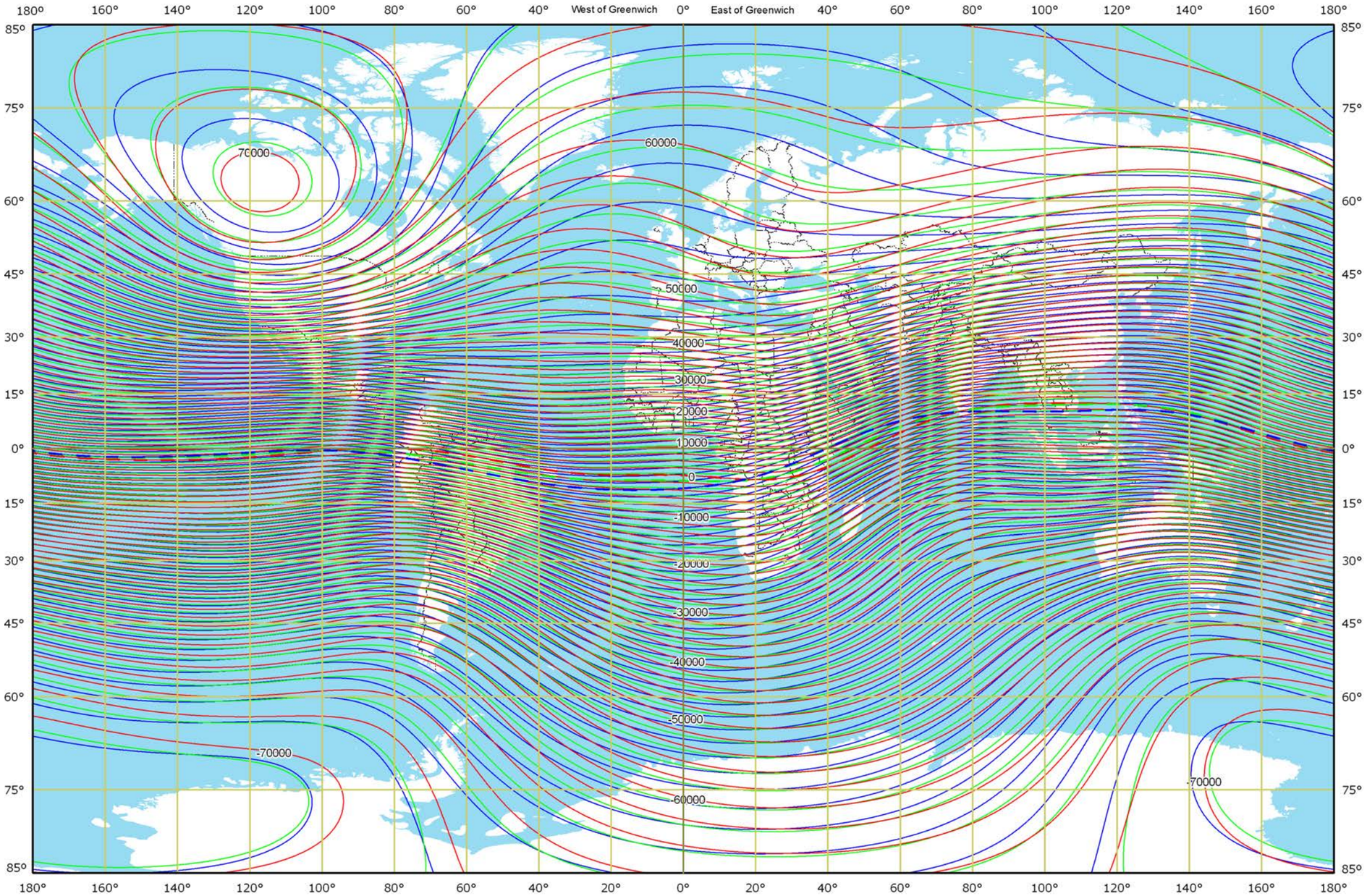

Years	Isolines	Geomagnetic equators
1650		1650
1675		1675
1700		1700

Example of magnetic field component value, nT

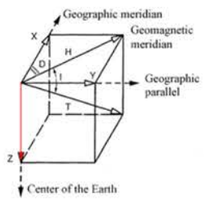

MGMF vector components

D Declination
I Inclination
H Horizontal component
T Total intensity
X North component
Y East component
Z Vertical component

Scale 1: 120 000 000

Projection: Miller cylindrical

VERTICAL COMPONENT OF MGMF

MGMF- 1700, 1725, 1750 – DZ

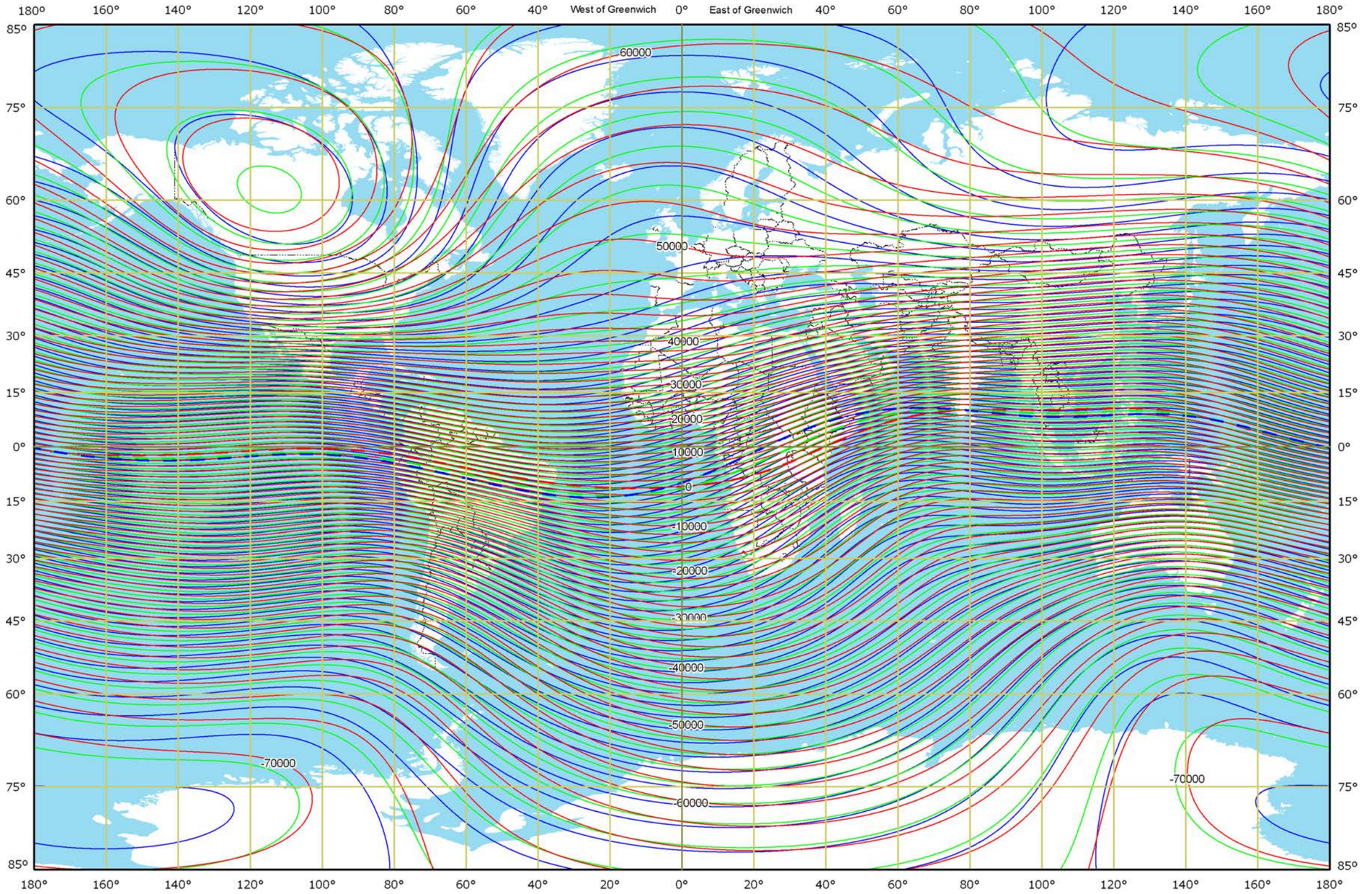

Years	Isolines	Geomagnetic equators
1700		1700
1725		1725
1750		1750

Example of magnetic field component value, nT

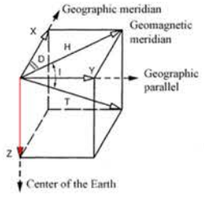

MGMF vector components

D Declination
I Inclination
H Horizontal component
T Total intensity
X North component
Y East component
Z Vertical component

Scale 1: 120 000 000

Projection: Miller cylindrical

VERTICAL COMPONENT OF MGMF

MGMF - 1750, 1775, 1800 – DZ

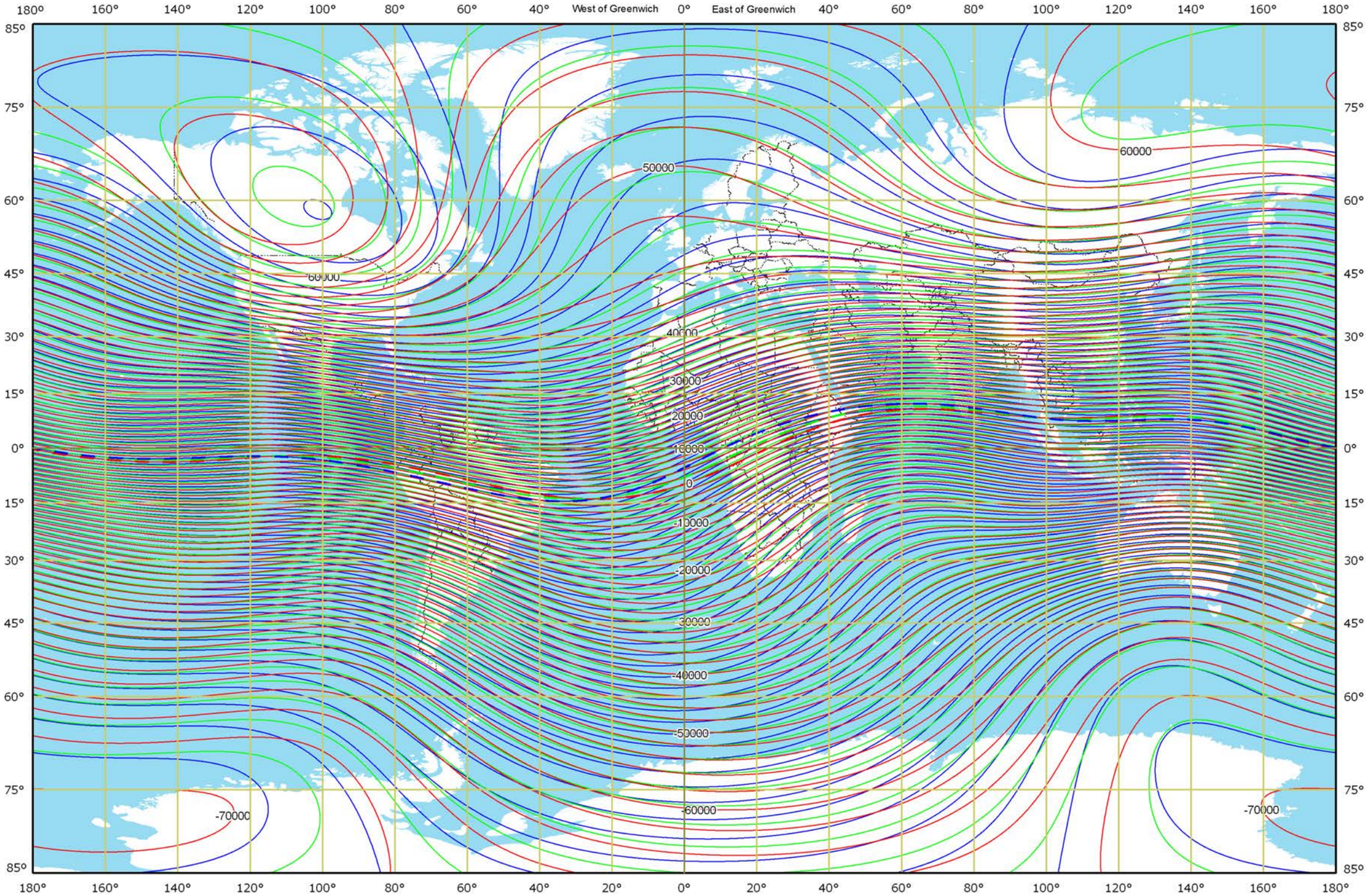

Years	Isolines	Geomagnetic equators
1750		1750
1775		1775
1800		1800

Example of magnetic field component value, nT

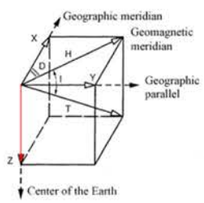

MGMF vector components

D Declination
I Inclination
H Horizontal component
T Total intensity
X North component
Y East component
Z Vertical component

Scale 1: 120 000 000

Projection: Miller cylindrical

VERTICAL COMPONENT OF MGMF

MGMF- 1800, 1825, 1850 – DZ

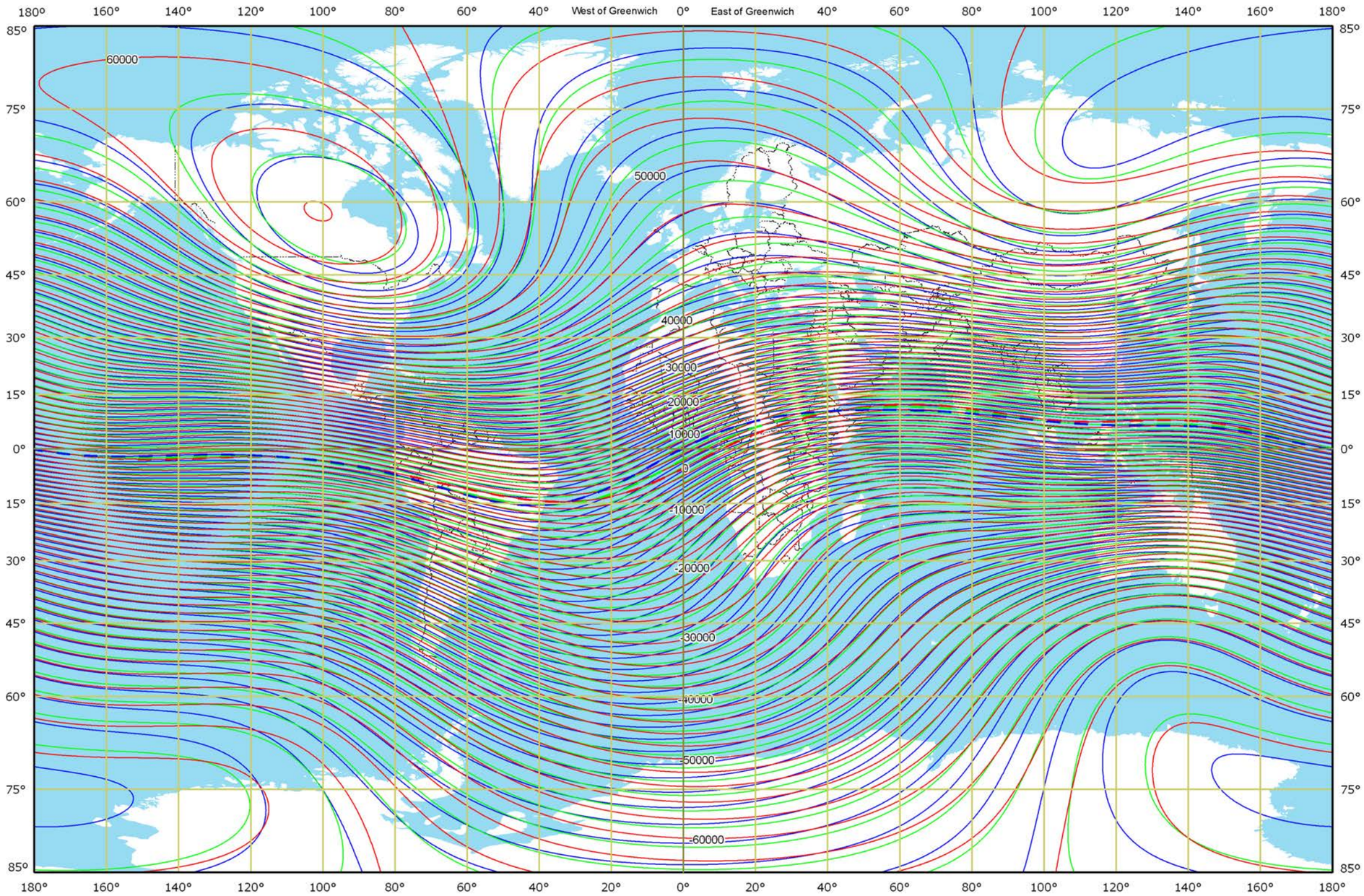

Years	Isolines	Geomagnetic equators
1800		1800
1825		1825
1850		1850

Example of magnetic field component value, nT

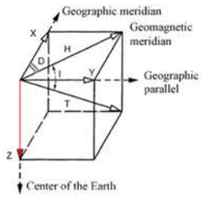

MGMF vector components

D Declination
I Inclination
H Horizontal component
T Total intensity
X North component
Y East component
Z Vertical component

Scale 1: 120 000 000

Projection: Miller cylindrical

VERTICAL COMPONENT OF MGMF

MGMF- 1850, 1875, 1900 – DZ

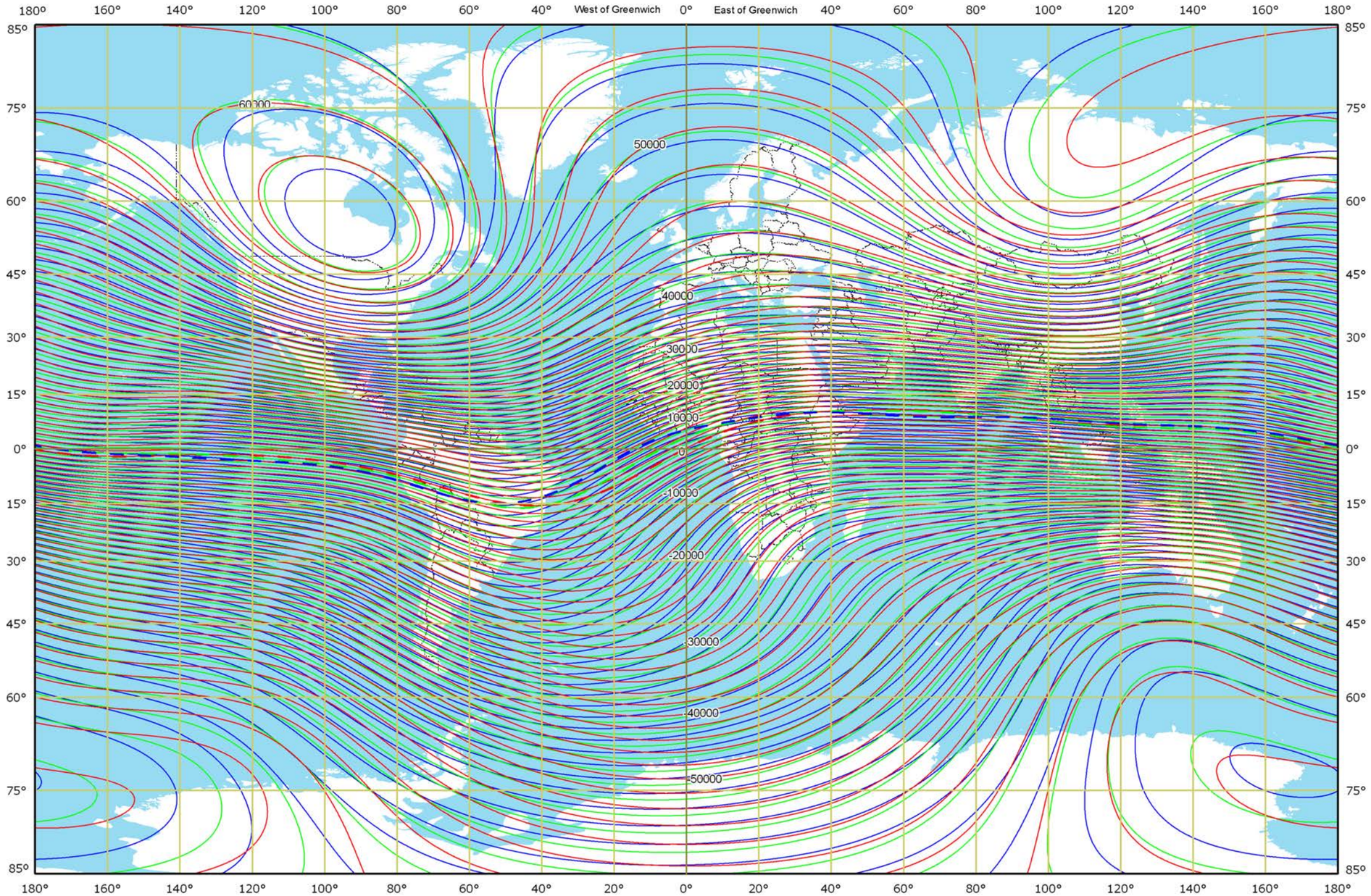

Years	Isolines	Geomagnetic equators
1850		1850
1875		1875
1900		1900

Example of magnetic field component value, nT

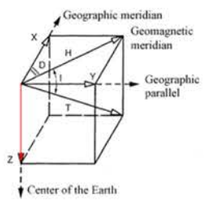

MGMF vector components

D Declination
I Inclination
H Horizontal component
T Total intensity
X North component
Y East component
Z Vertical component

Scale 1: 120 000 000

Projection: Miller cylindrical

HORIZONTAL COMPONENT OF MGMF

MGMF – 1500, 1525, 1550 – H

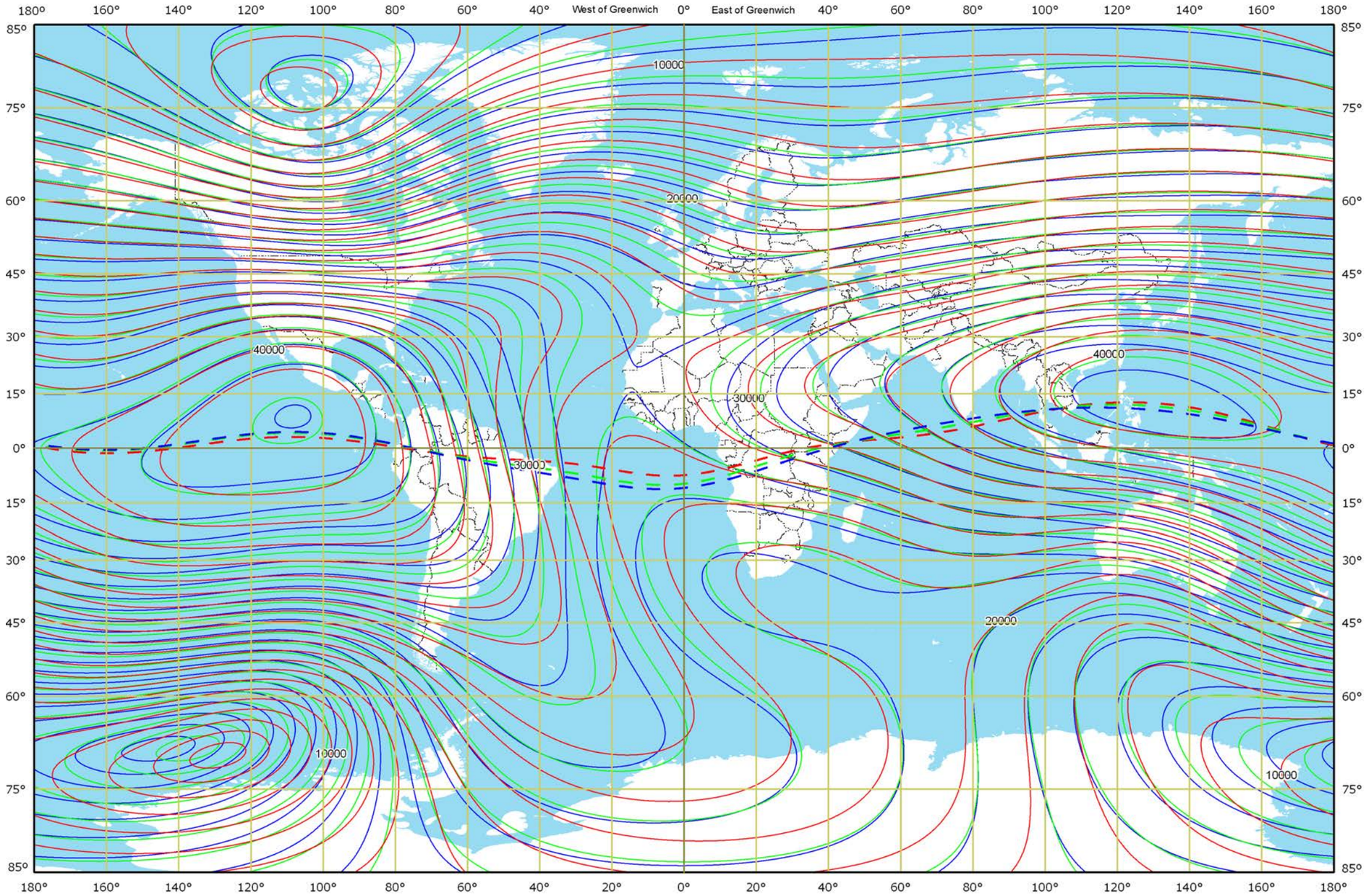

Years	Isolines	Geomagnetic equators
1500		1500
1525		1525
1550		1550

Example of magnetic field component value, nT

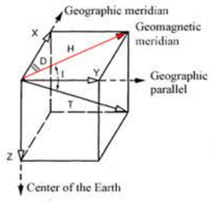

MGMF vector components

D Declination
I Inclination
H Horizontal component
T Total intensity
X North component
Y East component
Z Vertical component

Scale 1: 120 000 000

Projection: Miller cylindrical

HORIZONTAL COMPONENT OF MGMF

MGMF– 1550, 1575, 1600 – H

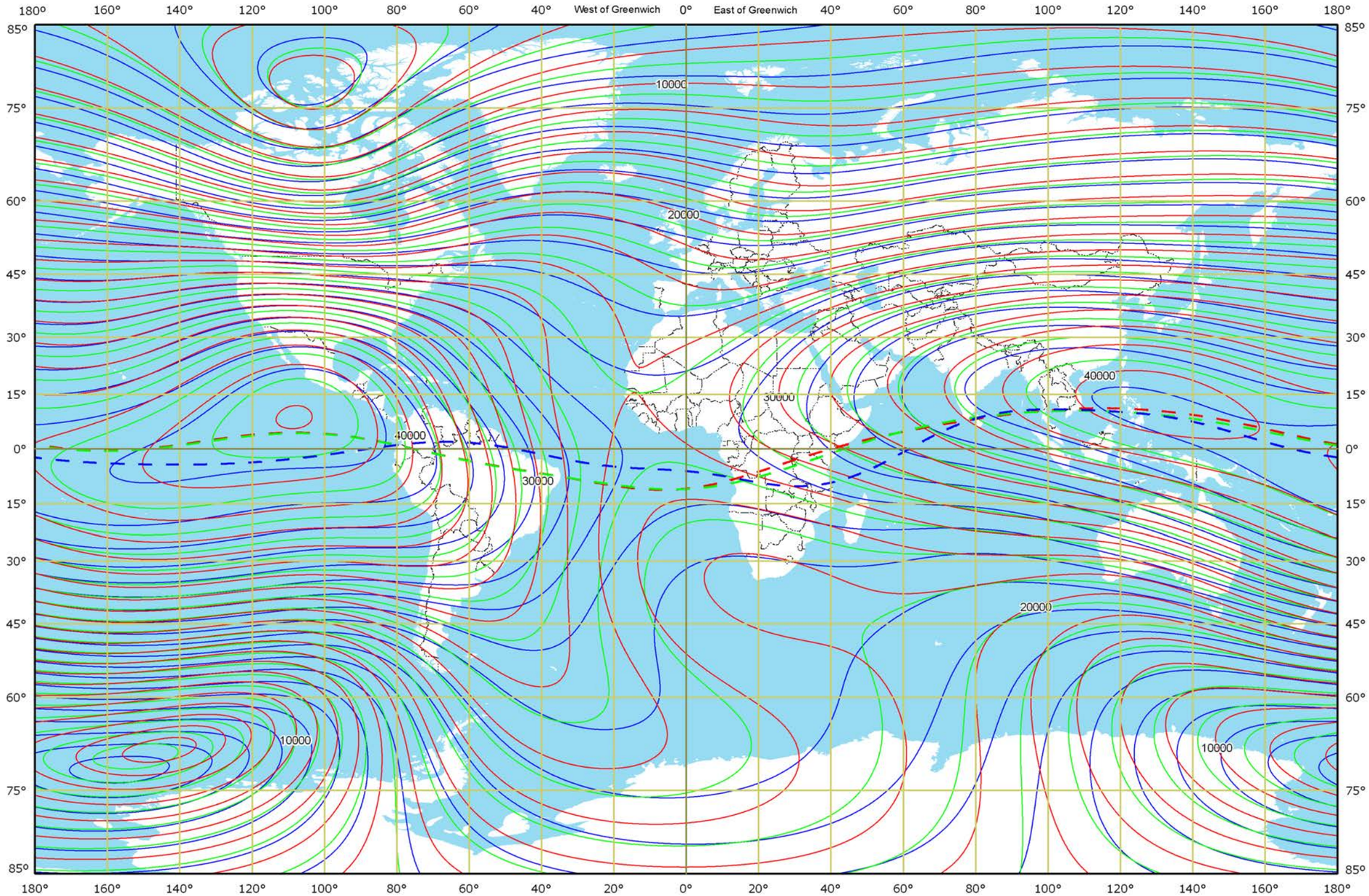

Years	Isolines	Geomagnetic equators
1550		1550
1575		1575
1600		1600

Example of magnetic field component value, nT

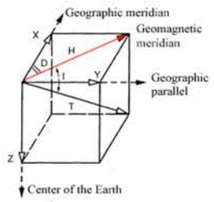

MGMF vector components

D Declination
I Inclination
H Horizontal component
T Total intensity
X North component
Y East component
Z Vertical component

Scale 1: 120 000 000

Projection: Miller cylindrical

HORIZONTAL COMPONENT OF MGMF

MGMF – 1600, 1625, 1650 – H

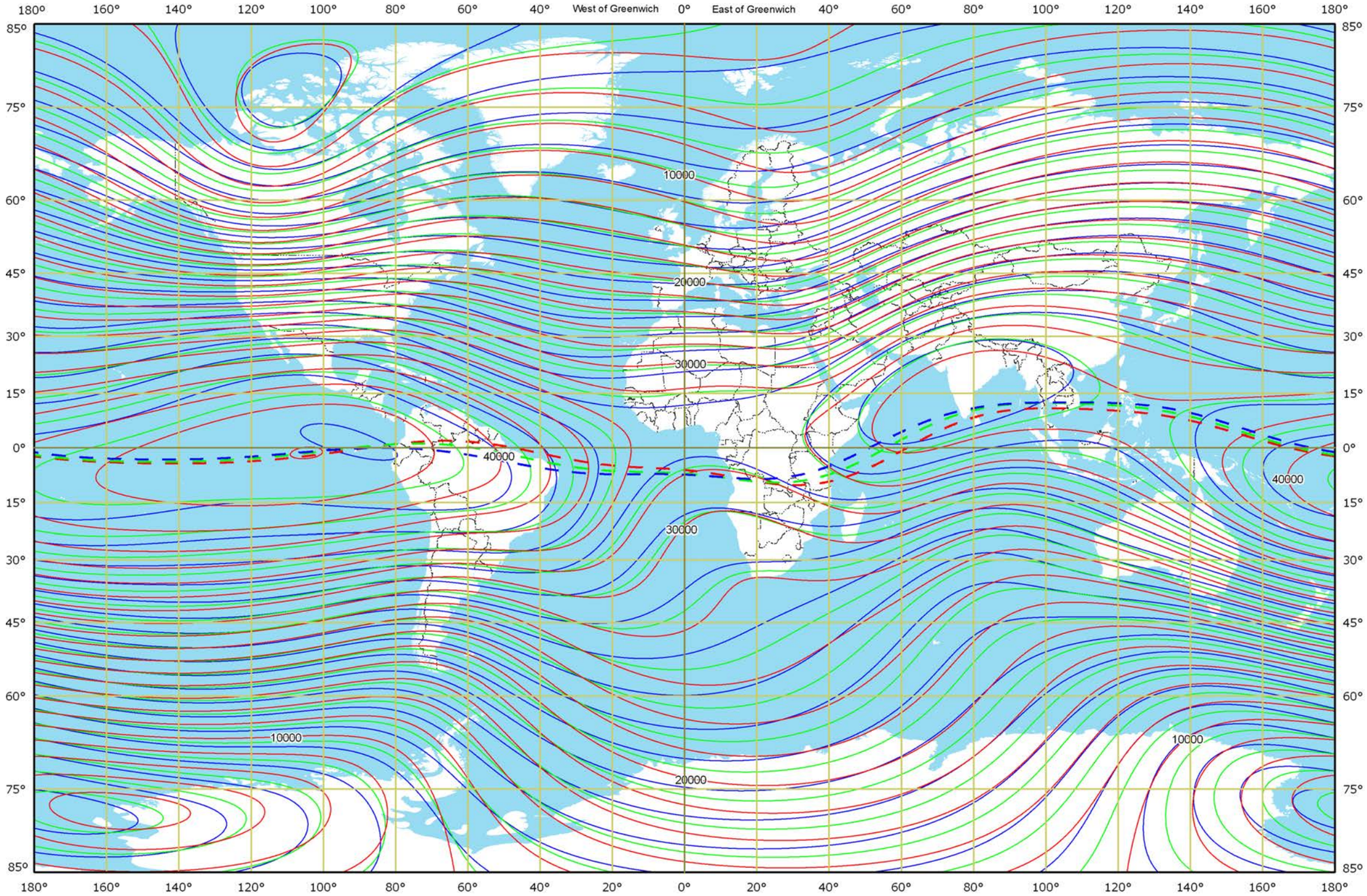

Years	Isolines	Geomagnetic equators
1600		1600
1625		1625
1650		1650

Example of magnetic field component value, nT

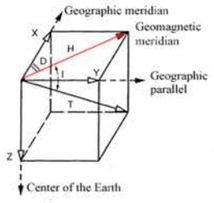

MGMF vector components

D Declination
I Inclination
H Horizontal component
T Total intensity
X North component
Y East component
Z Vertical component

Scale 1: 120 000 000

Projection: Miller cylindrical

HORIZONTAL COMPONENT OF MGMF

MGMF– 1650, 1675, 1700 – H

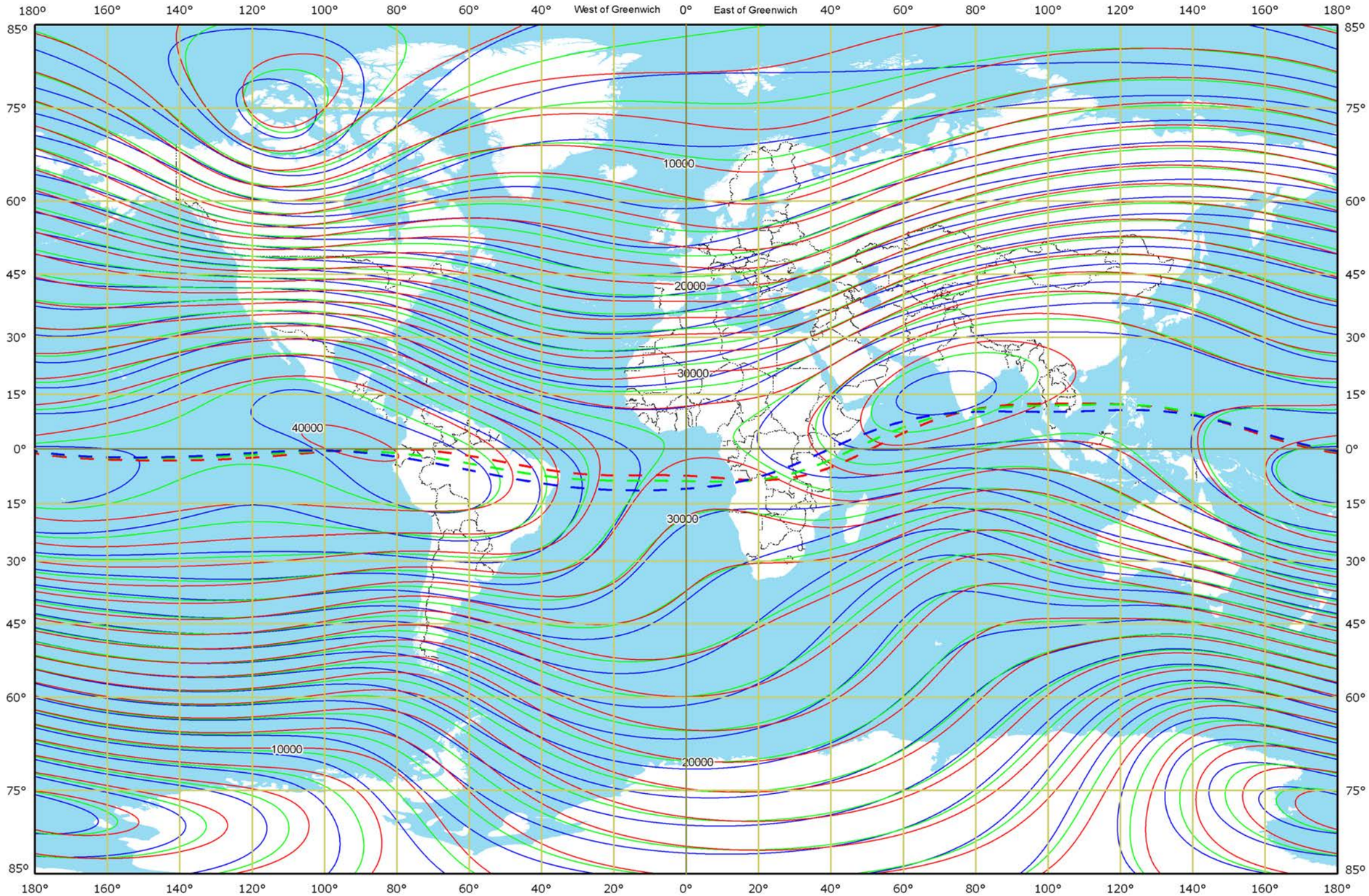

Years	Isolines	Geomagnetic equators
1650		1650
1675		1675
1700		1700

Example of magnetic field component value, nT

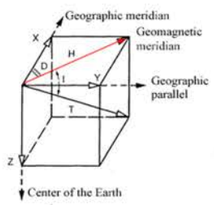

MGMF vector components

D Declination
I Inclination
H Horizontal component
T Total intensity
X North component
Y East component
Z Vertical component

Scale 1: 120 000 000

Projection: Miller cylindrical

HORIZONTAL COMPONENT OF MGMF

MGMF – 1700, 1725, 1750 – H

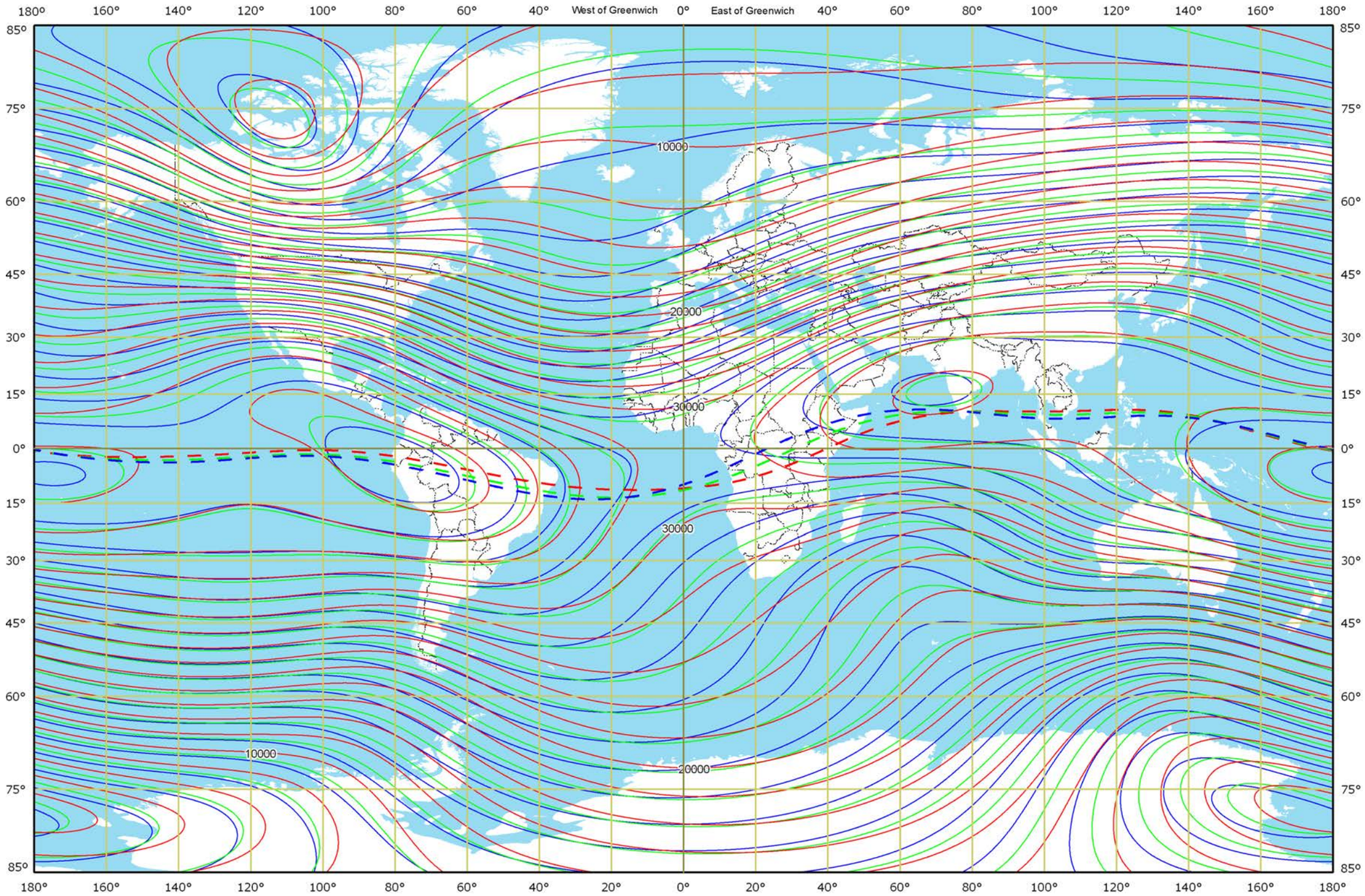

Years	Isolines	Geomagnetic equators
1700		1700
1725		1725
1750		1750

Example of magnetic field component value, nT

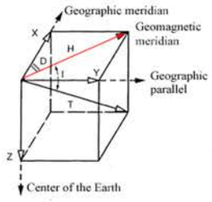

MGMF vector components

D Declination
I Inclination
H Horizontal component
T Total intensity
X North component
Y East component
Z Vertical component

Scale 1: 120 000 000

Projection: Miller cylindrical

HORIZONTAL COMPONENT OF MGMF

MGMF – 1750, 1775, 1800 – H

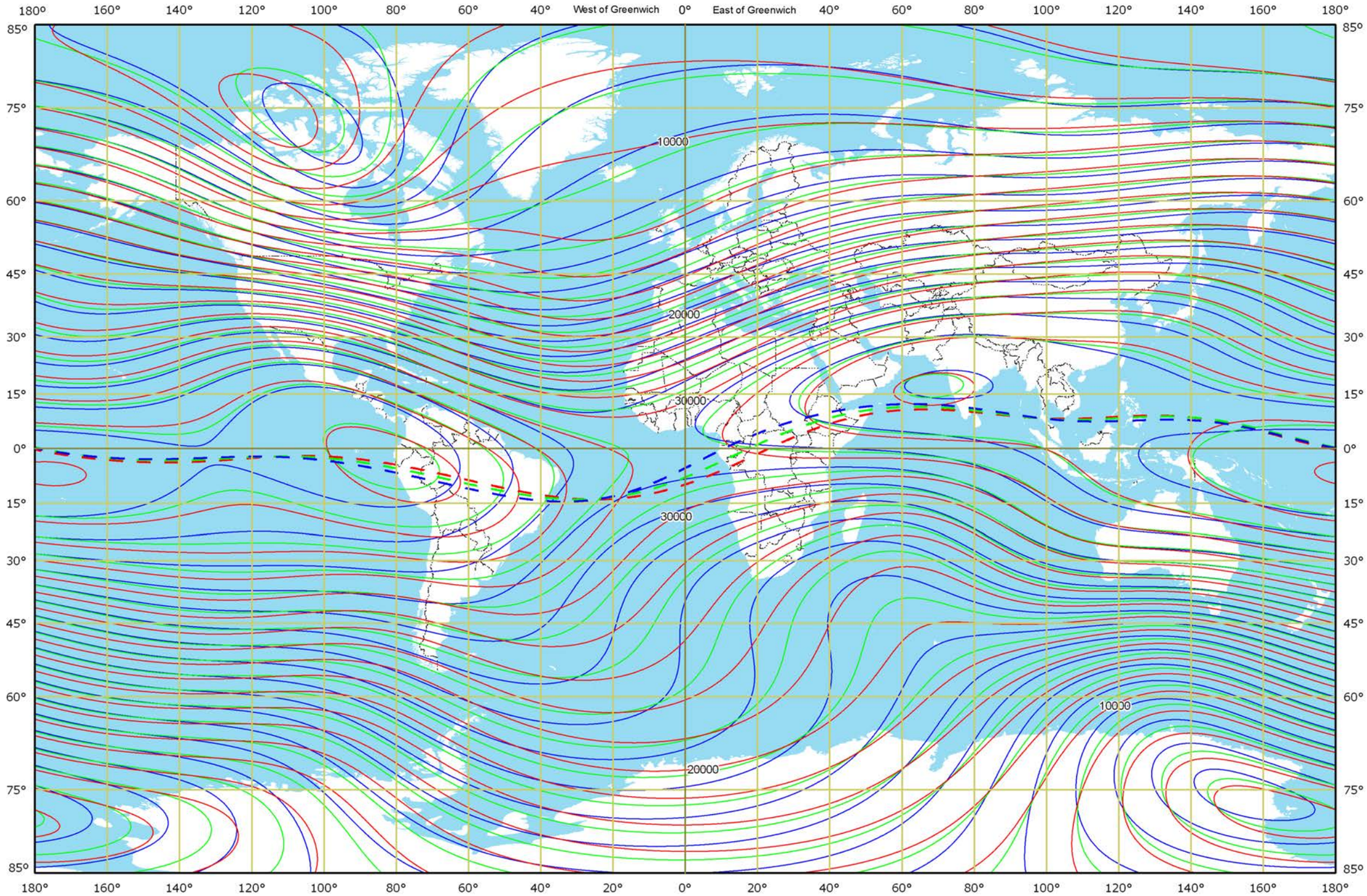

Years	Isolines	Geomagnetic equators
1750		1750
1775		1775
1800		1800

Example of magnetic field component value, nT

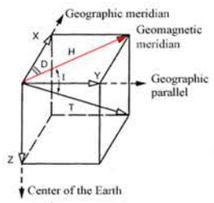

MGMF vector components

D Declination
I Inclination
H Horizontal component
T Total intensity
X North component
Y East component
Z Vertical component

Scale 1: 120 000 000

Projection: Miller cylindrical

HORIZONTAL COMPONENT OF MGMF

MGMF – 1800, 1825, 1850 – H

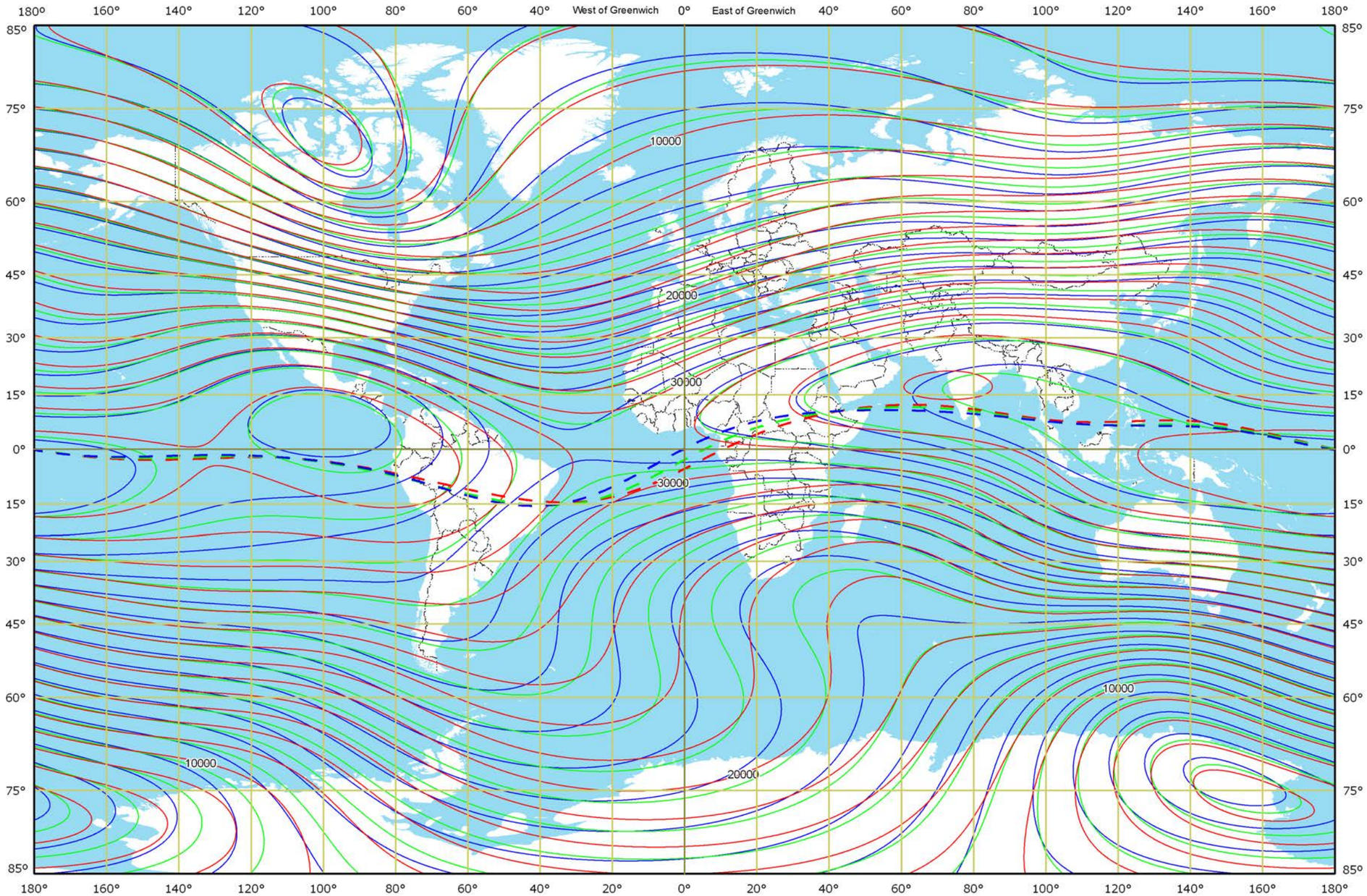

Years	Isolines	Geomagnetic equators
1800		1800
1825		1825
1850		1850

Example of magnetic field component value, nT

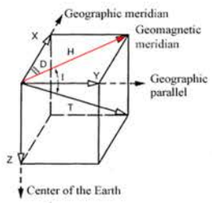

MGMF vector components

D Declination
I Inclination
H Horizontal component
T Total intensity
X North component
Y East component
Z Vertical component

Scale 1: 120 000 000

Projection: Miller cylindrical

HORIZONTAL COMPONENT OF MGMF

MGMF– 1850, 1875, 1900 – H

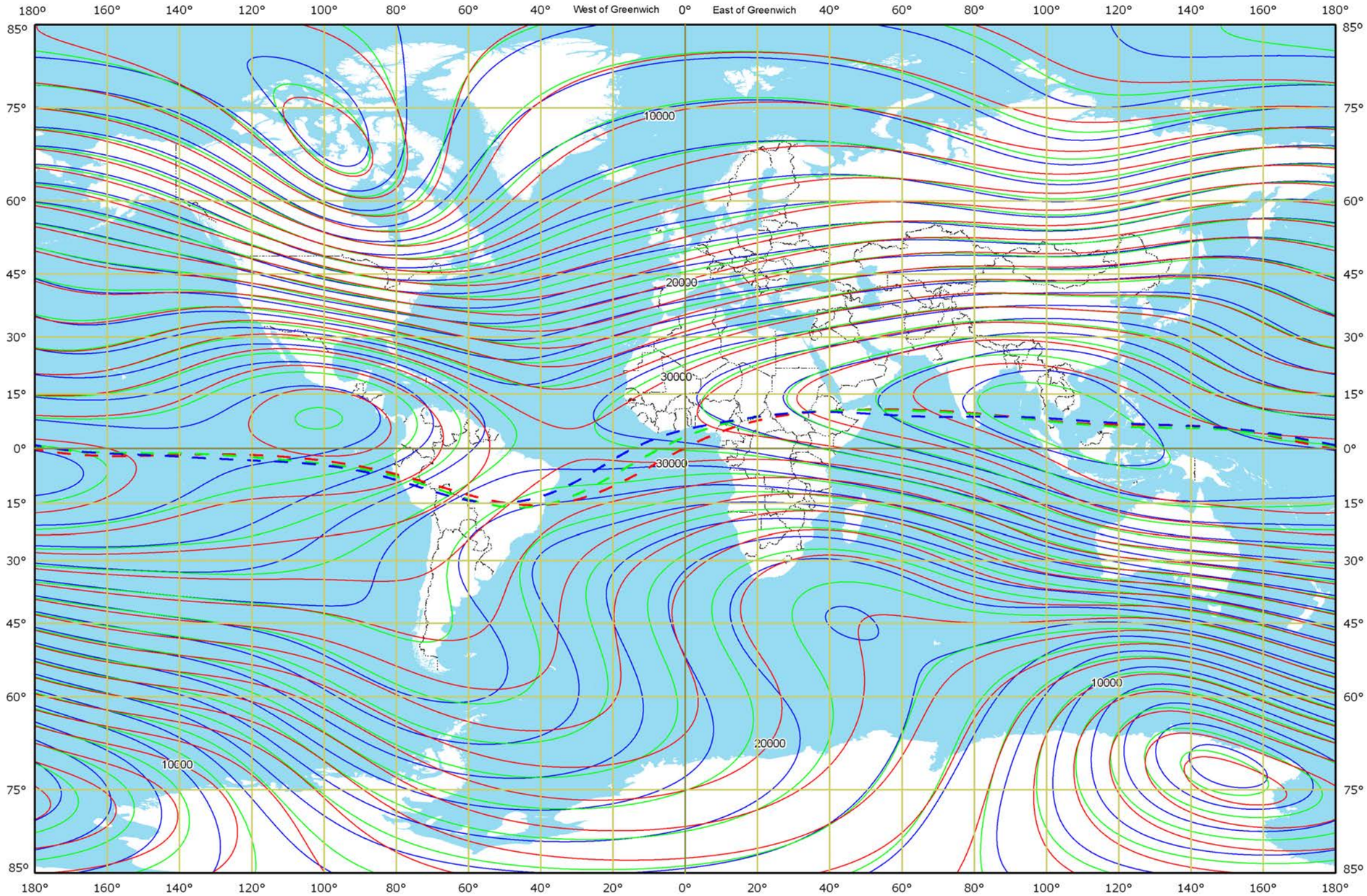

Years	Isolines	Geomagnetic equators
1850		1850
1875		1875
1900		1900

Example of magnetic field component value, nT

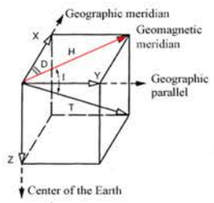

MGMF vector components

D Declination
I Inclination
H Horizontal component
T Total intensity
X North component
Y East component
Z Vertical component

Scale 1: 120 000 000

Projection: Miller cylindrical

MGMF TOTAL INTENSITY

MGMF – 1500, 1525, 1550 – FM (T)

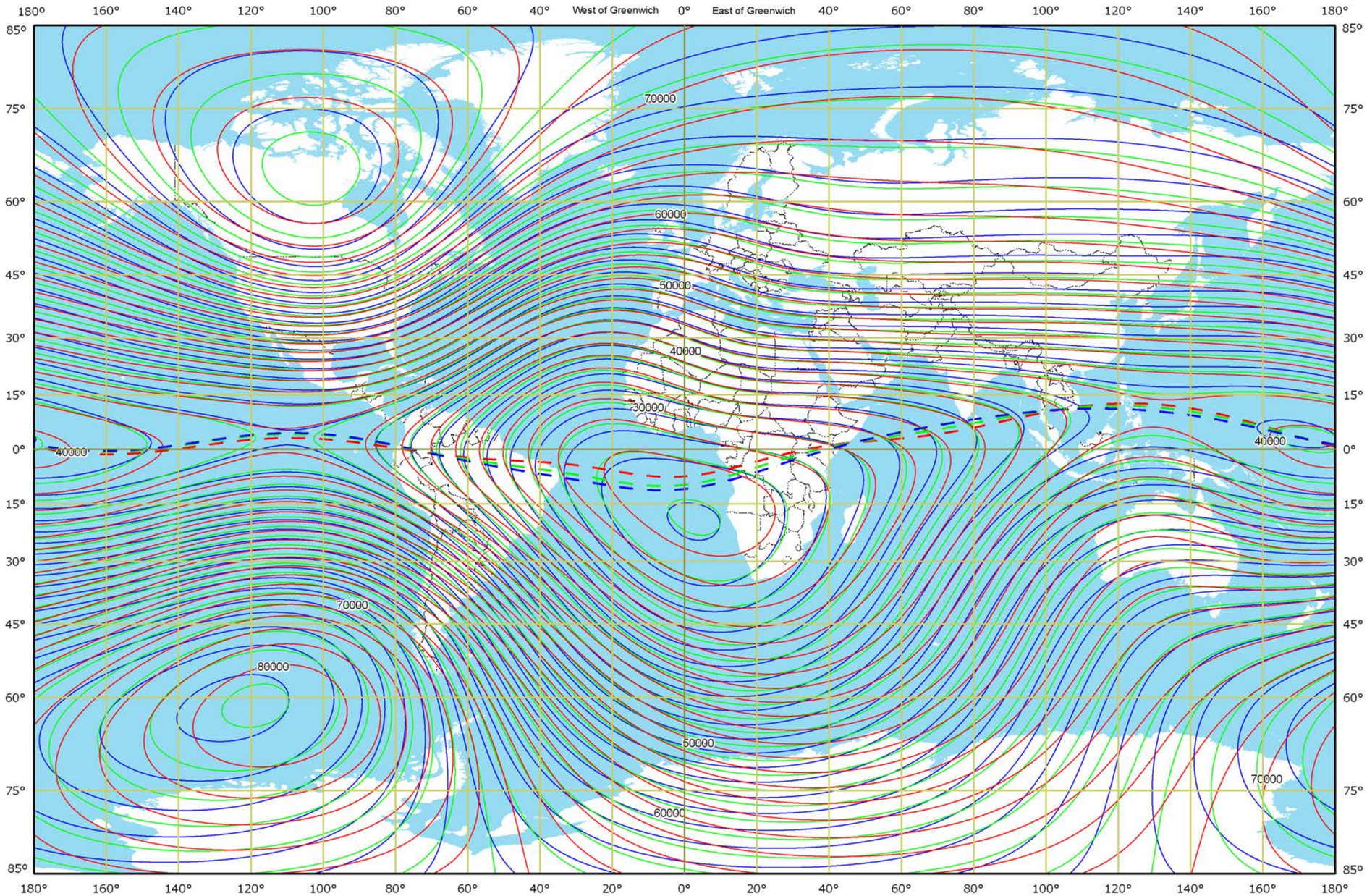

Years | Isolines | Geomagnetic equators

1500
1525
1550

1500
1525
1550

Example of magnetic total intensity value, nT

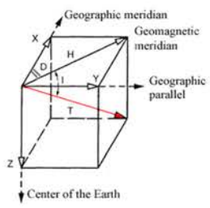

MGMF vector components

D Declination
I Inclination
H Horizontal component
T Total intensity
X North component
Y East component
Z Vertical component

Scale 1: 120 000 000

Projection: Miller cylindrical

MGMF TOTAL INTENSITY

MGMF – 1550, 1575, 1600 – FM (T)

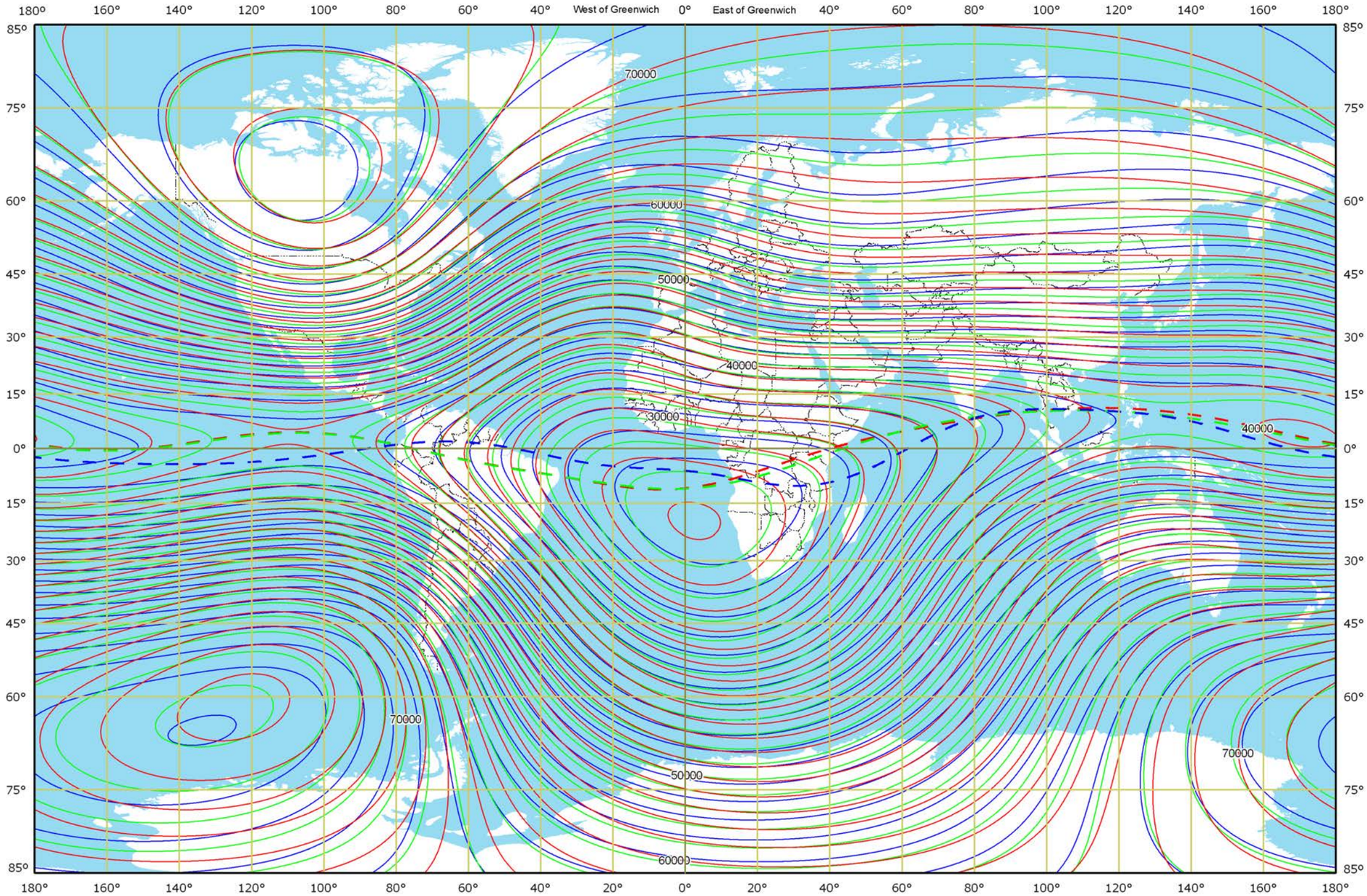

Years	Isolines	Geomagnetic equators
1550		1550
1575		1575
1600		1600

Example of magnetic total intensity value, nT

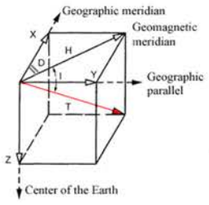

MGMF vector components

D Declination
I Inclination
H Horizontal component
T Total intensity
X North component
Y East component
Z Vertical component

Scale 1: 120 000 000

Projection: Miller cylindrical

MGMF TOTAL INTENSITY

MGMF – 1600, 1625, 1650 – FM (T)

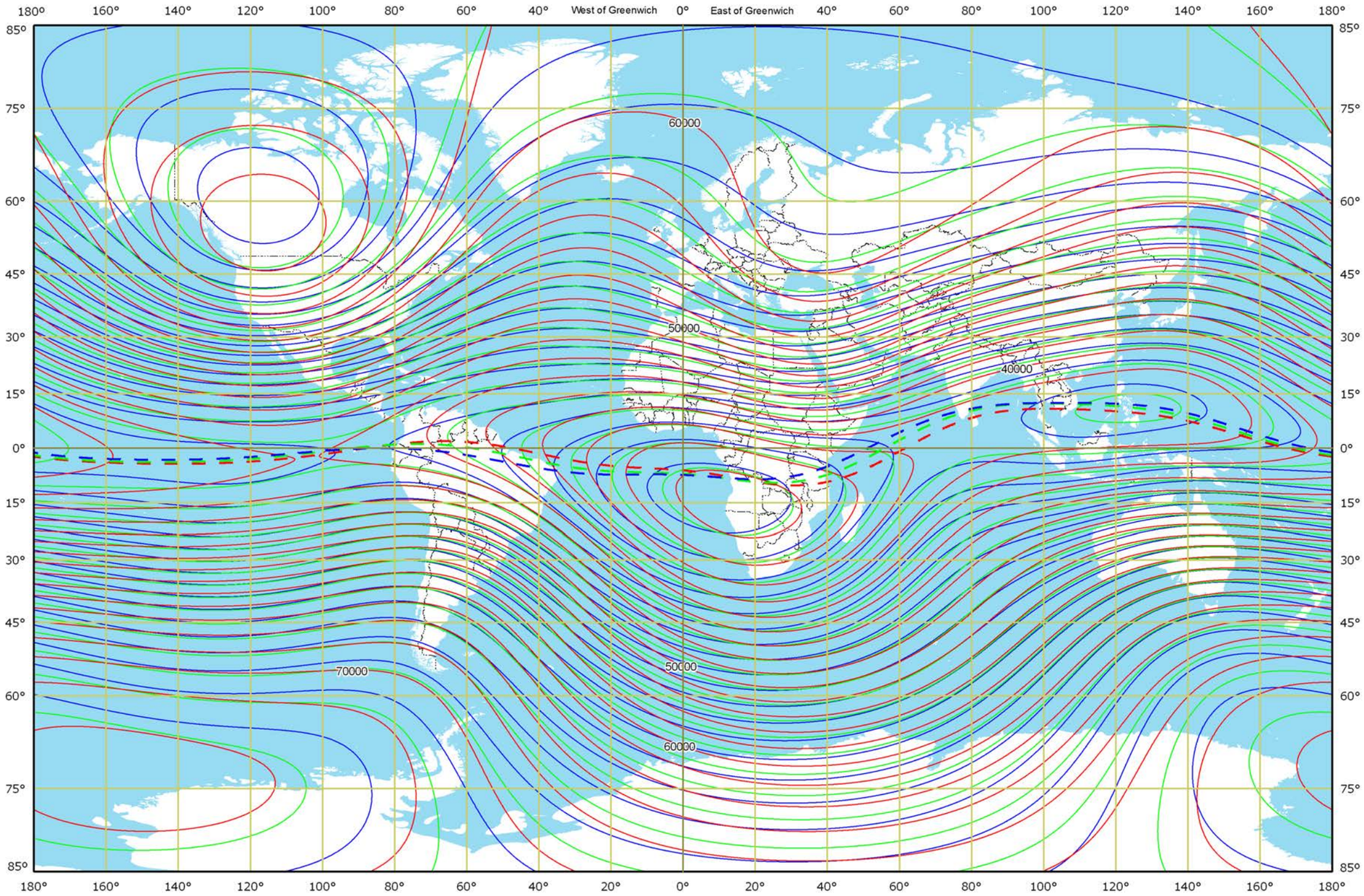

Years	Isolines	Geomagnetic equators
1600		1600
1625		1625
1650		1650

Example of magnetic total intensity value, nT

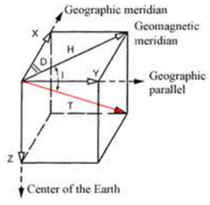

MGMF vector components

D Declination
I Inclination
H Horizontal component
T Total intensity
X North component
Y East component
Z Vertical component

Scale 1: 120 000 000

Projection: Miller cylindrical

MGMF TOTAL INTENSITY

MGMF – 1650, 1675, 1700 – FM (T)

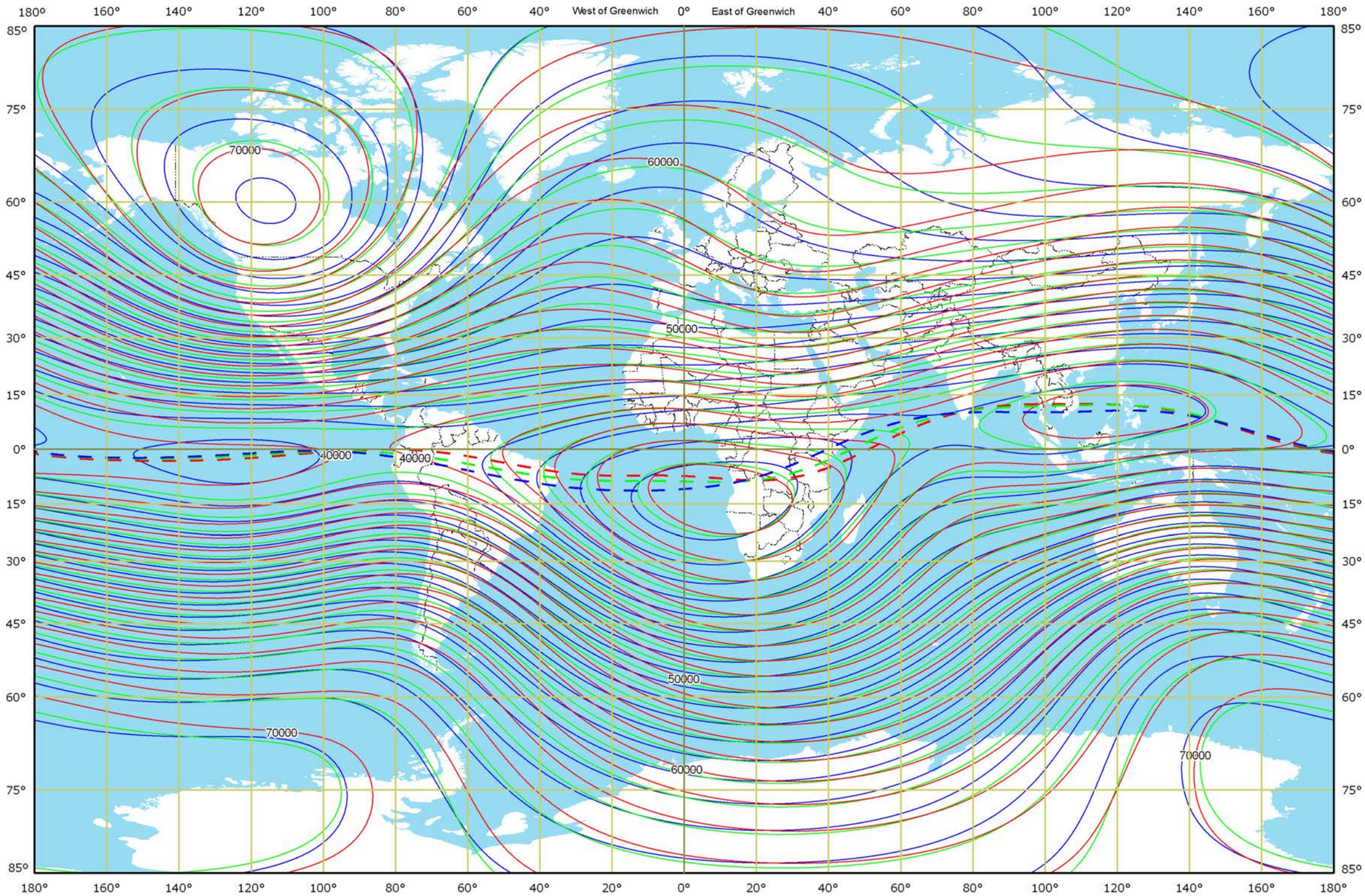

Years	Isolines	Geomagnetic equators
1650		1650
1675		1675
1700		1700

Example of magnetic total intensity value, nT

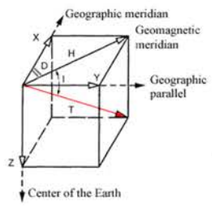

MGMF vector components

D Declination
I Inclination
H Horizontal component
T Total intensity
X North component
Y East component
Z Vertical component

Scale 1: 120 000 000

Projection: Miller cylindrical

MGMF TOTAL INTENSITY

MGMF – 1700, 1725, 1750 – FM (T)

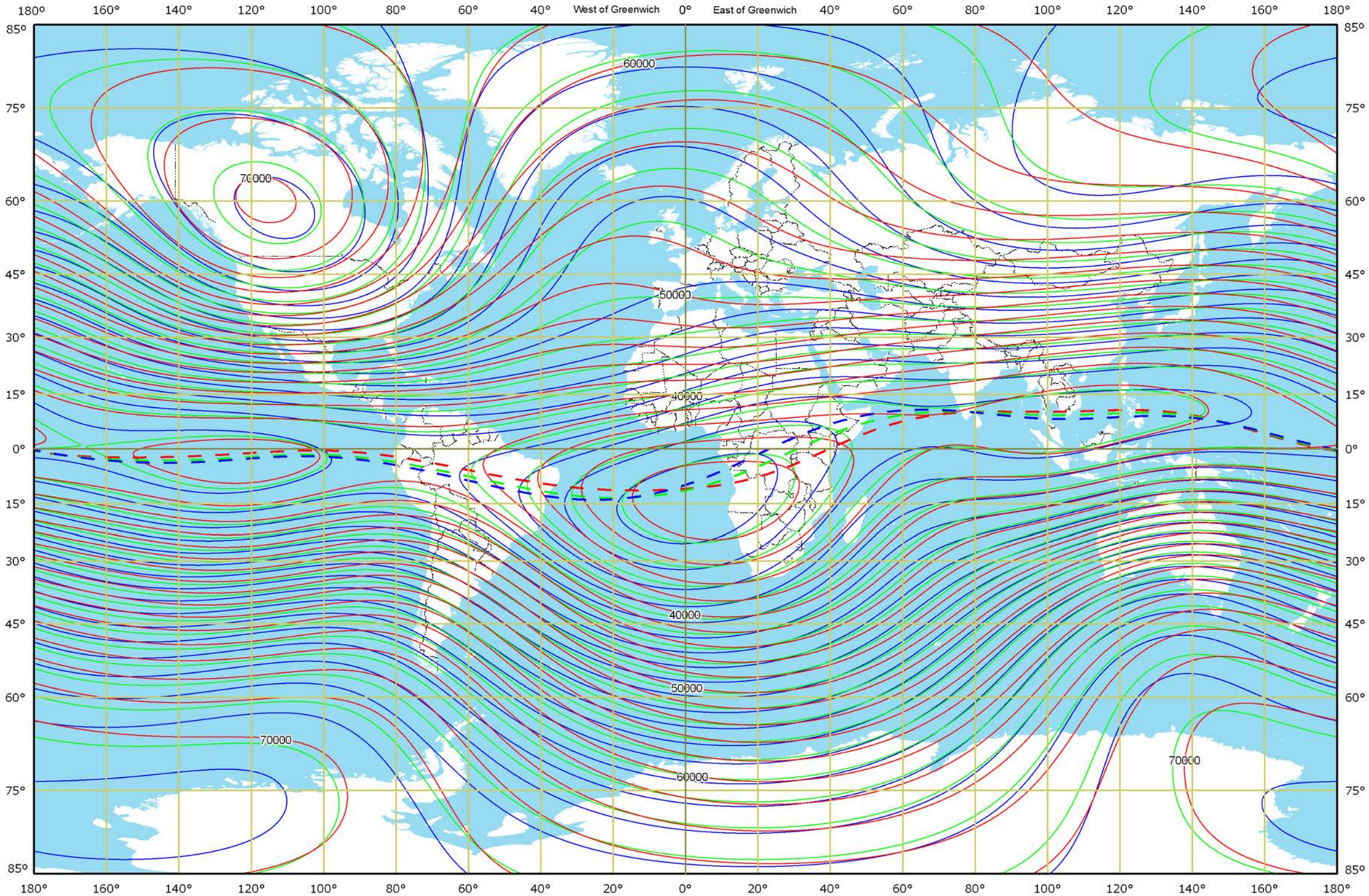

Years Isolines Geomagnetic equators

1700 1700
1725 1725
1750 1750

Example of magnetic total intensity value, nT

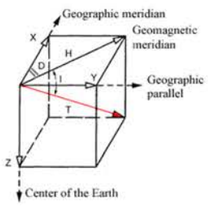

MGMF vector components

D Declination
I Inclination
H Horizontal component
T Total intensity
X North component
Y East component
Z Vertical component

Scale 1: 120 000 000

Projection: Miller cylindrical

MGMF TOTAL INTENSITY

MGMF – 1750, 1775, 1800 – FM (T)

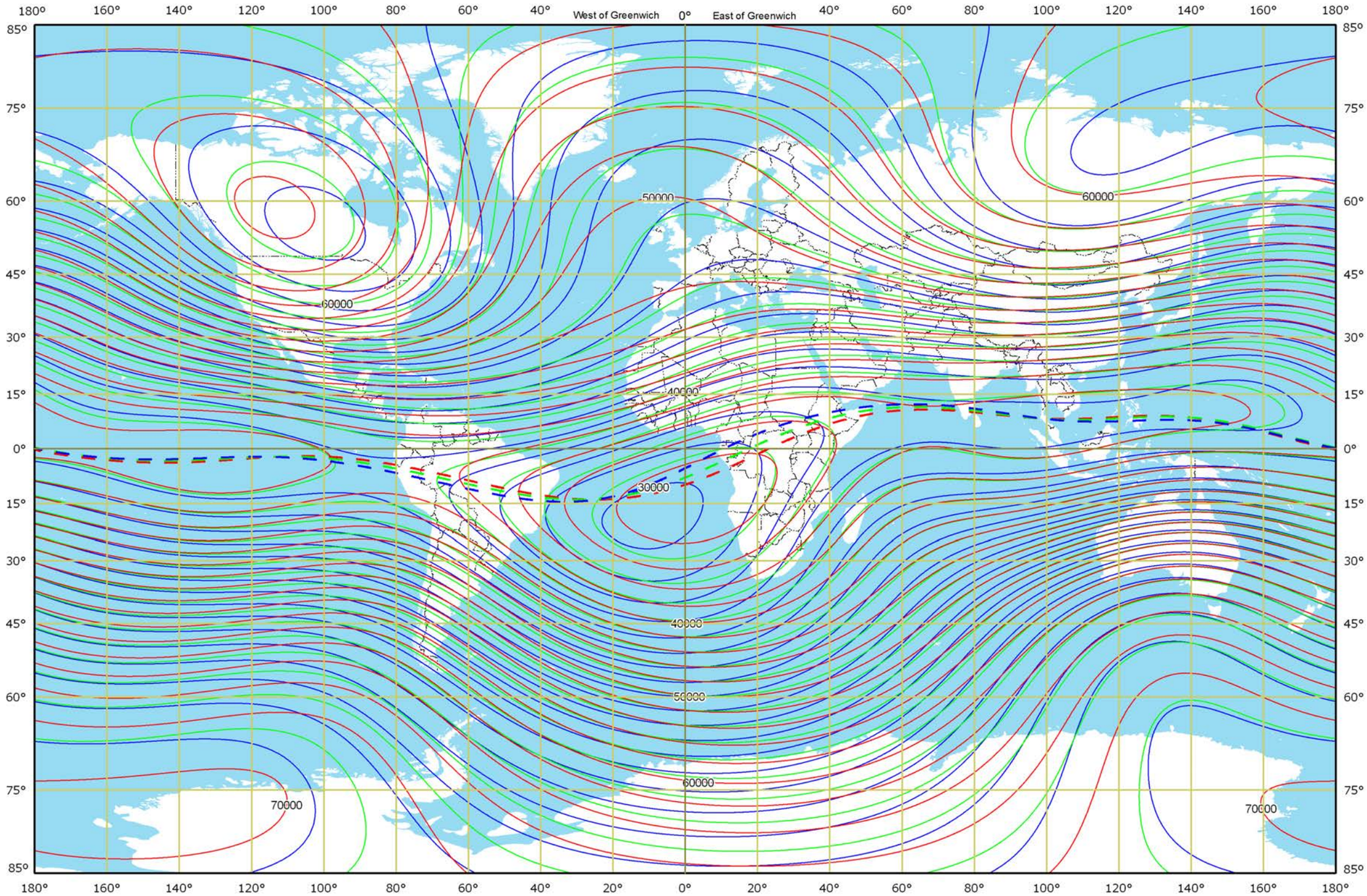

Years	Isolines	Geomagnetic equators
1800		1800
1825		1825
1850		1850

Example of magnetic total intensity value, nT

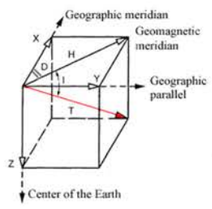

MGMF vector components

D Declination
I Inclination
H Horizontal component
T Total intensity
X North component
Y East component
Z Vertical component

Scale 1: 120 000 000

Projection: Miller cylindrical

MGMF TOTAL INTENSITY

MGMF – 1800, 1825, 1850 – FM (T)

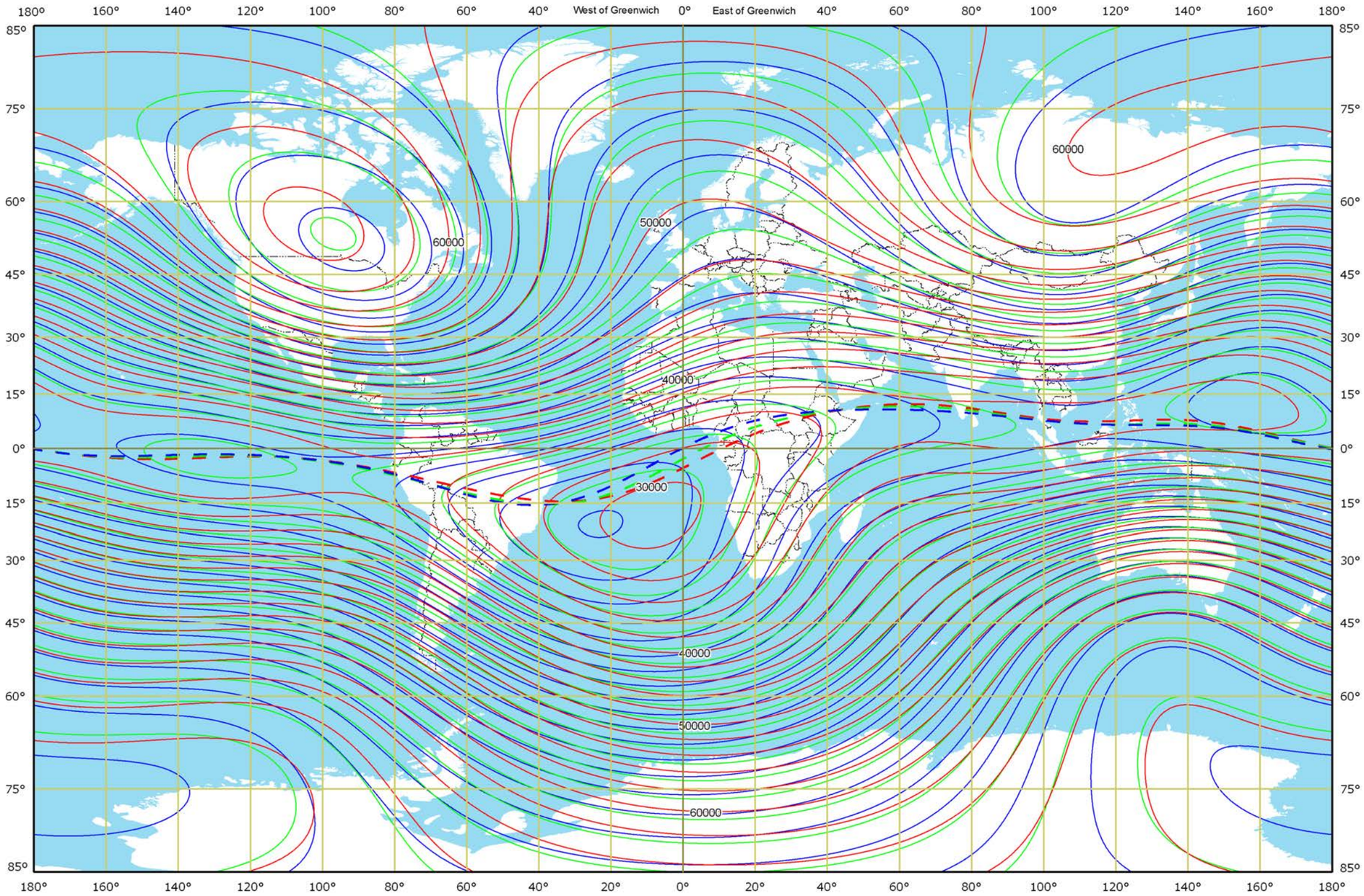

Years	Isolines	Geomagnetic equators
1800		1800
1825		1825
1850		1850

Example of magnetic total intensity value, nT

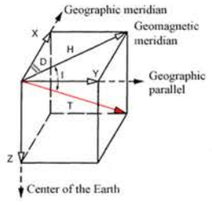

MGMF vector components

D Declination
I Inclination
H Horizontal component
T Total intensity
X North component
Y East component
Z Vertical component

Scale 1: 120 000 000

Projection: Miller cylindrical

MGMF TOTAL INTENSITY

MGMF – 1850, 1875, 1900 – FM (T)

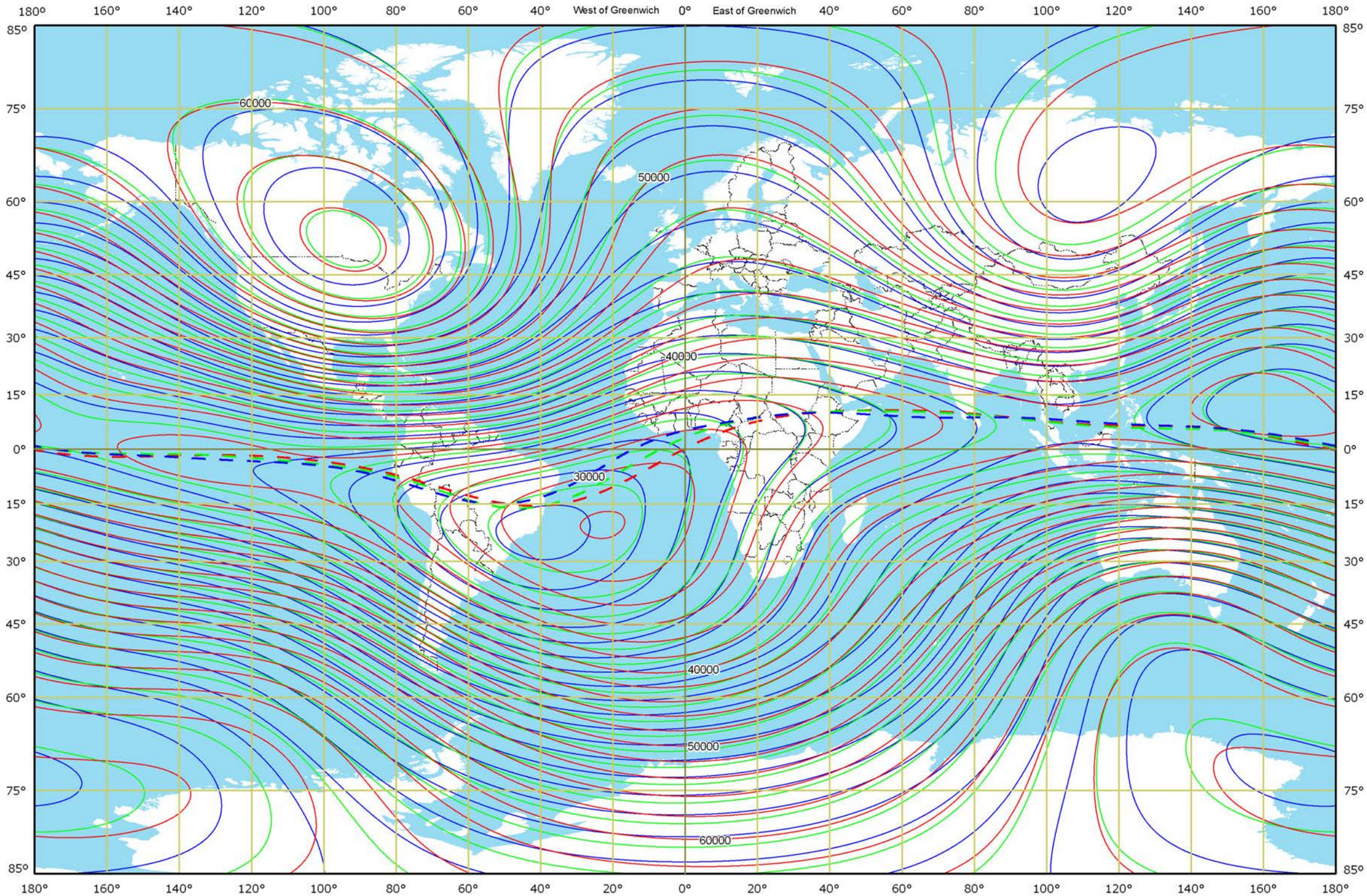

Years	Isolines	Geomagnetic equators
1850		1850
1875		1875
1900		1900

Example of magnetic total intensity value, nT

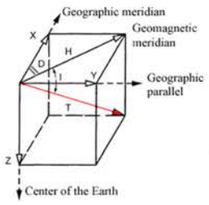

MGMF vector components

D Declination
I Inclination
H Horizontal component
T Total intensity
X North component
Y East component
Z Vertical component

Scale 1: 120 000 000

Projection: Miller cylindrical

SECULAR VARIATION OF VERTICAL COMPONENT OF MGMF

SV – 1902, 1907 – Z

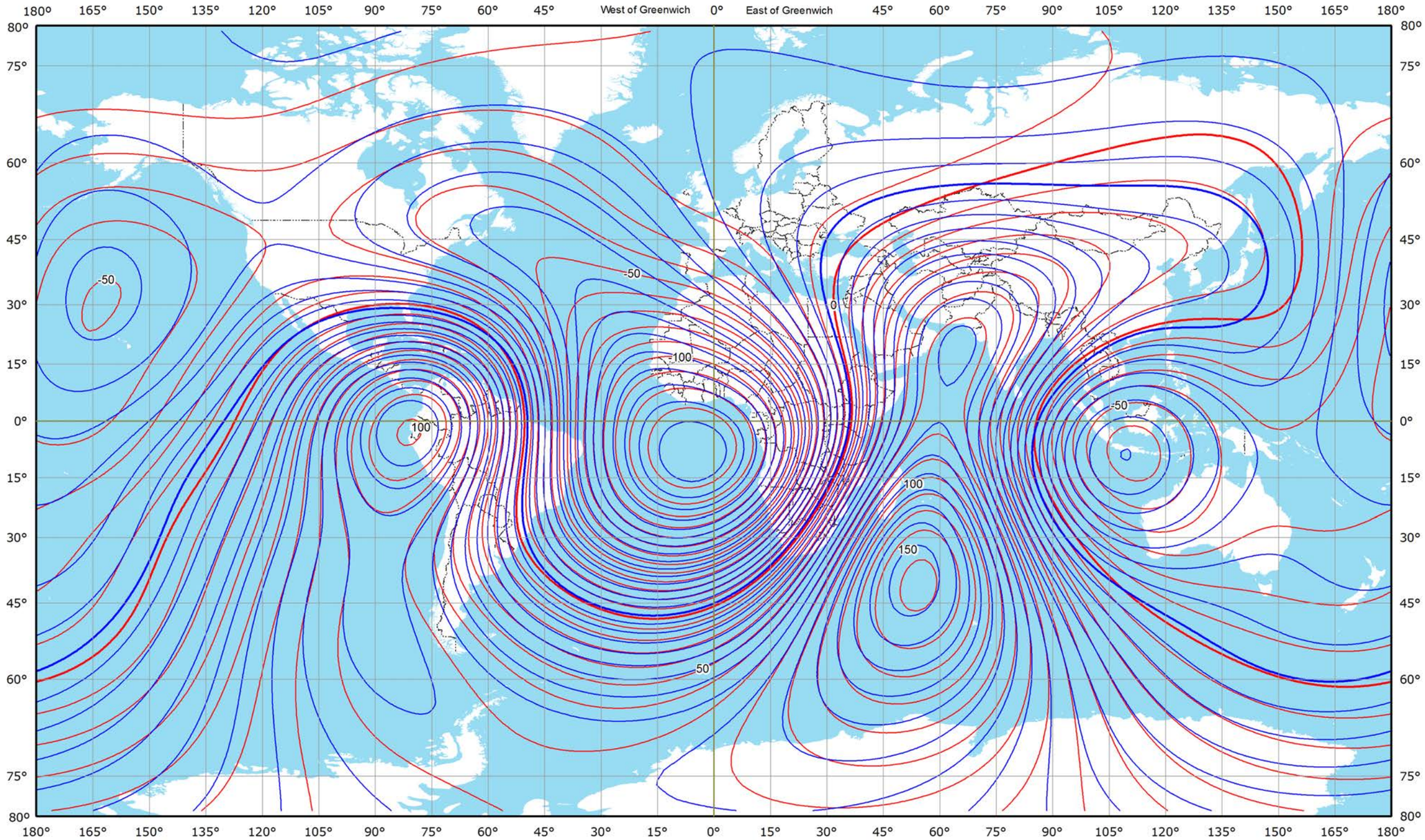

Epoch Isopors

1902
1907

Example. Secular variation value of vertical component of MGMF (nT/year)

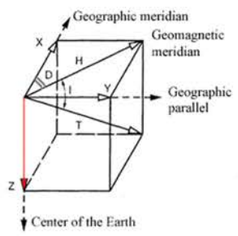

MGMF vector components

D Declination
I Inclination
H Horizontal component
T Total intensity
X North component
Y East component
Z Vertical component

Scale 1: 120 000 000

Projection: Miller cylindrical

SECULAR VARIATION OF VERTICAL COMPONENT OF MGMF

SV – 1907, 1912 – Z

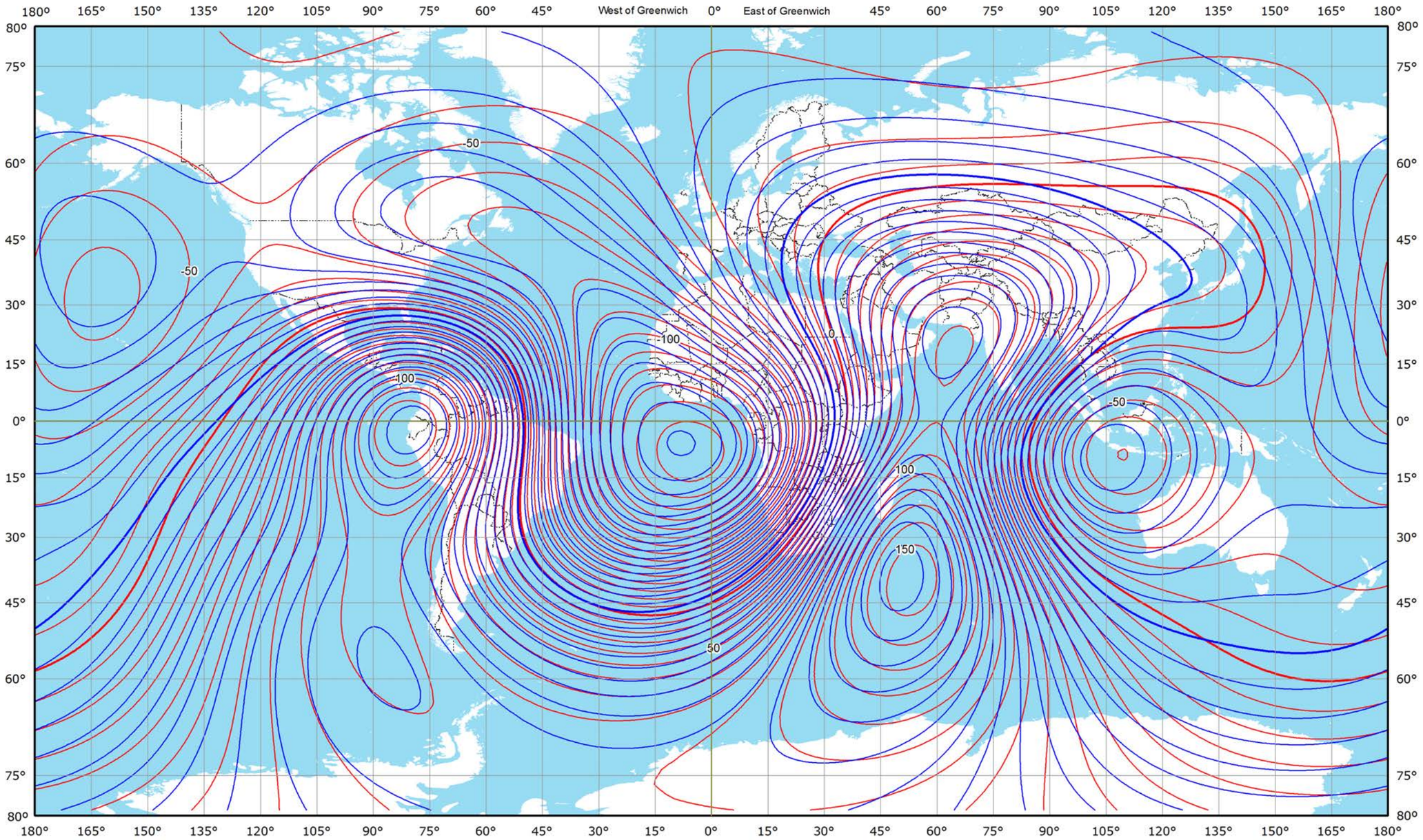

Epoch Isopors

1907
1912

Example. Secular variation value of vertical component of MGMF (nT/year)

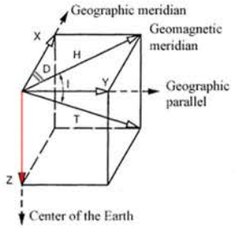

MGMF vector components

D Declination
I Inclination
H Horizontal component
T Total intensity
X North component
Y East component
Z Vertical component

Scale 1: 120 000 000

Projection: Miller cylindrical

SECULAR VARIATION OF VERTICAL COMPONENT OF MGMF

SV – 1912, 1917 – Z

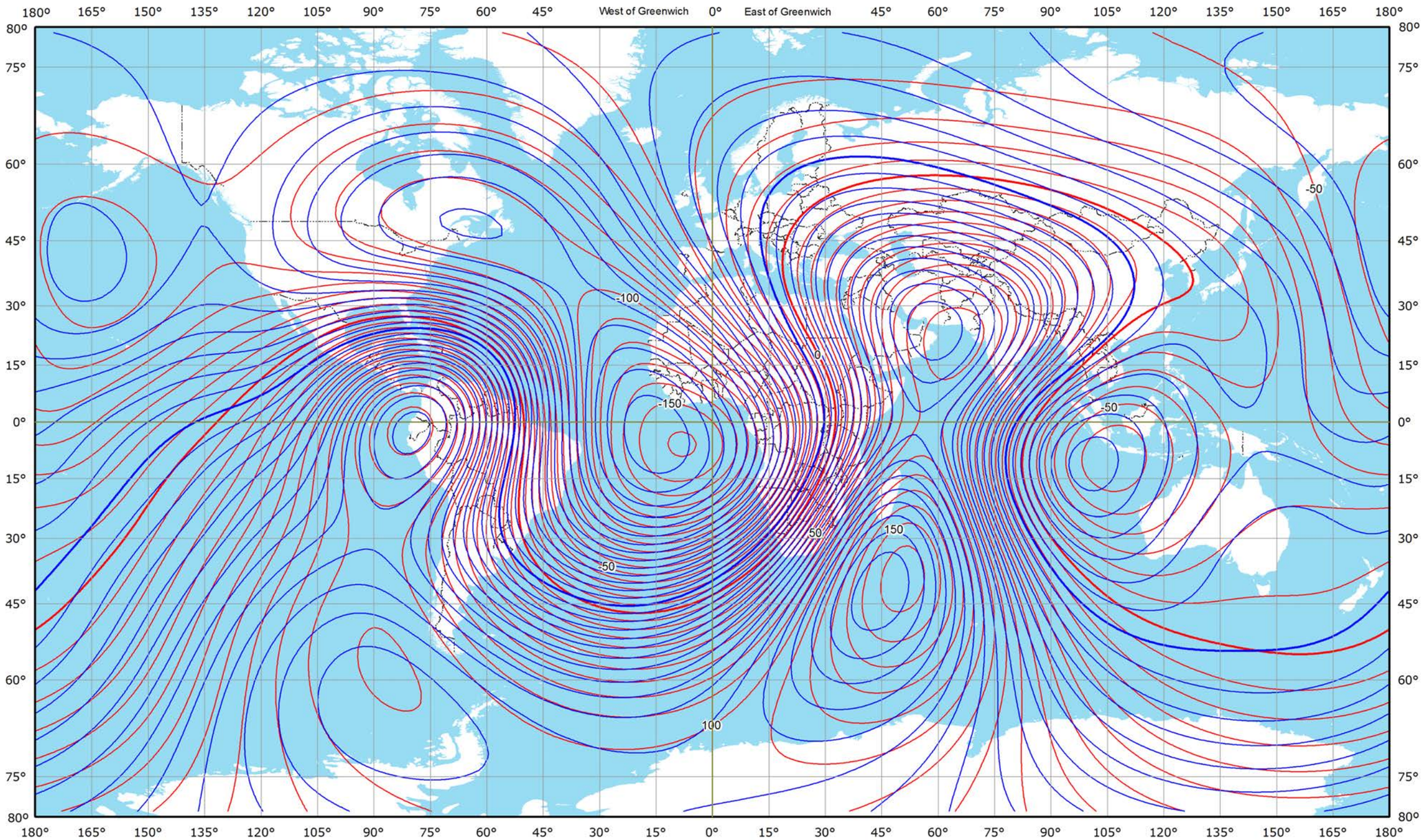

Epoch Isopors

1912
1917

Example. Secular variation value of vertical component of MGMF (nT/year)

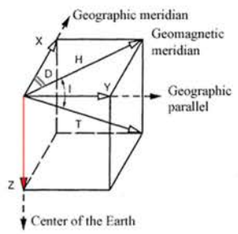

MGMF vector components

D Declination
I Inclination
H Horizontal component
T Total intensity
X North component
Y East component
Z Vertical component

Scale 1: 120 000 000

Projection: Miller cylindrical

SECULAR VARIATION OF VERTICAL COMPONENT OF MGMF

SV – 1917, 1922 – Z

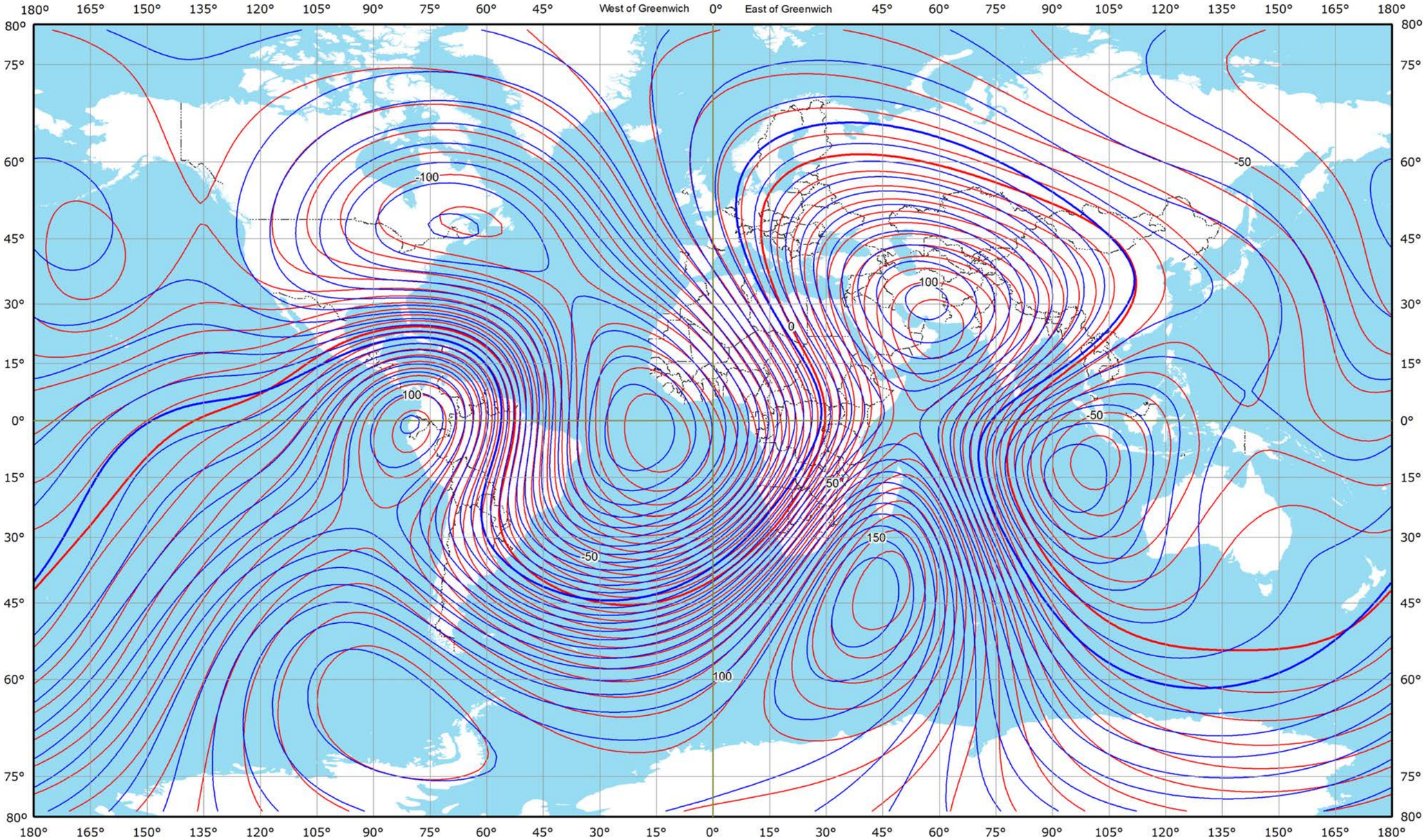

Epoch Isopors

1917
1922

Example. Secular variation value of vertical component of MGMF (nT/year)

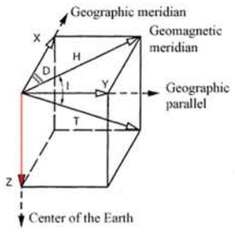

MGMF vector components

D Declination
I Inclination
H Horizontal component
T Total intensity
X North component
Y East component
Z Vertical component

Scale 1: 120 000 000

Projection: Miller cylindrical

SECULAR VARIATION OF VERTICAL COMPONENT OF MGMF

SV – 1922, 1927 – Z

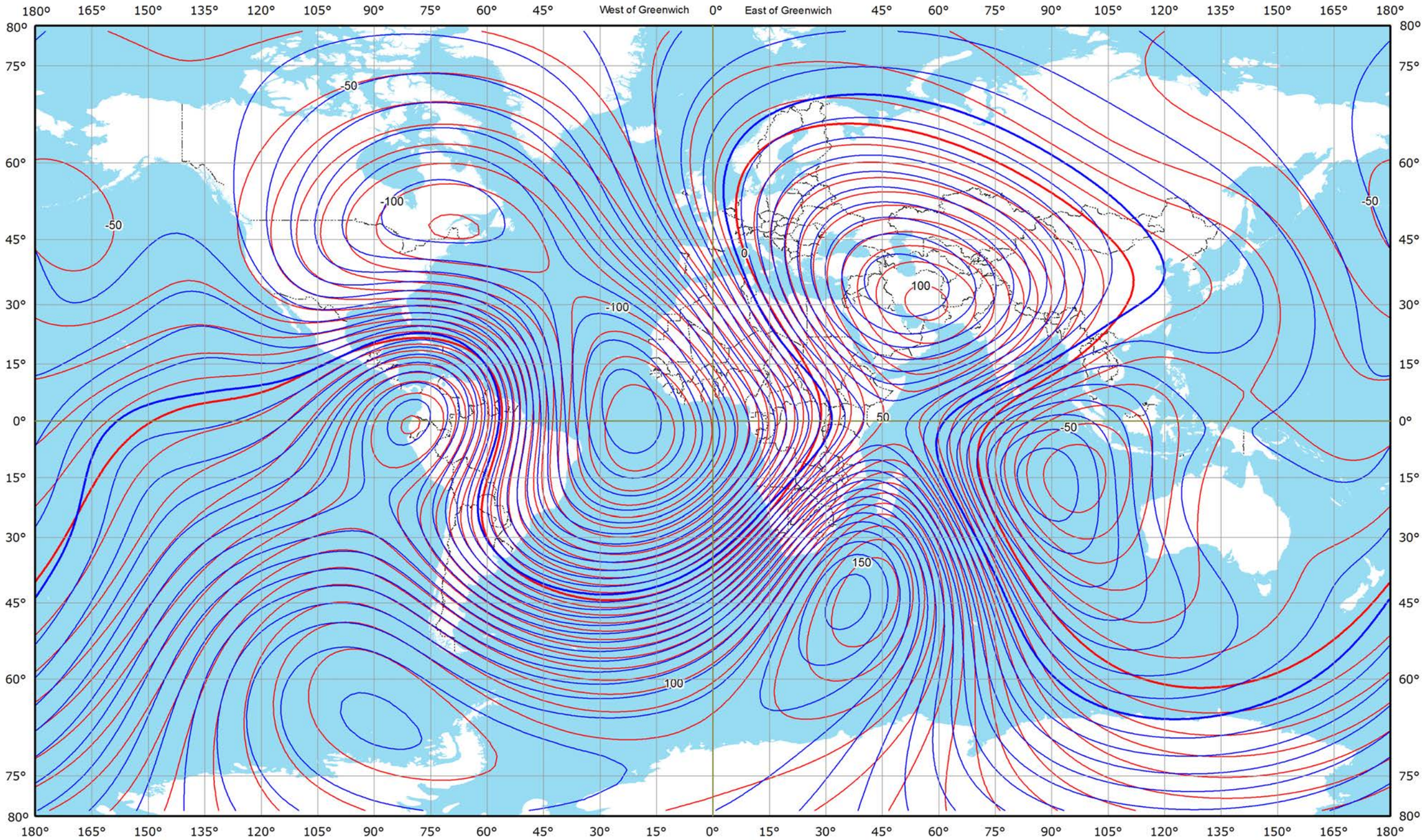

Epoch Isopors

1922
1927

Example. Secular variation value of vertical component of MGMF (nT/year)

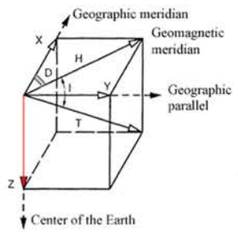

MGMF vector components

D Declination
I Inclination
H Horizontal component
T Total intensity
X North component
Y East component
Z Vertical component

Scale 1: 120 000 000

Projection: Miller cylindrical

SECULAR VARIATION OF VERTICAL COMPONENT OF MGMF

SV – 1927, 1932 – Z

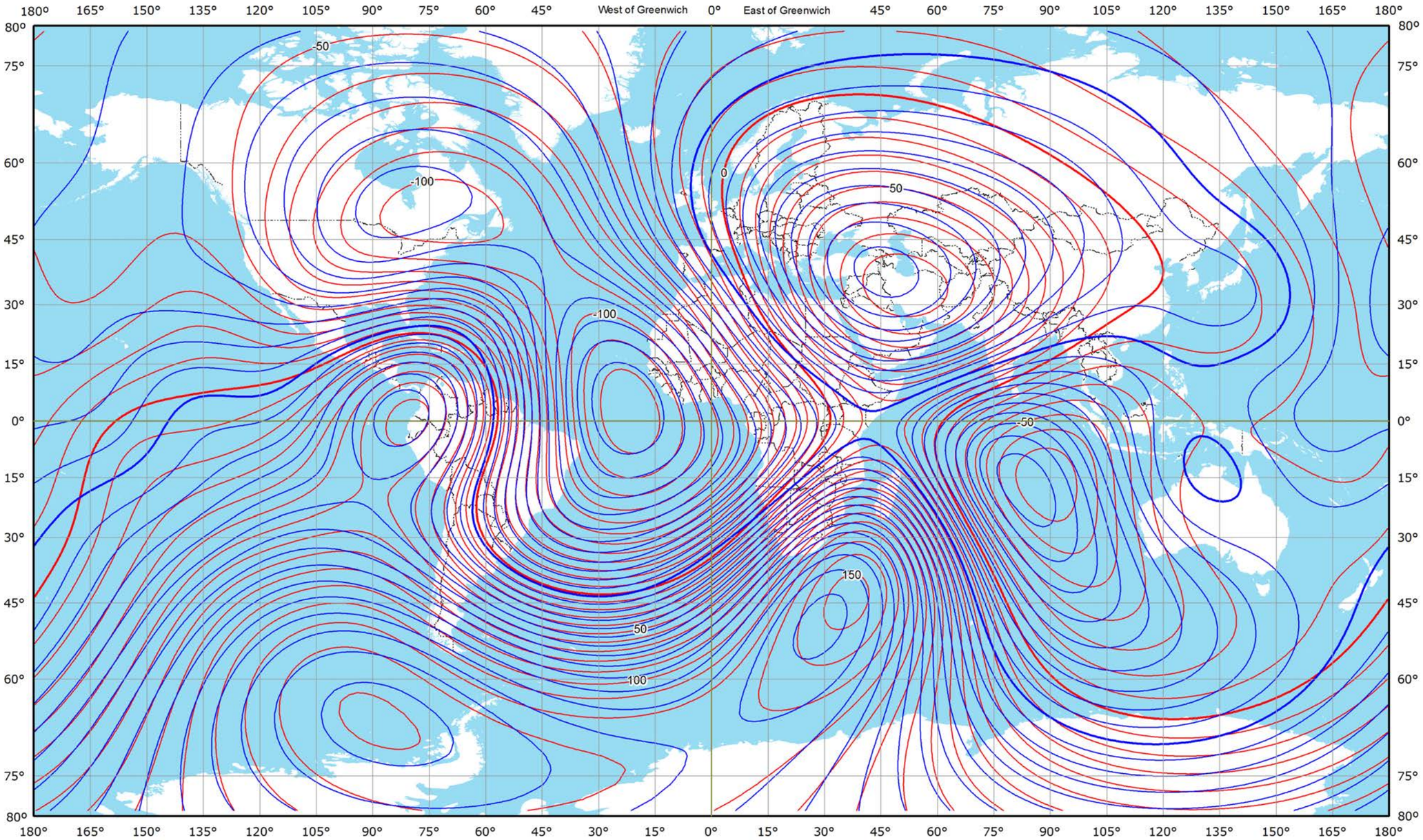

Epoch Isopors

1927
1932

Example. Secular variation value of vertical component of MGMF (nT/year)

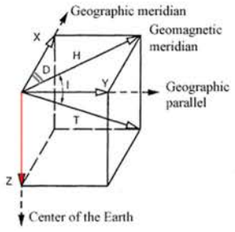

MGMF vector components

D Declination
I Inclination
H Horizontal component
T Total intensity
X North component
Y East component
Z Vertical component

Scale 1: 120 000 000

Projection: Miller cylindrical

SECULAR VARIATION OF VERTICAL COMPONENT OF MGMF

SV – 1932, 1937 – Z

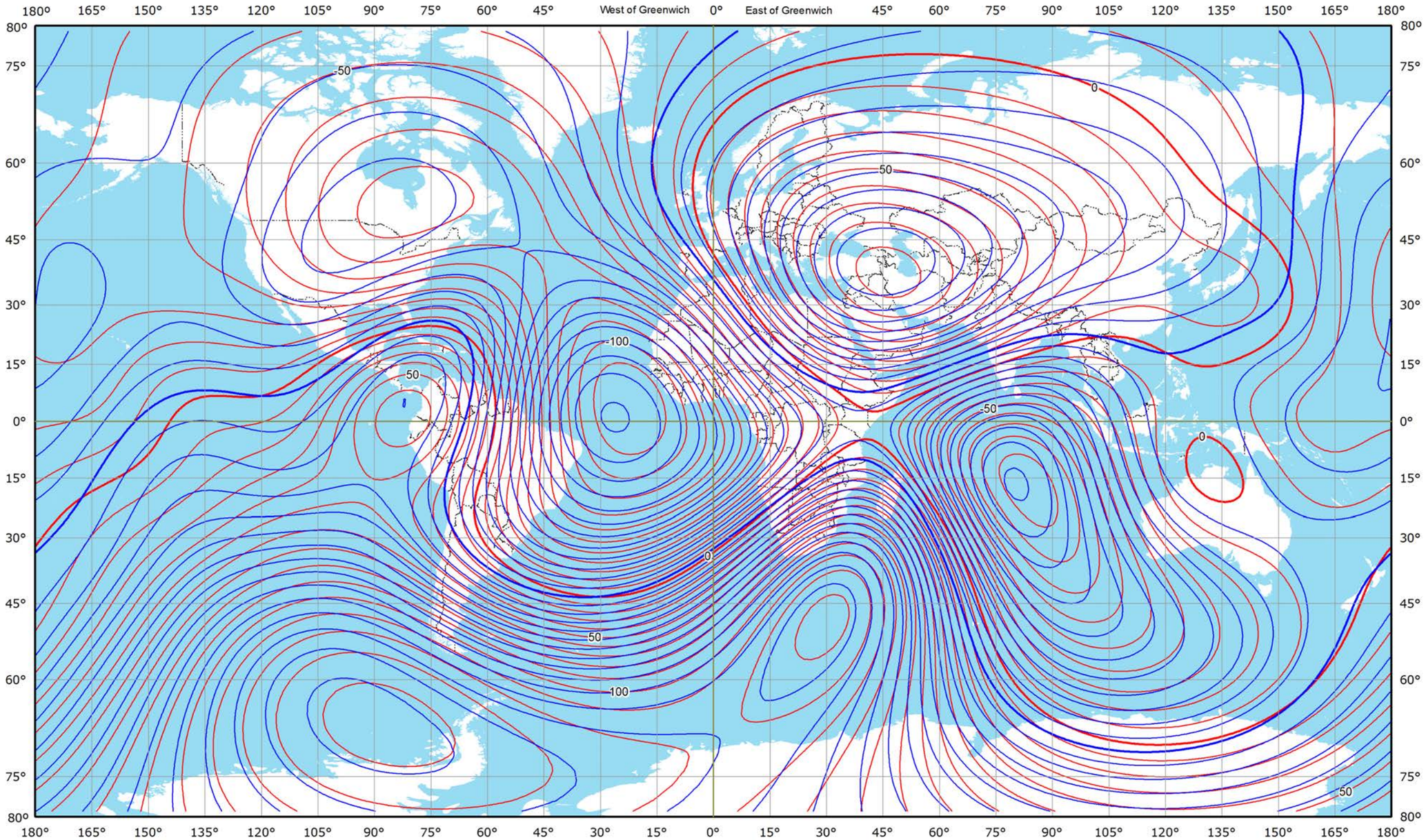

Epoch Isopors

1932
1937

Example. Secular variation value of vertical component of MGMF (nT/year)

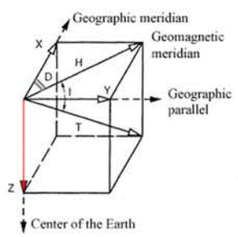

MGMF vector components

D Declination
I Inclination
H Horizontal component
T Total intensity
X North component
Y East component
Z Vertical component

Scale 1: 120 000 000

Projection: Miller cylindrical

SECULAR VARIATION OF VERTICAL COMPONENT OF MGMF

SV – 1937, 1942 – Z

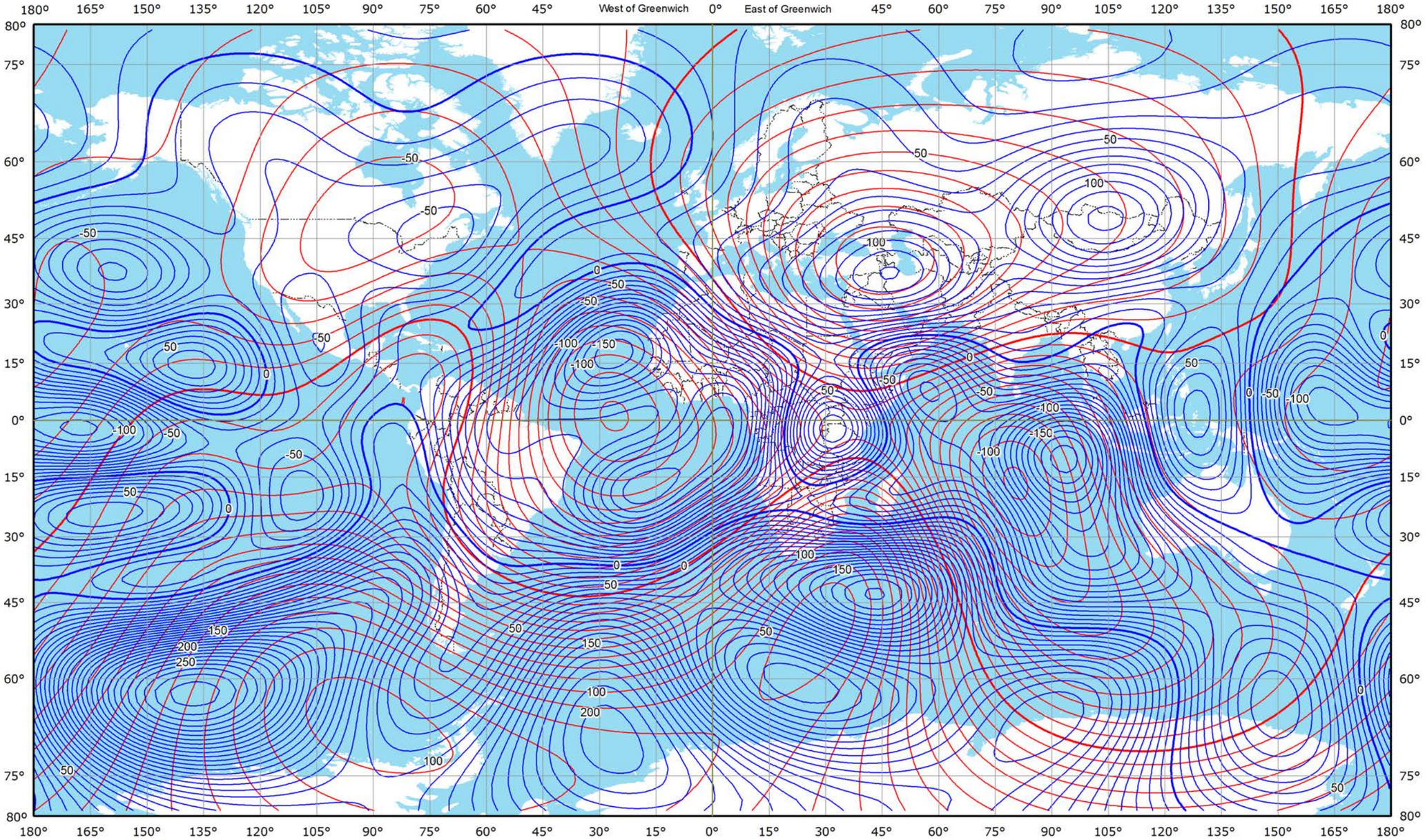

Epoch Isopors

1937
1942

Example. Secular variation value of vertical component of MGMF (nT/year)

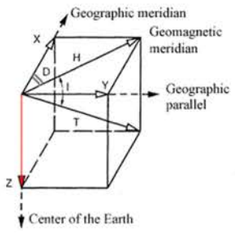

MGMF vector components

D Declination
I Inclination
H Horizontal component
T Total intensity
X North component
Y East component
Z Vertical component

Scale 1: 120 000 000

Projection: Miller cylindrical

SECULAR VARIATION OF VERTICAL COMPONENT OF MGMF

SV – 1942, 1947 – Z

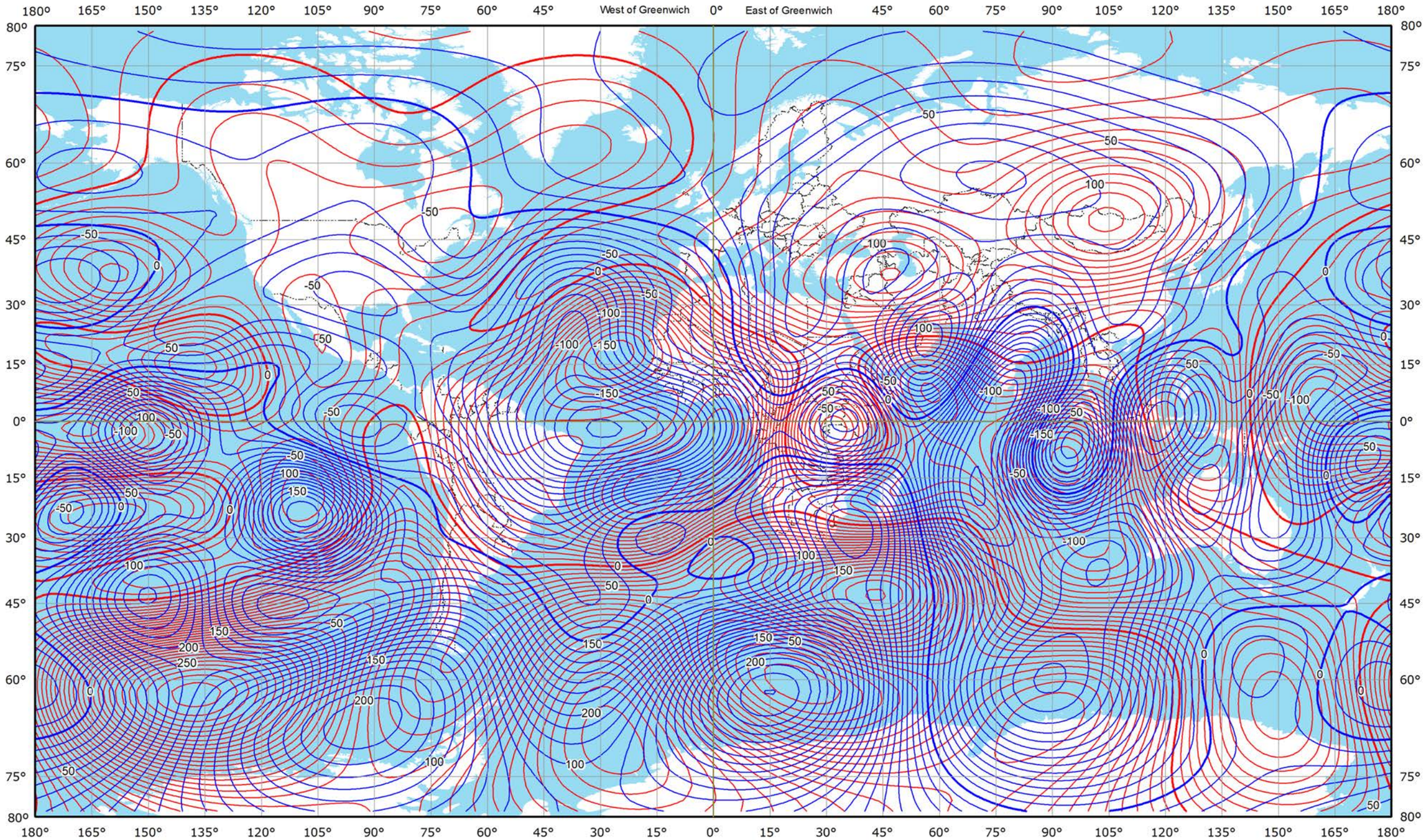

Epoch Isopors

1942
1947

Example. Secular variation value of vertical component of MGMF (nT/year)

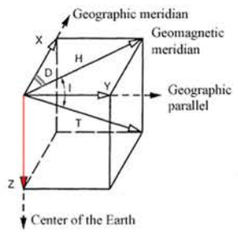

MGMF vector components

D Declination
I Inclination
H Horizontal component
T Total intensity
X North component
Y East component
Z Vertical component

Scale 1: 120 000 000

Projection: Miller cylindrical

SECULAR VARIATION OF VERTICAL COMPONENT OF MGMF

SV – 1947, 1952 – Z

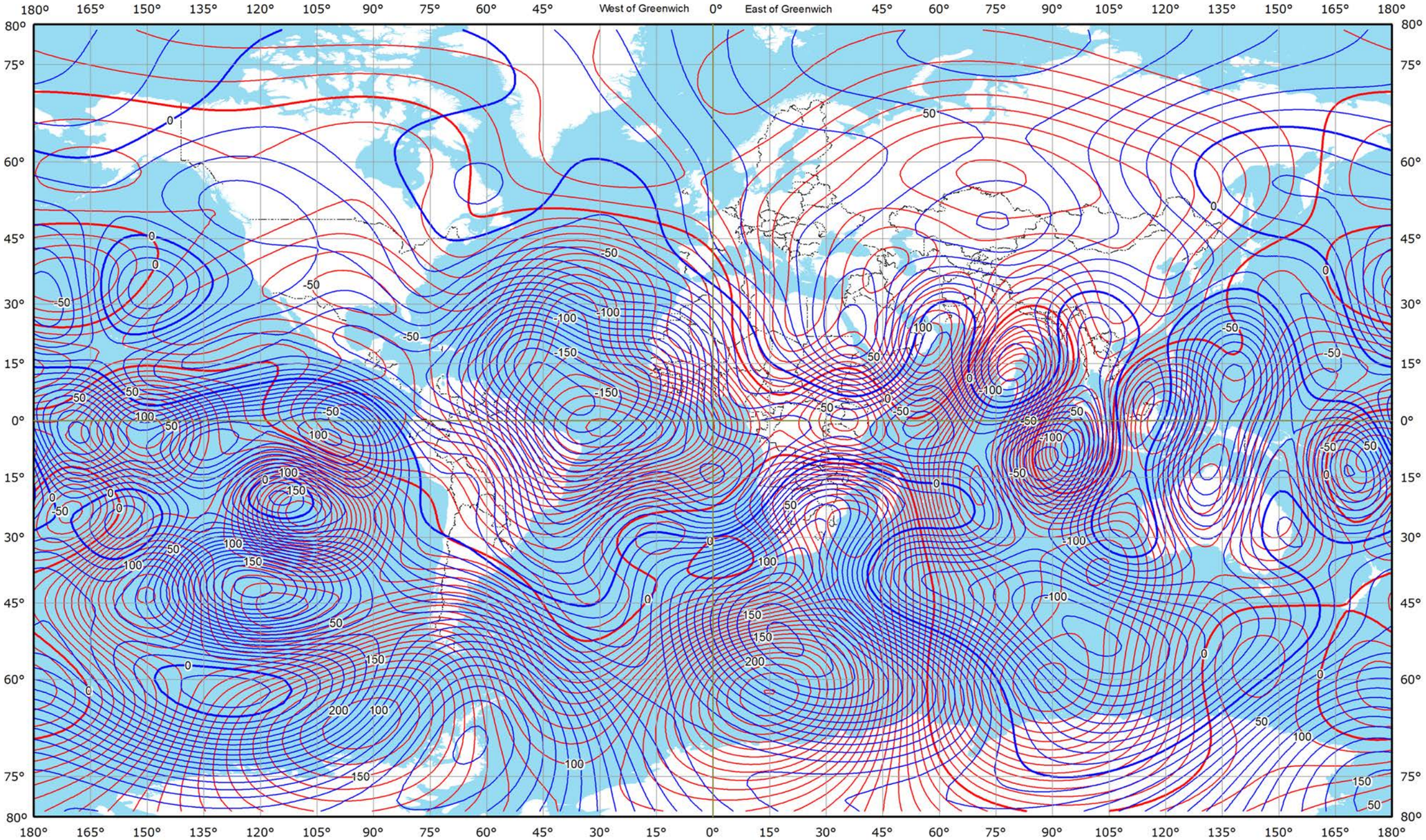

Epoch Isopors

1947
1952

Example. Secular variation value of vertical component of MGMF (nT/year)

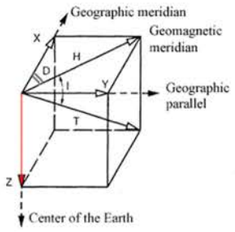

MGMF vector components

D Declination
I Inclination
H Horizontal component
T Total intensity
X North component
Y East component
Z Vertical component

Scale 1: 120 000 000

Projection: Miller cylindrical

SECULAR VARIATION OF VERTICAL COMPONENT OF MGMF

SV – 1952, 1957 – Z

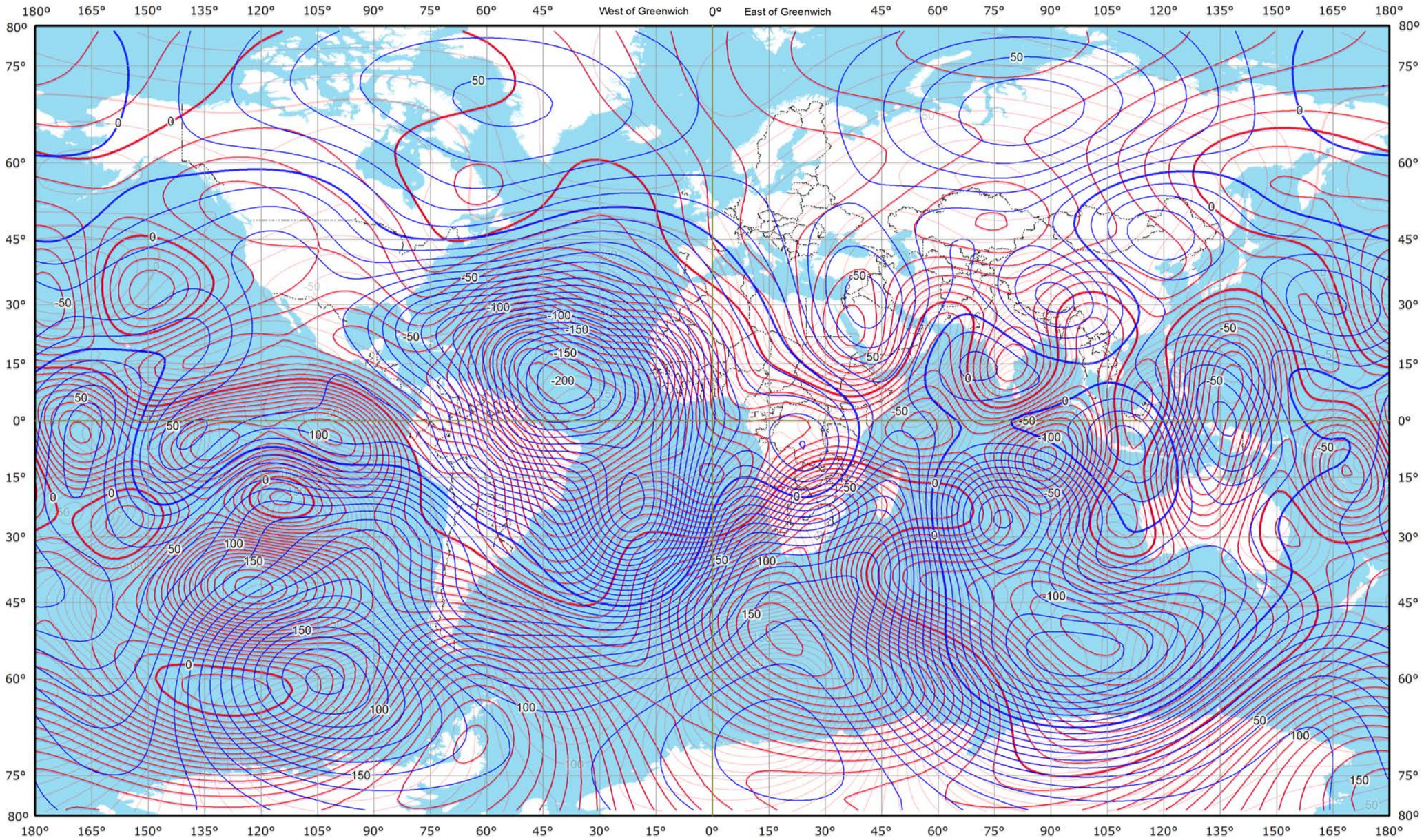

Epoch Isopors

1952
1957

Example. Secular variation value of vertical component of MGMF (nT/year)

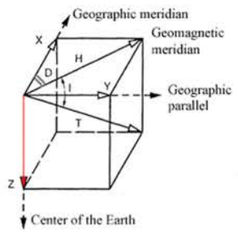

MGMF vector components

D Declination
I Inclination
H Horizontal component
T Total intensity
X North component
Y East component
Z Vertical component

Scale 1: 120 000 000

Projection: Miller cylindrical

SECULAR VARIATION OF VERTICAL COMPONENT OF MGMF

SV – 1957, 1962 – Z

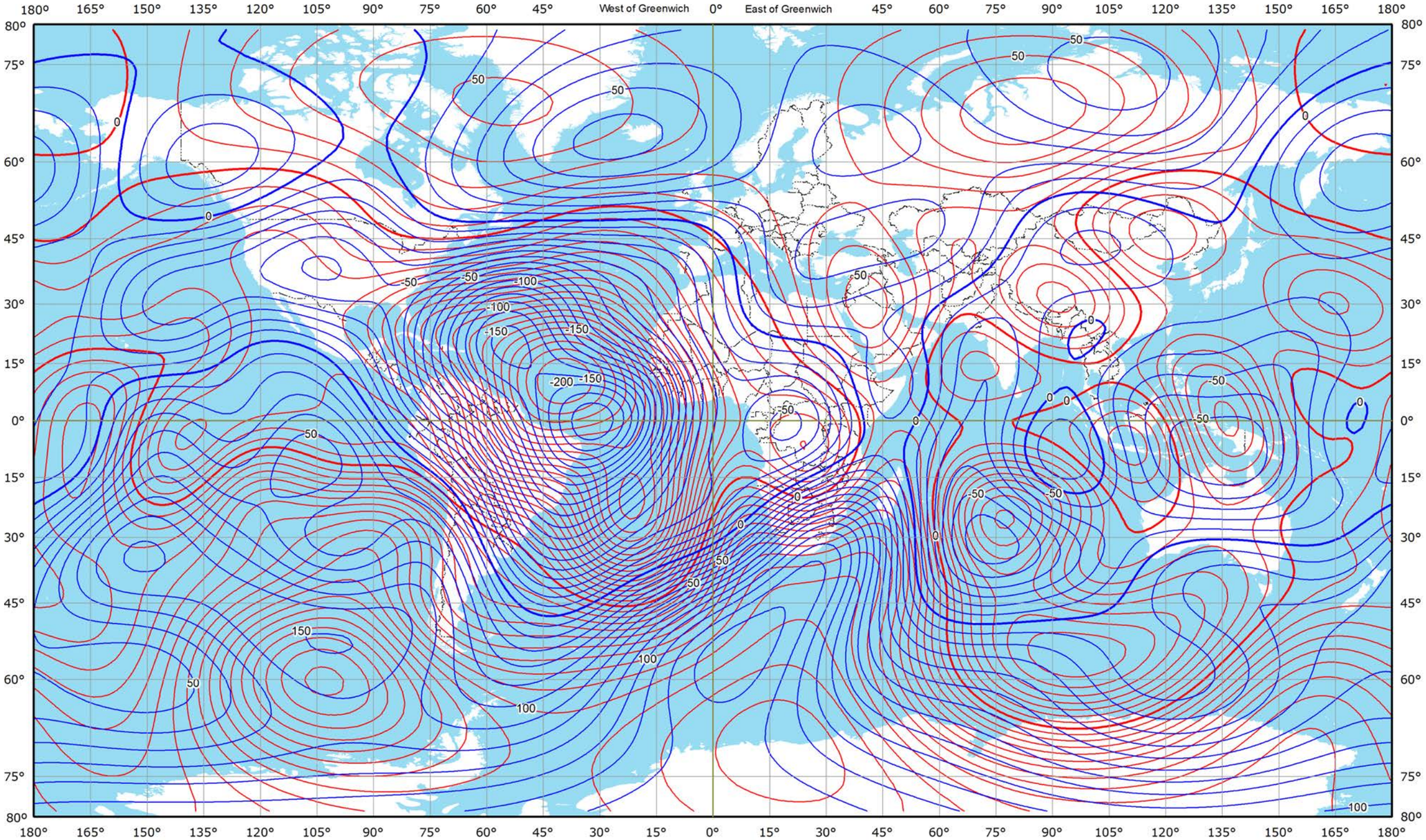

Epoch Isopors

1957
1962

Example. Secular variation value of vertical component of MGMF (nT/year)

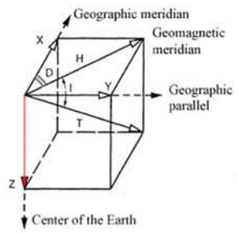

MGMF vector components

D Declination
I Inclination
H Horizontal component
T Total intensity
X North component
Y East component
Z Vertical component

Scale 1: 120 000 000

Projection: Miller cylindrical

SECULAR VARIATION OF VERTICAL COMPONENT OF MGMF

SV – 1962, 1967 – Z

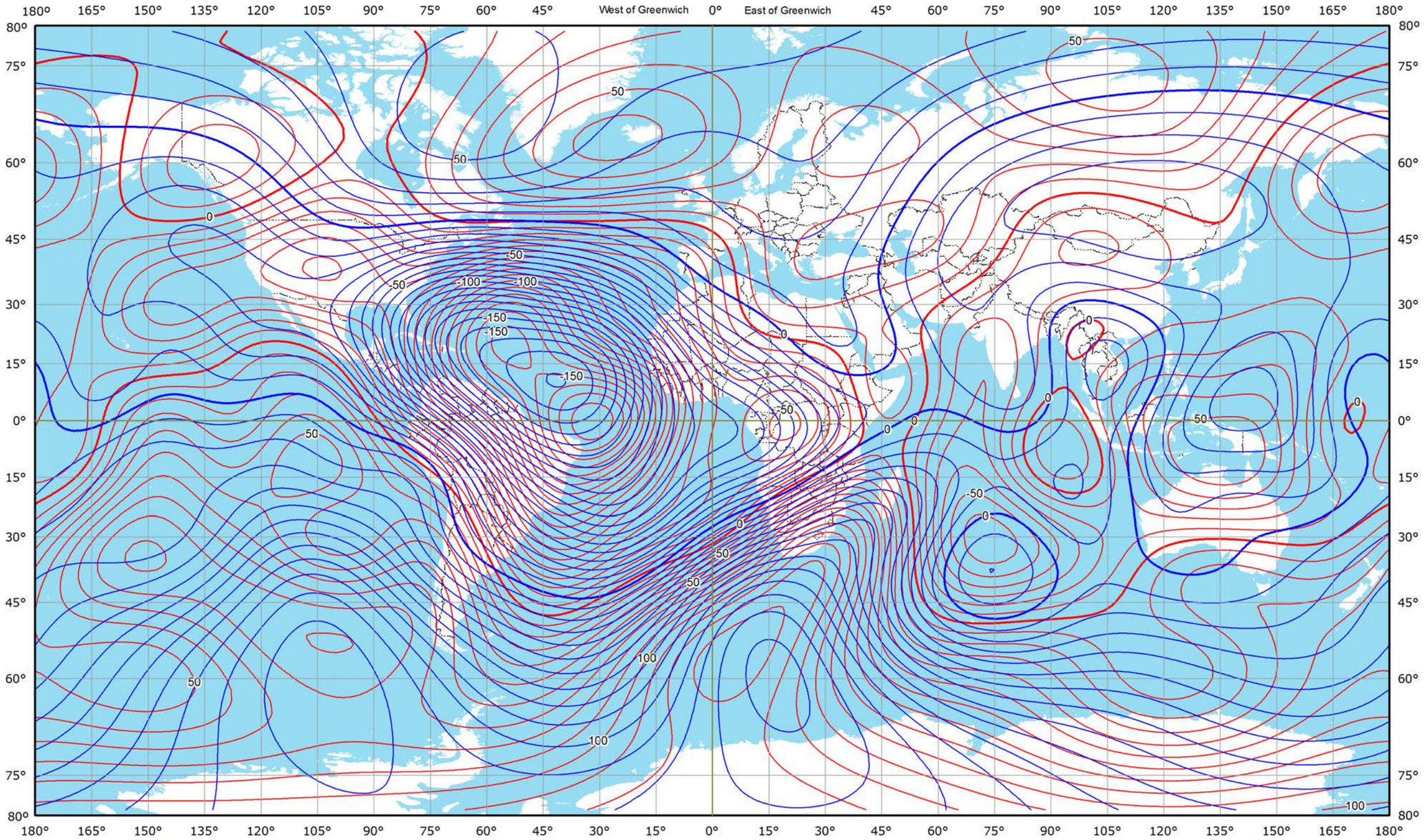

Epoch Isopors

1962
1967

Example. Secular variation value of vertical component of MGMF (nT/year)

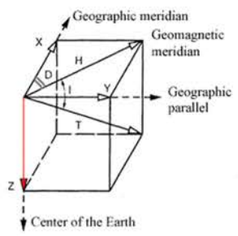

MGMF vector components

D Declination
I Inclination
H Horizontal component
T Total intensity
X North component
Y East component
Z Vertical component

Scale 1: 120 000 000

Projection: Miller cylindrical

SECULAR VARIATION OF VERTICAL COMPONENT OF MGMF

SV – 1967, 1972 – Z

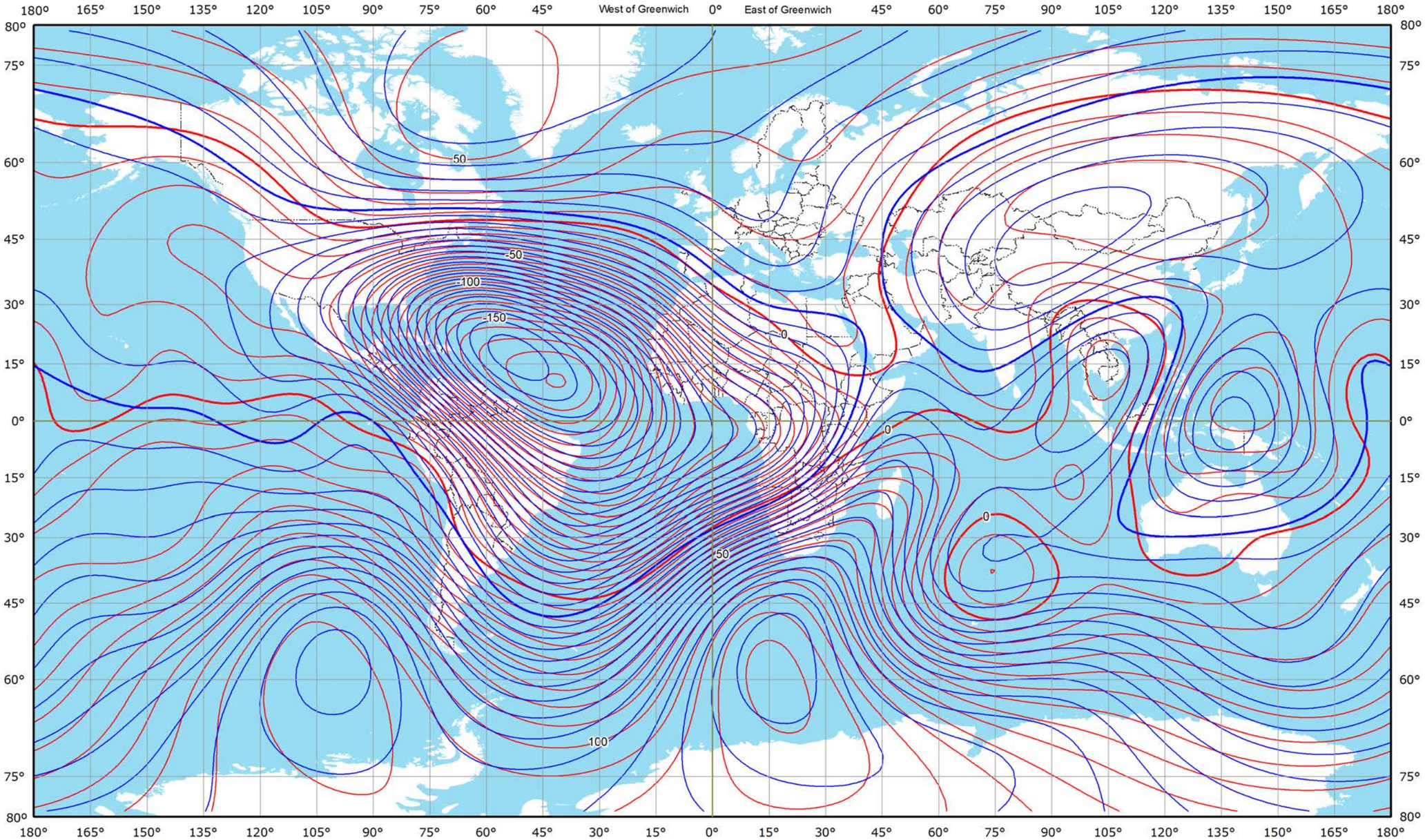

Epoch Isopors

1967
1972

Example. Secular variation value of vertical component of MGMF (nT/year)

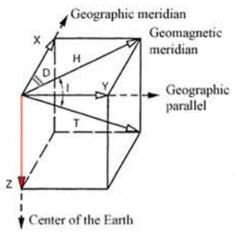

MGMF vector components

D Declination
I Inclination
H Horizontal component
T Total intensity
X North component
Y East component
Z Vertical component

Scale 1: 120 000 000

Projection: Miller cylindrical

SECULAR VARIATION OF VERTICAL COMPONENT OF MGMF

SV – 1972, 1977 – Z

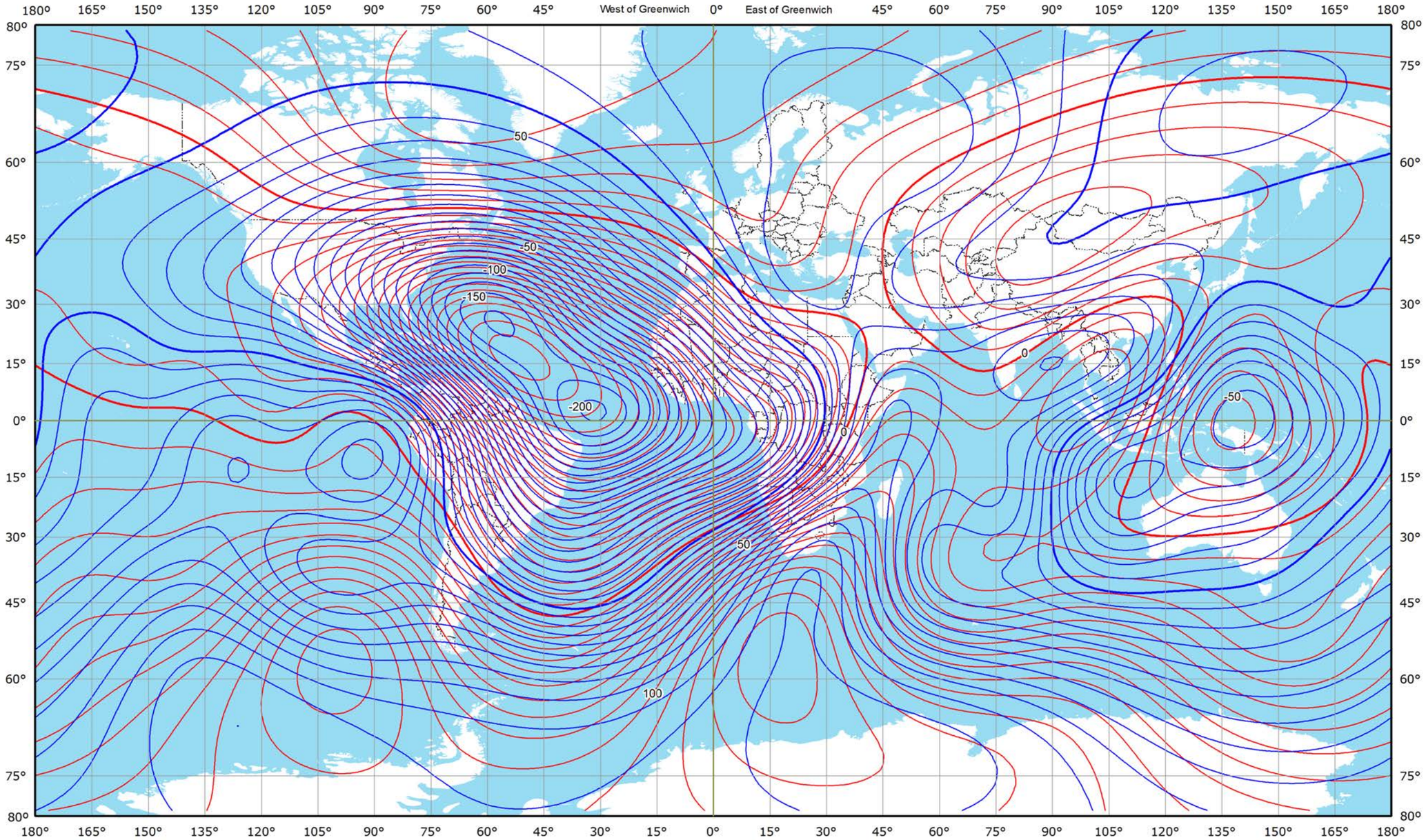

Epoch Isopors

1972
1977

Example. Secular variation value of vertical component of MGMF (nT/year)

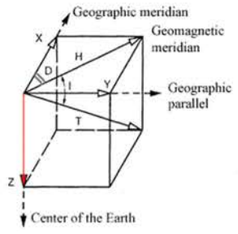

MGMF vector components

D Declination
I Inclination
H Horizontal component
T Total intensity
X North component
Y East component
Z Vertical component

Scale 1: 120 000 000

Projection: Miller cylindrical

SECULAR VARIATION OF VERTICAL COMPONENT OF MGMF

SV – 1977, 1982 – Z

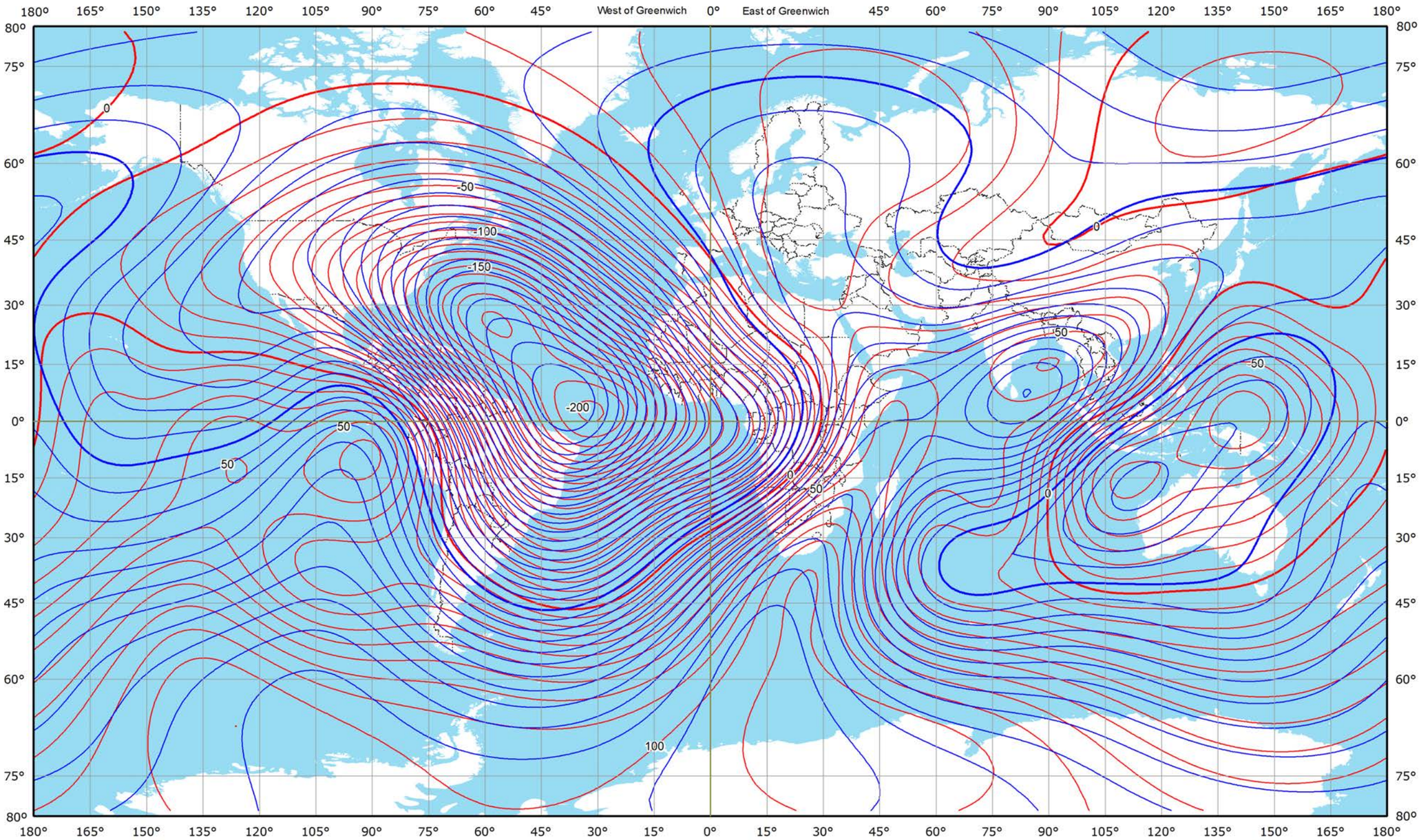

Epoch Isopors

1977
1982

Example. Secular variation value of vertical component of MGMF (nT/year)

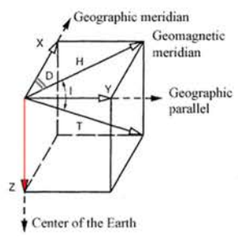

MGMF vector components

D Declination
I Inclination
H Horizontal component
T Total intensity
X North component
Y East component
Z Vertical component

Scale 1: 120 000 000

Projection: Miller cylindrical

SECULAR VARIATION OF VERTICAL COMPONENT OF MGMF

SV – 1982, 1987 – Z

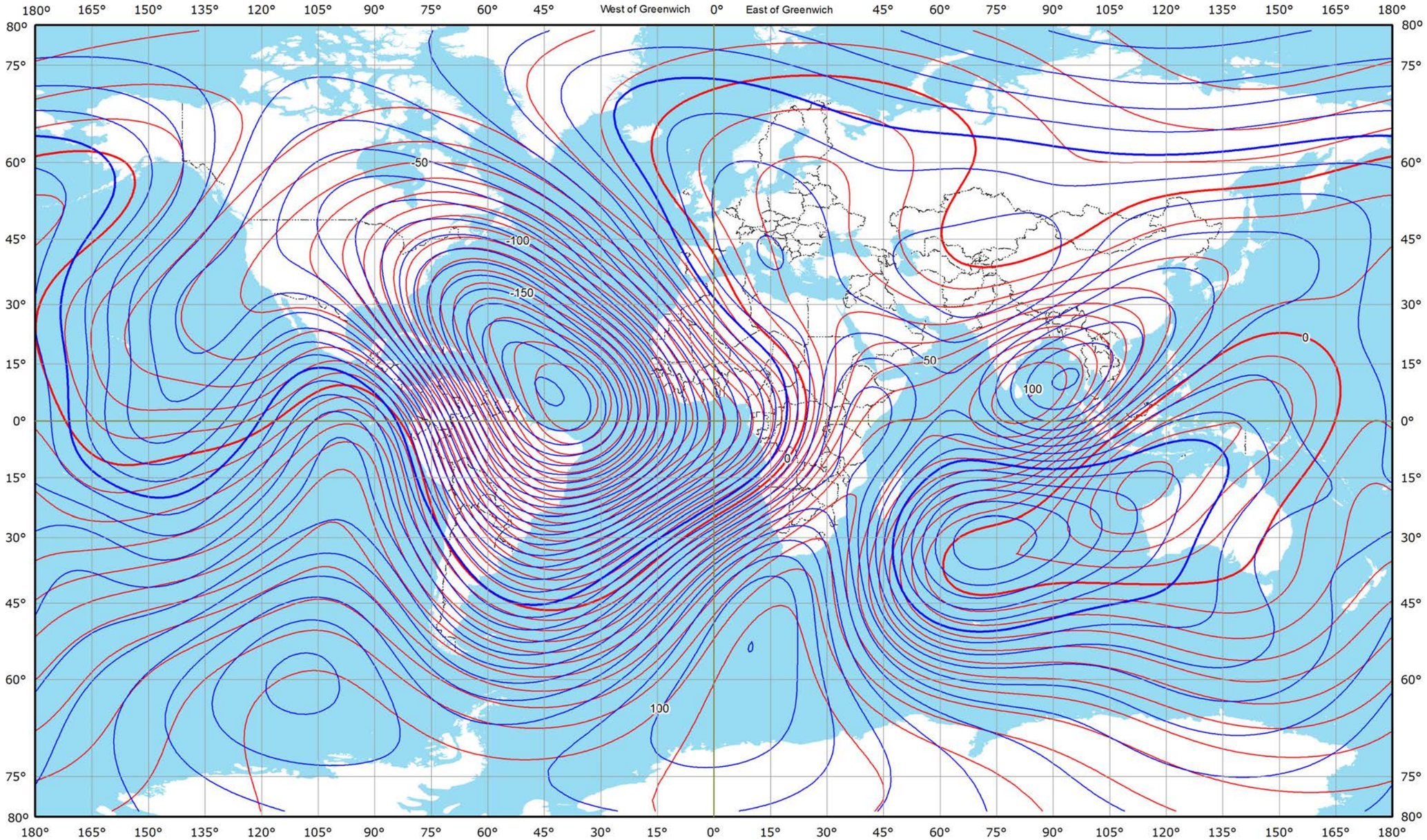

Epoch Isopors

1982
1987

Example. Secular variation value of vertical component of MGMF (nT/year)

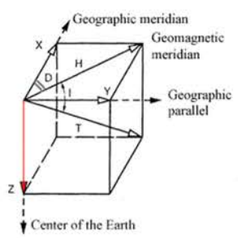

MGMF vector components

D Declination
I Inclination
H Horizontal component
T Total intensity
X North component
Y East component
Z Vertical component

Scale 1: 120 000 000

Projection: Miller cylindrical

SECULAR VARIATION OF VERTICAL COMPONENT OF MGMF

SV – 1987, 1992 – Z

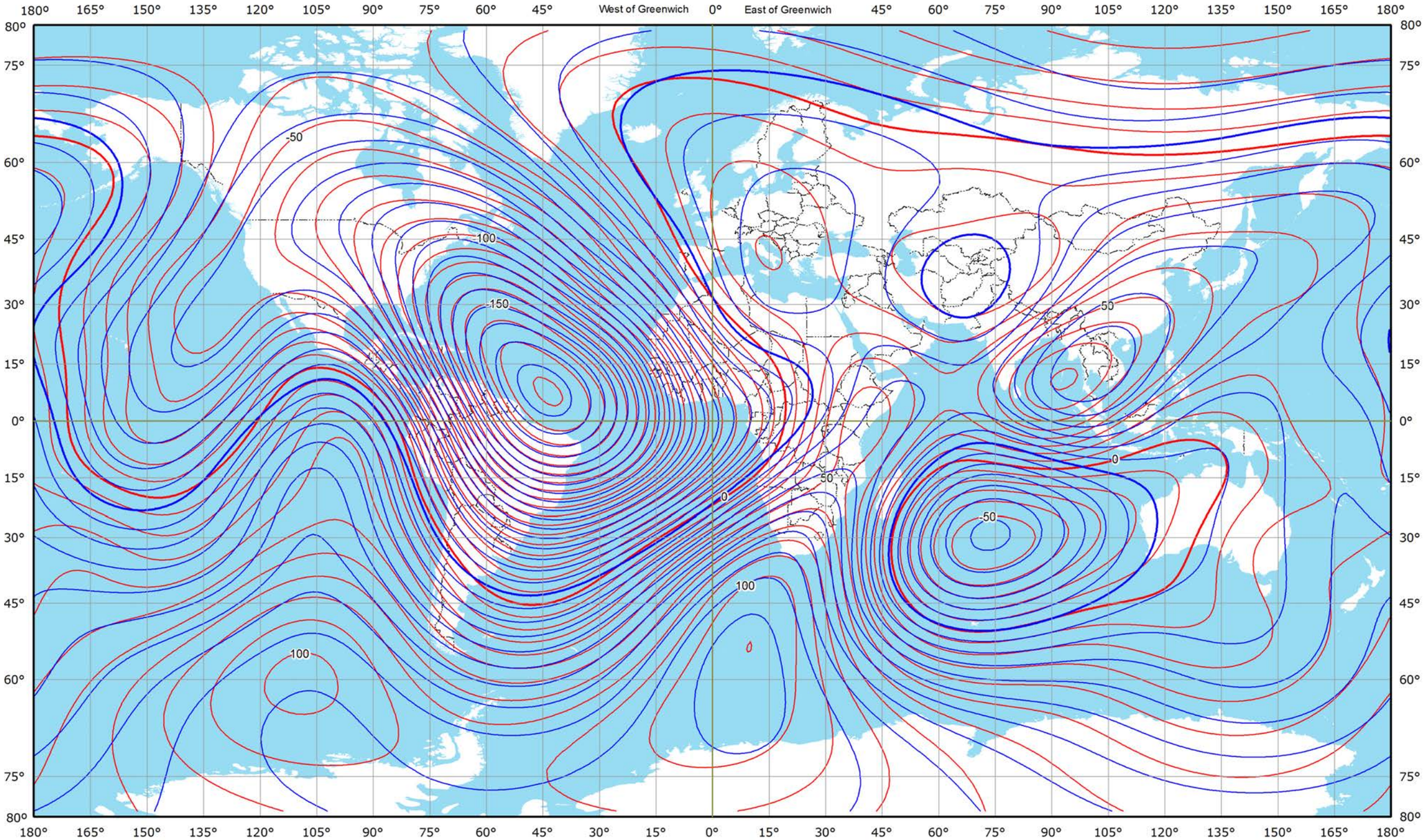

Epoch Isopors

1987
1992

Example. Secular variation value of vertical component of MGMF (nT/year)

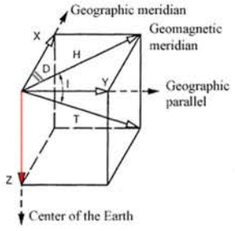

MGMF vector components

D Declination
I Inclination
H Horizontal component
T Total intensity
X North component
Y East component
Z Vertical component

Scale 1: 120 000 000

Projection: Miller cylindrical

SECULAR VARIATION OF VERTICAL COMPONENT OF MGMF

SV – 1992, 1997 – Z

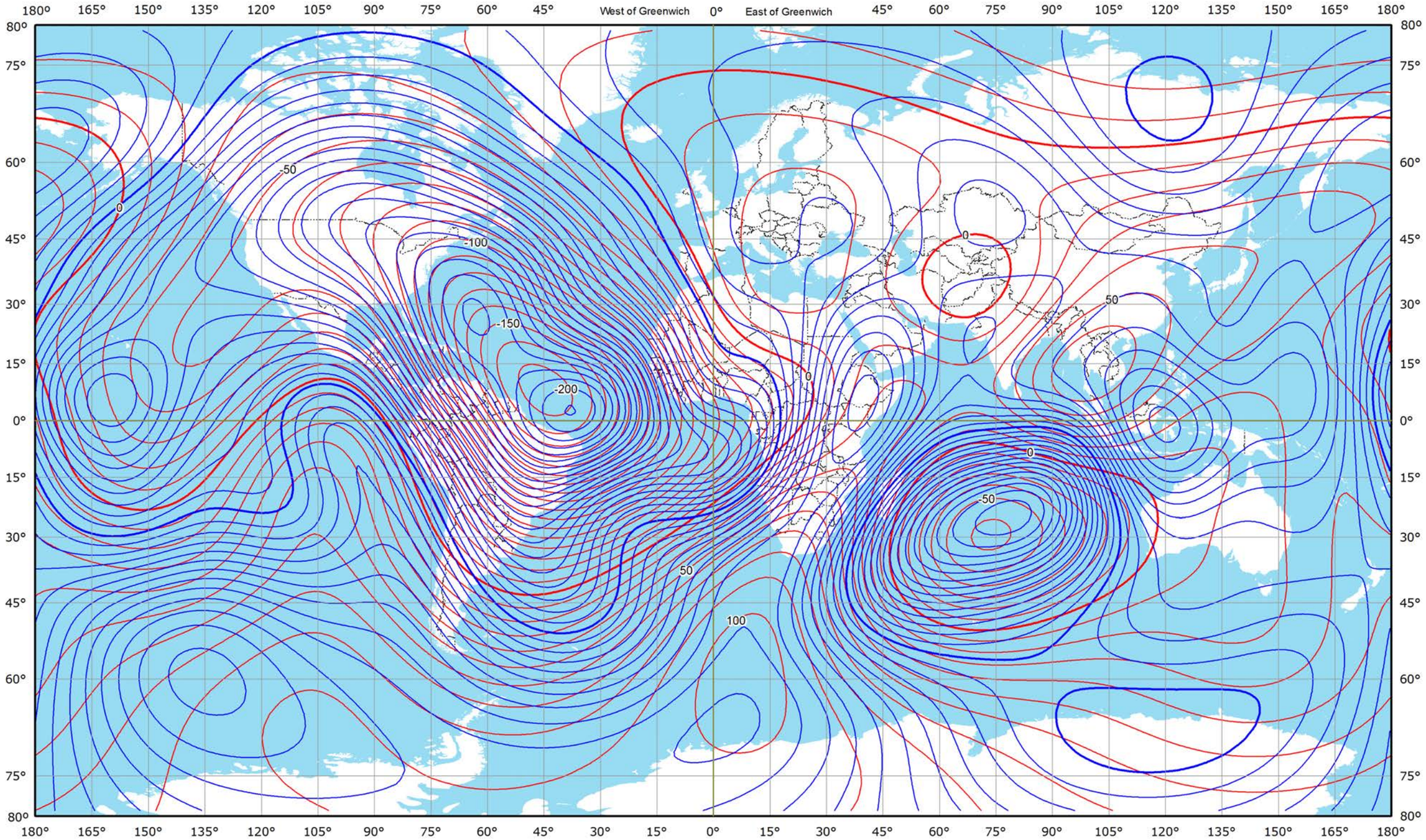

Epoch Isopors

1992
1997

Example. Secular variation value of vertical component of MGMF (nT/year)

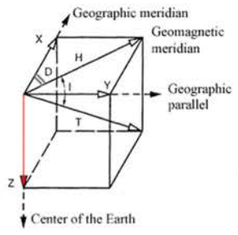

MGMF vector components

D Declination
I Inclination
H Horizontal component
T Total intensity
X North component
Y East component
Z Vertical component

Scale 1: 120 000 000

Projection: Miller cylindrical

SECULAR VARIATION OF VERTICAL COMPONENT OF MGMF

SV – 1997, 2002 – Z

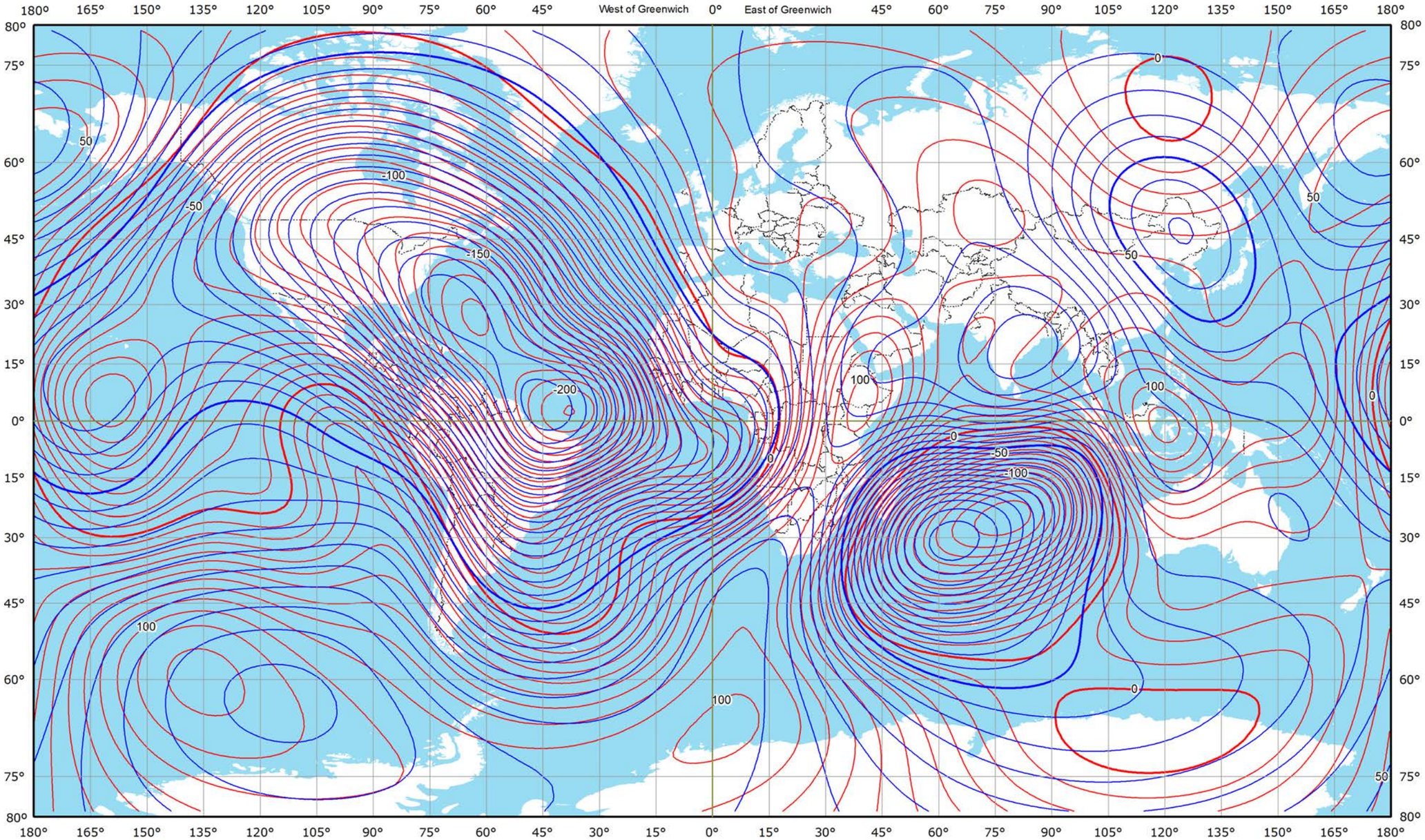

Epoch Isopors

1997
2002

Example. Secular variation value of vertical component of MGMF (nT/year)

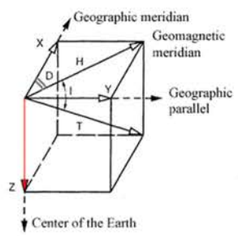

MGMF vector components

D Declination
I Inclination
H Horizontal component
T Total intensity
X North component
Y East component
Z Vertical component

Scale 1: 120 000 000

Projection: Miller cylindrical

SECULAR VARIATION OF VERTICAL COMPONENT OF MGMF

SV – 2002, 2007 – Z

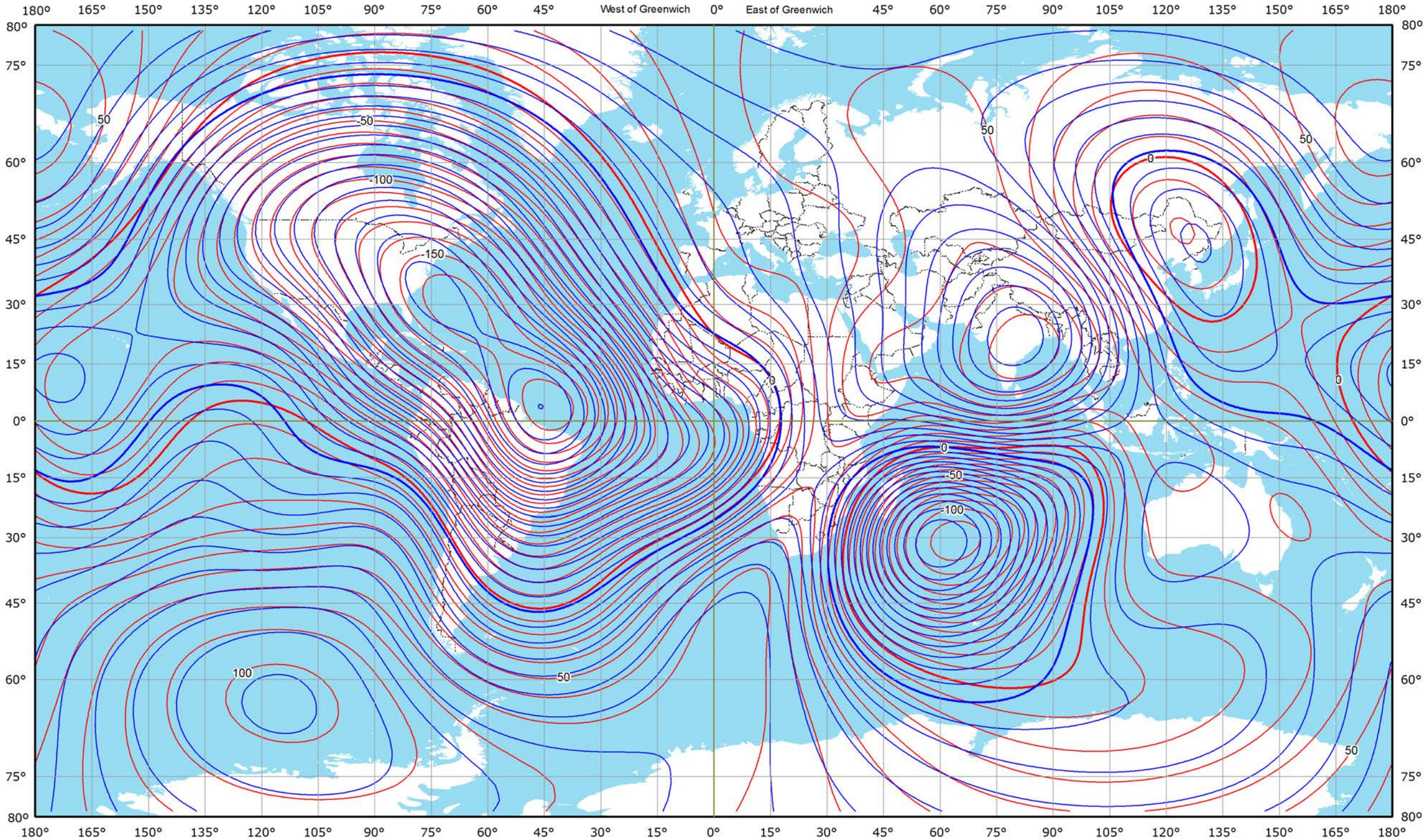

Epoch Isopors

2002
2007

Example. Secular variation value of vertical component of MGMF (nT/year)

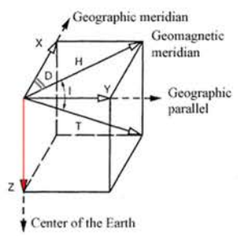

MGMF vector components

D Declination
I Inclination
H Horizontal component
T Total intensity
X North component
Y East component
Z Vertical component

Scale 1: 120 000 000

Projection: Miller cylindrical

SECULAR VARIATION OF HORIZONTAL COMPONENT OF MGMF

SV – 1902, 1907 – H

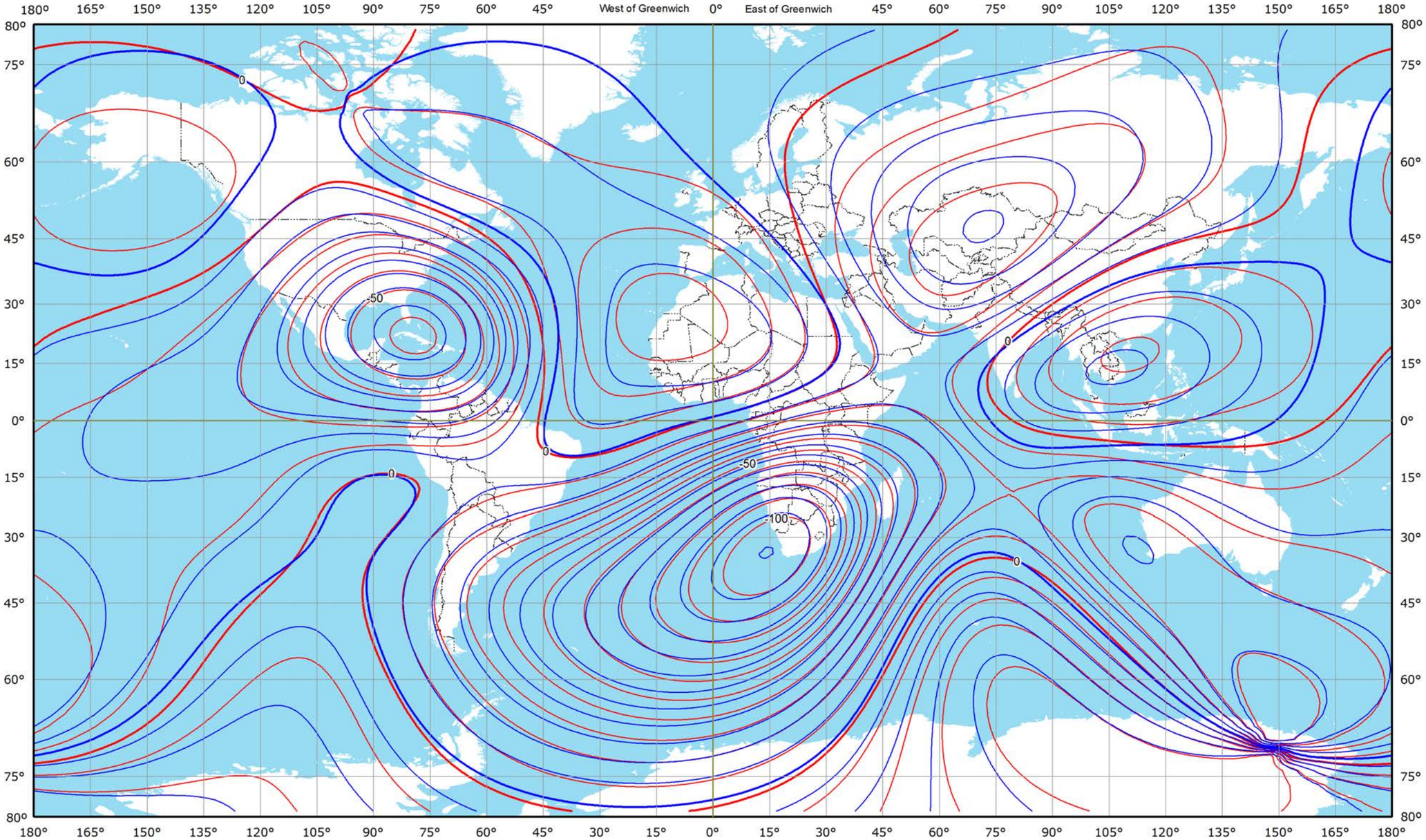

Epoch Isopors

1902
1907

Example. Secular variation value of horizontal component of MGMF (nT/year)

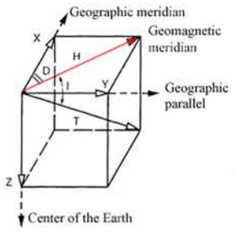

MGMF vector components

D Declination
I Inclination
H Horizontal component
T Total intensity
X North component
Y East component
Z Vertical component

Scale 1: 120 000 000

Projection: Miller cylindrical

SECULAR VARIATION OF HORIZONTAL COMPONENT OF MGMF

SV – 1907, 1912 – H

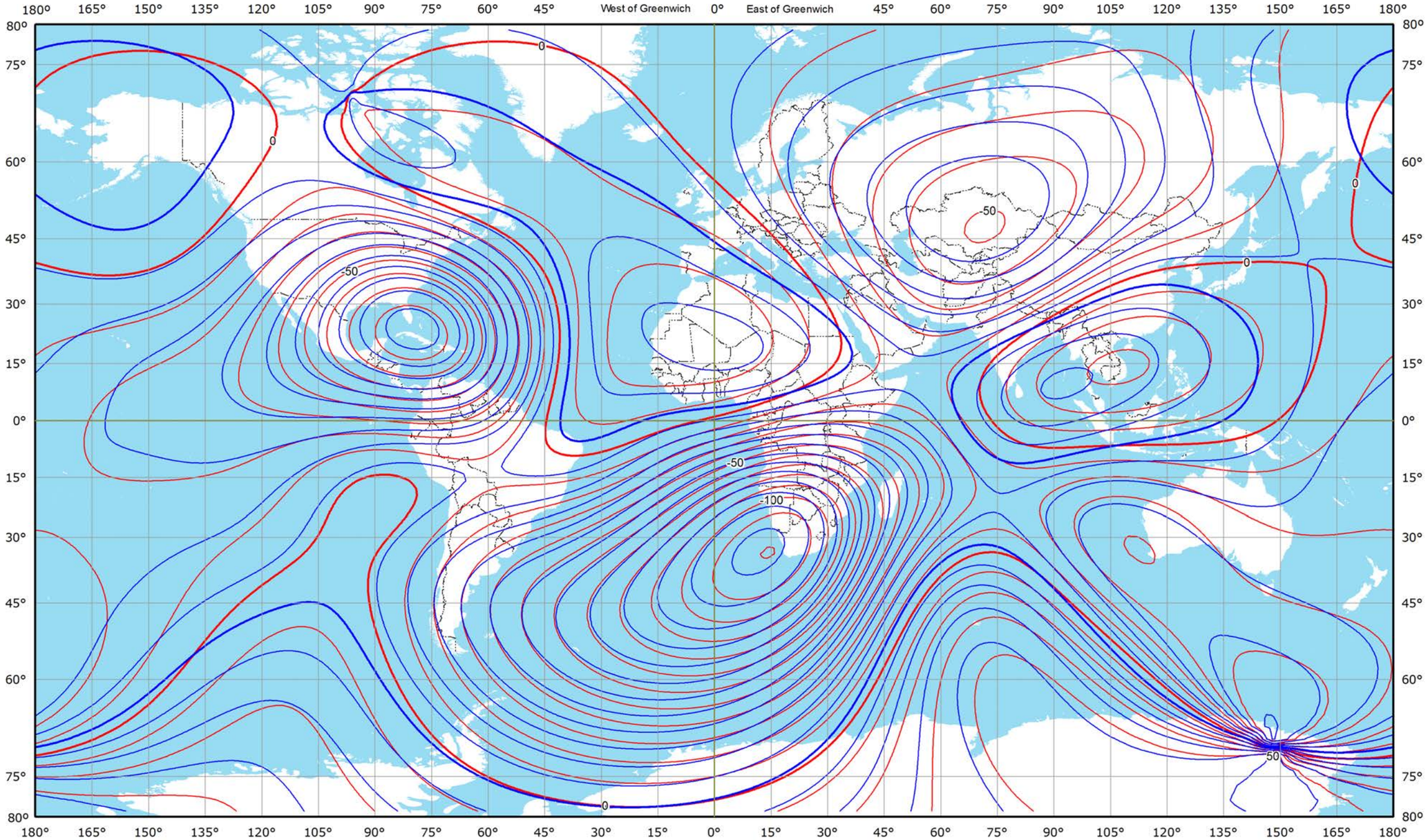

Epoch Isopors

1907
1912

Example. Secular variation value of horizontal component of MGMF (nT/year)

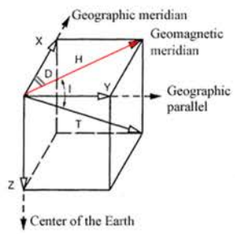

MGMF vector components

D Declination
I Inclination
H Horizontal component
T Total intensity
X North component
Y East component
Z Vertical component

Scale 1: 120 000 000

Projection: Miller cylindrical

SECULAR VARIATION OF HORIZONTAL COMPONENT OF MGMF

SV – 1912, 1917 – H

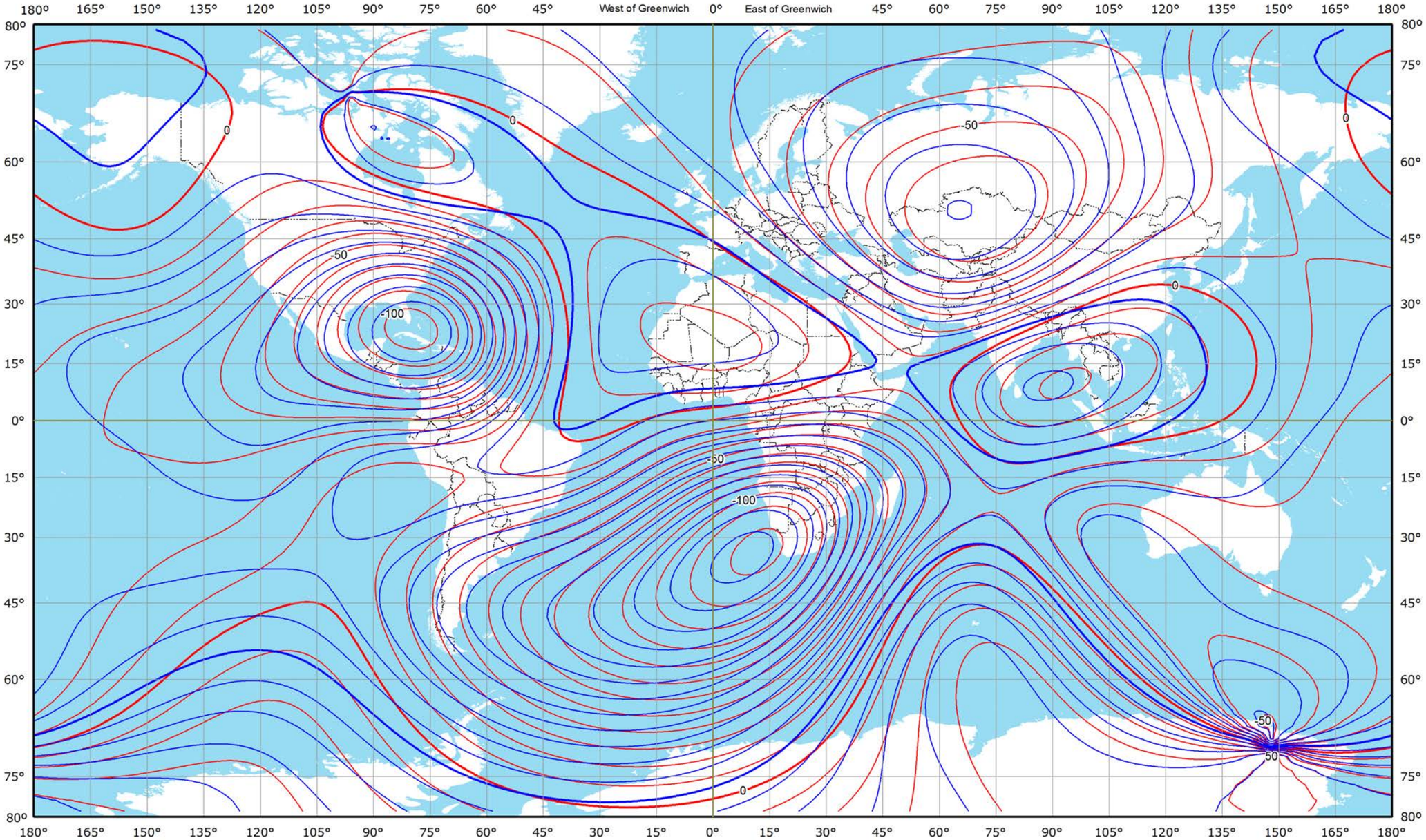

Epoch Isopors

1912
1917

Example. Secular variation value of horizontal component of MGMF (nT/year)

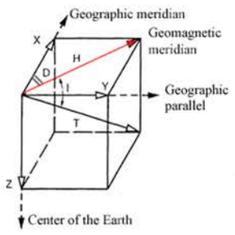

MGMF vector components

D Declination
I Inclination
H Horizontal component
T Total intensity
X North component
Y East component
Z Vertical component

Scale 1: 120 000 000

Projection: Miller cylindrical

SECULAR VARIATION OF HORIZONTAL COMPONENT OF MGMF

SV – 1917, 1922 – H

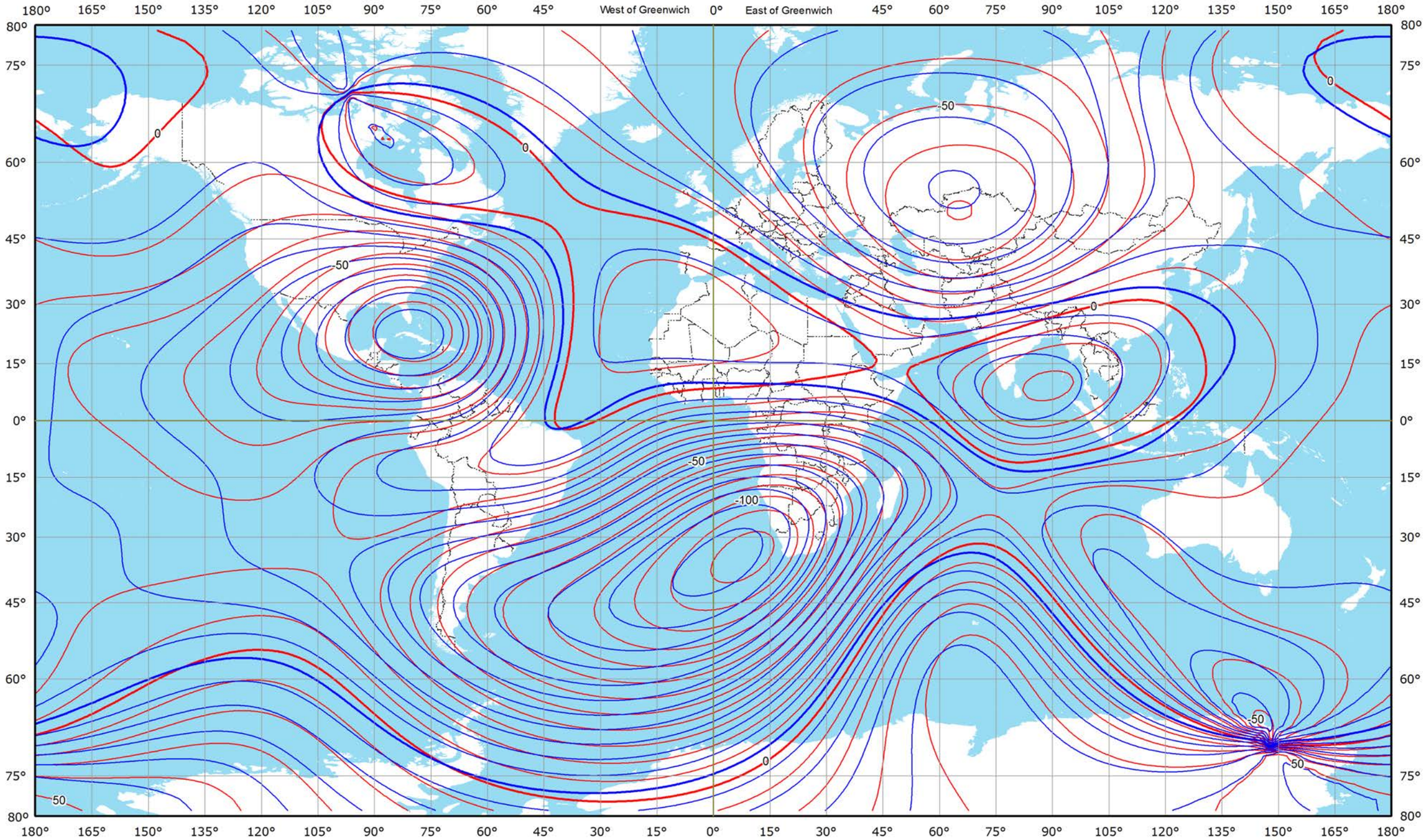

Epoch Isopors

1917
1922

Example. Secular variation value of horizontal component of MGMF (nT/year)

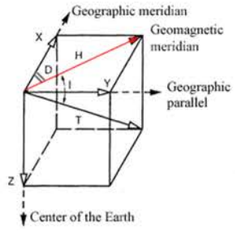

MGMF vector components

D Declination
I Inclination
H Horizontal component
T Total intensity
X North component
Y East component
Z Vertical component

Scale 1: 120 000 000

Projection: Miller cylindrical

SECULAR VARIATION OF HORIZONTAL COMPONENT OF MGMF

SV – 1922, 1927 – H

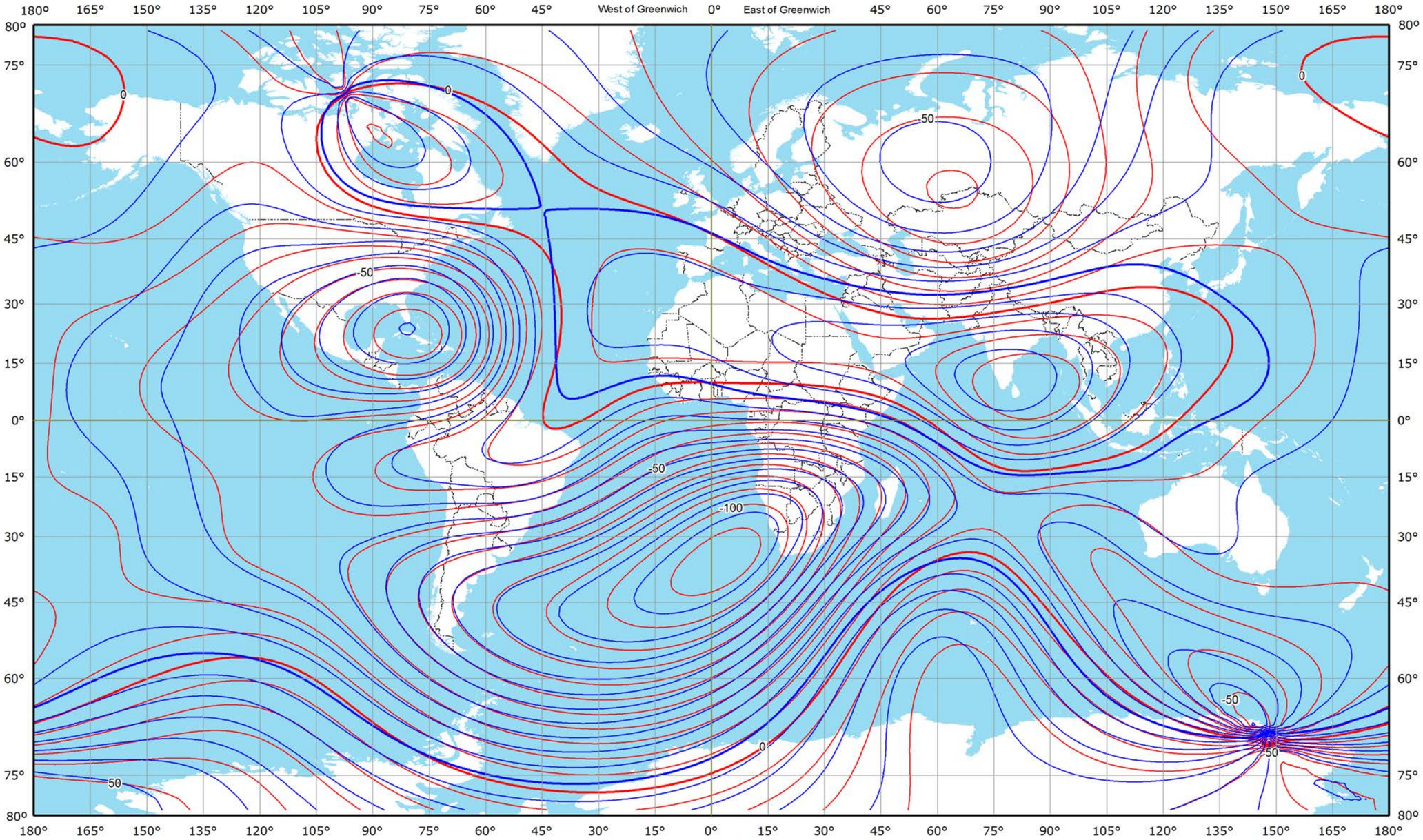

Epoch Isopors

1922
1927

Example. Secular variation value of horizontal component of MGMF (nT/year)

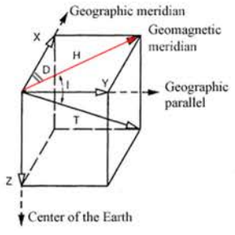

MGMF vector components

D Declination
I Inclination
H Horizontal component
T Total intensity
X North component
Y East component
Z Vertical component

Scale 1: 120 000 000

Projection: Miller cylindrical

SECULAR VARIATION OF HORIZONTAL COMPONENT OF MGMF

SV – 1927, 1932 – H

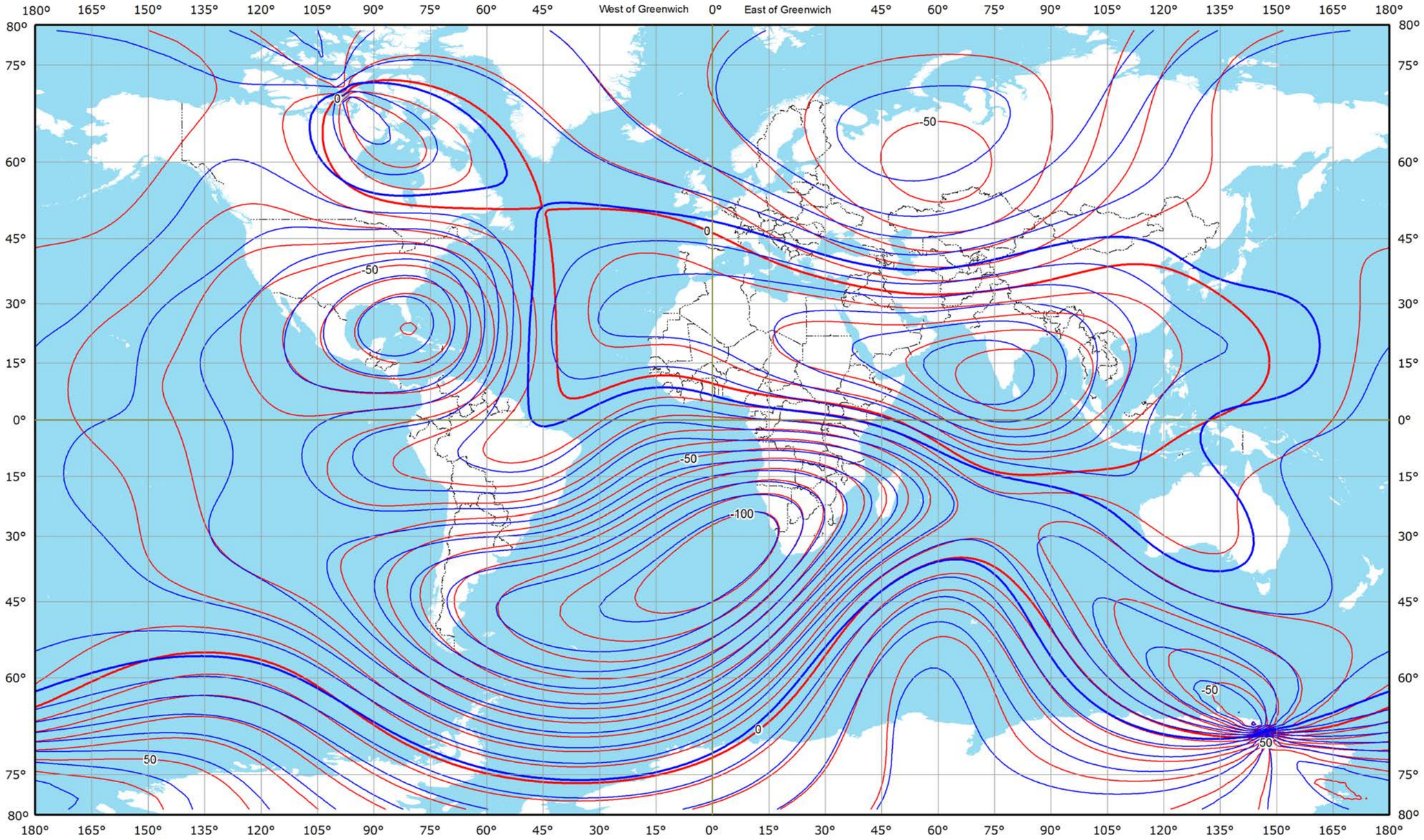

Epoch Isopors

1927
1932

Example. Secular variation value of horizontal component of MGMF (nT/year)

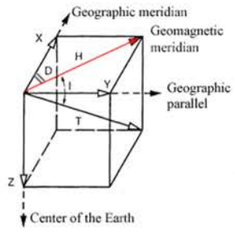

MGMF vector components

D Declination
I Inclination
H Horizontal component
T Total intensity
X North component
Y East component
Z Vertical component

Scale 1: 120 000 000

Projection: Miller cylindrical

SECULAR VARIATION OF HORIZONTAL COMPONENT OF MGMF

SV – 1932, 1937 – H

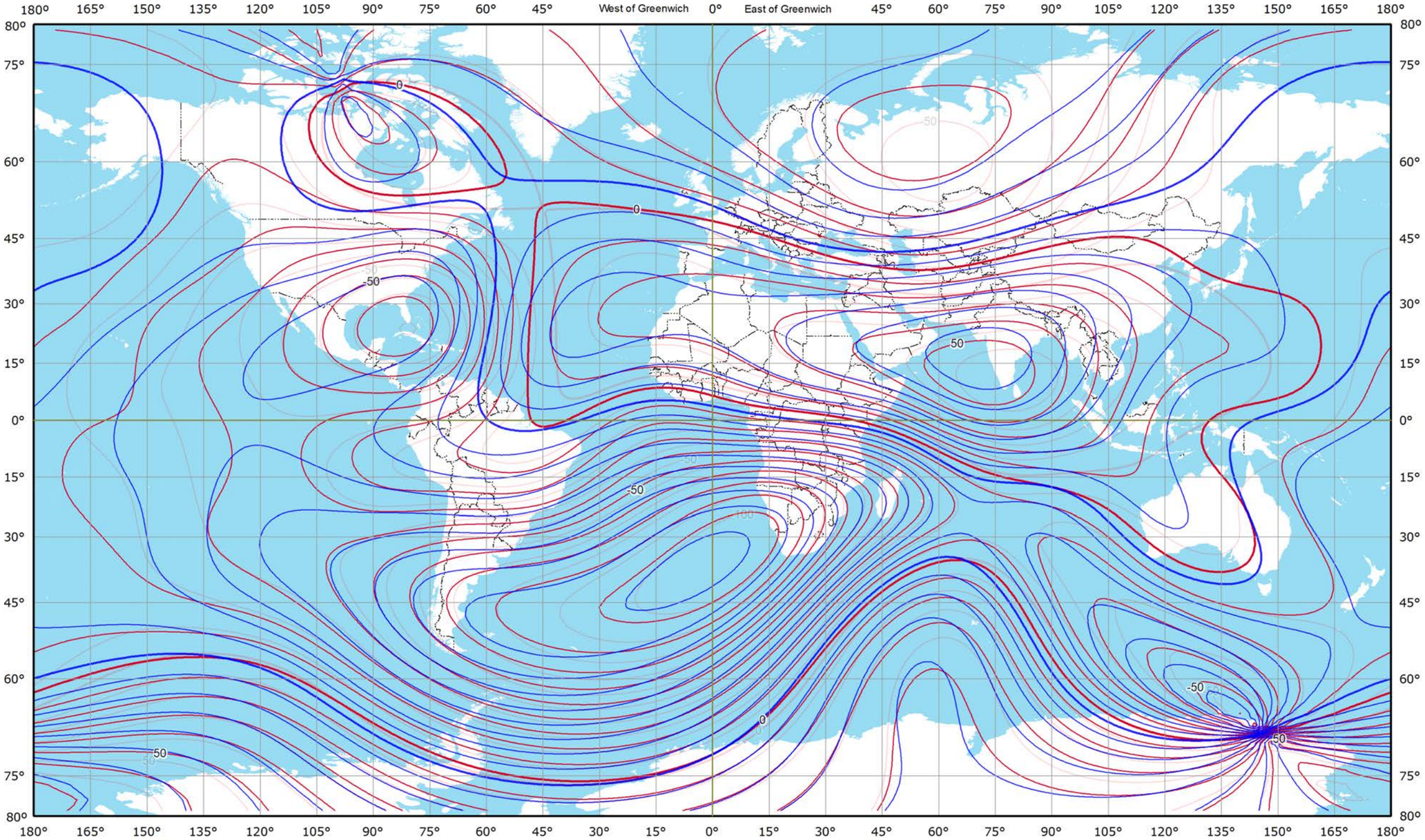

Epoch Isopors

1932
1937

Example. Secular variation value of horizontal component of MGMF (nT/year)

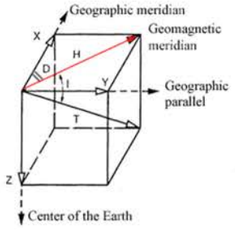

MGMF vector components

D Declination
I Inclination
H Horizontal component
T Total intensity
X North component
Y East component
Z Vertical component

Scale 1: 120 000 000

Projection: Miller cylindrical

SECULAR VARIATION OF HORIZONTAL COMPONENT OF MGMF

SV – 1937, 1942 – H

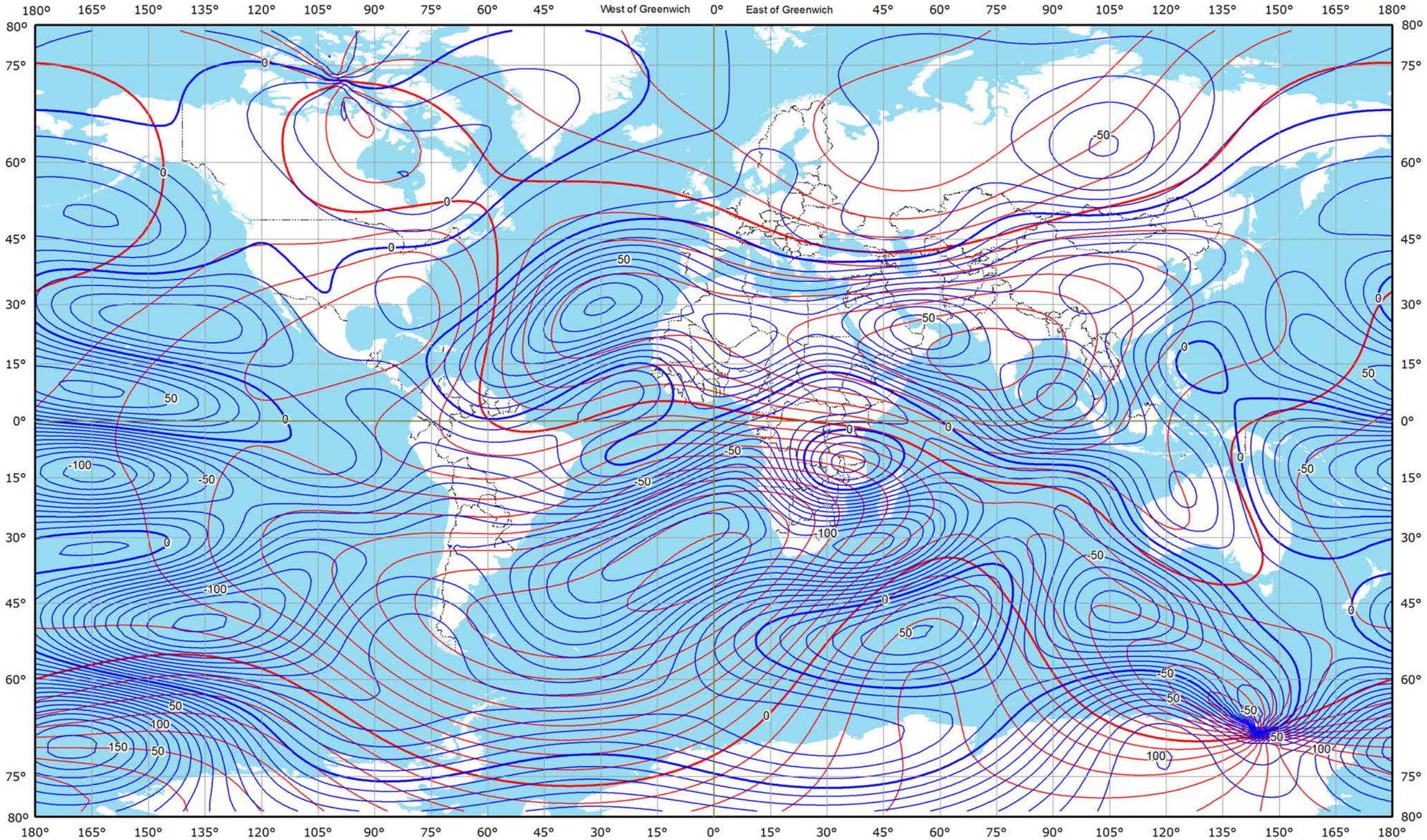

Epoch Isopors

1937
1942

Example. Secular variation value of horizontal component of MGMF (nT/year)

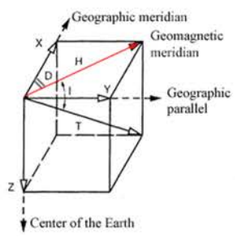

MGMF vector components

D Declination
I Inclination
H Horizontal component
T Total intensity
X North component
Y East component
Z Vertical component

Scale 1: 120 000 000

Projection: Miller cylindrical

SECULAR VARIATION OF HORIZONTAL COMPONENT OF MGMF

SV – 1942, 1947 – H

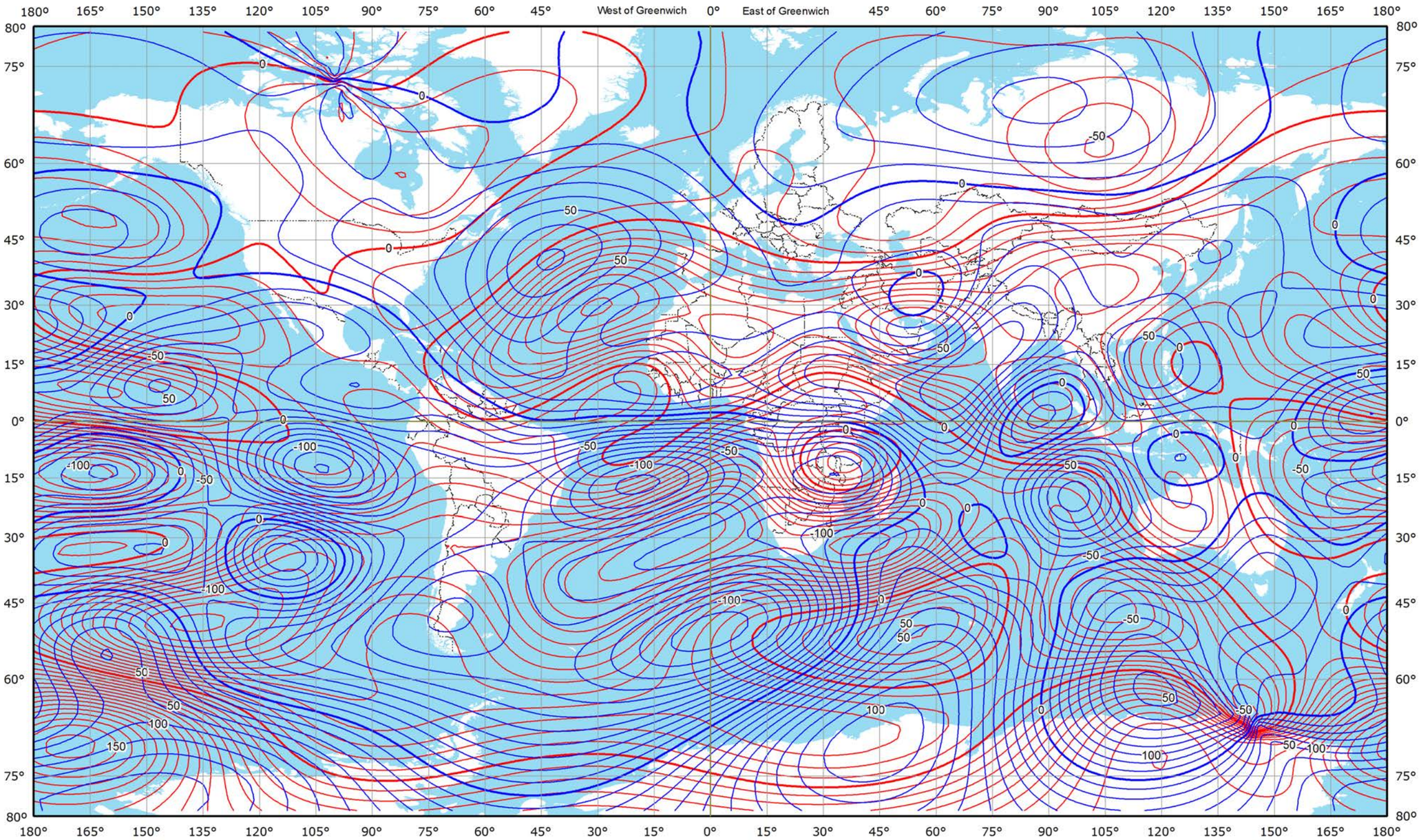

Epoch Isopors

1942
1947

Example. Secular variation value of horizontal component of MGMF (nT/year)

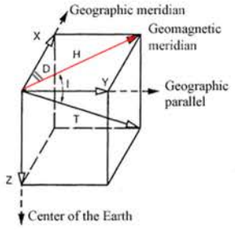

MGMF vector components

D Declination
I Inclination
H Horizontal component
T Total intensity
X North component
Y East component
Z Vertical component

Scale 1: 120 000 000

Projection: Miller cylindrical

SECULAR VARIATION OF HORIZONTAL COMPONENT OF MGMF

SV – 1947, 1952 – H

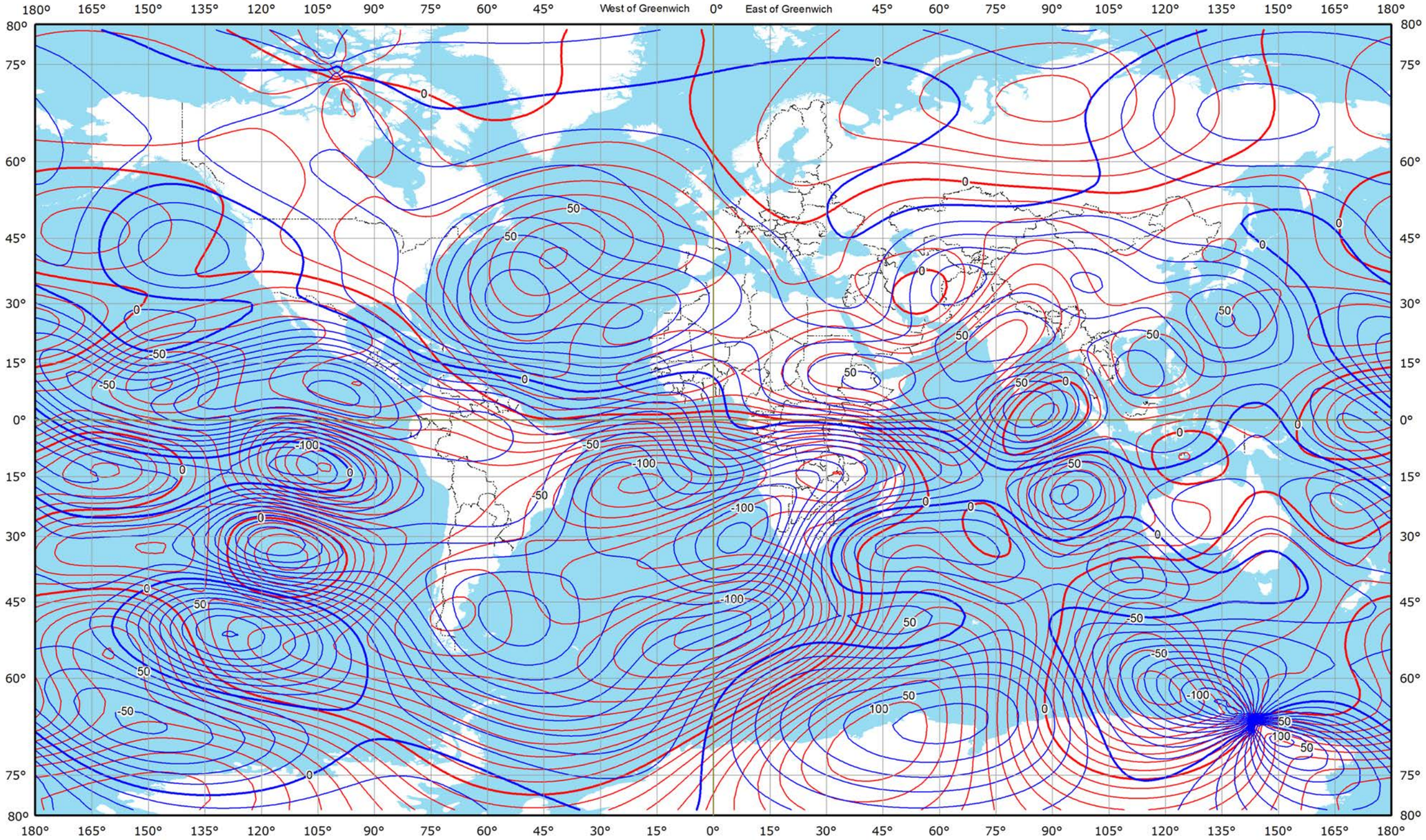

Epoch Isopors

1947
1952

Example. Secular variation value of horizontal component of MGMF (nT/year)

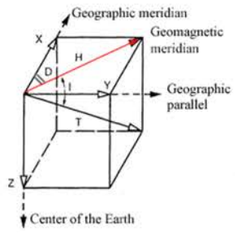

MGMF vector components

D Declination
I Inclination
H Horizontal component
T Total intensity
X North component
Y East component
Z Vertical component

Scale 1: 120 000 000

Projection: Miller cylindrical

SECULAR VARIATION OF HORIZONTAL COMPONENT OF MGMF

SV – 1952, 1957 – H

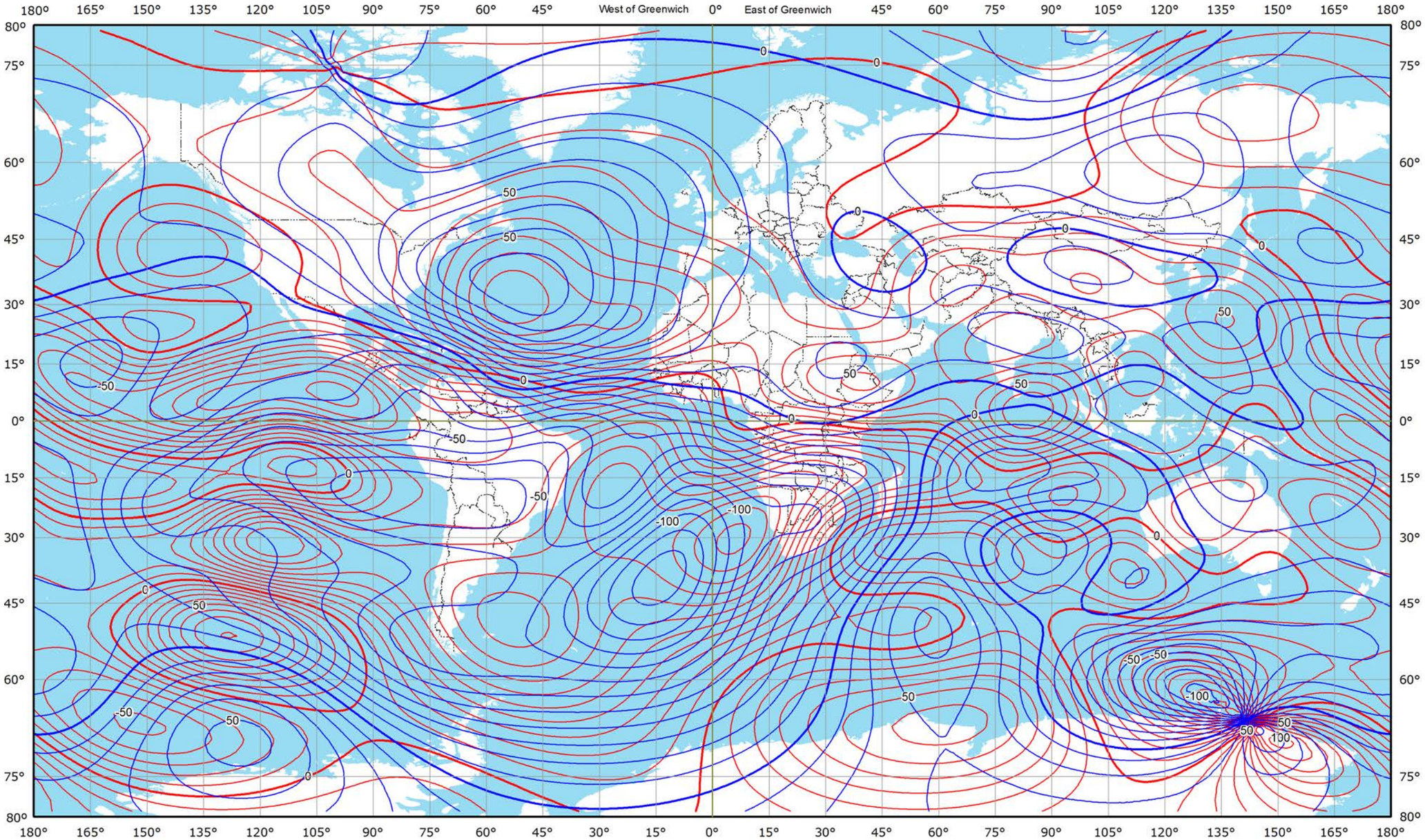

Epoch Isopors

1952
1957

Example. Secular variation value of horizontal component of MGMF (nT/year)

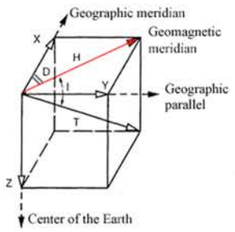

MGMF vector components

D Declination
I Inclination
H Horizontal component
T Total intensity
X North component
Y East component
Z Vertical component

Scale 1: 120 000 000

Projection: Miller cylindrical

SECULAR VARIATION OF HORIZONTAL COMPONENT OF MGMF

SV – 1957, 1962 – H

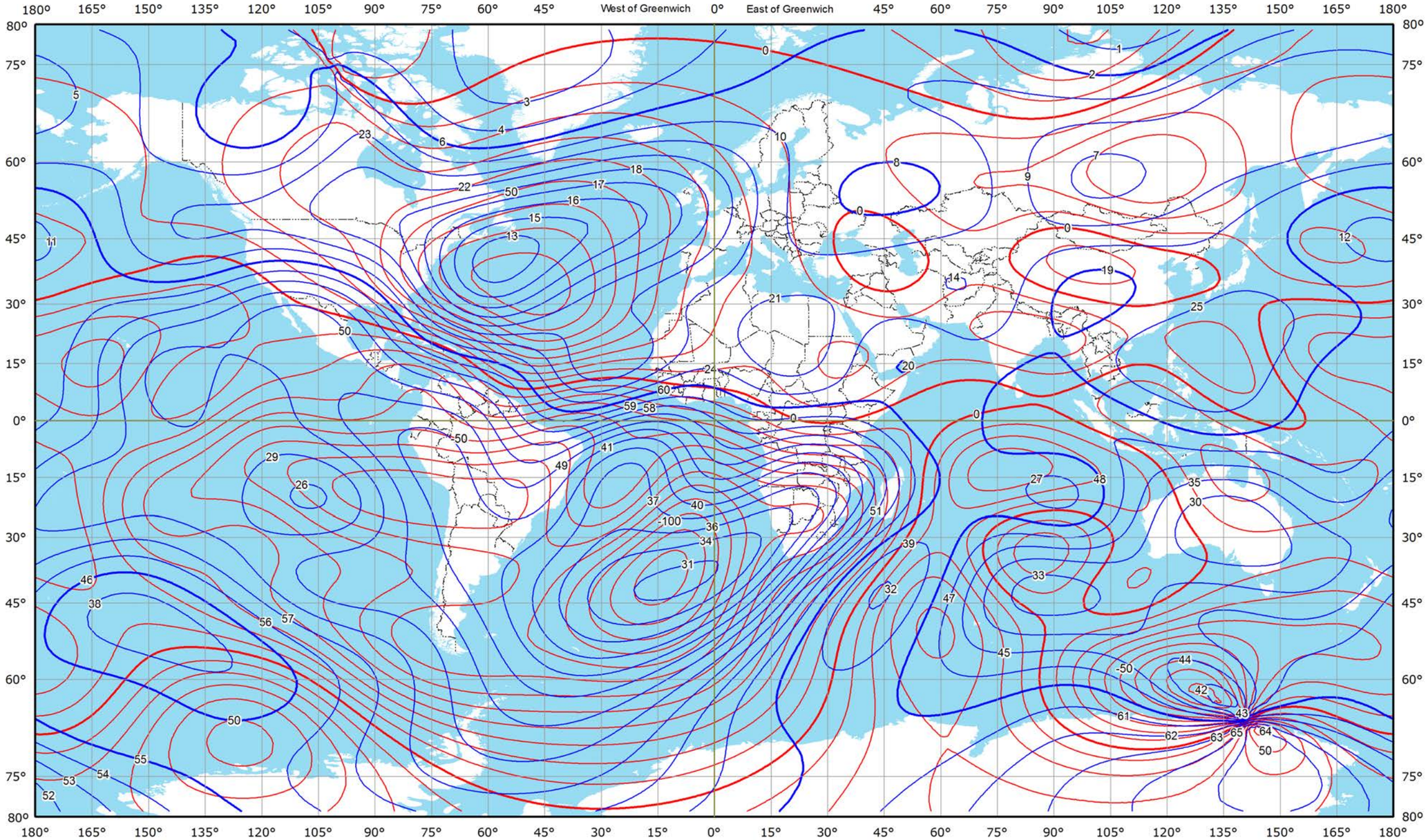

Epoch Isopors

1957
1962

Example. Secular variation value of horizontal component of MGMF (nT/year)

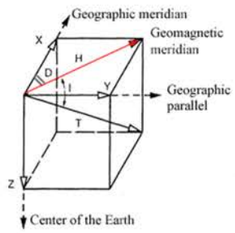

MGMF vector components

D Declination
I Inclination
H Horizontal component
T Total intensity
X North component
Y East component
Z Vertical component

Scale 1: 120 000 000

Projection: Miller cylindrical

SECULAR VARIATION OF HORIZONTAL COMPONENT OF MGMF

SV – 1962, 1967 – H

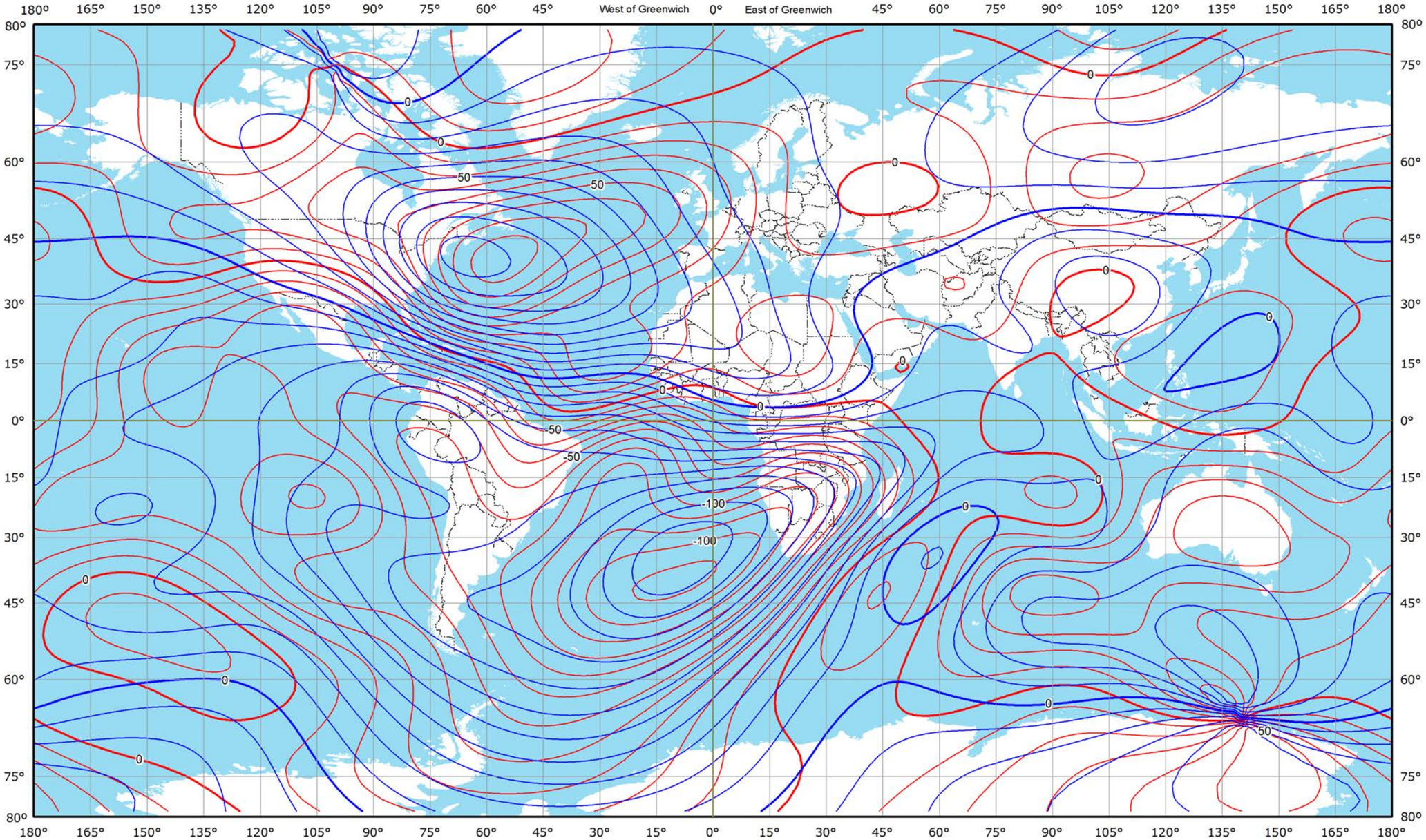

Epoch Isopors

1962
1967

Example. Secular variation value of horizontal component of MGMF (nT/year)

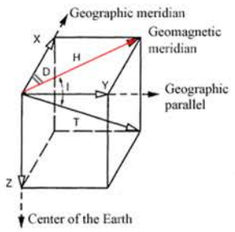

MGMF vector components

D Declination
I Inclination
H Horizontal component
T Total intensity
X North component
Y East component
Z Vertical component

Scale 1: 120 000 000

Projection: Miller cylindrical

SECULAR VARIATION OF HORIZONTAL COMPONENT OF MGMF

SV – 1967, 1972 – H

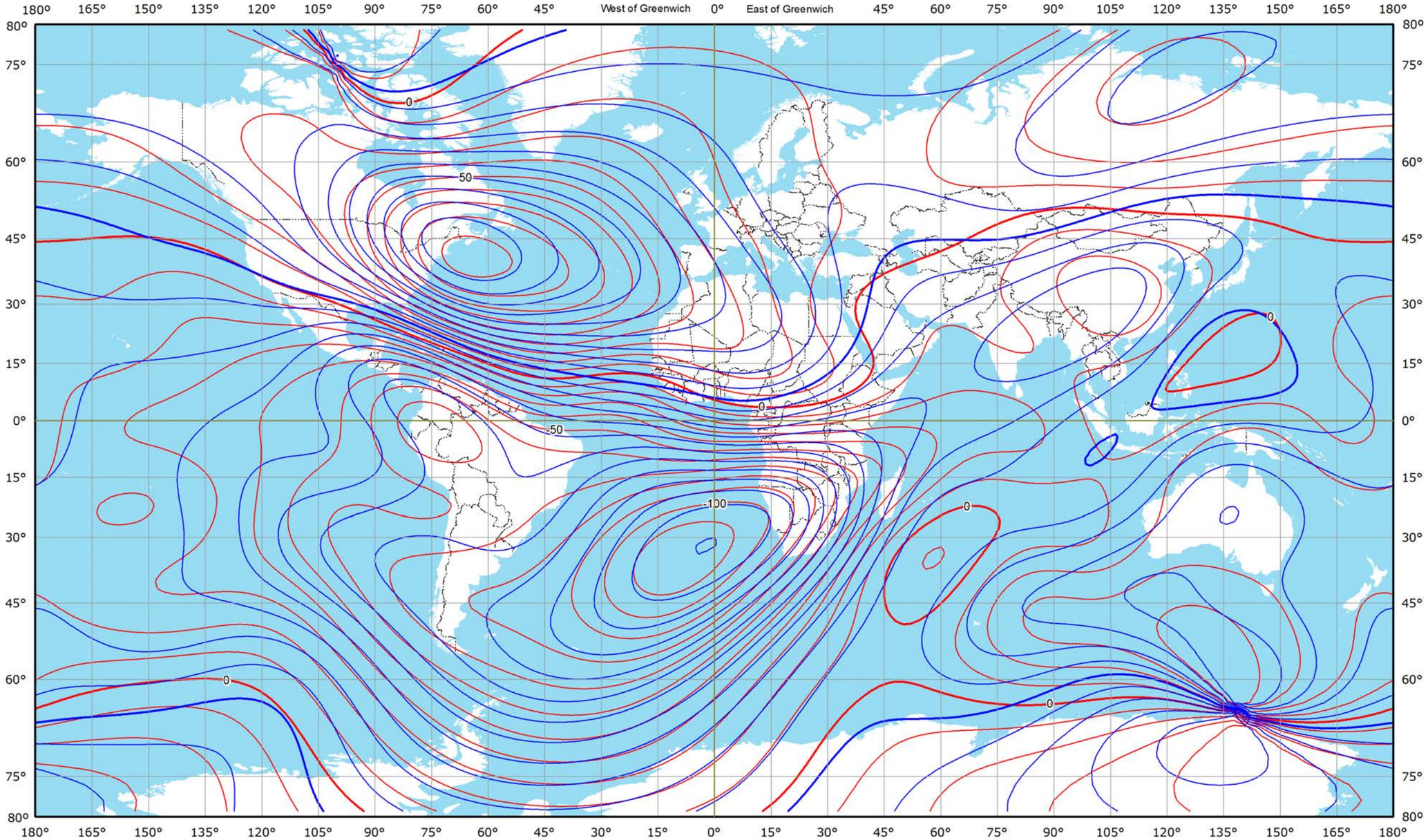

Epoch Isopors

1967
1972

Example. Secular variation value of horizontal component of MGMF (nT/year)

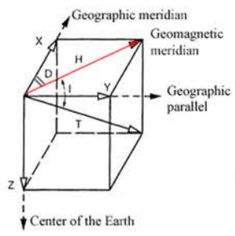

MGMF vector components

D Declination
I Inclination
H Horizontal component
T Total intensity
X North component
Y East component
Z Vertical component

Scale 1: 120 000 000

Projection: Miller cylindrical

SECULAR VARIATION OF HORIZONTAL COMPONENT OF MGMF

SV – 1972, 1977 – H

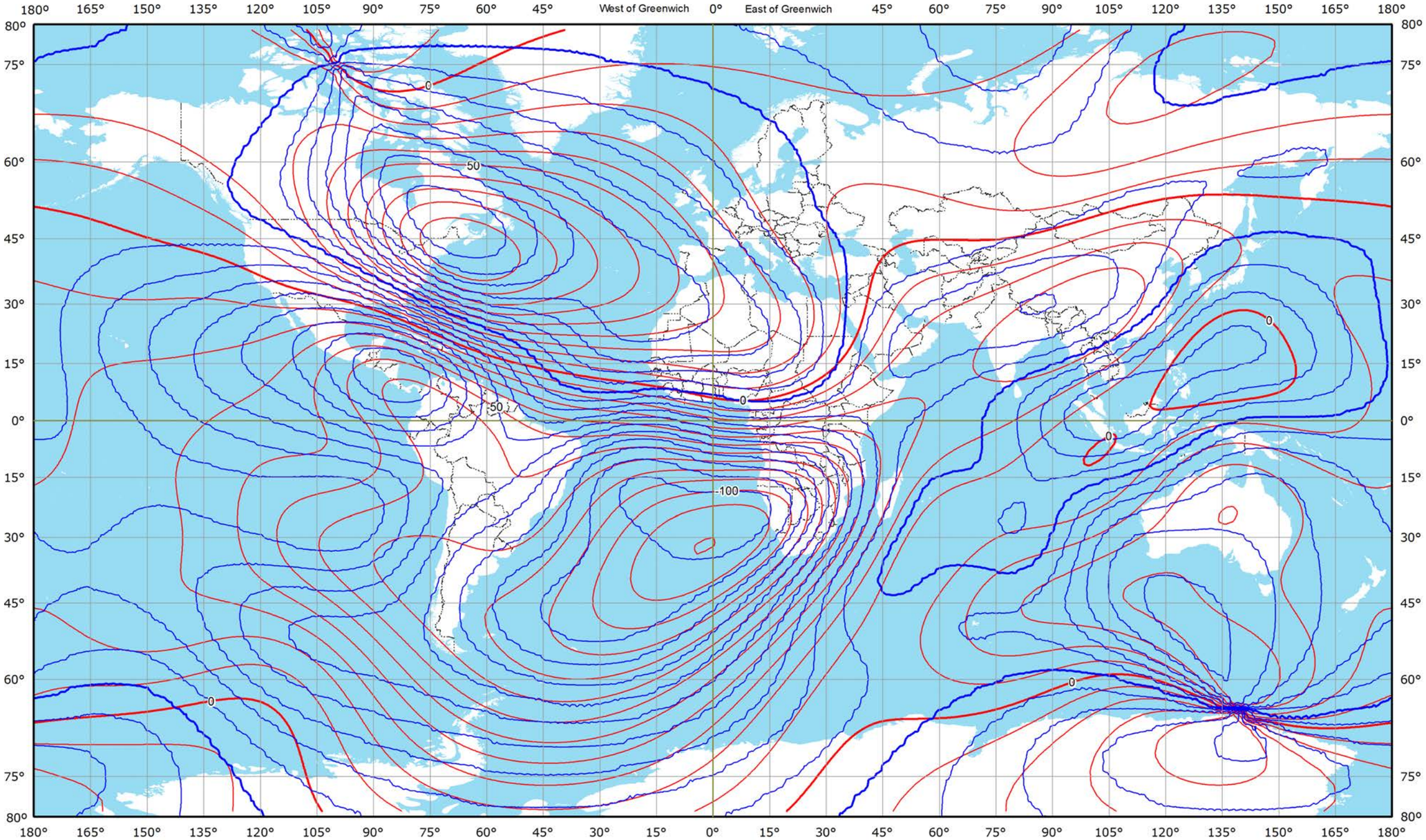

Epoch Isopors

1972
1977

Example. Secular variation value of horizontal component of MGMF (nT/year)

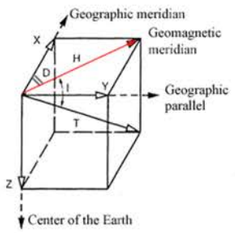

MGMF vector components

D Declination
I Inclination
H Horizontal component
T Total intensity
X North component
Y East component
Z Vertical component

Scale 1: 120 000 000

Projection: Miller cylindrical

SECULAR VARIATION OF HORIZONTAL COMPONENT OF MGMF

SV – 1977, 1982 – H

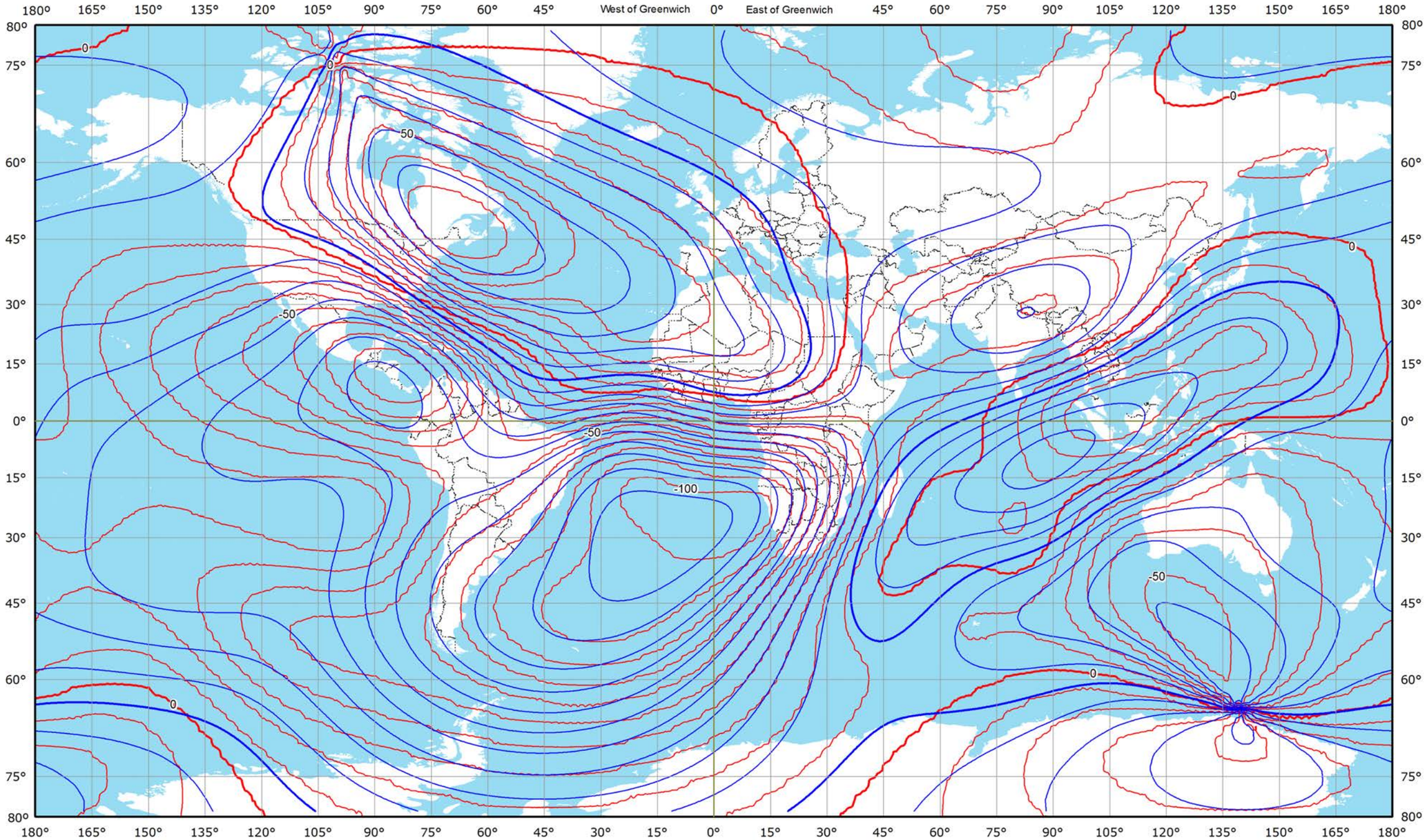

Epoch Isopors

1977
1982

Example. Secular variation value of horizontal component of MGMF (nT/year)

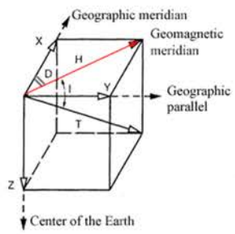

MGMF vector components

D Declination
I Inclination
H Horizontal component
T Total intensity
X North component
Y East component
Z Vertical component

Scale 1: 120 000 000

Projection: Miller cylindrical

SECULAR VARIATION OF HORIZONTAL COMPONENT OF MGMF

SV – 1982, 1987 – H

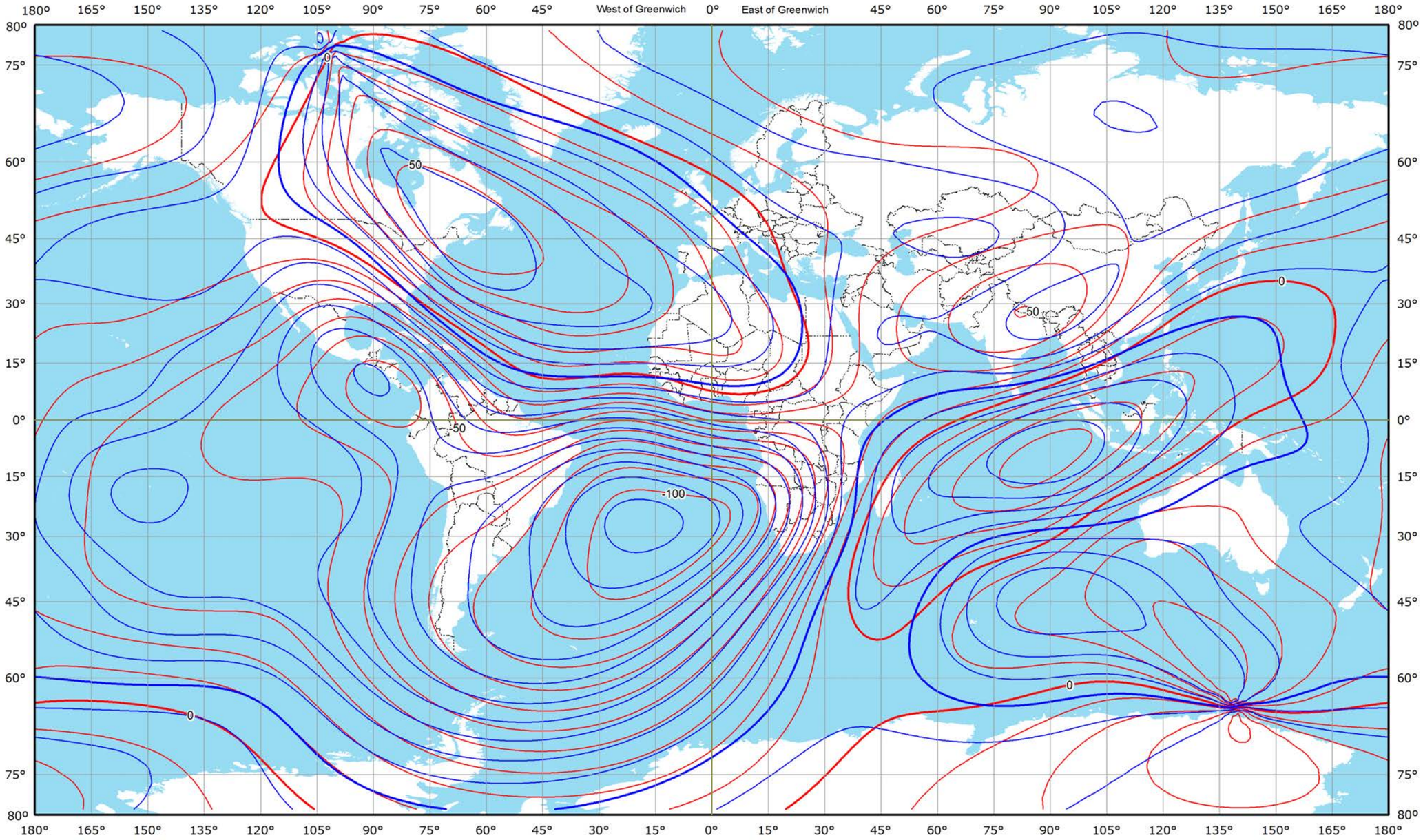

Epoch Isopors

1982
1987

Example. Secular variation value of horizontal component of MGMF (nT/year)

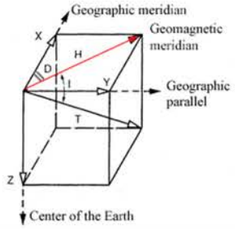

MGMF vector components

D Declination
I Inclination
H Horizontal component
T Total intensity
X North component
Y East component
Z Vertical component

Scale 1: 120 000 000

Projection: Miller cylindrical

SECULAR VARIATION OF HORIZONTAL COMPONENT OF MGMF

SV – 1987, 1992 – H

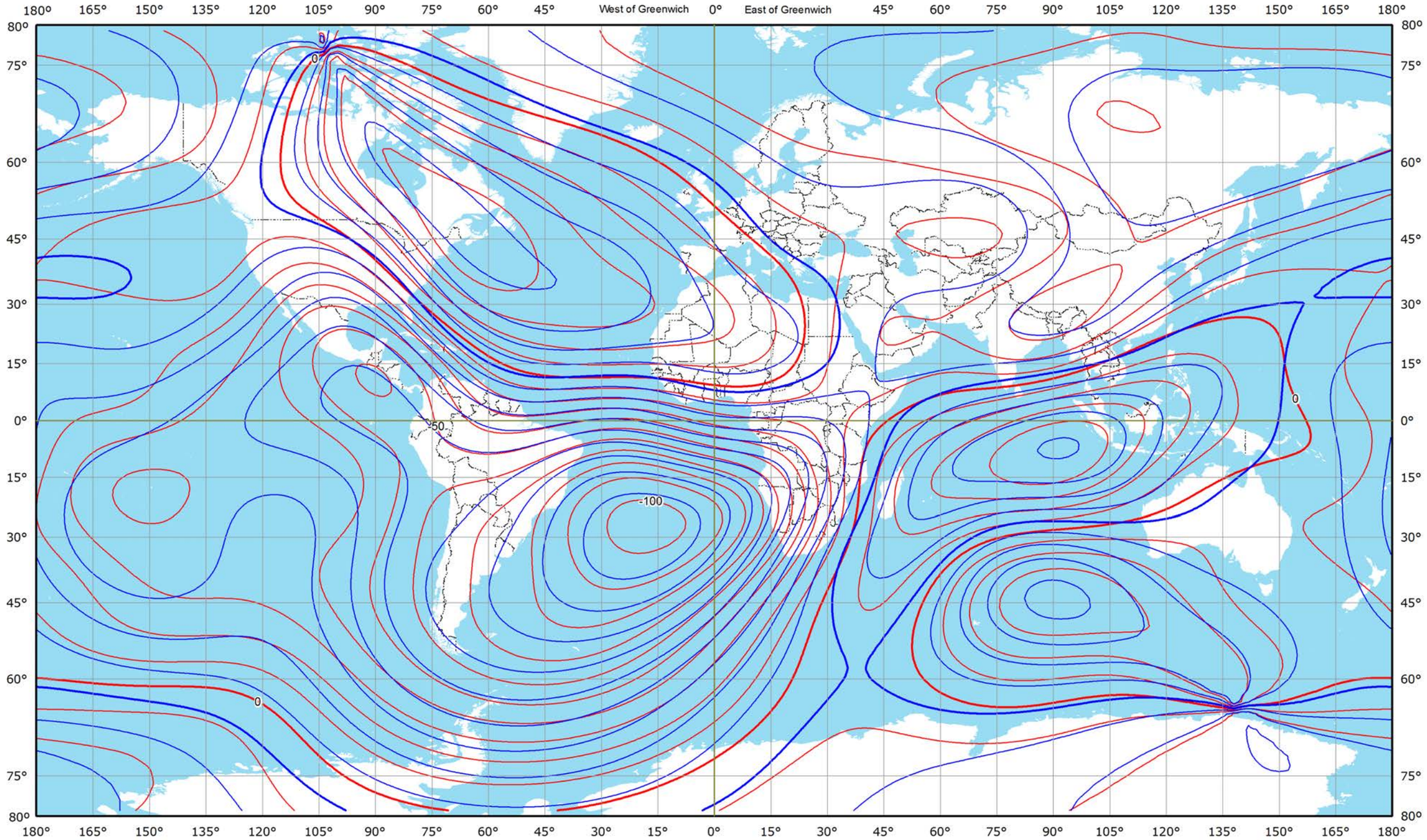

Epoch Isopors

1987
1992

Example. Secular variation value of horizontal component of MGMF (nT/year)

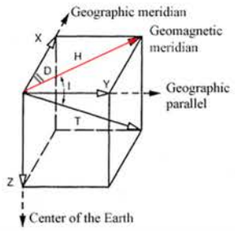

MGMF vector components

D Declination
I Inclination
H Horizontal component
T Total intensity
X North component
Y East component
Z Vertical component

Scale 1: 120 000 000

Projection: Miller cylindrical

SECULAR VARIATION OF HORIZONTAL COMPONENT OF MGMF

SV – 1992, 1997 – H

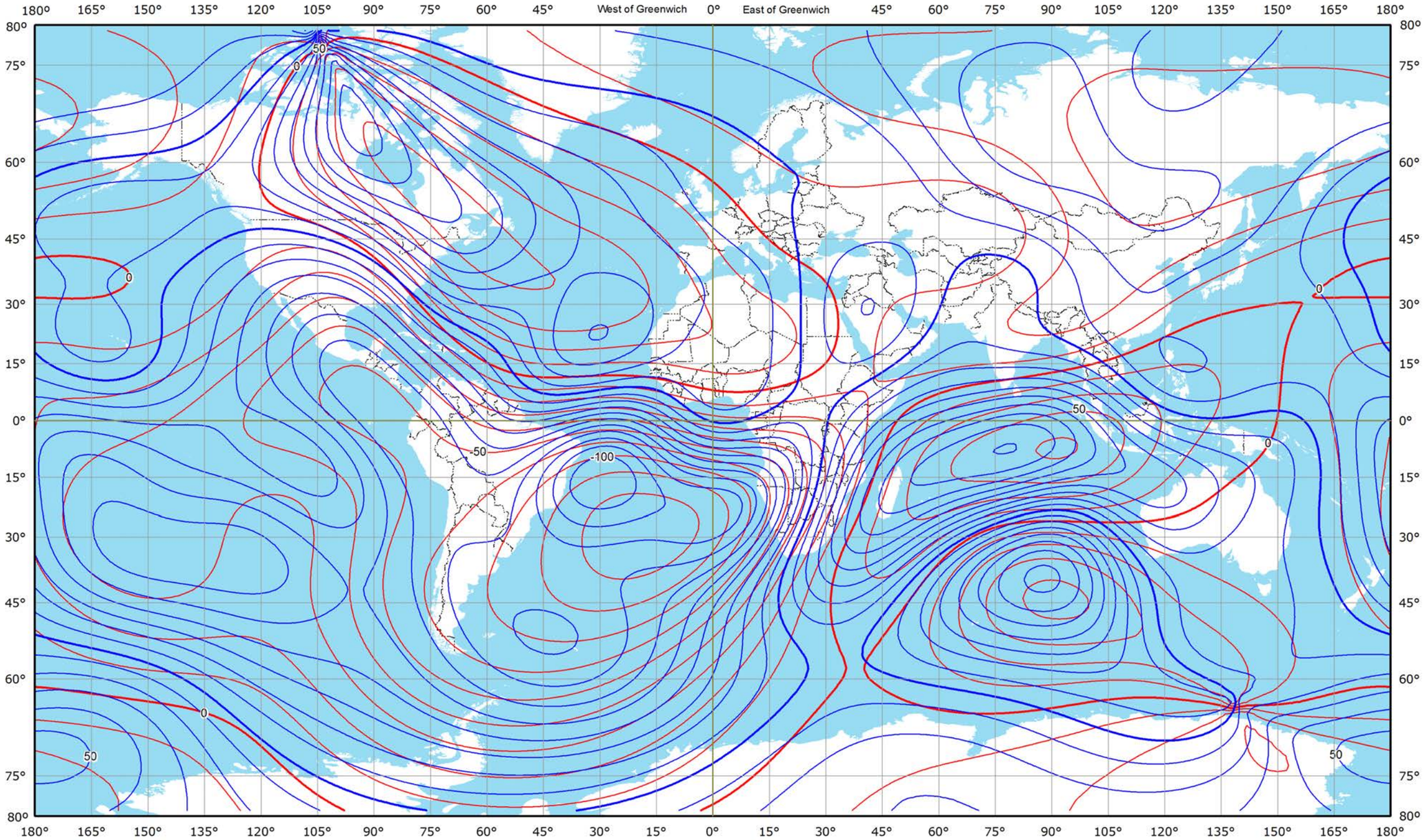

Epoch Isopors

1992
1997

Example. Secular variation value of horizontal component of MGMF (nT/year)

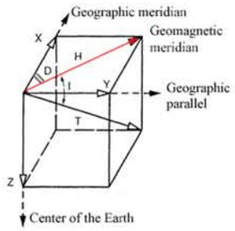

MGMF vector components

D Declination
I Inclination
H Horizontal component
T Total intensity
X North component
Y East component
Z Vertical component

Scale 1: 120 000 000

Projection: Miller cylindrical

SECULAR VARIATION OF HORIZONTAL COMPONENT OF MGMF

SV – 1997, 2002 – H

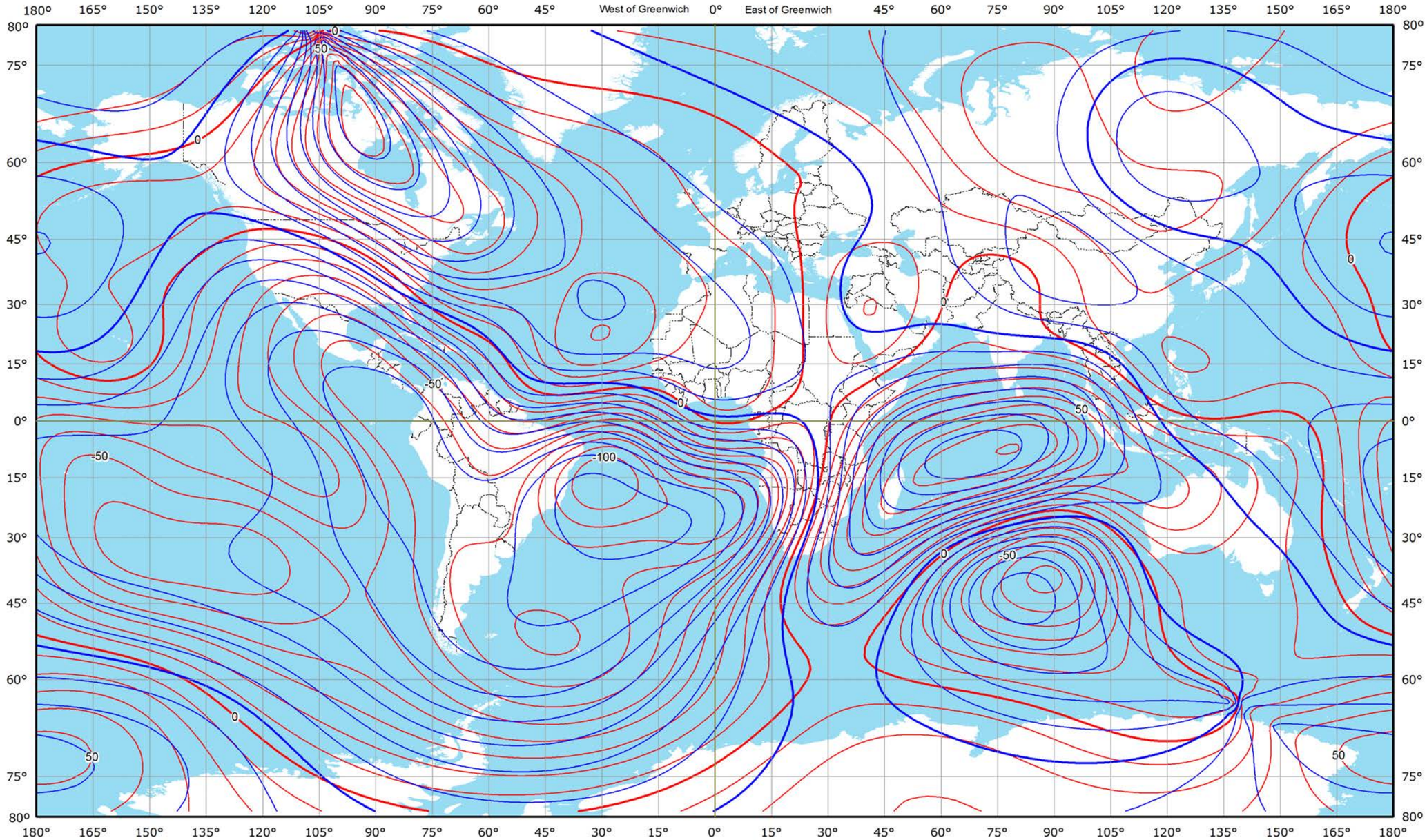

Epoch Isopors

1997
2002

Example. Secular variation value of horizontal component of MGMF (nT/year)

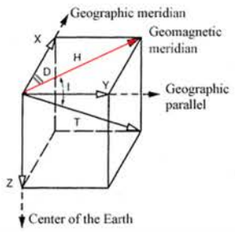

MGMF vector components

D Declination
I Inclination
H Horizontal component
T Total intensity
X North component
Y East component
Z Vertical component

Scale 1: 120 000 000

Projection: Miller cylindrical

SECULAR VARIATION OF HORIZONTAL COMPONENT OF MGMF

SV – 2002, 2007 – H

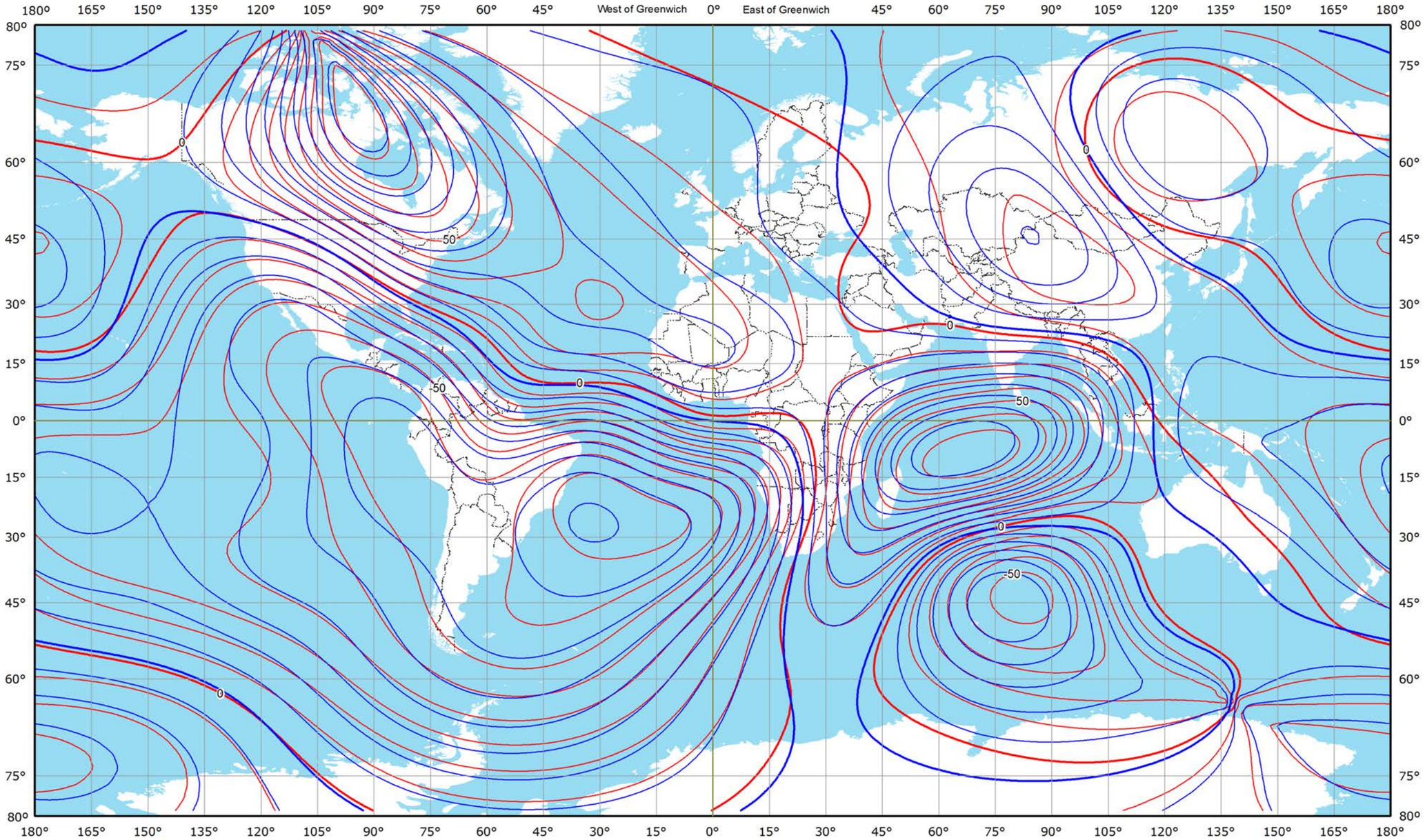

Epoch Isopors

2002
2007

Example. Secular variation value of horizontal component of MGMF (nT/year)

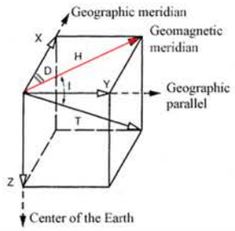

MGMF vector components

D Declination
I Inclination
H Horizontal component
T Total intensity
X North component
Y East component
Z Vertical component

Scale 1: 120 000 000

Projection: Miller cylindrical

SECULAR VARIATION OF MGMF TOTAL INTENSITY

SV – 1902, 1907 – T

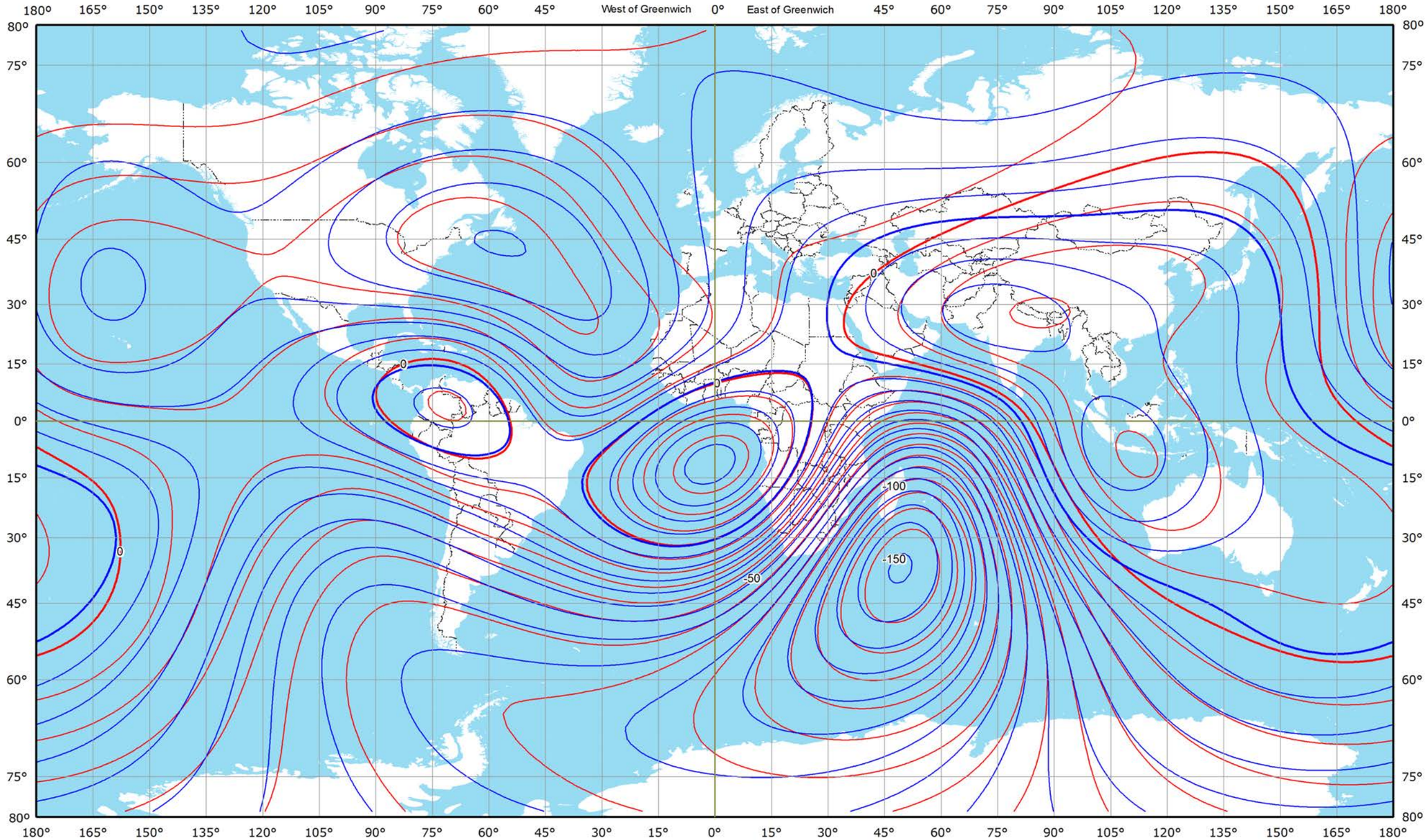

Epoch Isopors

1902
1907

Example. Secular variation value of MGMF total intensity (nT/year)

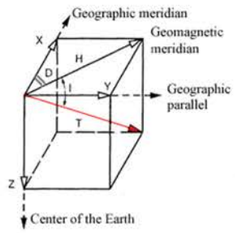

MGMF vector components

D Declination
I Inclination
H Horizontal component
T Total intensity
X North component
Y East component
Z Vertical component

Scale 1: 120 000 000

Projection: Miller cylindrical

SECULAR VARIATION OF MGMF TOTAL INTENSITY

SV – 1907, 1912 – T

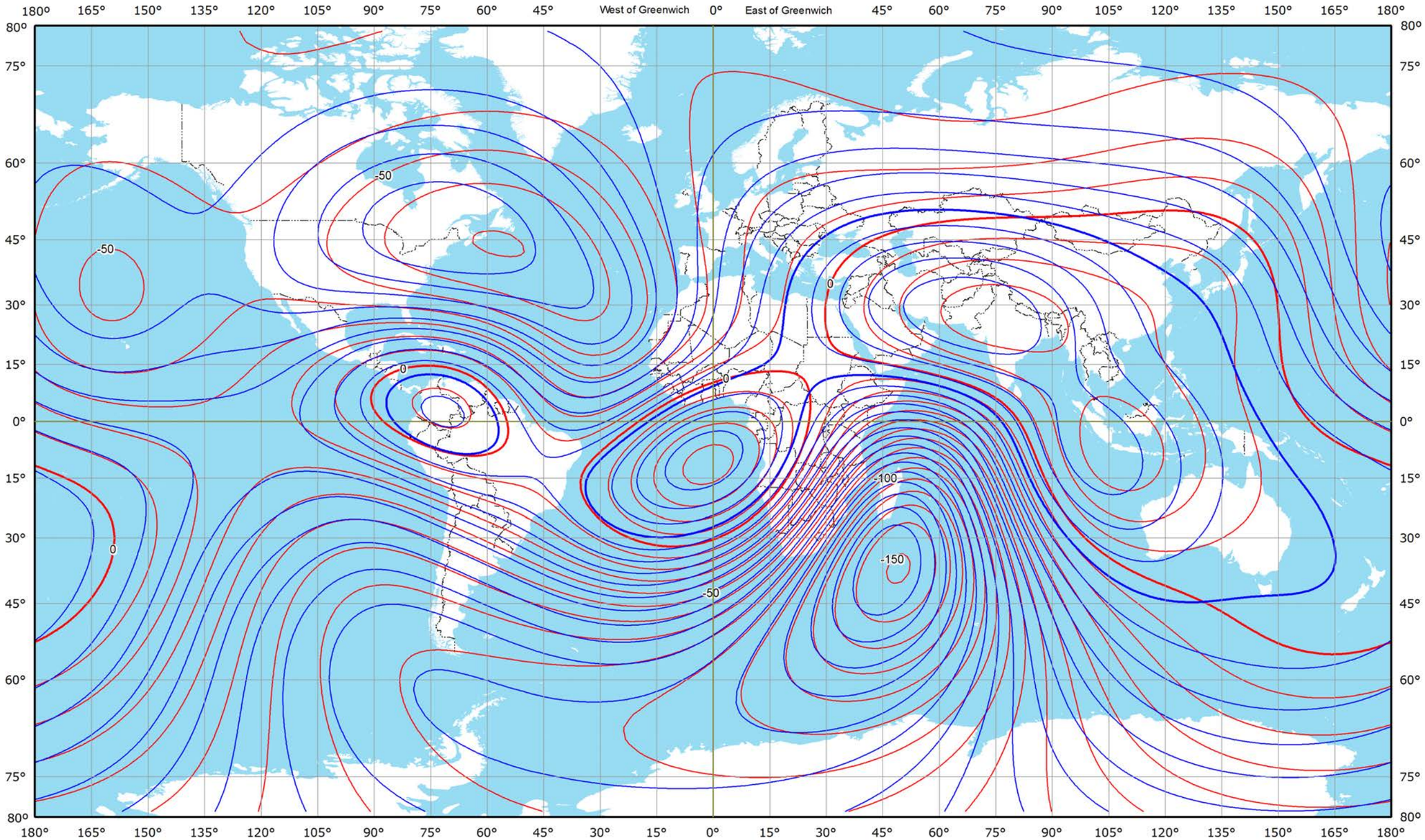

Epoch Isopors

1907
1912

Example. Secular variation value of MGMF total intensity (nT/year)

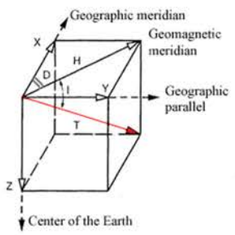

MGMF vector components

D Declination
I Inclination
H Horizontal component
T Total intensity
X North component
Y East component
Z Vertical component

Scale 1: 120 000 000

Projection: Miller cylindrical

SECULAR VARIATION OF MGMF TOTAL INTENSITY

SV – 1912, 1917 – T

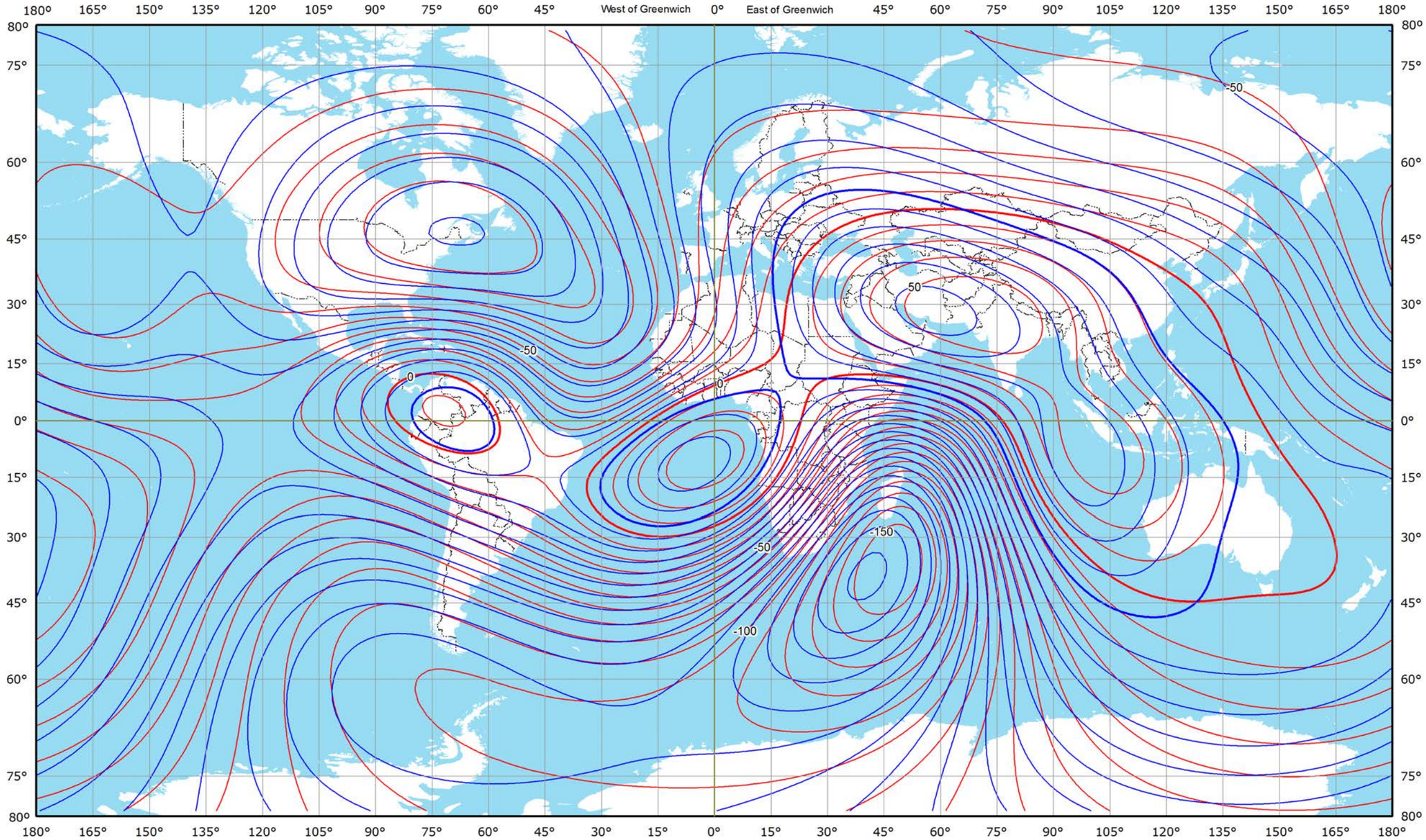

Epoch Isopors

1912
1917

Example. Secular variation value of MGMF total intensity (nT/year)

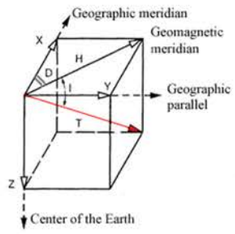

MGMF vector components

D Declination
I Inclination
H Horizontal component
T Total intensity
X North component
Y East component
Z Vertical component

Scale 1: 120 000 000

Projection: Miller cylindrical

SECULAR VARIATION OF MGMF TOTAL INTENSITY

SV – 1917, 1922 – T

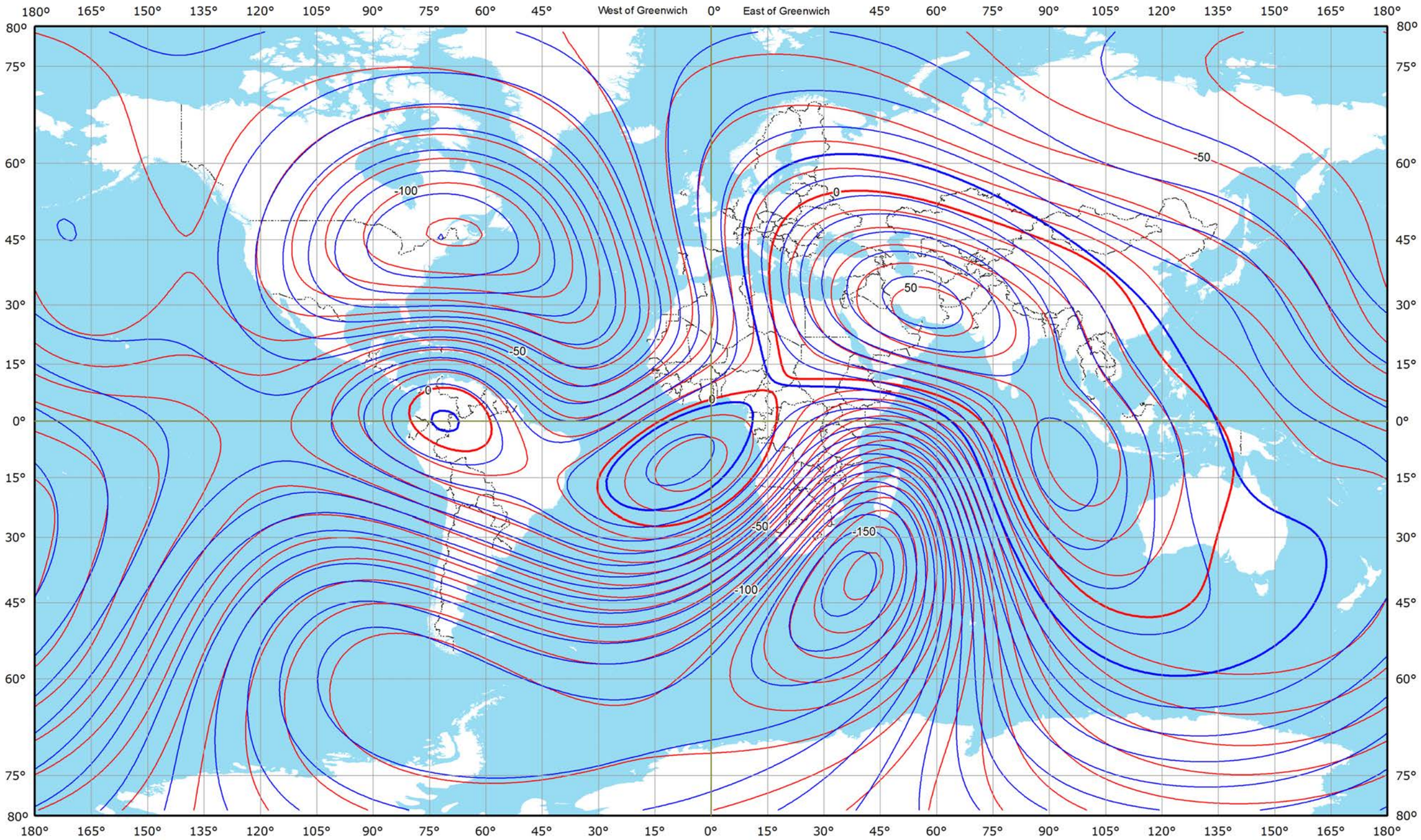

Epoch Isopors

1917
1922

Example. Secular variation value of MGMF total intensity (nT/year)

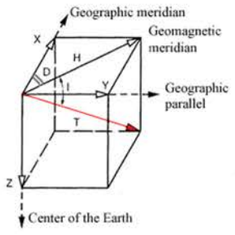

MGMF vector components

D Declination
I Inclination
H Horizontal component
T Total intensity
X North component
Y East component
Z Vertical component

Scale 1: 120 000 000

Projection: Miller cylindrical

SECULAR VARIATION OF MGMF TOTAL INTENSITY

SV – 1922, 1927 – T

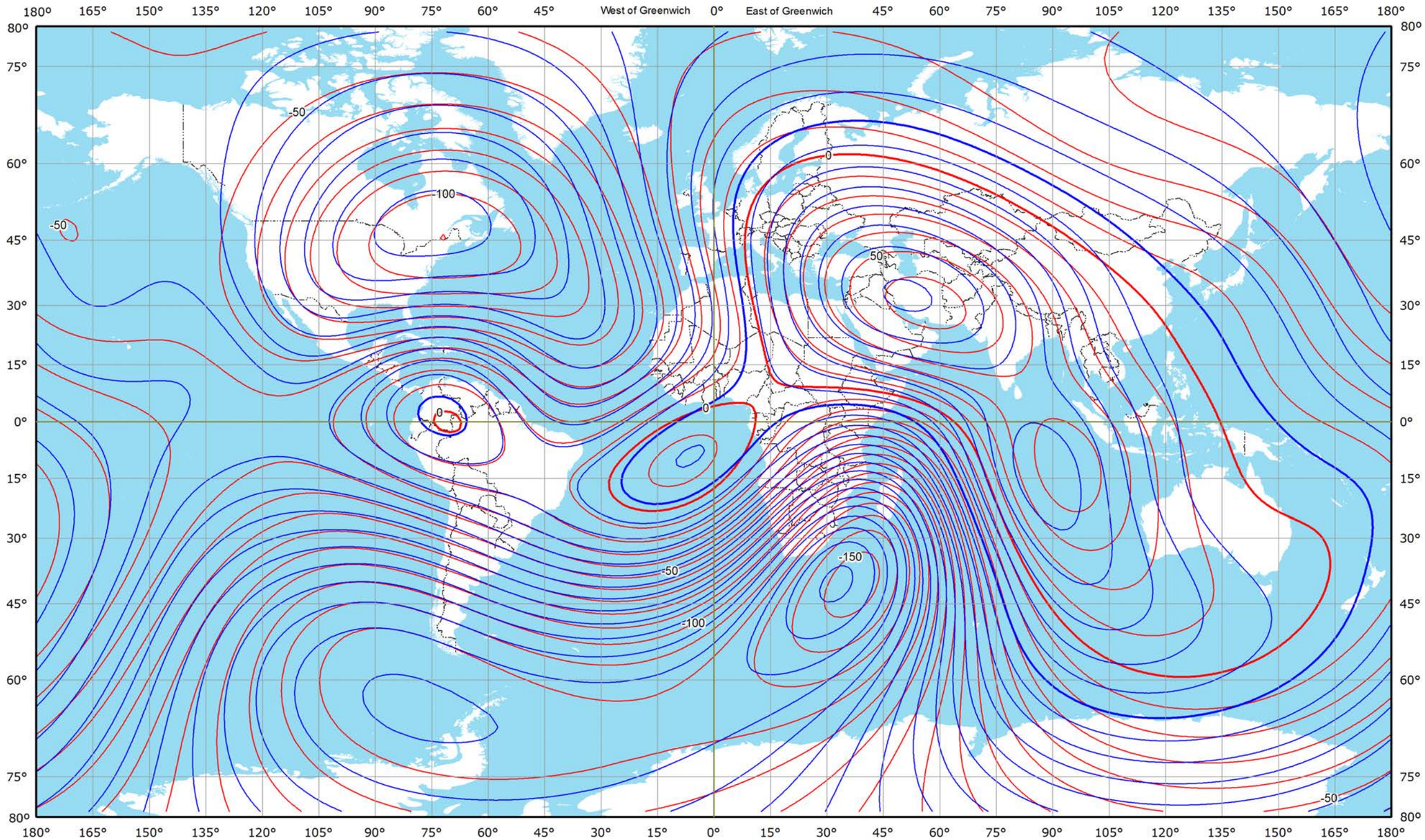

Epoch Isopors

1922
1927

Example. Secular variation value of MGMF total intensity (nT/year)

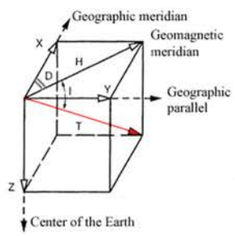

MGMF vector components

D Declination
I Inclination
H Horizontal component
T Total intensity
X North component
Y East component
Z Vertical component

Scale 1: 120 000 000

Projection: Miller cylindrical

SECULAR VARIATION OF MGMF TOTAL INTENSITY

SV – 1927, 1932 – T

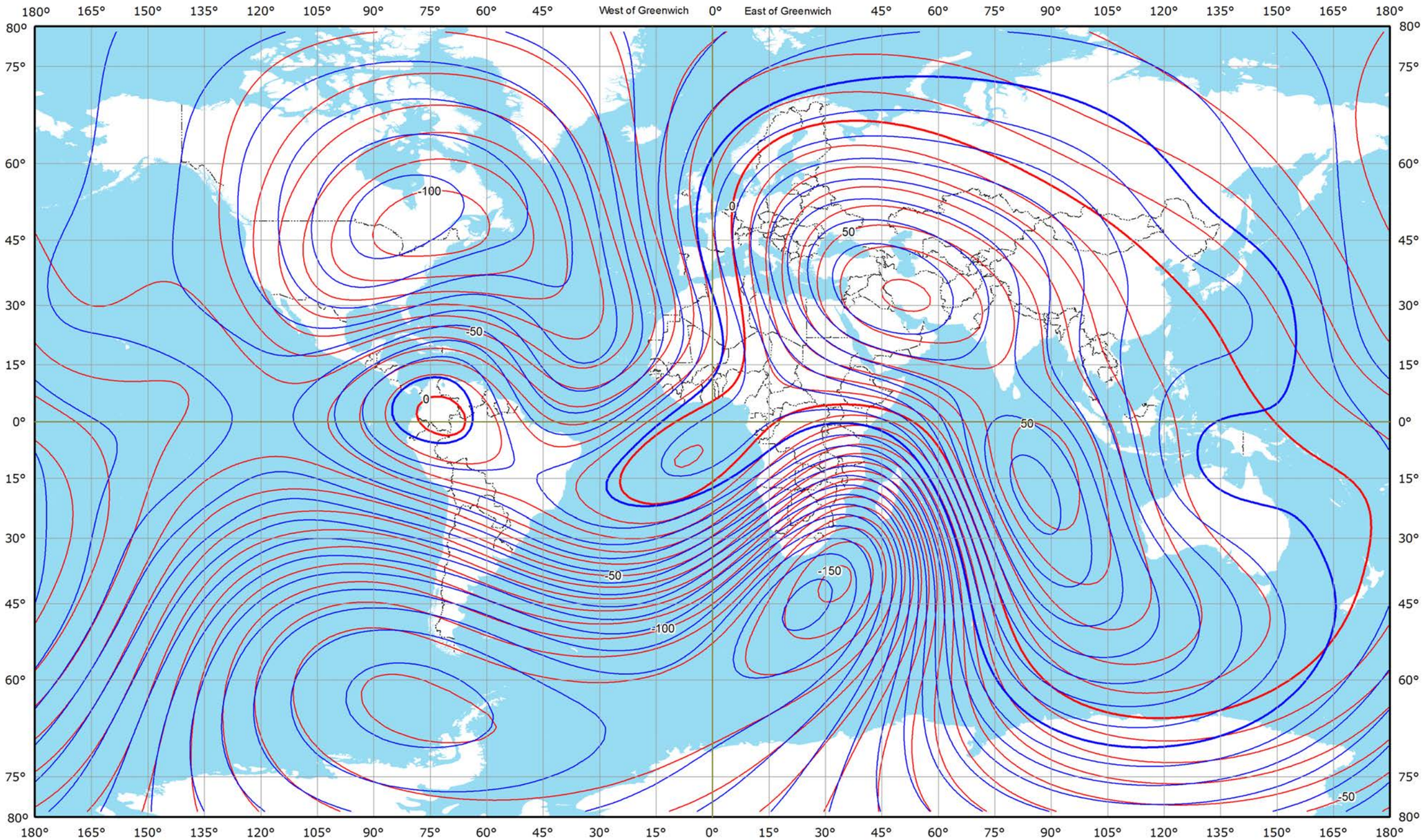

Epoch Isopors

1927
1932

Example. Secular variation value of MGMF total intensity (nT/year)

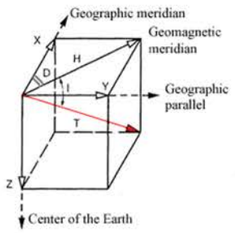

MGMF vector components

D Declination
I Inclination
H Horizontal component
T Total intensity
X North component
Y East component
Z Vertical component

Scale 1: 120 000 000

Projection: Miller cylindrical

SECULAR VARIATION OF MGMF TOTAL INTENSITY

SV – 1932, 1937 – T

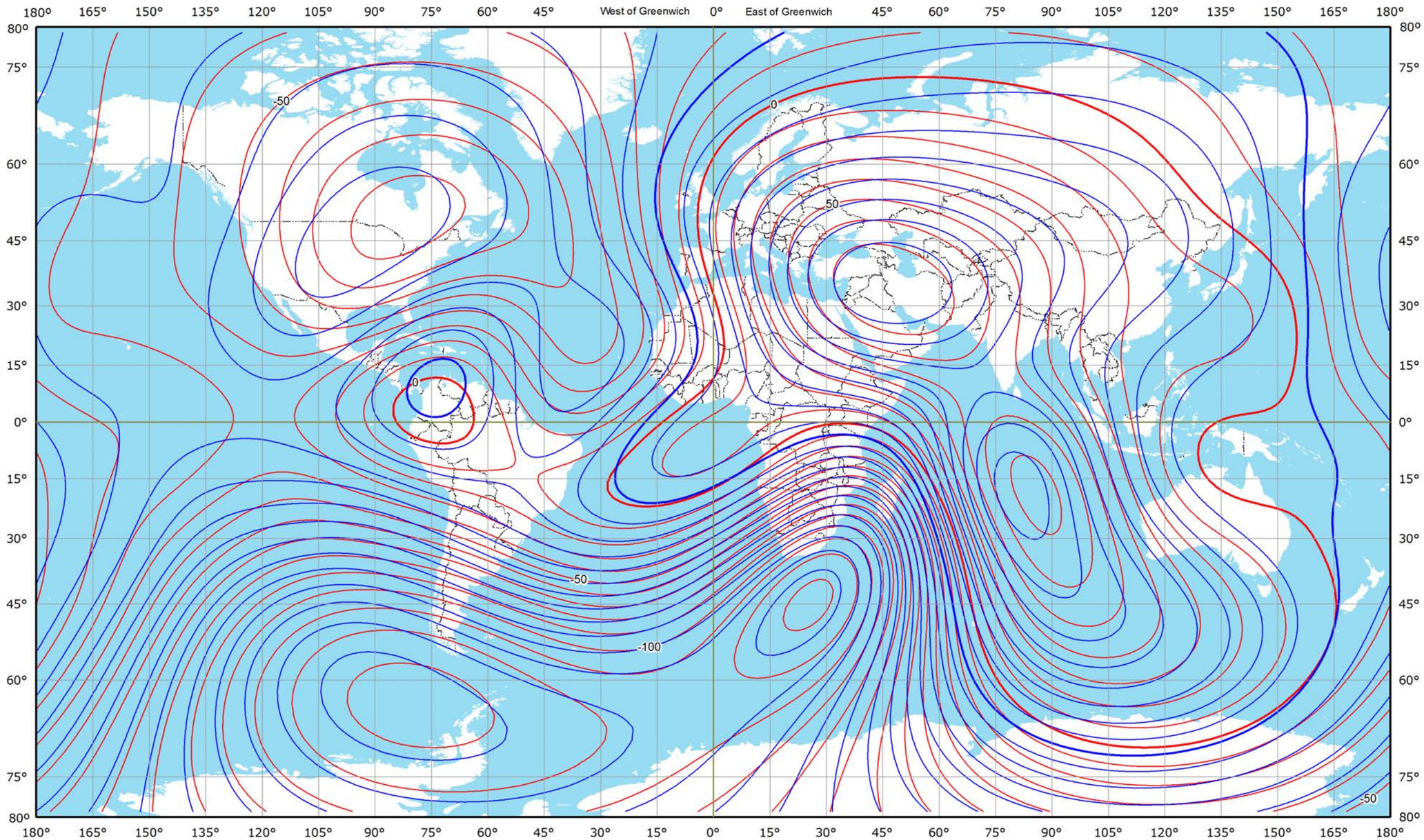

Epoch Isopors

1932
1937

Example. Secular variation value of MGMF total intensity (nT/year)

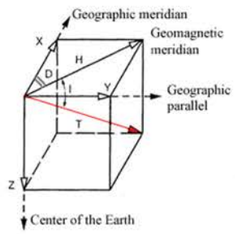

MGMF vector components

D Declination
I Inclination
H Horizontal component
T Total intensity
X North component
Y East component
Z Vertical component

Scale 1: 120 000 000

Projection: Miller cylindrical

SECULAR VARIATION OF MGMF TOTAL INTENSITY

SV – 1937, 1942 – T

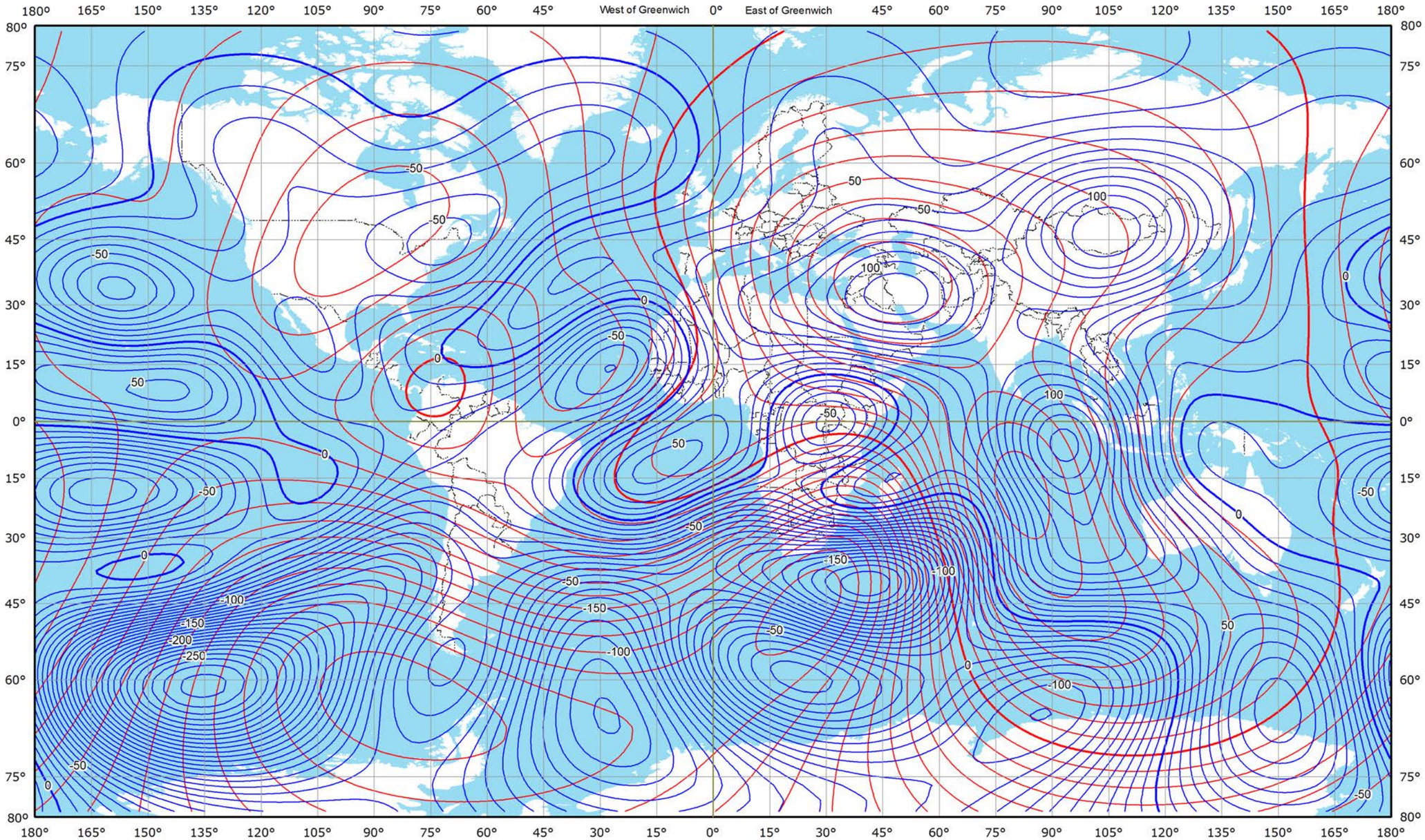

Epoch Isopors

1937
1942

Example. Secular variation value of MGMF total intensity (nT/year)

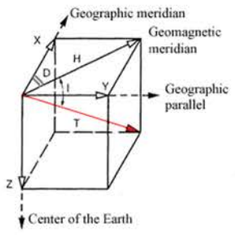

MGMF vector components

D Declination
I Inclination
H Horizontal component
T Total intensity
X North component
Y East component
Z Vertical component

Scale 1: 120 000 000

Projection: Miller cylindrical

SECULAR VARIATION OF MGMF TOTAL INTENSITY

SV – 1942, 1947 – T

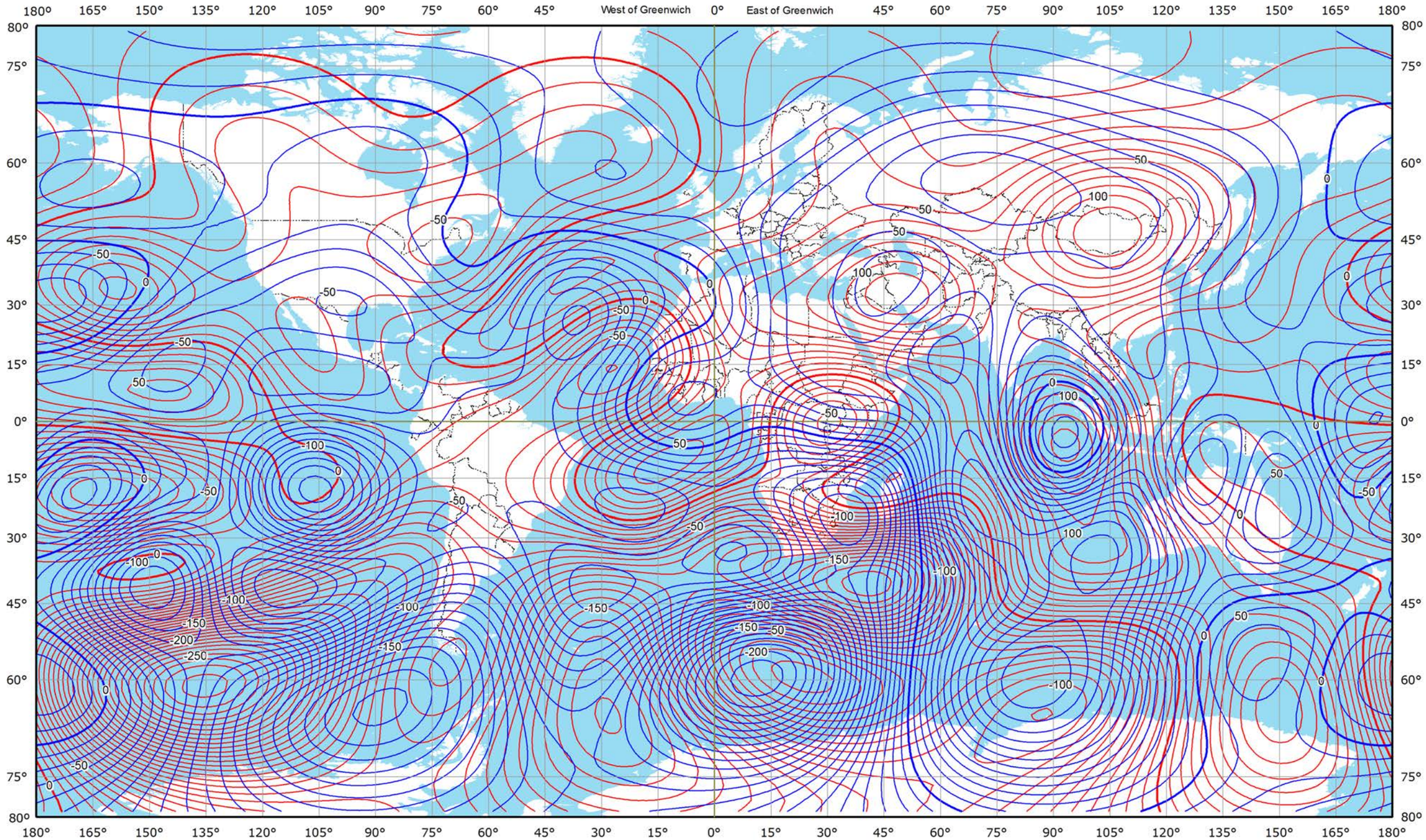

Epoch Isopors

1942
1947

Example. Secular variation value of MGMF total intensity (nT/year)

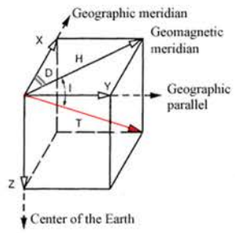

MGMF vector components

D Declination
I Inclination
H Horizontal component
T Total intensity
X North component
Y East component
Z Vertical component

Scale 1: 120 000 000

Projection: Miller cylindrical

SECULAR VARIATION OF MGMF TOTAL INTENSITY

SV – 1947, 1952 – T

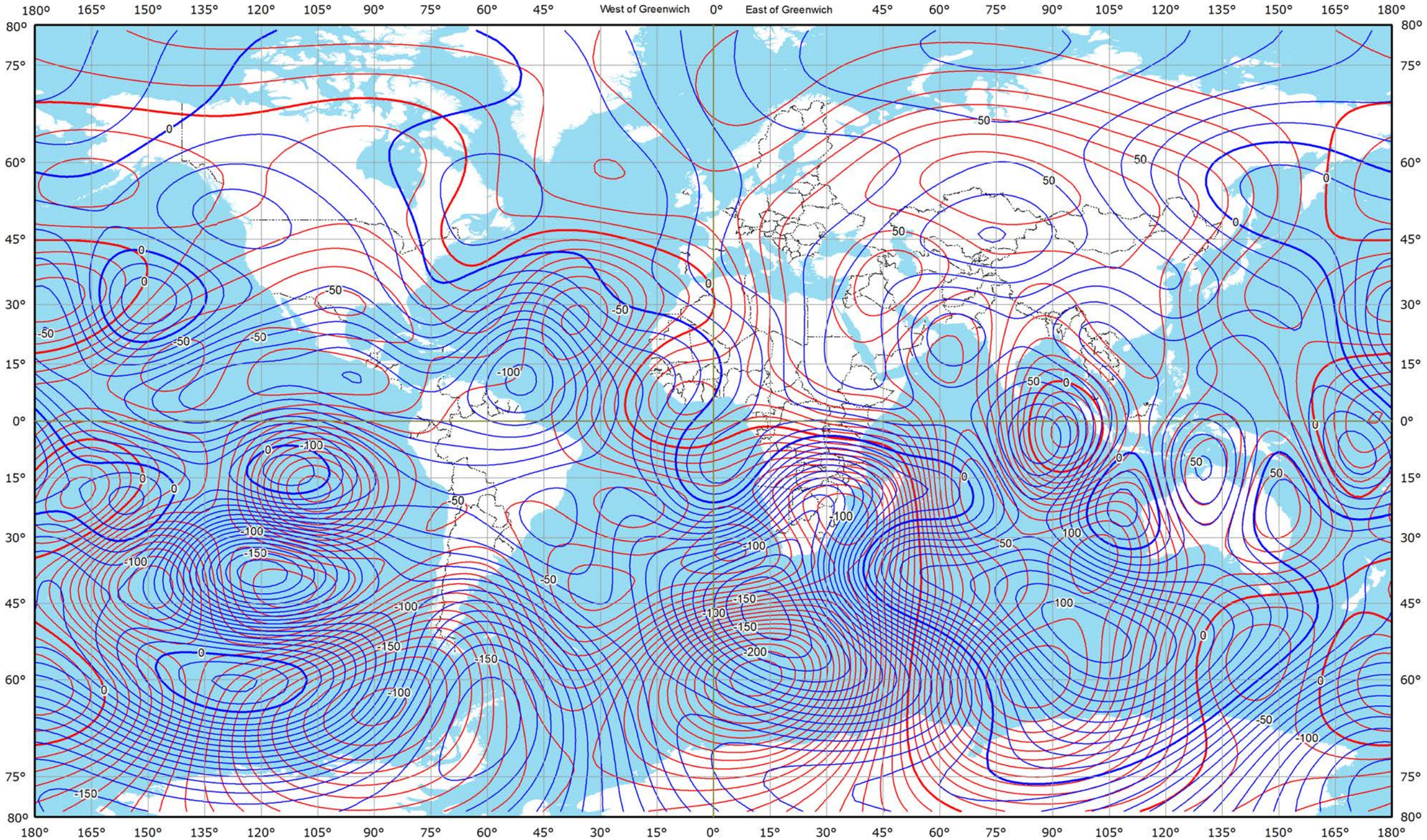

Epoch Isopors

1947
1952

Example. Secular variation value of MGMF total intensity (nT/year)

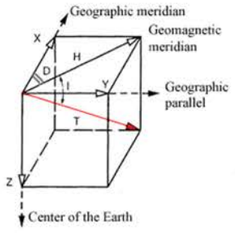

MGMF vector components

D Declination
I Inclination
H Horizontal component
T Total intensity
X North component
Y East component
Z Vertical component

Scale 1: 120 000 000

Projection: Miller cylindrical

SECULAR VARIATION OF MGMF TOTAL INTENSITY

SV – 1952, 1957 – T

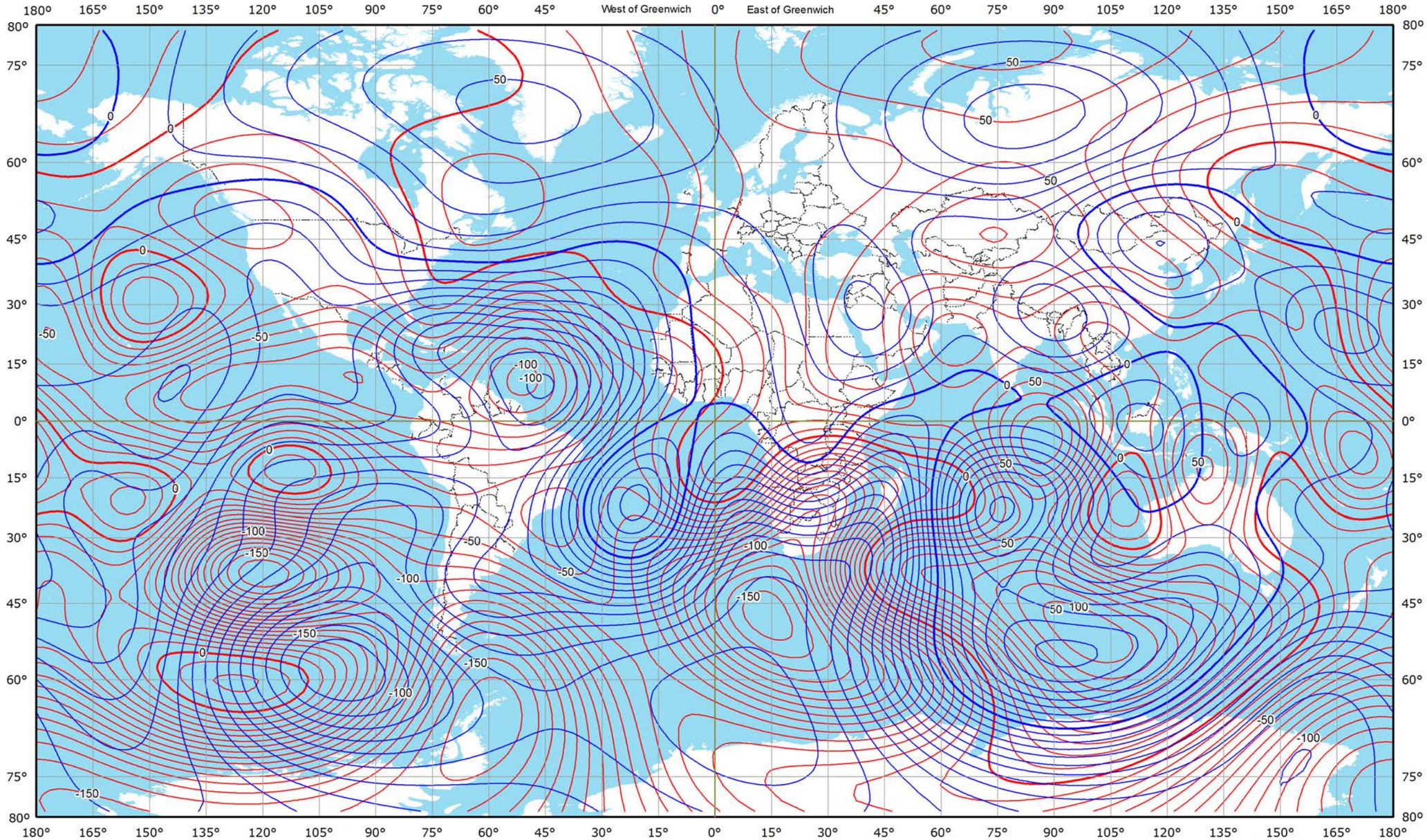

Epoch Isopors

1952
1957

Example. Secular variation value of MGMF total intensity (nT/year)

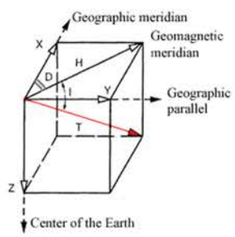

MGMF vector components

D Declination
I Inclination
H Horizontal component
T Total intensity
X North component
Y East component
Z Vertical component

Scale 1: 120 000 000

Projection: Miller cylindrical

SECULAR VARIATION OF MGMF TOTAL INTENSITY

SV – 1957, 1962 – T

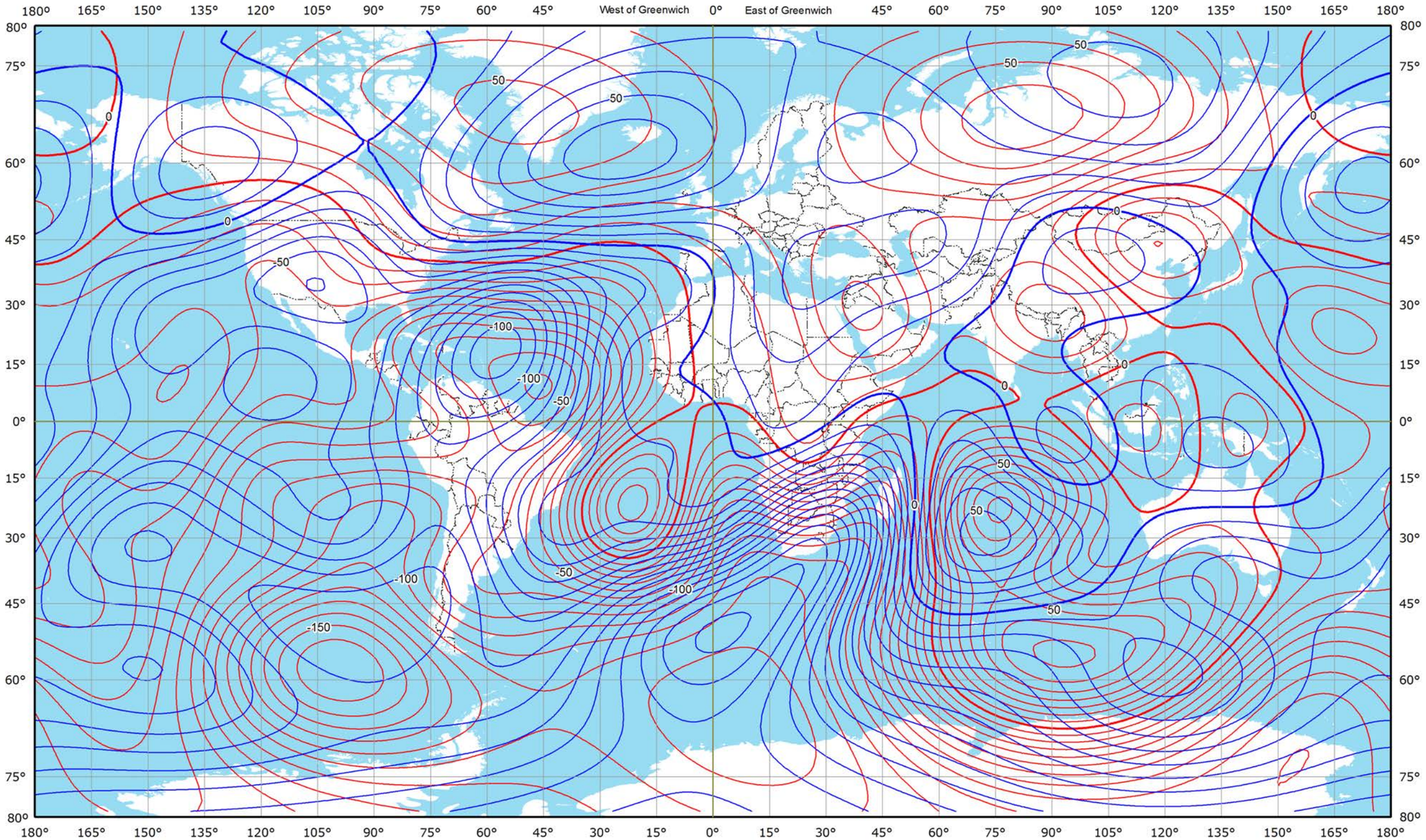

Epoch Isopors

1957
1962

Example. Secular variation value of MGMF total intensity (nT/year)

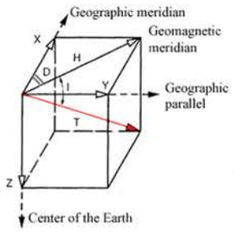

MGMF vector components

D Declination
I Inclination
H Horizontal component
T Total intensity
X North component
Y East component
Z Vertical component

Scale 1: 120 000 000

Projection: Miller cylindrical

SECULAR VARIATION OF MGMF TOTAL INTENSITY

SV – 1962, 1967 – T

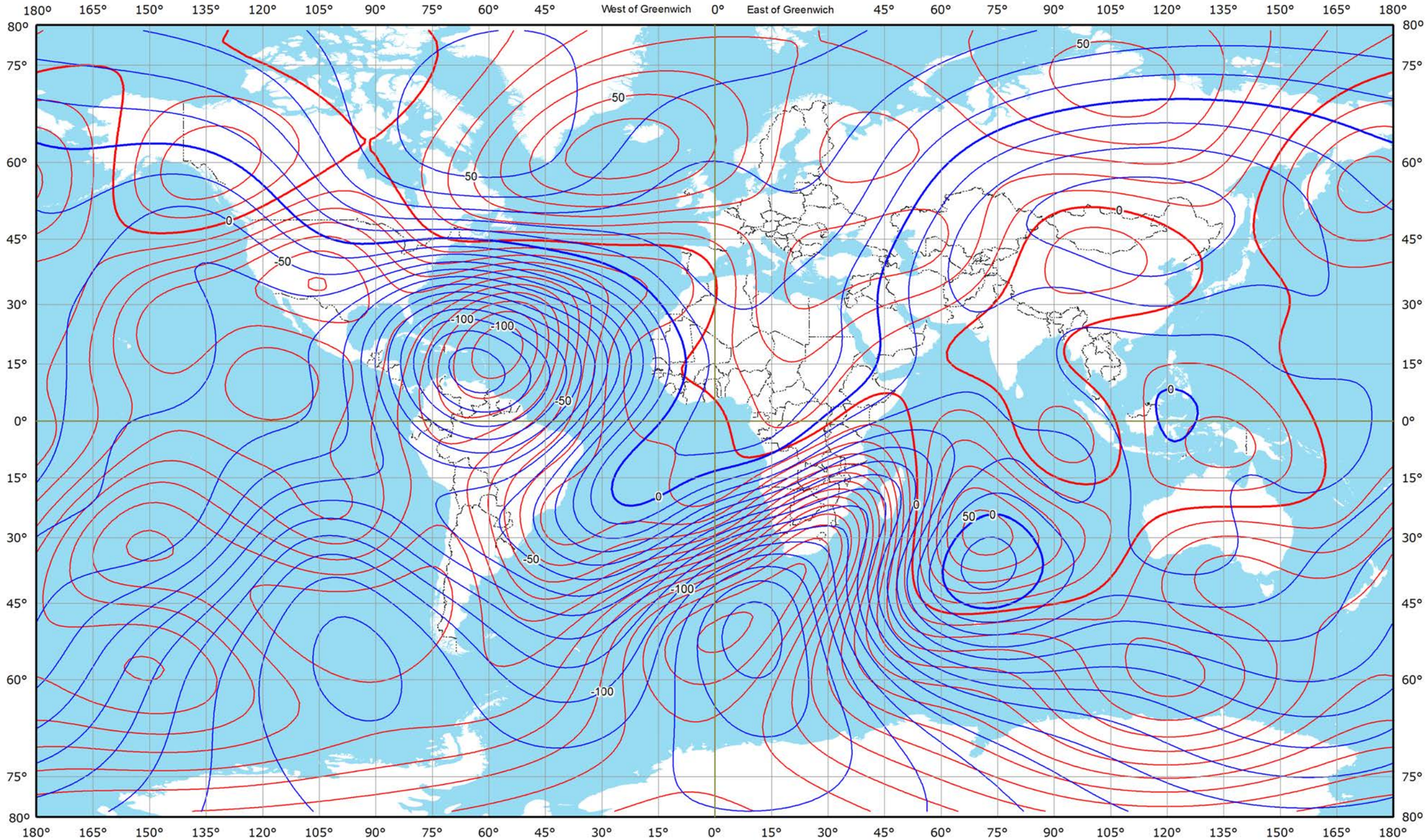

Epoch Isopors

1962
1967

Example. Secular variation value of MGMF total intensity (nT/year)

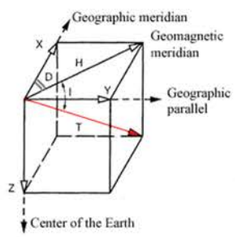

MGMF vector components

D Declination
I Inclination
H Horizontal component
T Total intensity
X North component
Y East component
Z Vertical component

Scale 1: 120 000 000

Projection: Miller cylindrical

SECULAR VARIATION OF MGMF TOTAL INTENSITY

SV – 1967, 1972 – T

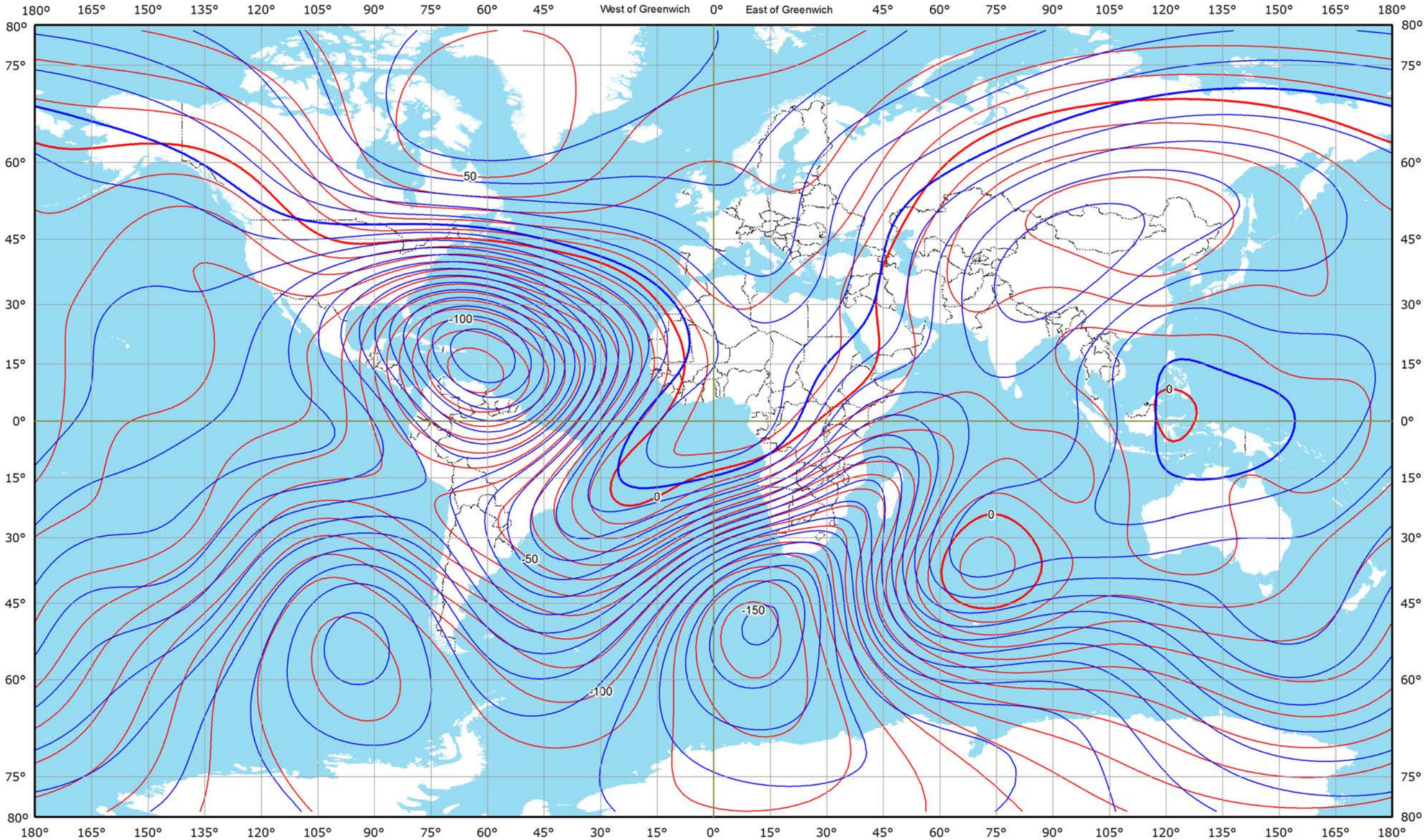

Epoch Isopors

1967
1972

Example. Secular variation value of MGMF total intensity (nT/year)

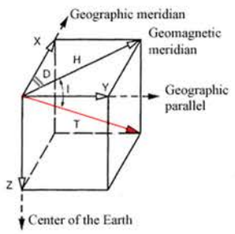

MGMF vector components

D Declination
I Inclination
H Horizontal component
T Total intensity
X North component
Y East component
Z Vertical component

Scale 1: 120 000 000

Projection: Miller cylindrical

SECULAR VARIATION OF MGMF TOTAL INTENSITY

SV – 1972, 1977 – T

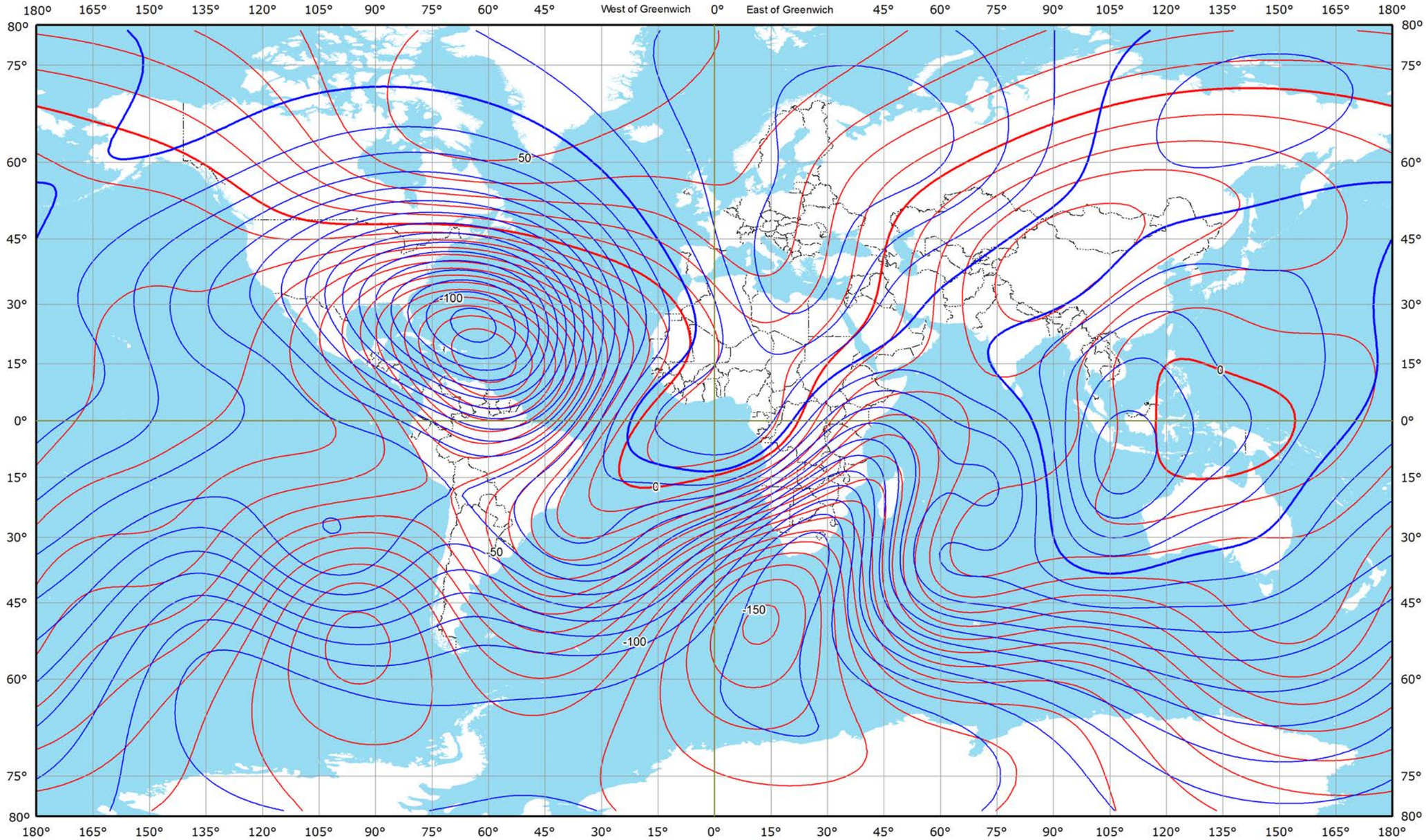

Epoch Isopors

1972
1977

Example. Secular variation value of MGMF total intensity (nT/year)

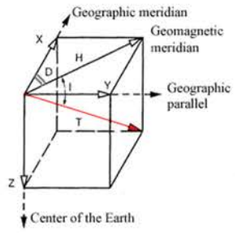

MGMF vector components

D Declination
I Inclination
H Horizontal component
T Total intensity
X North component
Y East component
Z Vertical component

Scale 1: 120 000 000

Projection: Miller cylindrical

SECULAR VARIATION OF MGMF TOTAL INTENSITY

SV – 1977, 1982 – T

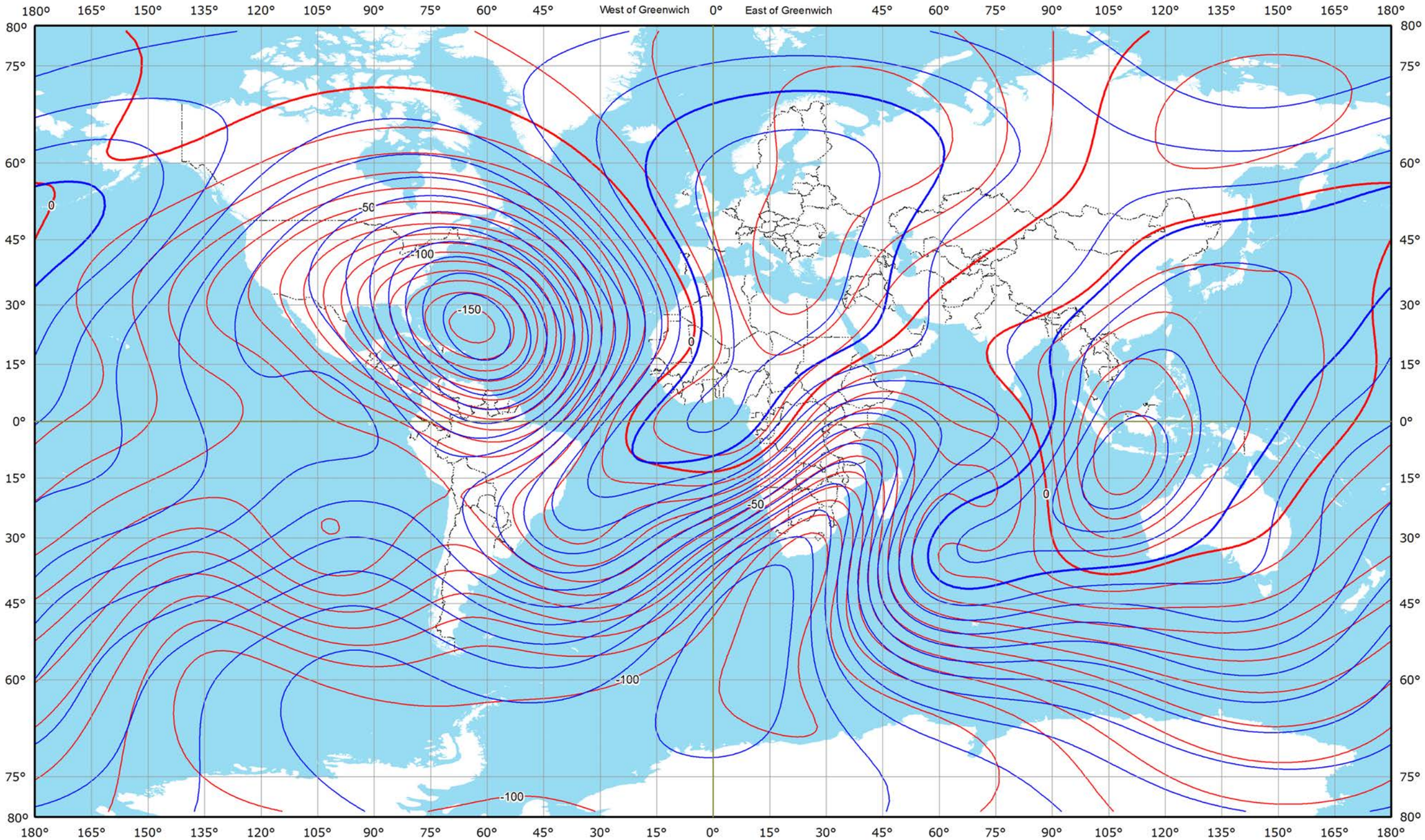

Epoch Isopors

1977
1982

Example. Secular variation value of MGMF total intensity (nT/year)

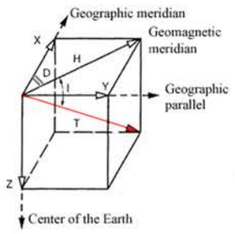

MGMF vector components

D Declination
I Inclination
H Horizontal component
T Total intensity
X North component
Y East component
Z Vertical component

Scale 1: 120 000 000

Projection: Miller cylindrical

SECULAR VARIATION OF MGMF TOTAL INTENSITY

SV – 1982, 1987 – T

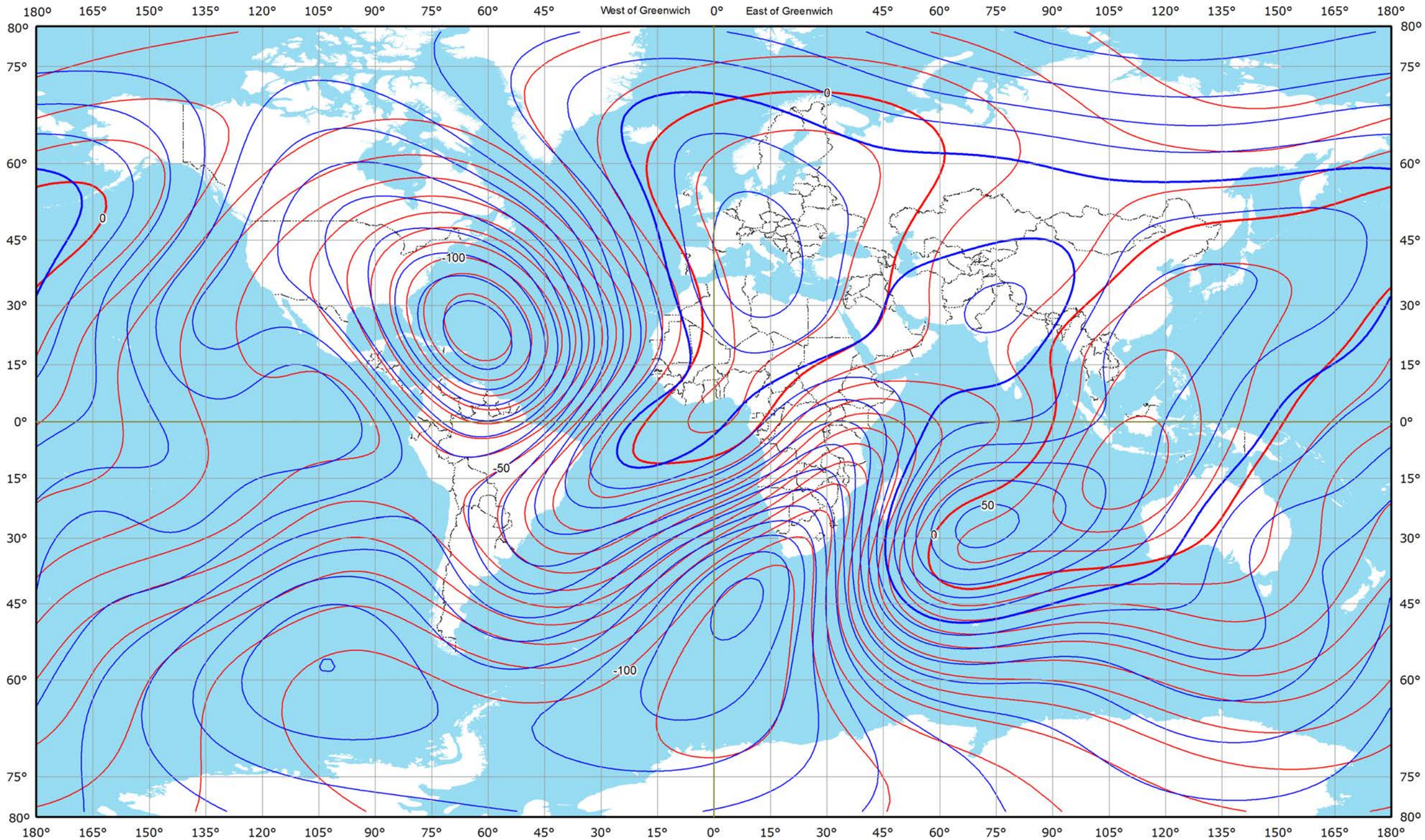

Epoch Isopors

1982
1987

Example. Secular variation value of MGMF total intensity (nT/year)

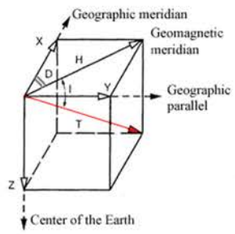

MGMF vector components

D Declination
I Inclination
H Horizontal component
T Total intensity
X North component
Y East component
Z Vertical component

Scale 1: 120 000 000

Projection: Miller cylindrical

SECULAR VARIATION OF MGMF TOTAL INTENSITY

SV – 1987, 1992 – T

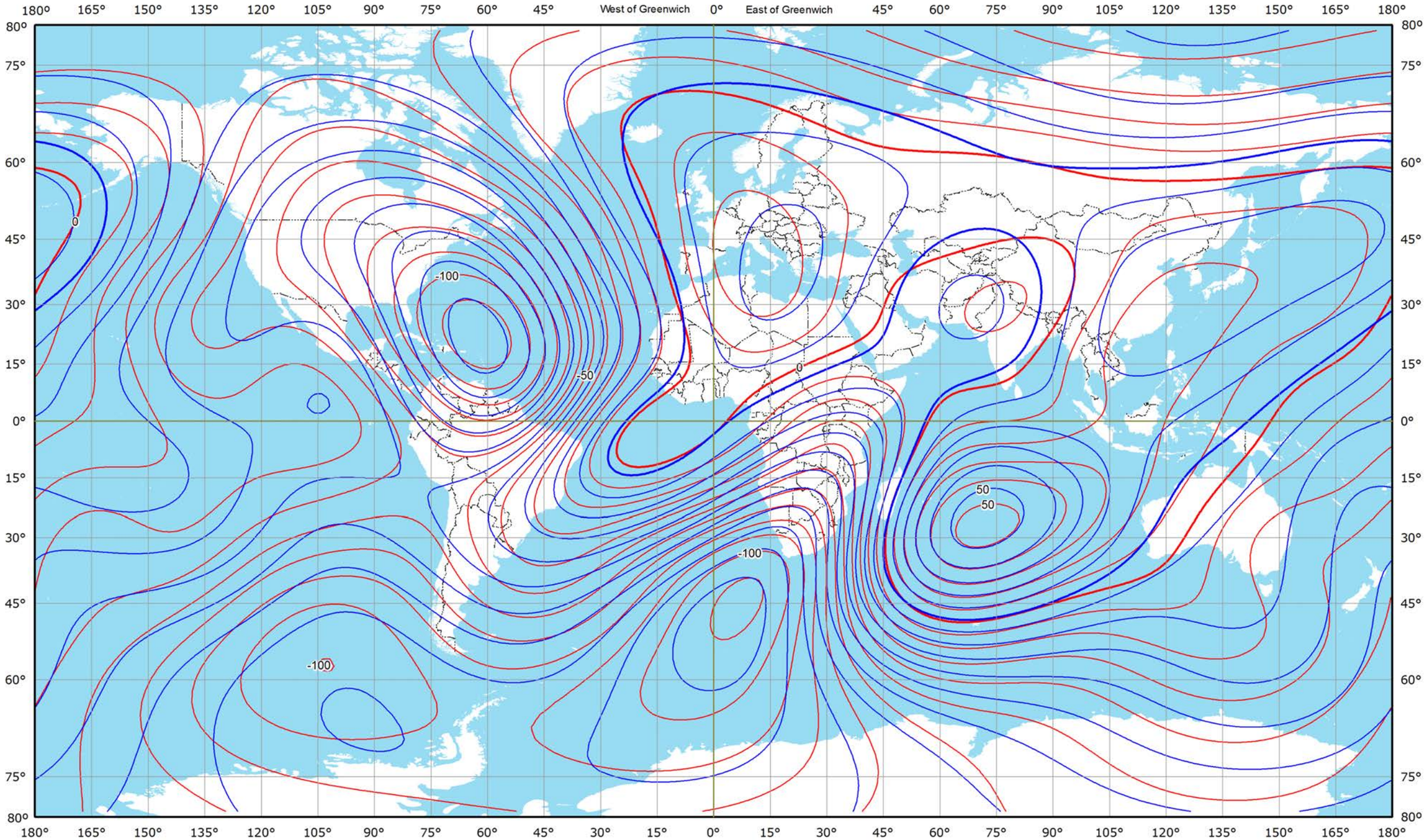

Epoch Isopors

1987
1992

Example. Secular variation value of MGMF total intensity (nT/year)

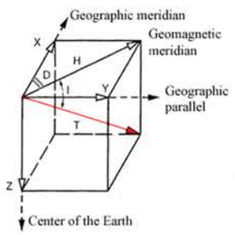

MGMF vector components

D Declination
I Inclination
H Horizontal component
T Total intensity
X North component
Y East component
Z Vertical component

Scale 1: 120 000 000

Projection: Miller cylindrical

SECULAR VARIATION OF MGMF TOTAL INTENSITY

SV – 1992, 1997 – T

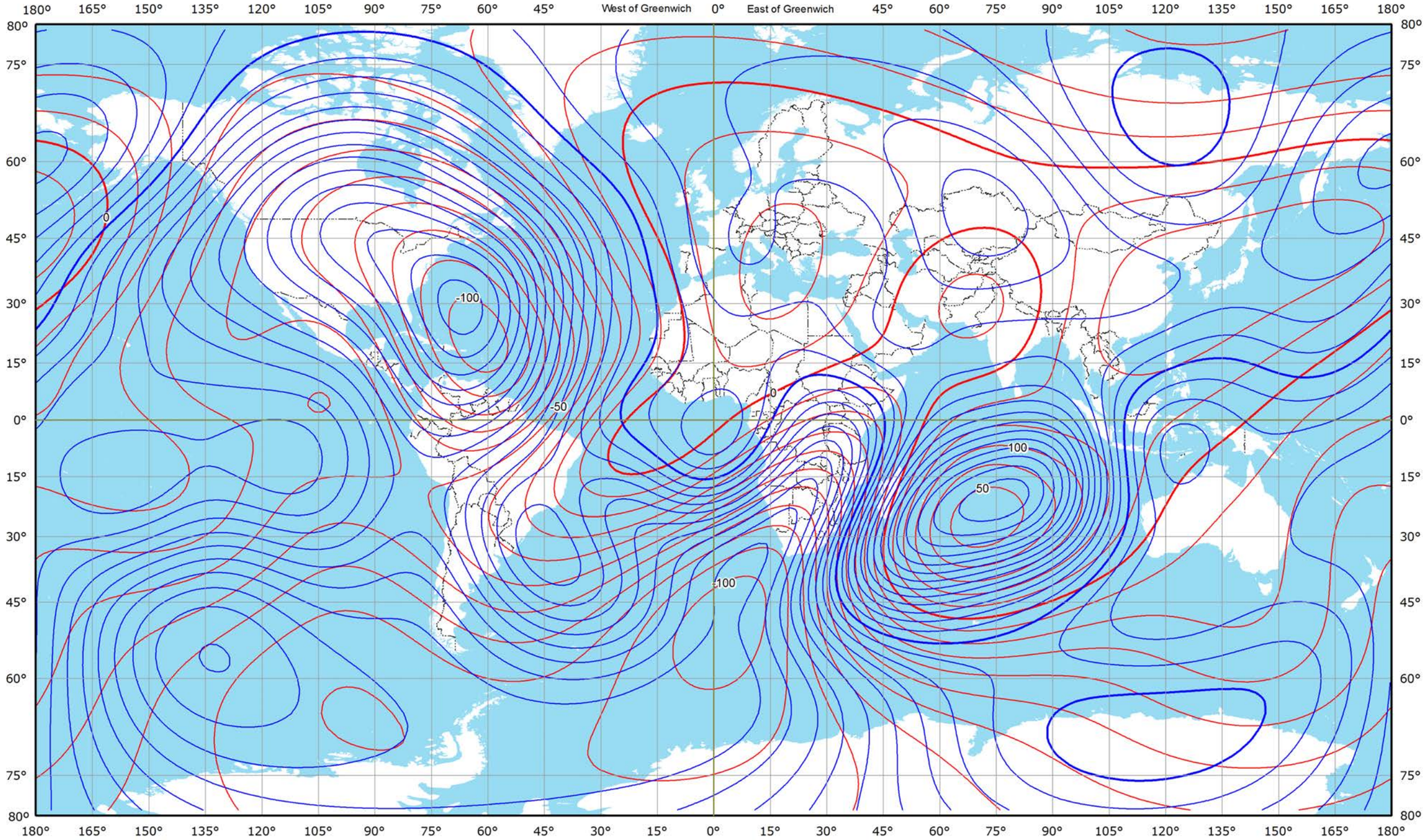

Epoch Isopors

1992
1997

Example. Secular variation value of MGMF total intensity (nT/year)

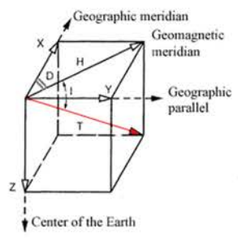

MGMF vector components

D Declination
I Inclination
H Horizontal component
T Total intensity
X North component
Y East component
Z Vertical component

Scale 1: 120 000 000

Projection: Miller cylindrical

SECULAR VARIATION OF MGMF TOTAL INTENSITY

SV – 1997, 2002 – T

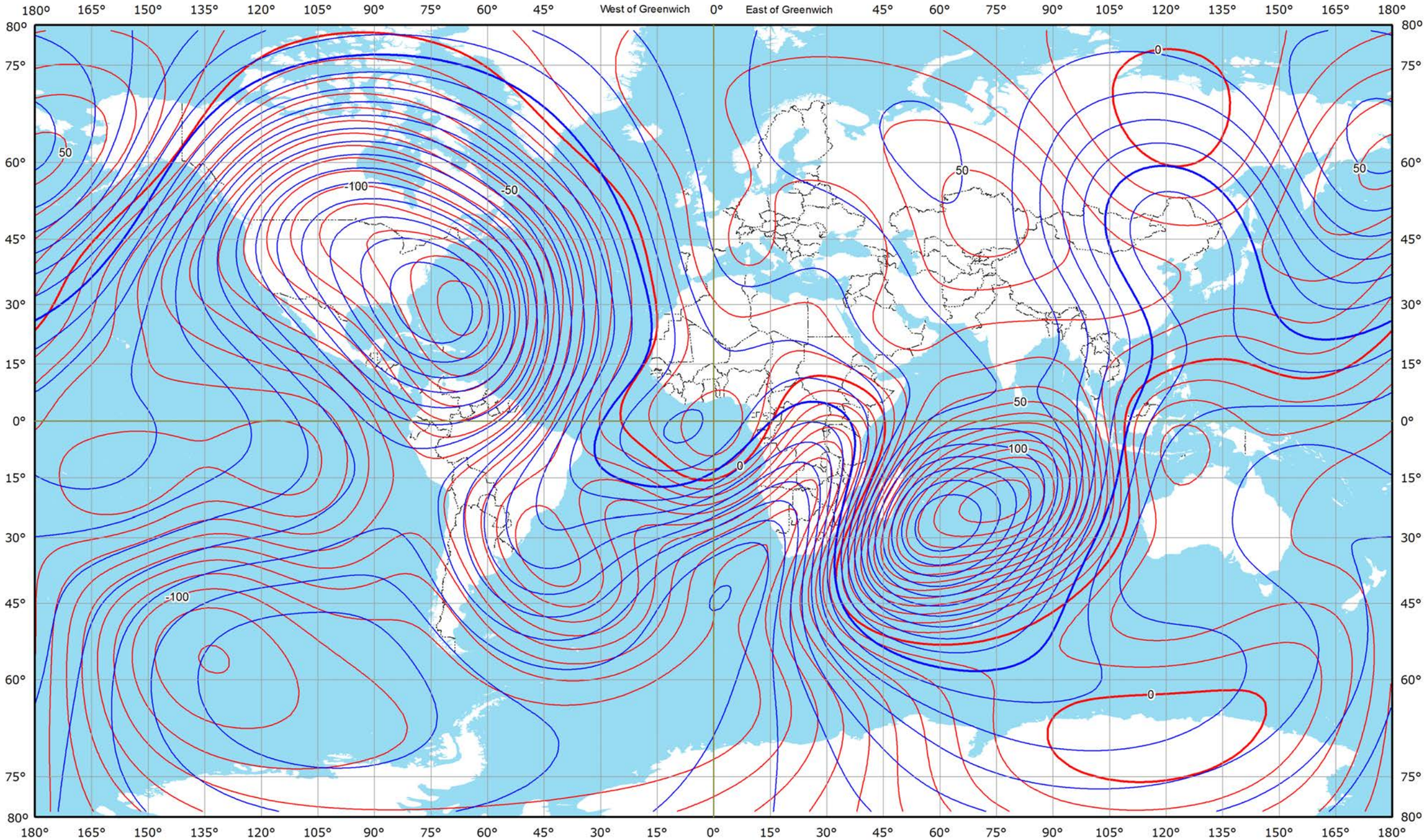

Epoch Isopors

1997
2002

Example. Secular variation value of MGMF total intensity (nT/year)

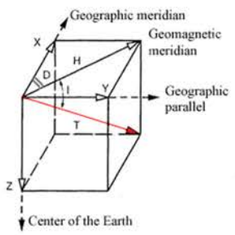

MGMF vector components

D Declination
I Inclination
H Horizontal component
T Total intensity
X North component
Y East component
Z Vertical component

Scale 1: 120 000 000

Projection: Miller cylindrical

SECULAR VARIATION OF MGMF TOTAL INTENSITY

SV – 2002, 2007 – T

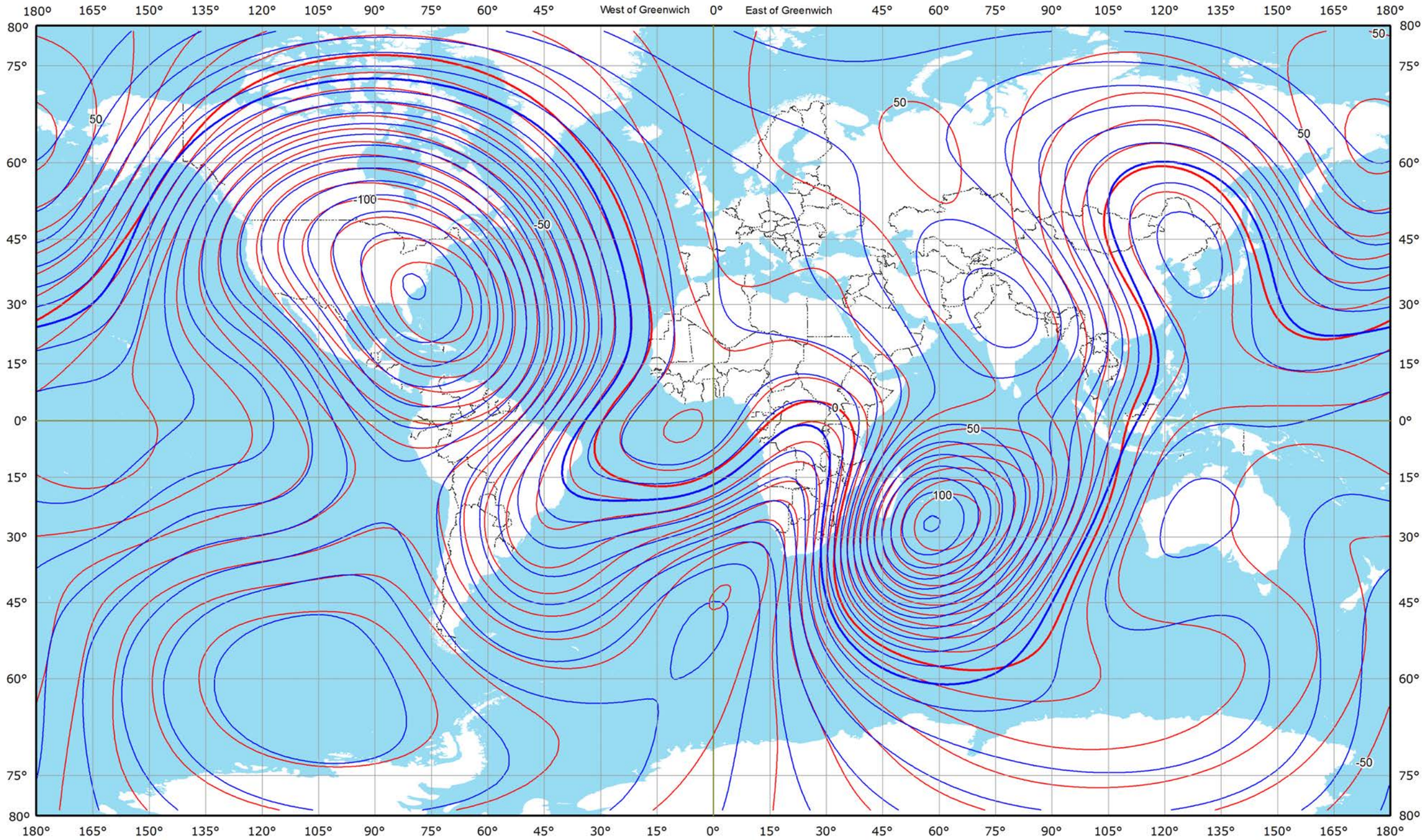

Epoch Isopors

2002
2007

Example. Secular variation value of MGMF total intensity (nT/year)

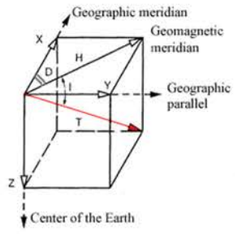

MGMF vector components

D Declination
I Inclination
H Horizontal component
T Total intensity
X North component
Y East component
Z Vertical component

Scale 1: 120 000 000

Projection: Miller cylindrical

MAGNETIC DECLINATION OF MGMF NONDIPOLE PART

MGMF – 1900, 1905, 1910 – D

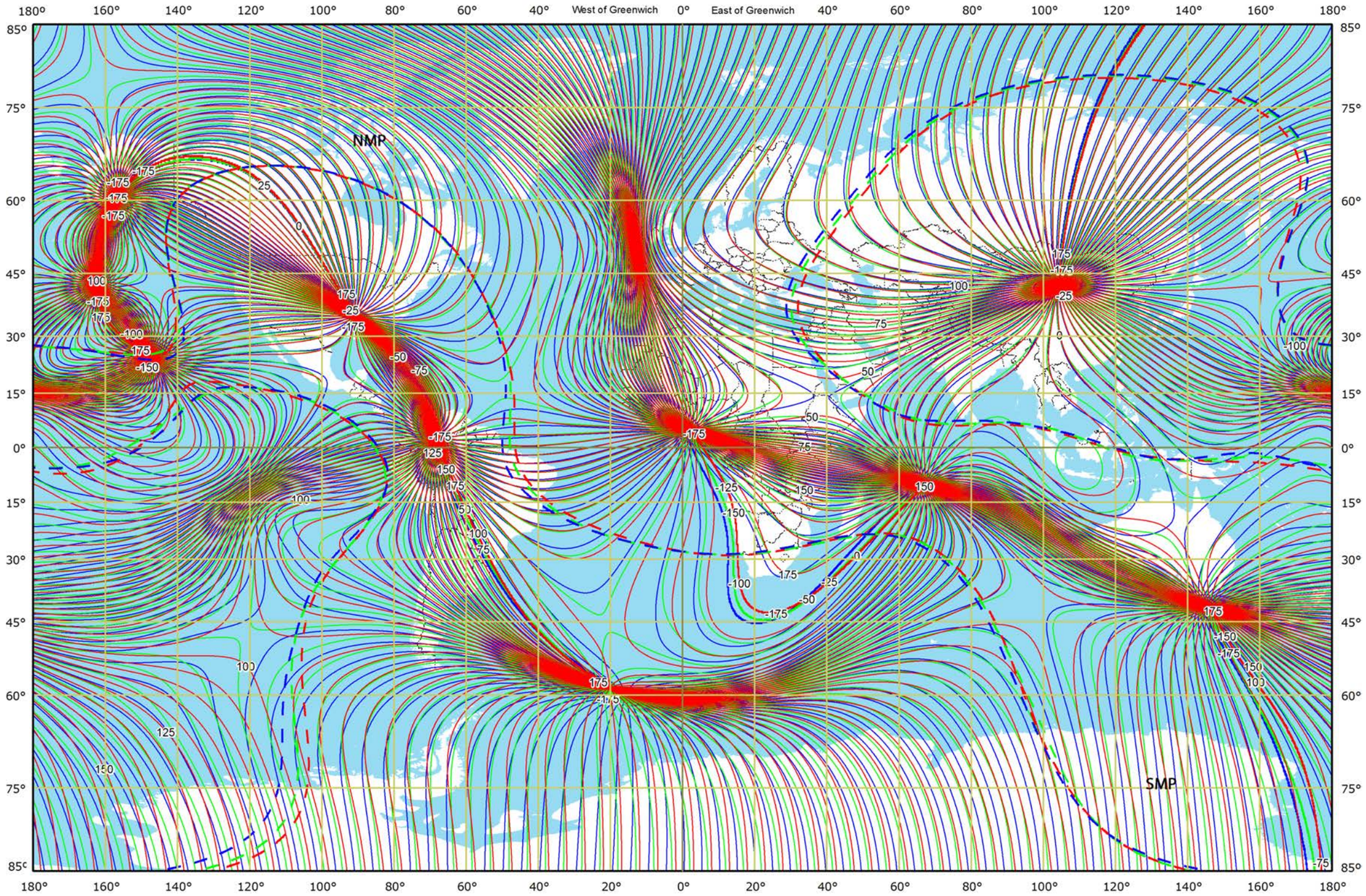

Years Isogons

1900
1905
1910

Geomagnetic equators

1900
1905
1910

Example of magnetic declination value, degree

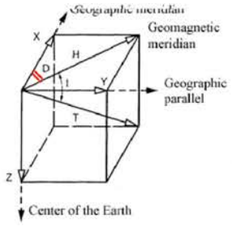

MGMF vector components

D Declination
I Inclination
H Horizontal component
T Total intensity
X North component
Y East component
Z Vertical component

Scale 1: 120 000 000

Projection: Miller cylindrical

MAGNETIC DECLINATION OF MGMF NONDIPOLE PART

MGMF – 1910, 1915, 1920 – D

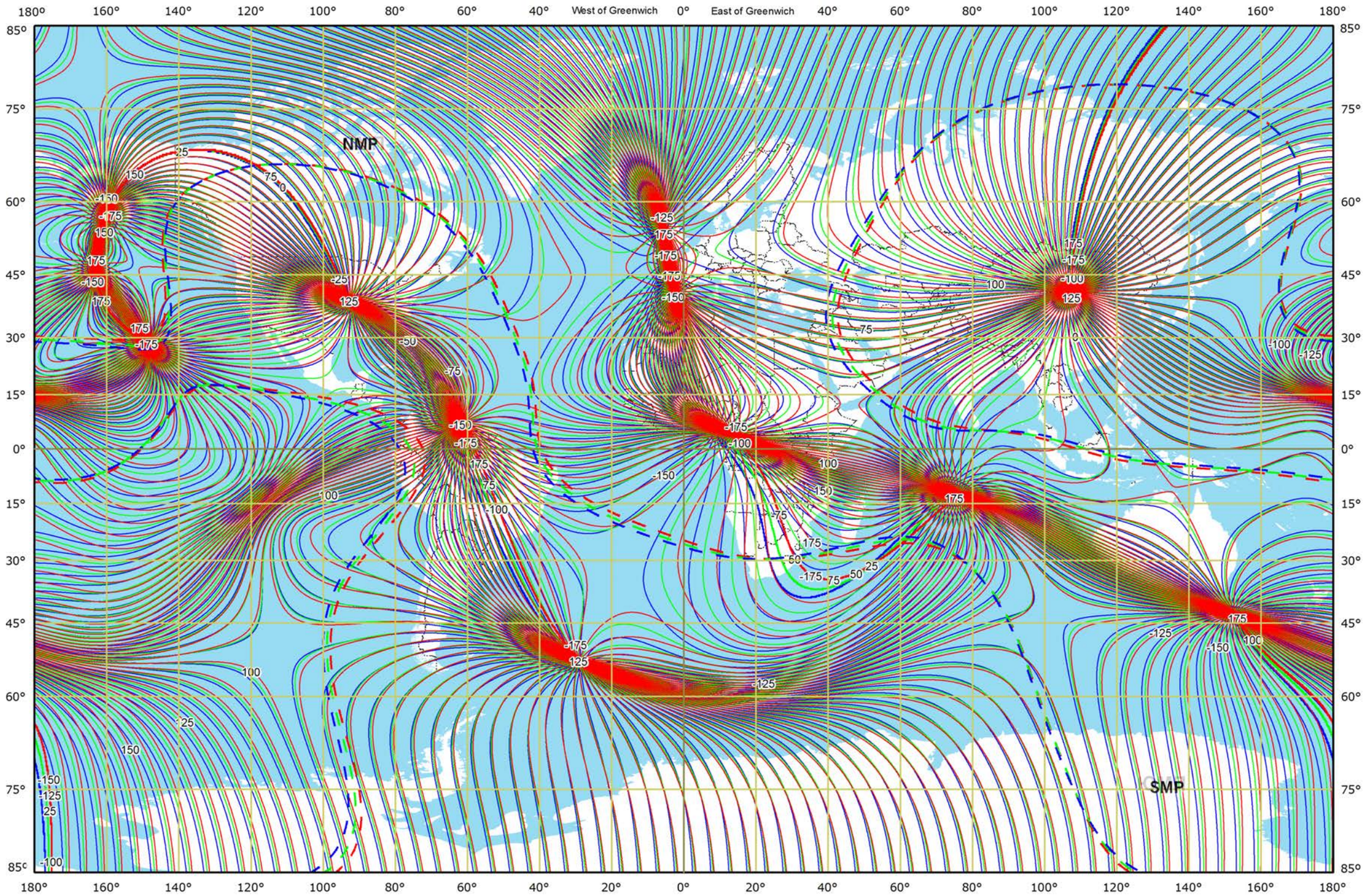

Years Isogons Geomagnetic equators

1910 1910
1915 1915
1920 1920

Example of magnetic declination value, degree

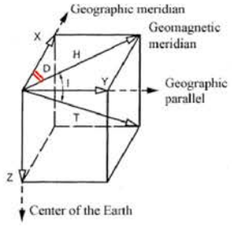

MGMF vector components

D Declination
I Inclination
H Horizontal component
T Total intensity
X North component
Y East component
Z Vertical component

Scale 1: 120 000 000

Projection: Miller cylindrical

MAGNETIC DECLINATION OF MGMF NONDIPOLE PART

MGMF – 1920, 1925, 1930 – D

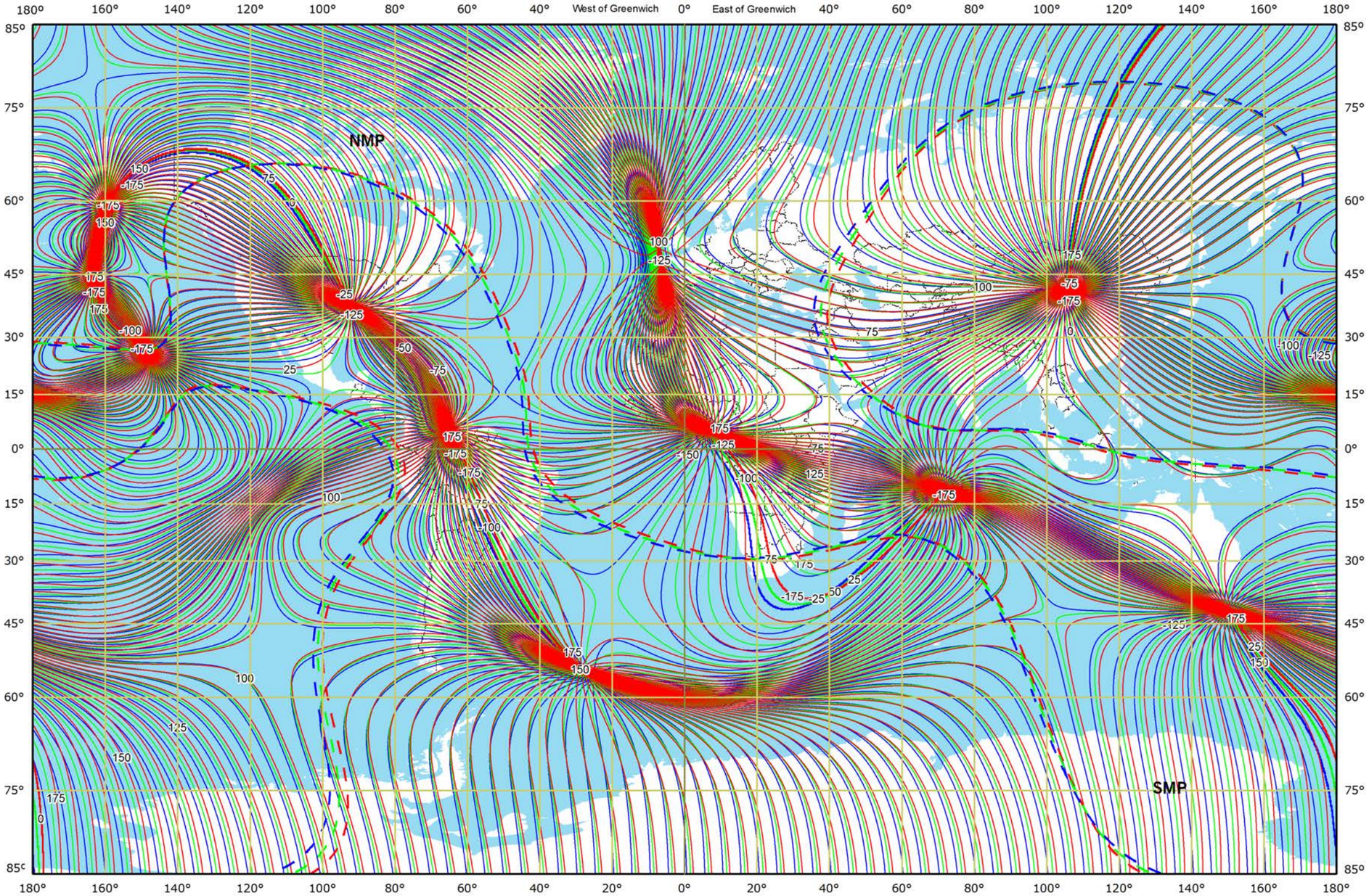

Years Isogons Geomagnetic equators

1920
1925
1930

1920
1925
1930

Example of magnetic declination value, degree

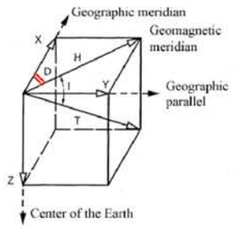

MGMF vector components

D Declination
I Inclination
H Horizontal component
T Total intensity
X North component
Y East component
Z Vertical component

Scale 1: 120 000 000

Projection: Miller cylindrical

MAGNETIC DECLINATION OF MGMF NONDIPOLE PART

MGMF – 1930, 1935, 1940 – D

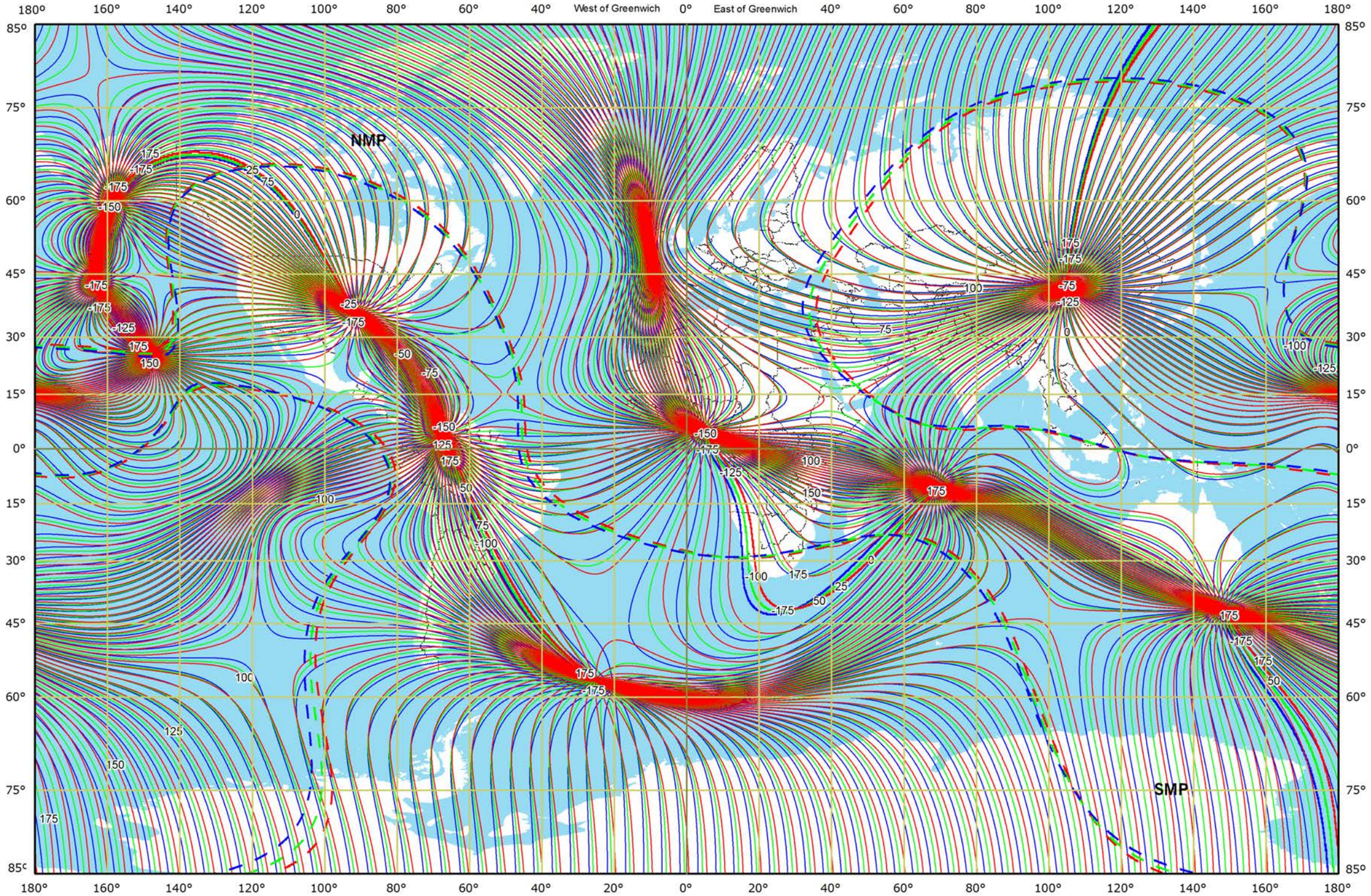

Years Isogons Geomagnetic equators

1930
1935
1940

1930
1935
1940

Example of magnetic declination value, degree

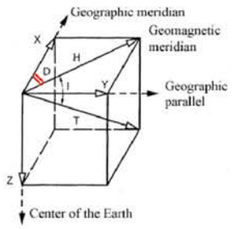

MGMF vector components

D Declination
I Inclination
H Horizontal component
T Total intensity
X North component
Y East component
Z Vertical component

Scale 1: 120 000 000

Projection: Miller cylindrical

MAGNETIC DECLINATION OF MGMF NONDIPOLE PART

MGMF – 1940, 1945, 1950 – D

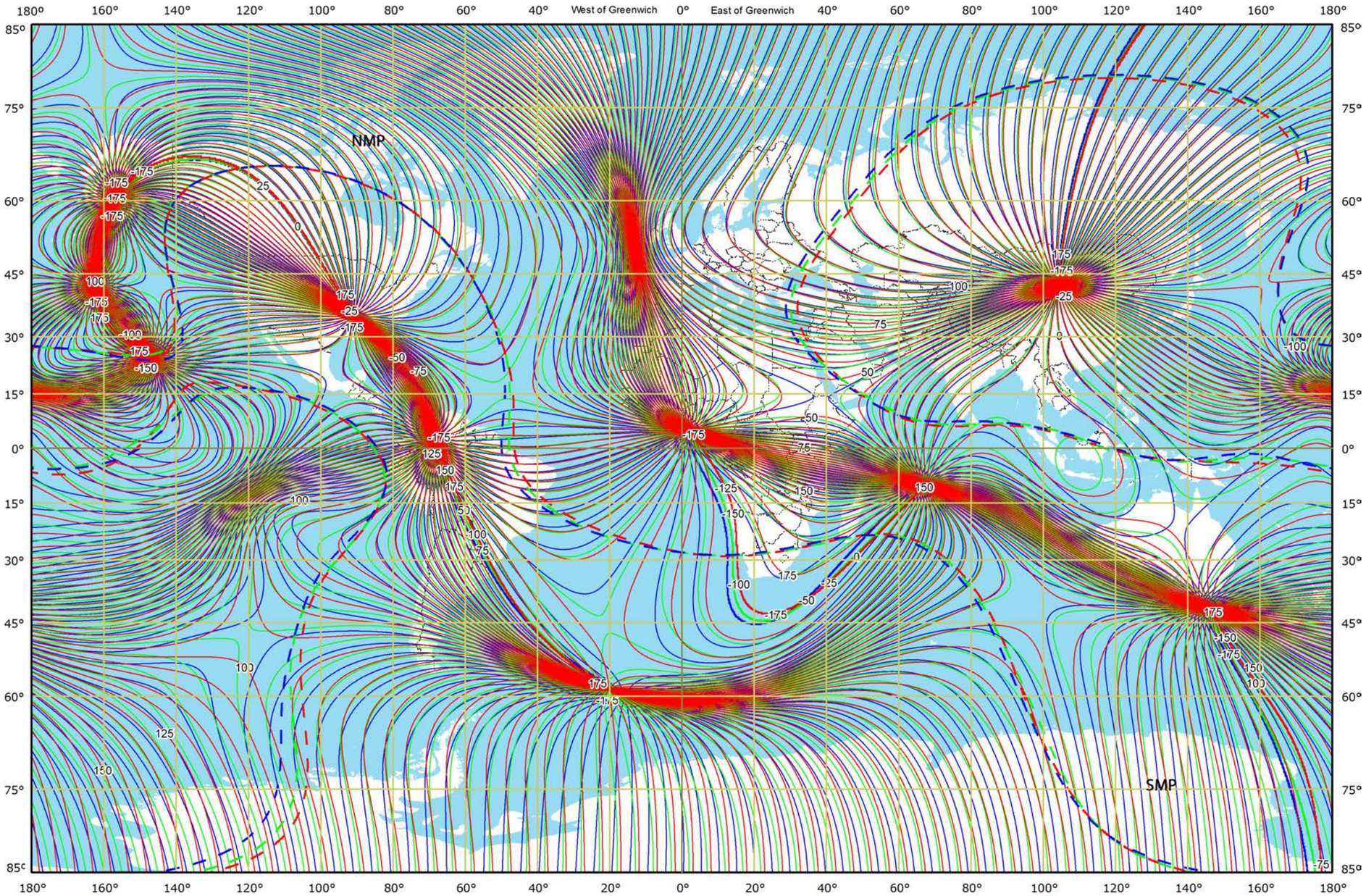

Years	Isogons	Geomagnetic equators
1940		1940
1945		1945
1950		1950

Example of magnetic declination value, degree

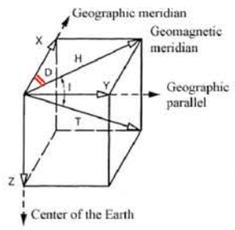

MGMF vector components

D Declination
I Inclination
H Horizontal component
T Total intensity
X North component
Y East component
Z Vertical component

Scale 1: 120 000 000

Projection: Miller cylindrical

MAGNETIC DECLINATION OF MGMF NONDIPOLE PART

MGMF – 1950, 1955, 1960 – D

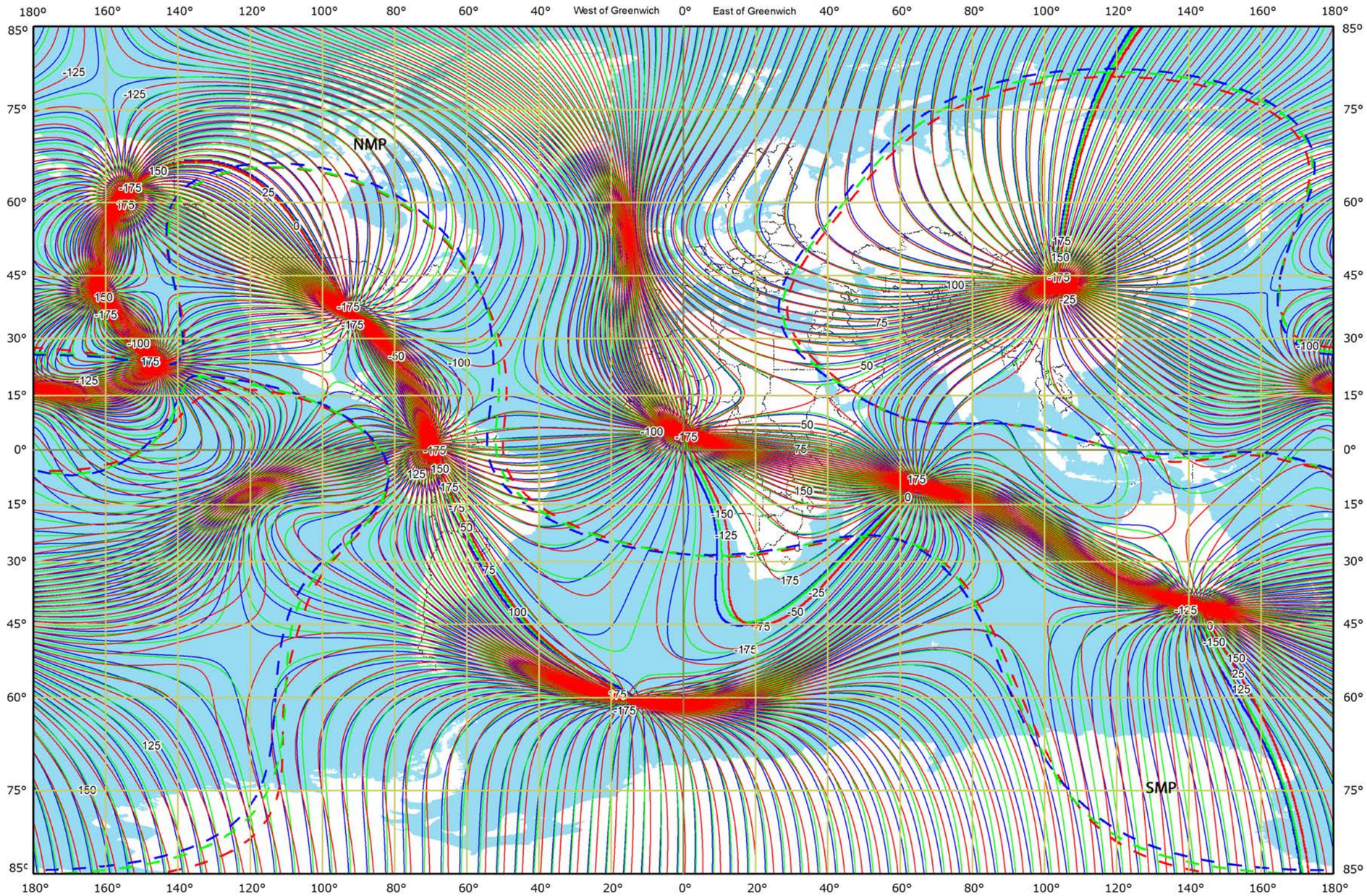

Years	Isogons	Geomagnetic equators
1950		1950
1955		1955
1960		1960

Example of magnetic declination value, degree

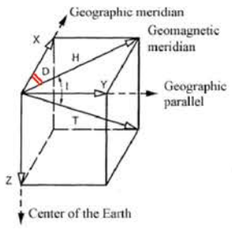

MGMF vector components

D Declination
I Inclination
H Horizontal component
T Total intensity
X North component
Y East component
Z Vertical component

Scale 1: 120 000 000

Projection: Miller cylindrical

MAGNETIC DECLINATION OF MGMF NONDIPOLE PART

MGMF – 1960, 1965, 1970 – D

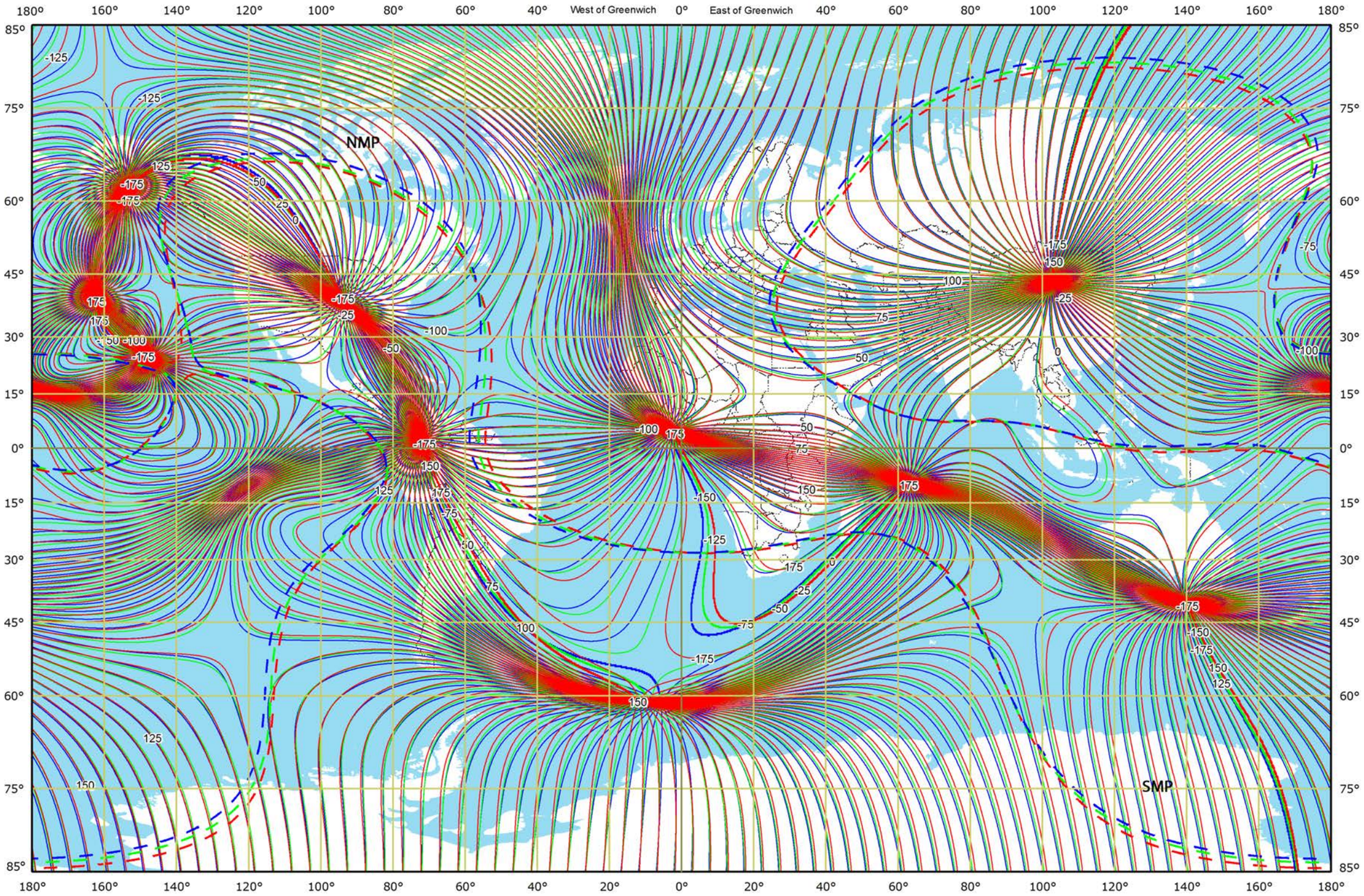

Years	Isogons	Geomagnetic equators
1960		1960
1965		1965
1970		1970

Example of magnetic declination value, degree

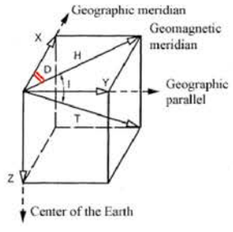

MGMF vector components

D Declination
I Inclination
H Horizontal component
T Total intensity
X North component
Y East component
Z Vertical component

Scale 1: 120 000 000

Projection: Miller cylindrical

MAGNETIC DECLINATION OF MGMF NONDIPOLE PART

MGMF – 1970, 1975, 1980 – D

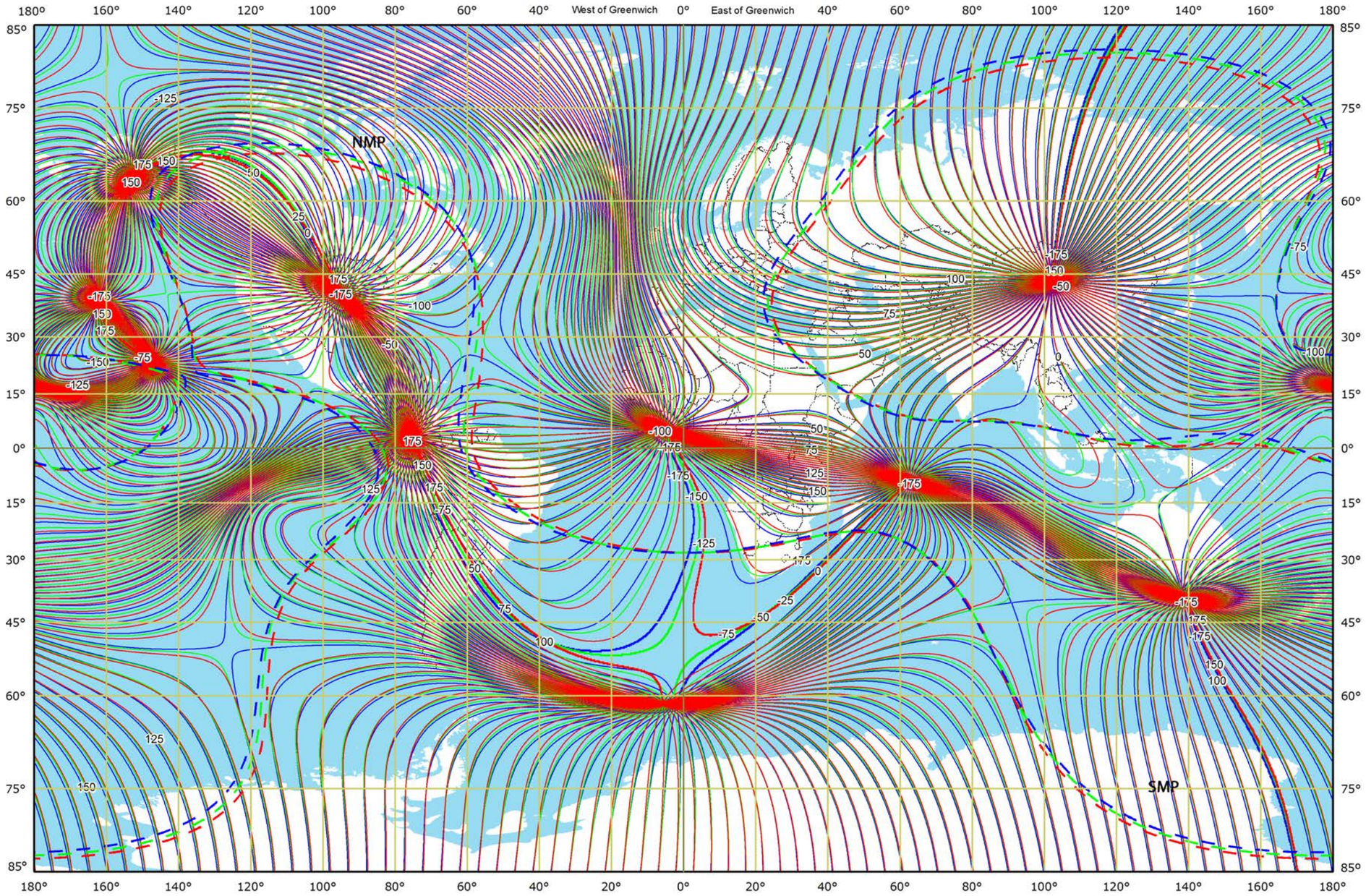

Years Isogons

1970
1975
1980

Geomagnetic equators

1970
1975
1980

Example of magnetic declination value, degree

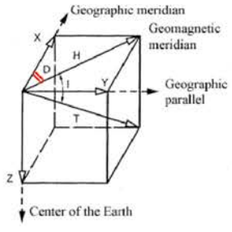

MGMF vector components

D Declination
I Inclination
H Horizontal component
T Total intensity
X North component
Y East component
Z Vertical component

Scale 1: 120 000 000

Projection: Miller cylindrical

MAGNETIC DECLINATION OF MGMF NONDIPOLE PART

MGMF – 1980, 1985, 1990 – D

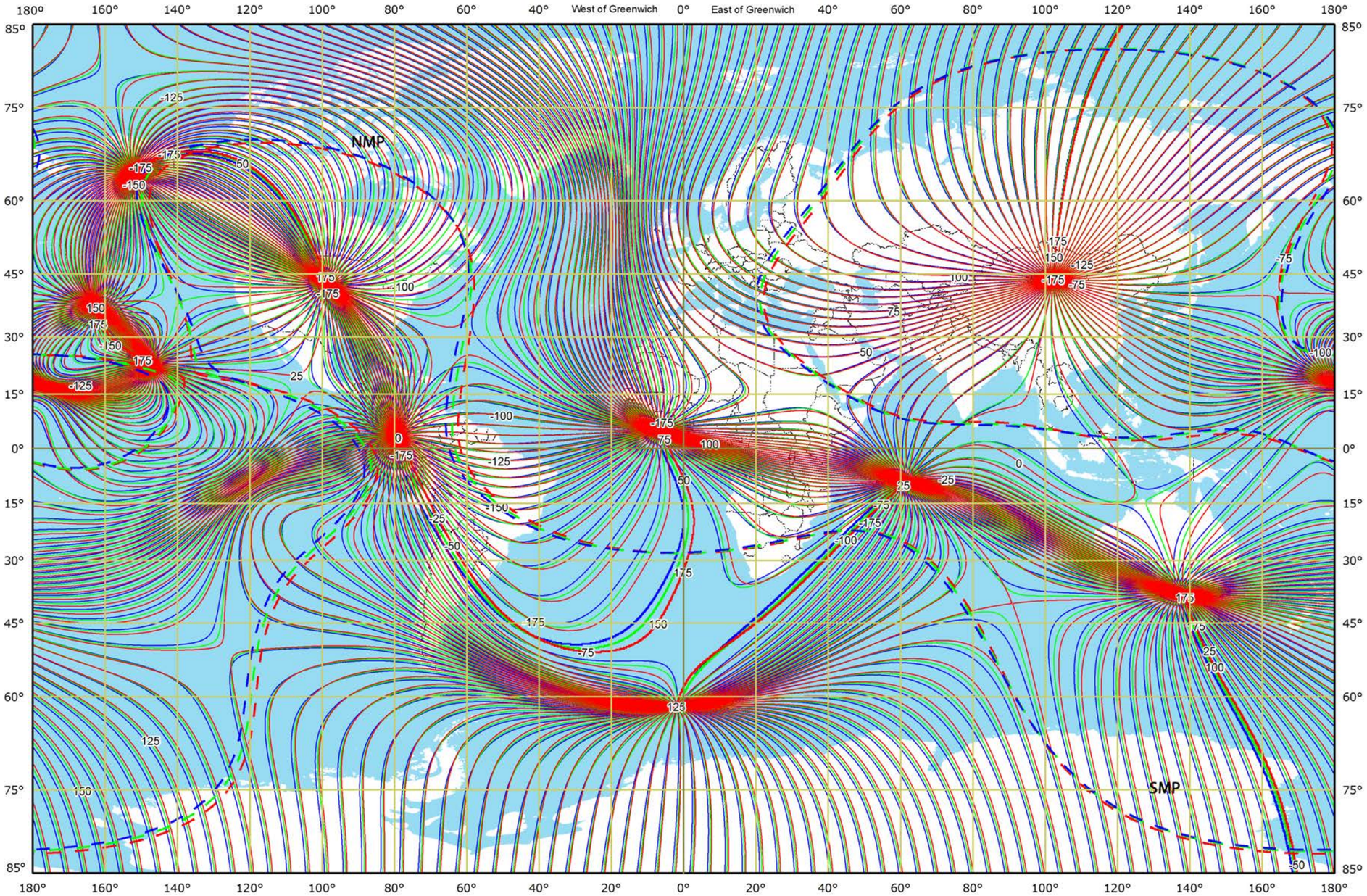

Years Isogons Geomagnetic equators

1980
1985
1990

1980
1985
1990

Example of magnetic declination value, degree

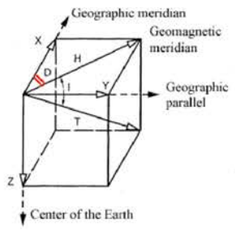

MGMF vector components

D Declination
I Inclination
H Horizontal component
T Total intensity
X North component
Y East component
Z Vertical component

Scale 1: 120 000 000

Projection: Miller cylindrical

MAGNETIC DECLINATION OF MGMF NONDIPOLE PART

MGMF – 1990, 1995, 2000 – D

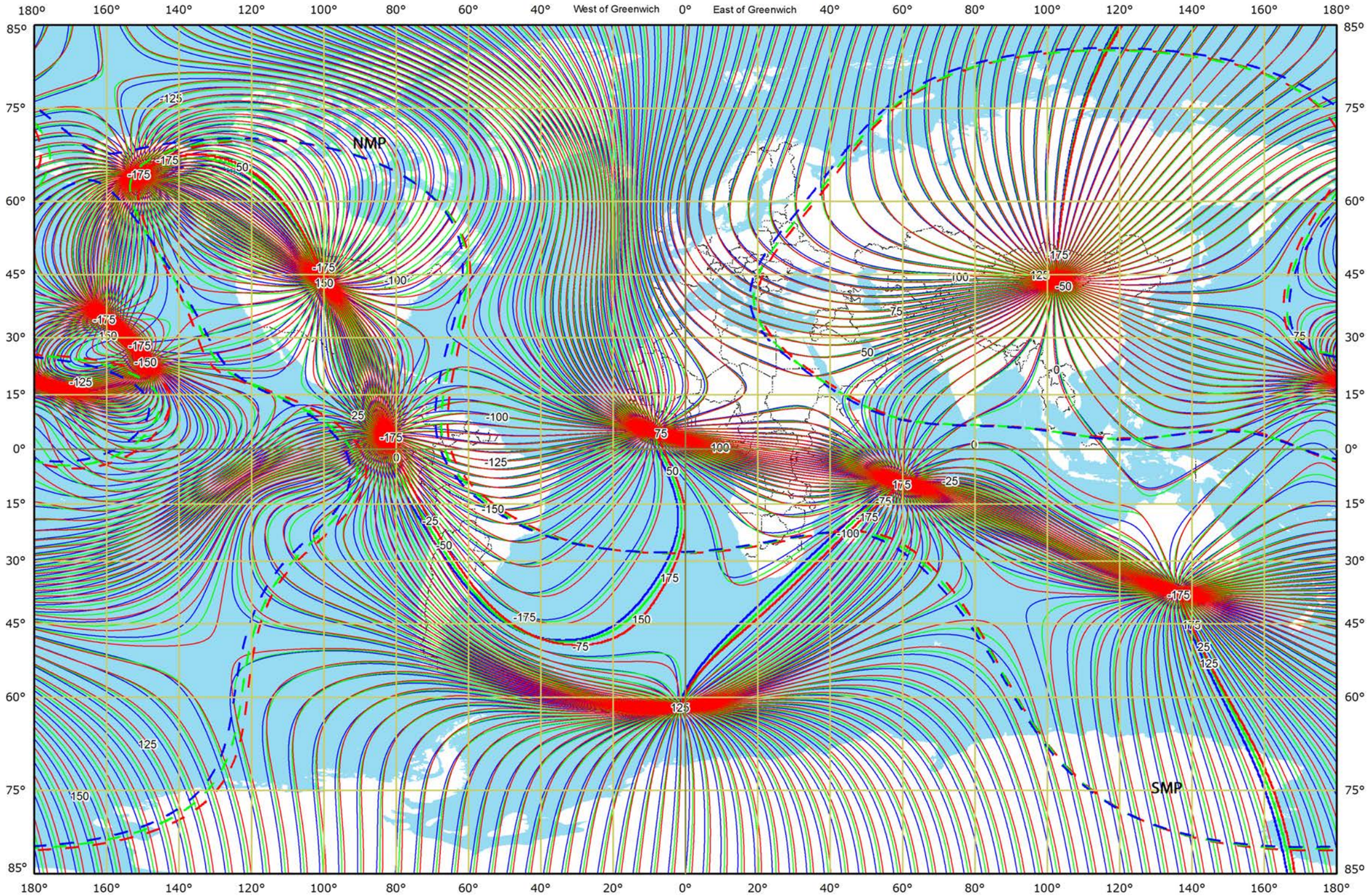

Years Isogons

1990
1995
2000

Geomagnetic equators

1990
1995
2000

Example of magnetic declination value, degree

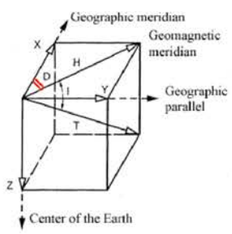

MGMF vector components

D Declination
I Inclination
H Horizontal component
T Total intensity
X North component
Y East component
Z Vertical component

Scale 1: 120 000 000

Projection: Miller cylindrical

MAGNETIC DECLINATION OF MGMF NONDIPOLE PART

MGMF – 2000, 2005, 2010 – D

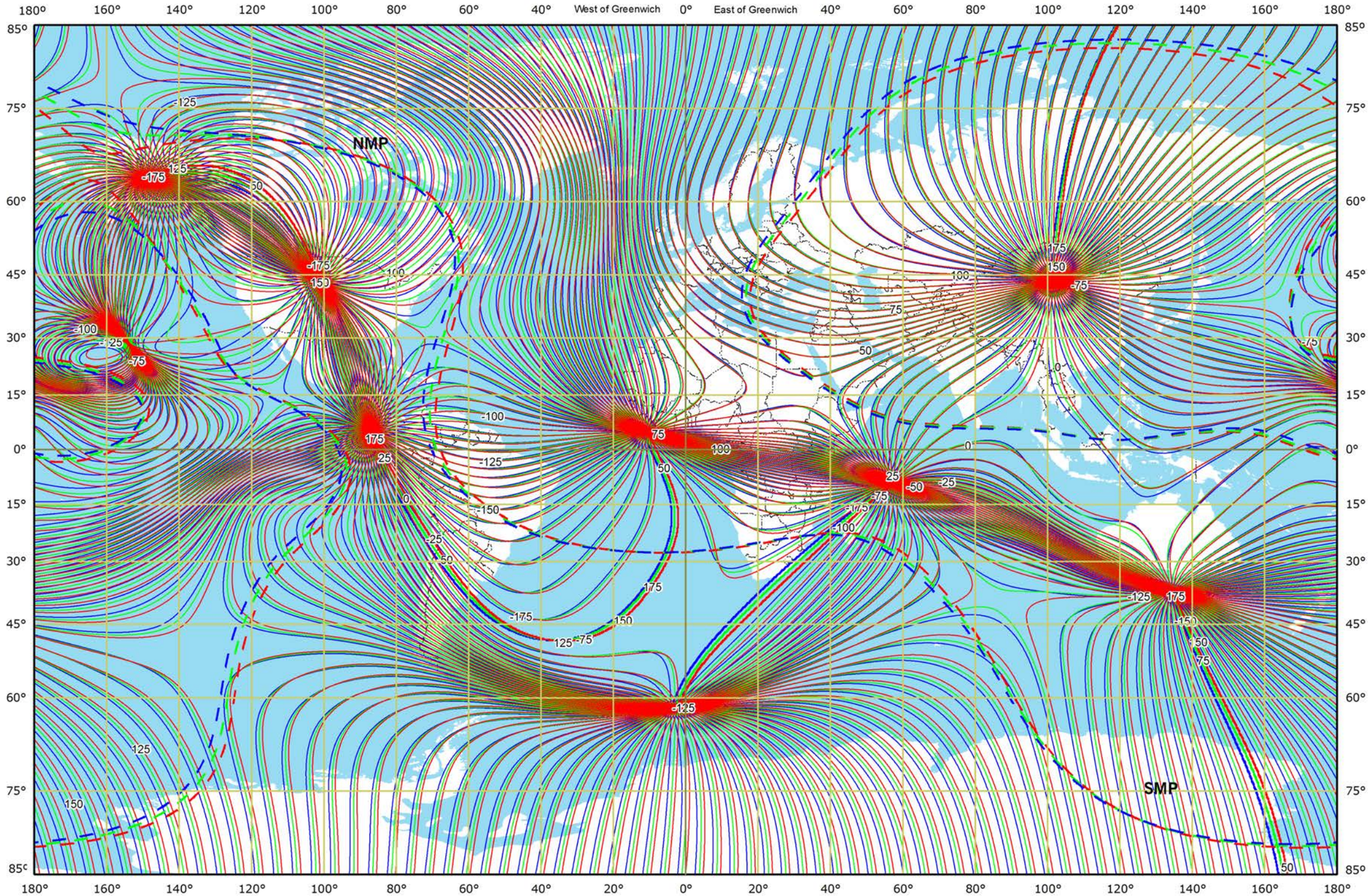

Years	Isogons	Geomagnetic equators
2000		2000
2005		2005
2010		2010

Example of magnetic declination value, degree

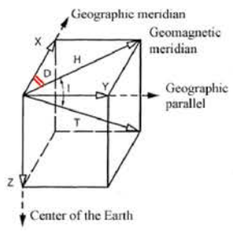

MGMF vector components

D Declination
I Inclination
H Horizontal component
T Total intensity
X North component
Y East component
Z Vertical component

Scale 1: 120 000 000

Projection: Miller cylindrical

MAGNETIC INCLINATION OF MGMF NONDIPOLE PART

MGMF– 1900, 1905, 1910 – I

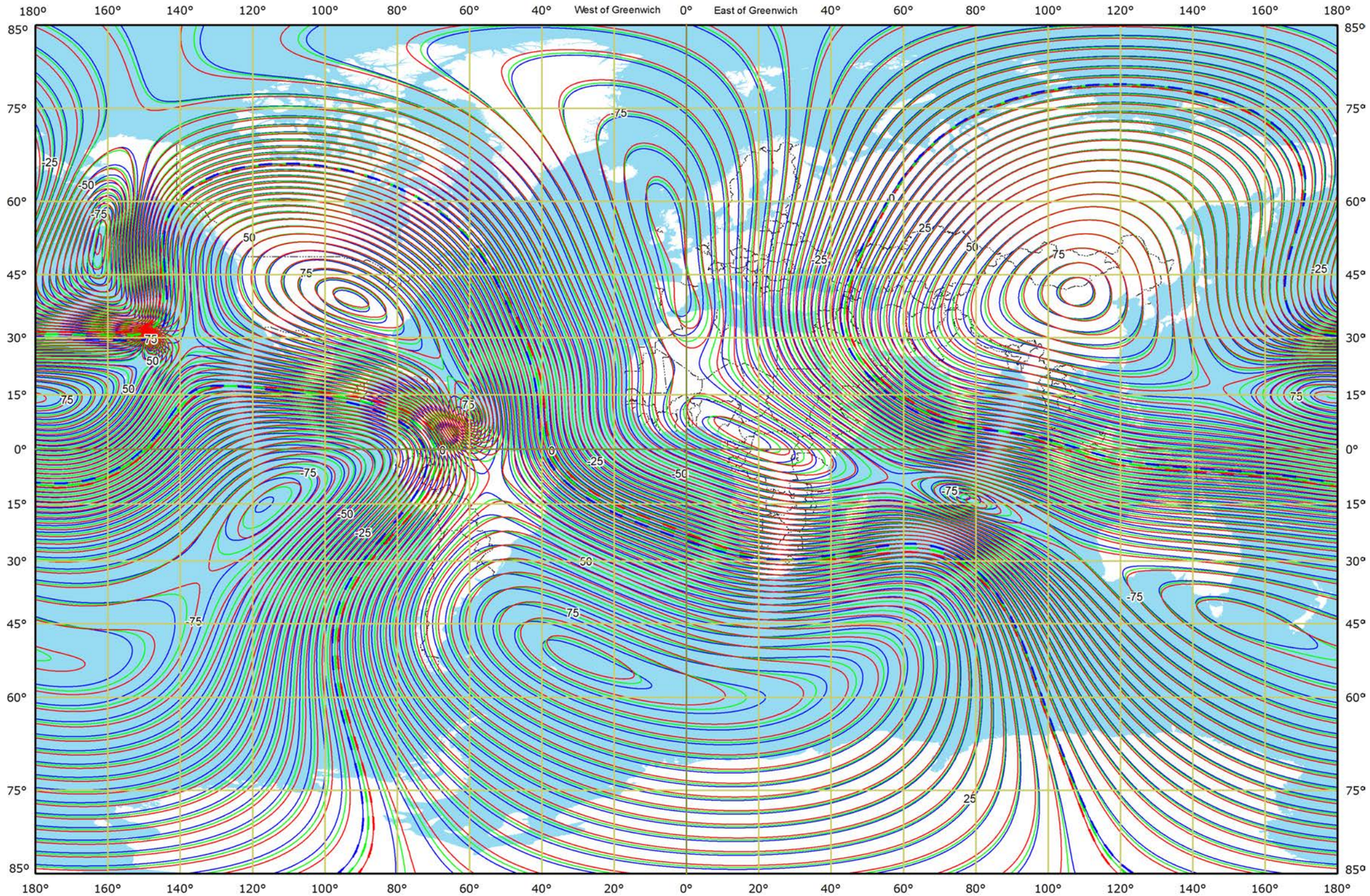

Years	Isoclines	Geomagnetic equators
1900		1900
1905		1905
1910		1910

Example of magnetic inclination value, degree

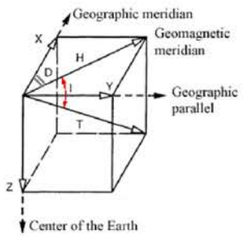

MGMF vector components

D Declination
I Inclination
H Horizontal component
T Total intensity
X North component
Y East component
Z Vertical component

Scale 1: 120 000 000

Projection: Miller cylindrical

MAGNETIC INCLINATION OF MGMF NONDIPOLE PART

MGMF– 1910, 1915, 1920 – I

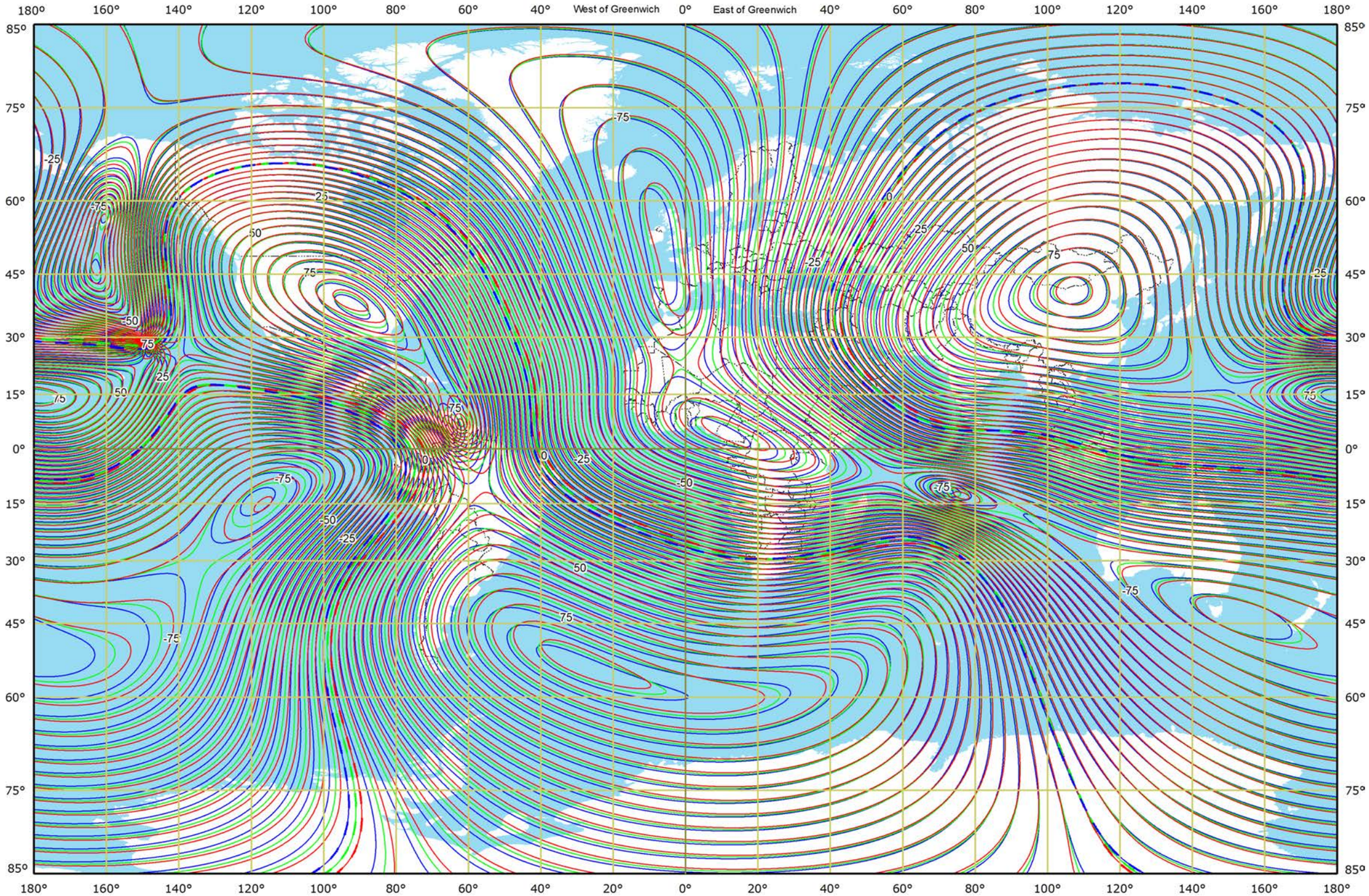

Years Isoclines Geomagnetic equators

1910
1915
1920

1910
1915
1920

Example of magnetic inclination value, degree

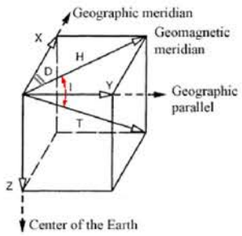

MGMF vector components

D Declination
I Inclination
H Horizontal component
T Total intensity
X North component
Y East component
Z Vertical component

Scale 1: 120 000 000

Projection: Miller cylindrical

MAGNETIC INCLINATION OF MGMF NONDIPOLE PART

MGMF– 1920, 1925, 1930 – I

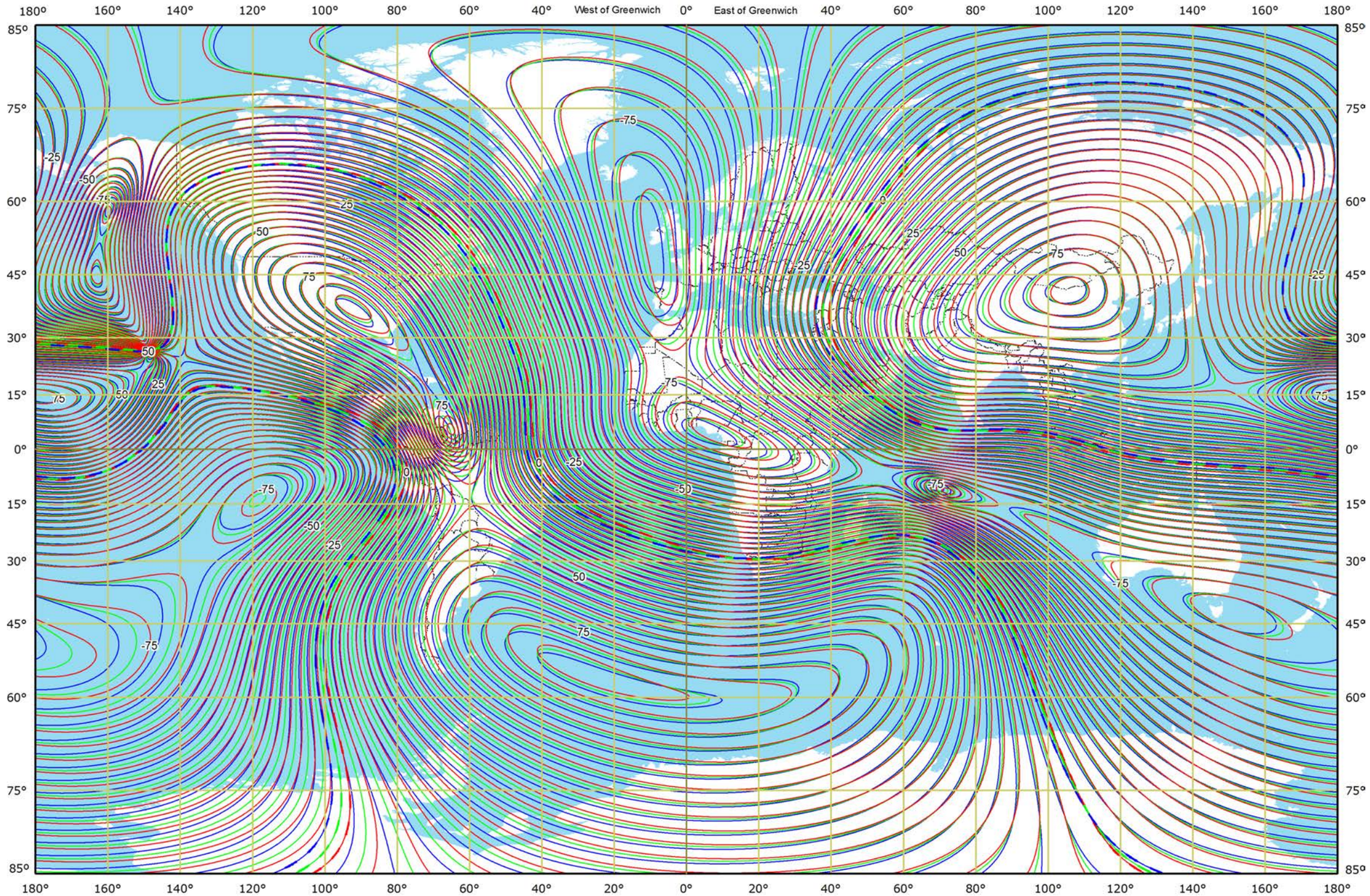

Years	Isoclines	Geomagnetic equators
1920		1920
1925		1925
1930		1930

Example of magnetic inclination value, degree

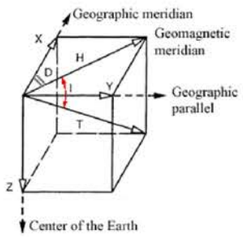

MGMF vector components

D Declination
I Inclination
H Horizontal component
T Total intensity
X North component
Y East component
Z Vertical component

Scale 1: 120 000 000

Projection: Miller cylindrical

MAGNETIC INCLINATION OF MGMF NONDIPOLE PART

MGMF– 1930, 1935, 1940 – I

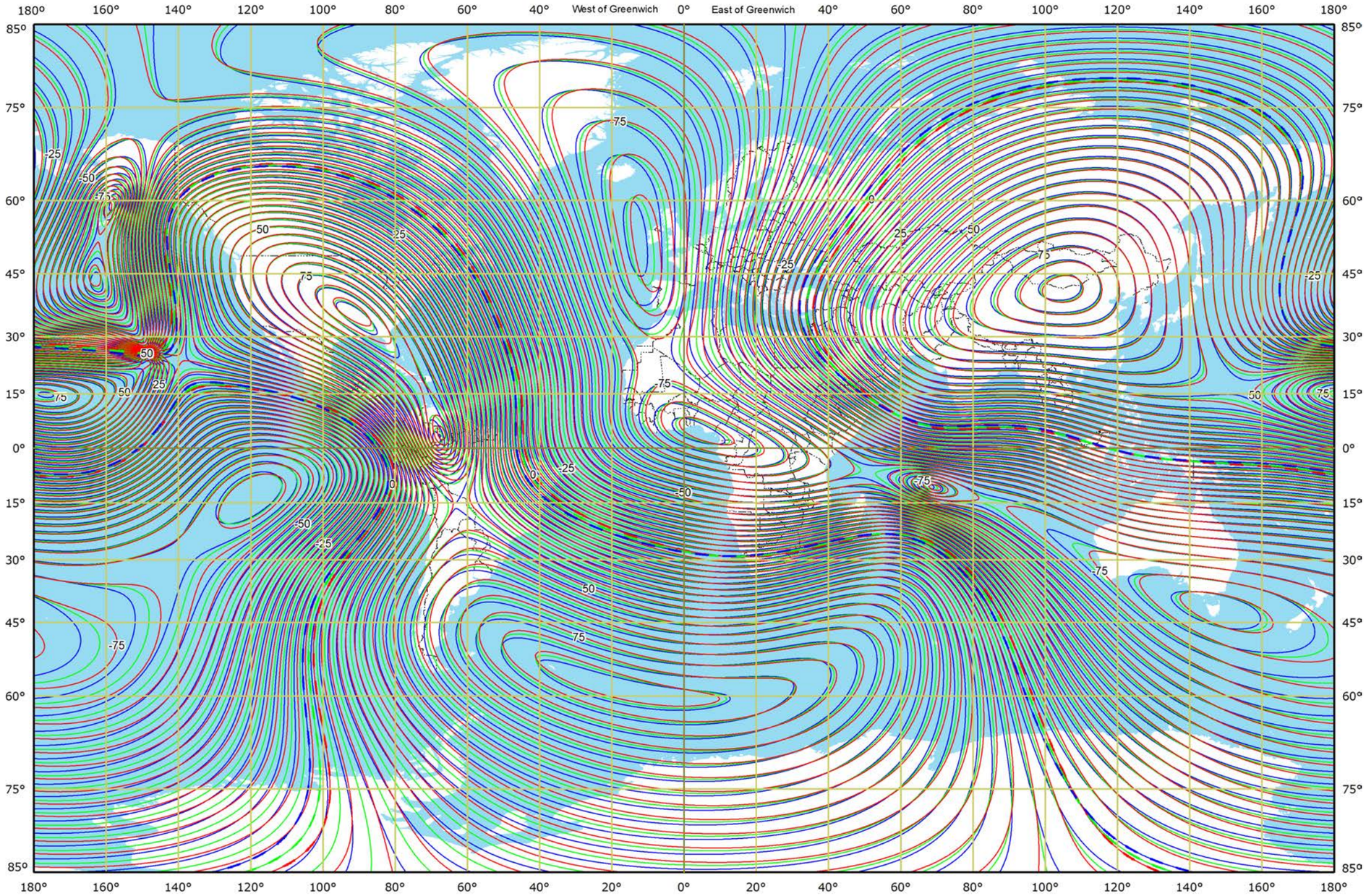

Years Isoclines Geomagnetic equators

1930 1930
1935 1935
1940 1940

Example of magnetic inclination value, degree

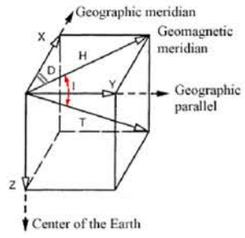

MGMF vector components

D Declination
I Inclination
H Horizontal component
T Total intensity
X North component
Y East component
Z Vertical component

Scale 1: 120 000 000

Projection: Miller cylindrical

MAGNETIC INCLINATION OF MGMF NONDIPOLE PART

MGMF– 1940, 1945, 1950 – I

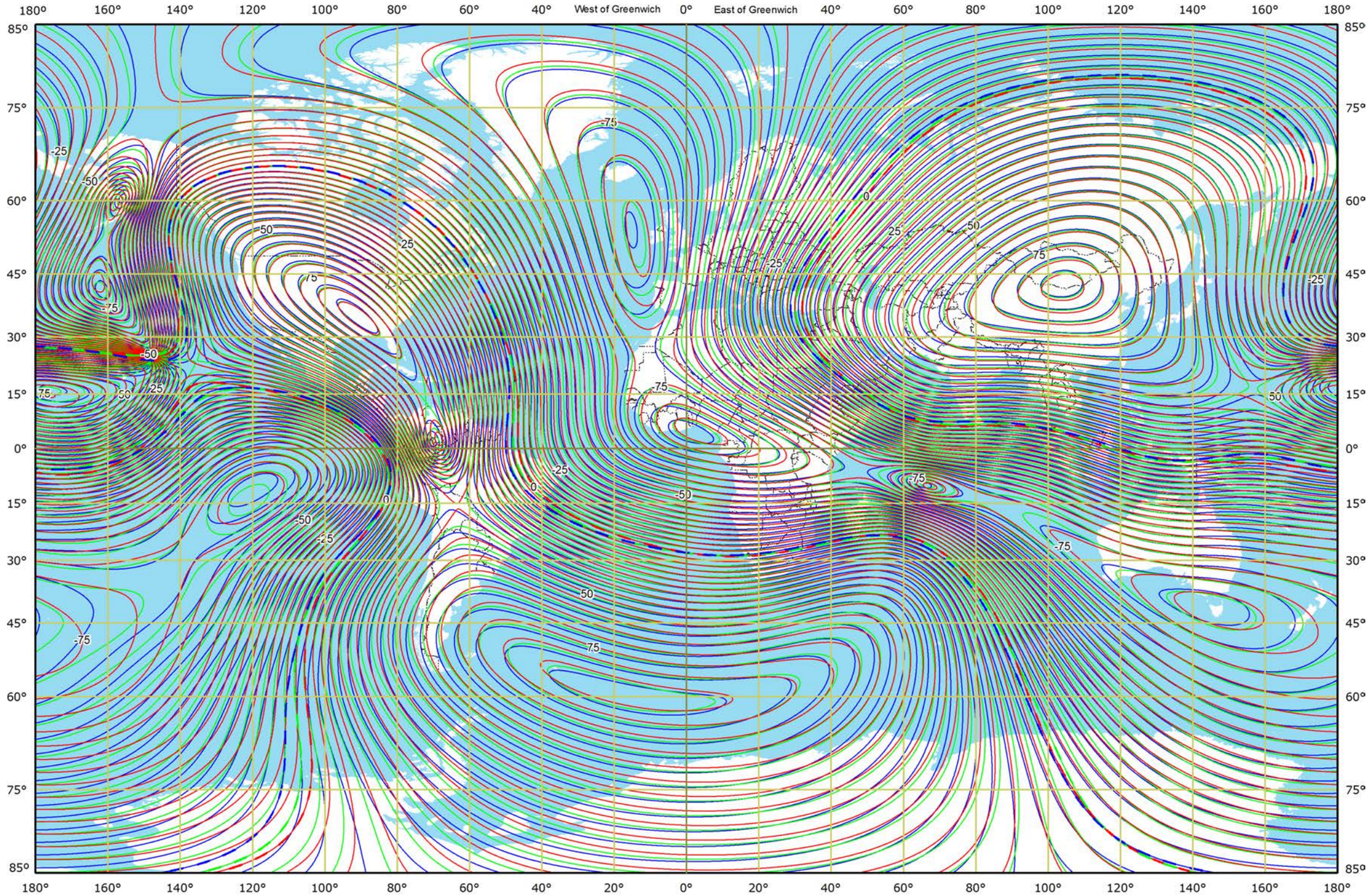

Years Isoclines

1940
1945
1950

Geomagnetic equators

1940
1945
1950

Example of magnetic inclination value, degree

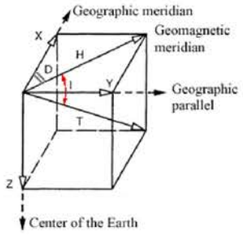

MGMF vector components

D Declination
I Inclination
H Horizontal component
T Total intensity
X North component
Y East component
Z Vertical component

Scale 1: 120 000 000

Projection: Miller cylindrical

MAGNETIC INCLINATION OF MGMF NONDIPOLE PART

MGMF– 1950, 1955, 1960 – I

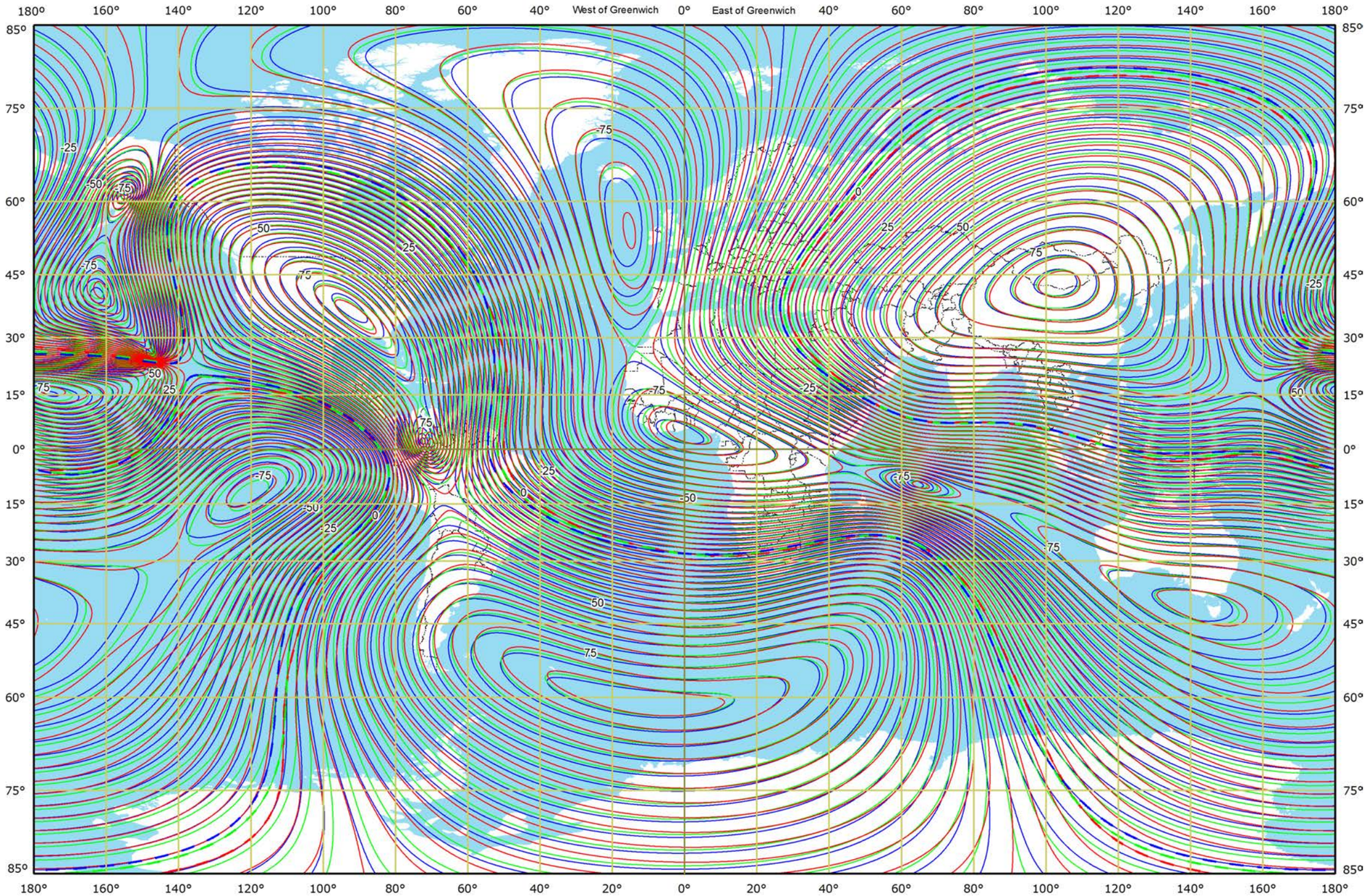

Years	Isoclines	Geomagnetic equators
1950		1950
1955		1955
1960		1960

Example of magnetic inclination value, degree

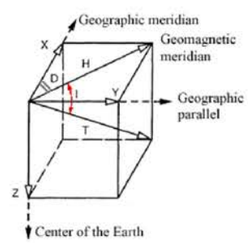

MGMF vector components

D Declination
I Inclination
H Horizontal component
T Total intensity
X North component
Y East component
Z Vertical component

Scale 1: 120 000 000

Projection: Miller cylindrical

MAGNETIC INCLINATION OF MGMF NONDIPOLE PART

MGMF– 1960, 1965, 1970 – I

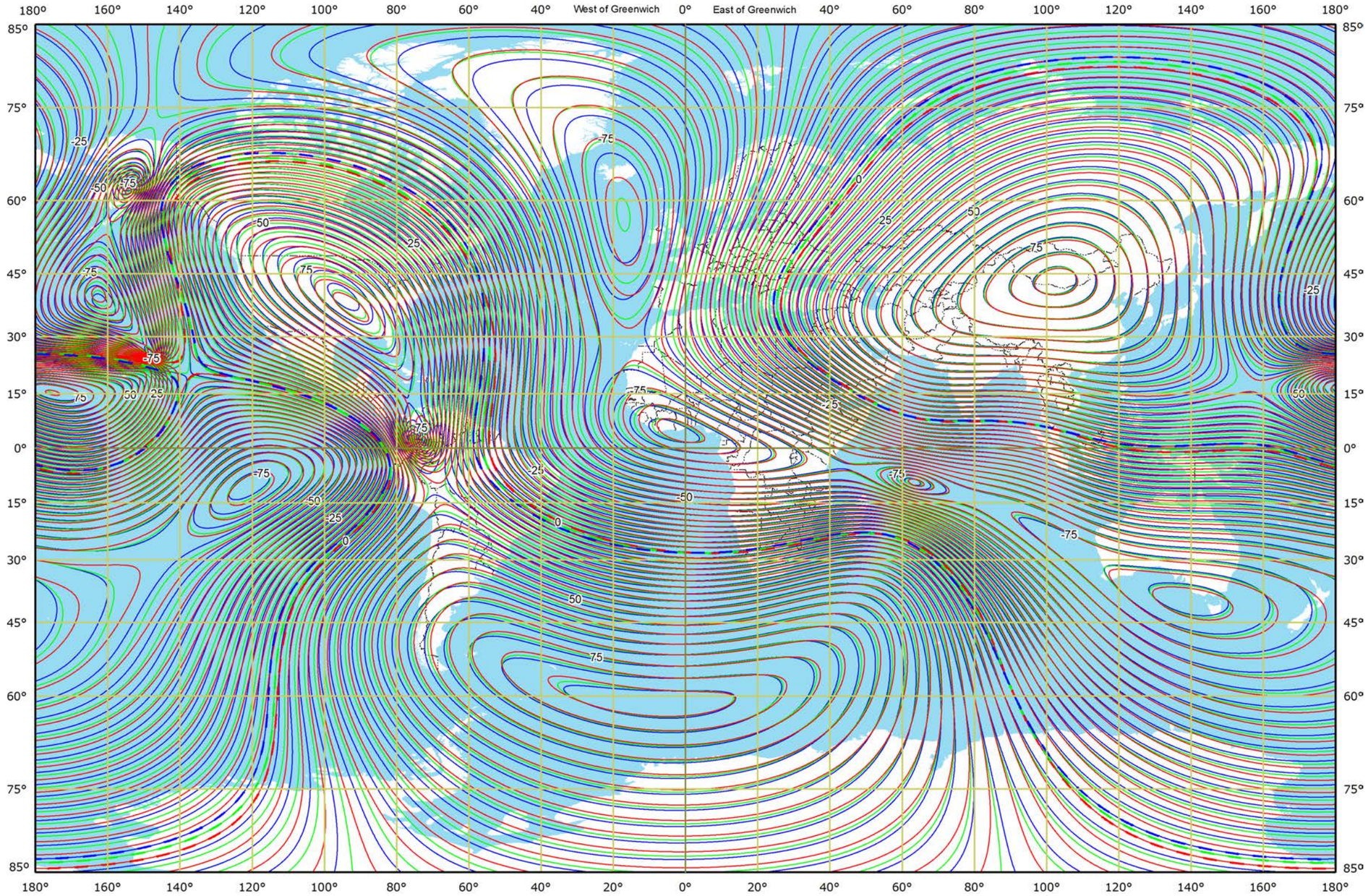

Years	Isoclines	Geomagnetic equators
1960		1960
1965		1965
1970		1970

Example of magnetic inclination value, degree

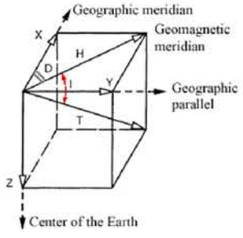

MGMF vector components

D Declination
I Inclination
H Horizontal component
T Total intensity
X North component
Y East component
Z Vertical component

Scale 1: 120 000 000

Projection: Miller cylindrical

MAGNETIC INCLINATION OF MGMF NONDIPOLE PART

MGMF– 1970, 1975, 1980 – I

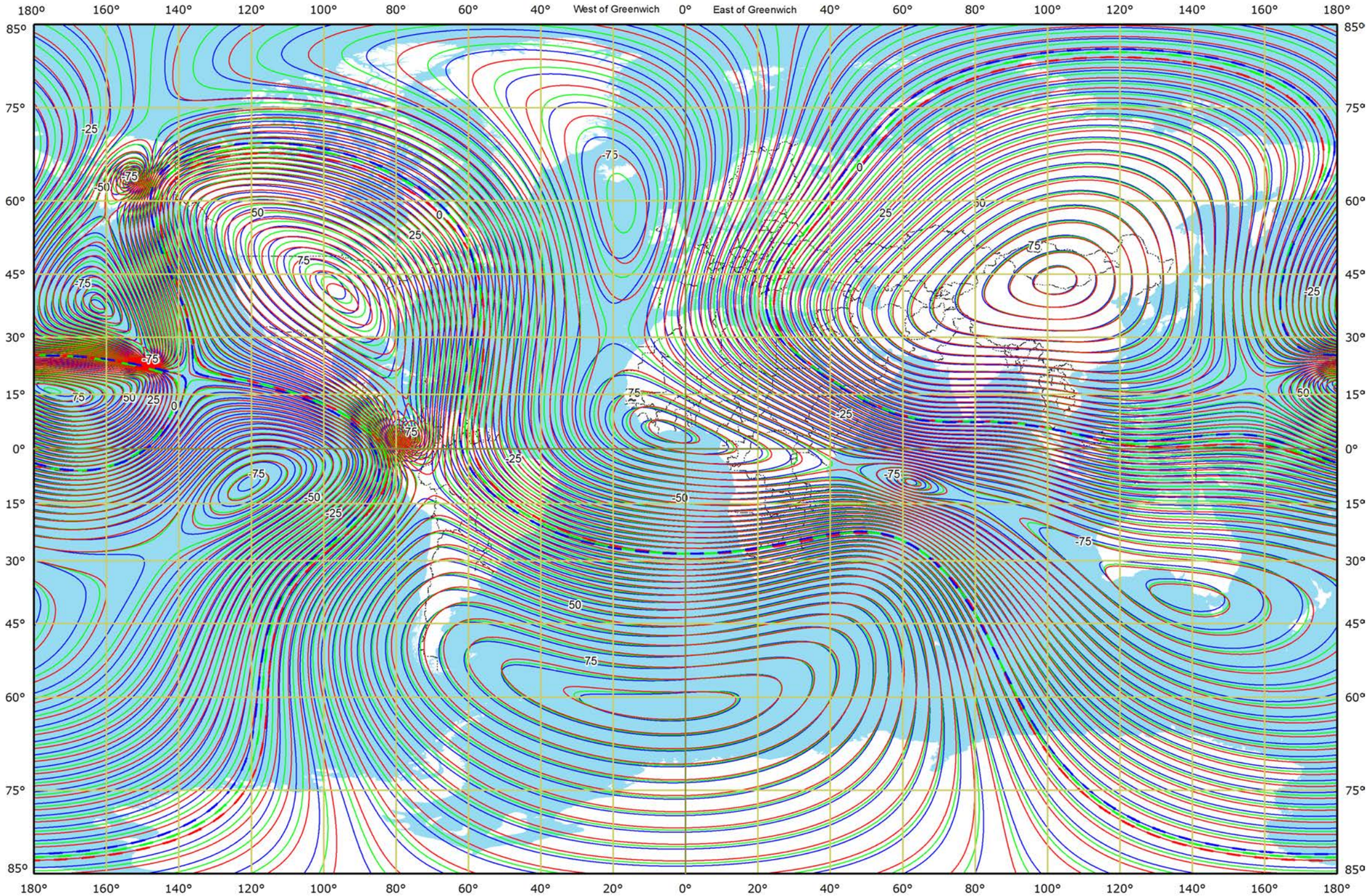

Years	Isoclines	Geomagnetic equators
1970		1970
1975		1975
1980		1980

Example of magnetic inclination value, degree

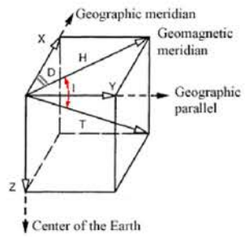

MGMF vector components

D Declination
I Inclination
H Horizontal component
T Total intensity
X North component
Y East component
Z Vertical component

Scale 1: 120 000 000

Projection: Miller cylindrical

MAGNETIC INCLINATION OF MGMF NONDIPOLE PART

MGMF– 1980, 1985, 1990 – I

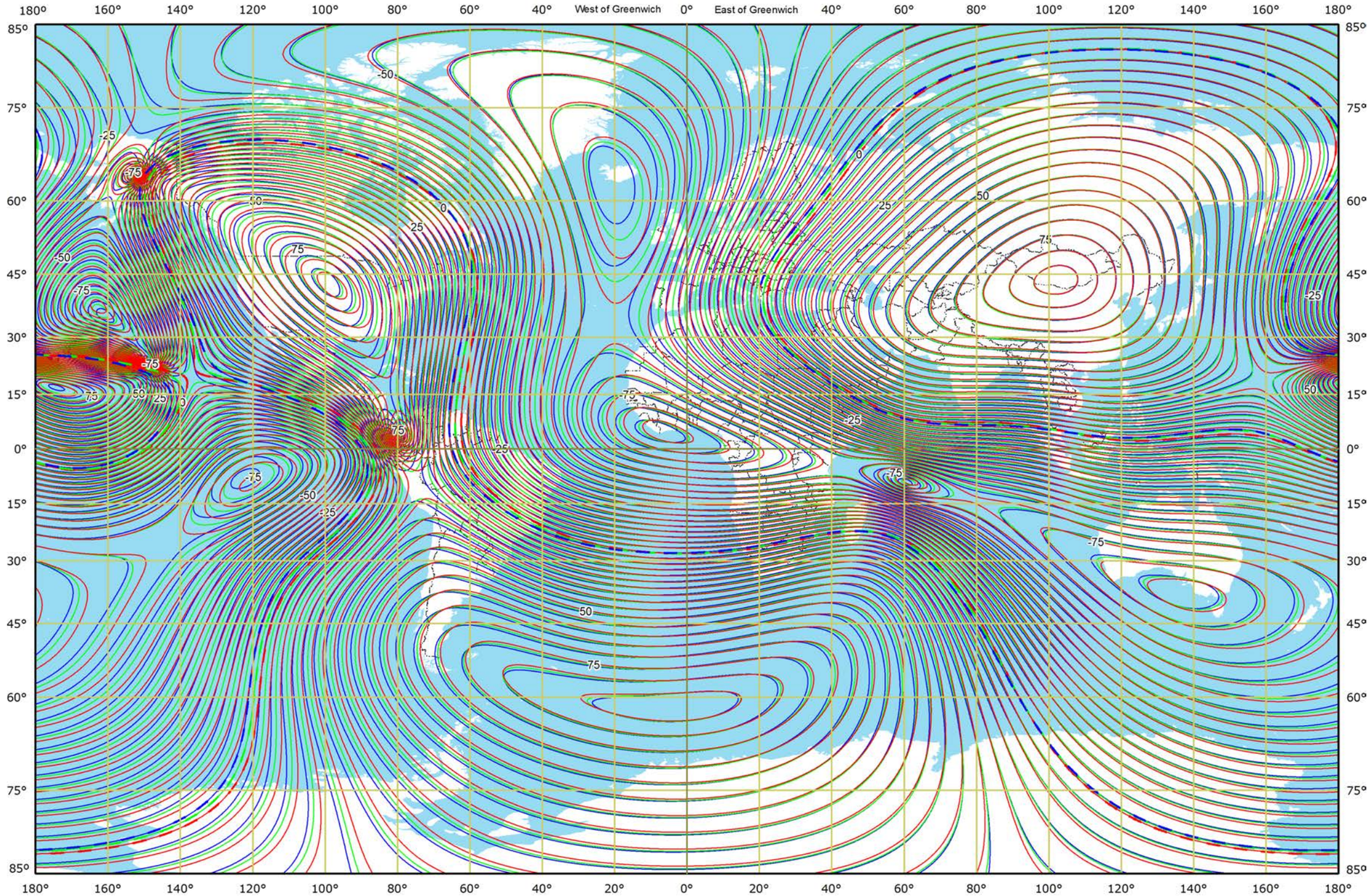

Years	Isoclines	Geomagnetic equators
1980		1980
1985		1985
1990		1990

Example of magnetic inclination value, degree

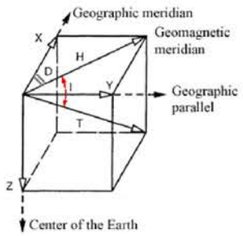

MGMF vector components

D Declination
I Inclination
H Horizontal component
T Total intensity
X North component
Y East component
Z Vertical component

Scale 1: 120 000 000

Projection: Miller cylindrical

MAGNETIC INCLINATION OF MGMF NONDIPOLE PART

MGMF– 1990, 1995, 2000 – I

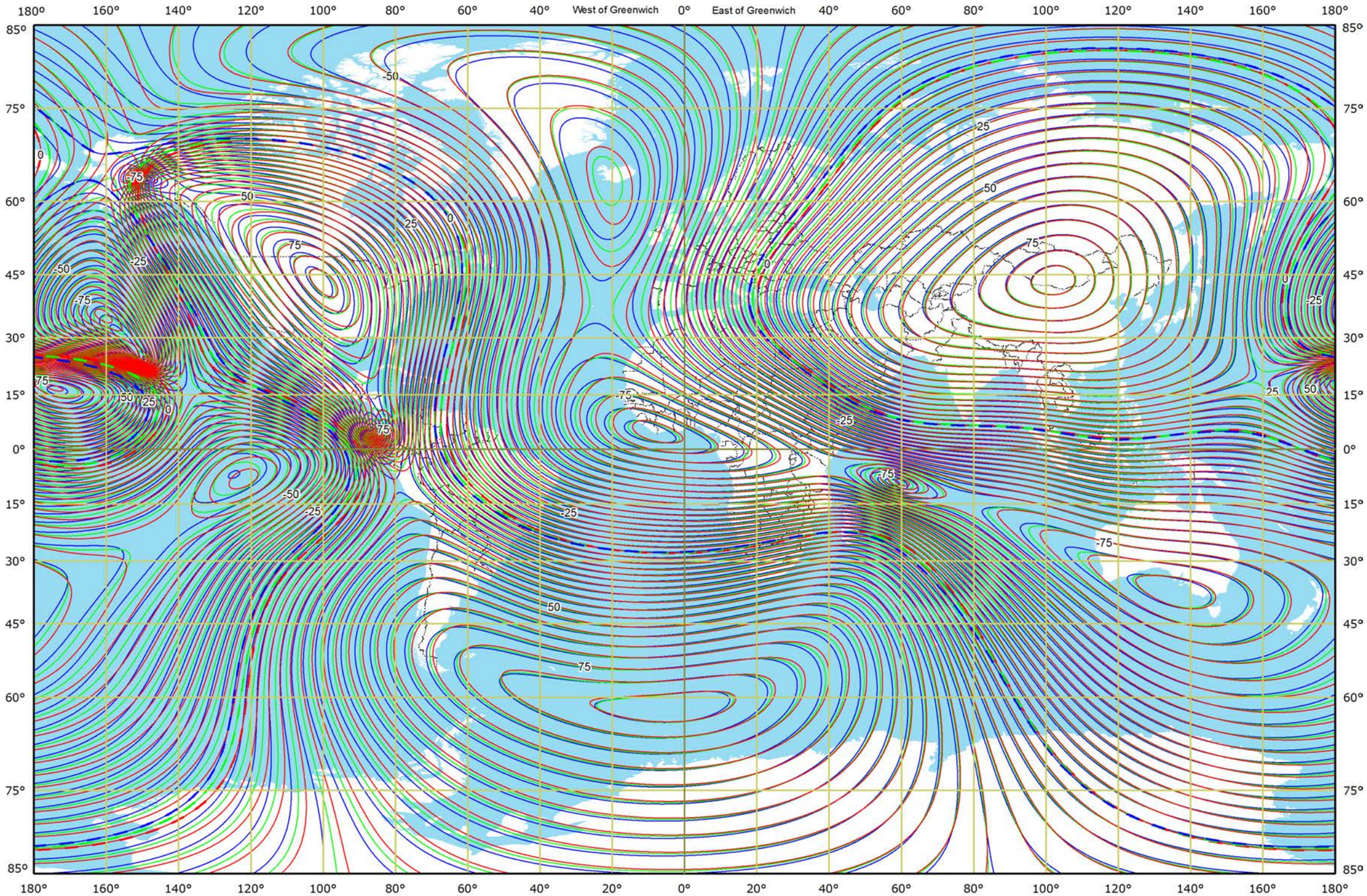

Years Isoclines Geomagnetic equators

1990
1995
2000

Example of magnetic inclination value, degree

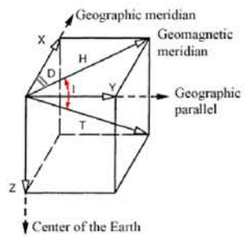

MGMF vector components

D Declination
I Inclination
H Horizontal component
T Total intensity
X North component
Y East component
Z Vertical component

Scale 1: 120 000 000

Projection: Miller cylindrical

MAGNETIC INCLINATION OF MGMF NONDIPOLE PART

MGMF– 2000, 2005, 2010 – I

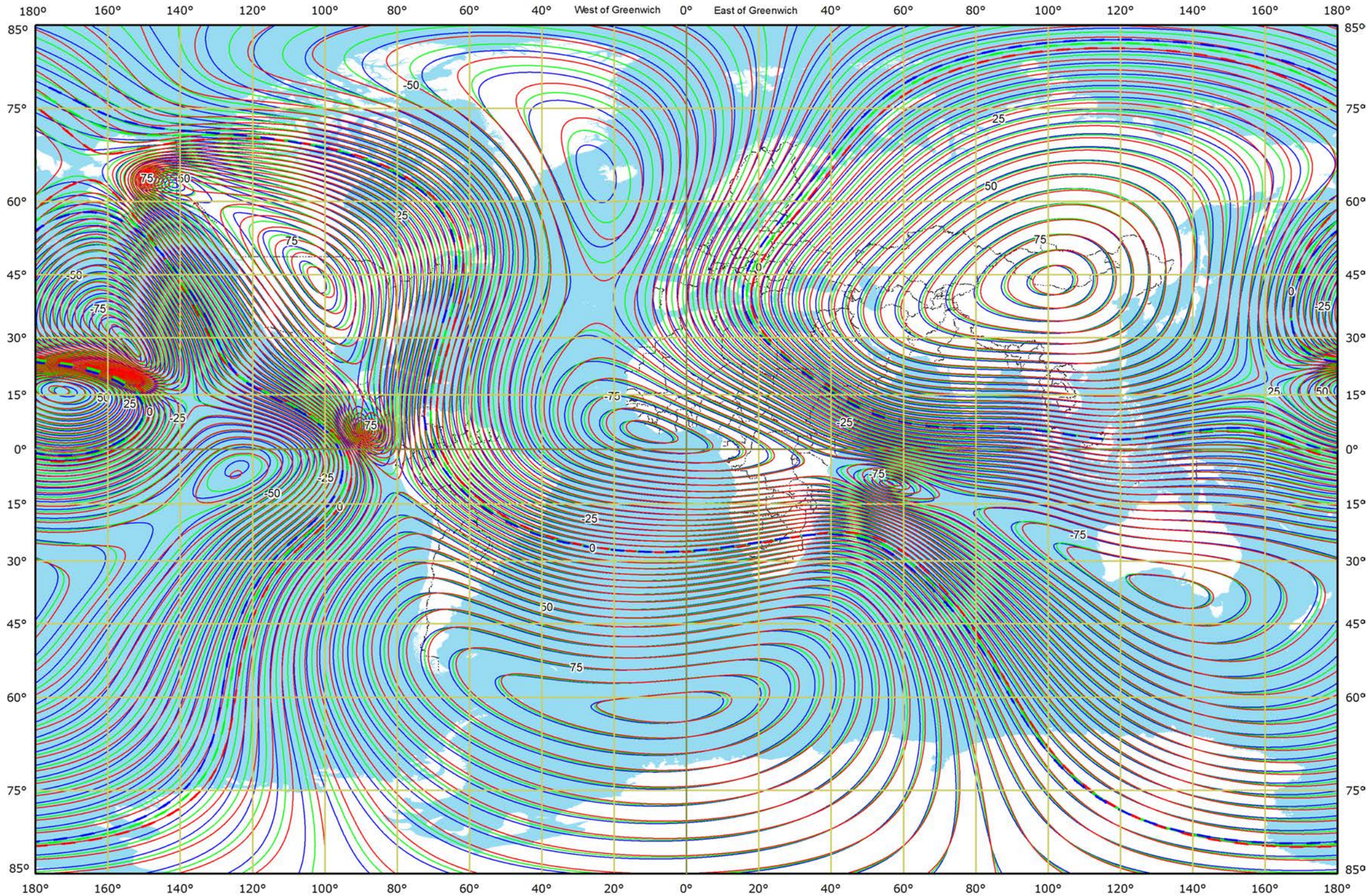

Years Isoclines

2000
2005
2010

Geomagnetic equators

2000
2005
2010

Example of magnetic inclination value, degree

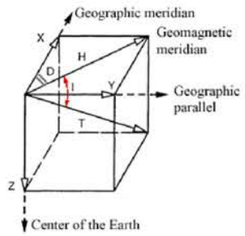

MGMF vector components

D Declination
I Inclination
H Horizontal component
T Total intensity
X North component
Y East component
Z Vertical component

Scale 1: 120 000 000

Projection: Miller cylindrical

NORTH COMPONENT OF MGMF NONDIPOLE PART

MGMF – 1900, 1905, 1910 – DX

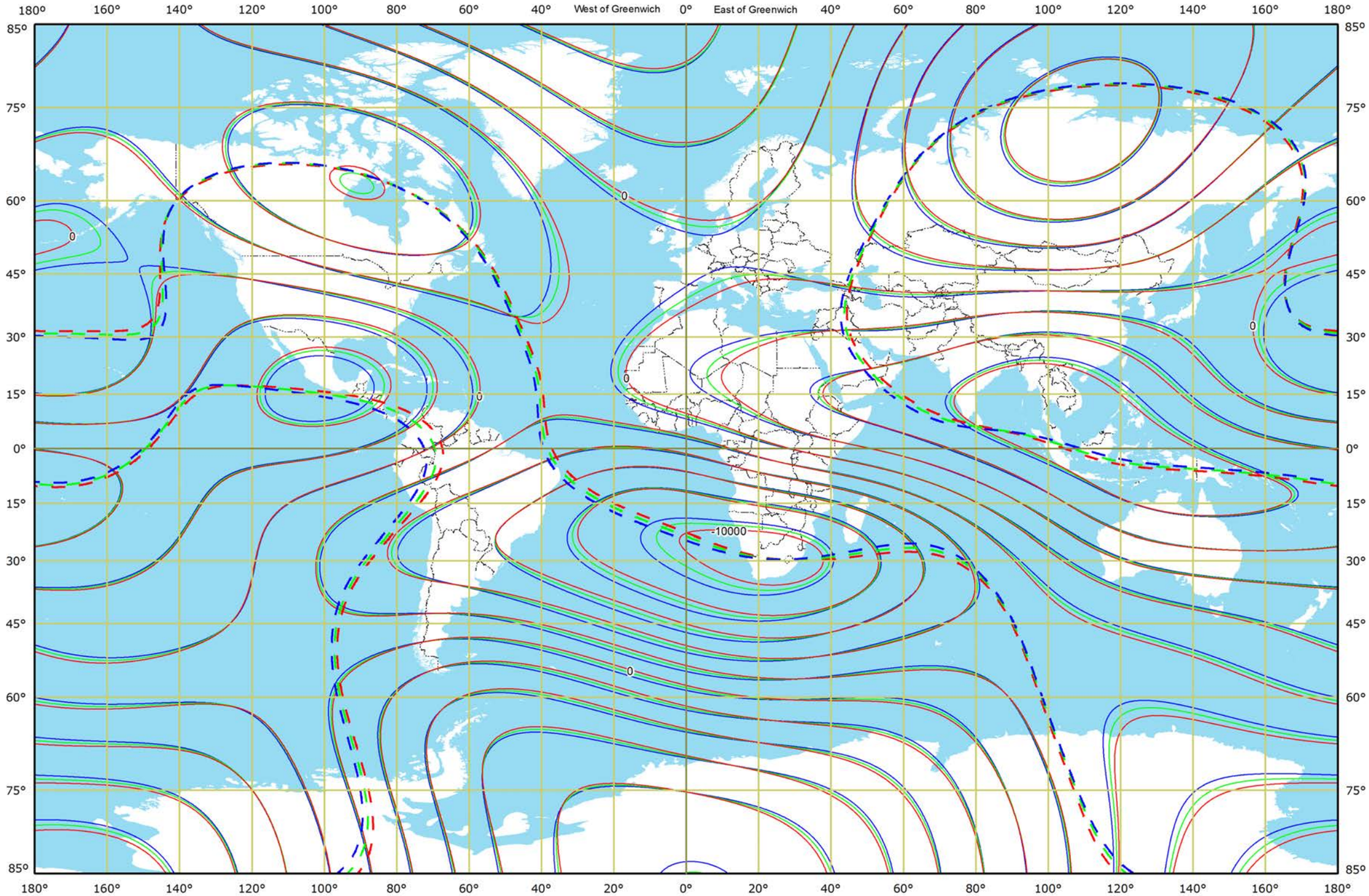

Years	Isolines	Geomagnetic equators
1900		1900
1905		1905
1910		1910

Example of magnetic field component value, nT

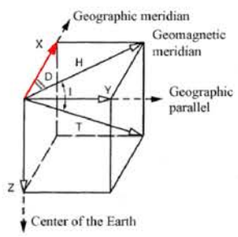

MGMF vector components

D Declination
I Inclination
H Horizontal component
T Total intensity
X North component
Y East component
Z Vertical component

Scale 1: 120 000 000

Projection: Miller cylindrical

NORTH COMPONENT OF MGMF NONDIPOLE PART

MGMF – 1910, 1915, 1920 – DX

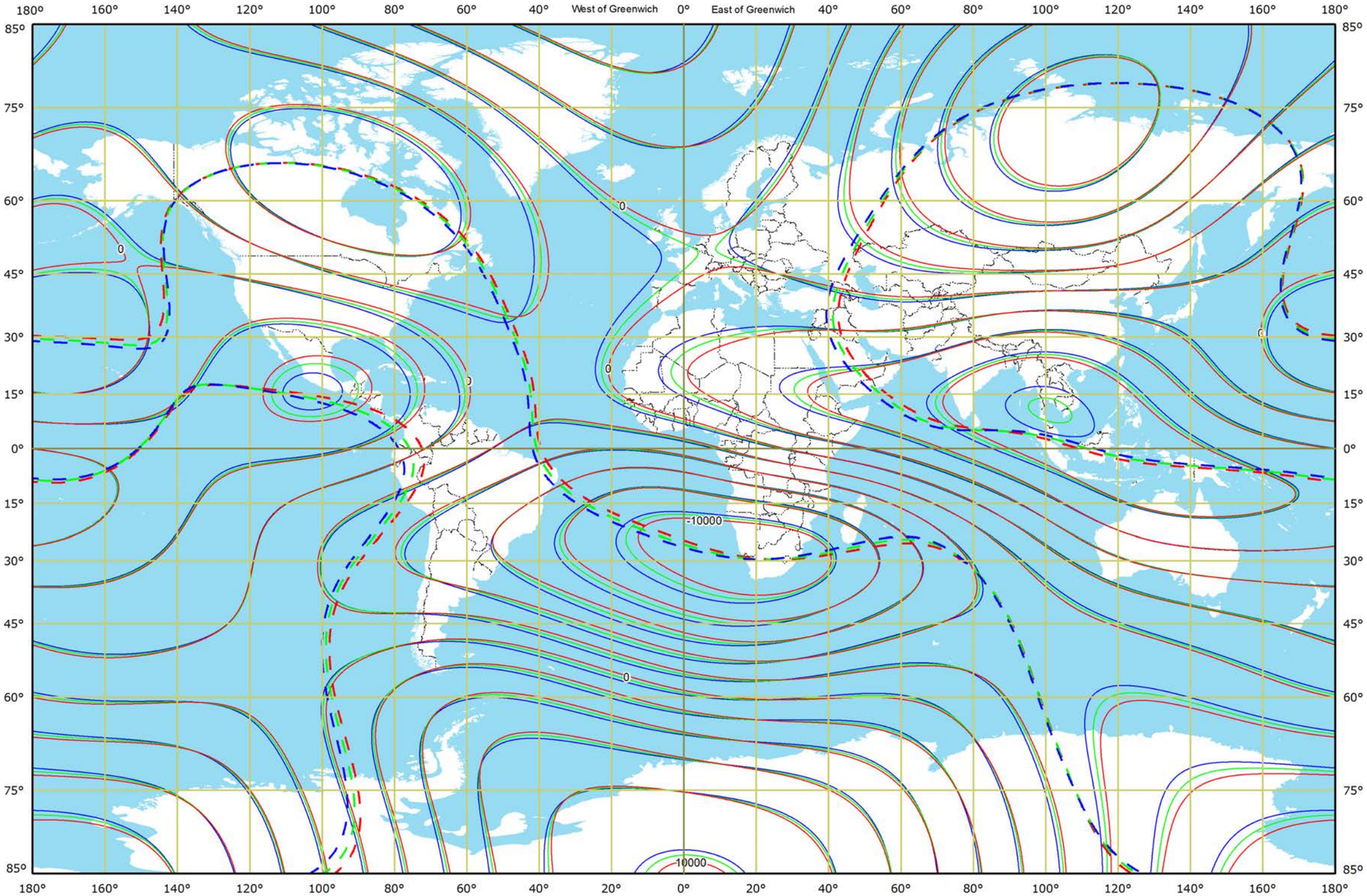

Years Isolines

1910
1915
1920

Geomagnetic equators

1910
1915
1920

Example of magnetic field component value, nT

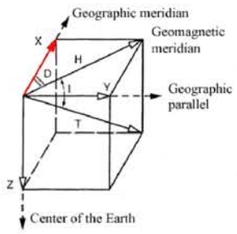

MGMF vector components

D Declination
I Inclination
H Horizontal component
T Total intensity
X North component
Y East component
Z Vertical component

Scale 1: 120 000 000

Projection: Miller cylindrical

NORTH COMPONENT OF MGMF NONDIPOLE PART

MGMF – 1920, 1925, 1930 – DX

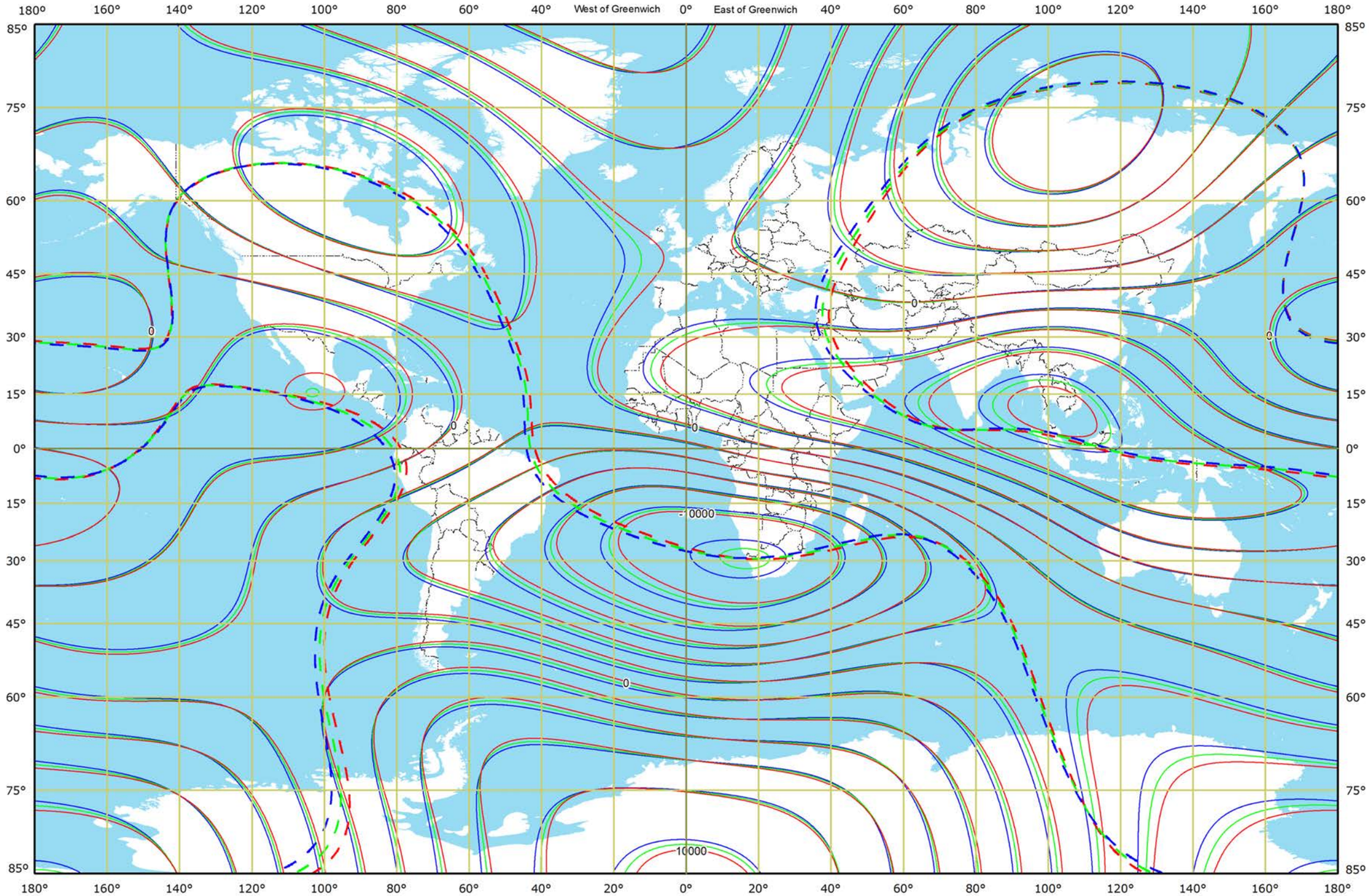

Years	Isolines	Geomagnetic equators
1920		1920
1925		1925
1930		1930

Example of magnetic field component value, nT

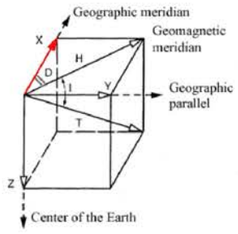

MGMF vector components

D Declination
I Inclination
H Horizontal component
T Total intensity
X North component
Y East component
Z Vertical component

Scale 1: 120 000 000

Projection: Miller cylindrical

NORTH COMPONENT OF MGMF NONDIPOLE PART

MGMF – 1930, 1935, 1940 – DX

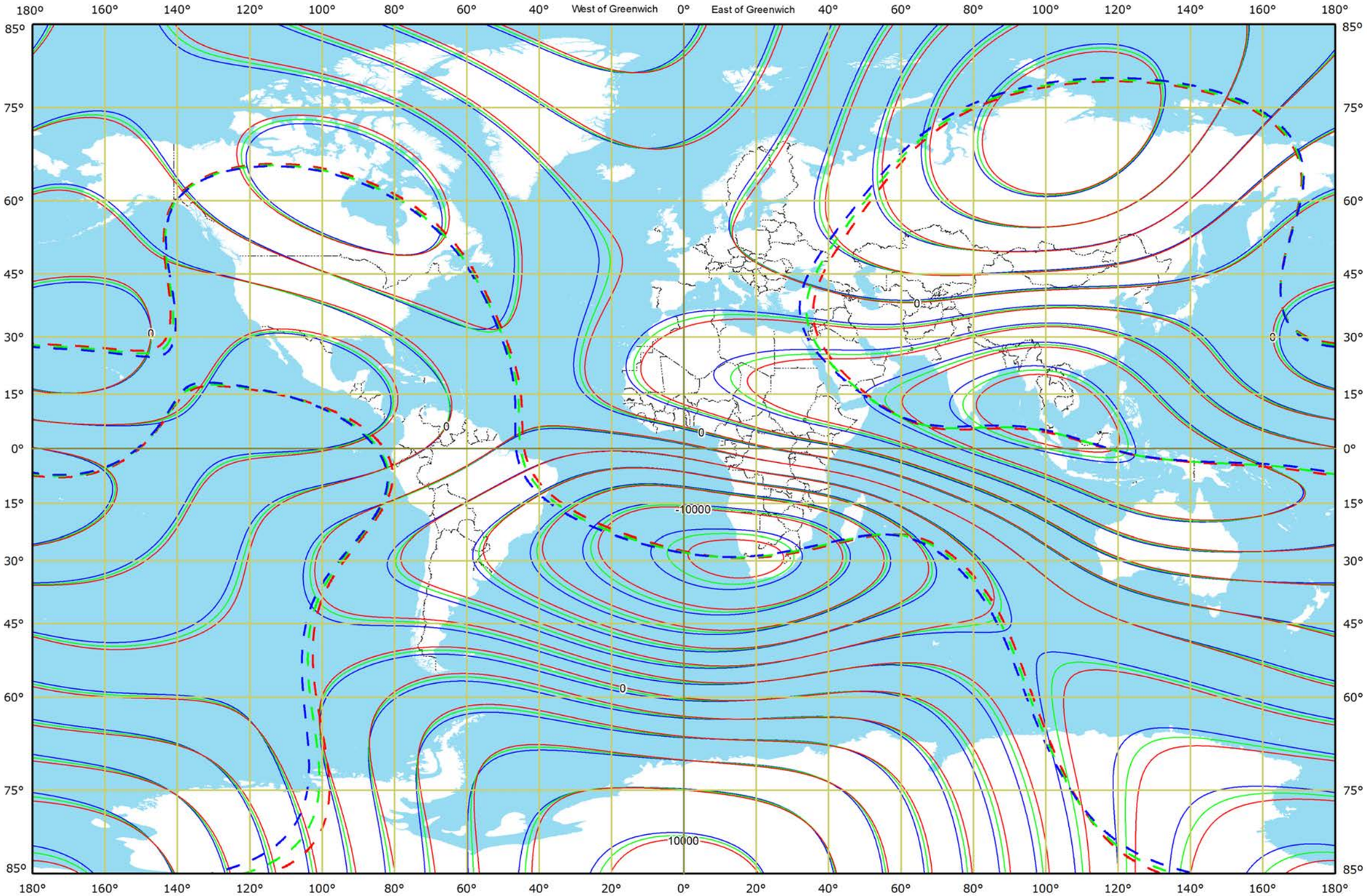

Years	Isolines	Geomagnetic equators
1930		1930
1935		1935
1940		1940

Example of magnetic field component value, nT

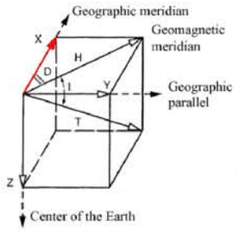

MGMF vector components

D Declination
I Inclination
H Horizontal component
T Total intensity
X North component
Y East component
Z Vertical component

Scale 1: 120 000 000

Projection: Miller cylindrical

NORTH COMPONENT OF MGMF NONDIPOLE PART

MGMF – 1940, 1945, 1950 – DX

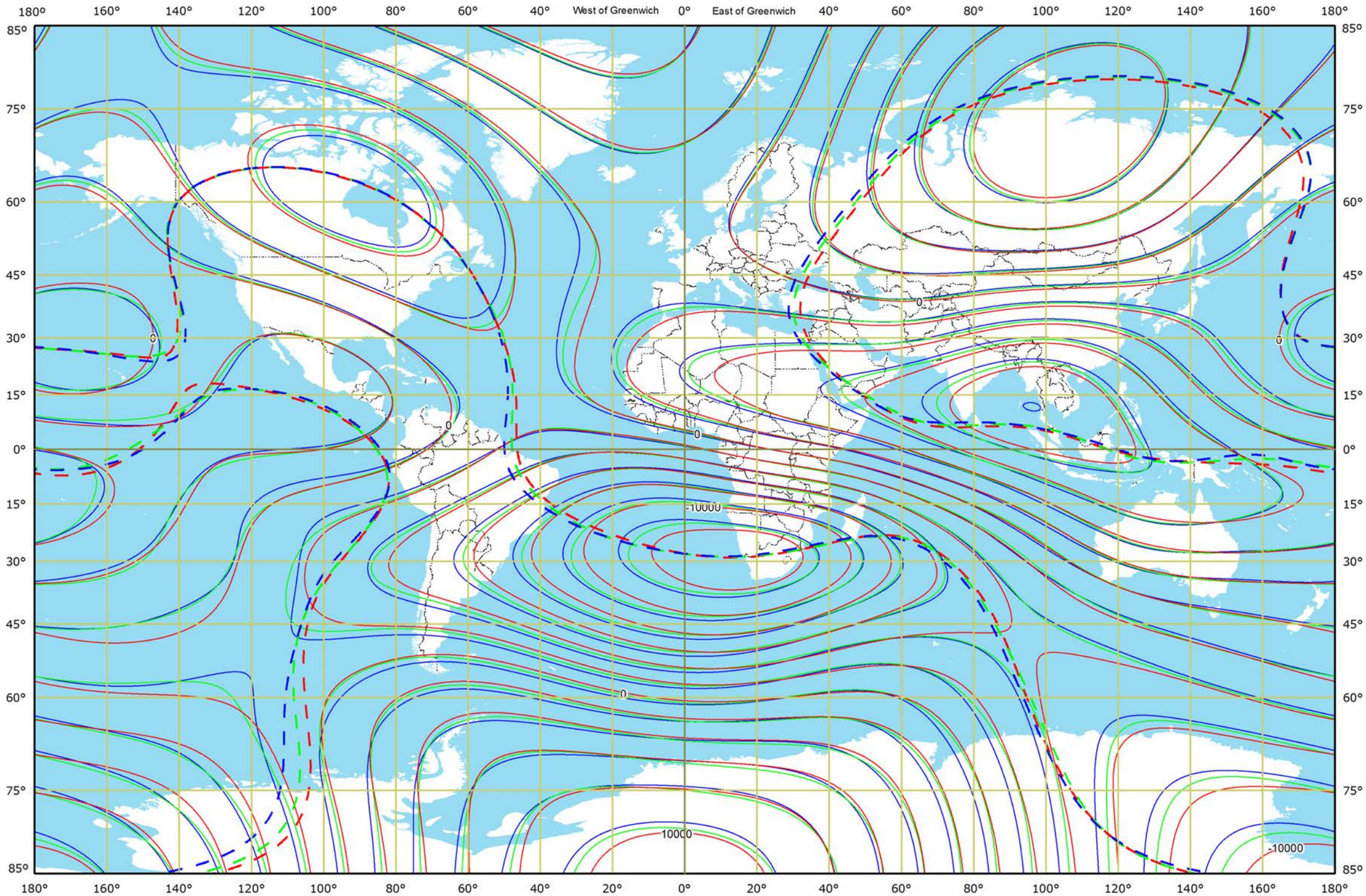

Years Isolines

1940
1945
1950

Geomagnetic equators

1940
1945
1950

Example of magnetic field component value, nT

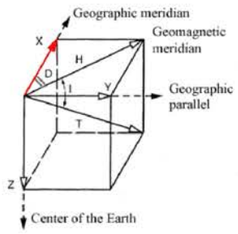

MGMF vector components

D Declination
I Inclination
H Horizontal component
T Total intensity
X North component
Y East component
Z Vertical component

Scale 1: 120 000 000

Projection: Miller cylindrical

NORTH COMPONENT OF MGMF NONDIPOLE PART

MGMF – 1950, 1955, 1960 – DX

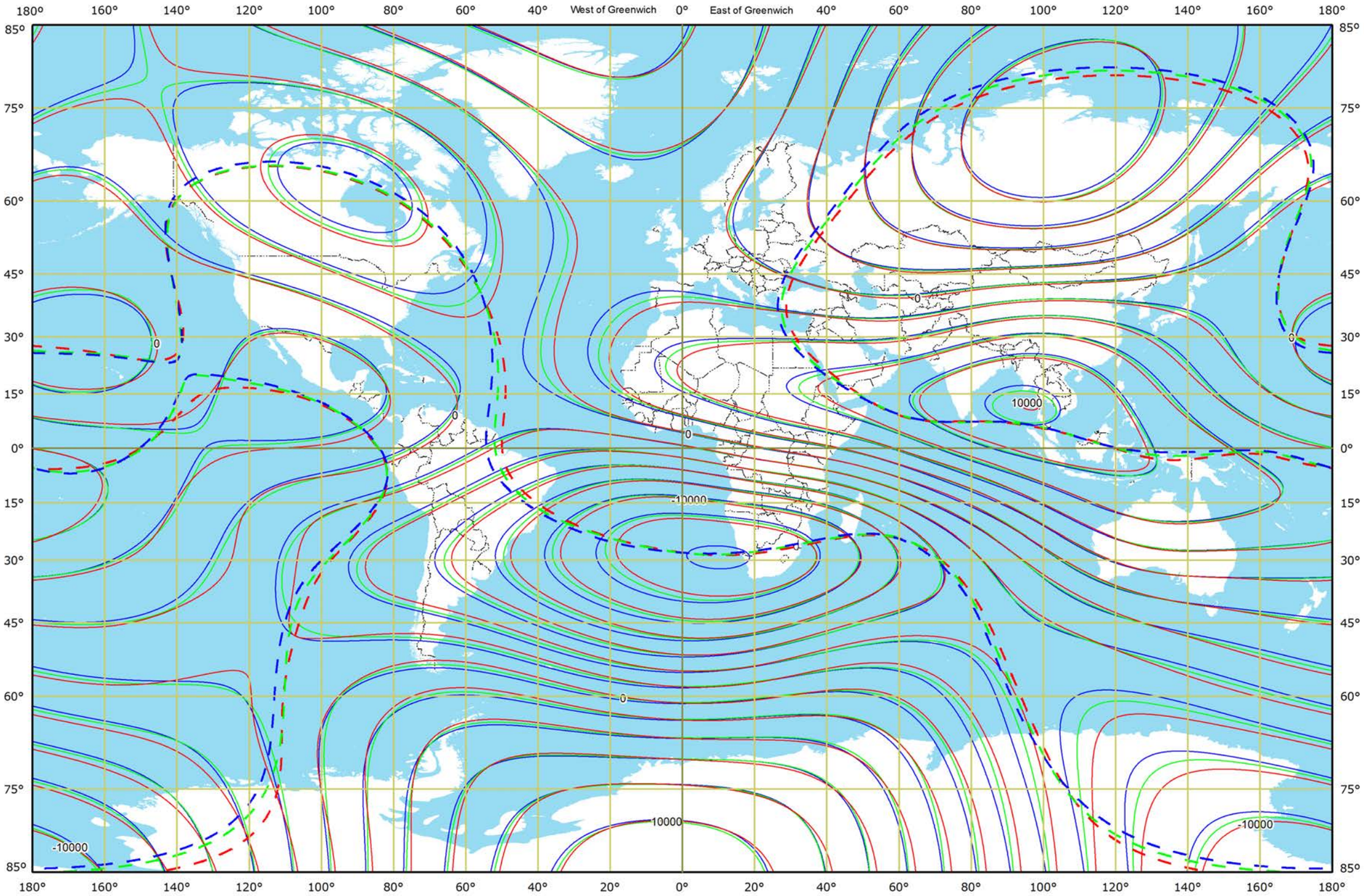

Years Isolines

1950
1955
1960

Geomagnetic equators

1950
1955
1960

Example of magnetic field component value, nT

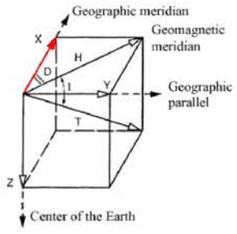

MGMF vector components

D Declination
I Inclination
H Horizontal component
T Total intensity
X North component
Y East component
Z Vertical component

Scale 1: 120 000 000

Projection: Miller cylindrical

NORTH COMPONENT OF MGMF NONDIPOLE PART

MGMF – 1960, 1965, 1970 – DX

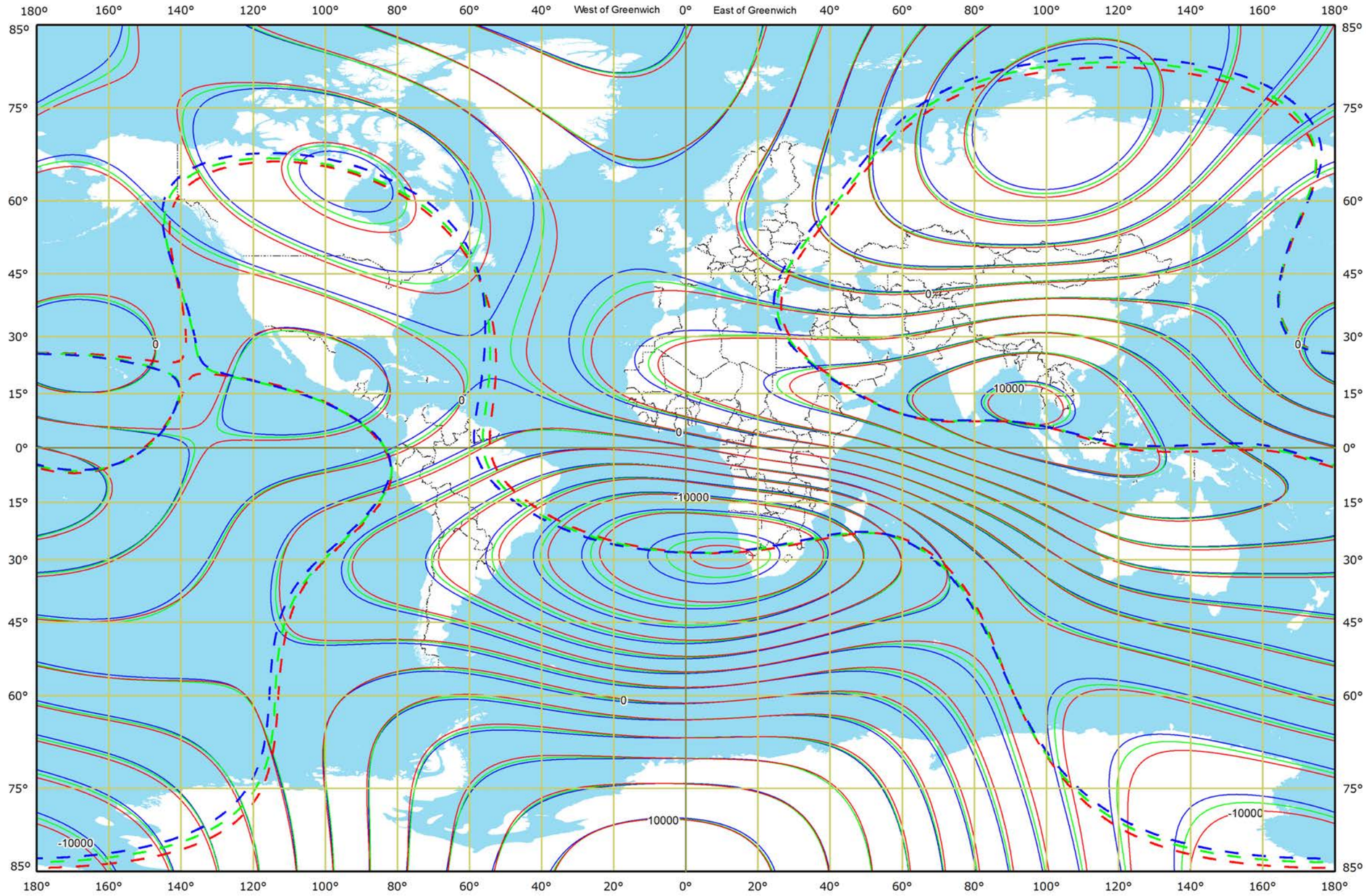

Years Isolines

1960
1965
1970

Geomagnetic equators

1960
1965
1970

Example of magnetic field component value, nT

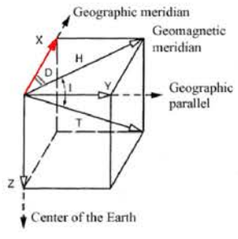

MGMF vector components

D Declination
I Inclination
H Horizontal component
T Total intensity
X North component
Y East component
Z Vertical component

Scale 1: 120 000 000

Projection: Miller cylindrical

NORTH COMPONENT OF MGMF NONDIPOLE PART

MGMF – 1970, 1975, 1980 – DX

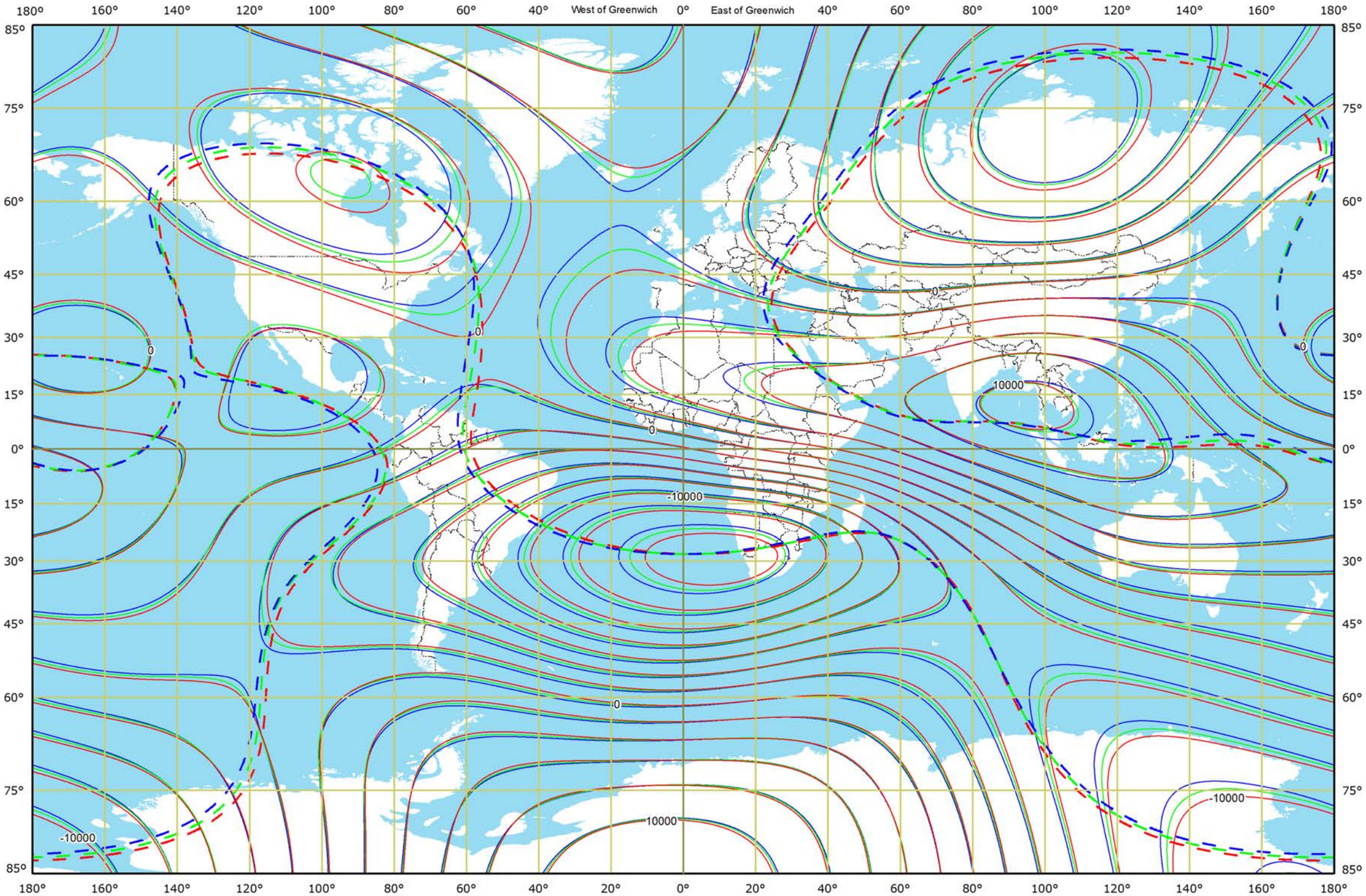

Years Isolines

1970
1975
1980

Geomagnetic equators

1970
1975
1980

Example of magnetic field component value, nT

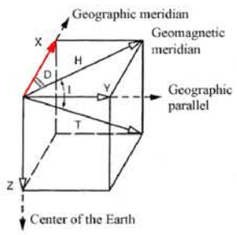

MGMF vector components

D Declination
I Inclination
H Horizontal component
T Total intensity
X North component
Y East component
Z Vertical component

Scale 1: 120 000 000

Projection: Miller cylindrical

NORTH COMPONENT OF MGMF NONDIPOLE PART

MGMF – 1980, 1985, 1990 – DX

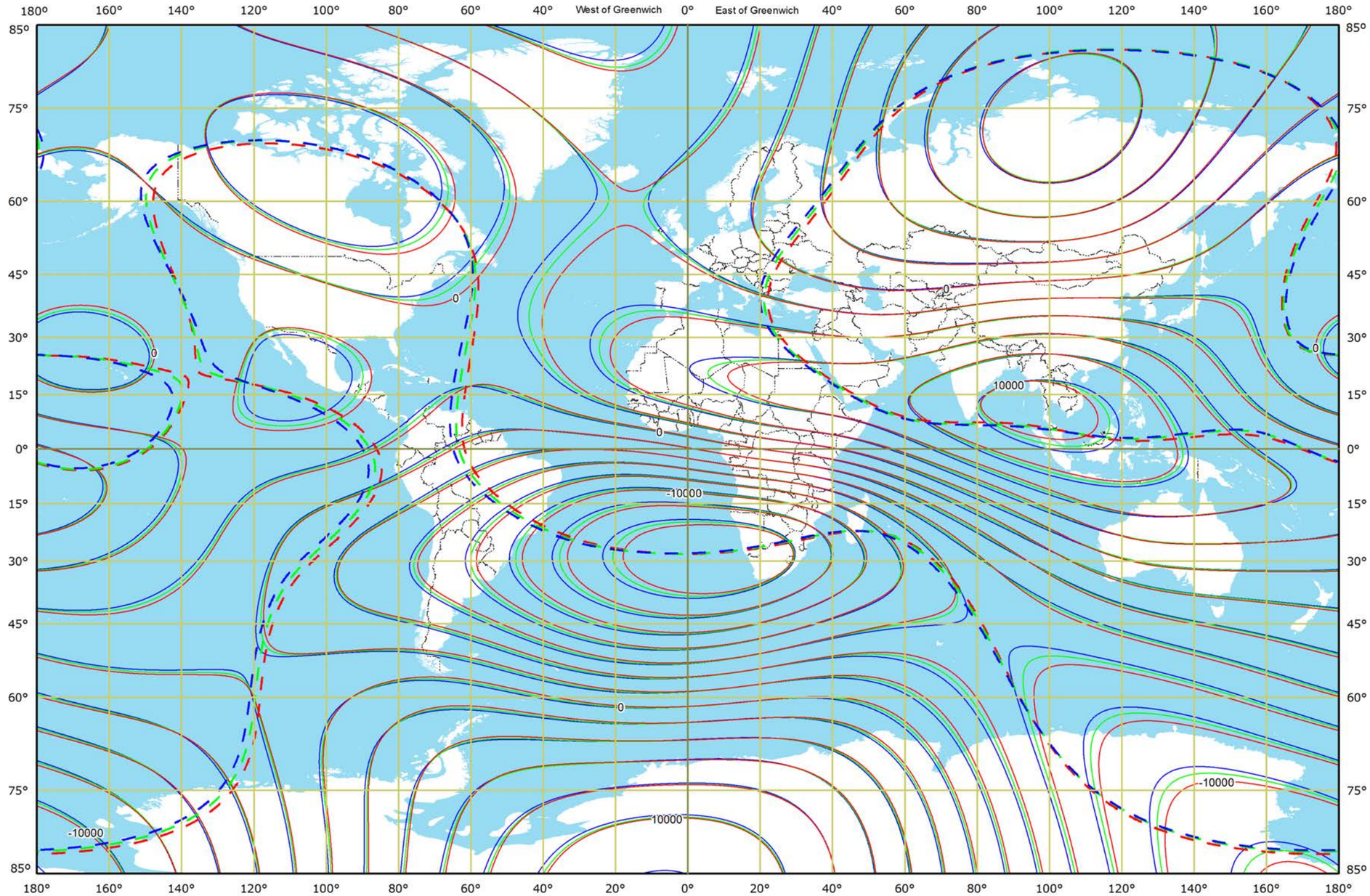

Years Isolines

1980
1985
1990

Geomagnetic equators

1980
1985
1990

Example of magnetic field component value, nT

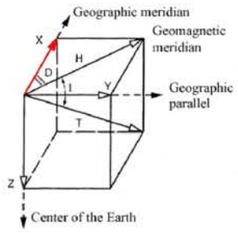

MGMF vector components

D Declination
I Inclination
H Horizontal component
T Total intensity
X North component
Y East component
Z Vertical component

Scale 1: 120 000 000

Projection: Miller cylindrical

NORTH COMPONENT OF MGMF NONDIPOLE PART

MGMF – 1990, 1995, 2000 – DX

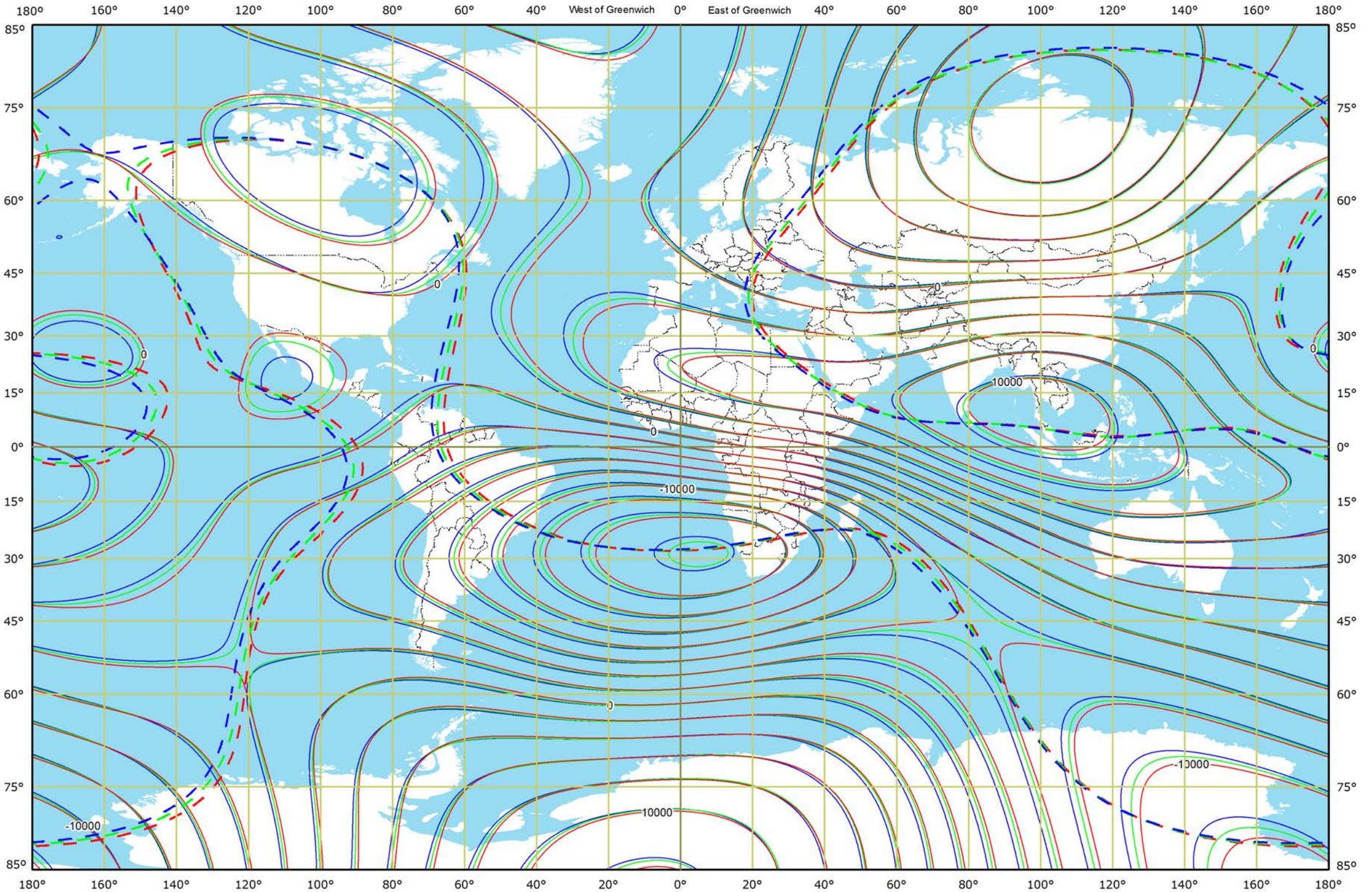

Years Isolines

1990
1995
2000

Geomagnetic equators

1990
1995
2000

Example of magnetic field component value, nT

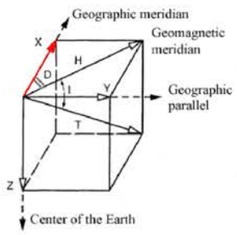

MGMF vector components

D Declination
I Inclination
H Horizontal component
T Total intensity
X North component
Y East component
Z Vertical component

Scale 1: 120 000 000

Projection: Miller cylindrical

NORTH COMPONENT OF MGMF NONDIPOLE PART

MGMF – 2000, 2005, 2010 – DX

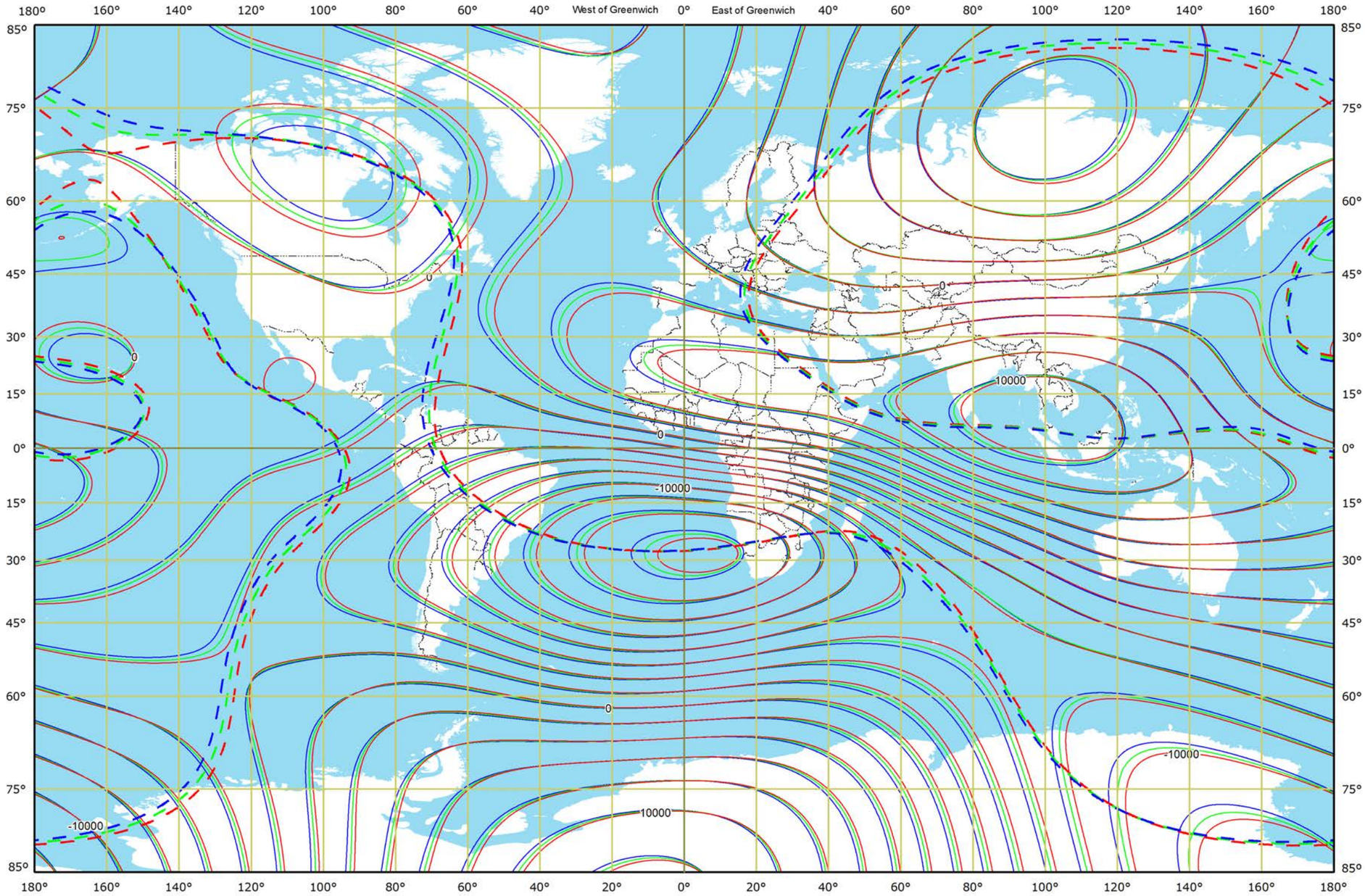

Years	Isolines	Geomagnetic equators
2000		2000
2005		2005
2010		2010

Example of magnetic field component value, nT

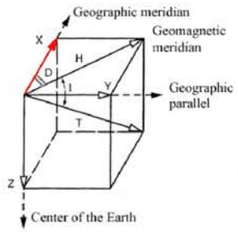

MGMF vector components

D Declination
I Inclination
H Horizontal component
T Total intensity
X North component
Y East component
Z Vertical component

Scale 1: 120 000 000

Projection: Miller cylindrical

EAST COMPONENT OF MGMF NONDIPOLE PART

MGMF – 1900, 1905, 1910 – DY

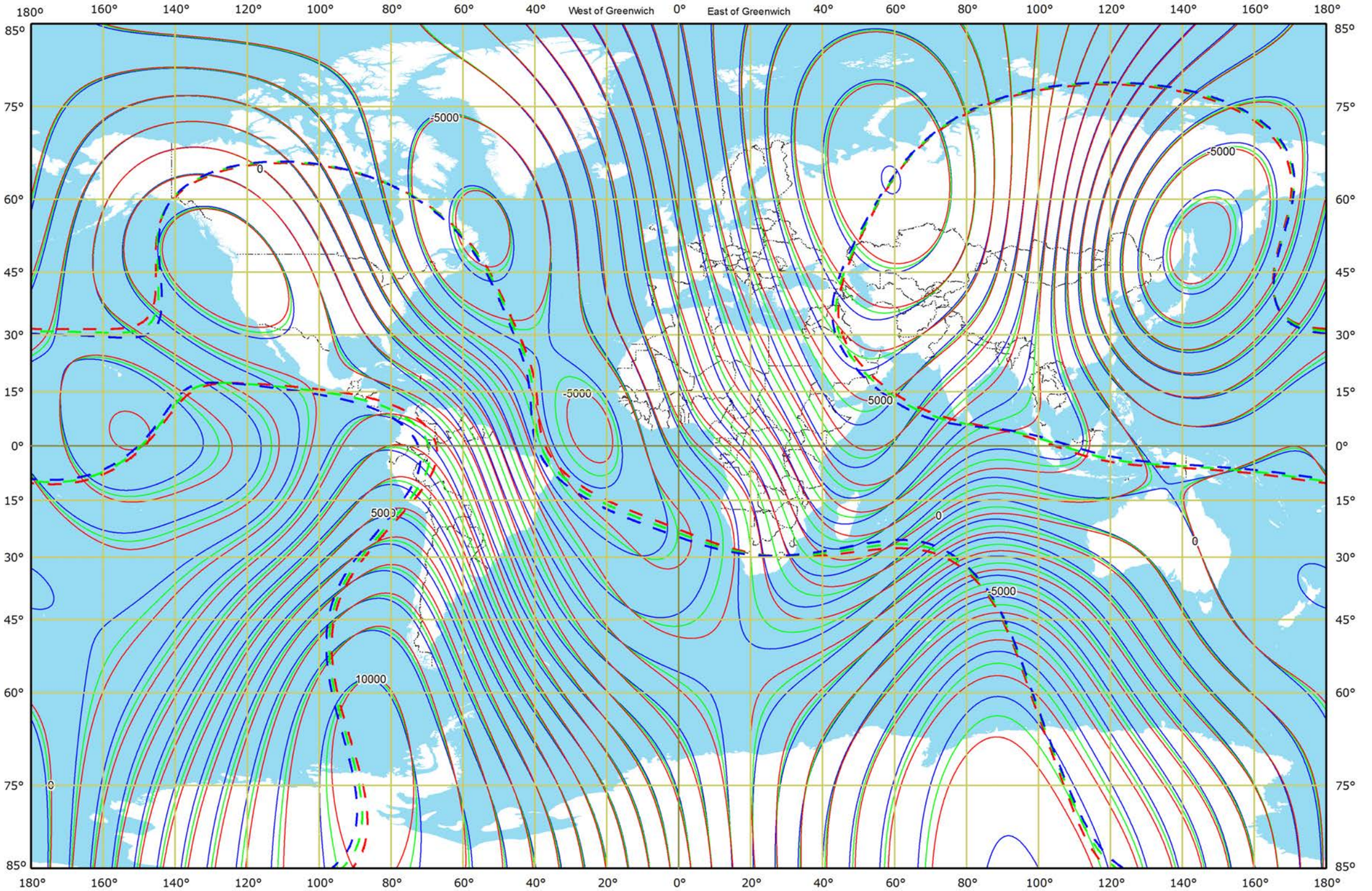

Years	Isolines	Geomagnetic equators
1910		1910
1915		1915
1920		1920

Example of magnetic field component value, nT

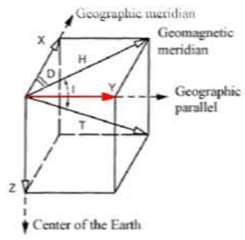

MGMF vector components

D Declination
I Inclination
H Horizontal component
T Total intensity
X North component
Y East component
Z Vertical component

Scale 1: 120 000 000

Projection: Miller cylindrical

EAST COMPONENT OF MGMF NONDIPOLE PART

MGMF – 1910, 1915, 1920 – DY

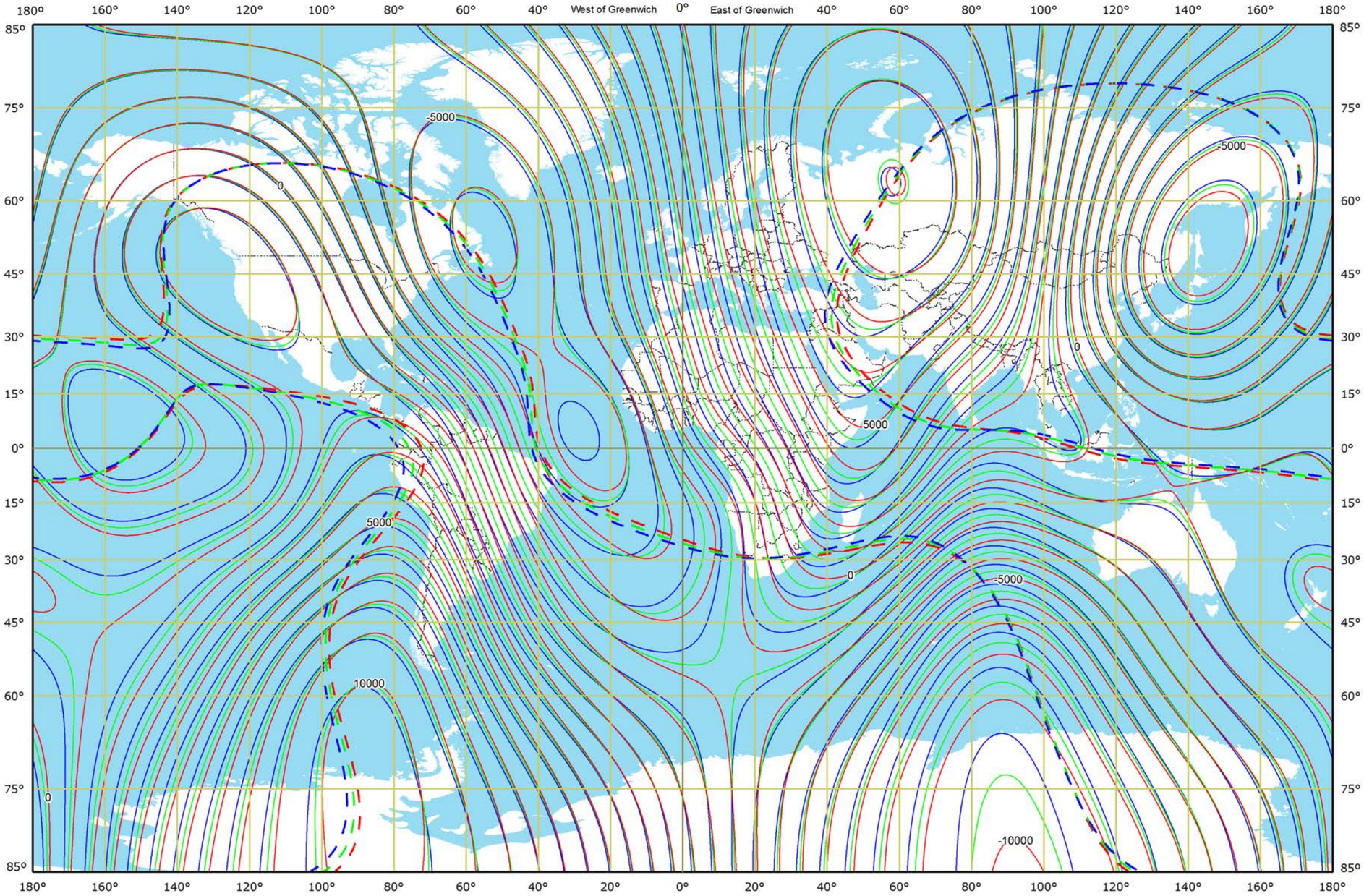

Years	Isolines	Geomagnetic equators
1910		1910
1915		1915
1920		1920

Example of magnetic field component value, nT

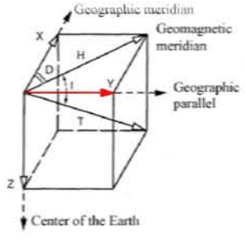

MGMF vector components

D Declination
I Inclination
H Horizontal component
T Total intensity
X North component
Y East component
Z Vertical component

Scale 1: 120 000 000

Projection: Miller cylindrical

EAST COMPONENT OF MGMF NONDIPOLE PART

MGMF – 1920, 1925, 1930 – DY

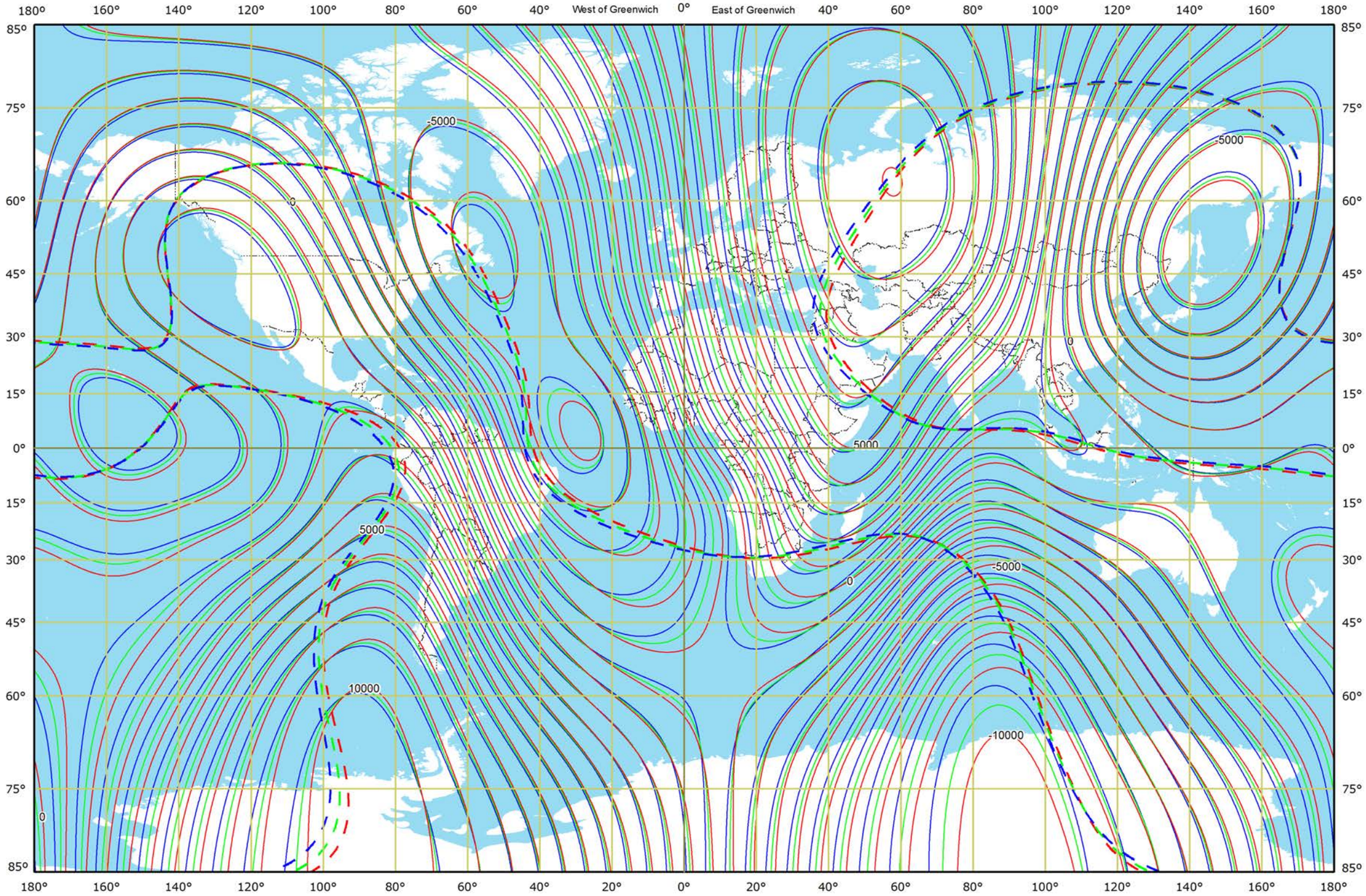

Years Isolines

1920
1925
1930

Geomagnetic equators

1920
1925
1930

Example of magnetic field component value, nT

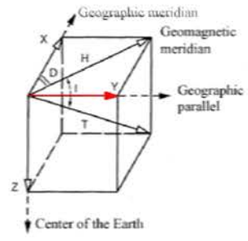

MGMF vector components

D Declination
I Inclination
H Horizontal component
T Total intensity
X North component
Y East component
Z Vertical component

Scale 1: 120 000 000

Projection: Miller cylindrical

EAST COMPONENT OF MGMF NONDIPOLE PART

MGMF – 1930, 1935, 1940 – DY

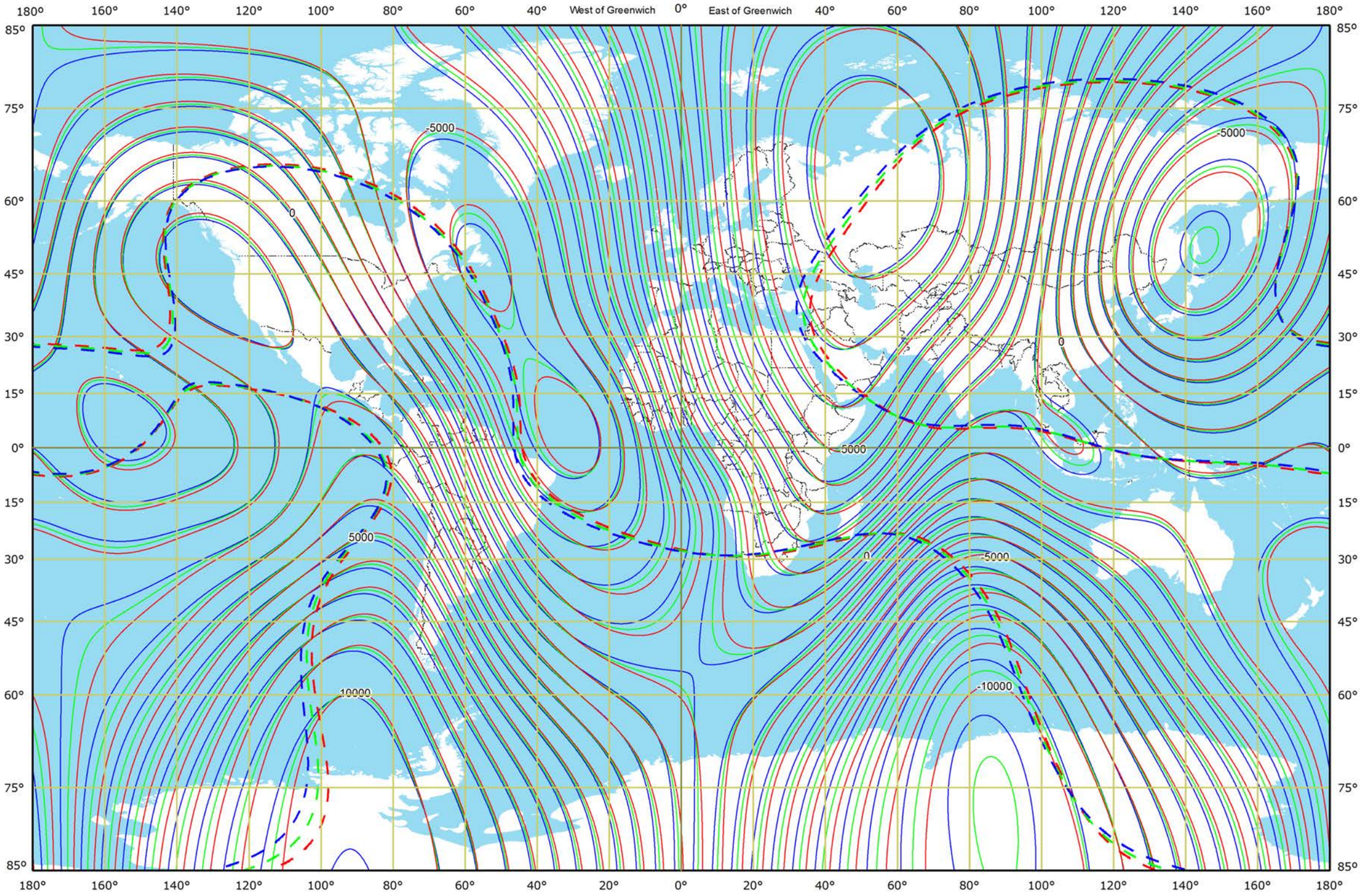

Years Isolines

1930
1935
1940

Geomagnetic equators

1930
1935
1940

Example of magnetic field component value, nT

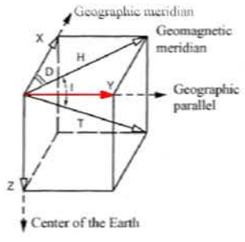

MGMF vector components

D Declination
I Inclination
H Horizontal component
T Total intensity
X North component
Y East component
Z Vertical component

Scale 1: 120 000 000

Projection: Miller cylindrical

EAST COMPONENT OF MGMF NONDIPOLE PART

MGMF – 1940, 1945, 1950 – DY

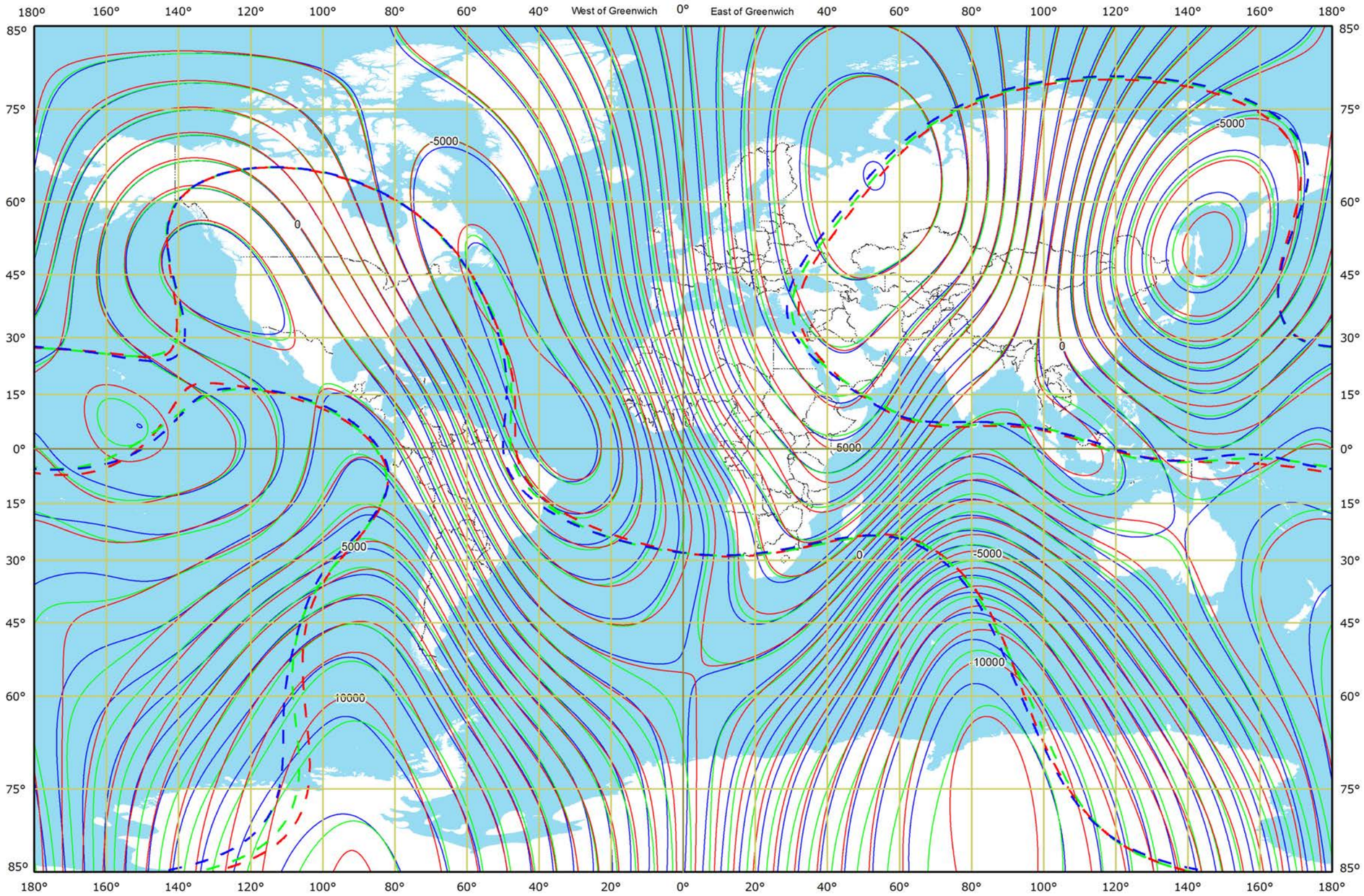

Years Isolines

1940
1945
1950

Geomagnetic equators

1940
1945
1950

Example of magnetic field component value, nT

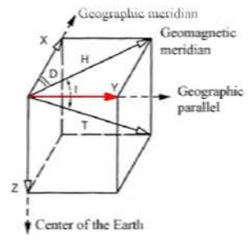

MGMF vector components

D Declination
I Inclination
H Horizontal component
T Total intensity
X North component
Y East component
Z Vertical component

Scale 1: 120 000 000

Projection: Miller cylindrical

EAST COMPONENT OF MGMF NONDIPOLE PART

MGMF – 1950, 1955, 1960 – DY

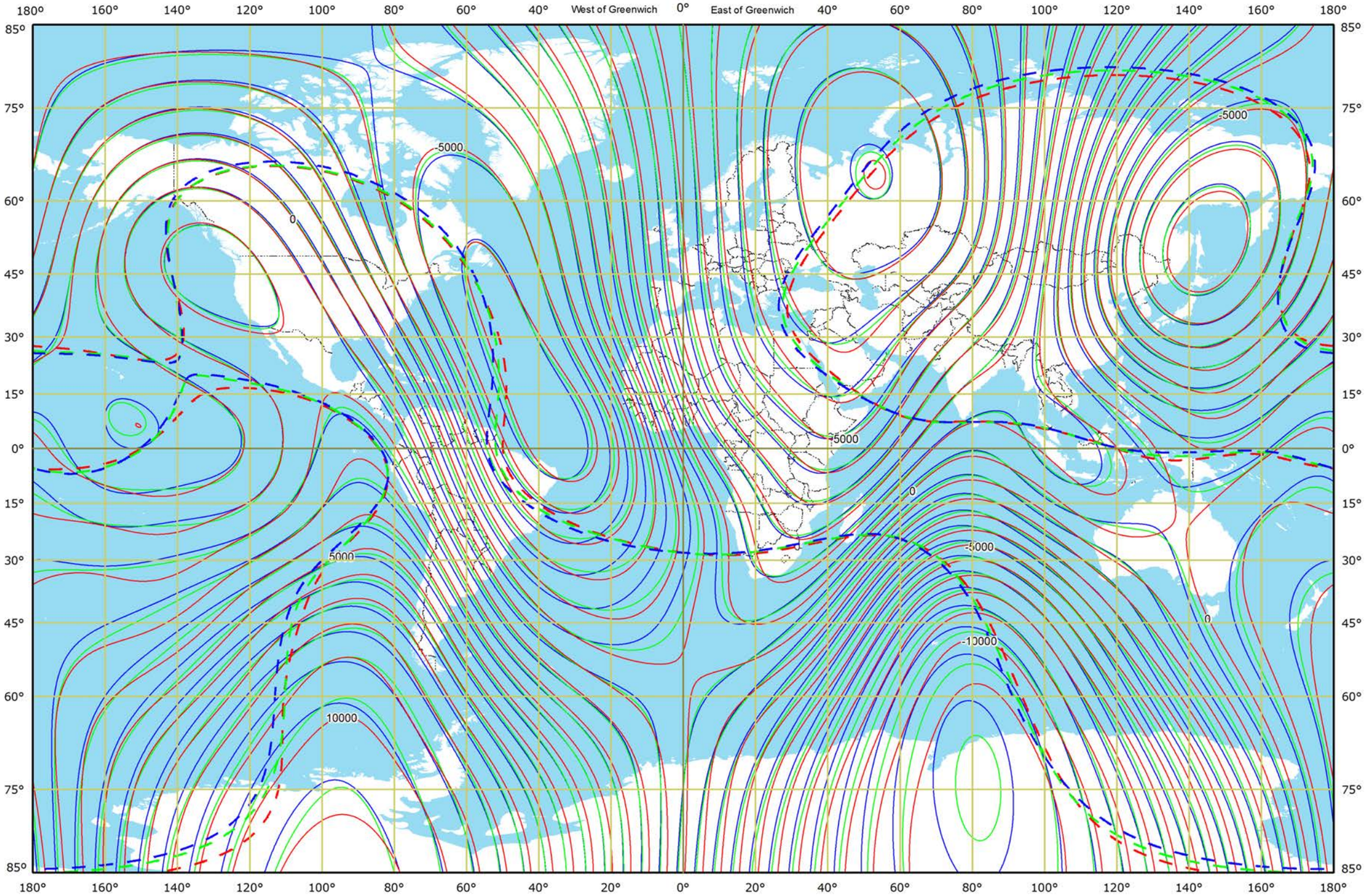

Years Isolines

1950
1955
1960

Geomagnetic equators

1950
1955
1960

Example of magnetic field component value, nT

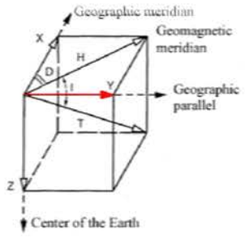

MGMF vector components

D Declination
I Inclination
H Horizontal component
T Total intensity
X North component
Y East component
Z Vertical component

Scale 1: 120 000 000

Projection: Miller cylindrical

EAST COMPONENT OF MGMF NONDIPOLE PART

MGMF – 1960, 1965, 1970 – DY

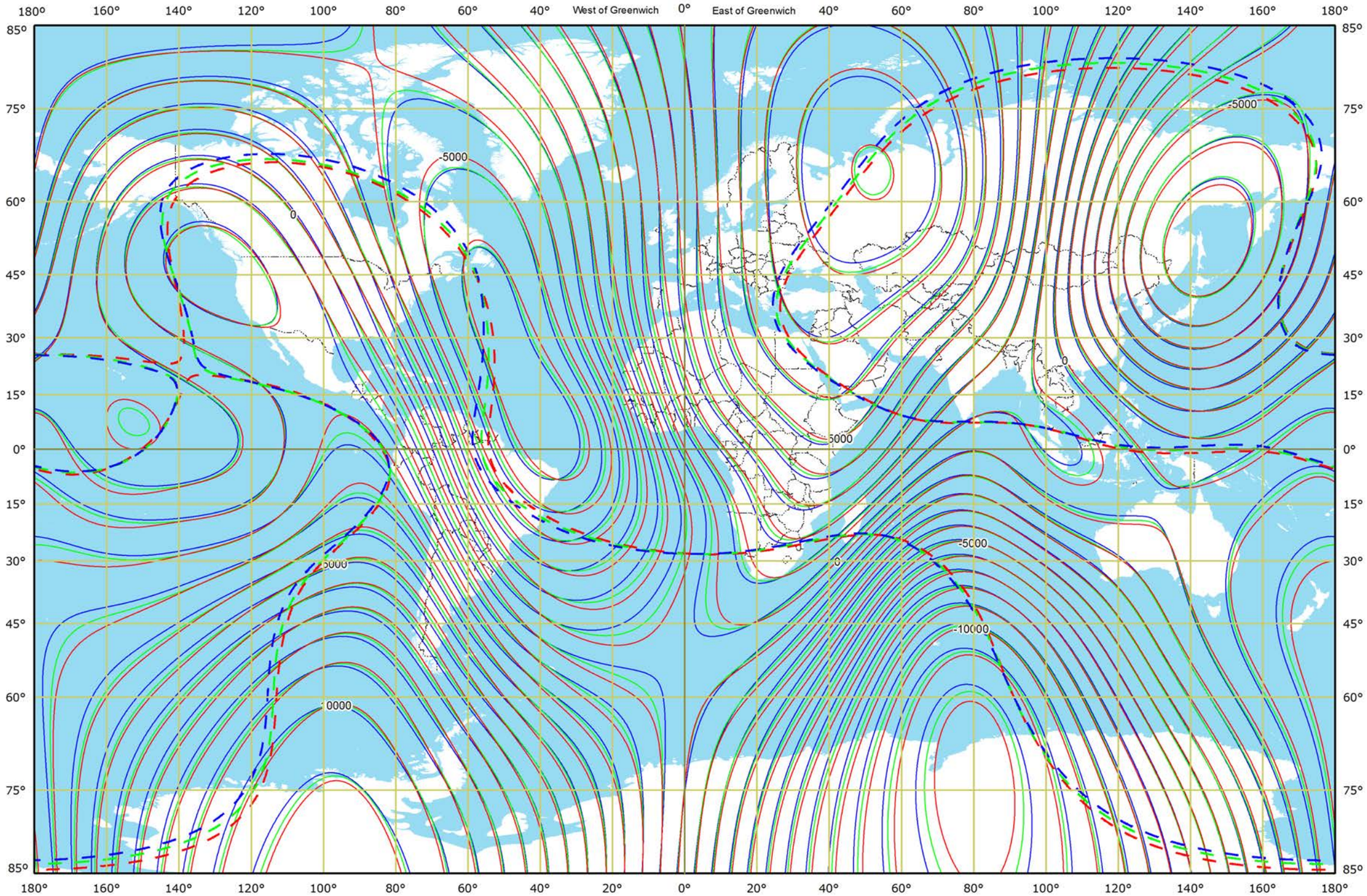

Years Isolines

1960
1965
1970

Geomagnetic equators

1960
1965
1970

Example of magnetic field component value, nT

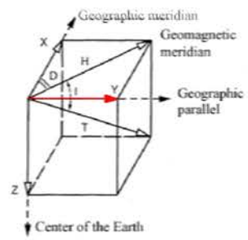

MGMF vector components

D Declination
I Inclination
H Horizontal component
T Total intensity
X North component
Y East component
Z Vertical component

Scale 1: 120 000 000

Projection: Miller cylindrical

EAST COMPONENT OF MGMF NONDIPOLE PART

MGMF – 1970, 1975, 1980 – DY

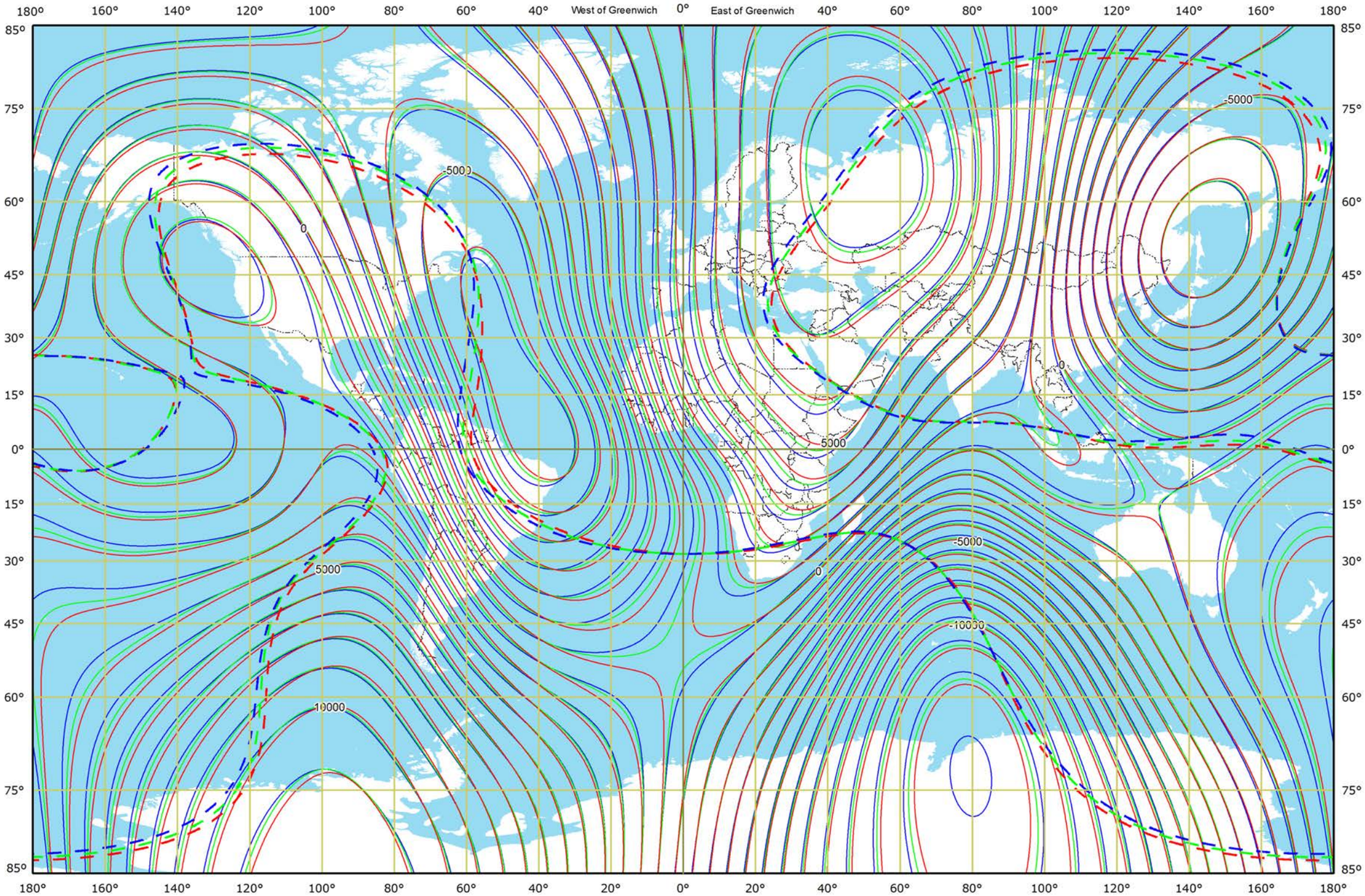

Years Isolines

1970
1975
1980

Geomagnetic equators

1970
1975
1980

Example of magnetic field component value, nT

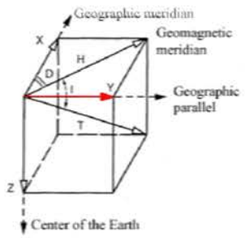

MGMF vector components

D Declination
I Inclination
H Horizontal component
T Total intensity
X North component
Y East component
Z Vertical component

Scale 1: 120 000 000

Projection: Miller cylindrical

EAST COMPONENT OF MGMF NONDIPOLE PART

MGMF – 1980, 1985, 1990 – DY

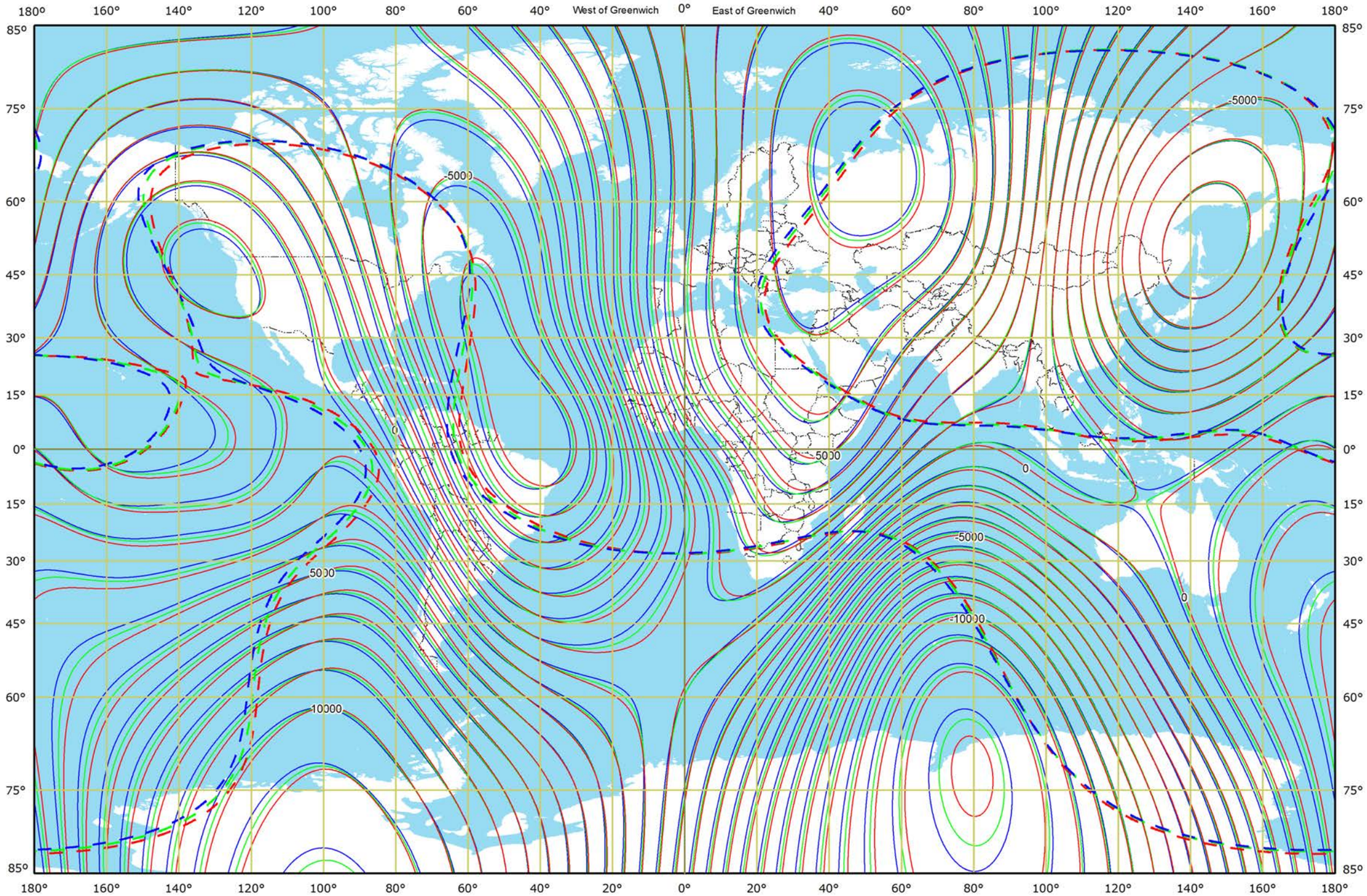

Years Isolines

1980
1985
1990

Geomagnetic equators

1980
1985
1990

Example of magnetic field component value, nT

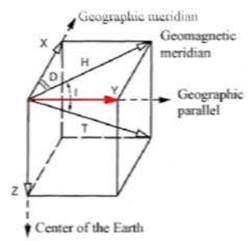

MGMF vector components

D Declination
I Inclination
H Horizontal component
T Total intensity
X North component
Y East component
Z Vertical component

Scale 1: 120 000 000

Projection: Miller cylindrical

EAST COMPONENT OF MGMF NONDIPOLE PART

MGMF – 1990, 1995, 2000 – DY

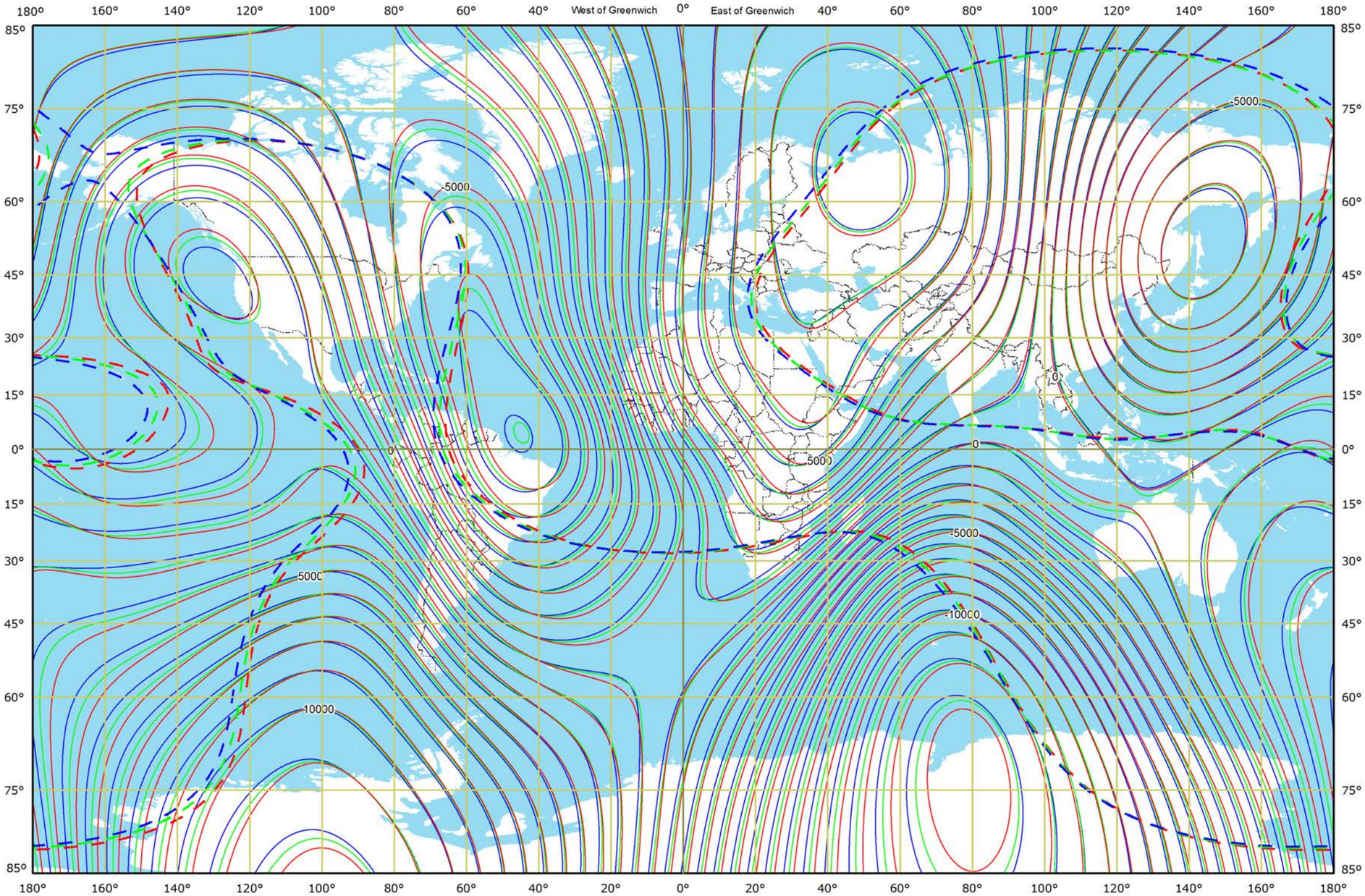

Years Isolines

1990
1995
2000

Geomagnetic equators

1990
1995
2000

Example of magnetic field component value, nT

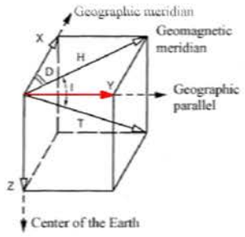

MGMF vector components

D Declination
I Inclination
H Horizontal component
T Total intensity
X North component
Y East component
Z Vertical component

Scale 1: 120 000 000

Projection: Miller cylindrical

EAST COMPONENT OF MGMF NONDIPOLE PART

MGMF – 2000, 2005, 2010 – DY

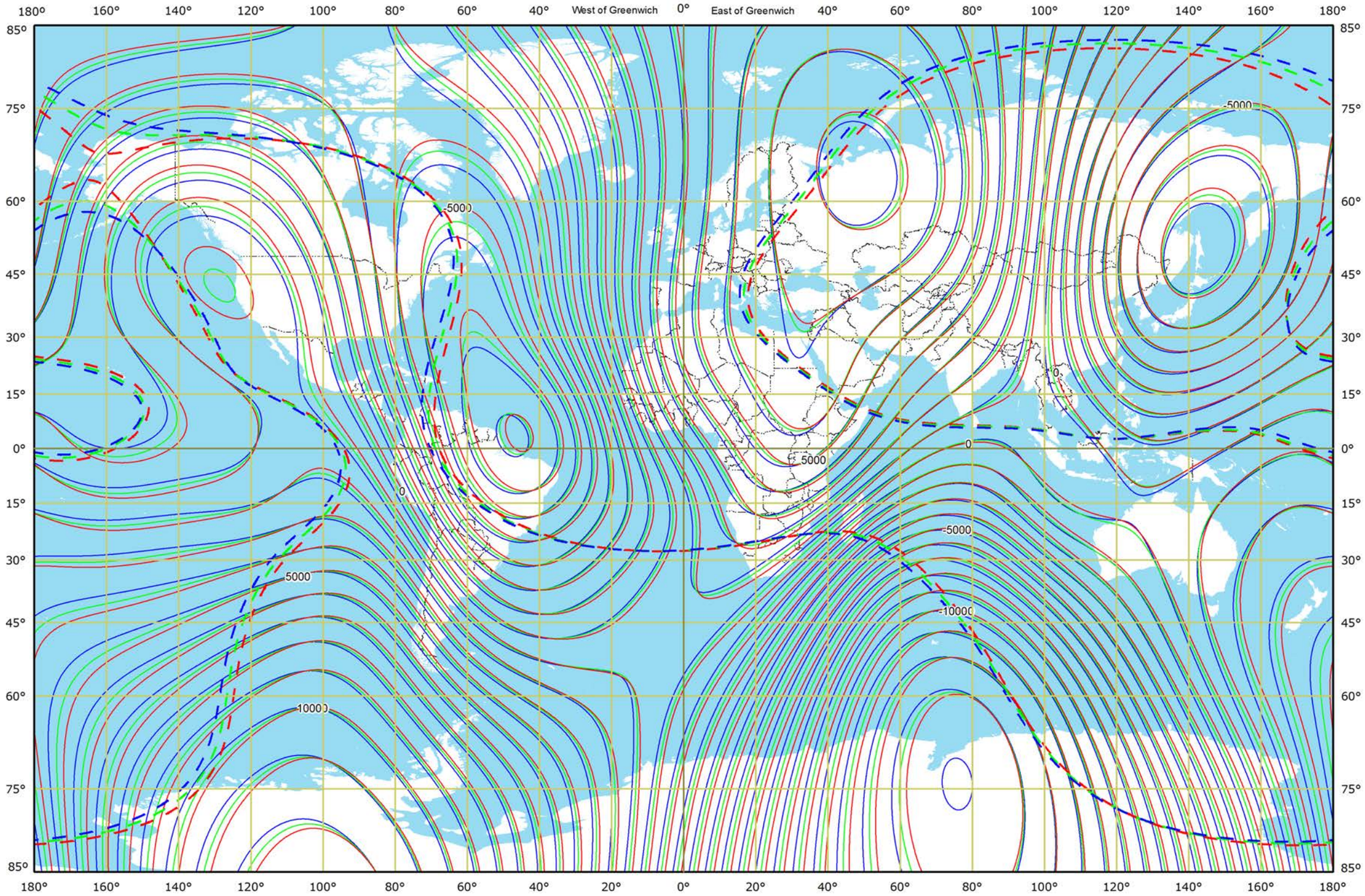

Years Isolines

2000
2005
2010

Geomagnetic equators

2000
2005
2010

Example of magnetic field component value, nT

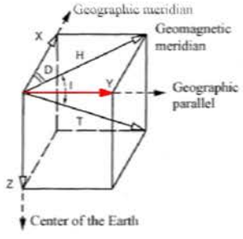

MGMF vector components

D Declination
I Inclination
H Horizontal component
T Total intensity
X North component
Y East component
Z Vertical component

Scale 1: 120 000 000

Projection: Miller cylindrical

VERTICAL COMPONENT OF MGMF NONDIPOLE PART

MGMF – 1900, 1905, 1910 – DZ

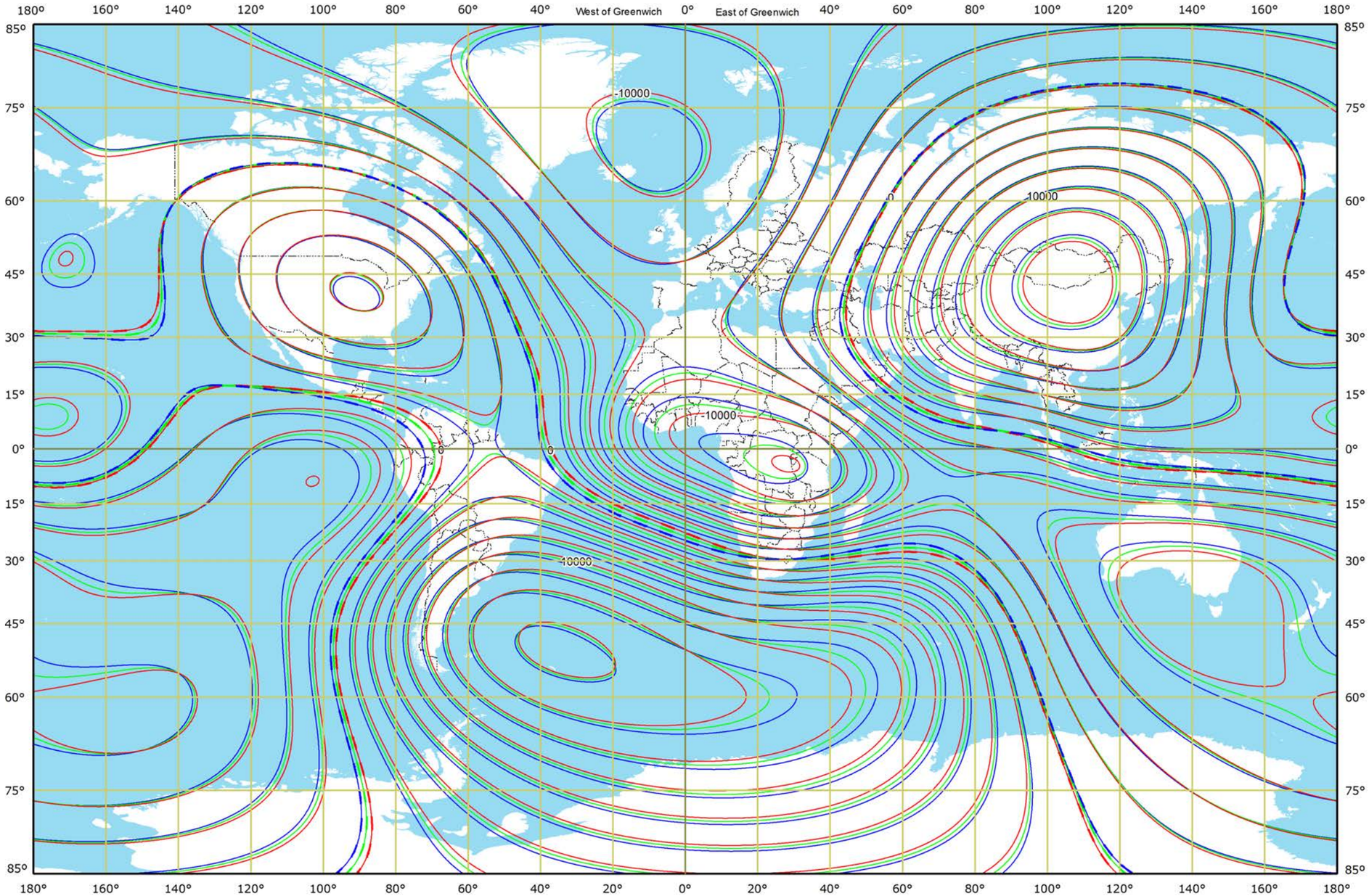

Years Isolines

1900
1905
1910

Geomagnetic equators

1900
1905
1910

Example of magnetic field component value, nT

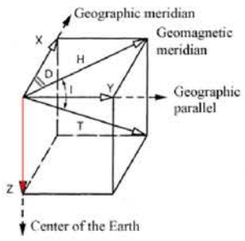

MGMF vector components

D Declination
I Inclination
H Horizontal component
T Total intensity
X North component
Y East component
Z Vertical component

Scale 1: 120 000 000

Projection: Miller cylindrical

VERTICAL COMPONENT OF MGMF NONDIPOLE PART

MGMF – 1910, 1915, 1920 – DZ

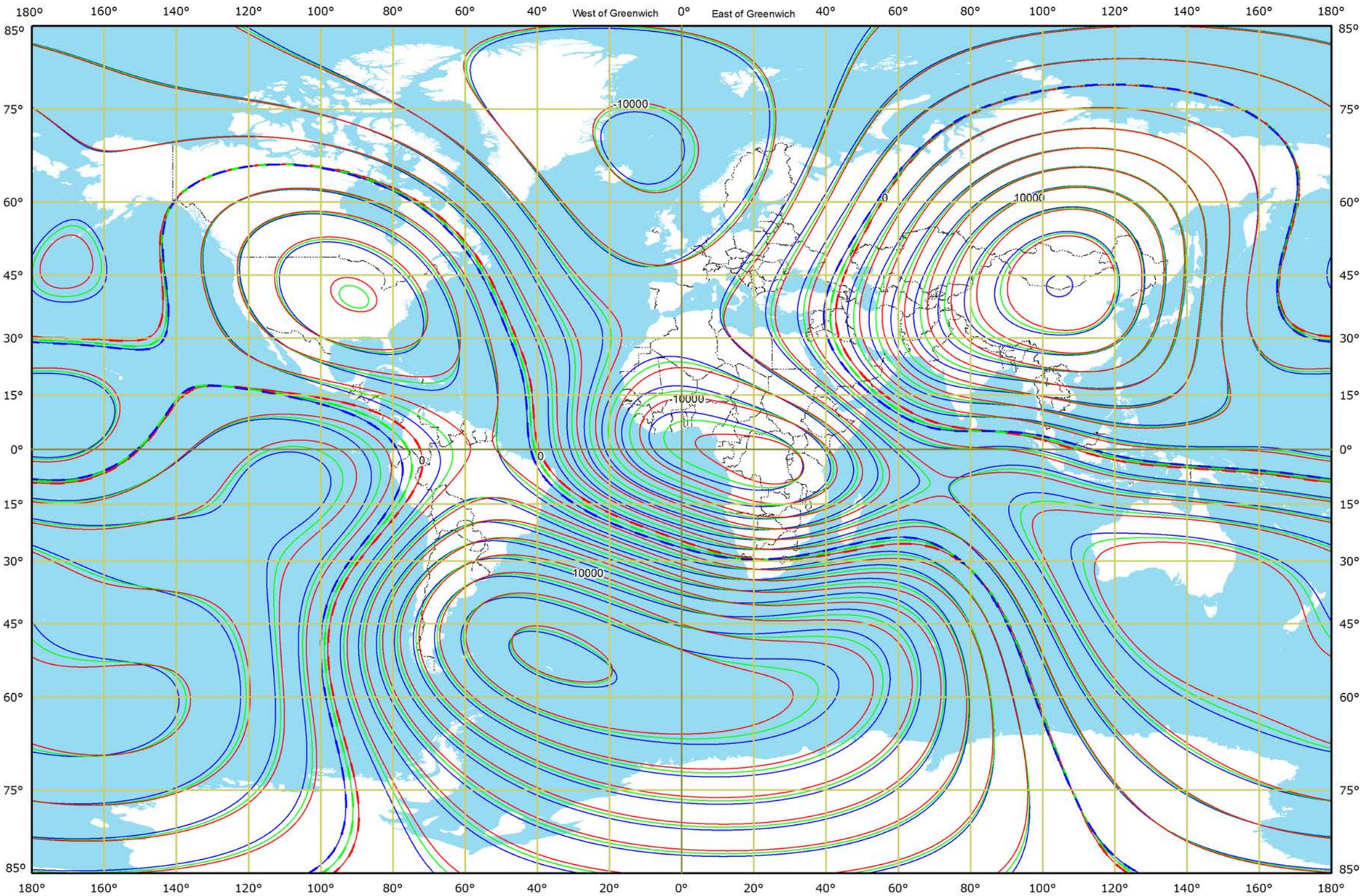

Years Isolines

1910
1915
1920

Geomagnetic equators

1910
1915
1920

Example of magnetic field component value, nT

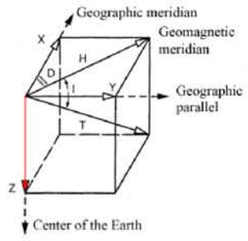

MGMF vector components

D Declination
I Inclination
H Horizontal component
T Total intensity
X North component
Y East component
Z Vertical component

Scale 1: 120 000 000

Projection: Miller cylindrical

VERTICAL COMPONENT OF MGMF NONDIPOLE PART

MGMF – 1920, 1925, 1930 – DZ

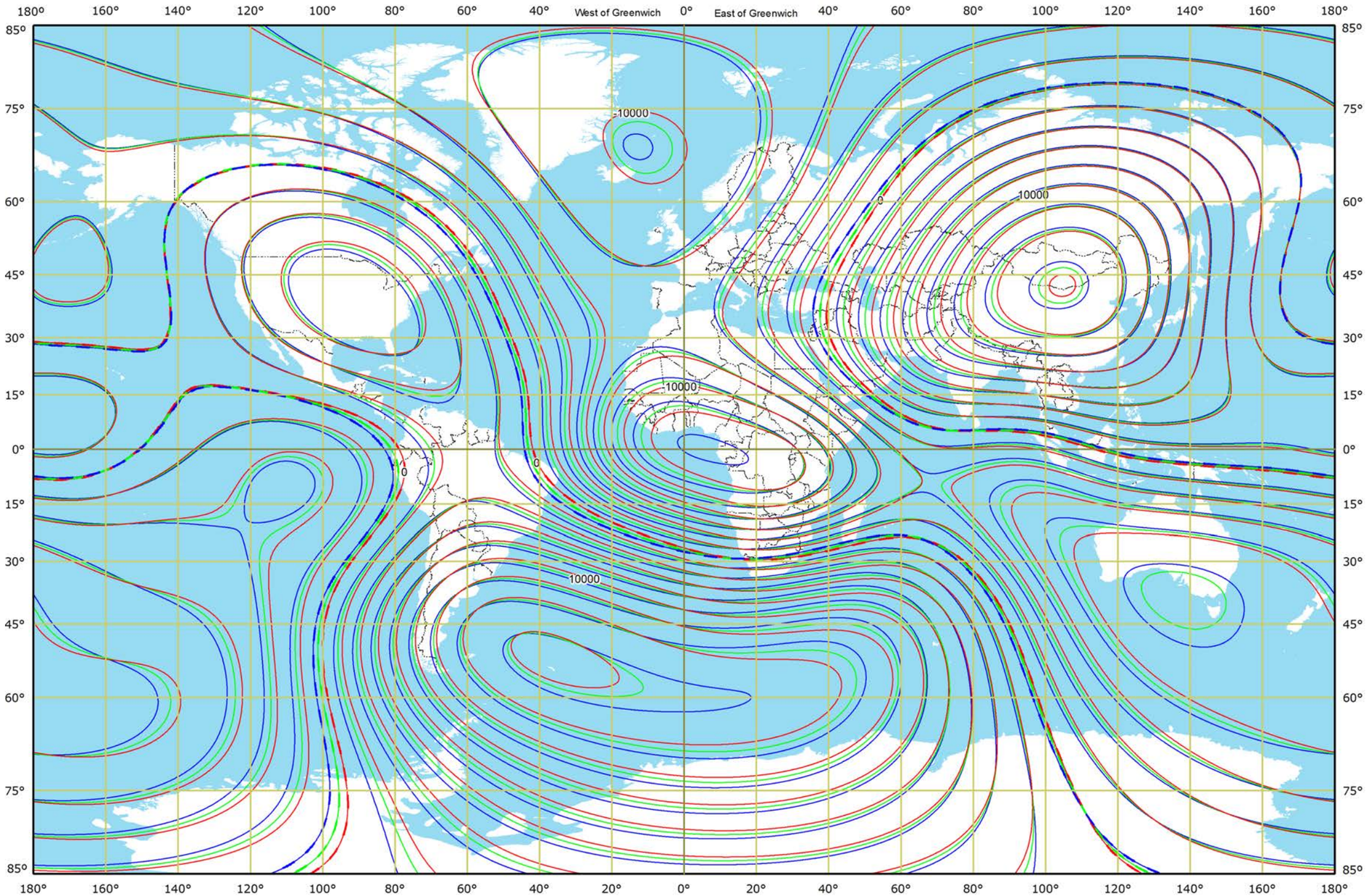

Years Isolines

1920
1925
1930

Geomagnetic equators

1920
1925
1930

Example of magnetic field component value, nT

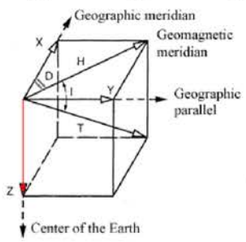

MGMF vector components

D Declination
I Inclination
H Horizontal component
T Total intensity
X North component
Y East component
Z Vertical component

Scale 1: 120 000 000

Projection: Miller cylindrical

VERTICAL COMPONENT OF MGMF NONDIPOLE PART

MGMF – 1930, 1935, 1940 – DZ

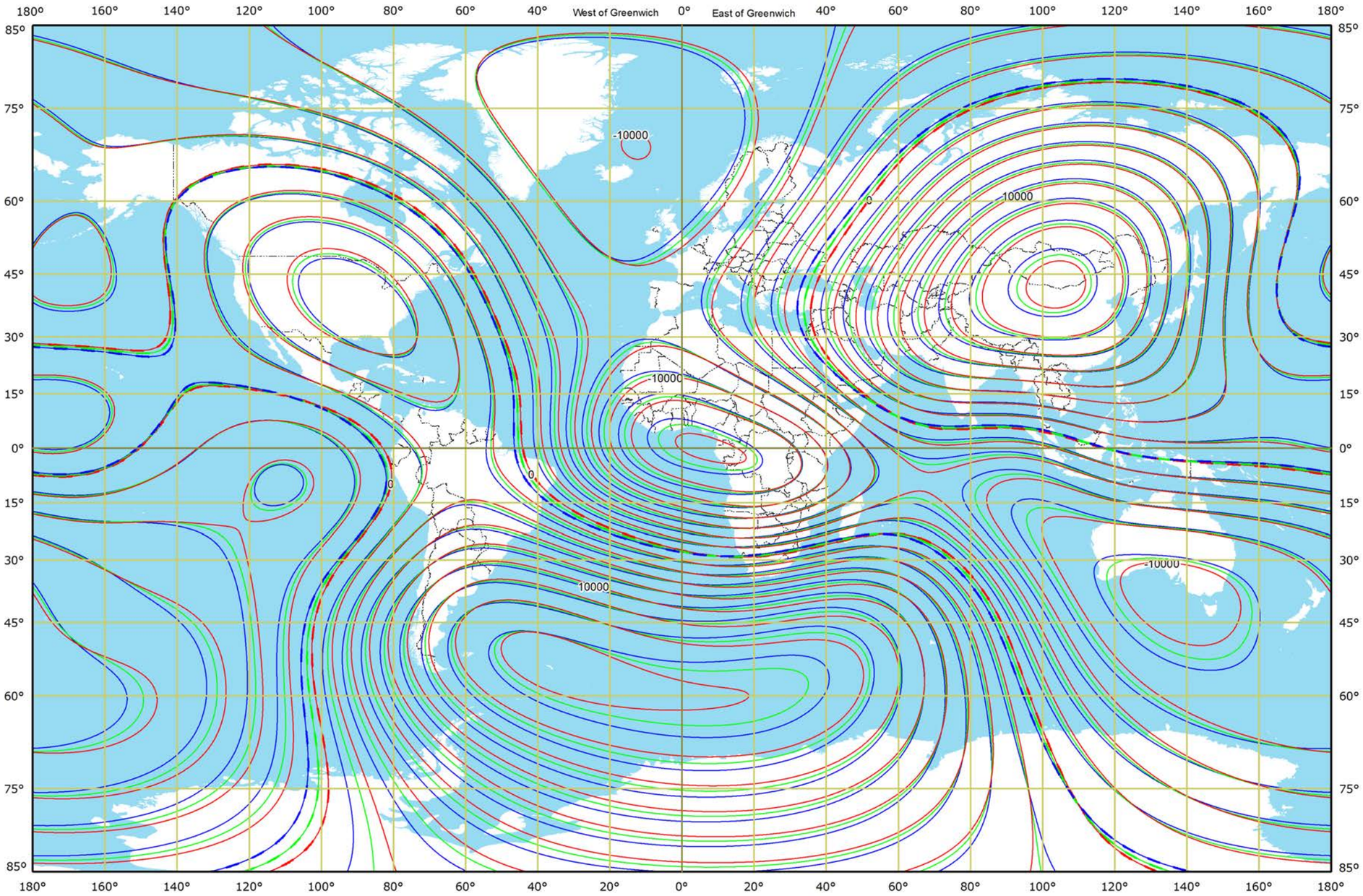

Years Isolines

1930
1935
1940

Geomagnetic equators

1930
1935
1940

Example of magnetic field component value, nT

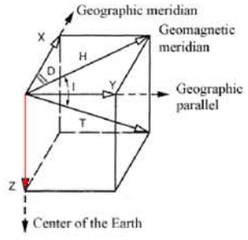

MGMF vector components

D Declination
I Inclination
H Horizontal component
T Total intensity
X North component
Y East component
Z Vertical component

Scale 1: 120 000 000

Projection: Miller cylindrical

VERTICAL COMPONENT OF MGMF NONDIPOLE PART

MGMF – 1940, 1945, 1950 – DZ

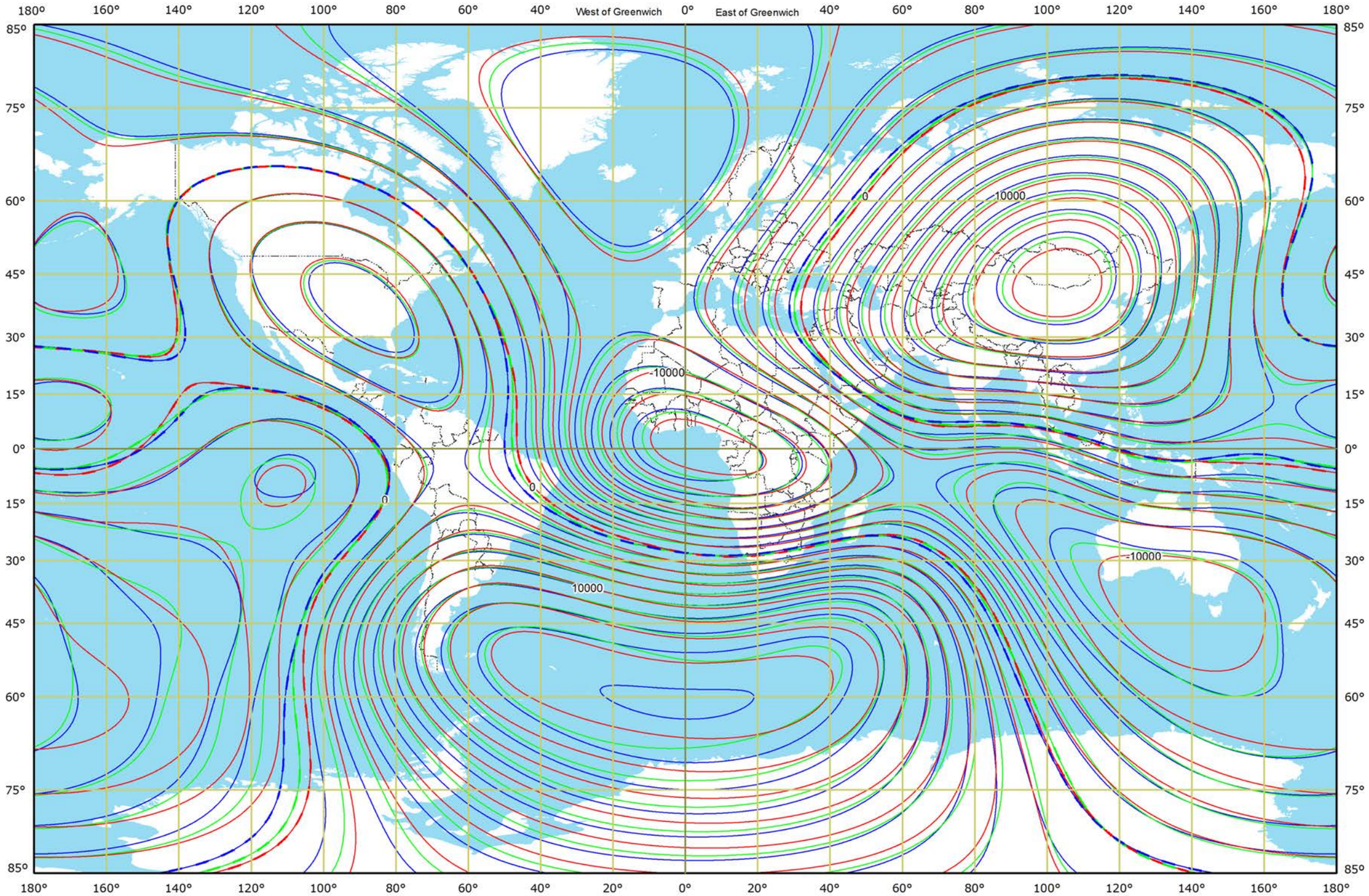

Years Isolines

1940
1945
1950

Geomagnetic equators

1940
1945
1950

Example of magnetic field component value, nT

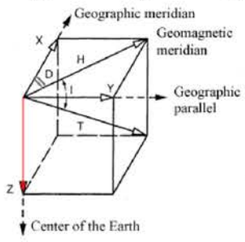

MGMF vector components

D Declination
I Inclination
H Horizontal component
T Total intensity
X North component
Y East component
Z Vertical component

Scale 1: 120 000 000

Projection: Miller cylindrical

VERTICAL COMPONENT OF MGMF NONDIPOLE PART

MGMF – 1950, 1955, 1960 – DZ

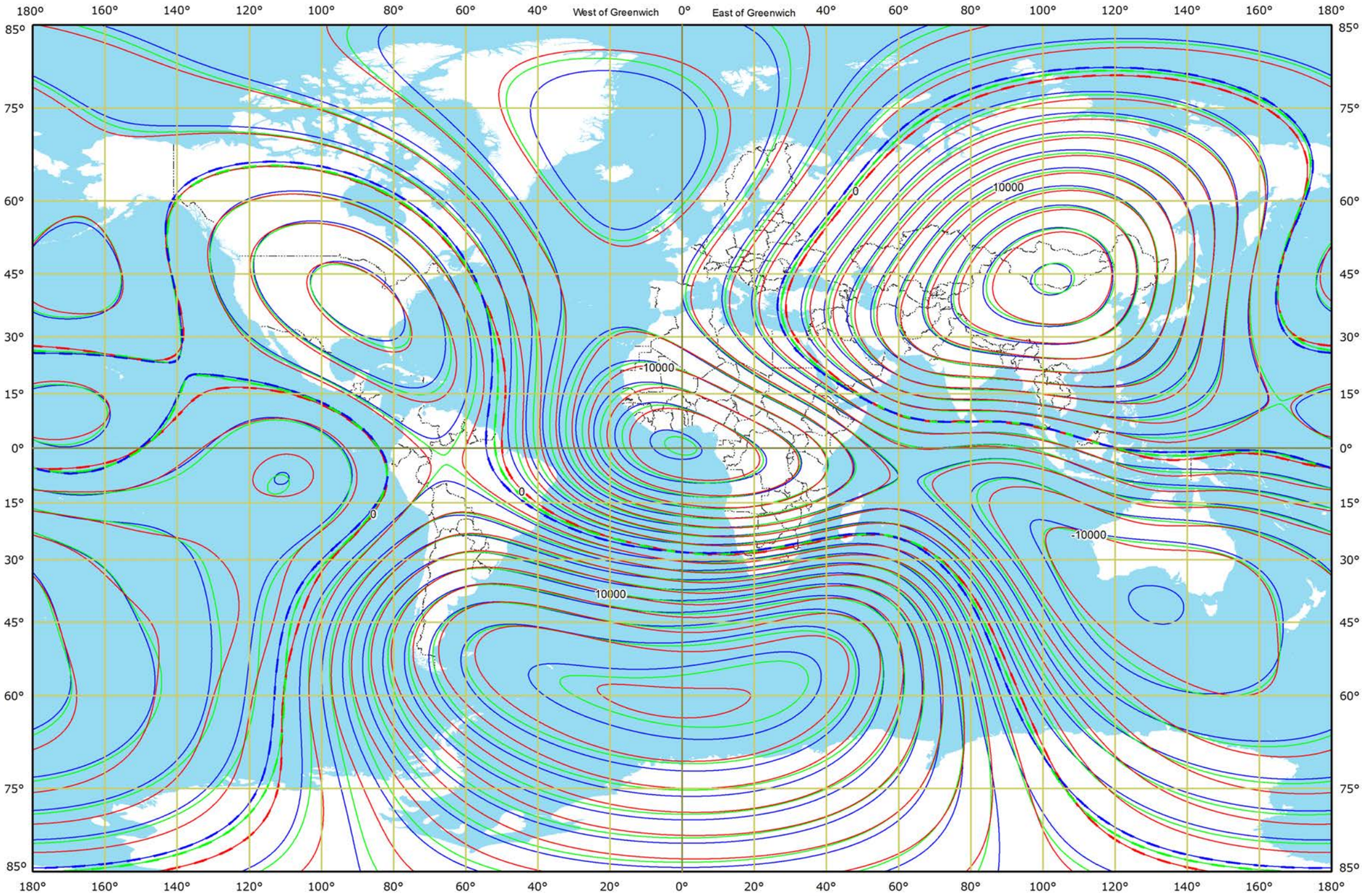

Years Isolines

1950
1955
1960

Geomagnetic equators

1950
1955
1960

Example of magnetic field component value, nT

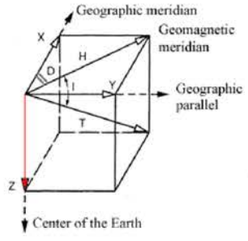

MGMF vector components

D Declination
I Inclination
H Horizontal component
T Total intensity
X North component
Y East component
Z Vertical component

Scale 1: 120 000 000

Projection: Miller cylindrical

VERTICAL COMPONENT OF MGMF NONDIPOLE PART

MGMF – 1960, 1965, 1970 – DZ

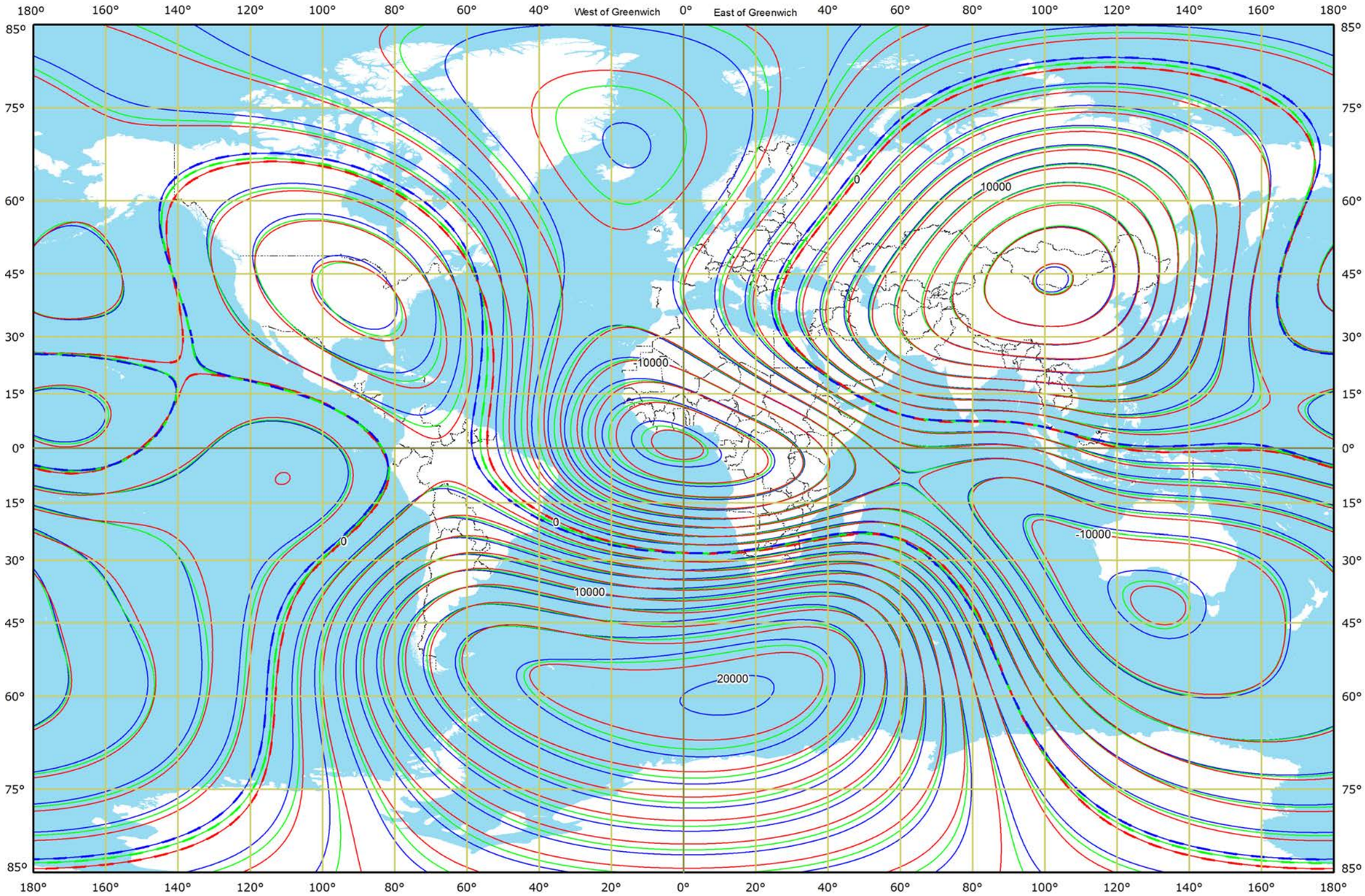

Years Isolines

1960
1965
1970

Geomagnetic equators

1960
1965
1970

Example of magnetic field component value, nT

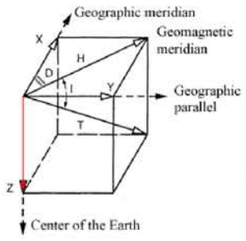

MGMF vector components

D Declination
I Inclination
H Horizontal component
T Total intensity
X North component
Y East component
Z Vertical component

Scale 1: 120 000 000

Projection: Miller cylindrical

VERTICAL COMPONENT OF MGMF NONDIPOLE PART

MGMF – 1970, 1975, 1980 – DZ

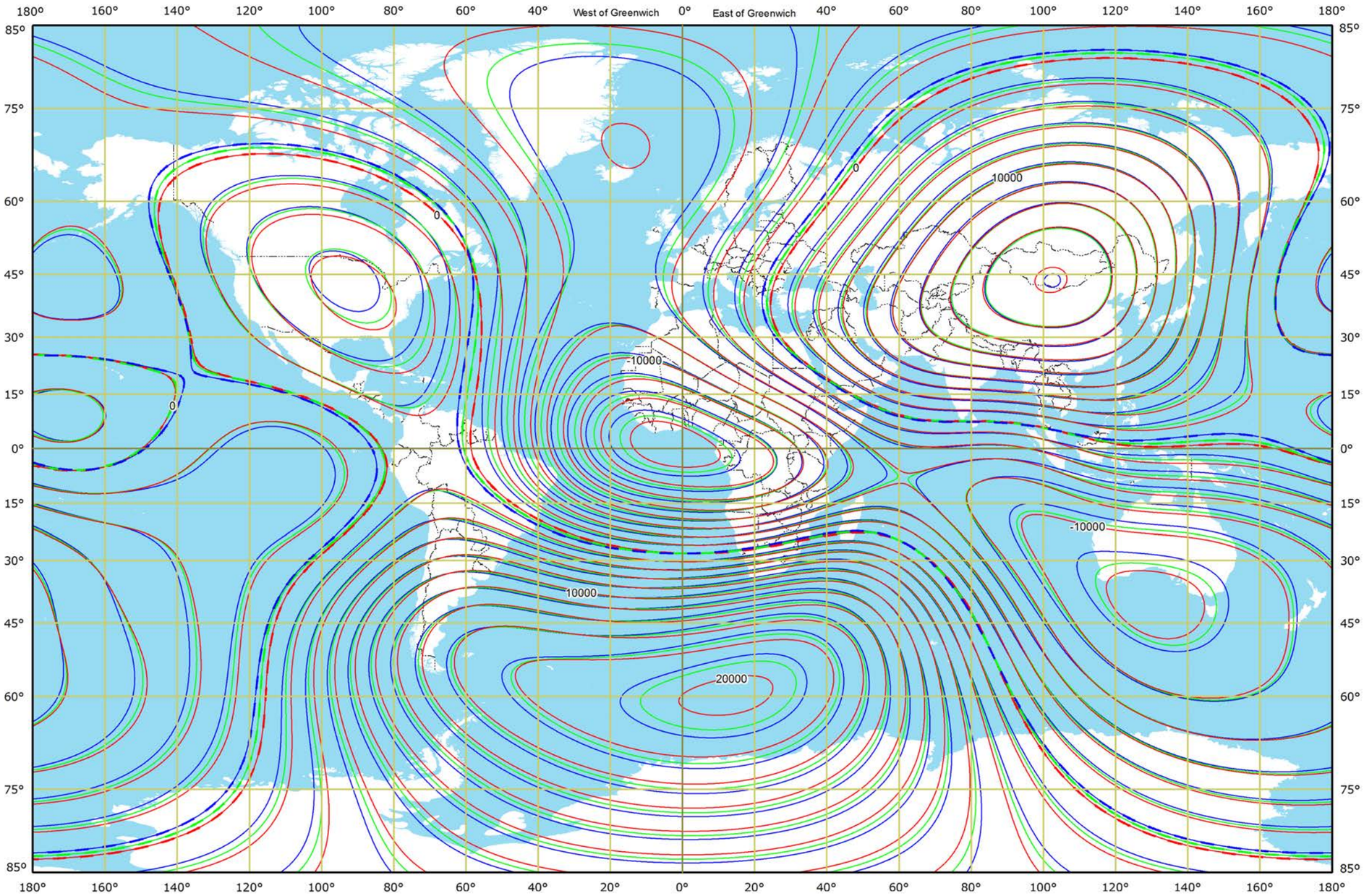

Years Isolines

1970
1975
1980

Geomagnetic equators

1970
1975
1980

Example of magnetic field component value, nT

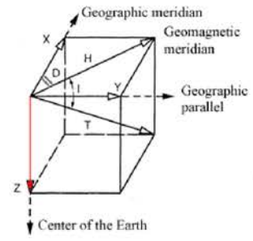

MGMF vector components

D Declination
I Inclination
H Horizontal component
T Total intensity
X North component
Y East component
Z Vertical component

Scale 1: 120 000 000

Projection: Miller cylindrical

VERTICAL COMPONENT OF MGMF NONDIPOLE PART

MGMF – 1980, 1985, 1990 – DZ

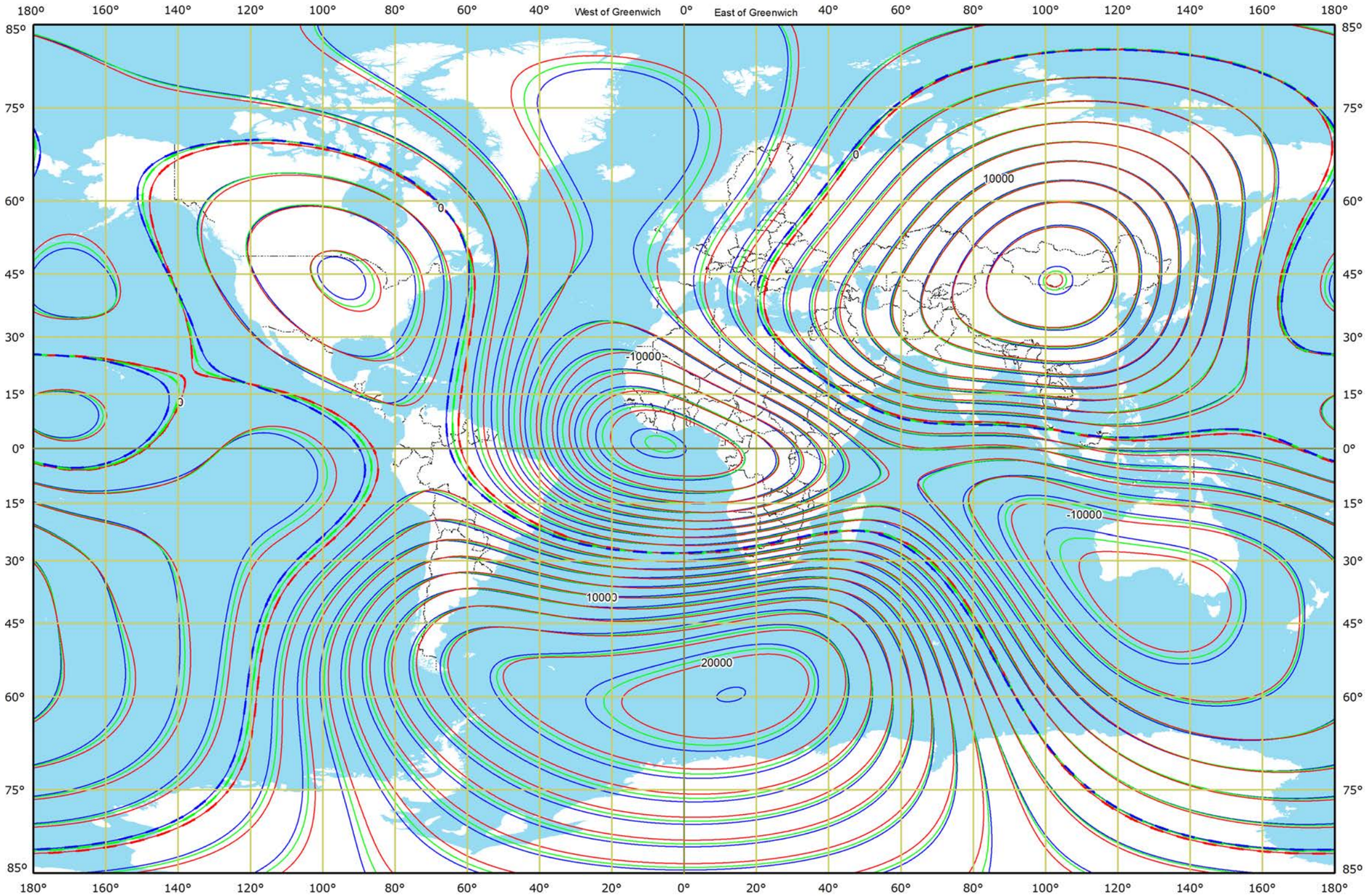

Years Isolines

1980
1985
1990

Geomagnetic equators

1980
1985
1990

Example of magnetic field component value, nT

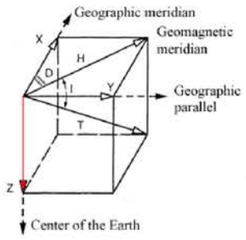

MGMF vector components

D Declination
I Inclination
H Horizontal component
T Total intensity
X North component
Y East component
Z Vertical component

Scale 1: 120 000 000

Projection: Miller cylindrical

VERTICAL COMPONENT OF MGMF NONDIPOLE PART

MGMF – 1990, 1995, 2000 – DZ

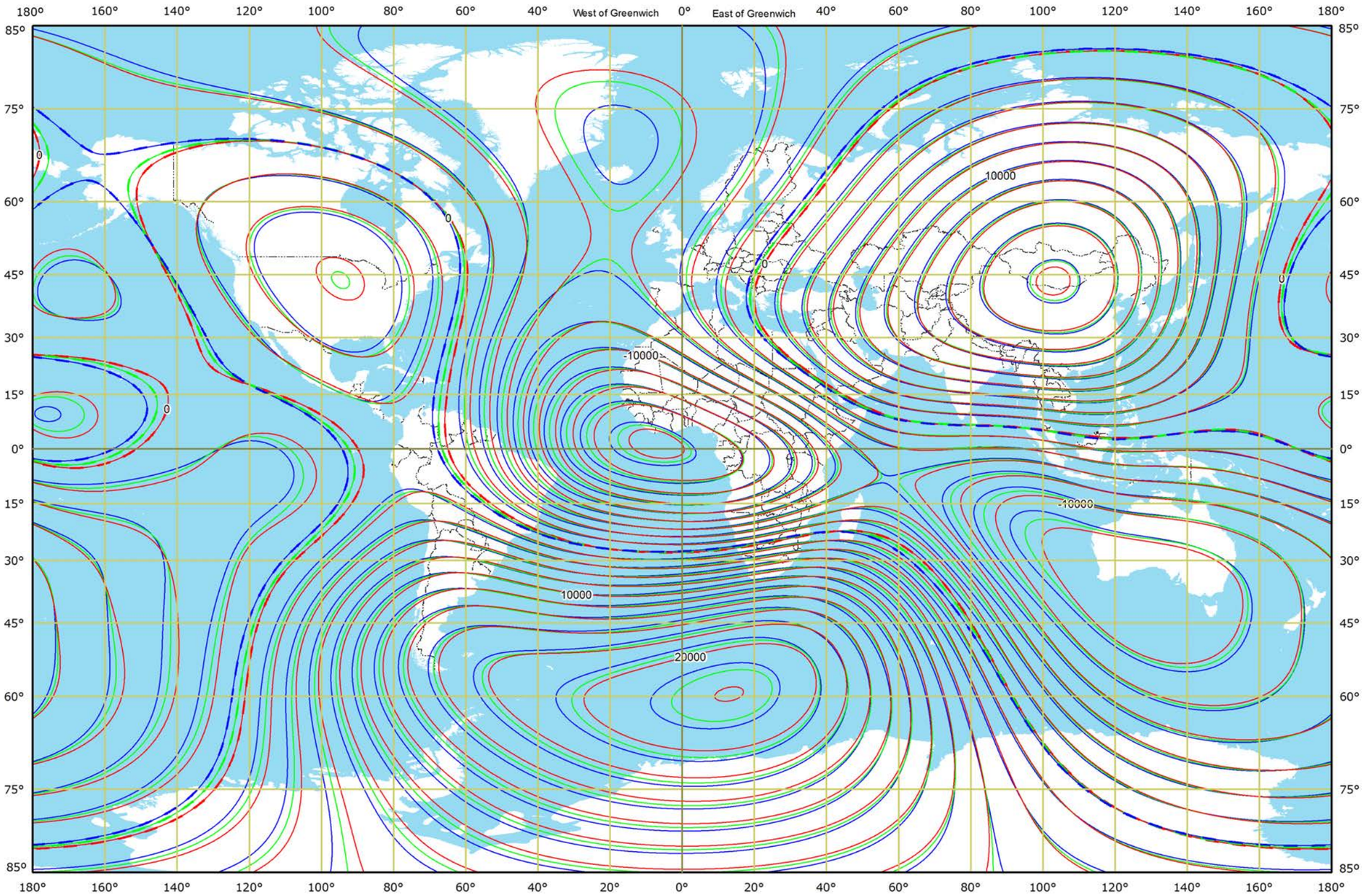

Years Isolines

1990
1995
2000

Geomagnetic equators

1990
1995
2000

Example of magnetic field component value, nT

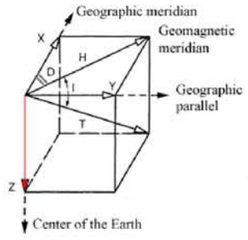

MGMF vector components

D Declination
I Inclination
H Horizontal component
T Total intensity
X North component
Y East component
Z Vertical component

Scale 1: 120 000 000

Projection: Miller cylindrical

VERTICAL COMPONENT OF MGMF NONDIPOLE PART

MGMF – 2000, 2005, 2010 – DZ

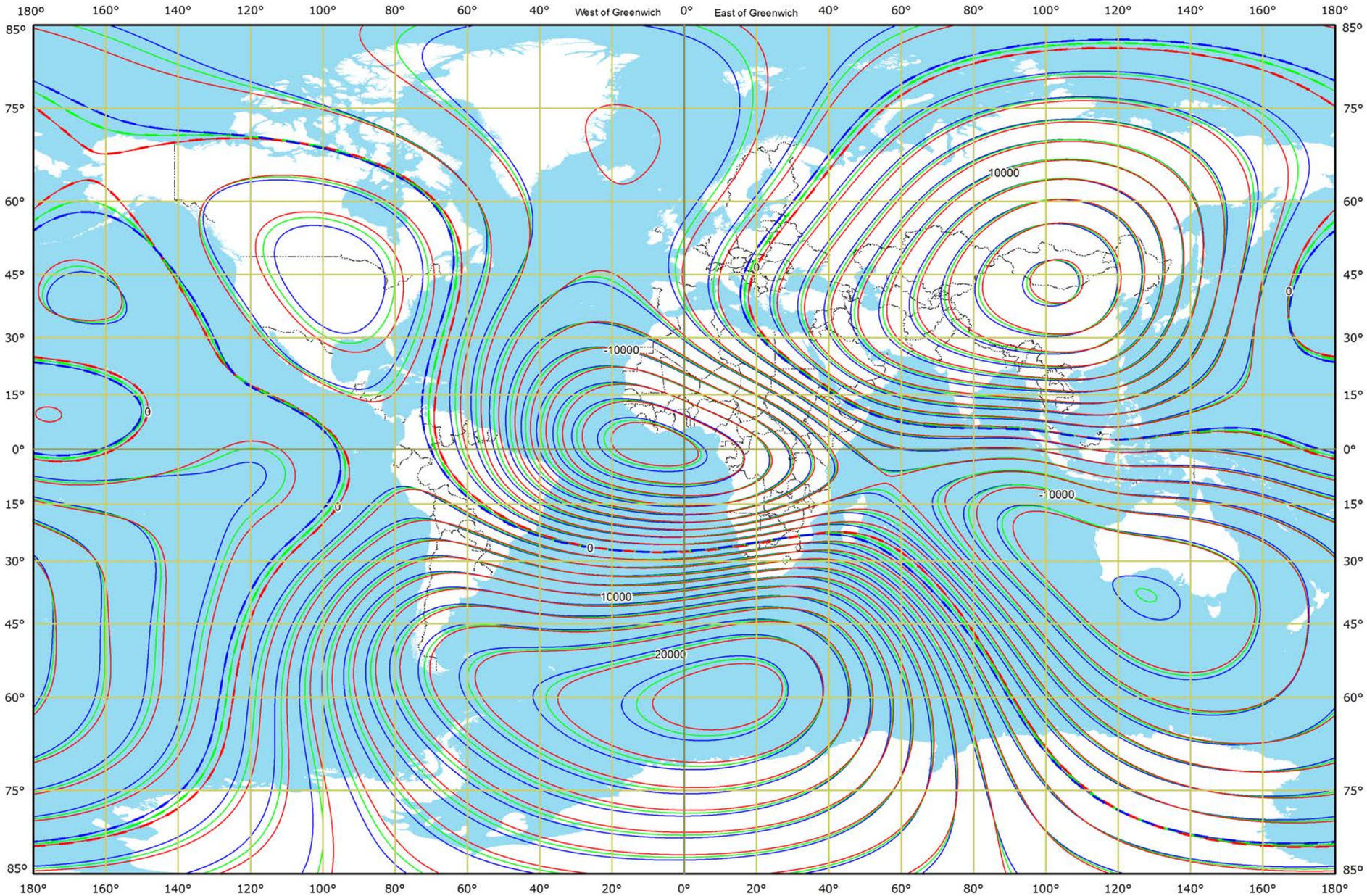

Years Isolines

2000
2005
2010

Geomagnetic equators

2000
2005
2010

Example of magnetic field component value, nT

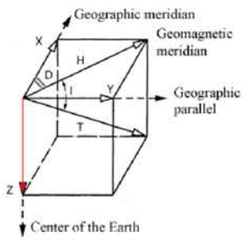

MGMF vector components

D Declination
I Inclination
H Horizontal component
T Total intensity
X North component
Y East component
Z Vertical component

Scale 1: 120 000 000

Projection: Miller cylindrical

HORIZONTAL COMPONENT OF MGMF NONDIPOLE PART

MGMF – 1900, 1905, 1910 – H

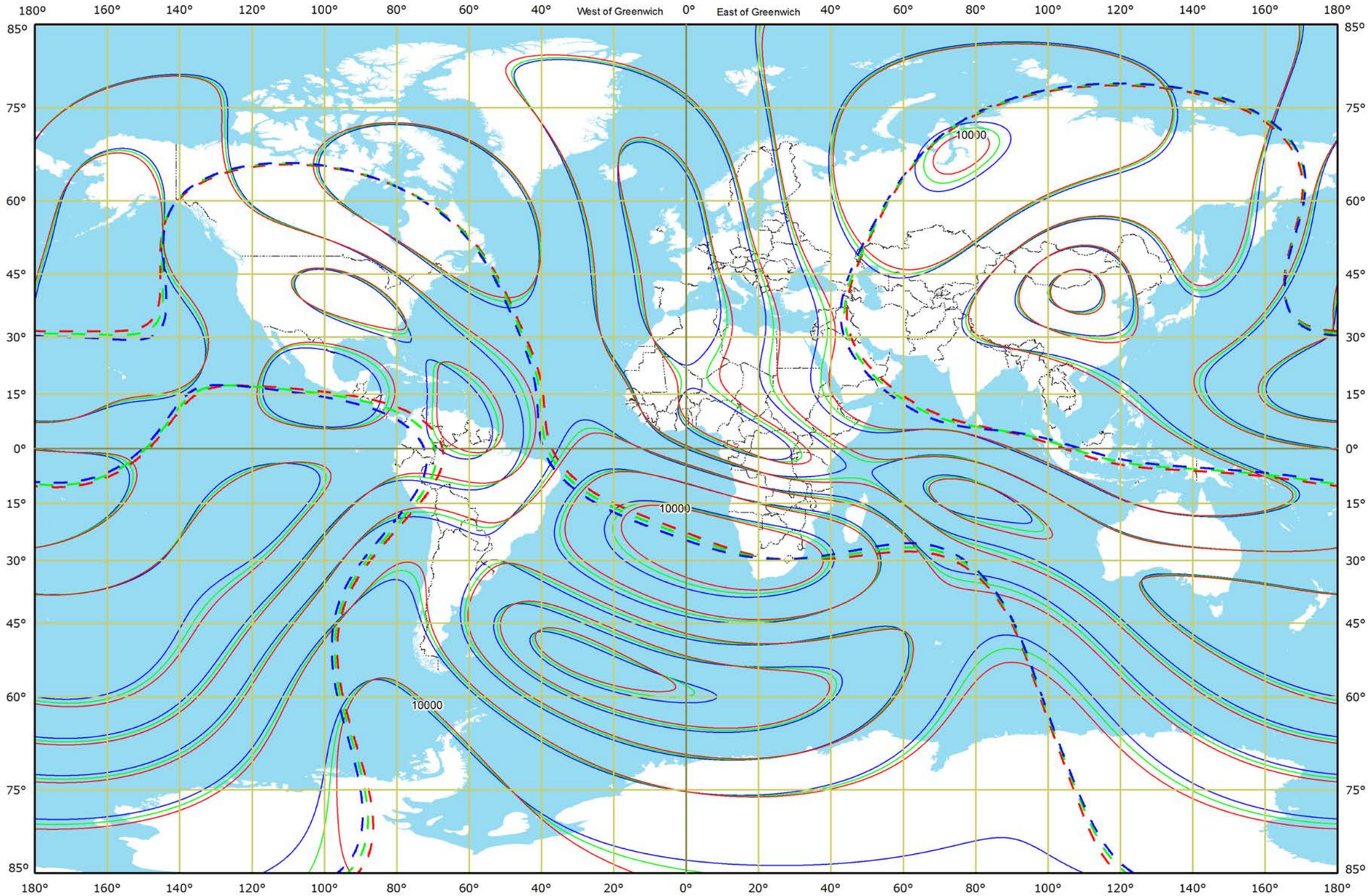

Years	Isolines	Geomagnetic equators
1900		1900
1905		1905
1910		1910

Example of magnetic field component value, nT

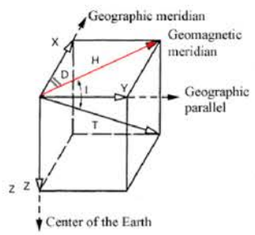

MGMF vector components

D Declination
I Inclination
H Horizontal component
T Total intensity
X North component
Y East component
Z Vertical component

Scale 1: 120 000 000

Projection: Miller cylindrical

HORIZONTAL COMPONENT OF MGMF NONDIPOLE PART

MGMF – 1910, 1915, 1920 – H

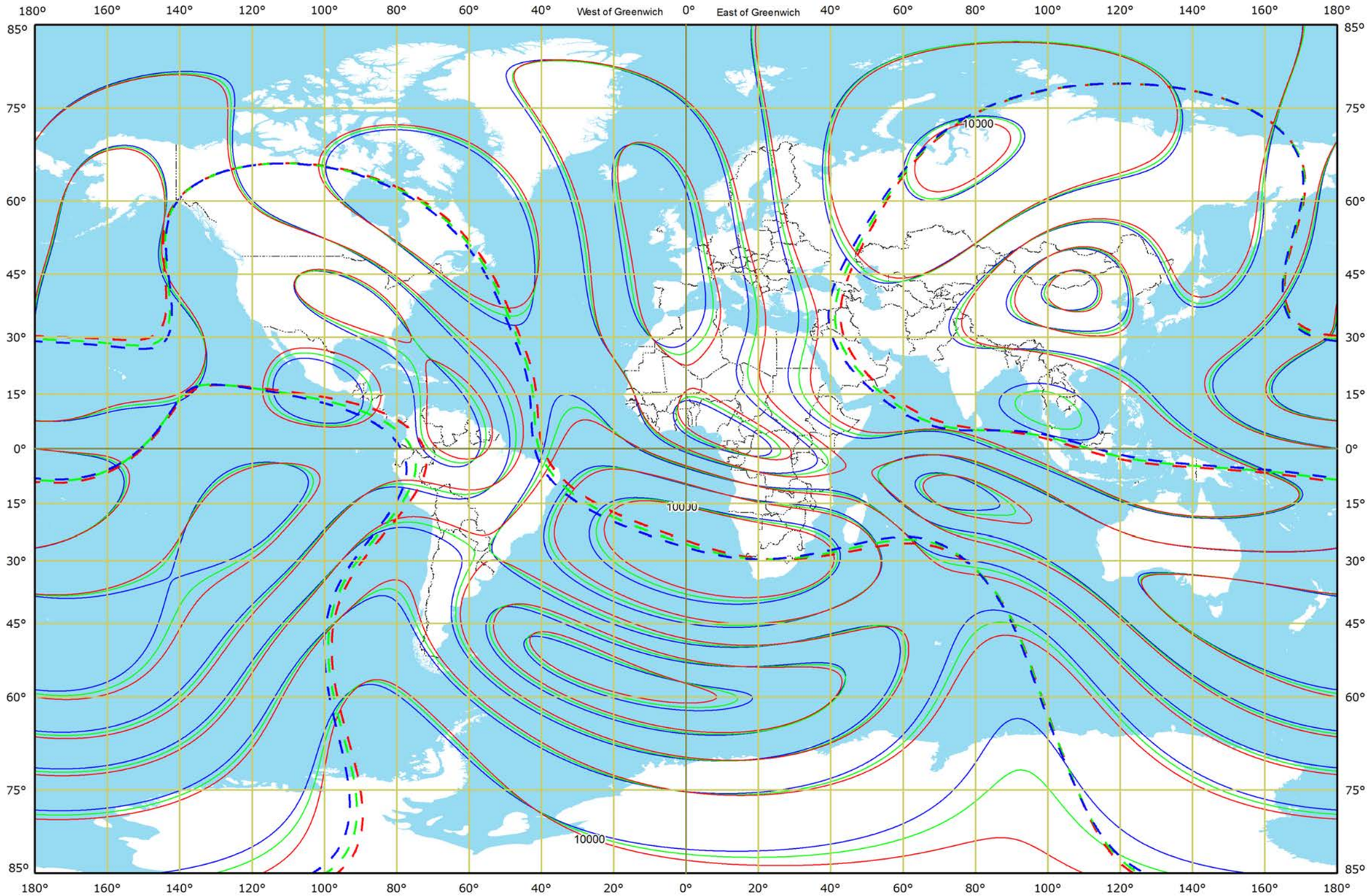

Years	Isolines	Geomagnetic equators
1910		1910
1915		1915
1920		1920

Example of magnetic field component value, nT

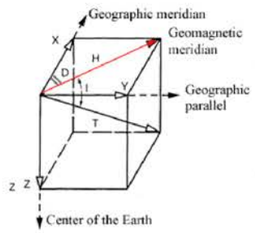

MGMF vector components

D Declination
I Inclination
H Horizontal component
T Total intensity
X North component
Y East component
Z Vertical component

Scale 1: 120 000 000

Projection: Miller cylindrical

HORIZONTAL COMPONENT OF MGMF NONDIPOLE PART

MGMF – 1920, 1925, 1930 – H

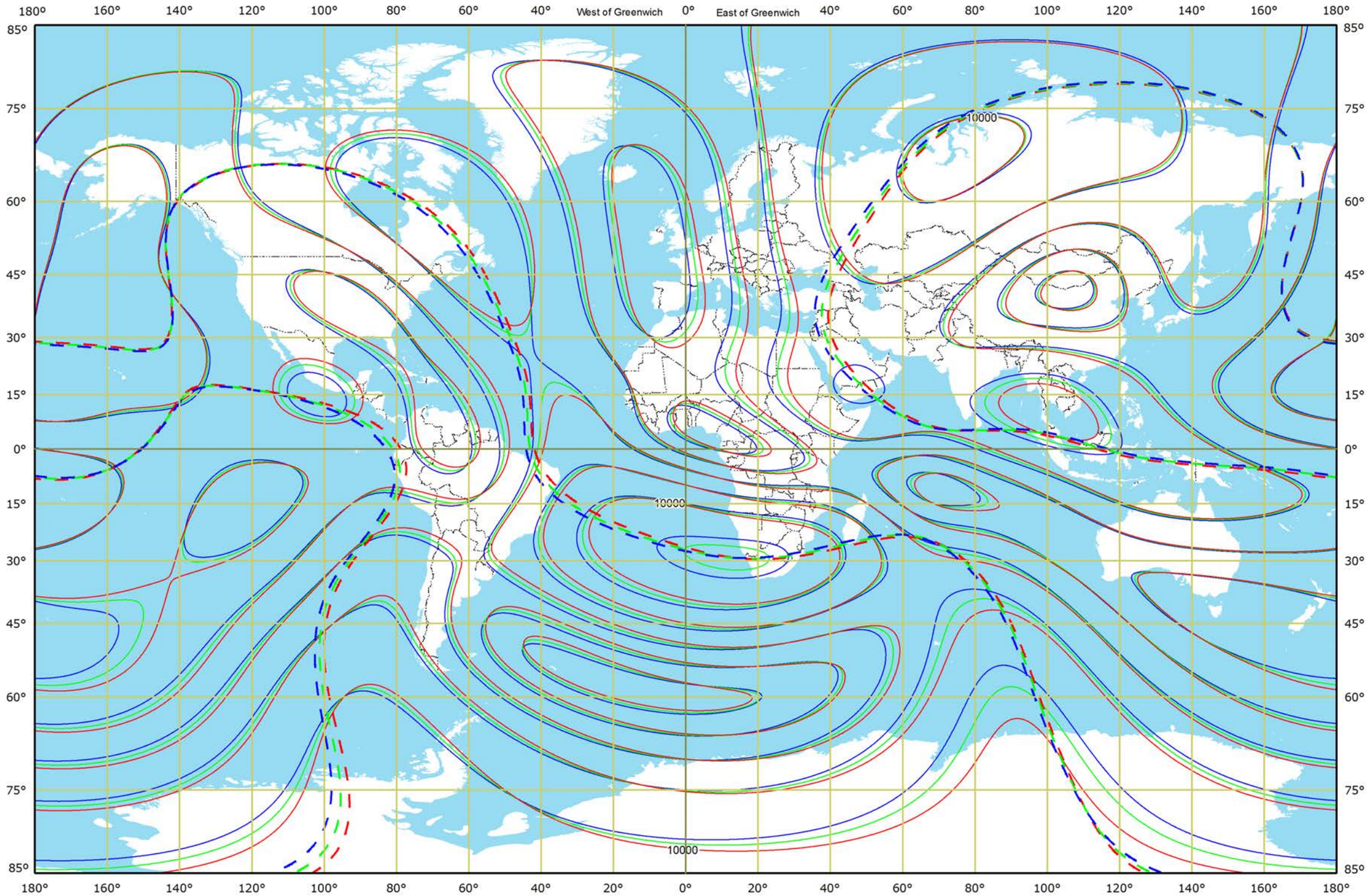

Years	Isolines	Geomagnetic equators
1920		1920
1925		1925
1930		1930

Example of magnetic field component value, nT

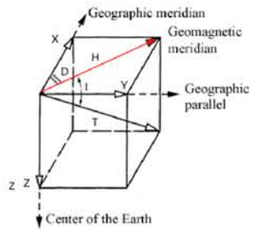

MGMF vector components

D Declination
I Inclination
H Horizontal component
T Total intensity
X North component
Y East component
Z Vertical component

Scale 1: 120 000 000

Projection: Miller cylindrical

HORIZONTAL COMPONENT OF MGMF NONDIPOLE PART

MGMF – 1930, 1935, 1940 – H

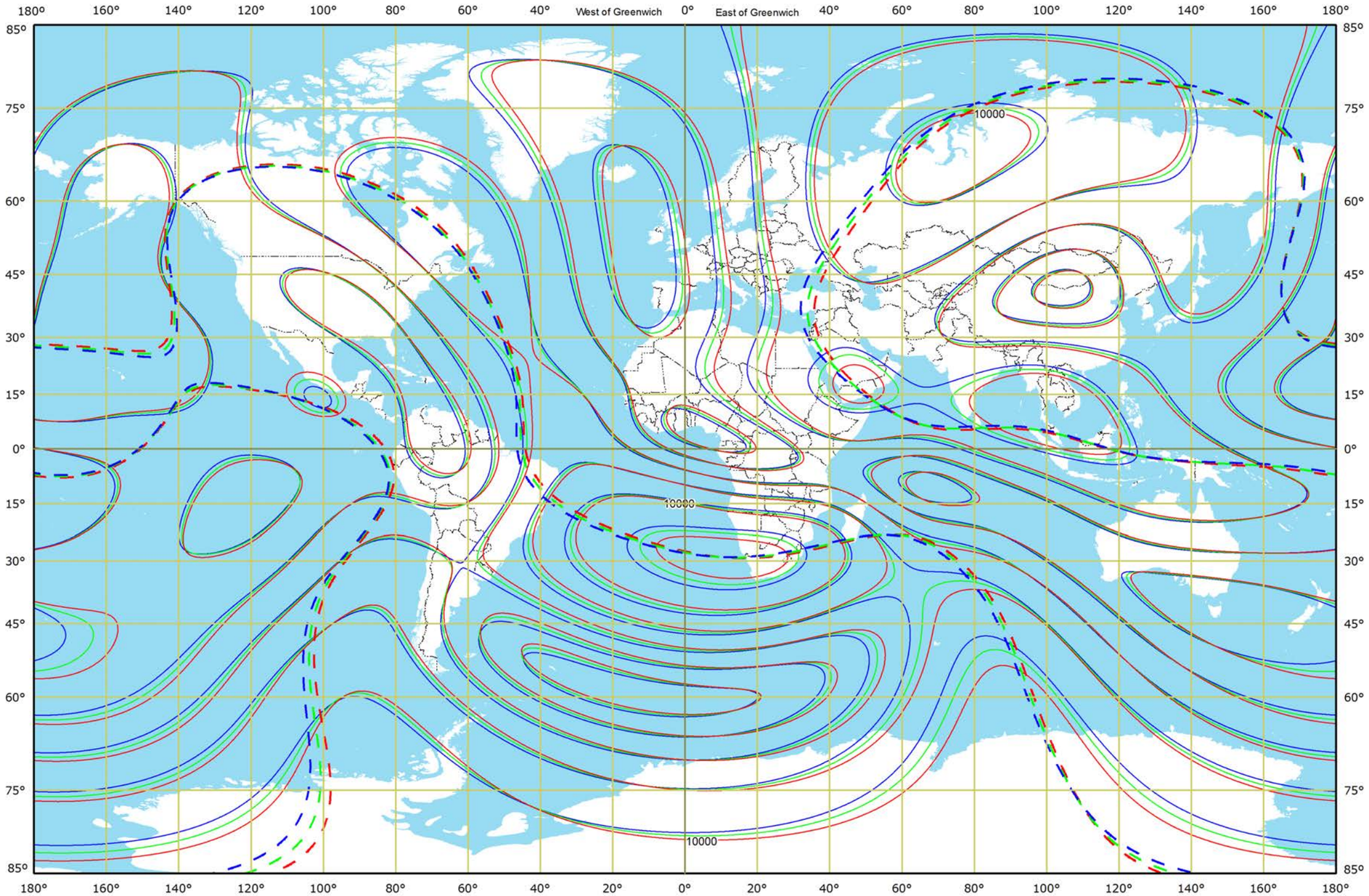

Years	Isolines	Geomagnetic equators
1930		1930
1935		1935
1940		1940

Example of magnetic field component value, nT

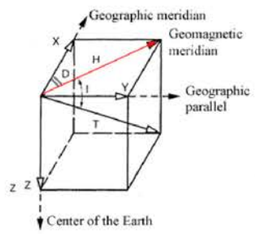

MGMF vector components

D Declination
I Inclination
H Horizontal component
T Total intensity
X North component
Y East component
Z Vertical component

Scale 1: 120 000 000

Projection: Miller cylindrical

HORIZONTAL COMPONENT OF MGMF NONDIPOLE PART

MGMF – 1940, 1945, 1950 – H

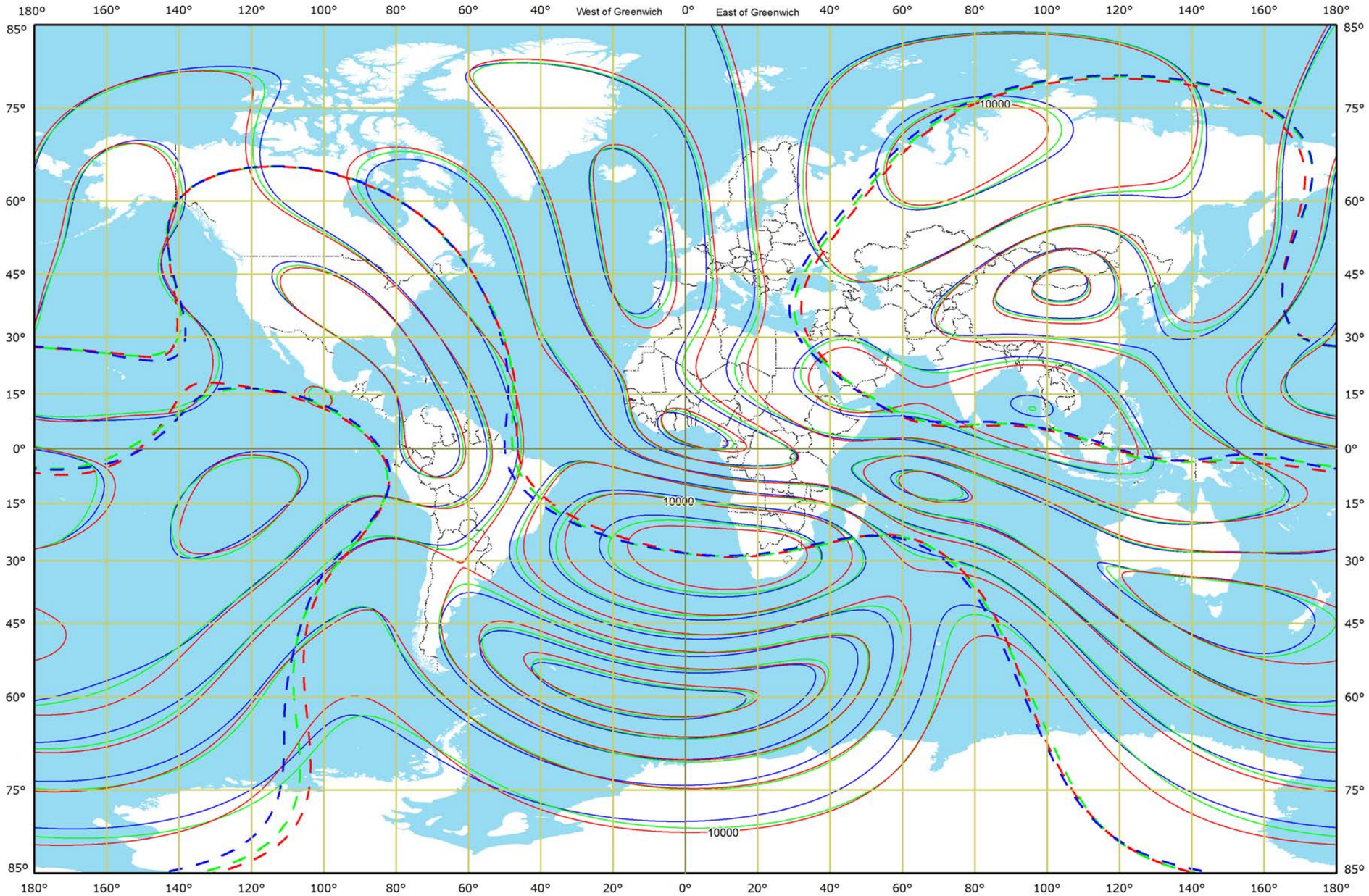

Years	Isolines	Geomagnetic equators
1940		1940
1945		1945
1950		1950

Example of magnetic field component value, nT

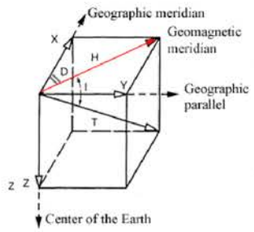

MGMF vector components

D Declination
I Inclination
H Horizontal component
T Total intensity
X North component
Y East component
Z Vertical component

Scale 1: 120 000 000

Projection: Miller cylindrical

HORIZONTAL COMPONENT OF MGMF NONDIPOLE PART

MGMF – 1950, 1955, 1960 – H

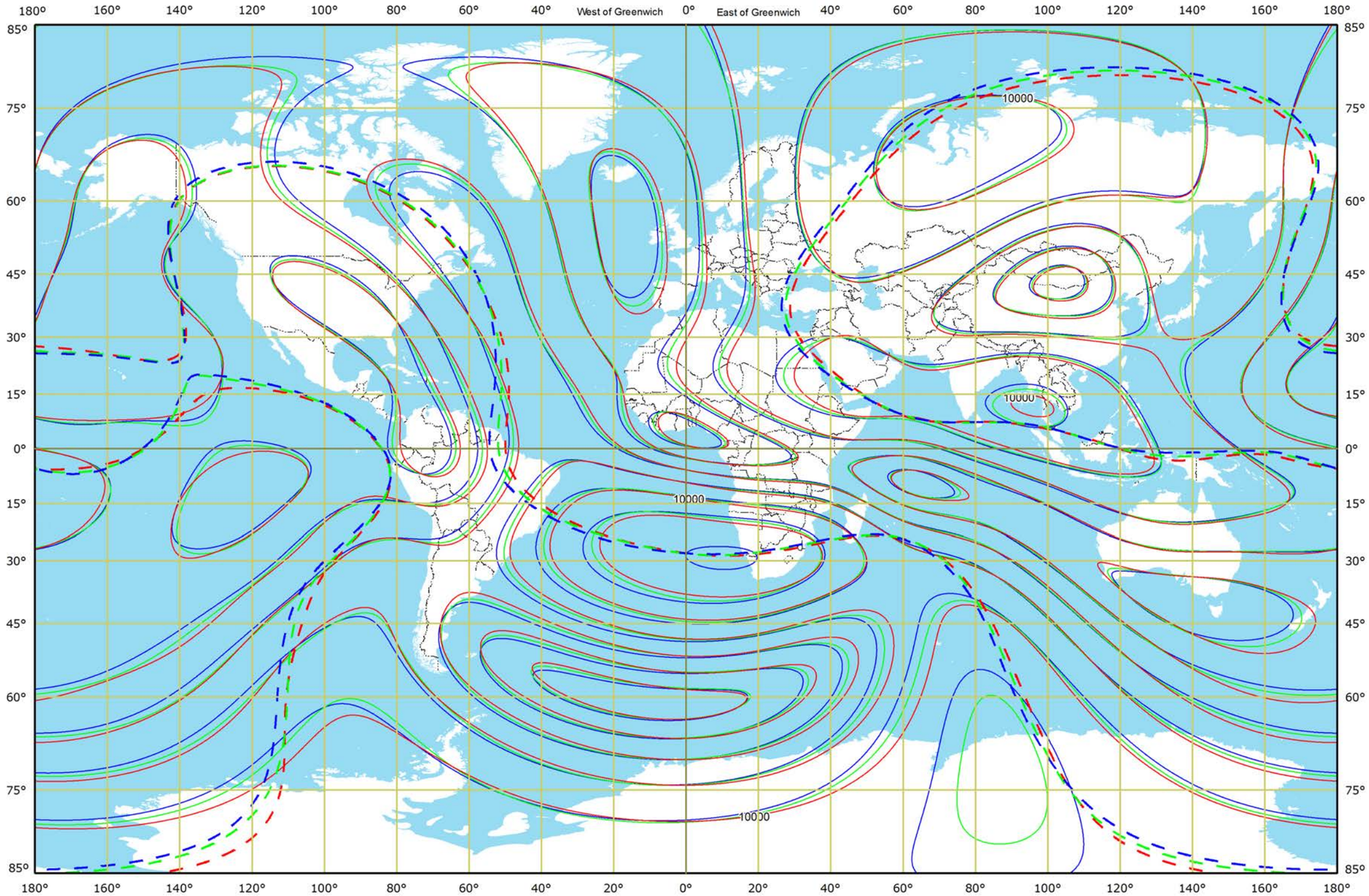

Years	Isolines	Geomagnetic equators
1950		1950
1955		1955
1960		1960

Example of magnetic field component value, nT

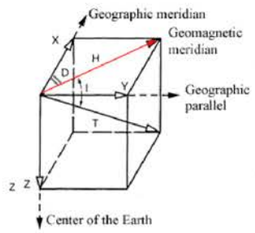

MGMF vector components

D Declination
I Inclination
H Horizontal component
T Total intensity
X North component
Y East component
Z Vertical component

Scale 1: 120 000 000

Projection: Miller cylindrical

HORIZONTAL COMPONENT OF MGMF NONDIPOLE PART

MGMF – 1960, 1965, 1970 – H

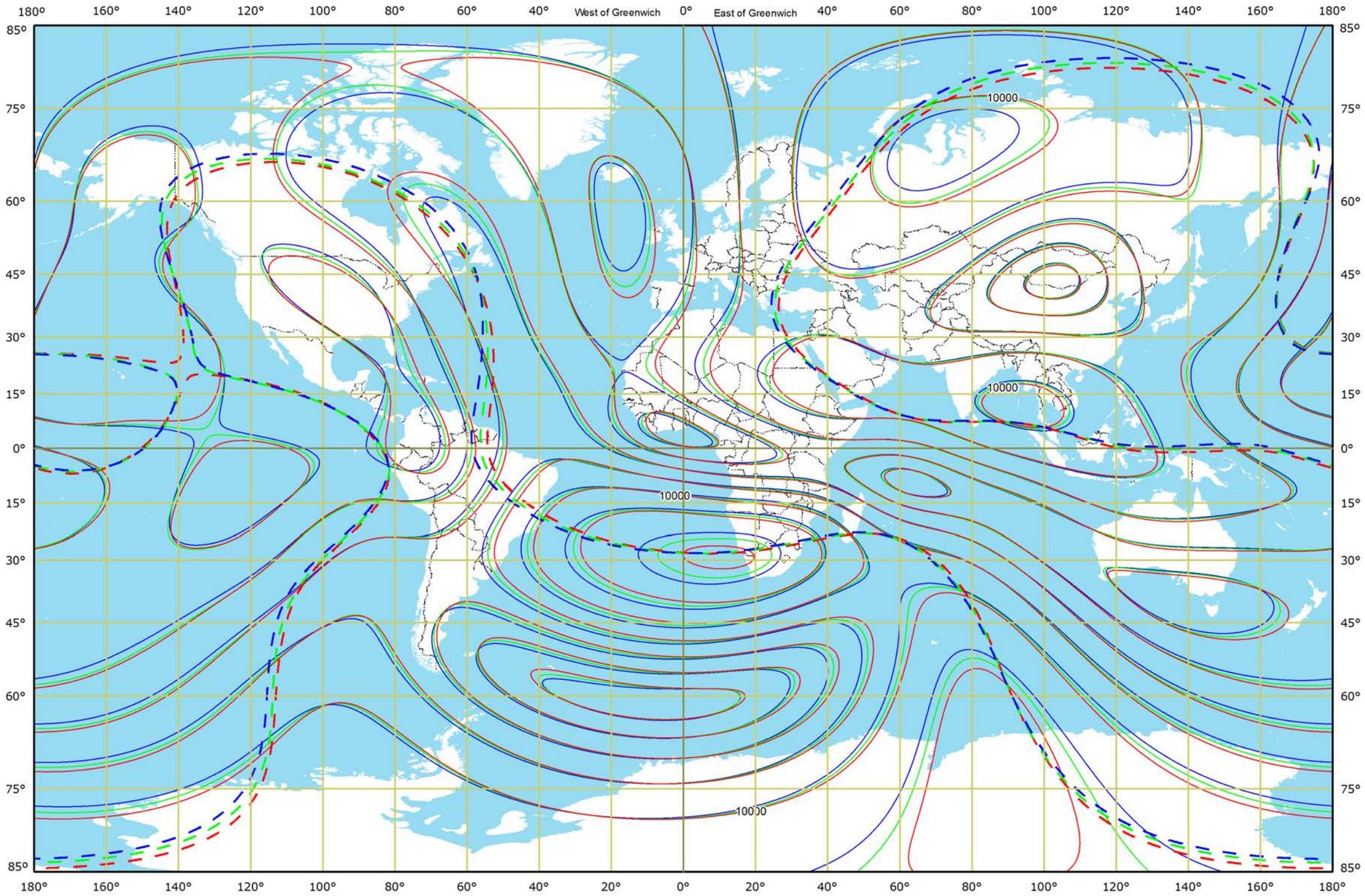

Years Isolines

1960
1965
1970

Geomagnetic equators

1960
1965
1970

Example of magnetic field component value, nT

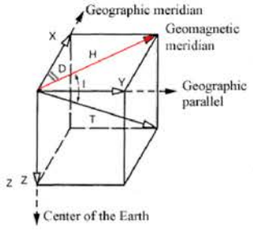

MGMF vector components

D Declination
I Inclination
H Horizontal component
T Total intensity
X North component
Y East component
Z Vertical component

Scale 1: 120 000 000

Projection: Miller cylindrical

HORIZONTAL COMPONENT OF MGMF NONDIPOLE PART

MGMF – 1970, 1975, 1980 – H

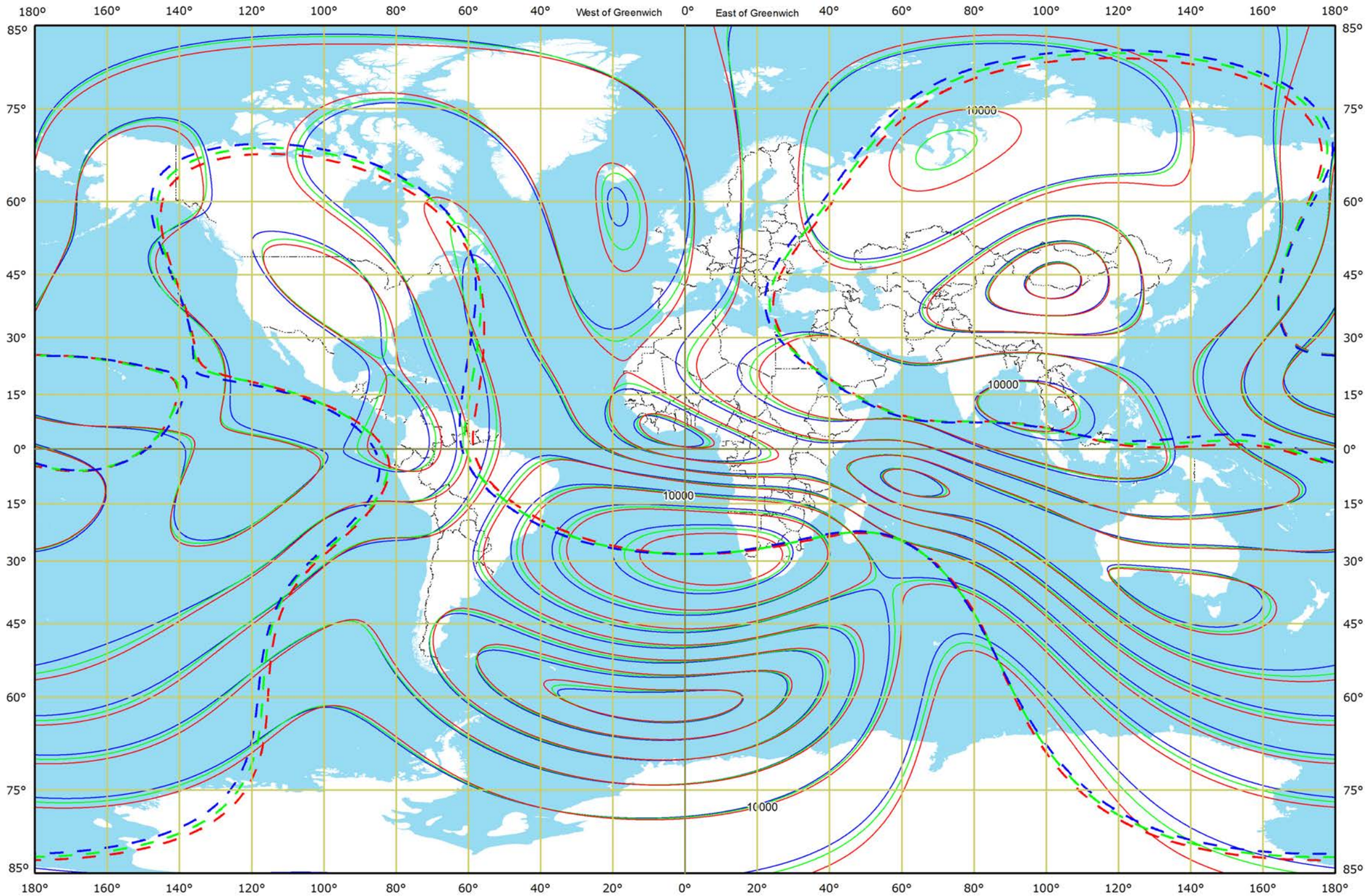

Years	Isolines	Geomagnetic equators
1970		1970
1975		1975
1980		1980

Example of magnetic field component value, nT

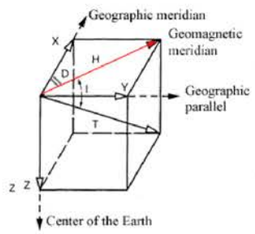

MGMF vector components

D Declination
I Inclination
H Horizontal component
T Total intensity
X North component
Y East component
Z Vertical component

Scale 1: 120 000 000

Projection: Miller cylindrical

HORIZONTAL COMPONENT OF MGMF NONDIPOLE PART

MGMF – 1980, 1985, 1990 – H

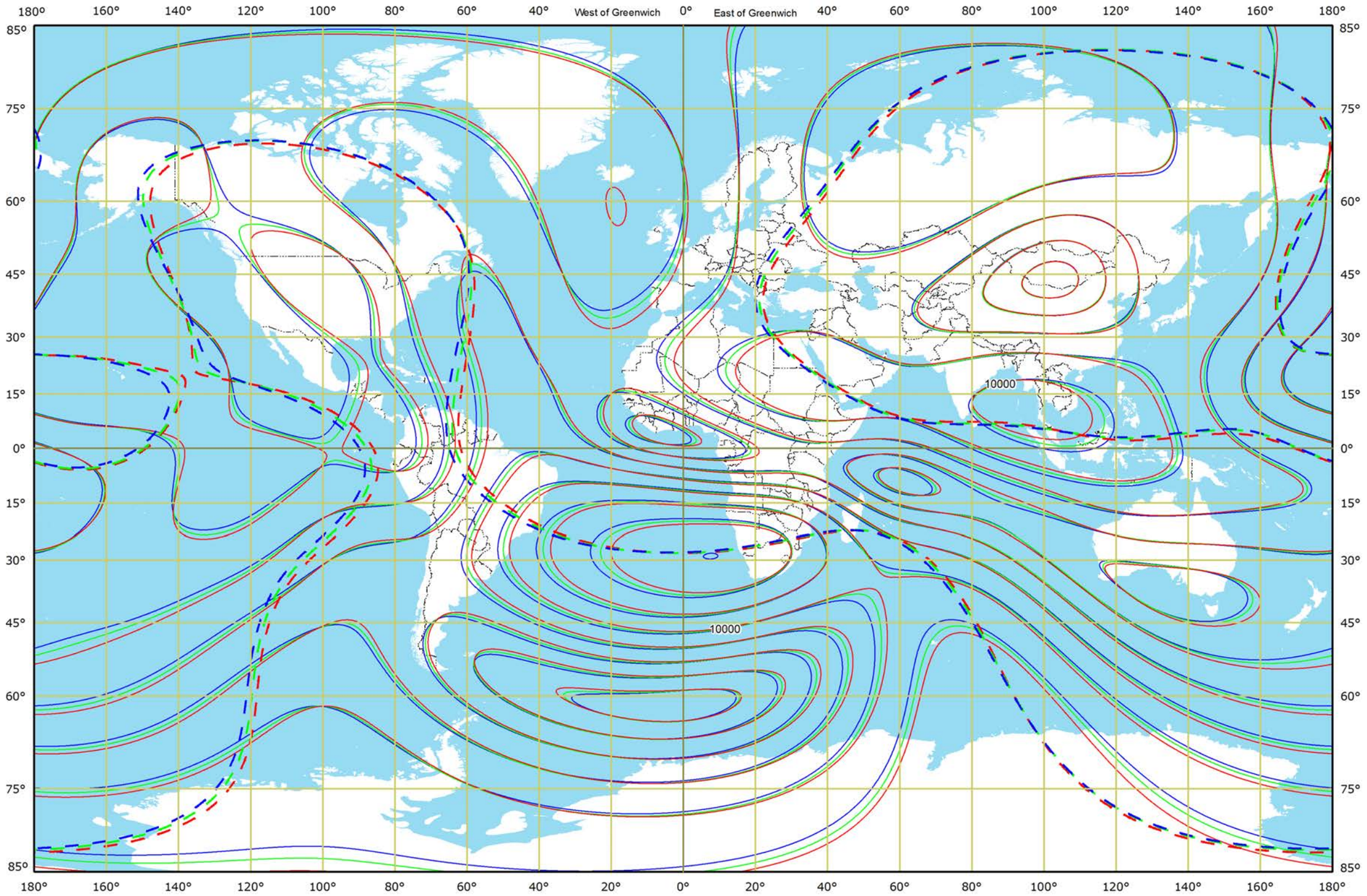

Years Isolines

1980
1985
1990

Geomagnetic equators

1980
1985
1990

Example of magnetic field component value, nT

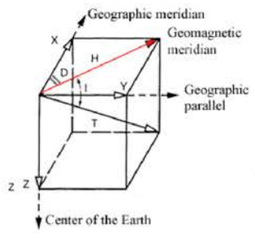

MGMF vector components

D Declination
I Inclination
H Horizontal component
T Total intensity
X North component
Y East component
Z Vertical component

Scale 1: 120 000 000

Projection: Miller cylindrical

HORIZONTAL COMPONENT OF MGMF NONDIPOLE PART

MGMF – 1990, 1995, 2000 – H

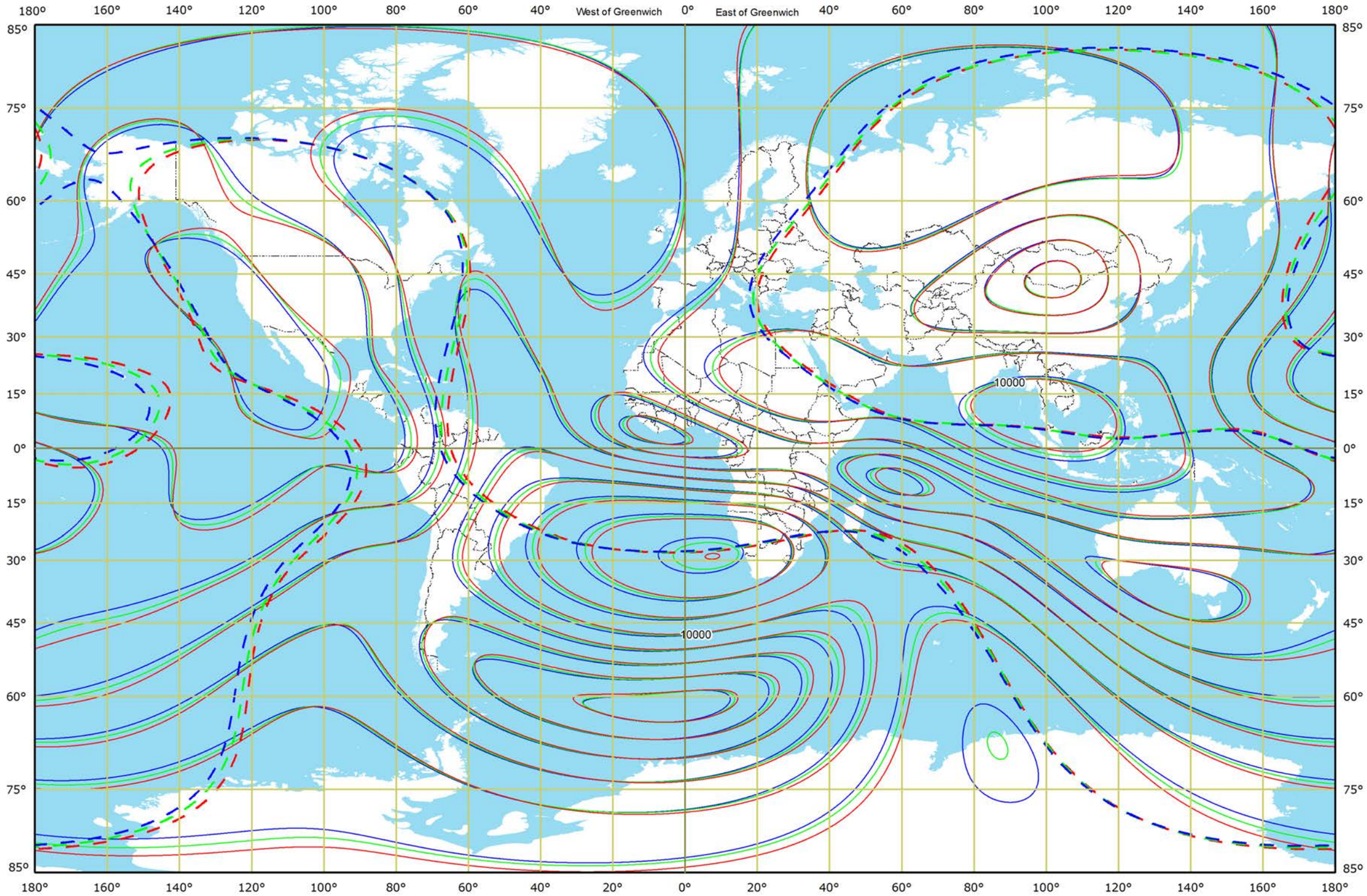

Years	Isolines	Geomagnetic equators
1990		1990
1995		1995
2000		2000

Example of magnetic field component value, nT

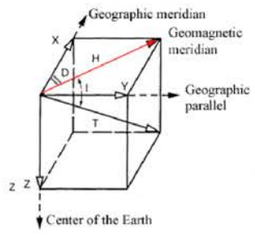

MGMF vector components

D Declination
I Inclination
H Horizontal component
T Total intensity
X North component
Y East component
Z Vertical component

Scale 1: 120 000 000

Projection: Miller cylindrical

HORIZONTAL COMPONENT OF MGMF NONDIPOLE PART

MGMF – 2000, 2005, 2010 – H

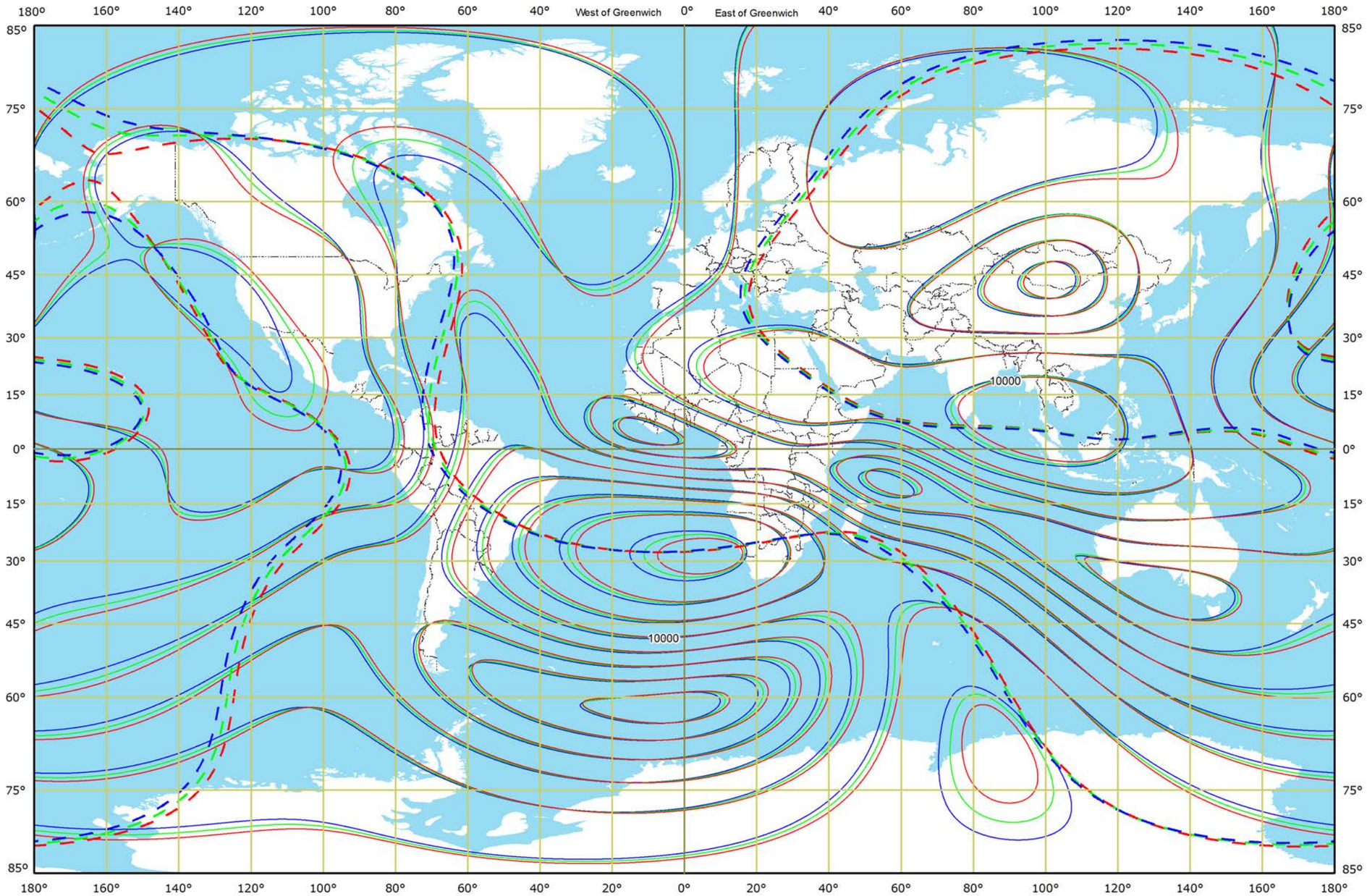

Years	Isolines	Geomagnetic equators
2000		2000
2005		2005
2010		2010

Example of magnetic field component value, nT

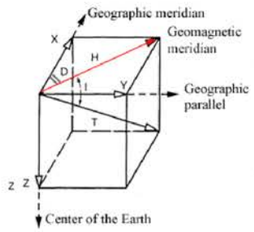

MGMF vector components

D Declination
I Inclination
H Horizontal component
T Total intensity
X North component
Y East component
Z Vertical component

Scale 1: 120 000 000

Projection: Miller cylindrical

TOTAL INTENSITY OF MGMF NONDIPOLE PART

MGMF – 1900, 1905, 1910 – FM (T)

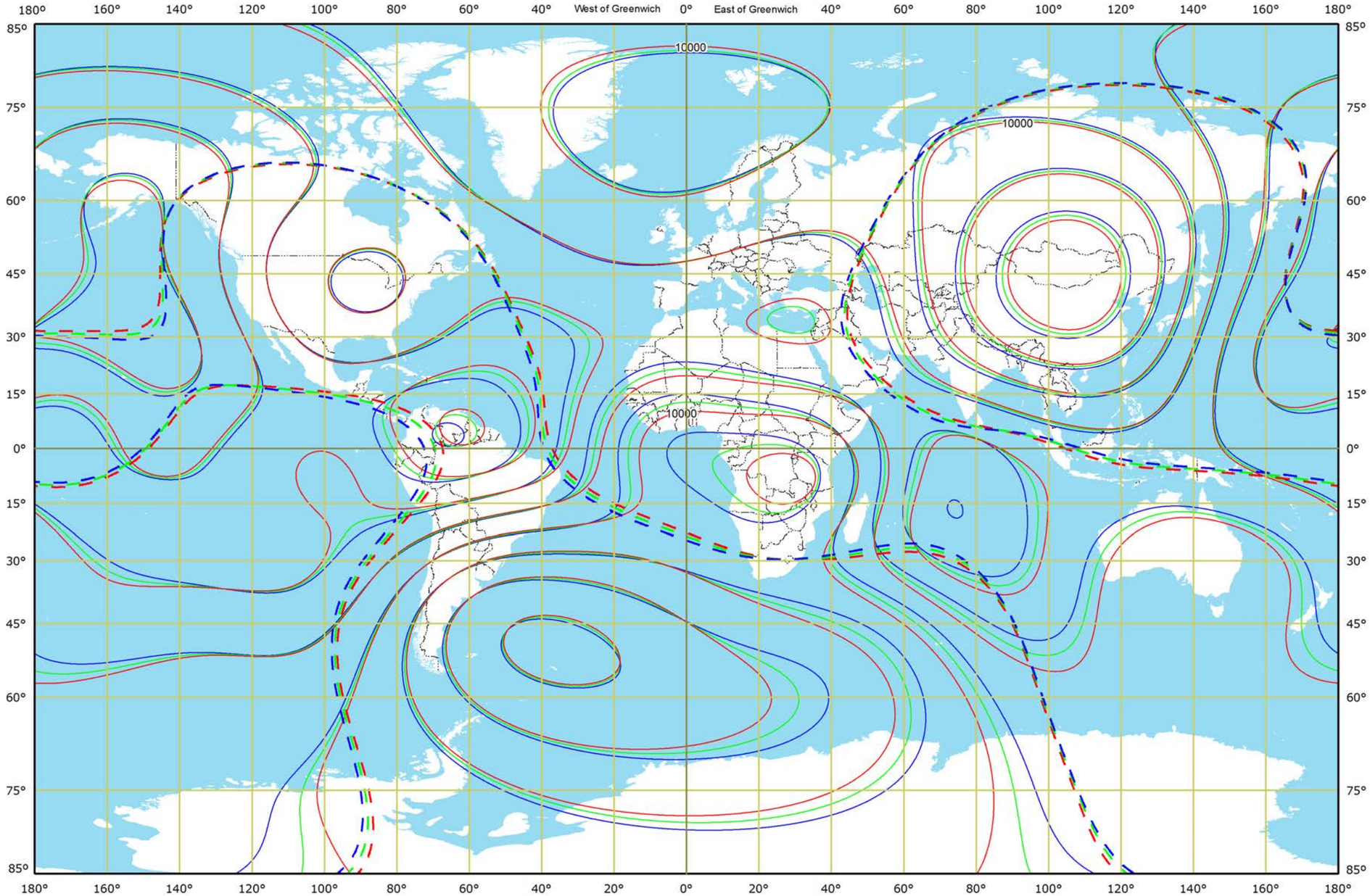

Years Isolines

1900
1905
1910

Geomagnetic equators

1900
1905
1910

Example of magnetic total intensity value, nT

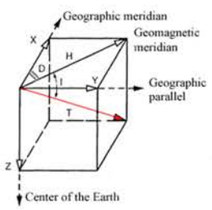

MGMF vector components

D Declination
I Inclination
H Horizontal component
T Total intensity
X North component
Y East component
Z Vertical component

Scale 1: 120 000 000

Projection: Miller cylindrical

TOTAL INTENSITY OF MGMF NONDIPOLE PART

MGMF – 1910, 1915, 1920 – FM (T)

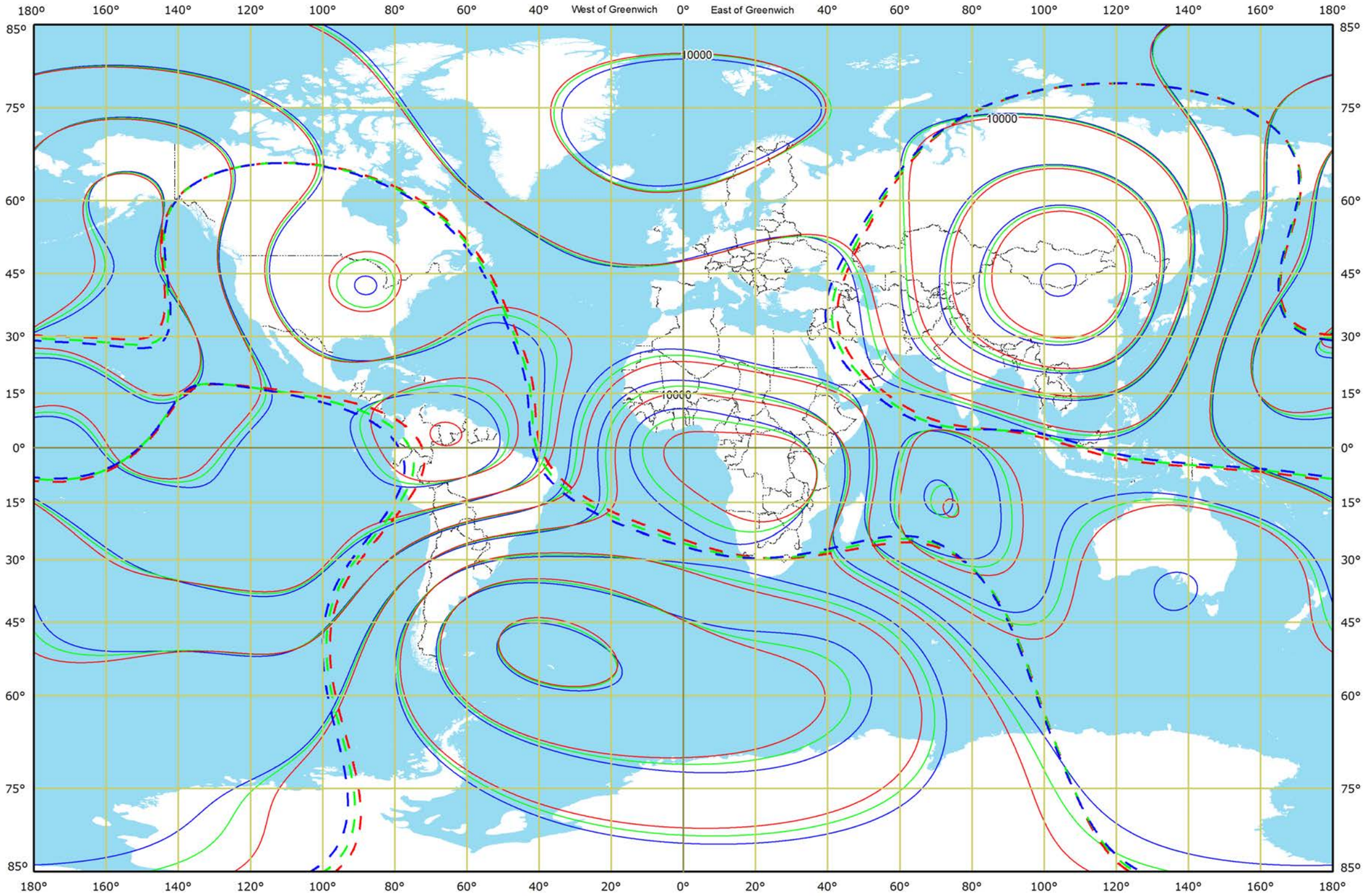

Years Isolines

1910
1915
1920

Geomagnetic equators

1910
1915
1920

Example of magnetic total intensity value, nT

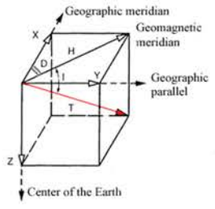

MGMF vector components

D Declination
I Inclination
H Horizontal component
T Total intensity
X North component
Y East component
Z Vertical component

Scale 1: 120 000 000

Projection: Miller cylindrical

TOTAL INTENSITY OF MGMF NONDIPOLE PART

MGMF – 1920, 1925, 1930 – FM (T)

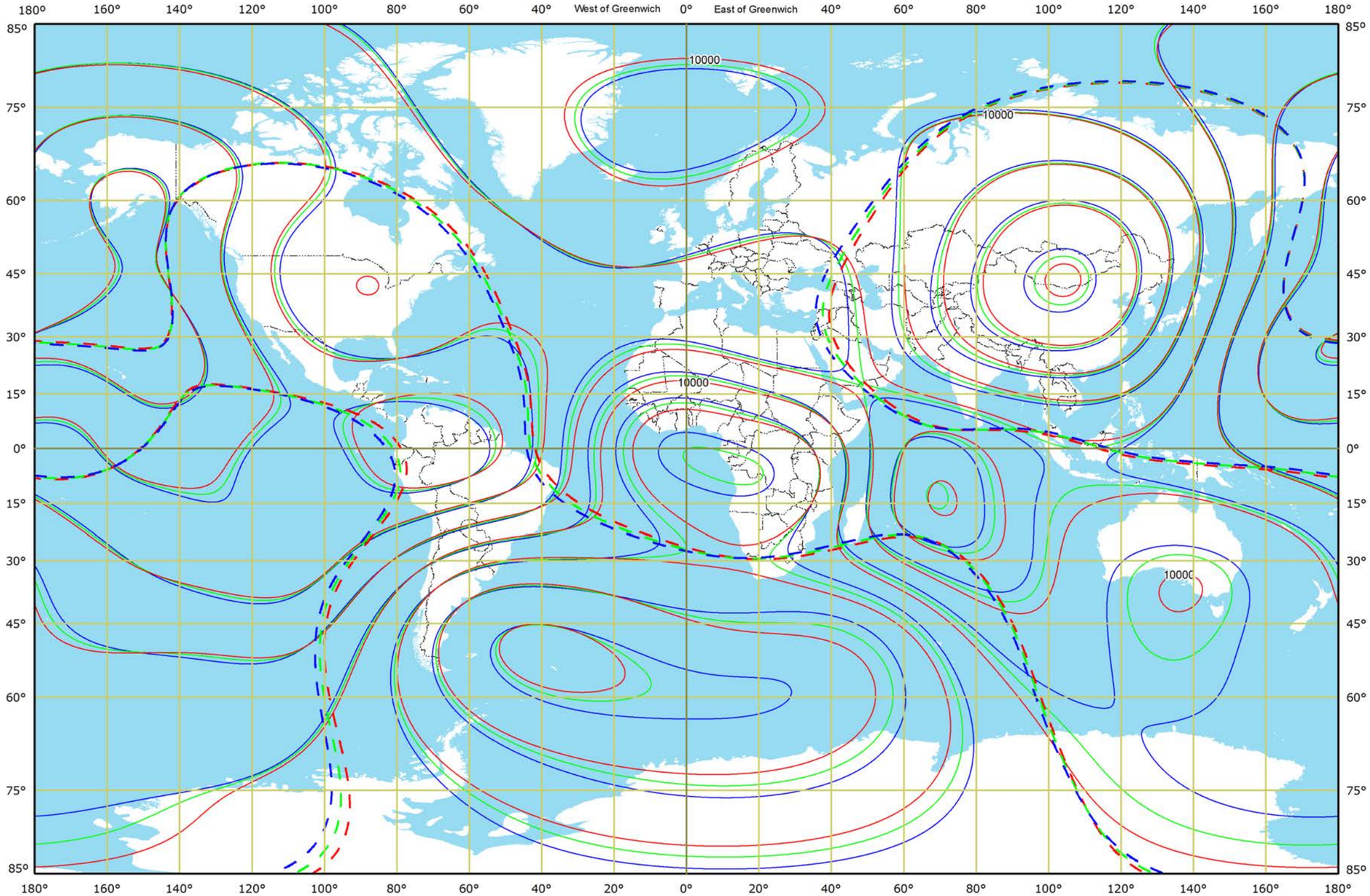

Years Isolines

1920
1925
1930

Geomagnetic equators

1920
1925
1930

Example of magnetic total intensity value, nT

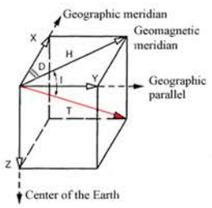

MGMF vector components

D Declination
I Inclination
H Horizontal component
T Total intensity
X North component
Y East component
Z Vertical component

Scale 1: 120 000 000

Projection: Miller cylindrical

TOTAL INTENSITY OF MGMF NONDIPOLE PART

MGMF – 1930, 1935, 1940 – FM (T)

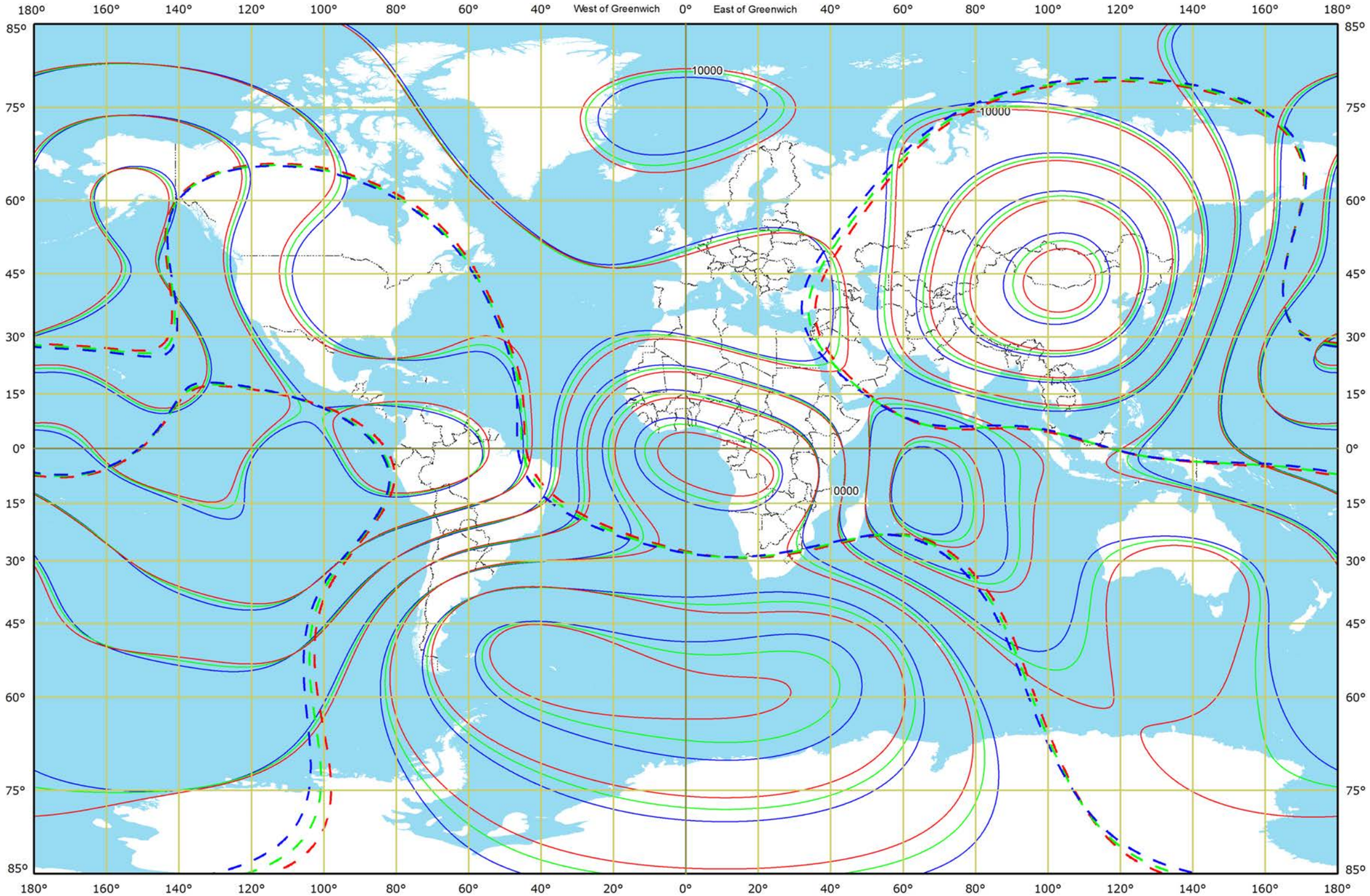

Years Isolines

1930
1935
1940

Geomagnetic equators

1930
1935
1940

Example of magnetic total intensity value, nT

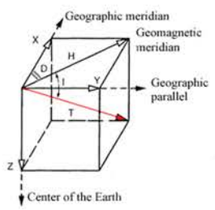

MGMF vector components

D Declination
I Inclination
H Horizontal component
T Total intensity
X North component
Y East component
Z Vertical component

Scale 1: 120 000 000

Projection: Miller cylindrical

TOTAL INTENSITY OF MGMF NONDIPOLE PART

MGMF – 1940, 1945, 1950 – FM (T)

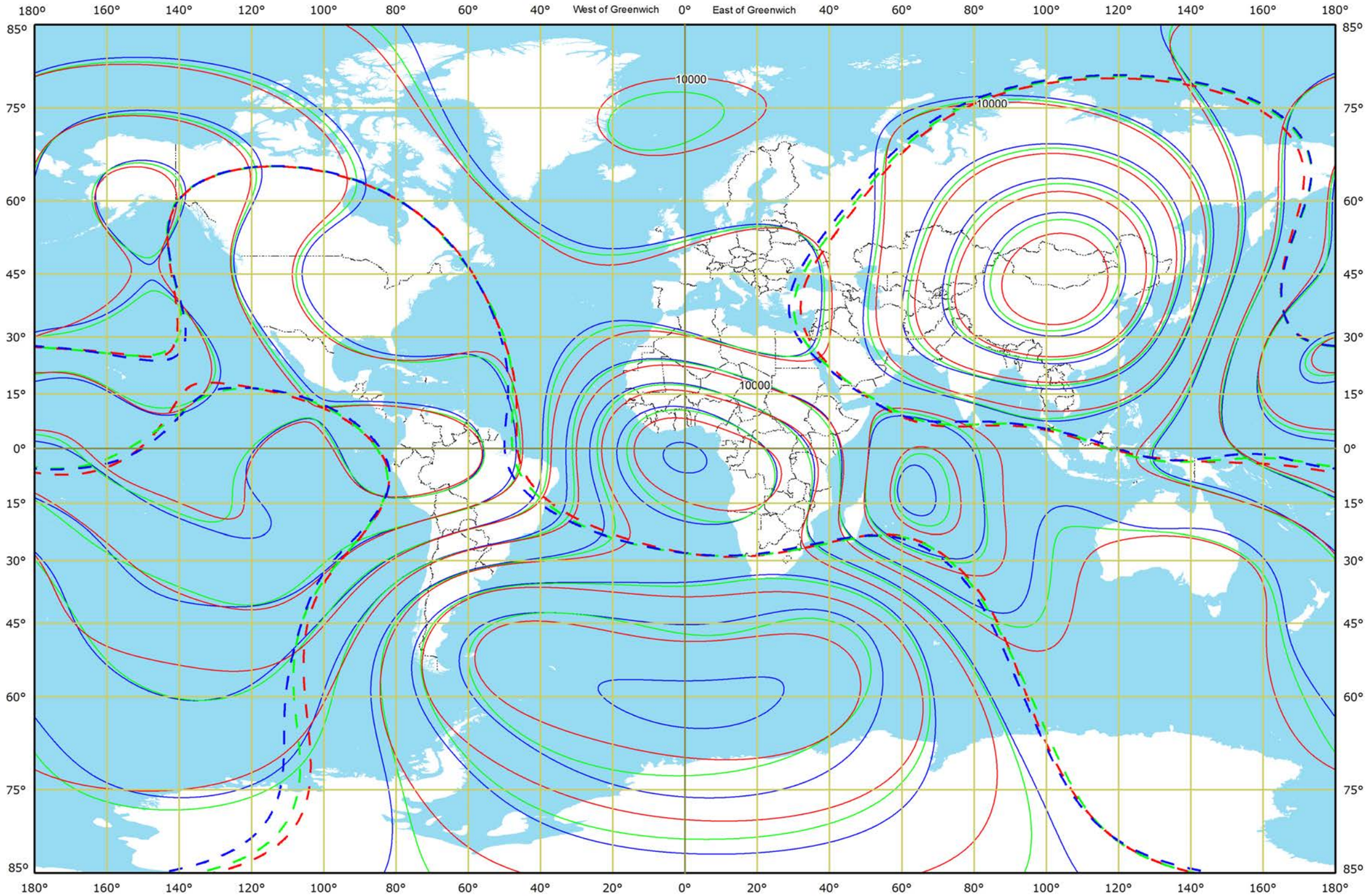

Years Isolines

1940
1945
1950

Geomagnetic equators

1940
1945
1950

Example of magnetic total intensity value, nT

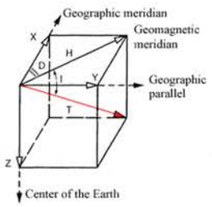

MGMF vector components

D Declination
I Inclination
H Horizontal component
T Total intensity
X North component
Y East component
Z Vertical component

Scale 1: 120 000 000

Projection: Miller cylindrical

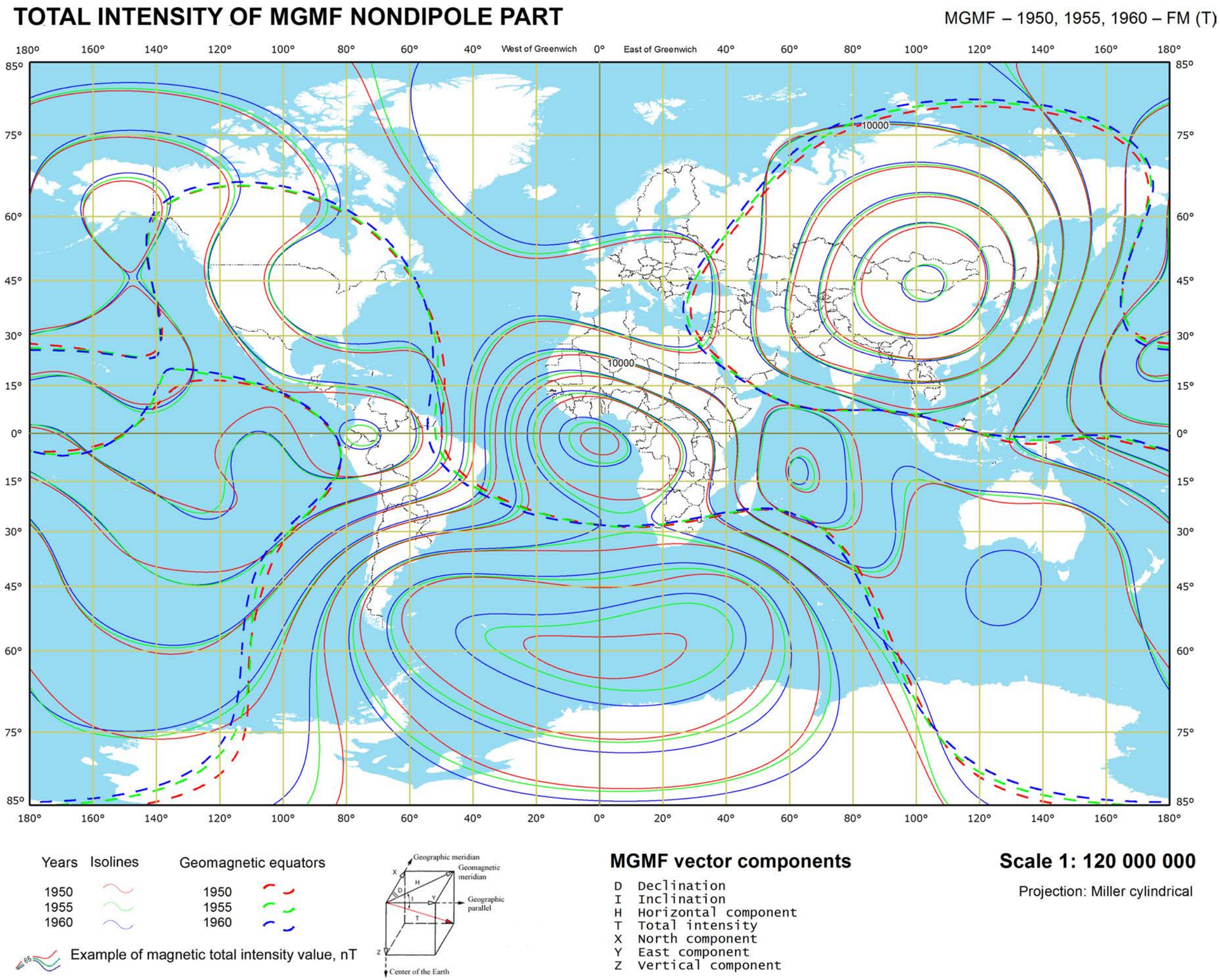
TOTAL INTENSITY OF MGMF NONDIPOLE PART
MGMF – 1950, 1955, 1960 – FM (T)
West of Greenwich
East of Greenwich
10000
10000
Years Isolines
1950
1955
1960
Geomagnetic equators
1950
1955
1960
Example of magnetic total intensity value, nT
Geographic meridian
Geomagnetic meridian
Geographic parallel
Center of the Earth
MGMF vector components
D Declination
I Inclination
H Horizontal component
T Total intensity
X North component
Y East component
Z Vertical component
Scale 1: 120 000 000
Projection: Miller cylindrical

TOTAL INTENSITY OF MGMF NONDIPOLE PART

MGMF – 1960, 1965, 1970 – FM (T)

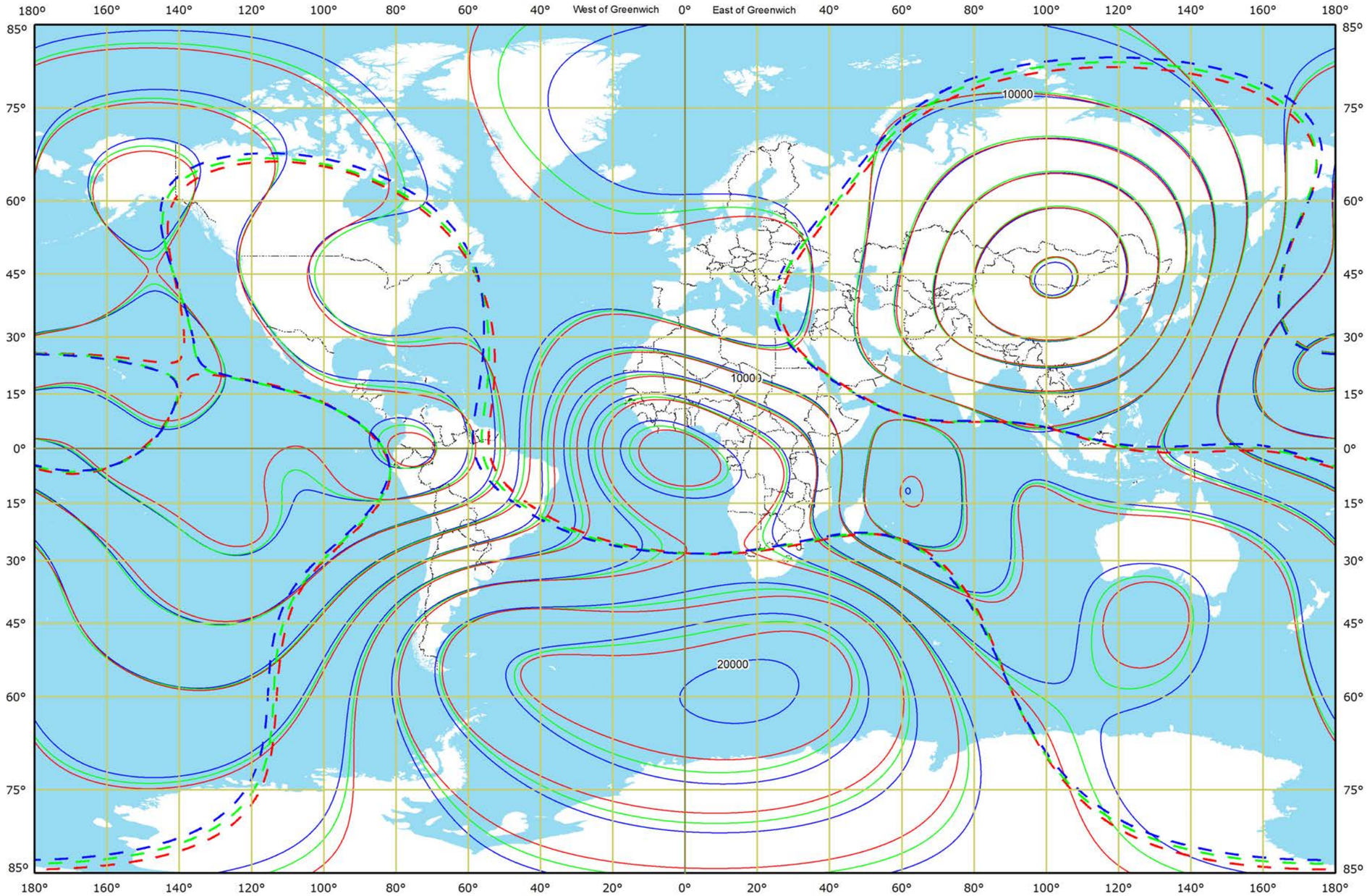

Years Isolines

1960
1965
1970

Geomagnetic equators

1960
1965
1970

Example of magnetic total intensity value, nT

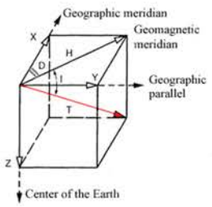

MGMF vector components

D Declination
I Inclination
H Horizontal component
T Total intensity
X North component
Y East component
Z Vertical component

Scale 1: 120 000 000

Projection: Miller cylindrical

TOTAL INTENSITY OF MGMF NONDIPOLE PART

MGMF – 1970, 1975, 1980 – FM (T)

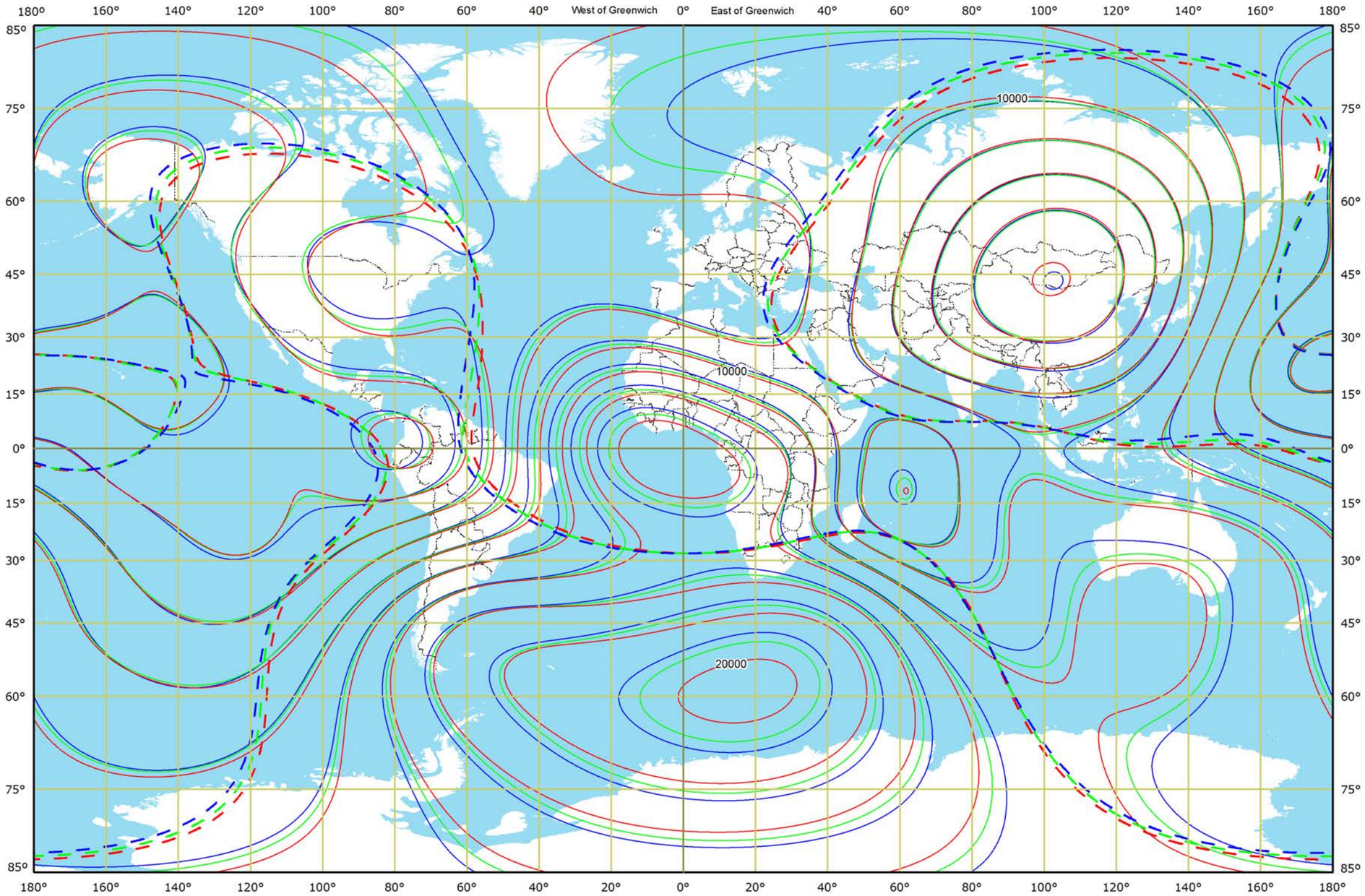

Years Isolines

1970
1975
1980

Geomagnetic equators

1970
1975
1980

Example of magnetic total intensity value, nT

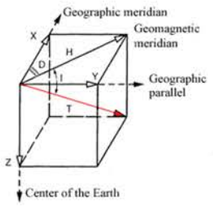

MGMF vector components

D Declination
I Inclination
H Horizontal component
T Total intensity
X North component
Y East component
Z Vertical component

Scale 1: 120 000 000

Projection: Miller cylindrical

TOTAL INTENSITY OF MGMF NONDIPOLE PART

MGMF – 1980, 1985, 1990 – FM (T)

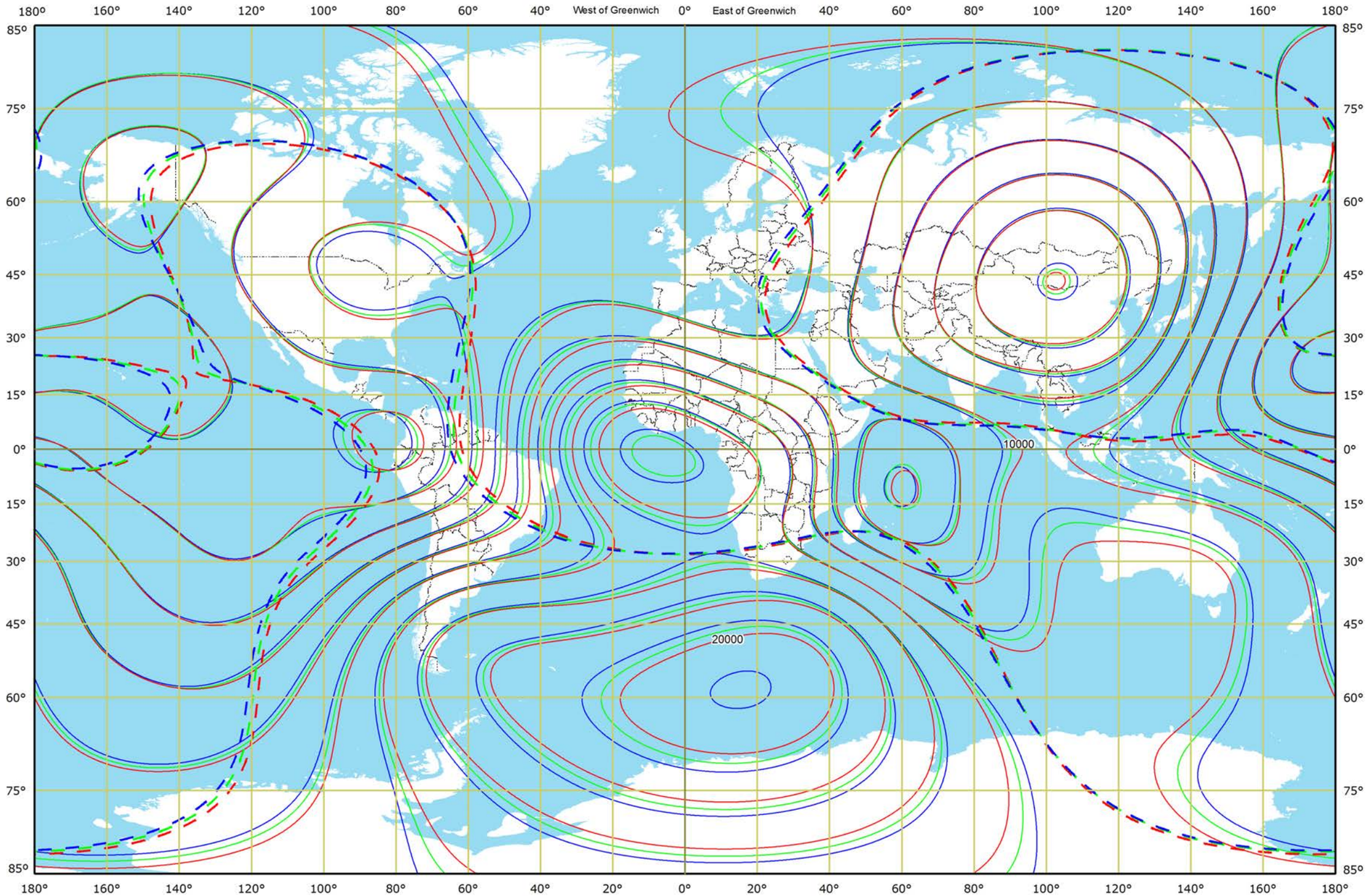

Years Isolines

1980
1985
1990

Geomagnetic equators

1980
1985
1990

Example of magnetic total intensity value, nT

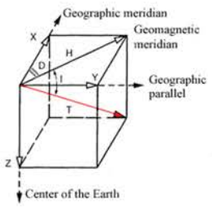

MGMF vector components

D Declination
I Inclination
H Horizontal component
T Total intensity
X North component
Y East component
Z Vertical component

Scale 1: 120 000 000

Projection: Miller cylindrical

TOTAL INTENSITY OF MGMF NONDIPOLE PART

MGMF – 1990, 1995, 2000 – FM (T)

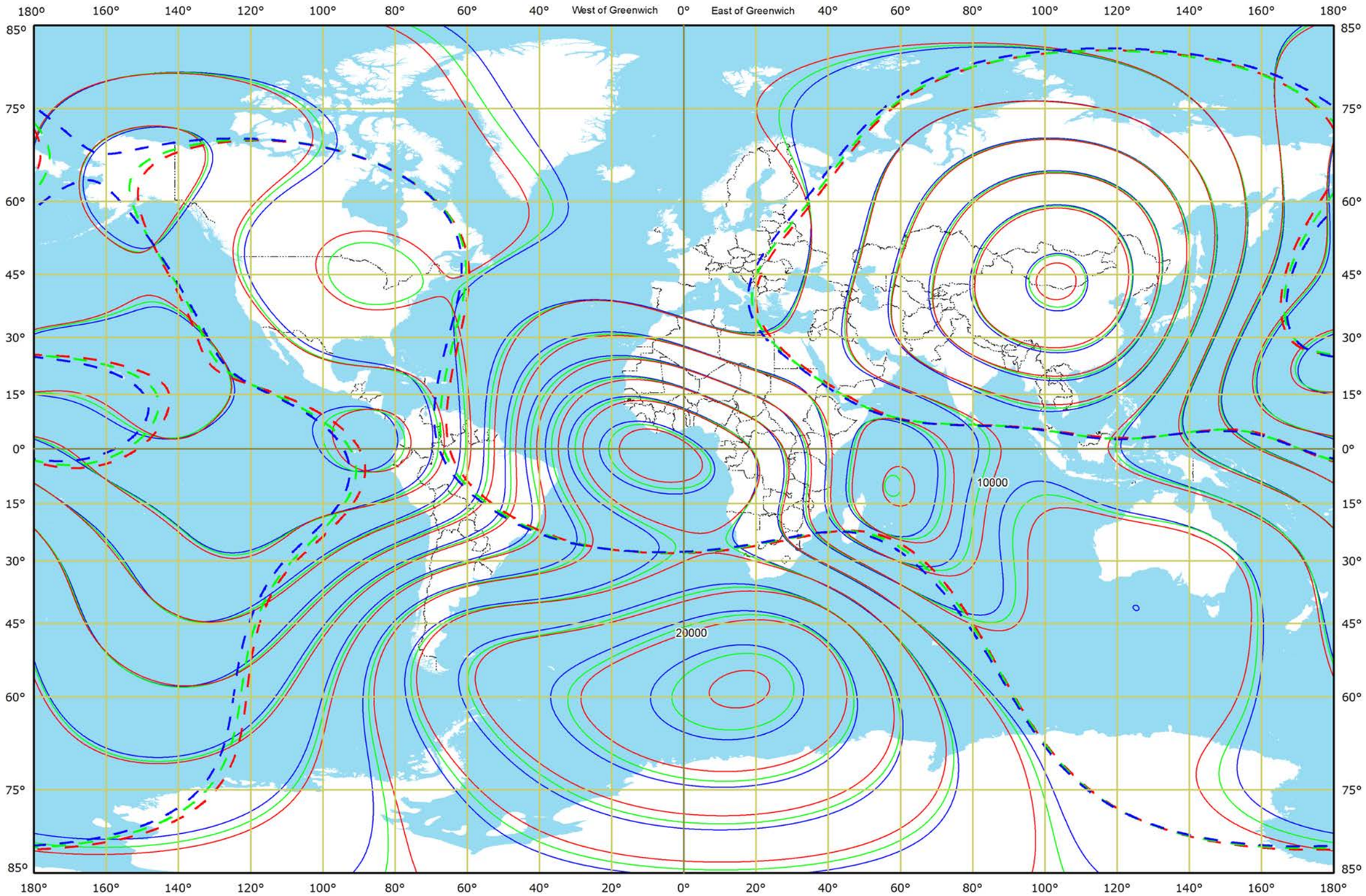

Years Isolines

1990
1995
2000

Geomagnetic equators

1990
1995
2000

Example of magnetic total intensity value, nT

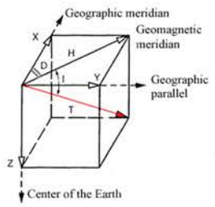

MGMF vector components

D Declination
I Inclination
H Horizontal component
T Total intensity
X North component
Y East component
Z Vertical component

Scale 1: 120 000 000

Projection: Miller cylindrical

TOTAL INTENSITY OF MGMF NONDIPOLE PART

MGMF – 2000, 2005, 2010 – FM (T)

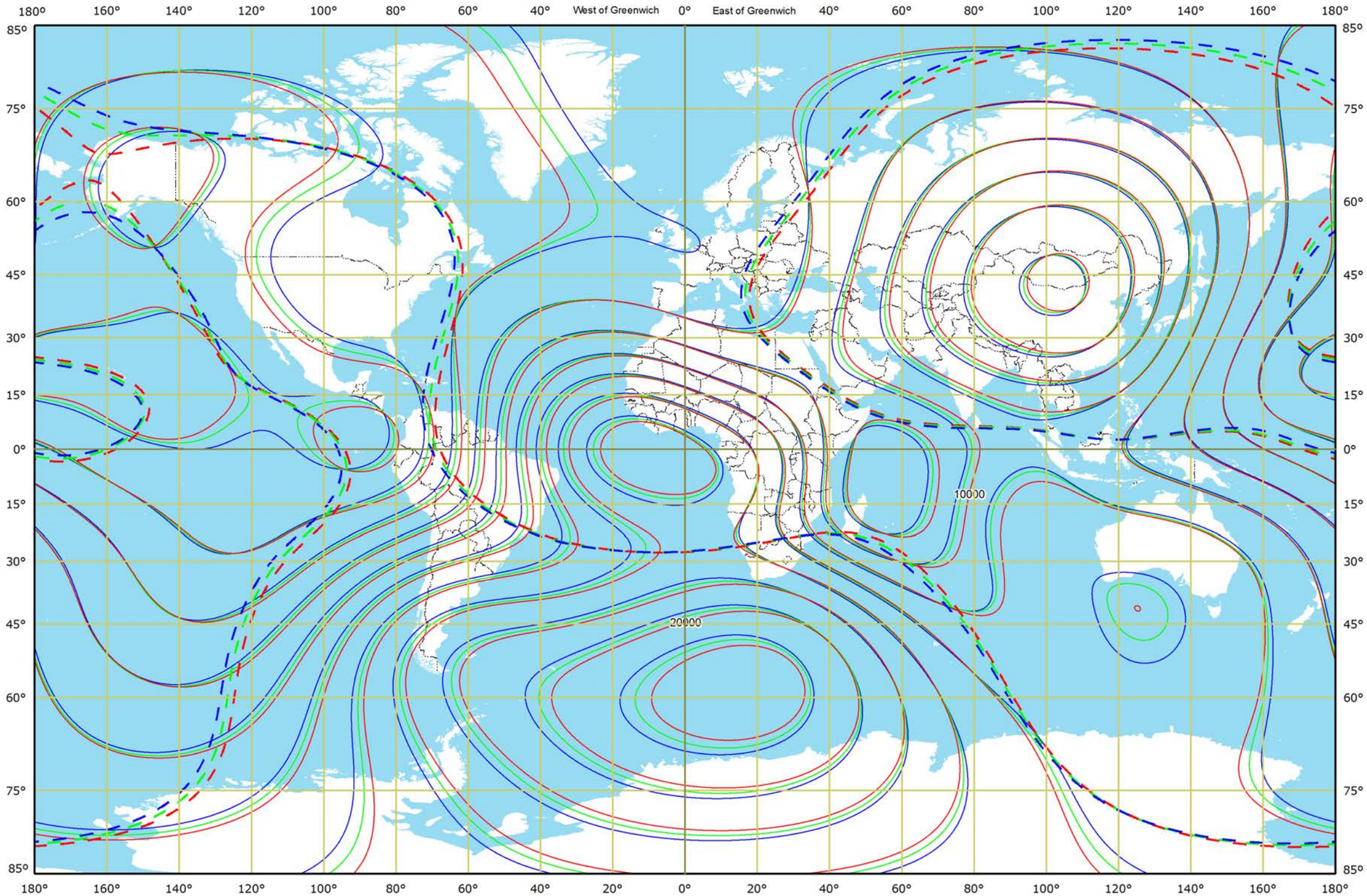

Years Isolines

2000
2005
2010

Geomagnetic equators

2000
2005
2010

Example of magnetic total intensity value, nT

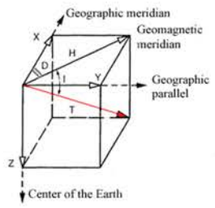

MGMF vector components

D Declination
I Inclination
H Horizontal component
T Total intensity
X North component
Y East component
Z Vertical component

Scale 1: 120 000 000

Projection: Miller cylindrical

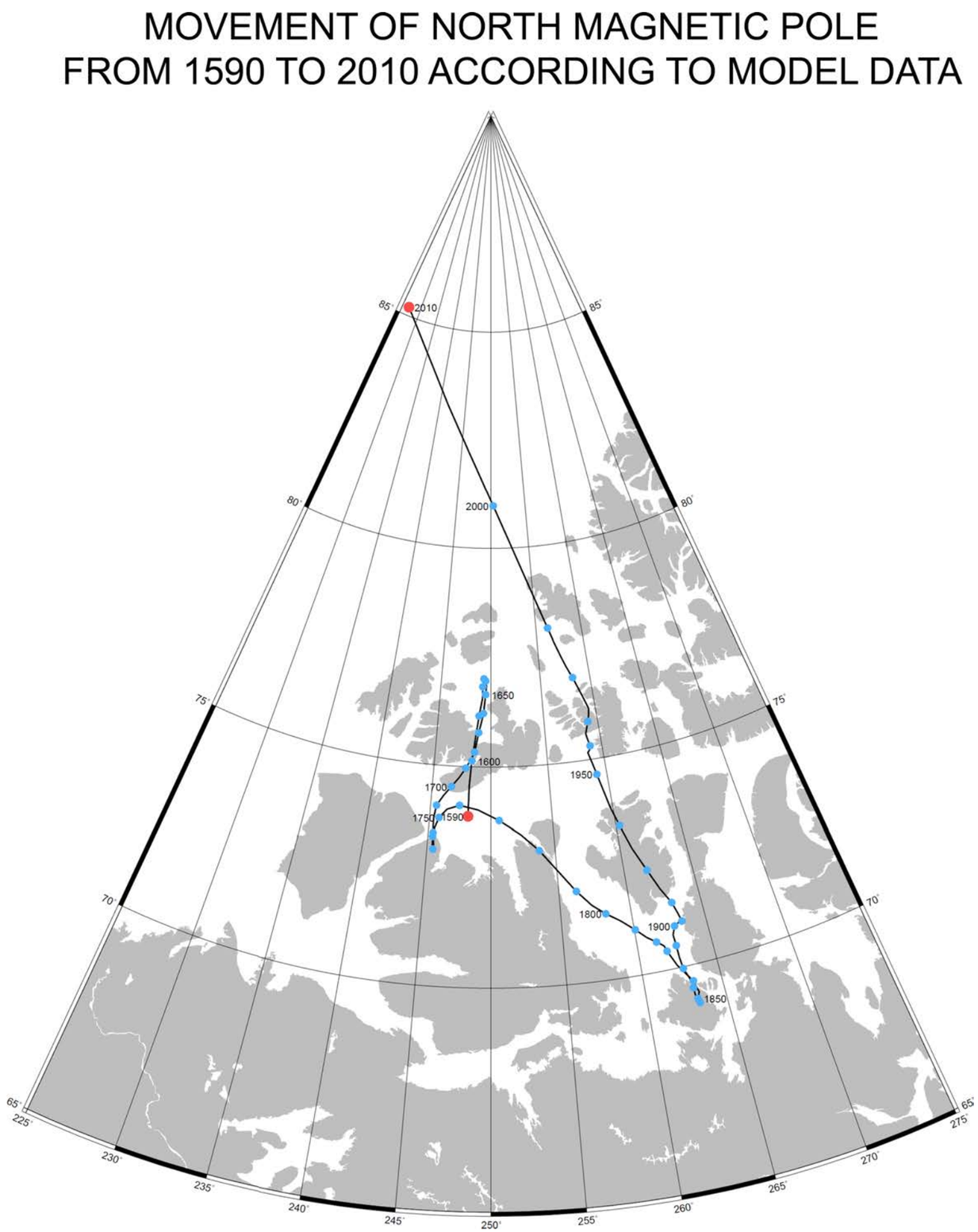
MOVEMENT OF NORTH MAGNETIC POLE
FROM 1590 TO 2010 ACCORDING TO MODEL DATA
2010
2000
1950
1900
1850
1800
1750
1700
1650
1600
1590
85°
80°
75°
70°
65°
225°
230°
235°
240°
245°
250°
255°
260°
265°
270°
275°

MOVEMENT OF SOUTH MAGNETIC POLE FROM 1590 TO 2010 ACCORDING TO MODEL DATA

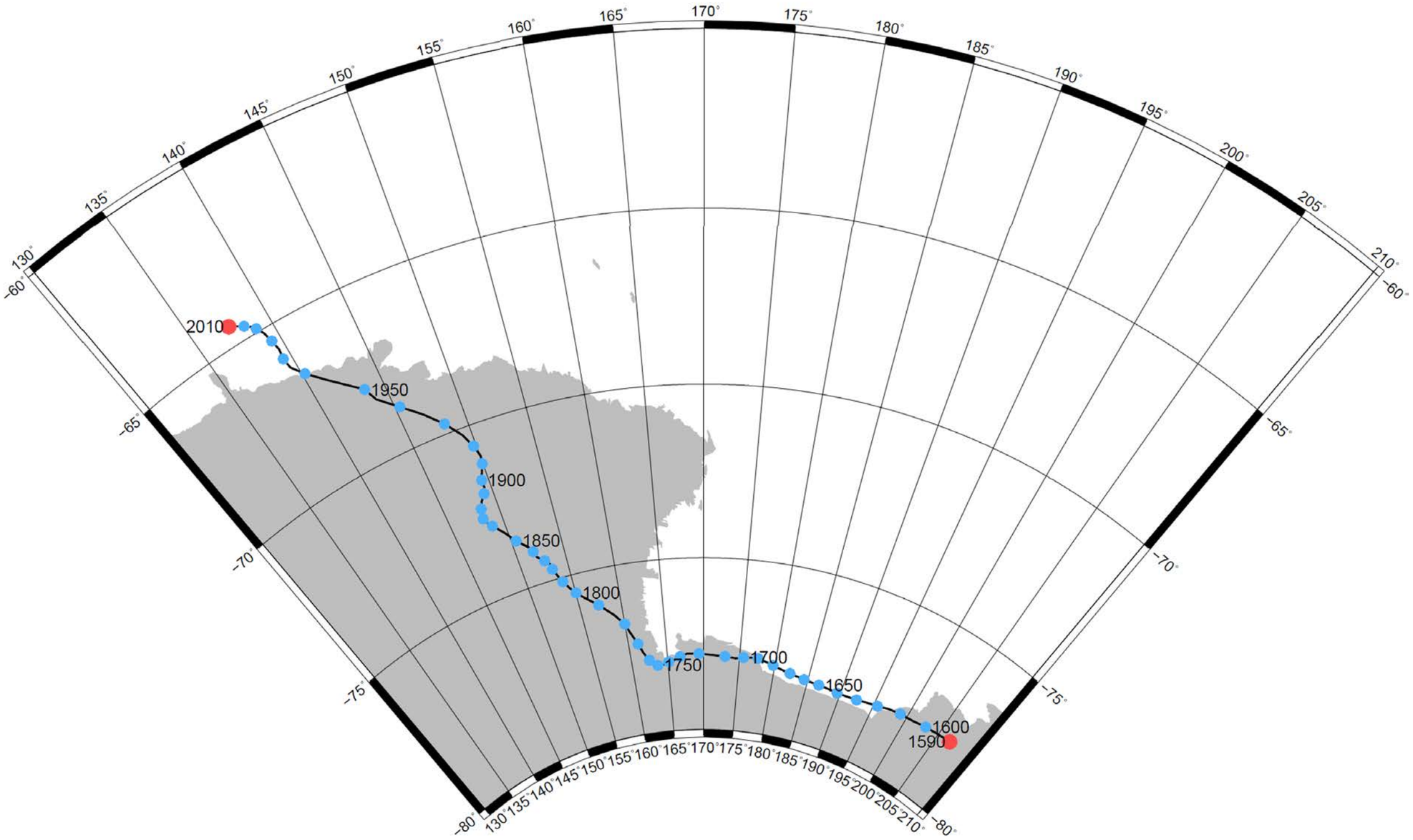

MOVEMENT OF THE NORTH MAGNETIC POLE FROM 1831 TO 2007 ACCORDING TO FIELD MEASUREMENTS

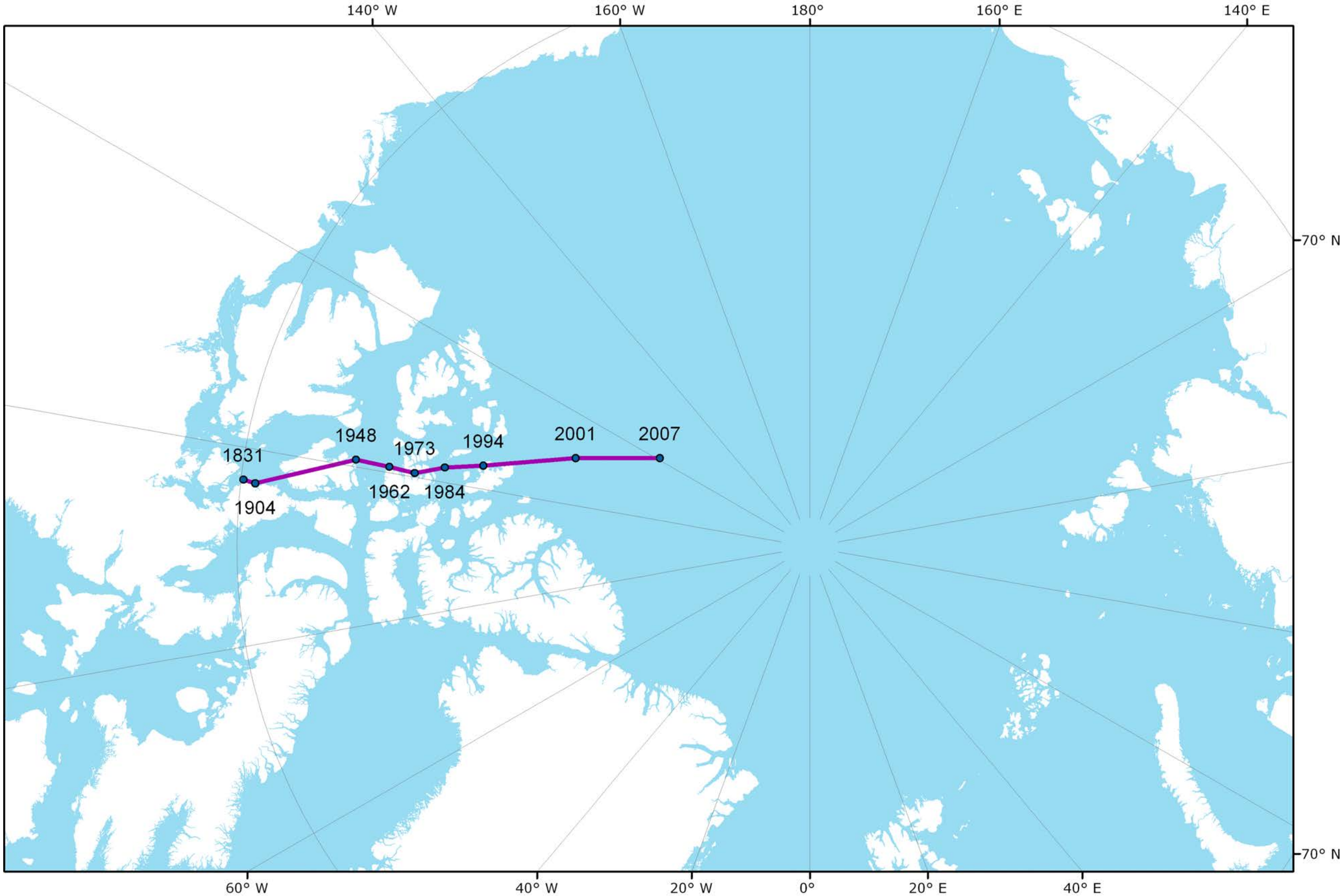

Scale 1: 15 000 000

Movement trajectory of the North magnetic pole from 1831 to 2007

Projection: Lambert Azimuthal Equal Area

MOVEMENT OF THE SOUTH MAGNETIC POLE FROM 1903 TO 2000 ACCORDING TO FIELD MEASUREMENTS

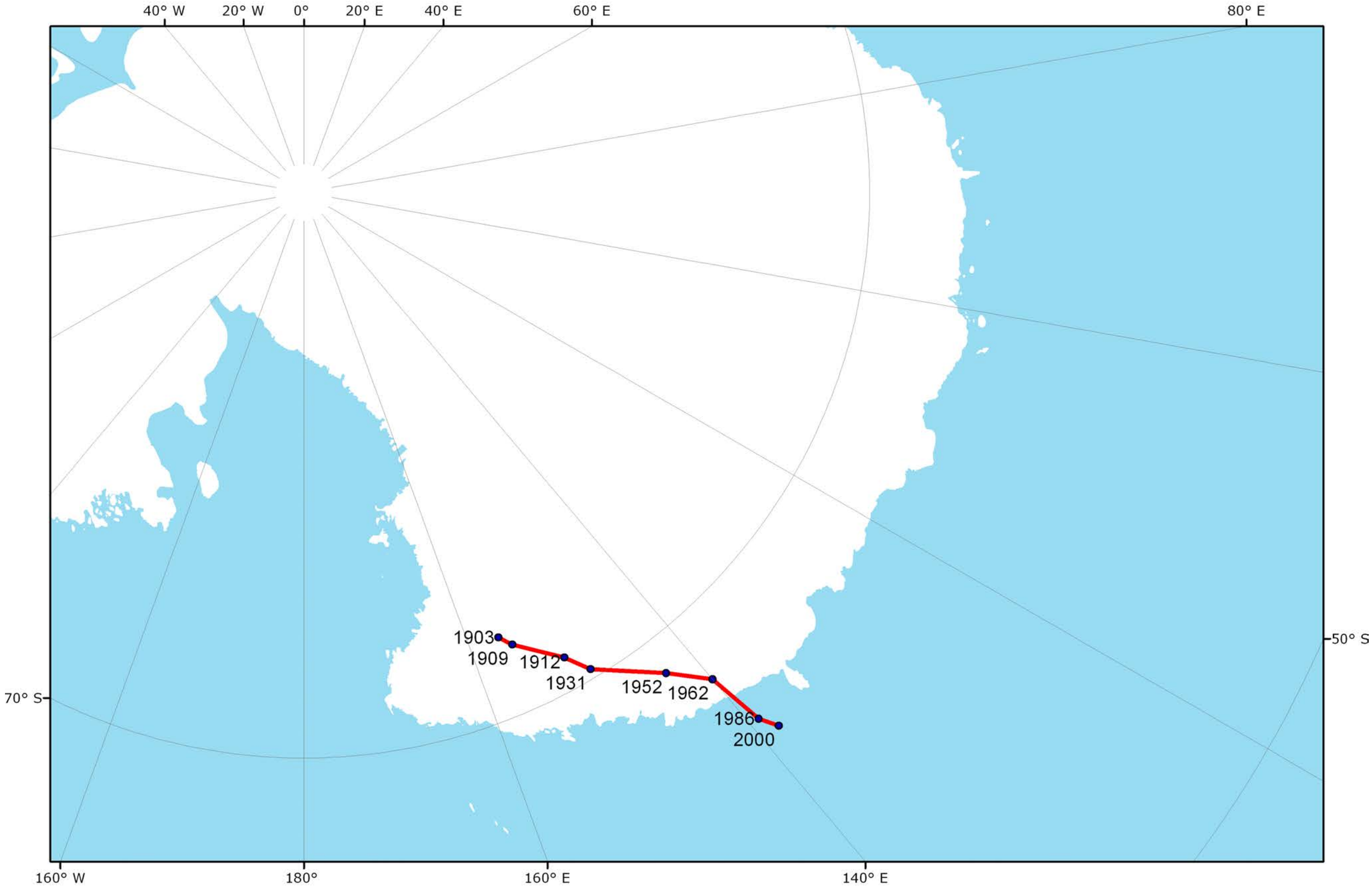

Scale 1: 15 000 000

Movement trajectory of the South magnetic pole from 1903 to 2000

Projection: Lambert Azimuthal Equal Area

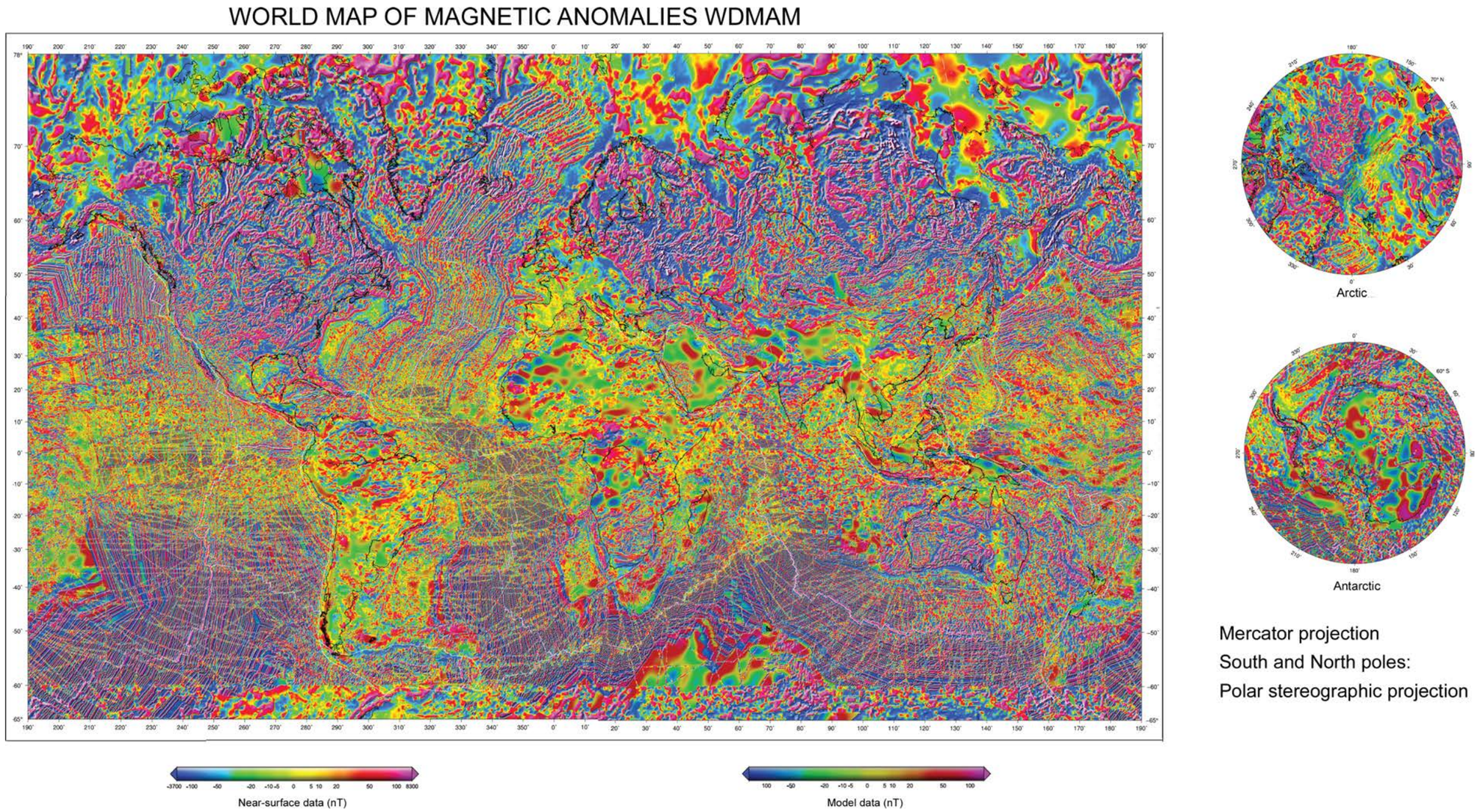
WORLD MAP OF MAGNETIC ANOMALIES WDMAM
Arctic
Antarctic
Mercator projection
South and North poles:
Polar stereographic projection
Near-surface data (nT)
Model data (nT)

DATA USED FOR PREPARATION OF THE MAP OF MAGNETIC ANOMALIES WDMAM

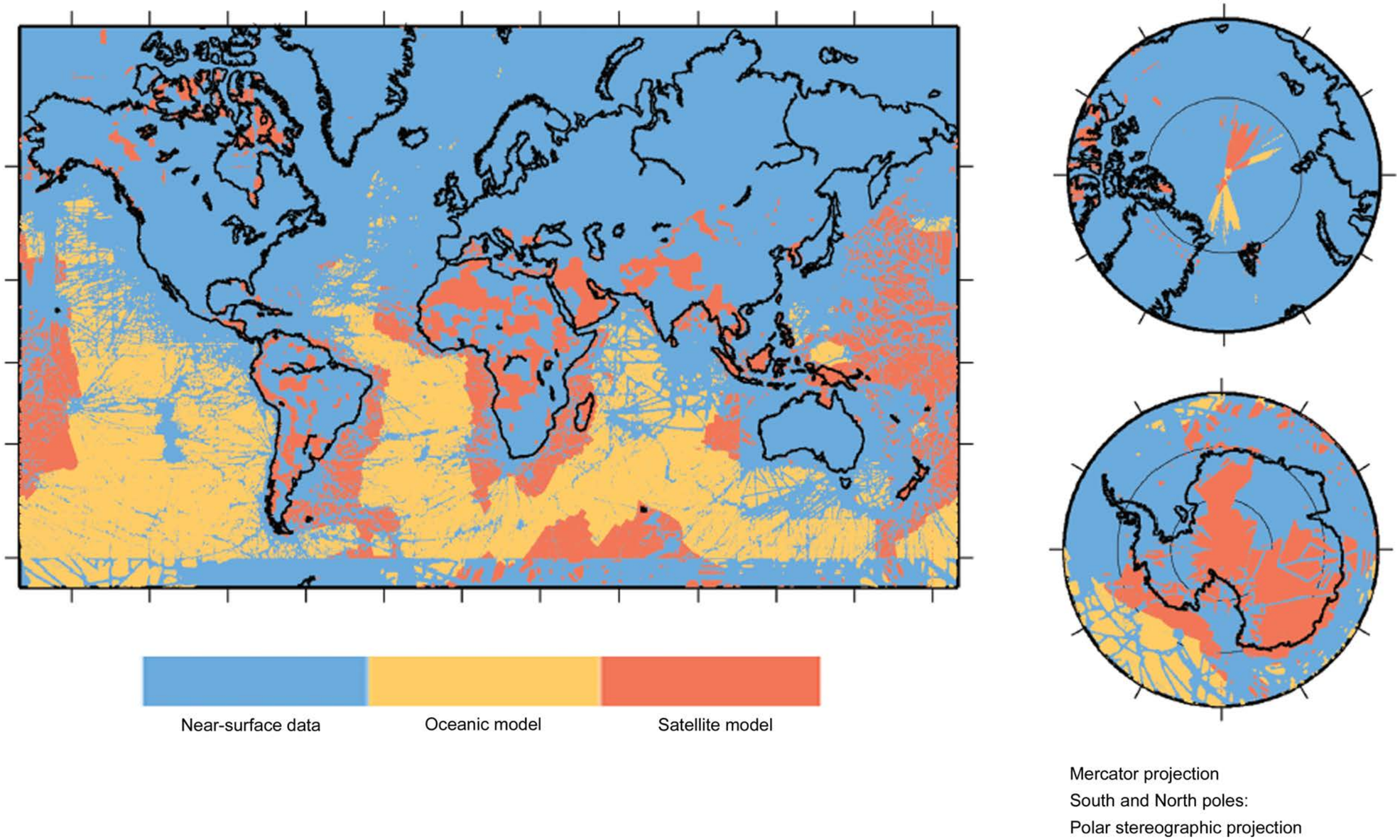

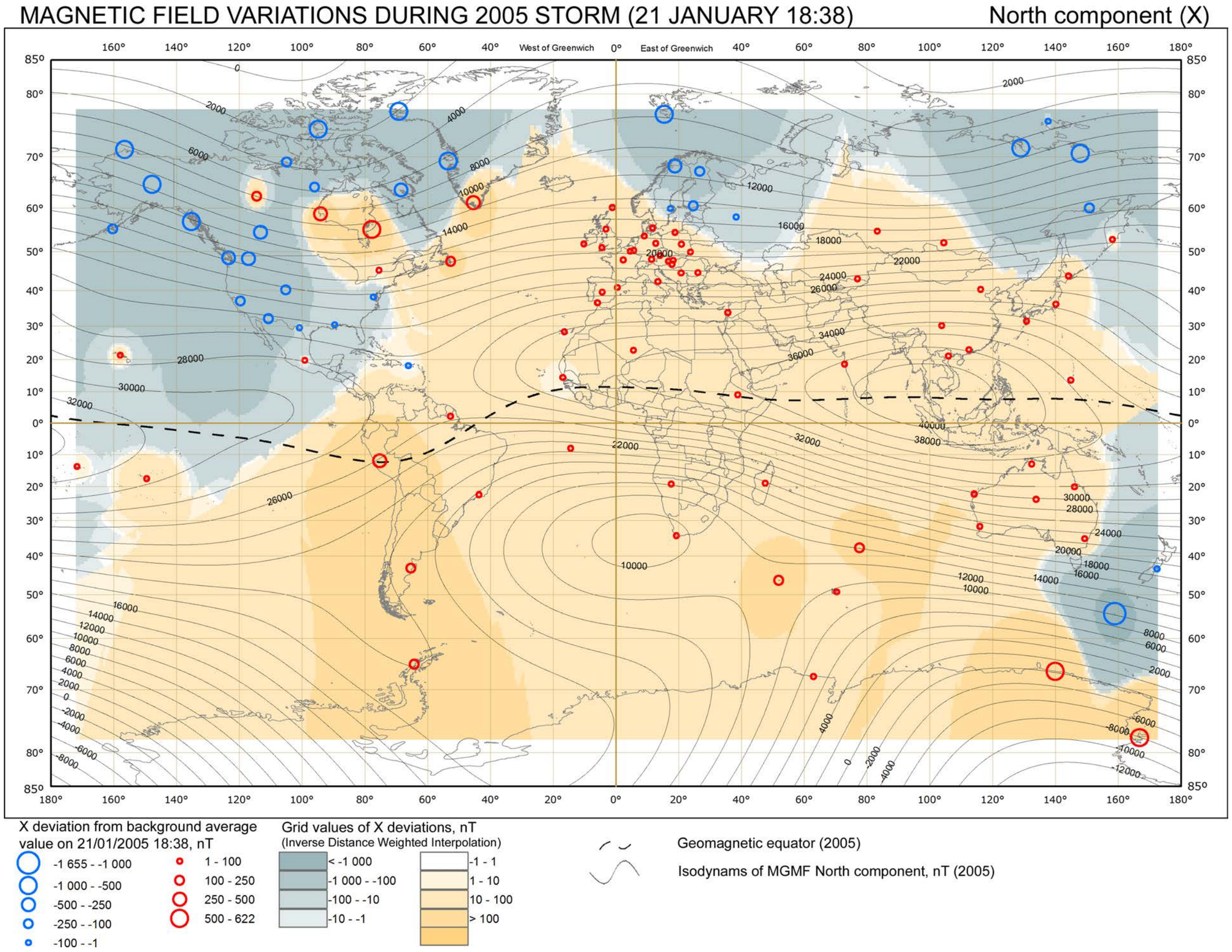
MAGNETIC FIELD VARIATIONS DURING 2005 STORM (21 JANUARY 18:38)
North component (X)
West of Greenwich
East of Greenwich
X deviation from background average value on 21/01/2005 18:38, nT
-1 655 - -1 000
-1 000 - -500
-500 - -250
-250 - -100
-100 - -1
1 - 100
100 - 250
250 - 500
500 - 622
Grid values of X deviations, nT
(Inverse Distance Weighted Interpolation)
< -1 000
-1 000 - -100
-100 - -10
-10 - -1
-1 - 1
1 - 10
10 - 100
> 100
Geomagnetic equator (2005)
Isodynams of MGMF North component, nT (2005)

MAGNETIC FIELD VARIATIONS DURING 2005 STORM (21 JANUARY 18:38) Vertical component (Z)

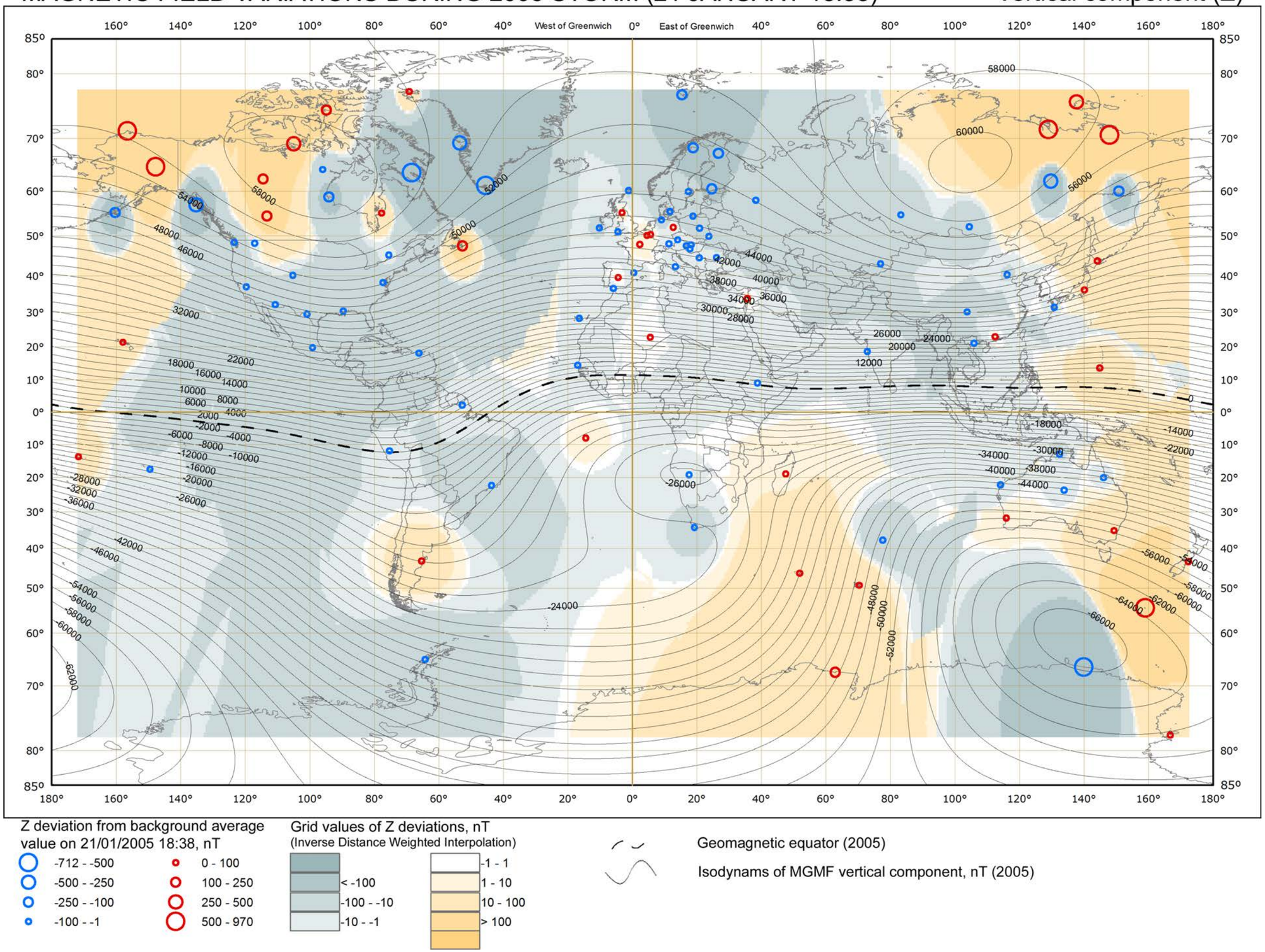

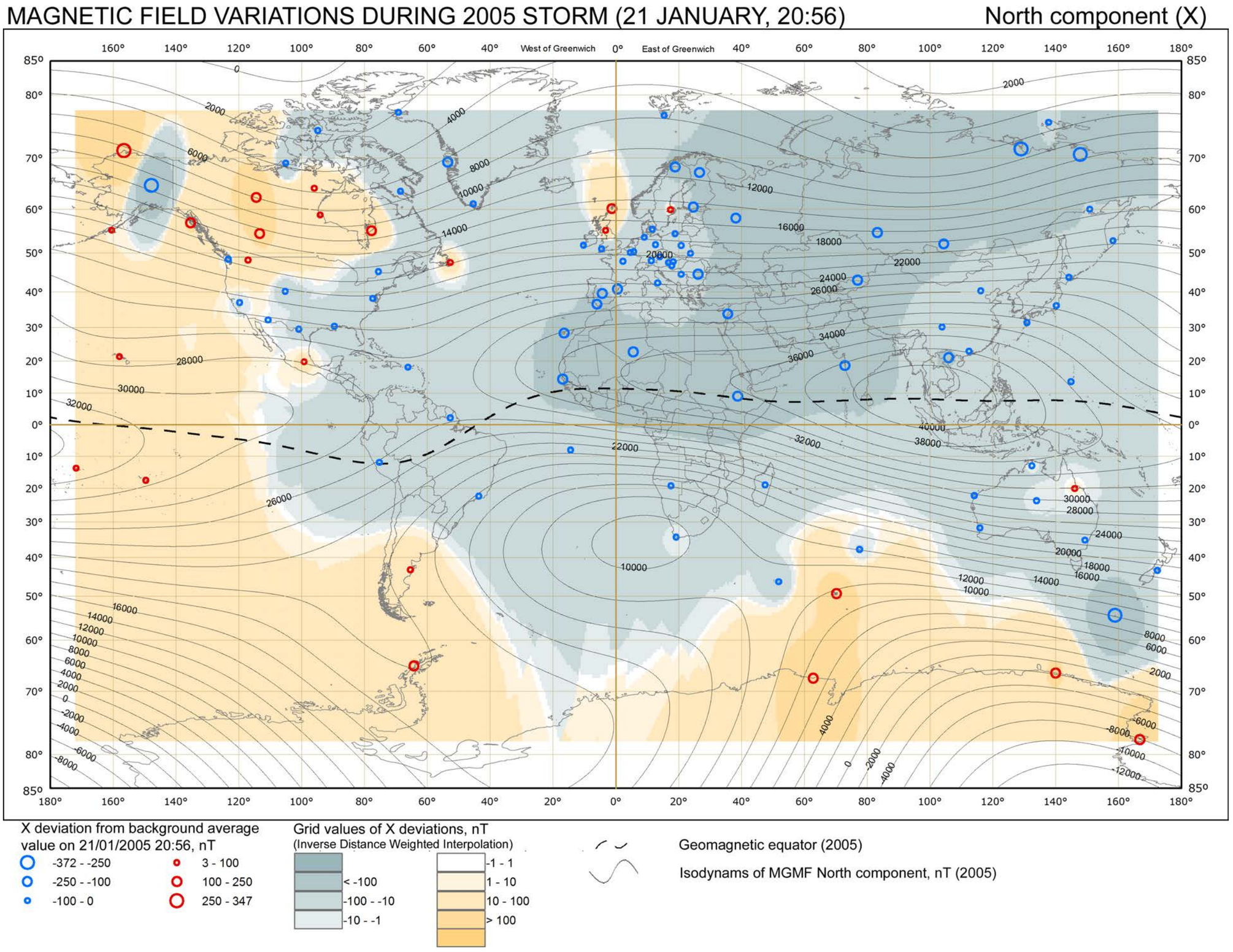
MAGNETIC FIELD VARIATIONS DURING 2005 STORM (21 JANUARY, 20:56)
North component (X)
West of Greenwich
East of Greenwich
X deviation from background average value on 21/01/2005 20:56, nT
-372 - -250
-250 - -100
-100 - 0
3 - 100
100 - 250
250 - 347
Grid values of X deviations, nT
(Inverse Distance Weighted Interpolation)
< -100
-100 - -10
-10 - -1
-1 - 1
1 - 10
10 - 100
> 100
Geomagnetic equator (2005)
Isodynams of MGMF North component, nT (2005)

MAGNETIC FIELD VARIATIONS DURING 2005 STORM (21 JANUARY 20:56) Vertical component (Z)

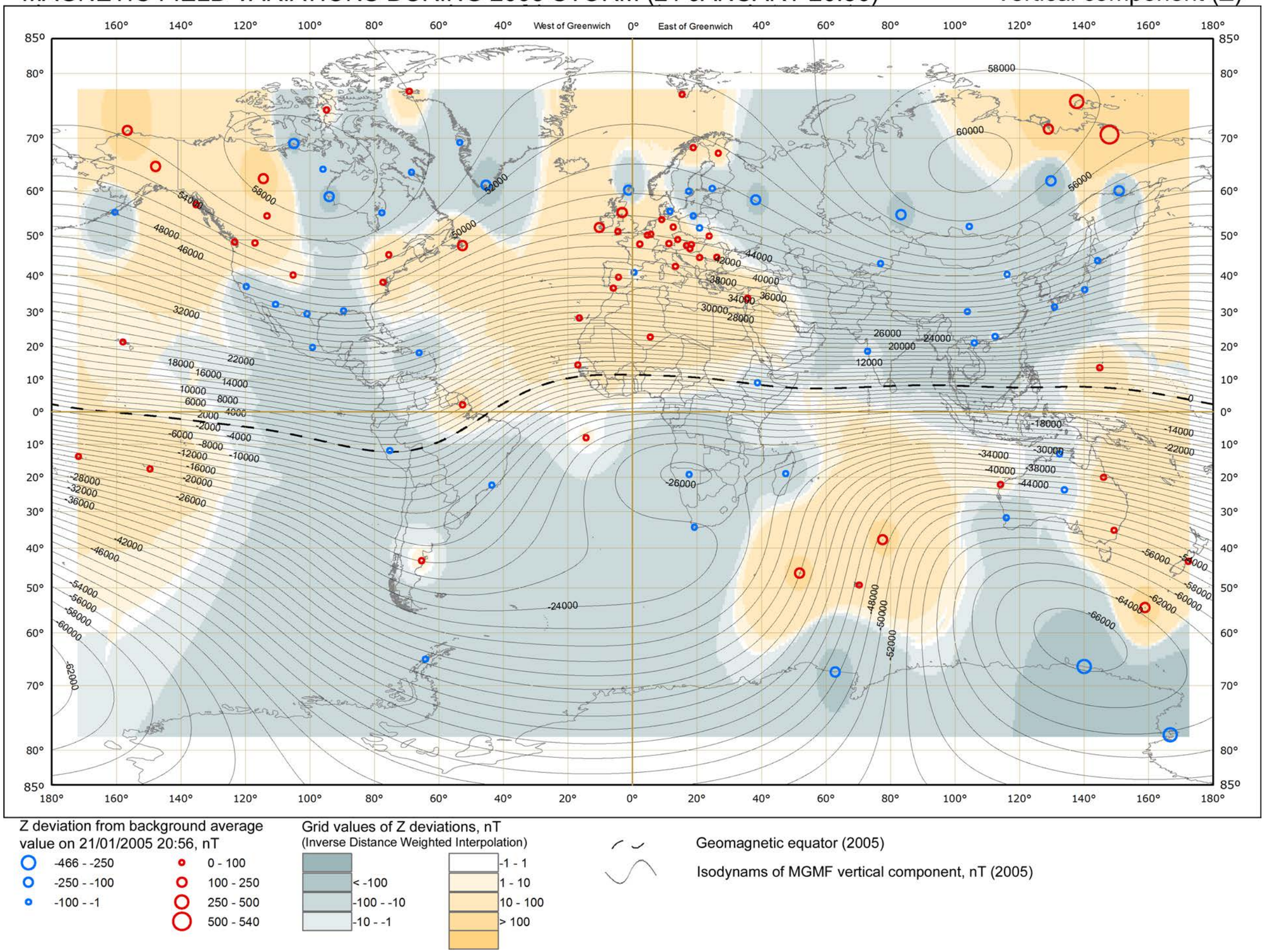

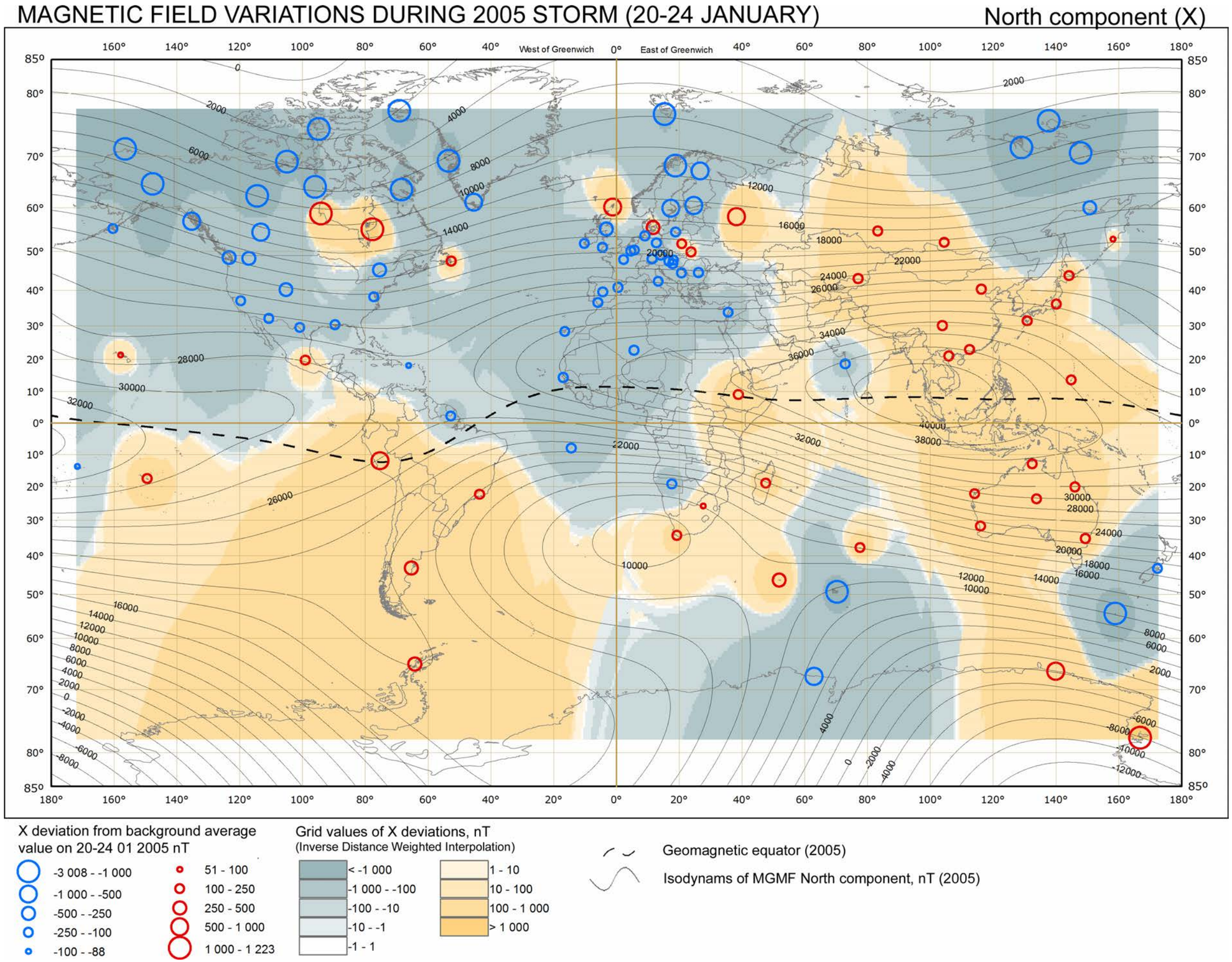
MAGNETIC FIELD VARIATIONS DURING 2005 STORM (20-24 JANUARY)
North component (X)
West of Greenwich
East of Greenwich
X deviation from background average value on 20-24 01 2005 nT
-3 008 - -1 000
-1 000 - -500
-500 - -250
-250 - -100
-100 - -88
51 - 100
100 - 250
250 - 500
500 - 1 000
1 000 - 1 223
Grid values of X deviations, nT
(Inverse Distance Weighted Interpolation)
< -1 000
-1 000 - -100
-100 - -10
-10 - -1
-1 - 1
1 - 10
10 - 100
100 - 1 000
> 1 000
Geomagnetic equator (2005)
Isodynams of MGMF North component, nT (2005)

MAGNETIC FIELD VARIATIONS DURING 2005 STORM (20-24 JANUARY) Vertical component (Z)

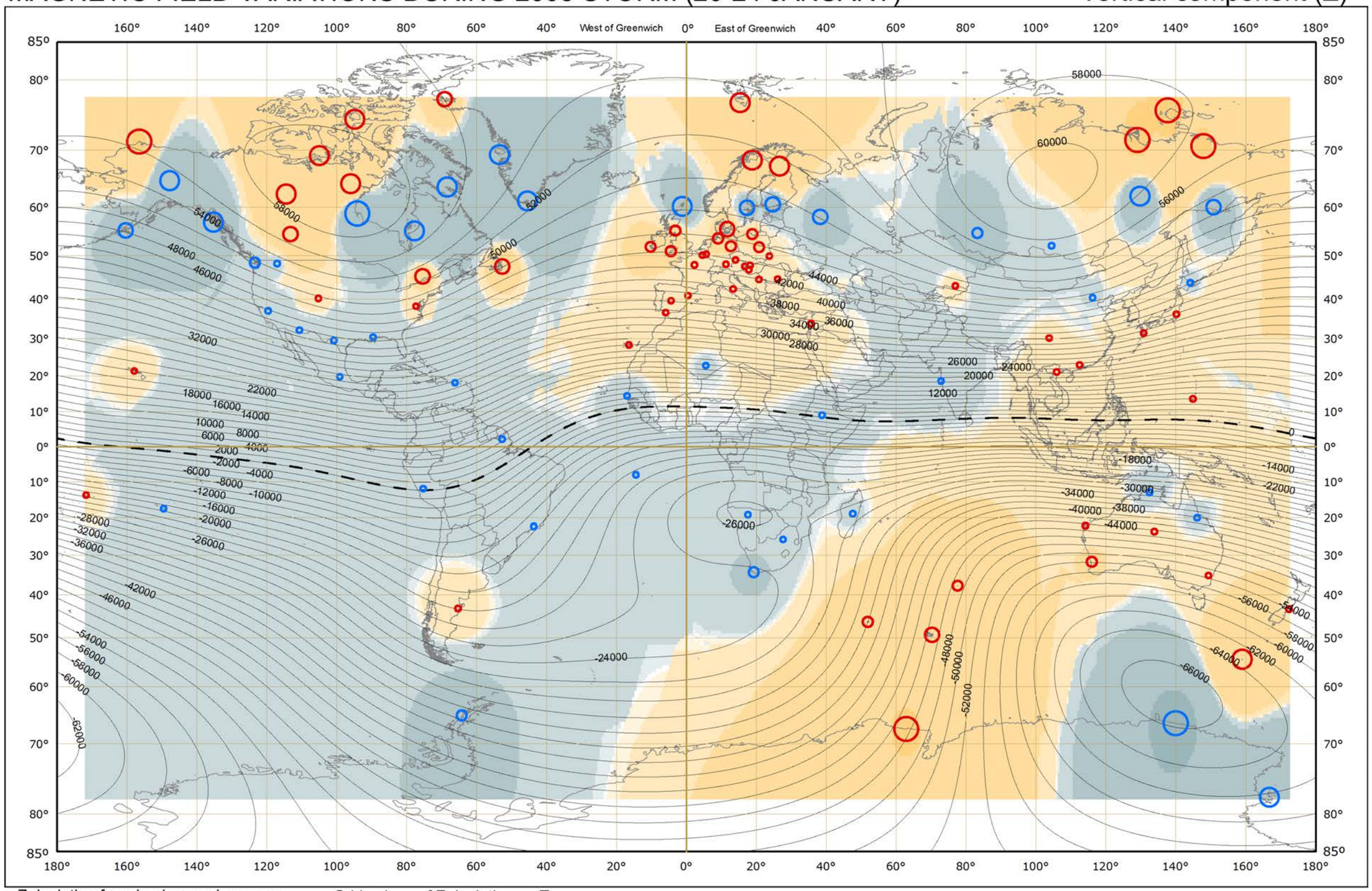

Annex 2. Historical Charts of the Earth's Magnetic Field

ORBIS TERRÆ COMPENDIOSA DESCRIPTIO EX PERITISSIMORVM TO
TIVS ORBIS GEOGRAPHORVM TABVLIS ET NOVISSIMIS OBSERVATIONIBVS DESVMPTA
HEMICICLVS MAGNEBOREVS PERVVIANVS
HEMICICLVS MAGNEBOREVS ASIATICVS
NOVA ZEMBLA
CIRCVLVS ARCTICVS
AMERICA SIVE INDIA NOVA
NOVA FRANCIA
TARTARIA
ASIA
EVROPA
NATOLIA
INDIA ORIENTALIS
CHINA
GVZARATE
ARABIA
AFRICA
NVBIA
ABISIMBA
MANICOMGO
MELINDE
MAR DEL NORT
CIRCVLVS ÆQVINOCTIALIS
TROPICVS CANCRI
TROPICVS CAPRICORNI
TROPICVS
MAGNETIS
MAR DEL ZVR
MAR DI INDIA
OCALETVR
PERV
CHICA
BRASILIA
ÆQVINOCTIALIS
MAGELLANICA REGIO
CIRCVLVS ANTARCTICVS
HIC EST
TERRA AVSTRALIS
NONDVM COGNITA
MARCPAVLINA REGIO
CIRCVLVS ANTARCTICVS
POLVS MAGNETIS
POLVS MAGNETIS PRIMVS
HEMICICLVS CONTRARIVS
MAGNETIS
MAGNETIS
LVCACH
Vetustissimas hic pestergiones ex M. Pauli Vonnet vartema scriptis Peregrinati omnibus constat
ET PVISSANT SEIGNEVR MESSIRE ANTOINE DE CARDAILLAC DE LEVI GENTIL HOMME ORDINAIRE DE LA CHAMBRE DV ROY, SEIGNEVR
ET BARON DE BIEVIL GAIS VILLENEVEVE MONTREDON ET C. DEDIOIT CETTE TABLE ET L'EXPOSITION DICELLE SON TRES HVMBLE SERVITEVR G. DE NAVTONIER

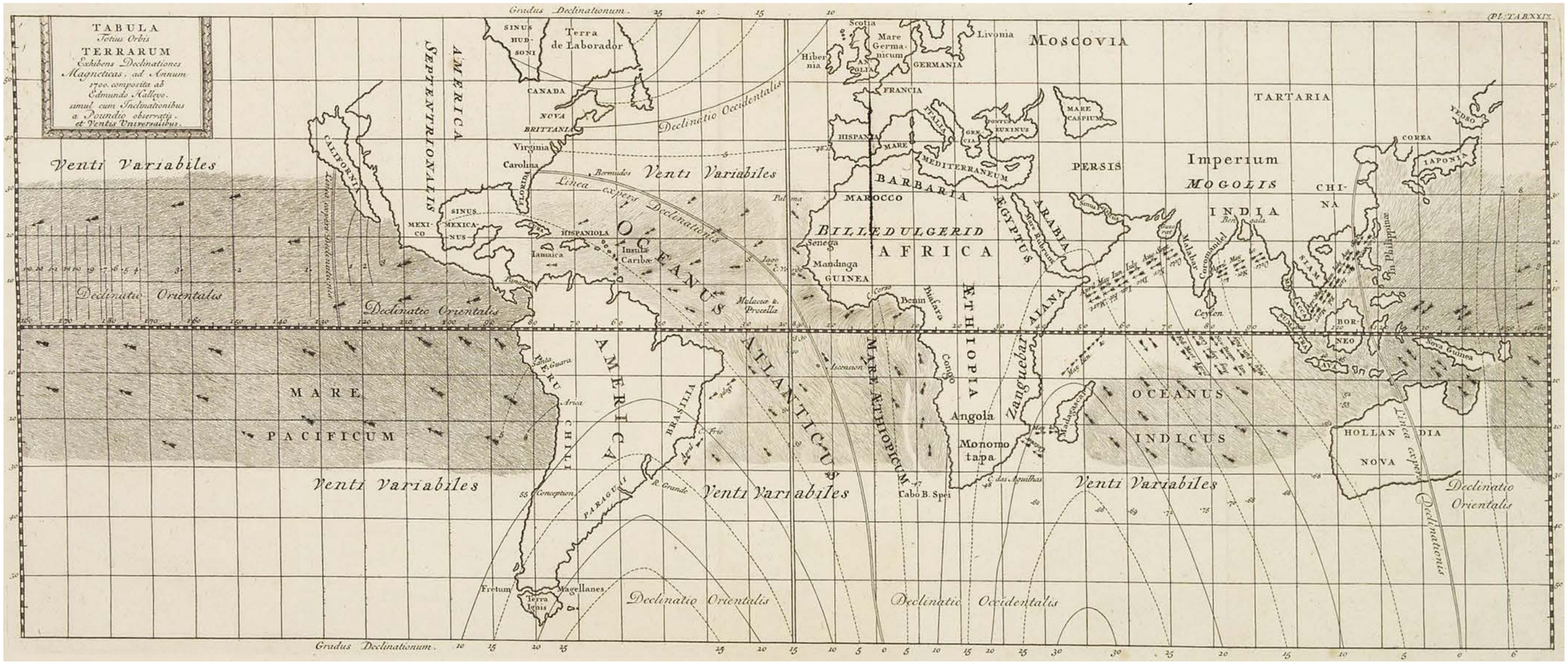
TABULA
Totius Orbis
TERRARUM
Exhibens Declinationes
Magneticas, ad Annum
1700. composita ab
Edmundo Halleyo.
simul cum Inclinationibus
a Poundio observatis,
et Ventis Universalibus.
(PL. TAB. XXIX.)
Gradus Declinationum.
Venti Variabiles
Declinatio Orientalis
Declinatio Occidentalis
Linea expers Declinationis
AMERICA SEPTENTRIONALIS
SINUS HUDSONI
Terra de Laborador
CANADA
NOVA BRITTANIA
Virginia
Carolina
FLORIDA
CALIFORNIA
SINUS MEXICANUS
MEXICO
HISPANIOLA
Jamaica
Insulæ Caribæ
Bermudes
Panama
Scotia
Hibernia
Mare Germanicum
ANGLIA
GERMANIA
Livonia
MOSCOVIA
FRANCIA
HISPANIA
MARE MEDITERRANEUM
ITALIA
GRECIA
PONTUS EUXINUS
MARE CASPIUM
TARTARIA
PERSIA
Imperium MOGOLIS
INDIA
CHINA
COREA
JAPONIA
YEDSO
BARBARIA
MAROCCO
BILLEDULGERID
AFRICA
Senega
Mandinga
GUINEA
Benin
Congo
ÆGYPTUS
ARABIA
ALANA
ÆTHIOPIA
Zanguebar
Malabar
Coromandel
Bengala
Ceylon
SIAM
Philippinæ
BORNEO
Nova Guinea
Malacca & Procella
Ascension
MARE ÆTHIOPICUM
Angola
Monomotapa
Cabo B. Spei
C. das Aguilhas
Madagascar
OCEANUS INDICUS
HOLLANDIA NOVA
MARE PACIFICUM
PERU
CHILI
Arica
Conception
PARAGUAI
R. Grande
BRASILIA
Frio
AMERICA
OCEANUS ATLANTICUS
Fretum Magellanes
Terra Ignis
Linea expers Declinationis

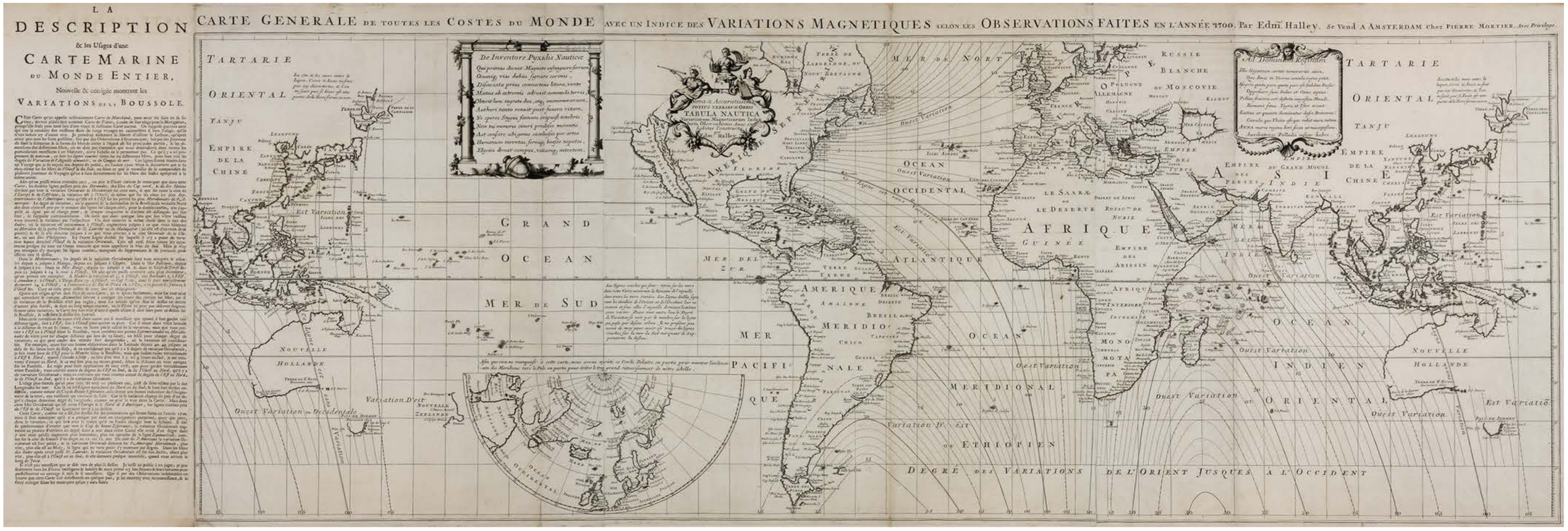
LA DESCRIPTION
& les Usages d'une
CARTE MARINE
DU MONDE ENTIER,
Nouvelle & corrigée montrant les
VARIATIONS DE LA BOUSSOLE.
CARTE GENERALE DE TOUTES LES COSTES DU MONDE AVEC UN INDICE DES VARIATIONS MAGNETIQUES SELON LES OBSERVATIONS FAITES EN L'ANNÉE 1700. Par Edm. Halley. Se Vend A AMSTERDAM Chez PIERRE MORTIER.
De Inventore Pyxidis Nauticae
TABULA NAUTICA
TARTARIE ORIENTAL
EMPIRE DE LA CHINE
GRAND OCEAN
MER DE SUD
NOUVELLE HOLLANDE
Ouest Variation
Est Variation
MER DE NORT
OCEAN OCCIDENTAL
MER DEL ZUR
MER PACIFIQUE
ATLANTIQUE
AMERIQUE MERIDIONALE
AFRIQUE
RUSSIE BLANCHE
EMPIRE DES TURCS
EMPIRE DES PERSES
INDE
ASIE
OCEAN INDIEN ORIENTAL
Variation D'est
DEGRÉ DES VARIATIONS DE L'ORIENT JUSQUES A L'OCCIDENT

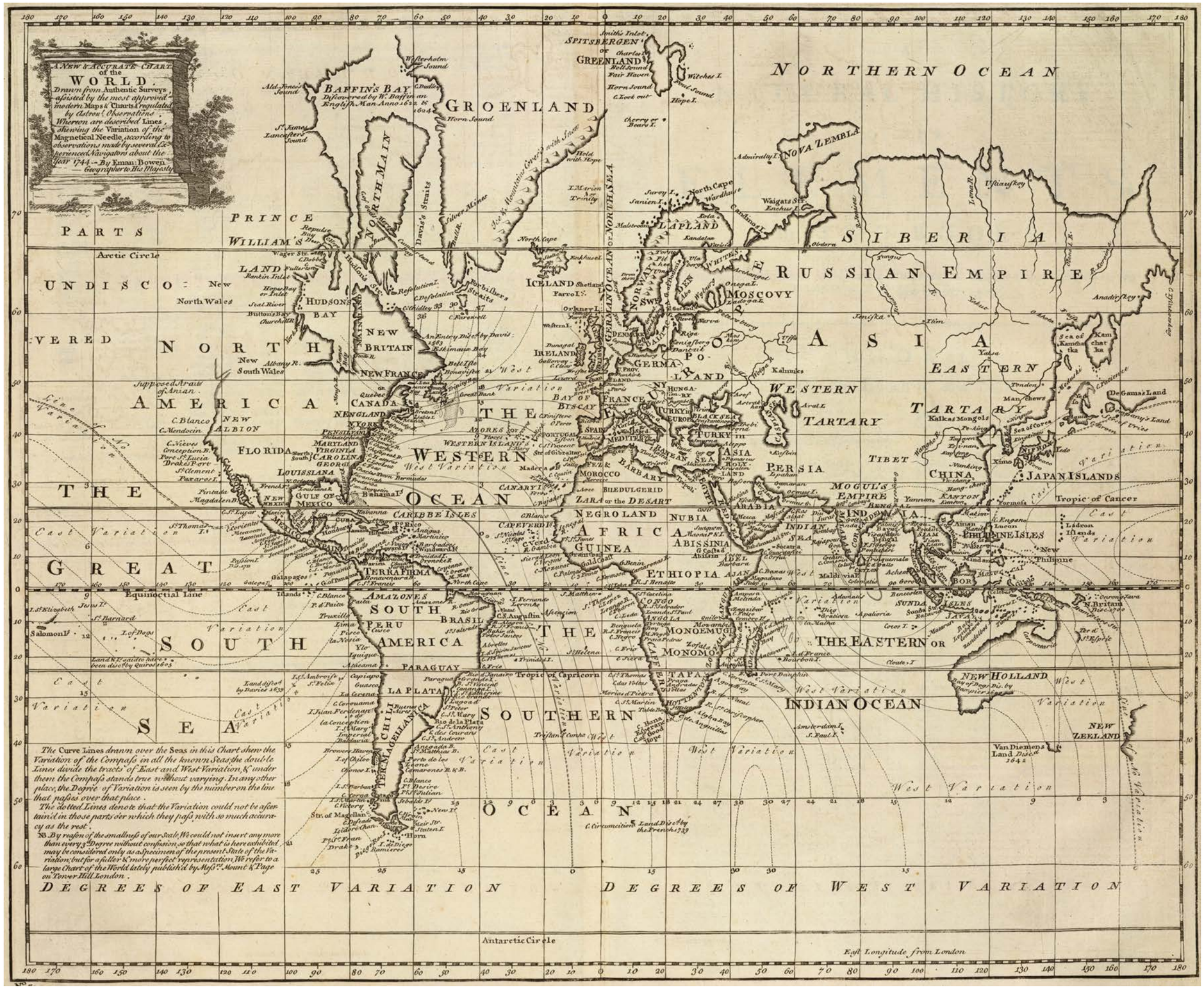
A New & Accurate Chart of the WORLD.
Drawn from Authentic Surveys, assisted by the most approved modern Maps & Charts regulated by Astron'l Observations; Wherein are described Lines shewing the Variation of the Magnetical Needle, according to observations made by several Experienced Navigators about the year 1744. — By Eman: Bowen Geographer to His Majesty.
NORTHERN OCEAN
GREENLAND
BAFFIN'S BAY
NORTH MAIN
PRINCE WILLIAM'S LAND
UNDISCOVERED NORTH AMERICA
HUDSON'S BAY
NEW BRITAIN
NEW FRANCE
CANADA
NEW ENGLAND
FLORIDA
LOUISIANA
GULF OF MEXICO
MEXICO
CARIBBE ISLES
TERRAFIRMA
AMAZONES
SOUTH AMERICA
PERU
BRASIL
PARAGUAY
LA PLATA
CHILI
TERRA MAGELLANICA
THE GREAT SOUTH SEA
THE WESTERN OCEAN
THE SOUTHERN OCEAN
ICELAND
IRELAND
GERMANY
FRANCE
SPAIN
PORTUGAL
MOROCCO
BARBARY
BIEDULGERID
LARA or the DESART
NEGROLAND
AFRICA
GUINEA
ETHIOPIA
CONGO
ANGOLA
MONOMOTAPA
HOTTENTOTS
NUBIA
ABISSINIA
ARABIA
INDIA
PERSIA
TURKY
TURKY in EUROPE
BLACK SEA
MOSCOVY
LAPLAND
NOVA ZEMBLA
SPITSBERGEN or GREENLAND
RUSSIAN EMPIRE
SIBERIA
ASIA
EASTERN TARTARY
WESTERN TARTARY
TIBET
CHINA
JAPAN ISLANDS
MOGUL'S EMPIRE
INDIA
PHILIPPINE ISLES
THE EASTERN OR INDIAN OCEAN
NEW HOLLAND
NEW ZEELAND
Van Diemen's Land Disc'd 1642
Tropic of Cancer
Tropic of Capricorn
Equinoctial Line
Arctic Circle
Antarctic Circle
East Longitude from London
The Curve Lines drawn over the Seas in this Chart shew the Variation of the Compass in all the known Seas; the double Lines divide the tracts of East and West Variation, & under them the Compass stands true without varying. In any other place, the Degree of Variation is seen by the number on the line that passes over that place.
The dotted Lines denote that the Variation could not be ascertained in those parts over which they pass, with so much accuracy as the rest.
NB. By reason of the smallness of our Scale, We could not insert any more than every 5 Degree without confusion, so that what is here exhibited may be considered only as a Specimen of the present State of the Variation; but for a fuller & more perfect representation, We refer to a large Chart of the World lately published by Mess.rs Mount & Page on Tower Hill London.
DEGREES OF EAST VARIATION
DEGREES OF WEST VARIATION

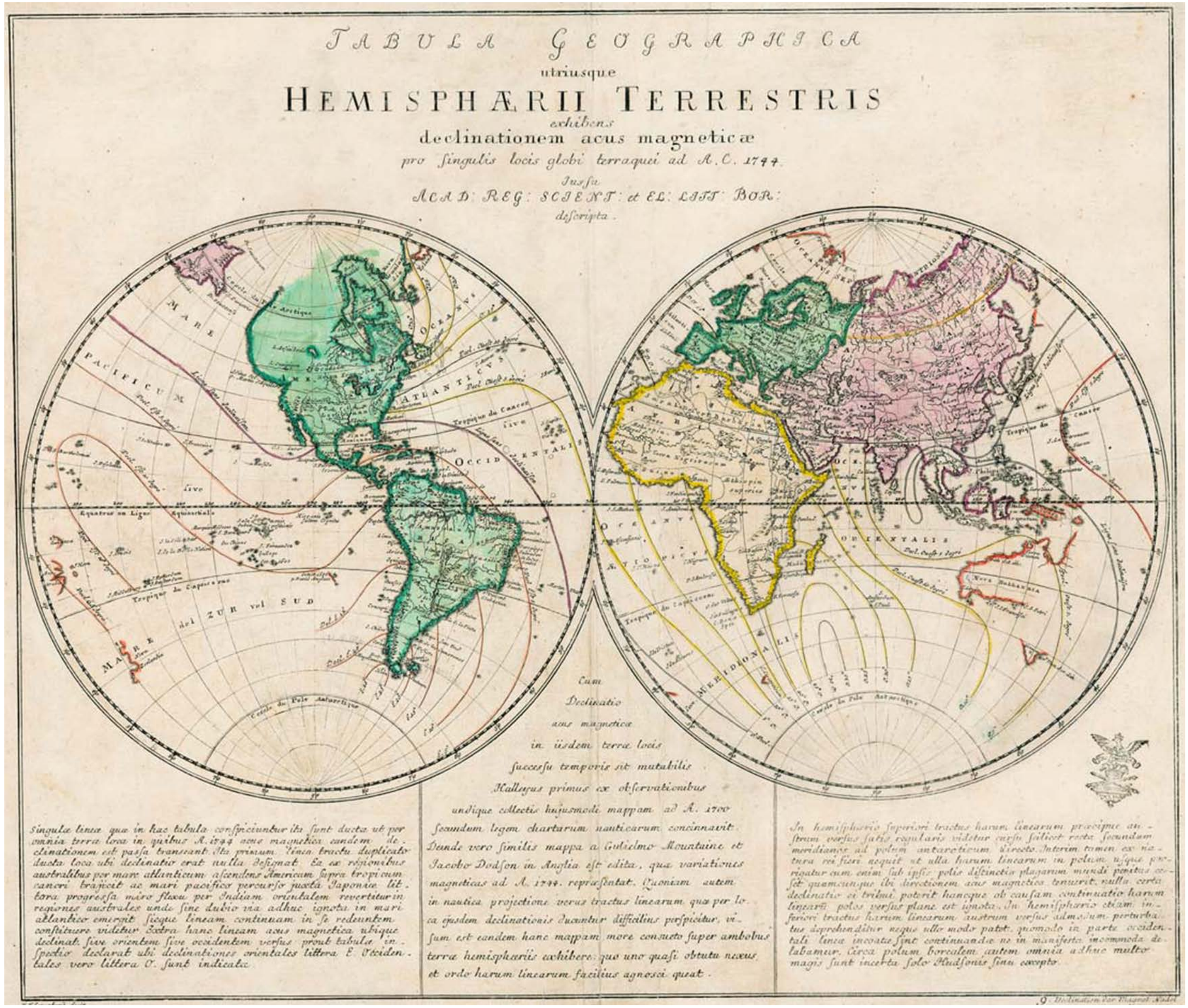
TABULA GEOGRAPHICA
utriusque
HEMISPHÆRII TERRESTRIS
exhibens
declinationem acus magneticæ
pro singulis locis globi terraquei ad A.C. 1744.
Jussu
ACAD: REG: SCIENT: et EL: LATT: BOR:
descripta.
MARE PACIFICUM
OCEANUS ATLANTICUS
OCCID
MARE del ZUR vel SUD
Equator ou Ligne
Equinoctiale
Tropique du Cancre
Tropique du Capricorne
Cercle du Pole Antarctique
OCEANUS ORIENTALIS
MERIDIONALIS
Cum
Declinatio
acus magnetica
in iisdem terræ locis
successu temporis sit mutabilis
Halleyus primus ex observationibus
undique collectis hujusmodi mappam ad A. 1700
secundum legem chartarum nauticarum concinnavit.
Deinde vero similis mappa a Gulielmo Mountaine et
Jacobo Dodson in Anglia est edita, qua variationes
magneticas ad A. 1744. repræsentat. Quoniam autem
in nautica projectione veras tractus linearum quæ per lo-
ca ejusdem declinationis ducuntur difficilius perspicitur, vi-
sum est eandem hanc mappam more consueto super ambobus
terræ hemisphæriis exhibere: quo uno quasi obtutu nexus
et ordo harum linearum facilius agnosci queat.
Singulæ linea quæ in hac tabula conspiciuntur ita sunt ducta ut per
omnia terræ loca in quibus A. 1744 acus magnetica eandem de-
clinationem est passa transeant. Sic primum linea tractu duplicato
ducta loca ubi declinatio erat nulla designat. Ea ex regionibus
australibus per mare atlanticum ascendens Americam supra tropicum
cancri bracicit ac mari pacifico percurso juxta Japonice lit-
tora progressa miro flexu per Indiam orientalem revertitur in
regiones australes unde sine dubio via adhuc ignota in mari
atlantico emergit sicque lineam continuam in se redeuntem
constituere videtur. Extra hanc lineam acus magnetica ubique
declinat sive orientem sive occidentem versus prout tabula in-
spectio declarat ubi declinationes orientales littera E. Occiden-
tales vero littera O. sunt indicata.
In hemisphærio superiori tractus harum linearum præcipue au-
strum versus satis regularis videtur cursu scilicet recta secundum
meridianos ad polum antarcticum directo. Interim tamen ex na-
tura rei fieri nequit ut ulla harum linearum in polum usque pro-
rigatur cum enim sub ipso polo distinctio plagarum mundi penitus ce-
sset quamcunque ibi directionem acus magnetica tenuerit, nulla certa
declinatio ei tribui poterit hanc que ob causam continuatio harum
linearum polos versus plane est ignota. In hemisphærio etiam in-
feriori tractus harum linearum austrum versus admodum perturba-
tus deprehenditur neque ullo modo patet quomodo in parte occiden-
tali lineæ incoatæ sint continuandæ ne in manifesta incommoda de-
labamur. Circa polum borealem autem omnia adhuc multo
magis sunt incerta solo Hudsonis sinu excepto.

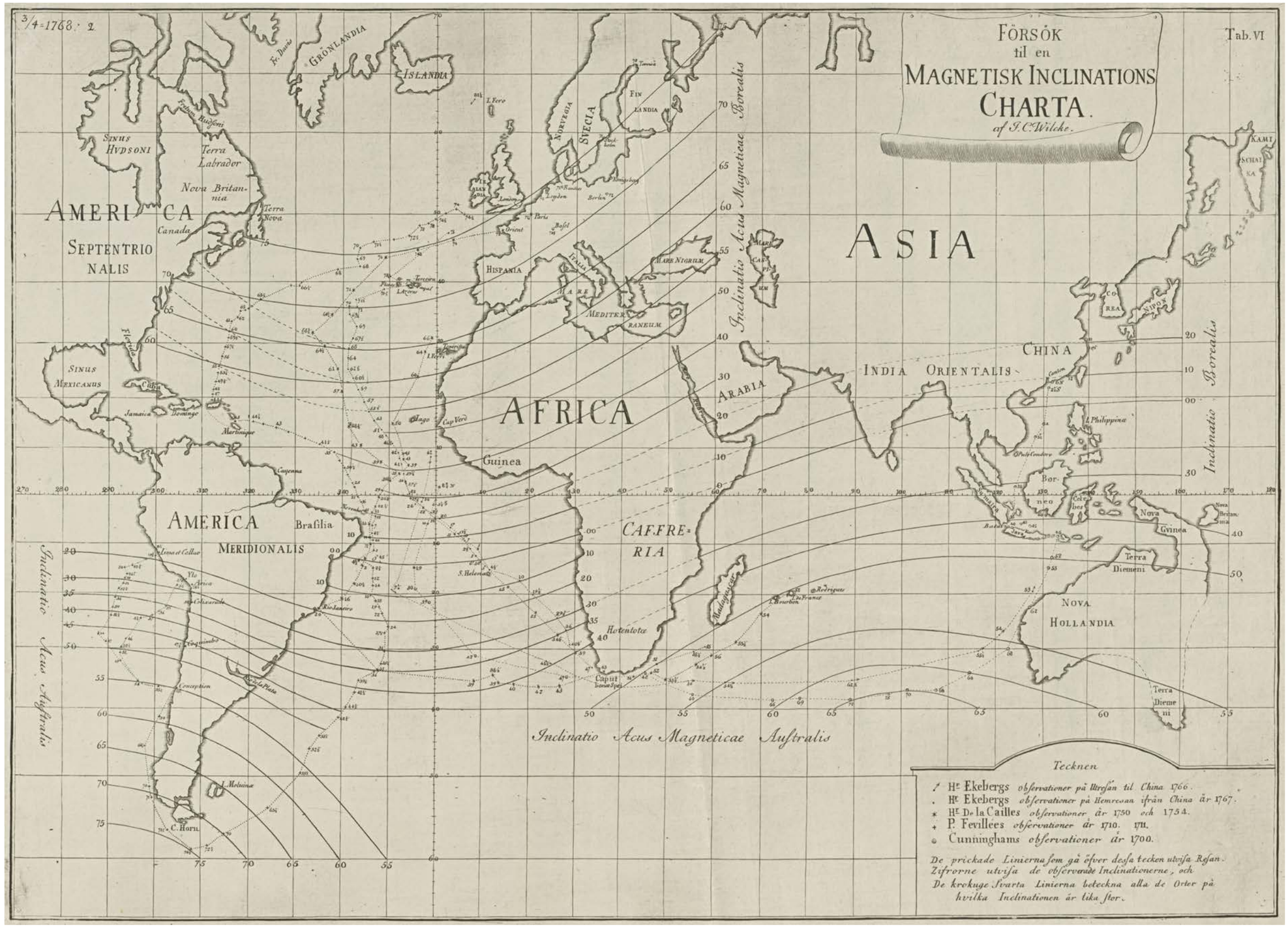
3/4-1768. 2
Tab. VI
FÖRSÖK
til en
MAGNETISK INCLINATIONS
CHARTA.
af J. C. Wilcke.
AMERICA
SEPTENTRIONALIS
ASIA
AFRICA
AMERICA
MERIDIONALIS
CAFFRERIA
NOVA
HOLLANDIA
CHINA
INDIA ORIENTALIS
ARABIA
GRÖNLANDIA
ISLANDIA
SVECIA
HISPANIA
Guinea
Brasilia
Hottentotæ
Inclinatio Acus Magneticae Borealis
Inclinatio Acus Magneticae Australis
Tecknen
Hr Ekebergs observationer på Utrefan til China 1766.
Hr Ekebergs observationer på Hemresan ifrån China år 1767.
Hr De la Cailles observationer år 1750 och 1754.
P. Fevillees observationer år 1710. 1711.
Cunninghams observationer år 1700.
De prickade Linierna som gå öfver dessa tecken utvisa Resan.
Siffrorne utvisa de observerade Inclinationerne, och
De krokige Svarta Linierna beteckna alla de Orter på
hvilka Inclinationen är lika stor.

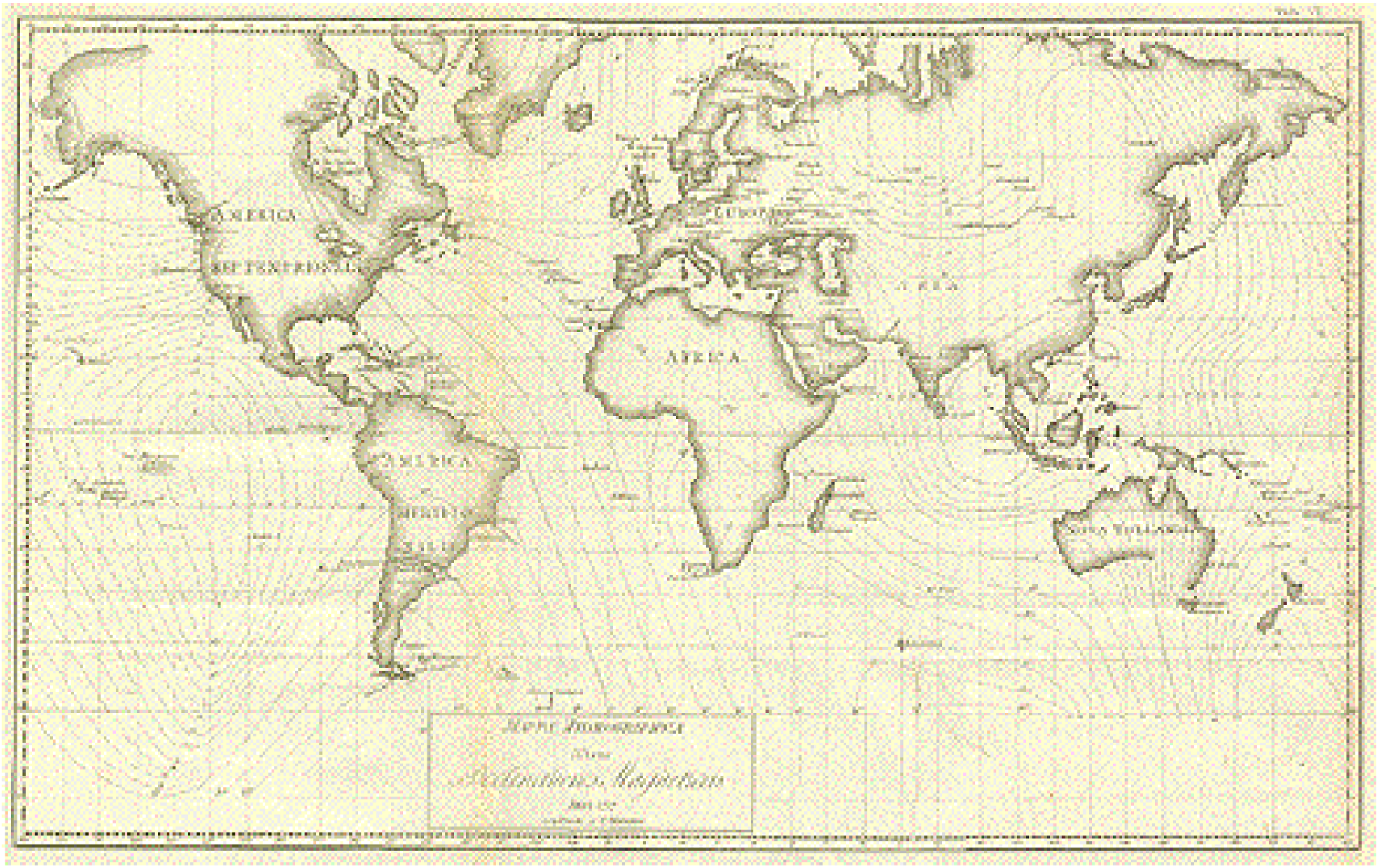
AMERICA
AMERICA
AFRICA
ASIA
EUROPA
NOVA HOLLANDIA

MAPPA HYDROGRAPHICA
Inclinationes Magneticas
AMERICA SEPTENTRIONALIS
EUROPA
AFRICA
AMERICA PERUVIA
NOVA HOLLANDIA

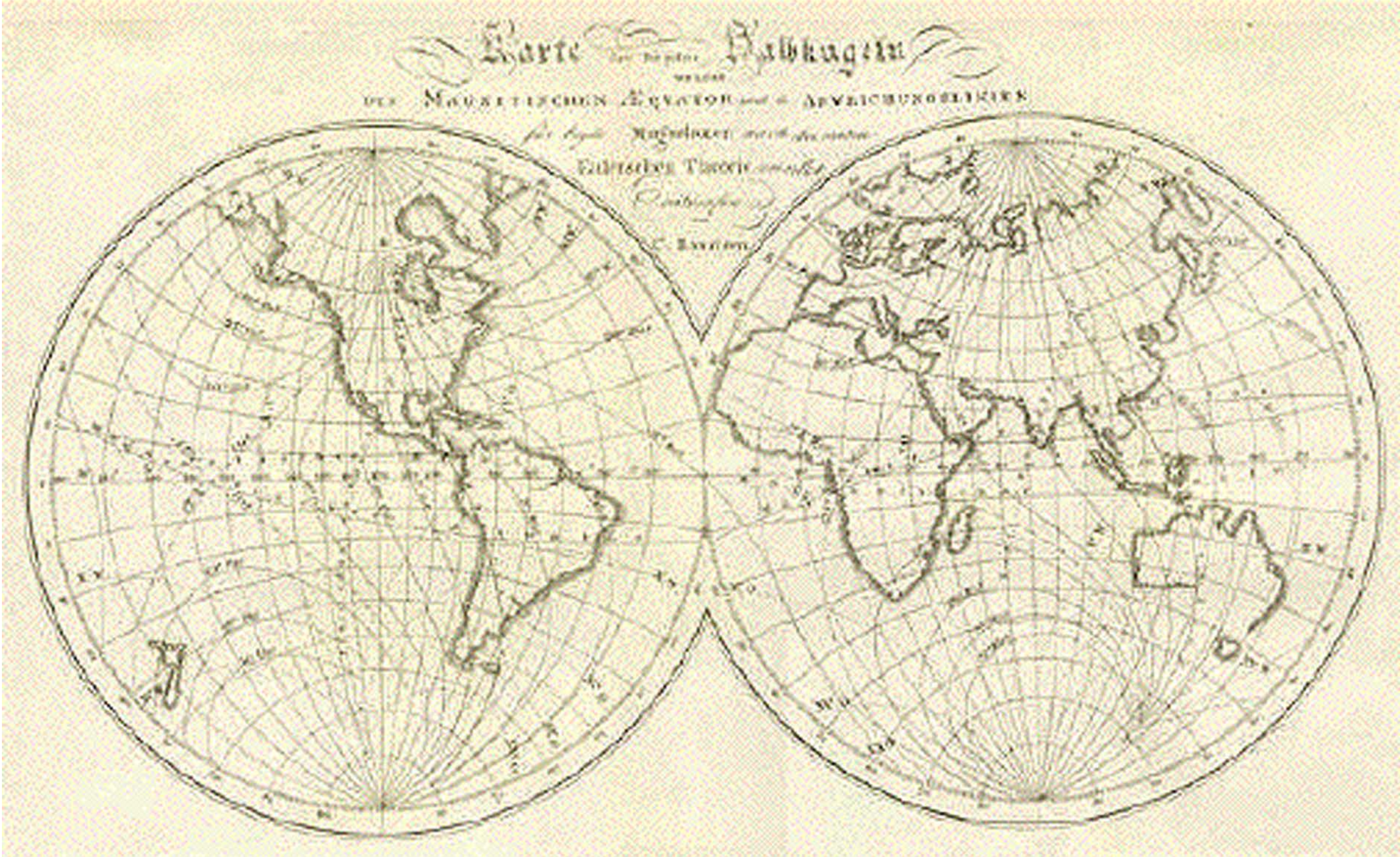
Karte
Abweichungslinien

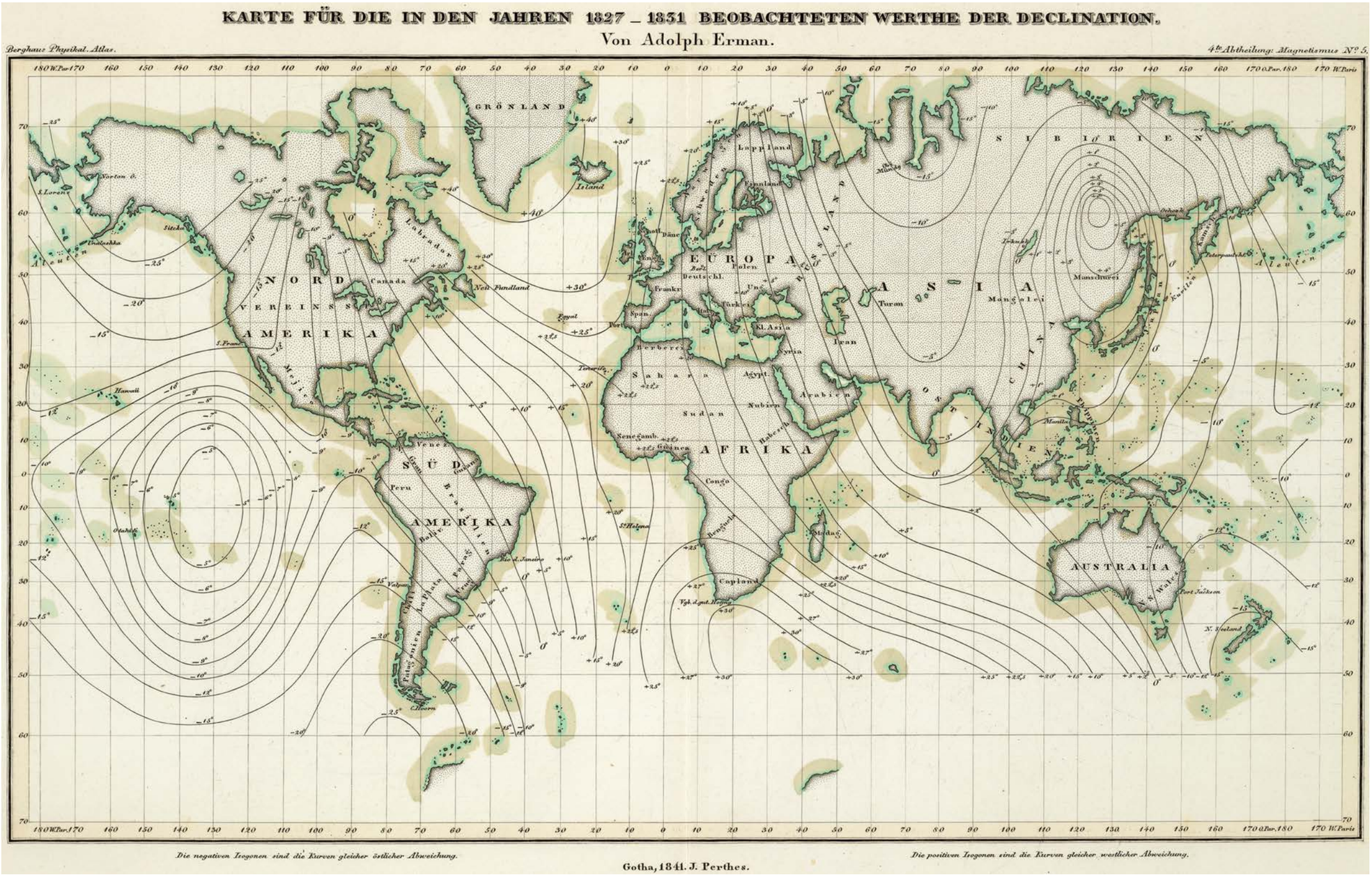
KARTE FÜR DIE IN DEN JAHREN 1827 – 1831 BEOBACHTETEN WERTHE DER DECLINATION.
Von Adolph Erman.
Berghaus Physikal. Atlas.
4te Abtheilung: Magnetismus No. 5.
GRÖNLAND
Island
NORD AMERIKA
Canada
Labrador
Neu Fundland
Norton ö.
Sitka
Unalaska
Aleuten
Hawaii
Mexico
Venez.
SÜD AMERIKA
Peru
Brasilien
Rio d. Janeiro
Patagonien
Chiloe
St. Helena
EUROPA
Lappland
Finnland
Schweden
Norwegen
Dänemark
Polen
Deutschl.
Frankr.
Span.
Port.
Türkei
Italien
Kl. Asien
Syrien
Egypt.
Nubien
Sudan
Senegamb.
Guinea
Congo
Capland
Madag.
AFRIKA
Sahara
Berberei
Arabien
Persien
Turan
Mongolei
Mandschurei
SIBIRIEN
Ochotsk
Kamtschatka
Tschukt.
Ostindien
Manilla
Philippinen
Japan
Kurile
Australien
Neu Wales
Port Jackson
N. Seeland
Die negativen Isogonen sind die Kurven gleicher östlicher Abweichung.
Die positiven Isogonen sind die Kurven gleicher westlicher Abweichung.
Gotha, 1841. J. Perthes.

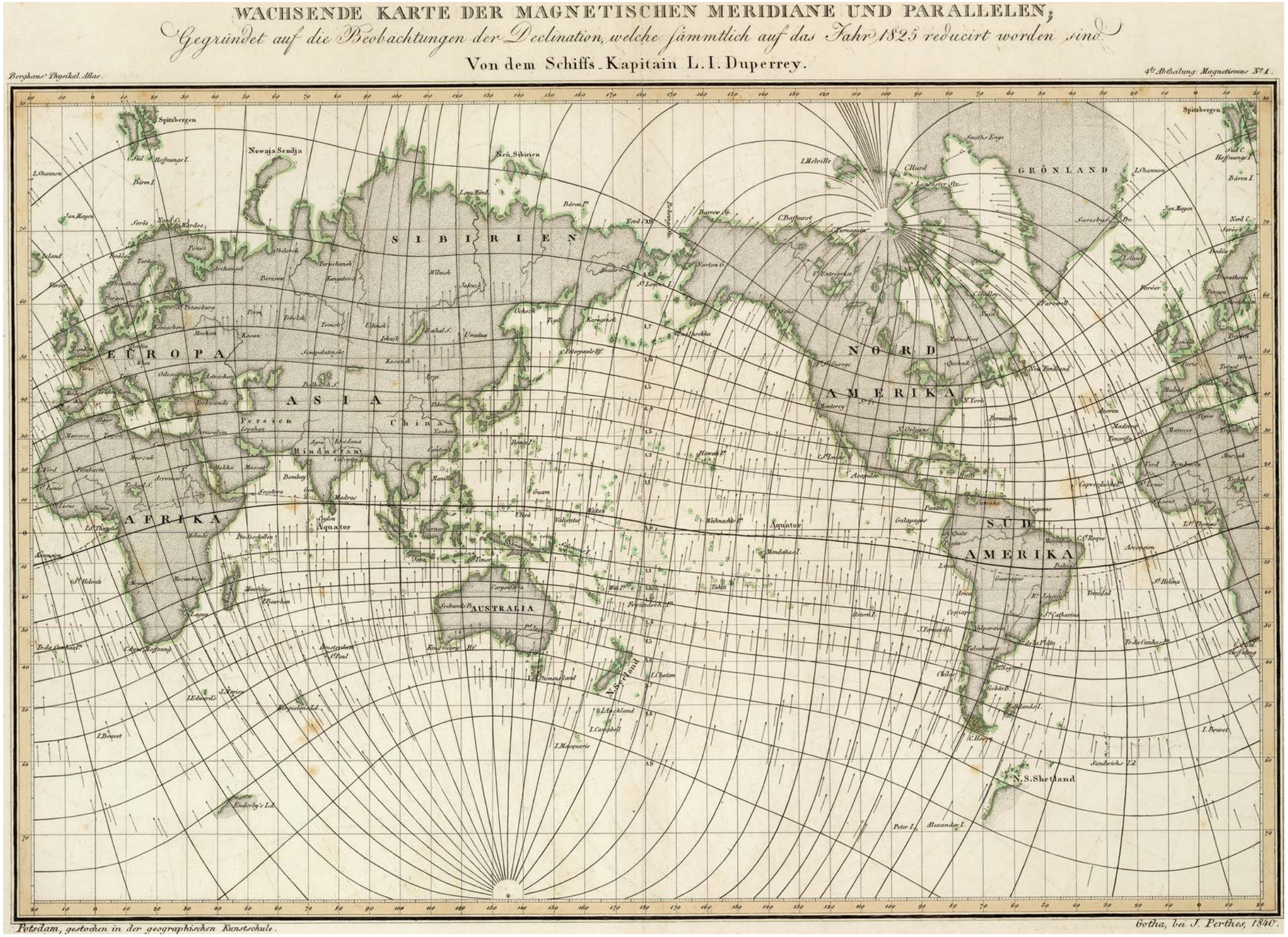
WACHSENDE KARTE DER MAGNETISCHEN MERIDIANE UND PARALLELEN;
Gegründet auf die Beobachtungen der Declination, welche sämmtlich auf das Jahr 1825 reducirt worden sind.
Von dem Schiffs-Kapitain L. I. Duperrey.
Berghaus' Physikal. Atlas.
4te Abtheilung: Magnetismus No 1.
SIBIRIEN
EUROPA
ASIA
AFRIKA
AUSTRALIA
GRÖNLAND
NORD AMERIKA
SÜD AMERIKA
Spitzbergen
Nowaja Semlja
Neü Sibirien
Hindustan
China
Persien
Äquator
N.S.Shetland
Potsdam, gestochen in der geographischen Kunstschule.
Gotha, bei J. Perthes, 1840.

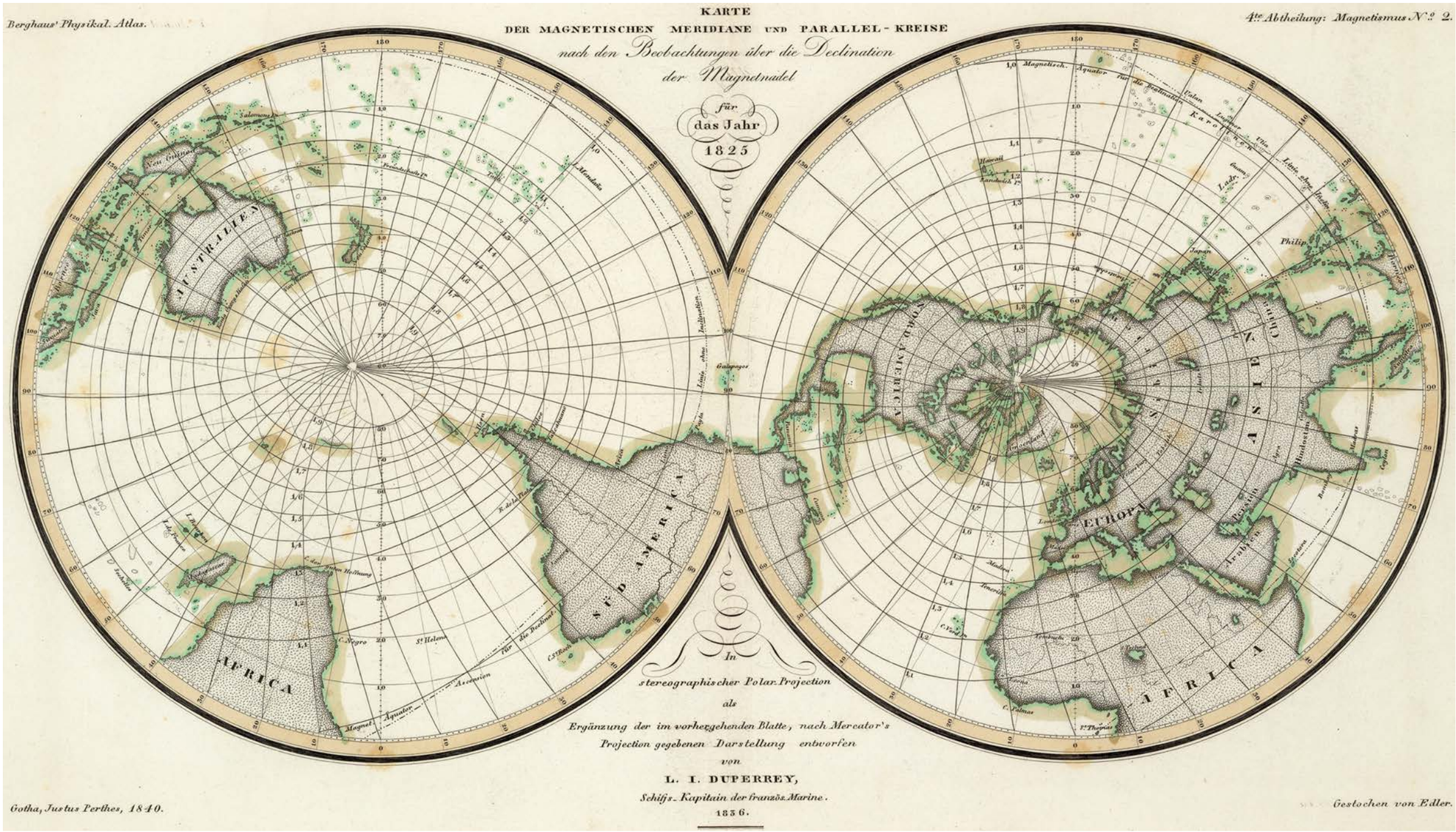
Berghaus' Physikal. Atlas.
4te Abtheilung: Magnetismus N.o 2.
KARTE
DER MAGNETISCHEN MERIDIANE UND PARALLEL-KREISE
nach den Beobachtungen über die Declination
der Magnetnadel
für
das Jahr
1825
In
stereographischer Polar-Projection
als
Ergänzung der im vorhergehenden Blatte, nach Mercator's
Projection gegebenen Darstellung entworfen
von
L. I. DUPERREY,
Schiffs-Kapitain der französ. Marine.
1836.
AUSTRALIEN
SÜD AMERICA
AFRICA
NORD AMERICA
EUROPA
ASIA
AFRICA
Gotha, Justus Perthes, 1840.
Gestochen von Edler.

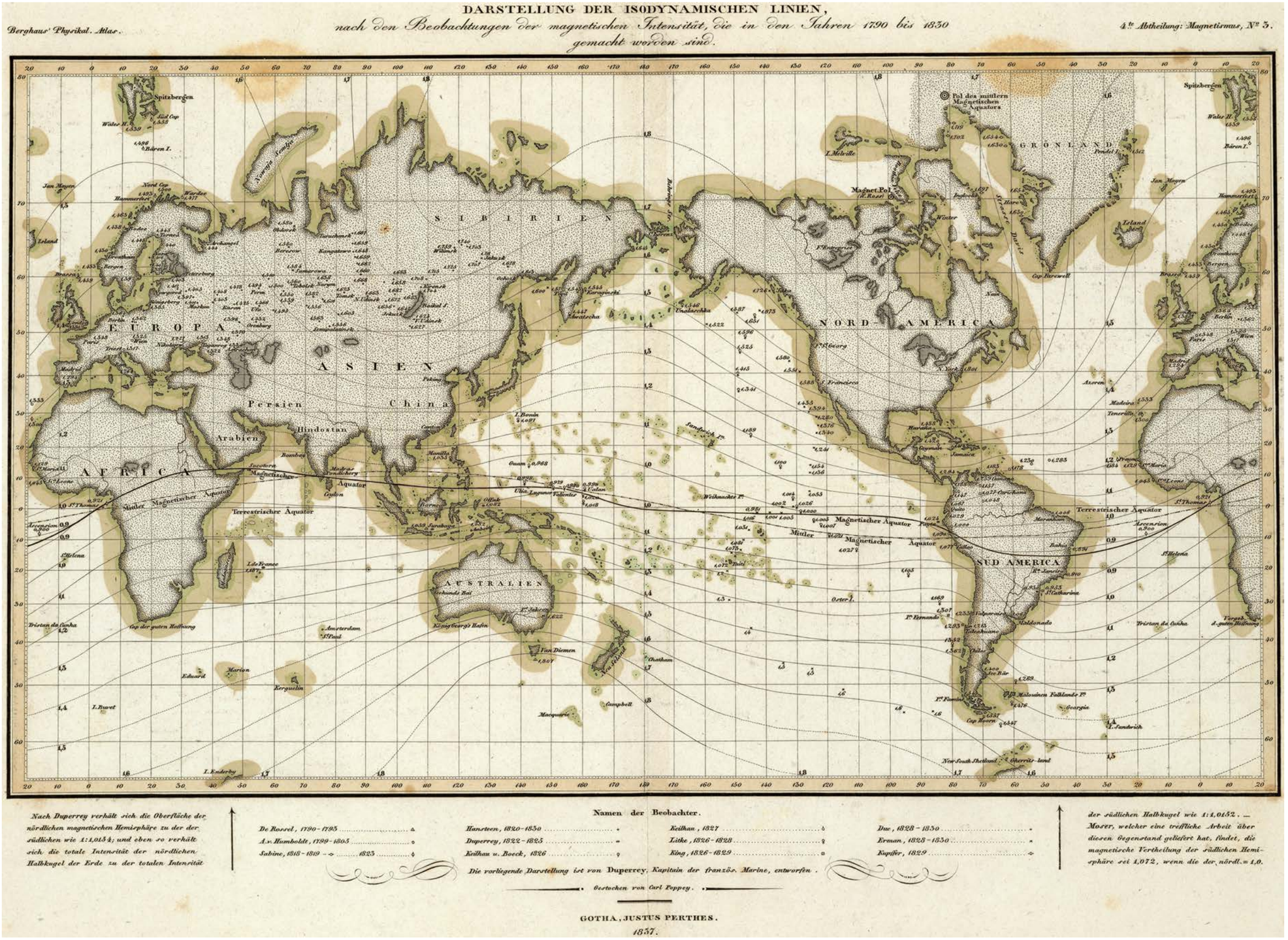
DARSTELLUNG DER ISODYNAMISCHEN LINIEN,
nach den Beobachtungen der magnetischen Intensität, die in den Jahren 1790 bis 1830 gemacht worden sind.
Berghaus' Physikal. Atlas.
4te Abtheilung: Magnetismus, No 3.
EUROPA
ASIEN
AFRICA
AUSTRALIEN
NORD AMERICA
SÜD AMERICA
GRÖNLAND
SIBIRIEN
China
Persien
Arabien
Hindostan
Terrestrischer Äquator
Magnetischer Äquator
Mittler Magnetischer Äquator
Pol des mittlern Magnetischen Äquators
Magnet. Pol
Nach Duperrey verhält sich die Oberfläche der nördlichen magnetischen Hemisphäre zu der der südlichen wie 1:1,015¼; und eben so verhält sich die totale Intensität der nördlichen Halbkugel der Erde zu der totalen Intensität der südlichen Halbkugel wie 1:1,0152. — Moser, welcher eine treffliche Arbeit über diesen Gegenstand geliefert hat, findet, die magnetische Vertheilung der südlichen Hemisphäre sei 1,072, wenn die der nördl. = 1,0.
Namen der Beobachter.
De Rossel, 1790-1795
A. v. Humboldt, 1799-1805
Sabine, 1818-1819 - 1825
Hansteen, 1820-1830
Duperrey, 1822-1825
Keilhau u. Boeck, 1826
Keilhau, 1827
Lütke, 1826-1828
King, 1826-1829
Due, 1828-1830
Erman, 1828-1830
Kupffer, 1829
Die vorliegende Darstellung ist von Duperrey, Kapitain der französ. Marine, entworfen.
Gestochen von Carl Poppey.
GOTHA, JUSTUS PERTHES.
1837.

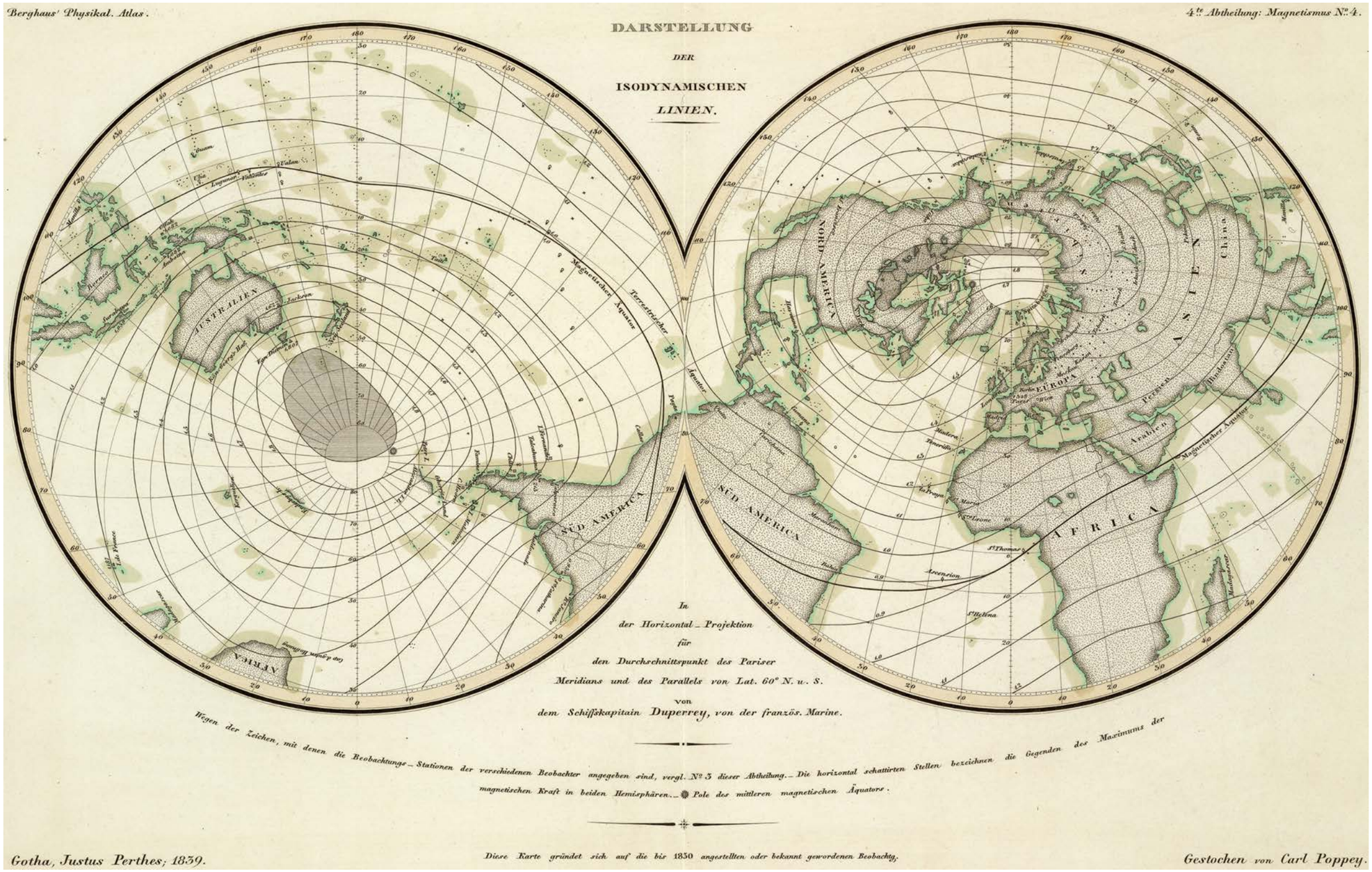
Berghaus' Physikal. Atlas.
4te Abtheilung: Magnetismus No. 4.
DARSTELLUNG
DER
ISODYNAMISCHEN
LINIEN.
In
der Horizontal-Projektion
für
den Durchschnittspunkt des Pariser
Meridians und des Parallels von Lat. 60° N. u. S.
von
dem Schiffskapitain Duperrey, von der französ. Marine.
Wegen der Zeichen, mit denen die Beobachtungs-Stationen der verschiedenen Beobachter angegeben sind, vergl. No. 3 dieser Abtheilung. – Die horizontal schattirten Stellen bezeichnen die Gegenden des Maximums der magnetischen Kraft in beiden Hemisphären. – Pole des mittleren magnetischen Äquators.
Gotha, Justus Perthes; 1839.
Diese Karte gründet sich auf die bis 1850 angestellten oder bekannt gewordenen Beobachtg.
Gestochen von Carl Poppey.
AUSTRALIEN
NORD AMERICA
SÜD AMERICA
EUROPA
ASIEN
China
Persien
Arabien
AFRICA
Magnetischer Äquator
Terrestrischer Äquator
Äquator

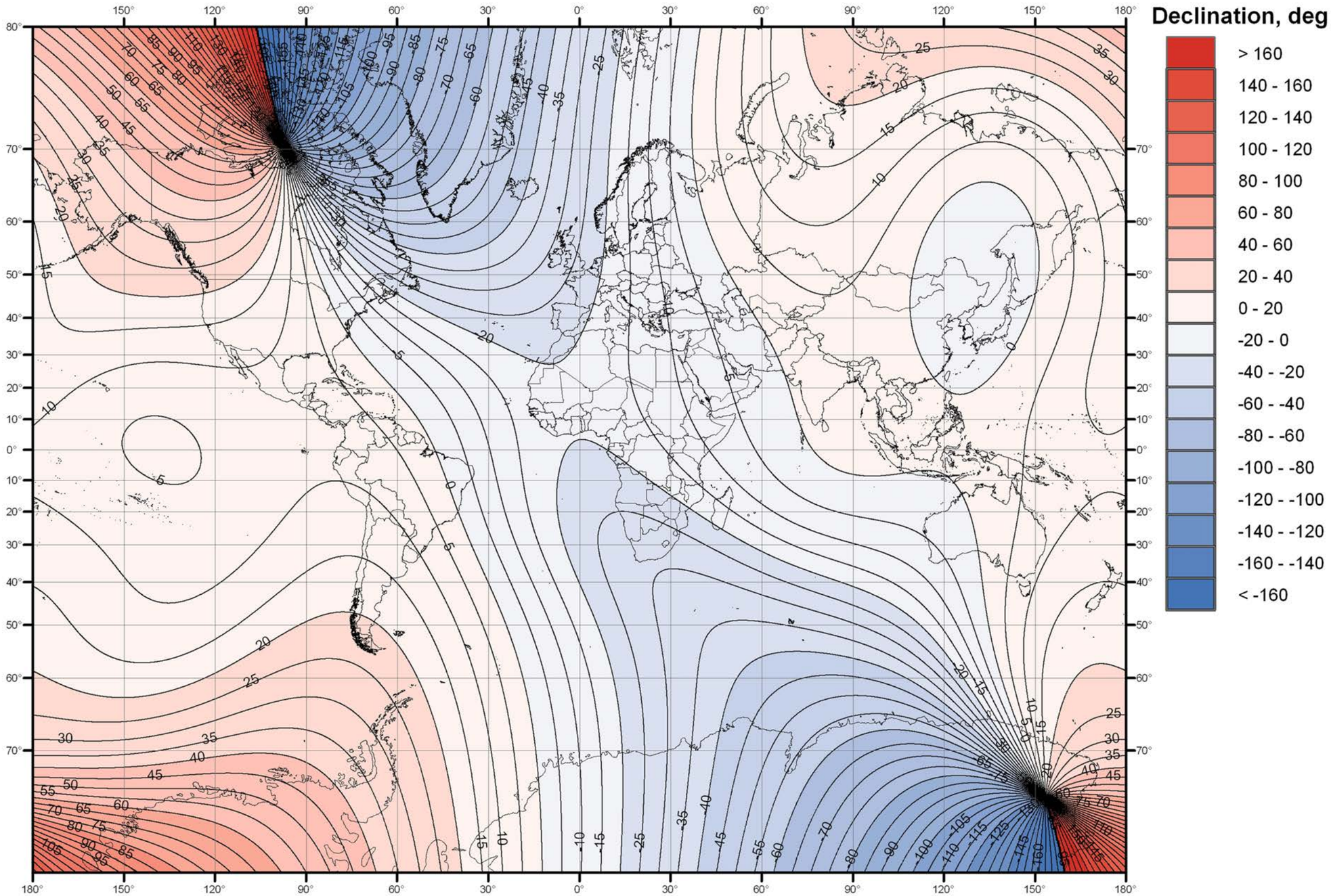
Declination, deg
> 160
140 - 160
120 - 140
100 - 120
80 - 100
60 - 80
40 - 60
20 - 40
0 - 20
-20 - 0
-40 - -20
-60 - -40
-80 - -60
-100 - -80
-120 - -100
-140 - -120
-160 - -140
< -160

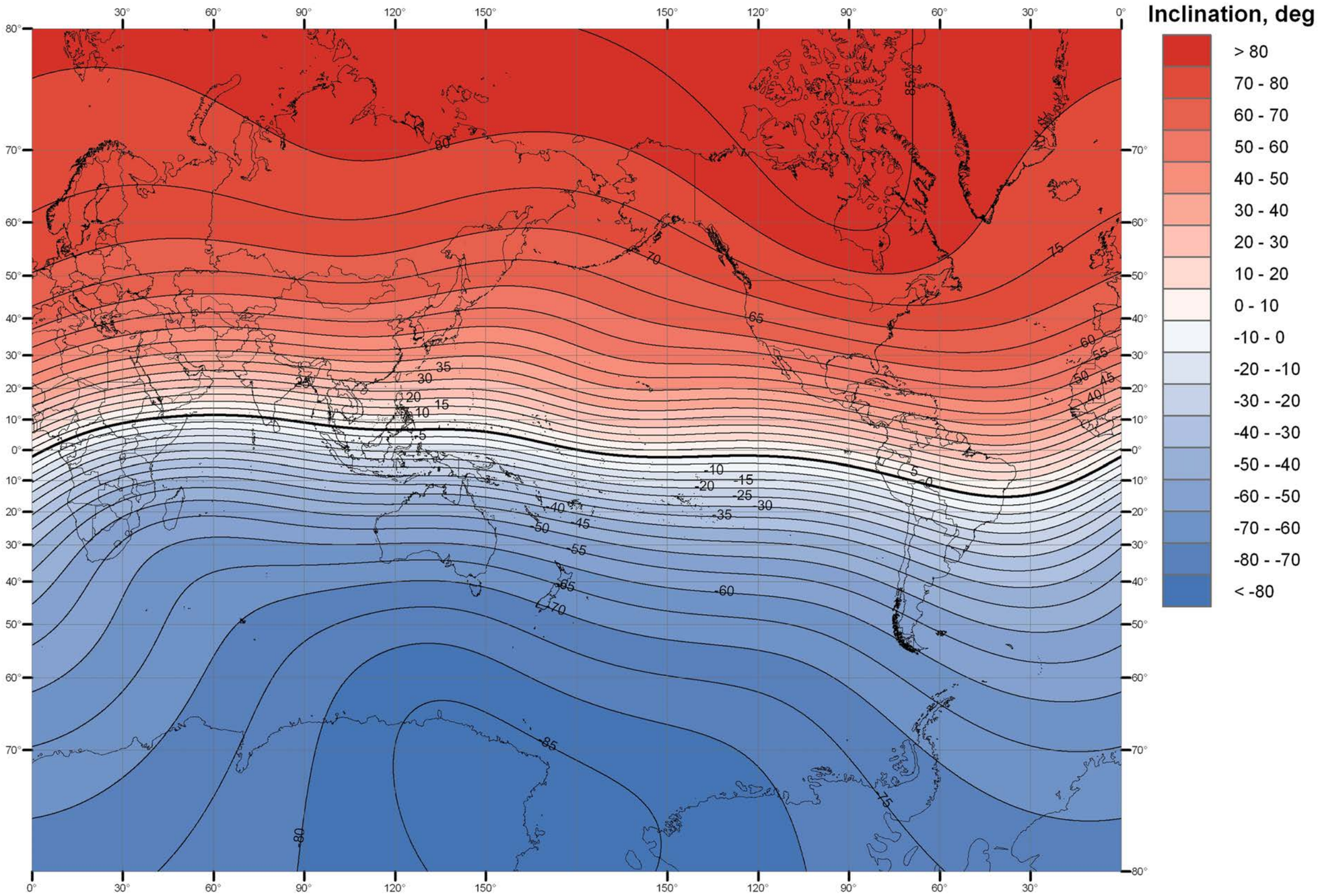
Inclination, deg
> 80
70 - 80
60 - 70
50 - 60
40 - 50
30 - 40
20 - 30
10 - 20
0 - 10
-10 - 0
-20 - -10
-30 - -20
-40 - -30
-50 - -40
-60 - -50
-70 - -60
-80 - -70
< -80

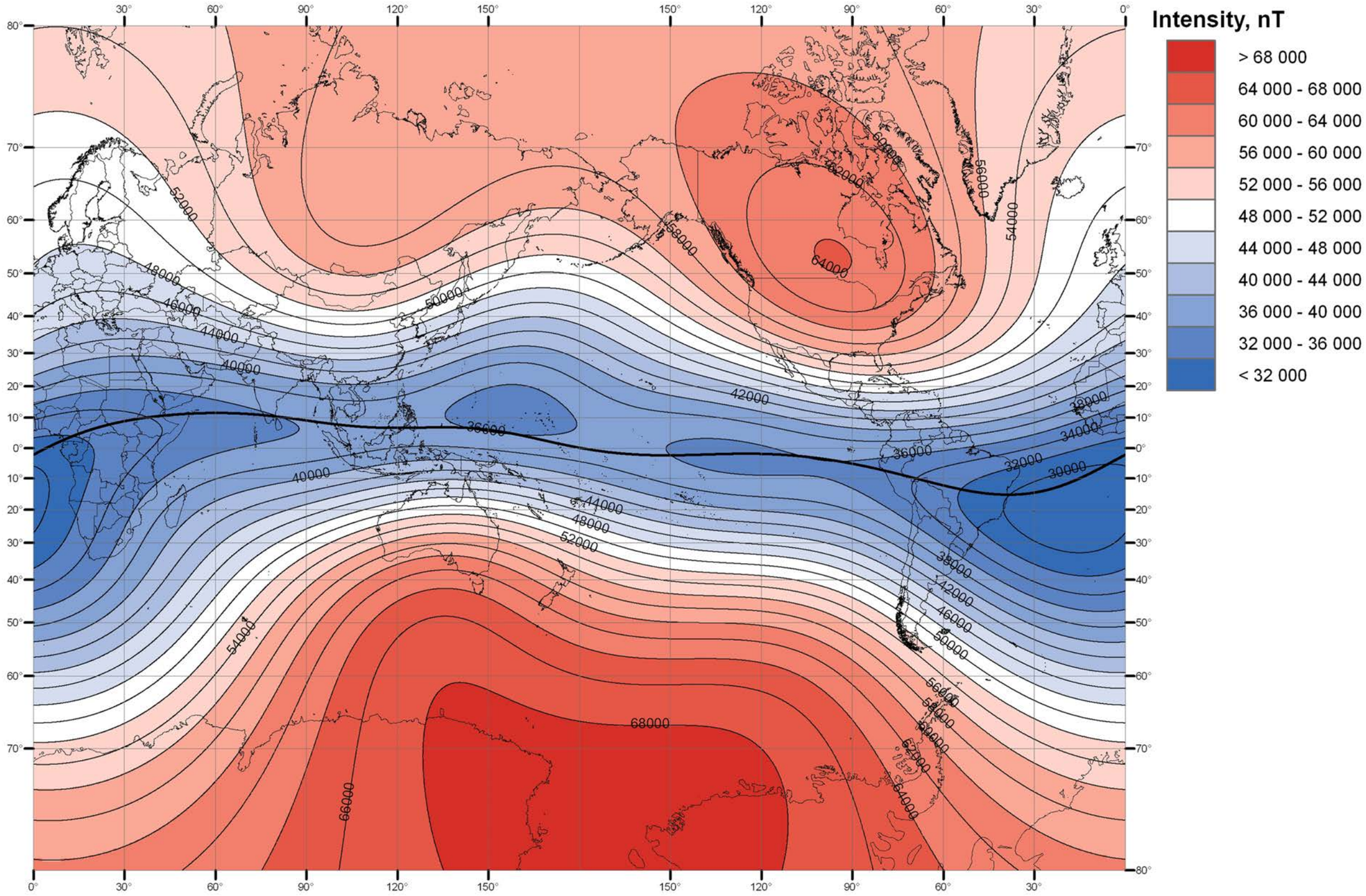
Intensity, nT
> 68 000
64 000 - 68 000
60 000 - 64 000
56 000 - 60 000
52 000 - 56 000
48 000 - 52 000
44 000 - 48 000
40 000 - 44 000
36 000 - 40 000
32 000 - 36 000
< 32 000

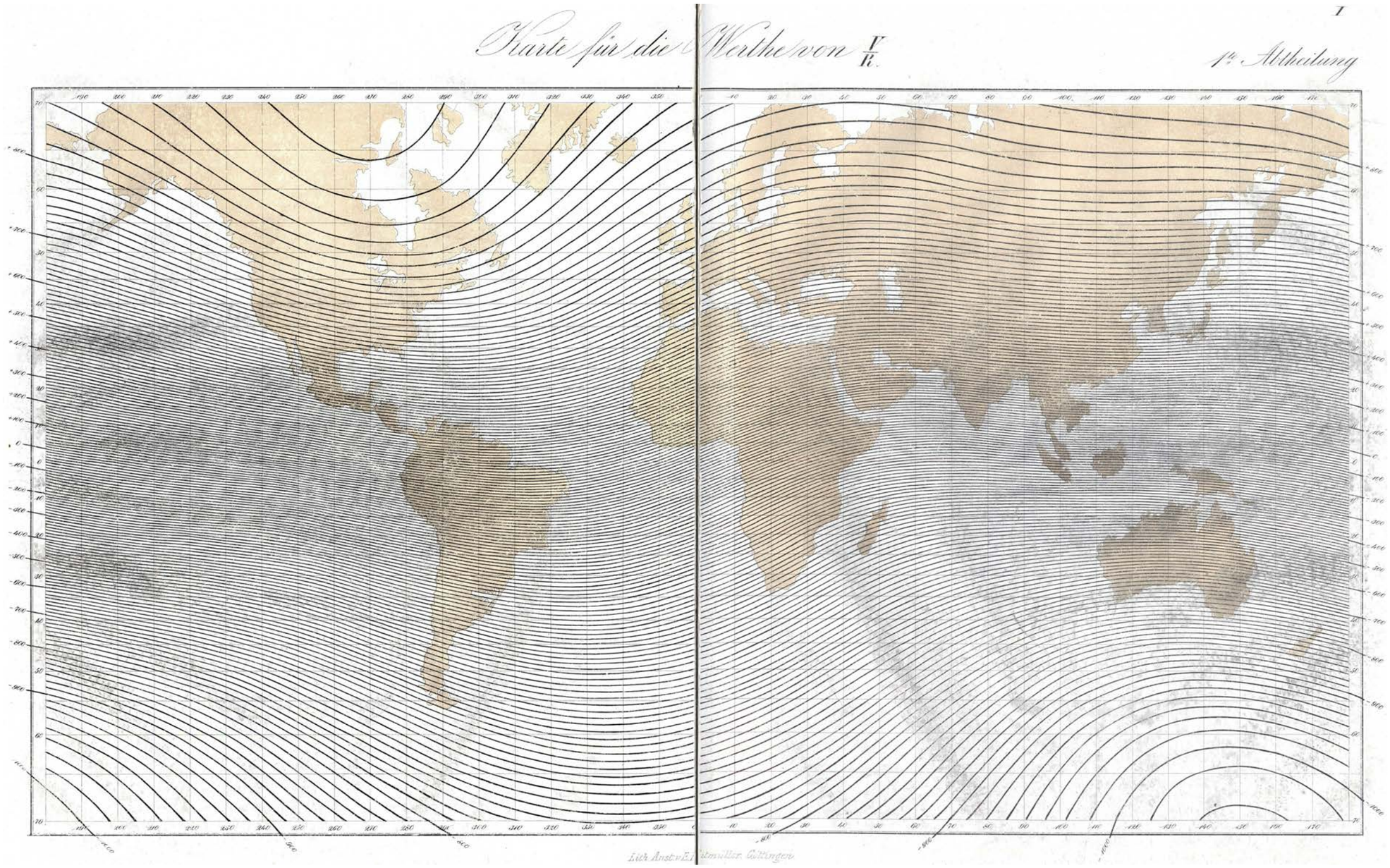

1. Map of the values of V/R (70°S–70°N).

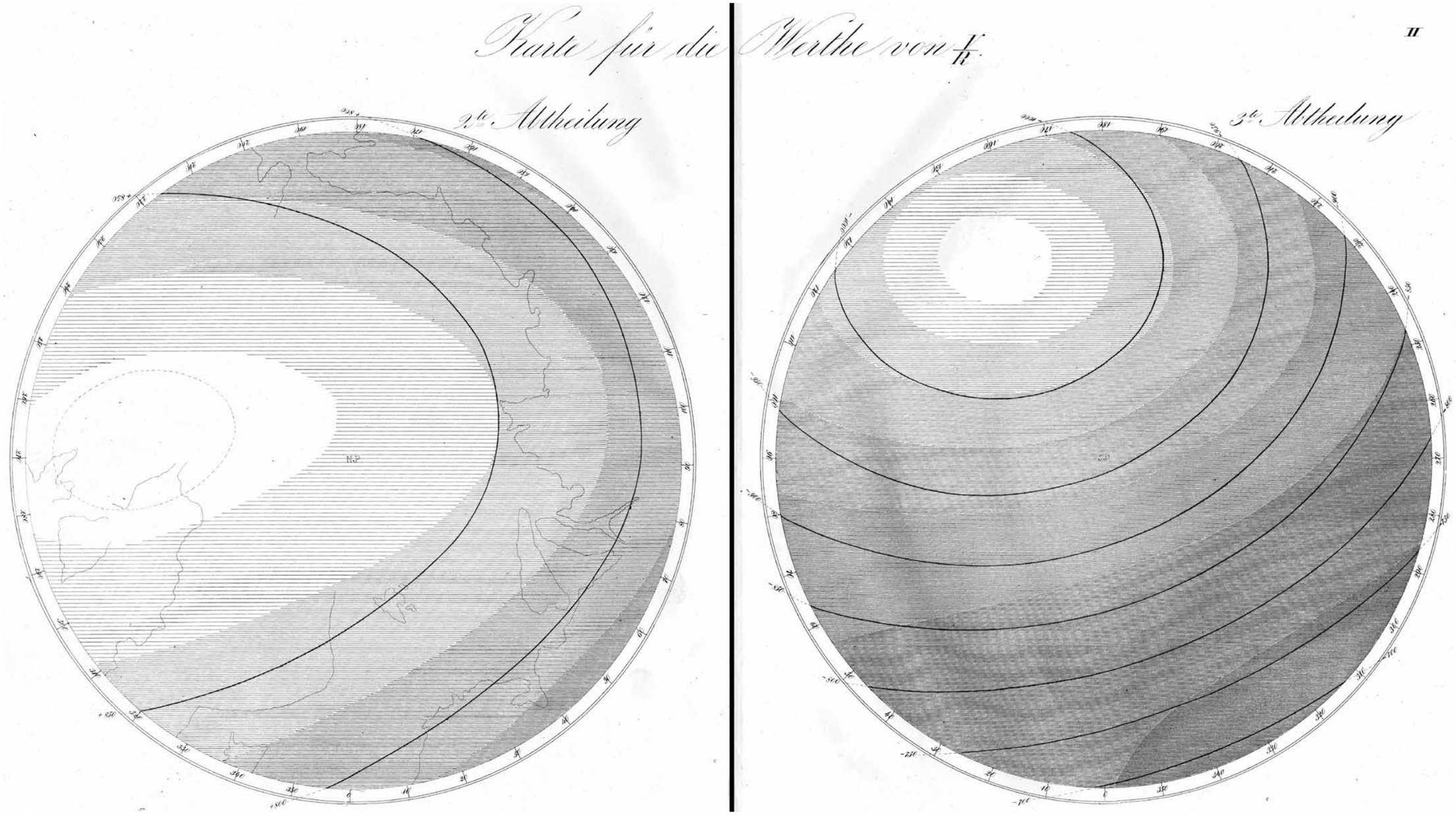

2. Map of the values of V/R (polar zones).

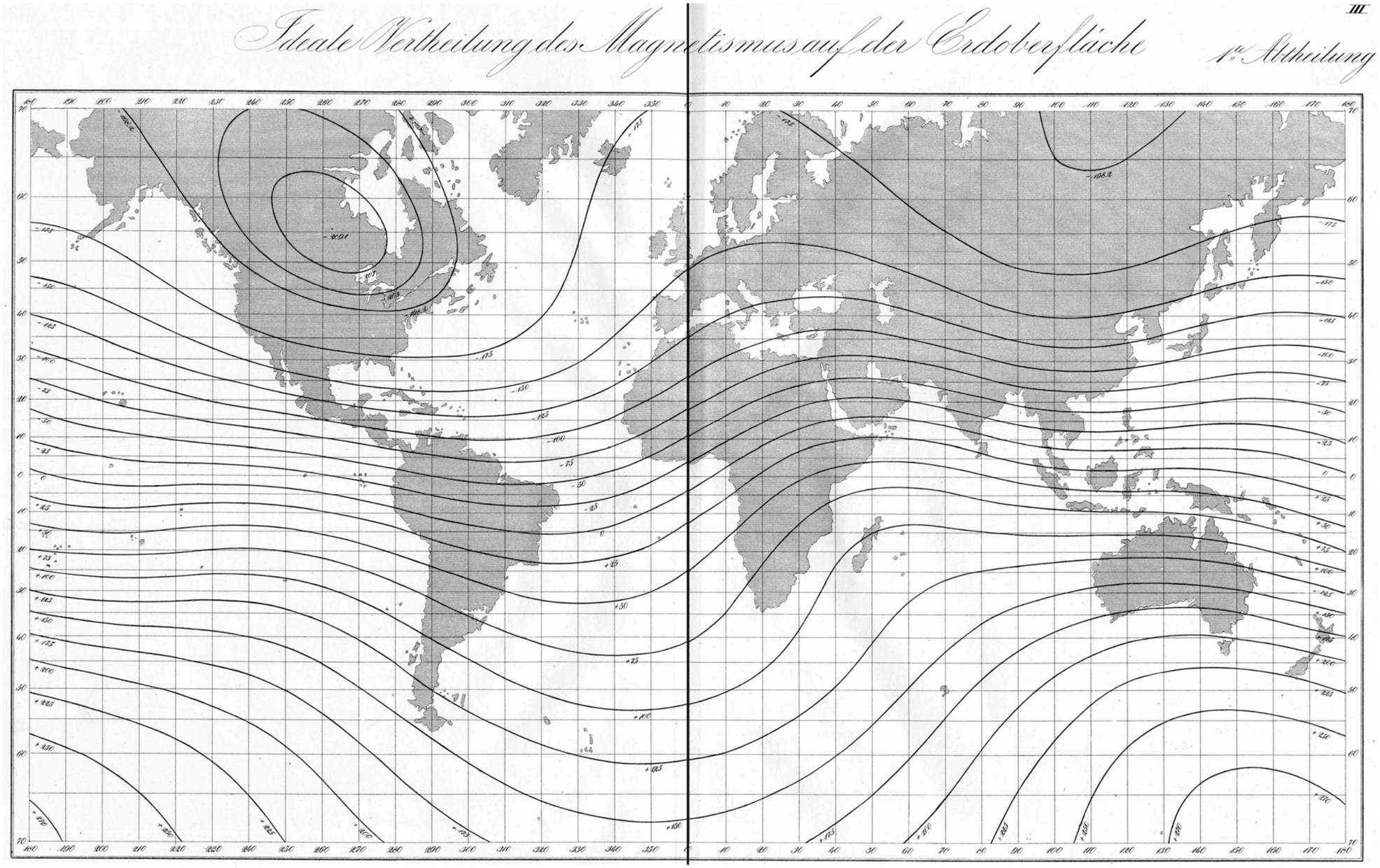

3. Ideal distribution of magnetism on the Earth's surface (70°S–70°N).

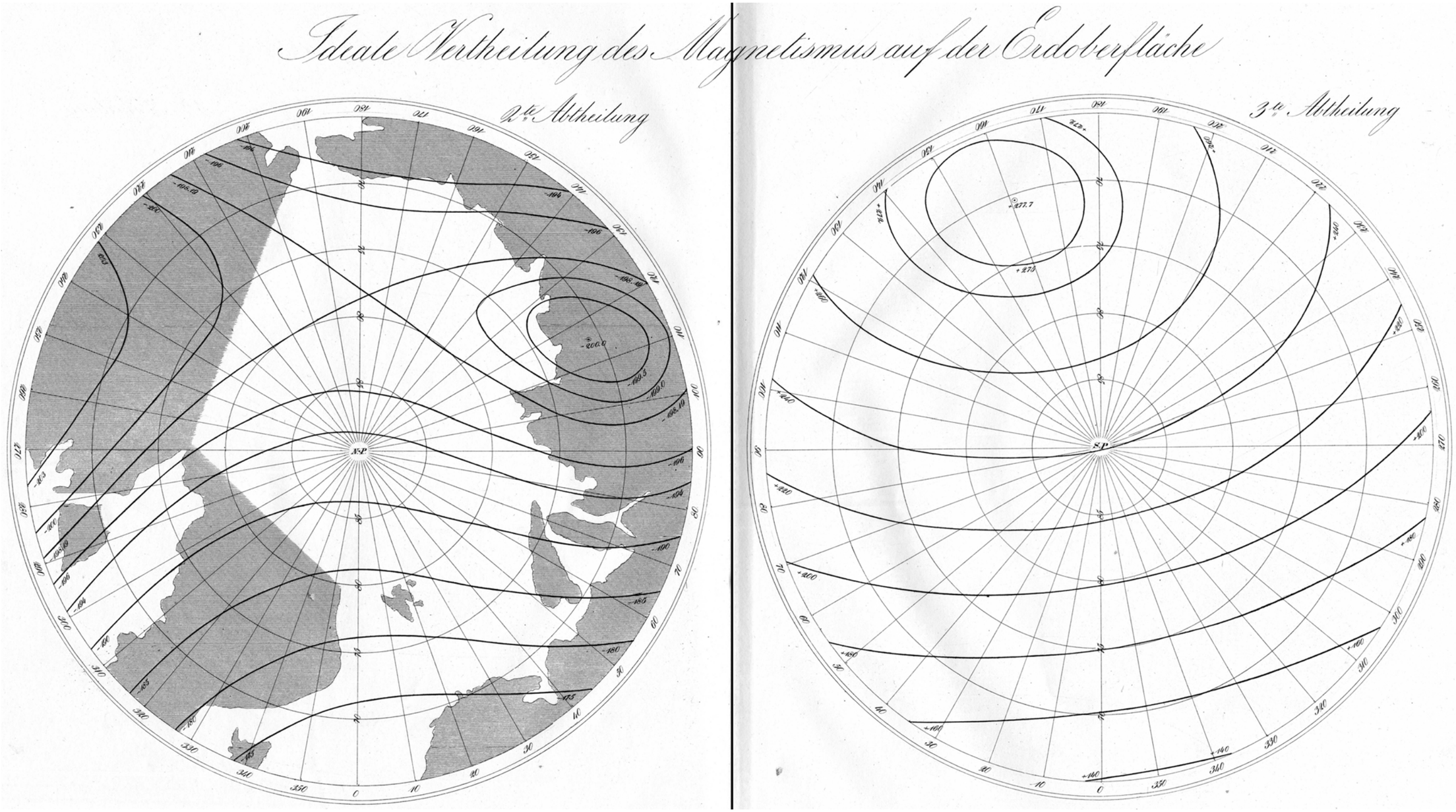

4. Ideal distribution of magnetism on the Earth's surface (polar zones).

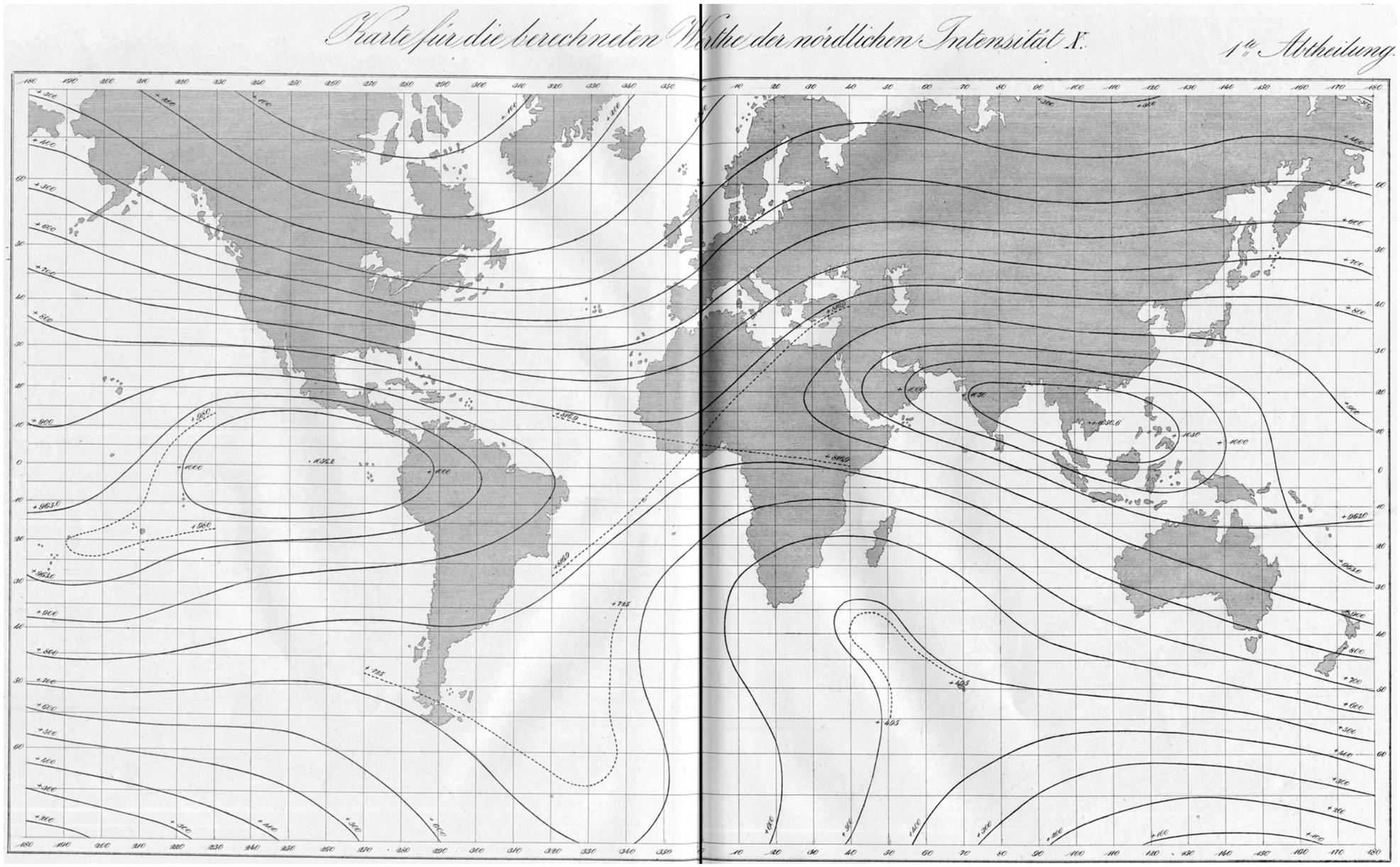

5. Map of the calculated values of the northward component X (70°S–70°N).

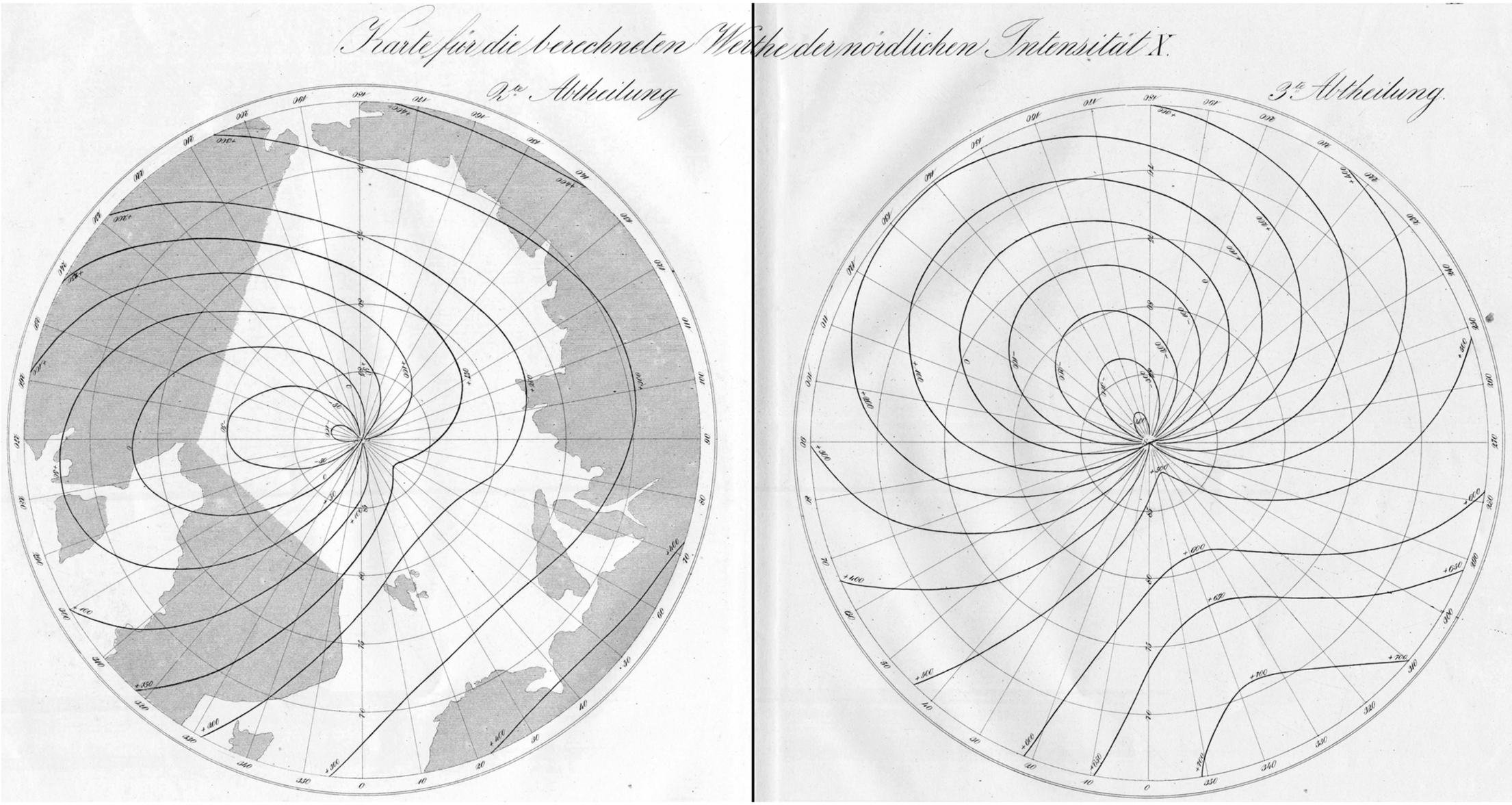

6. Map of the calculated values of the northward component X (polar zones).

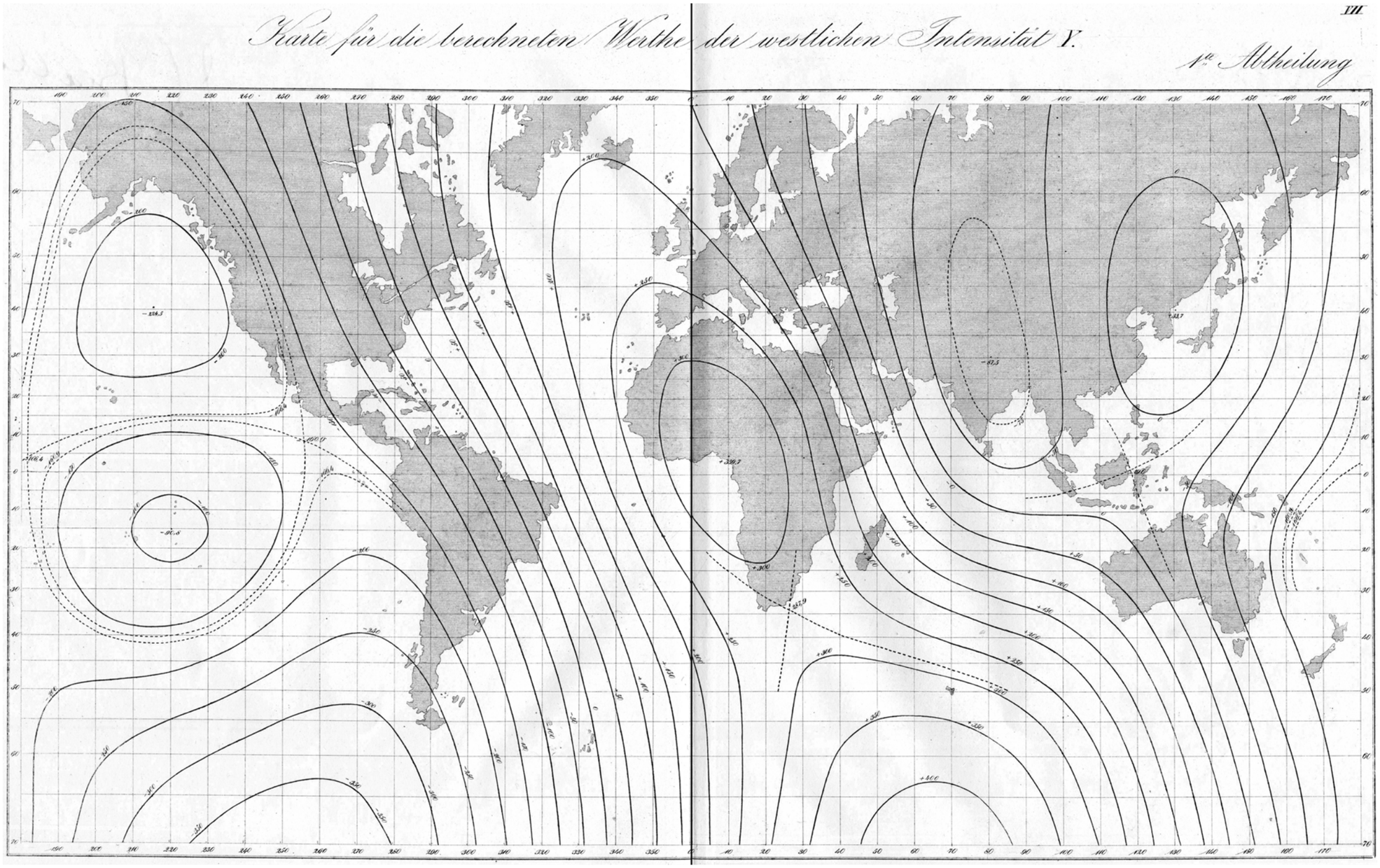

7. Map of the calculated values of the westward component Y (70°S–70°N).

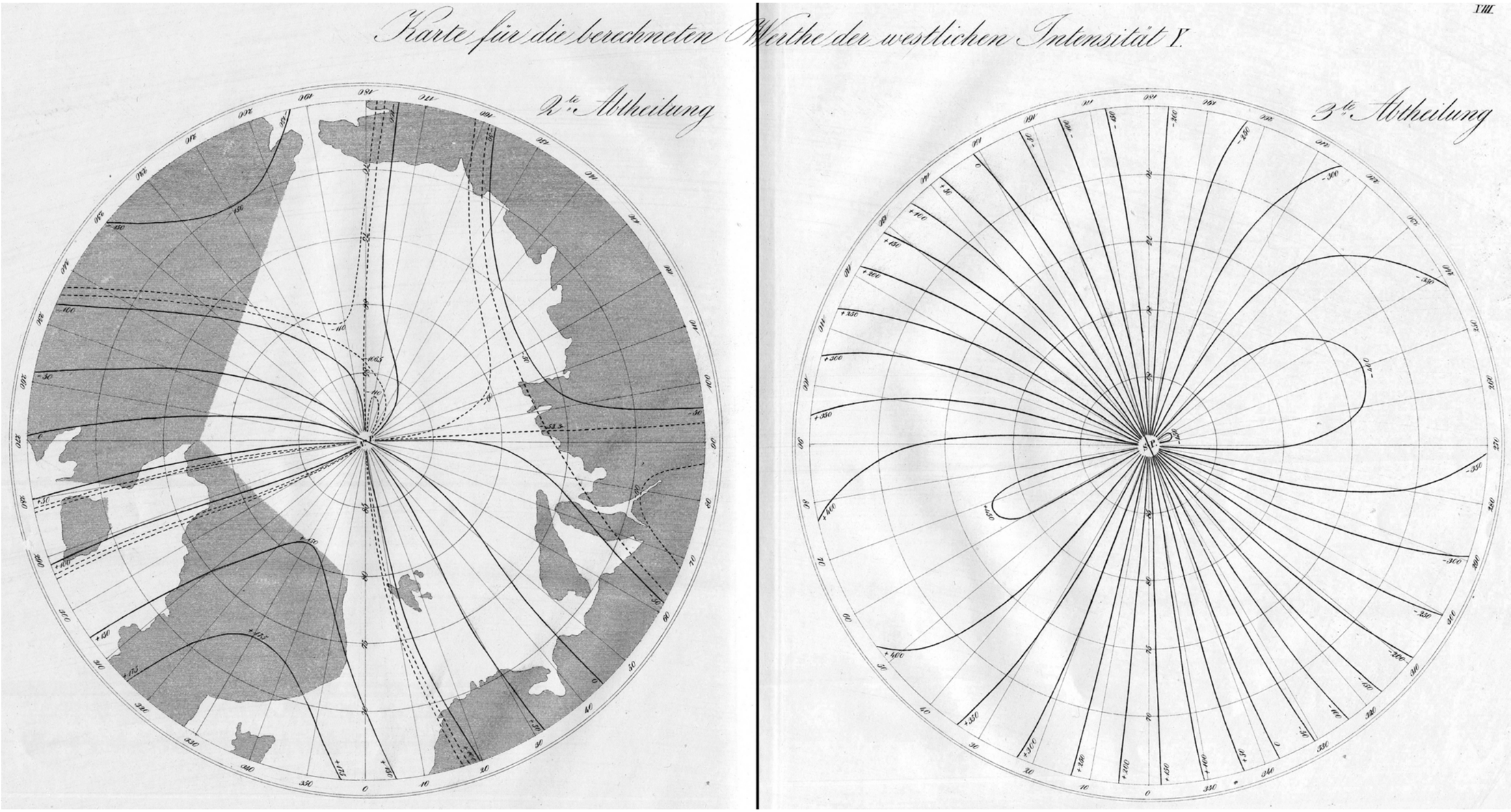

8. Map of the calculated values of the westward component Y (polar zones).

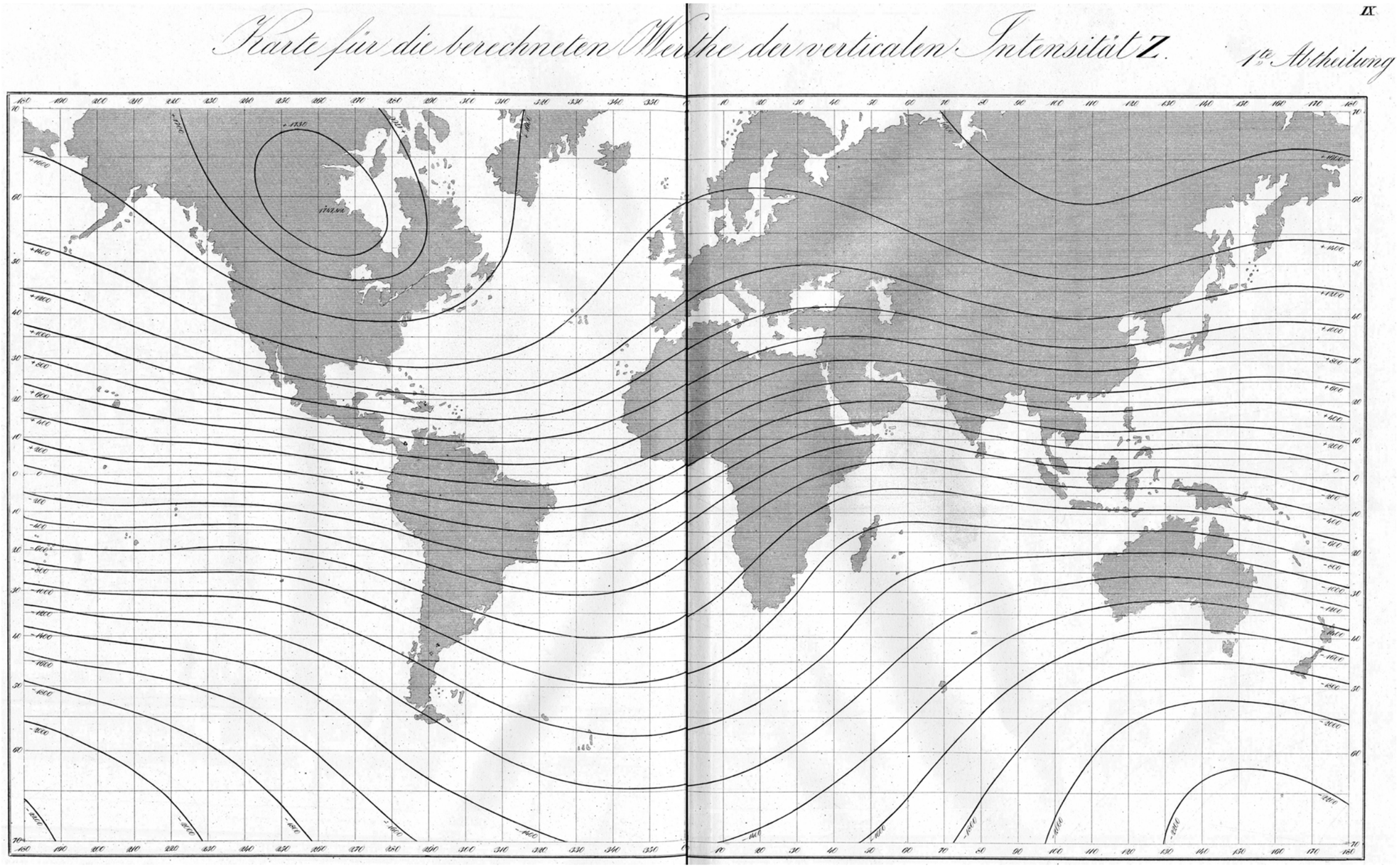

9. Map of the calculated values of the vertical component Z (70°S–70°N).

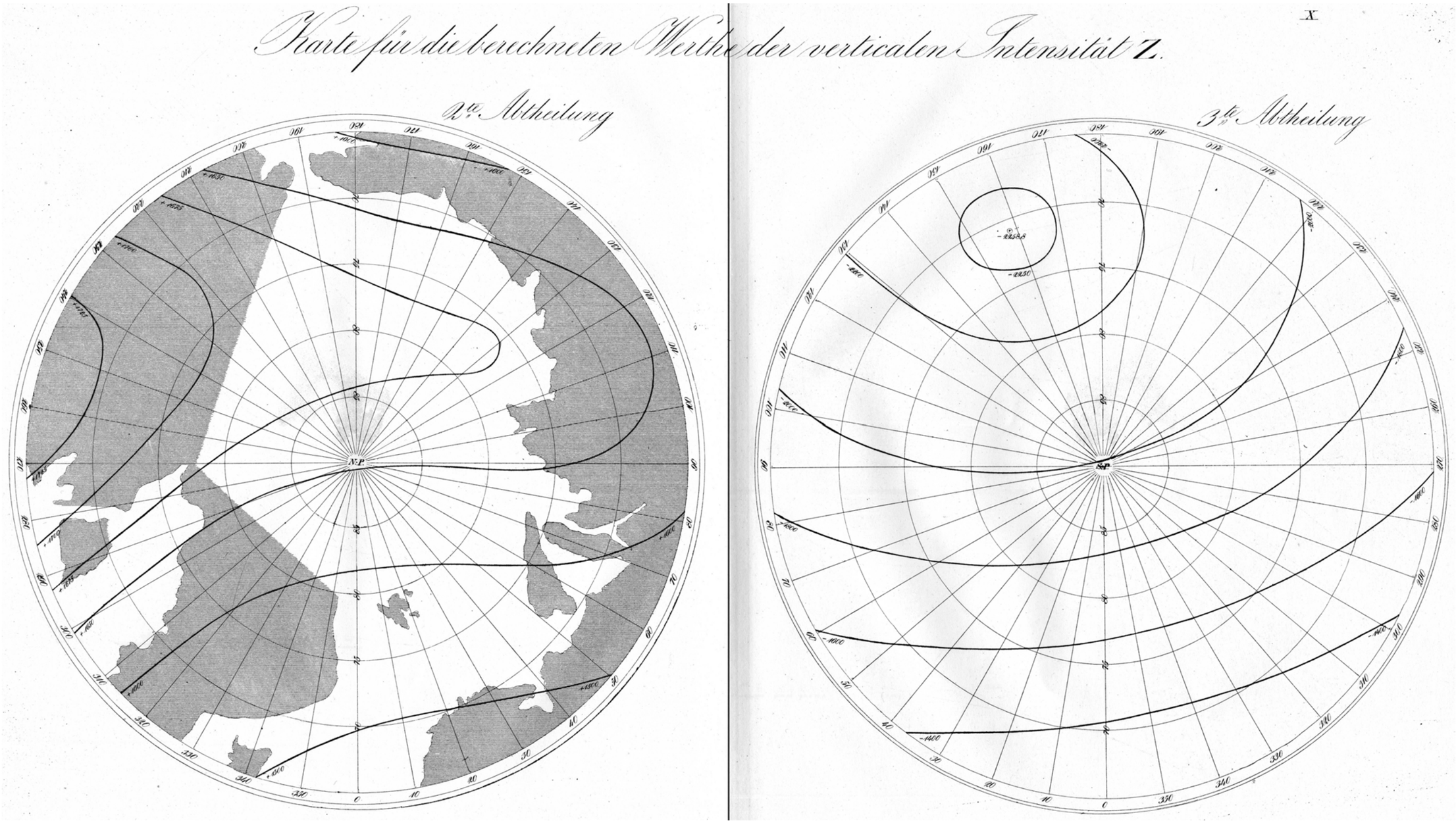

10. Map of the calculated values of the vertical component Z (polar zones).

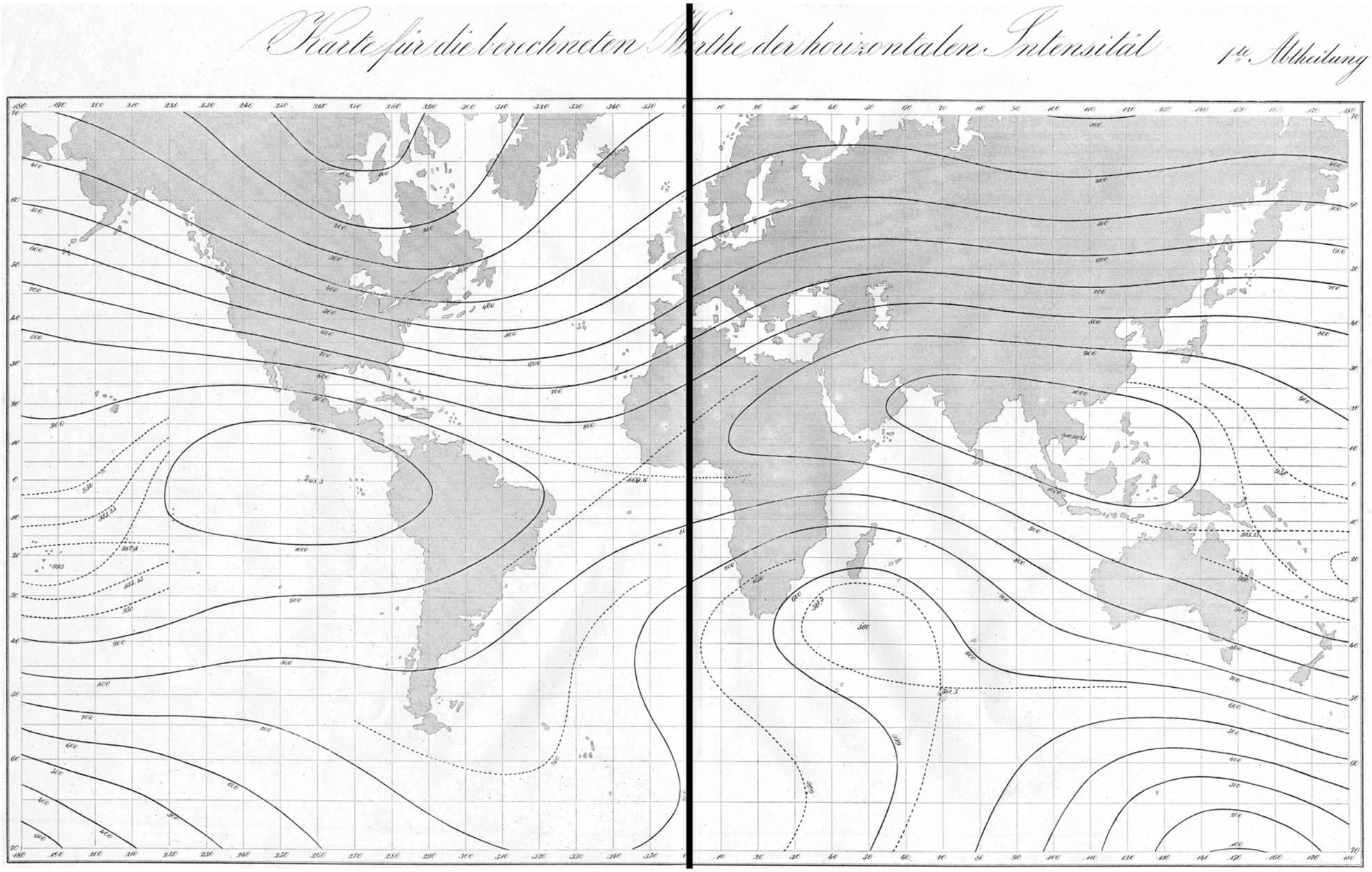

11. Map of the calculated values of the horizontal component (70°S–70°N).

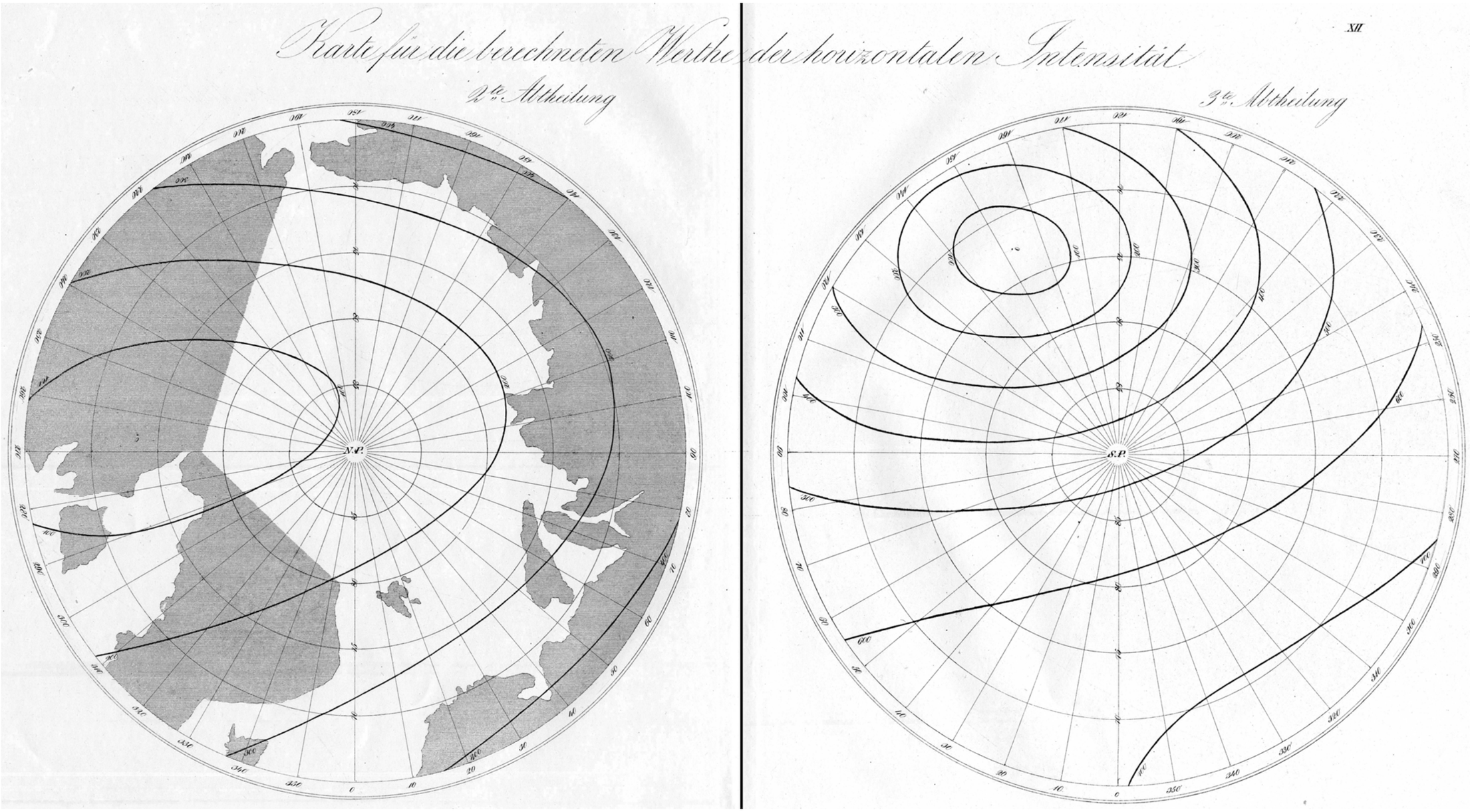

12. Map of the calculated values of the horizontal component (polar zones).

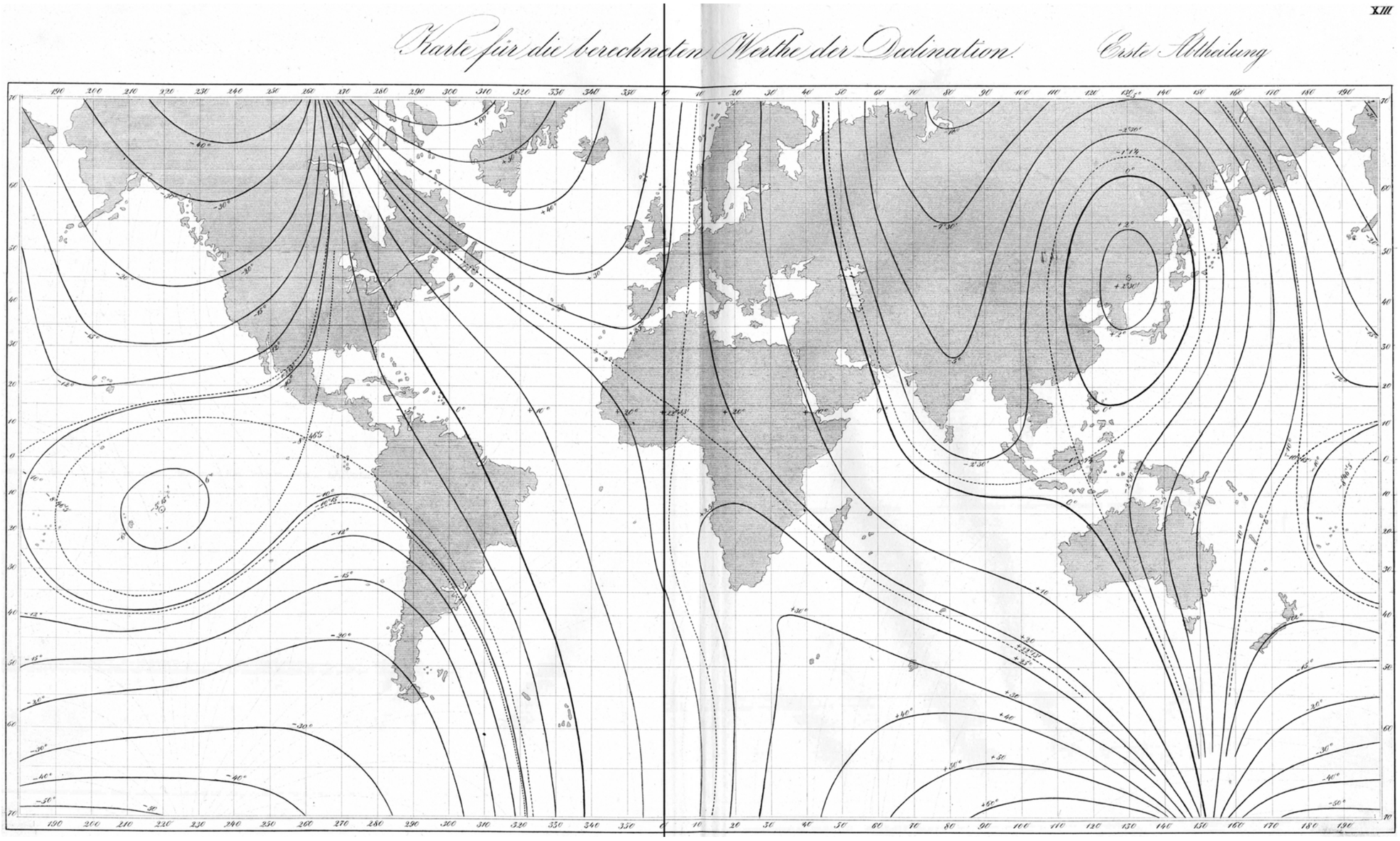

13. Map of the calculated values of the declination (70°S–70°N).

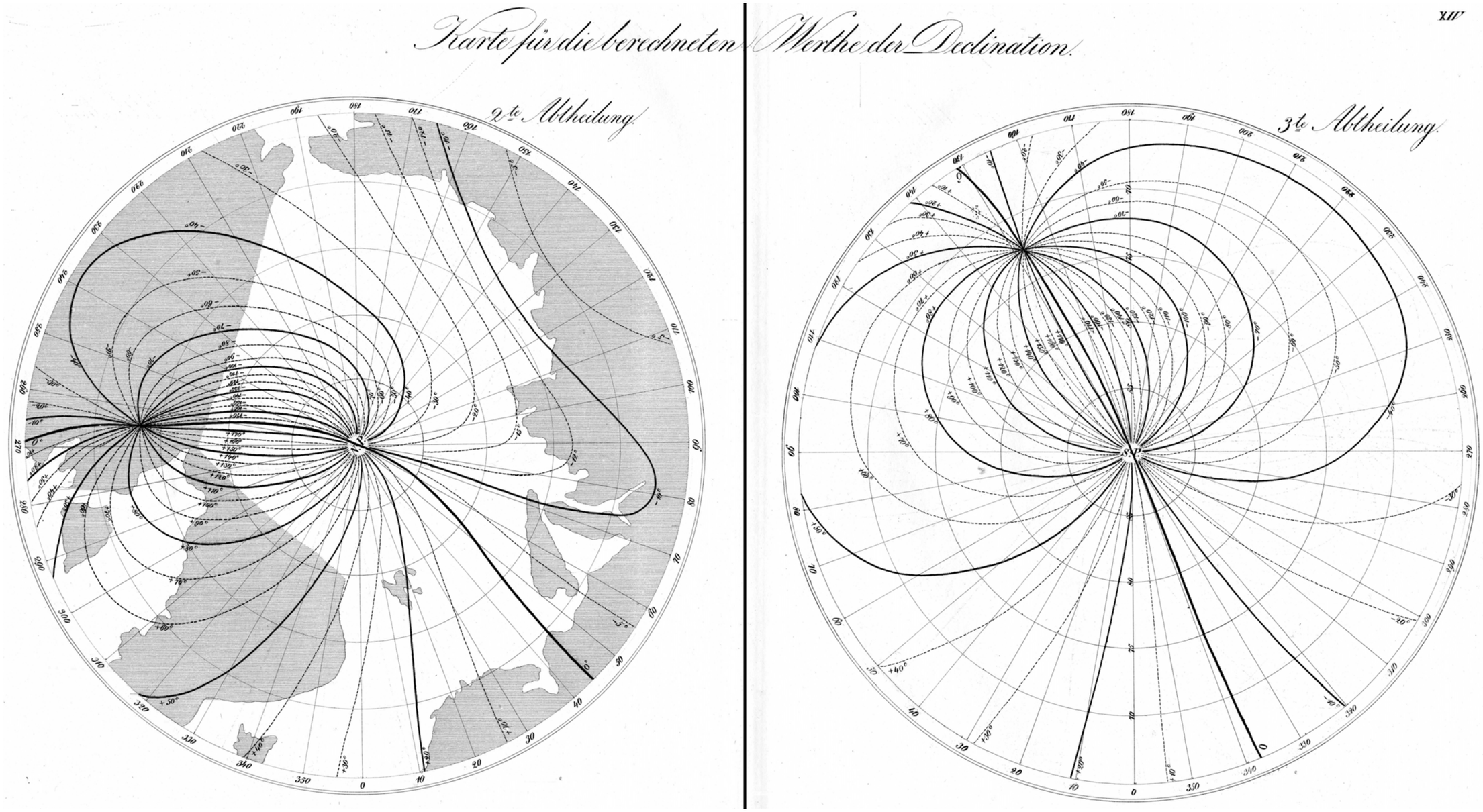

14. Map of the calculated values of the declination (polar zones).

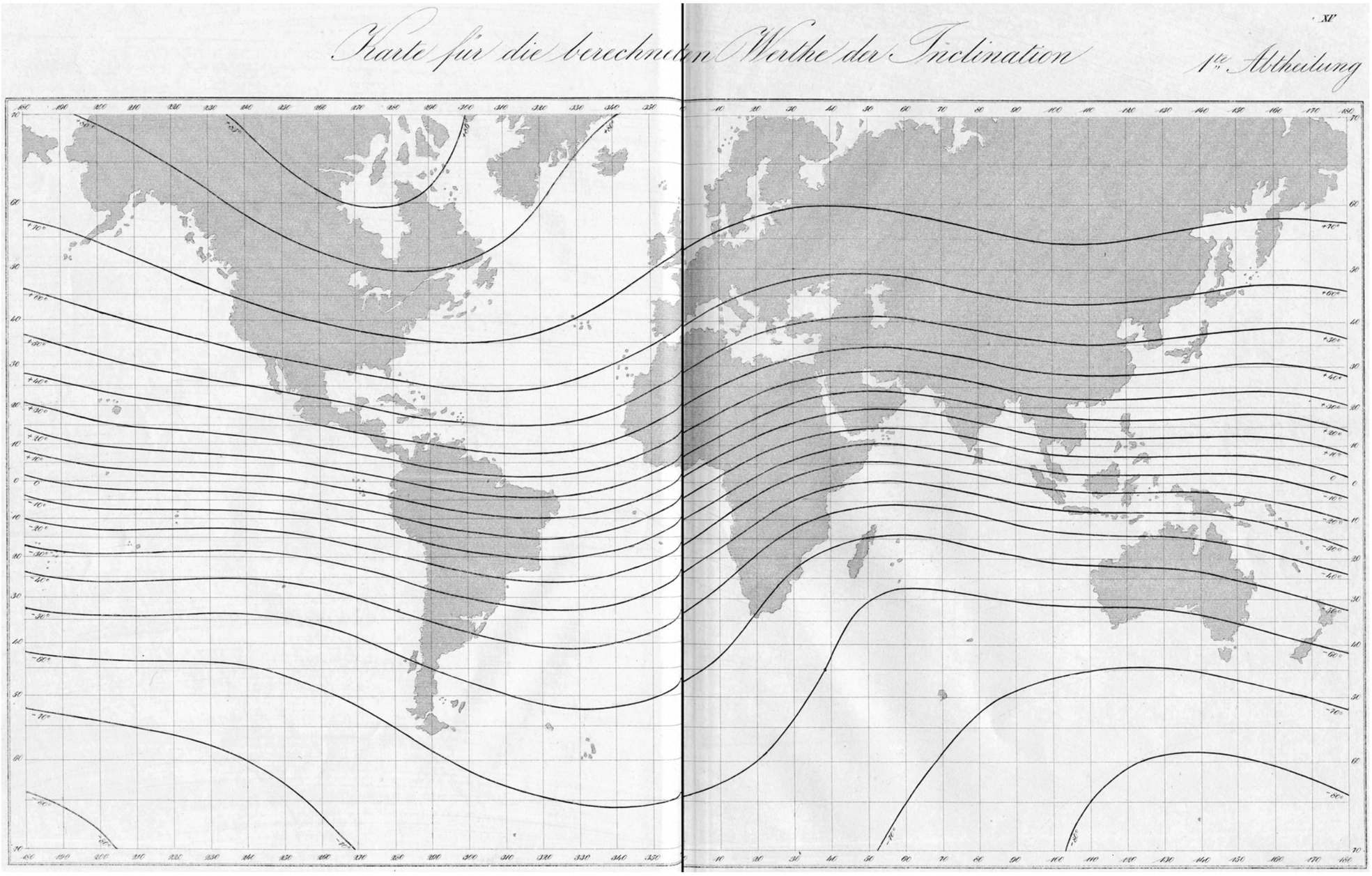

15. Map of the calculated values of the inclination (70°S–70°N).

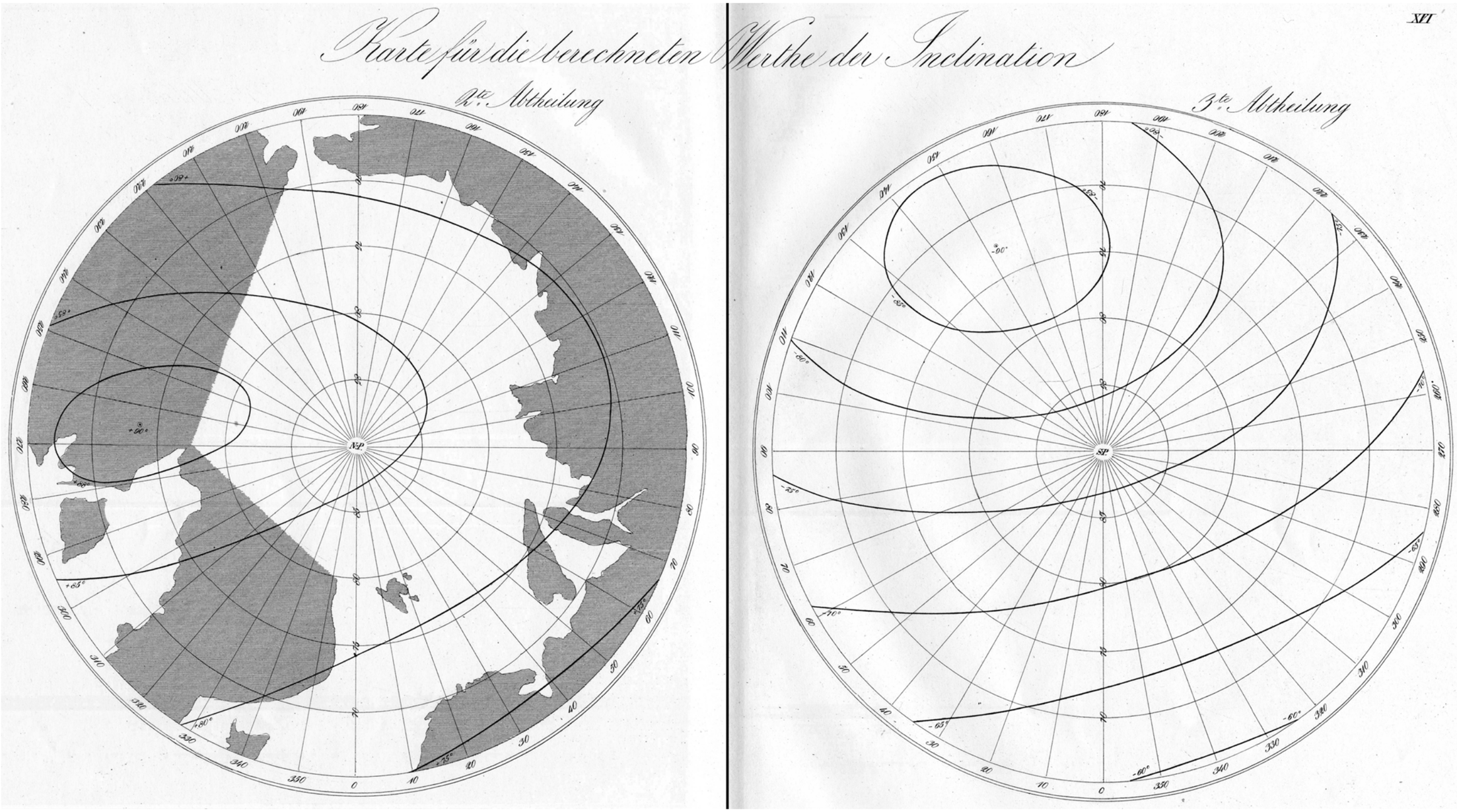

16. Map of the calculated values of the inclination (polar zones).

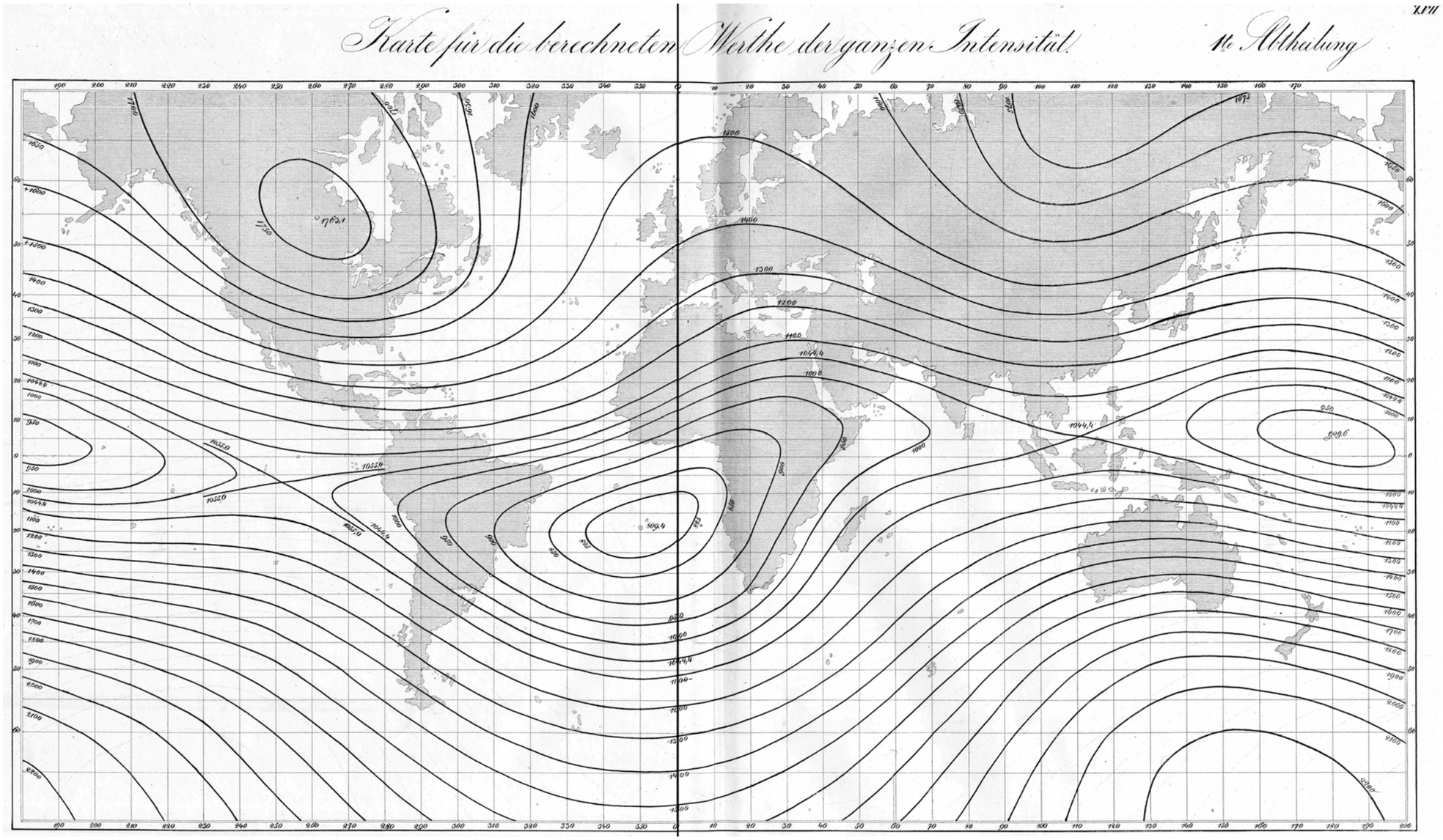

17. Map of the computed values of the total intensity (70°S–70°N).

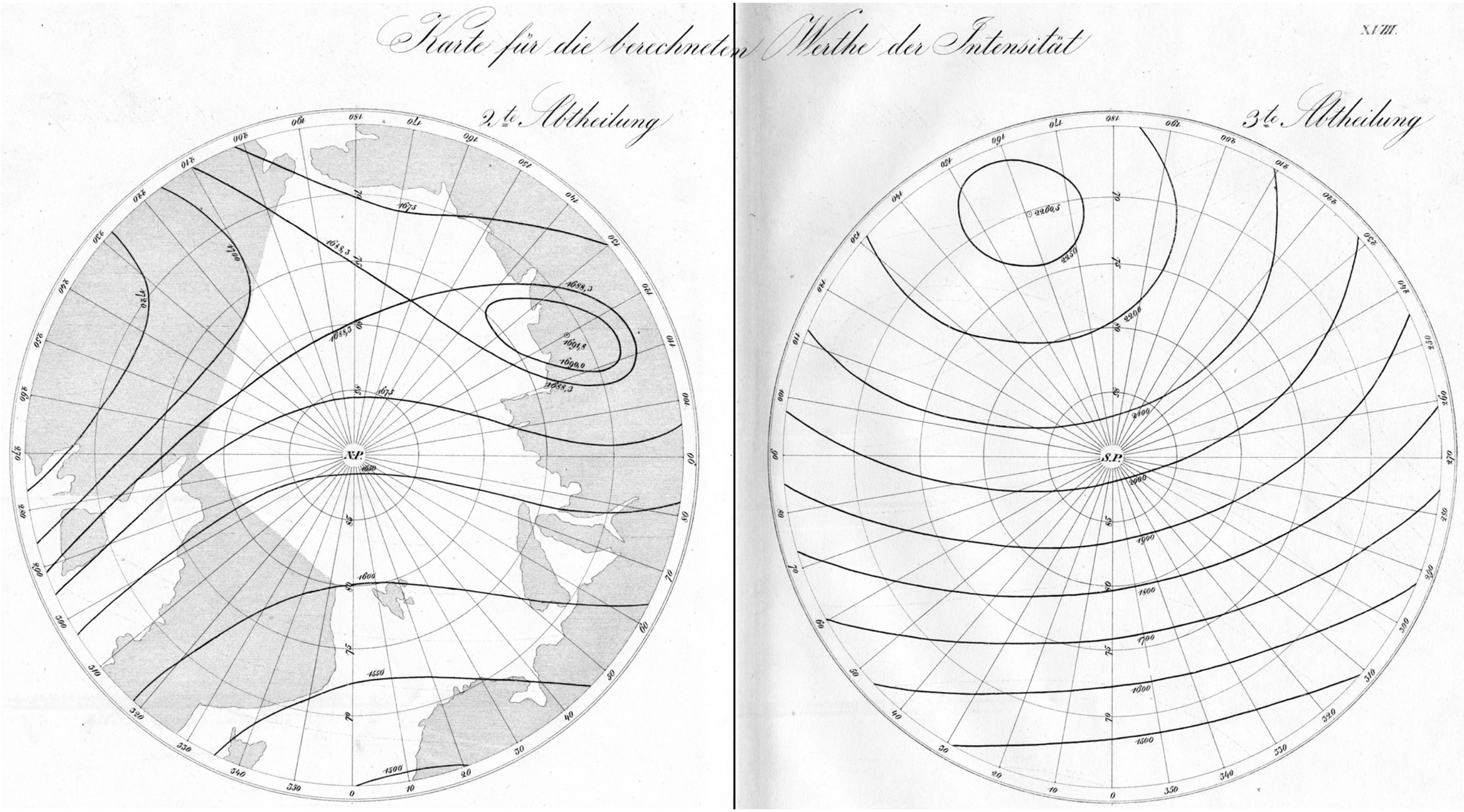

18. Map of the computed values of the total intensity (polar zones).

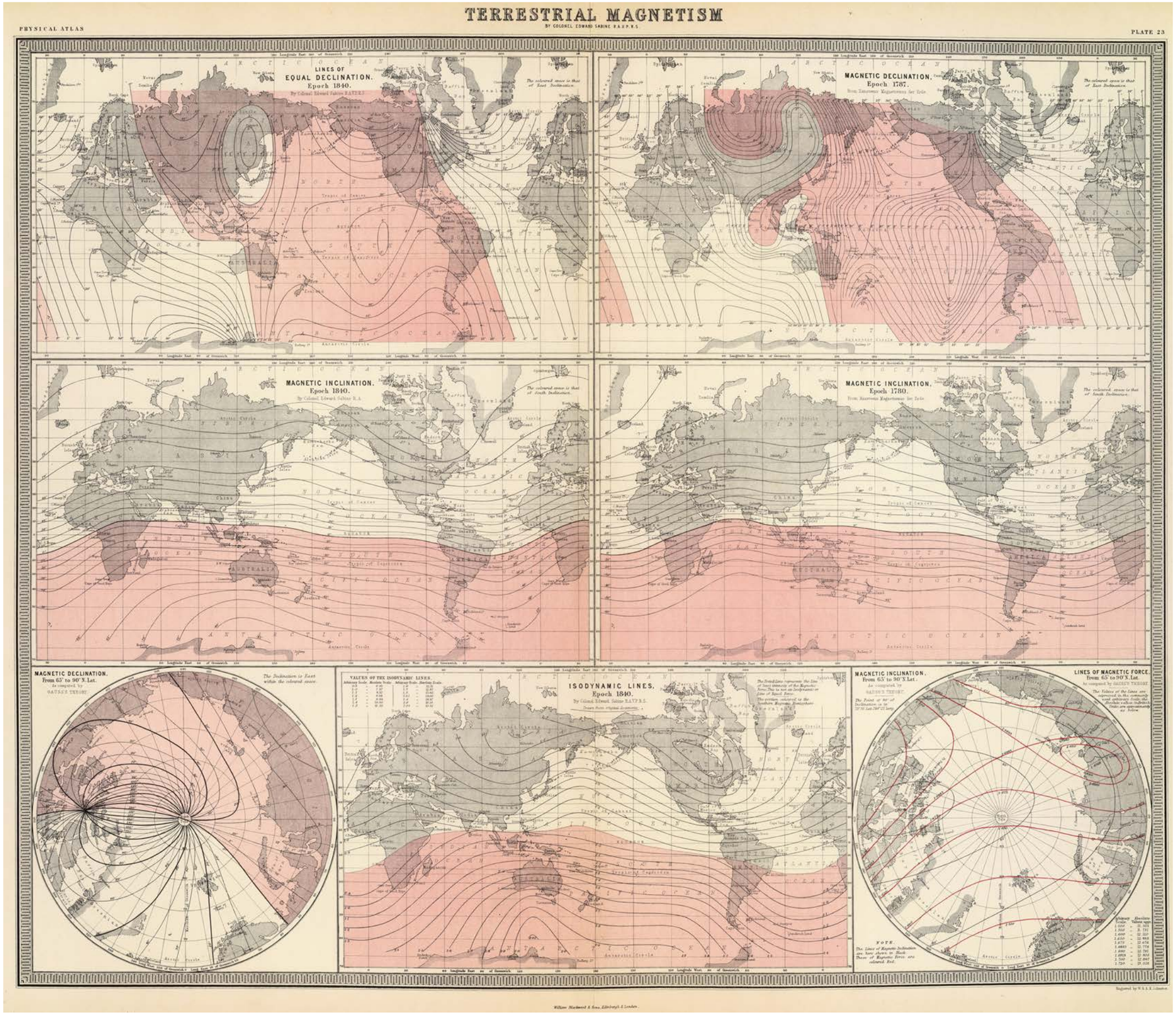
TERRESTRIAL MAGNETISM
PHYSICAL ATLAS
BY COLONEL EDWARD SABINE R.A.V.P.R.S.
PLATE 23
LINES OF EQUAL DECLINATION. Epoch 1840.
MAGNETIC DECLINATION. Epoch 1787.
MAGNETIC INCLINATION. Epoch 1840.
MAGNETIC INCLINATION. Epoch 1780.
MAGNETIC DECLINATION. From 65° to 90° N. Lat.
ISODYNAMIC LINES. Epoch 1840.
MAGNETIC INCLINATION. From 65° to 90° N. Lat.
LINES OF MAGNETIC FORCE. From 65° to 90° N. Lat.

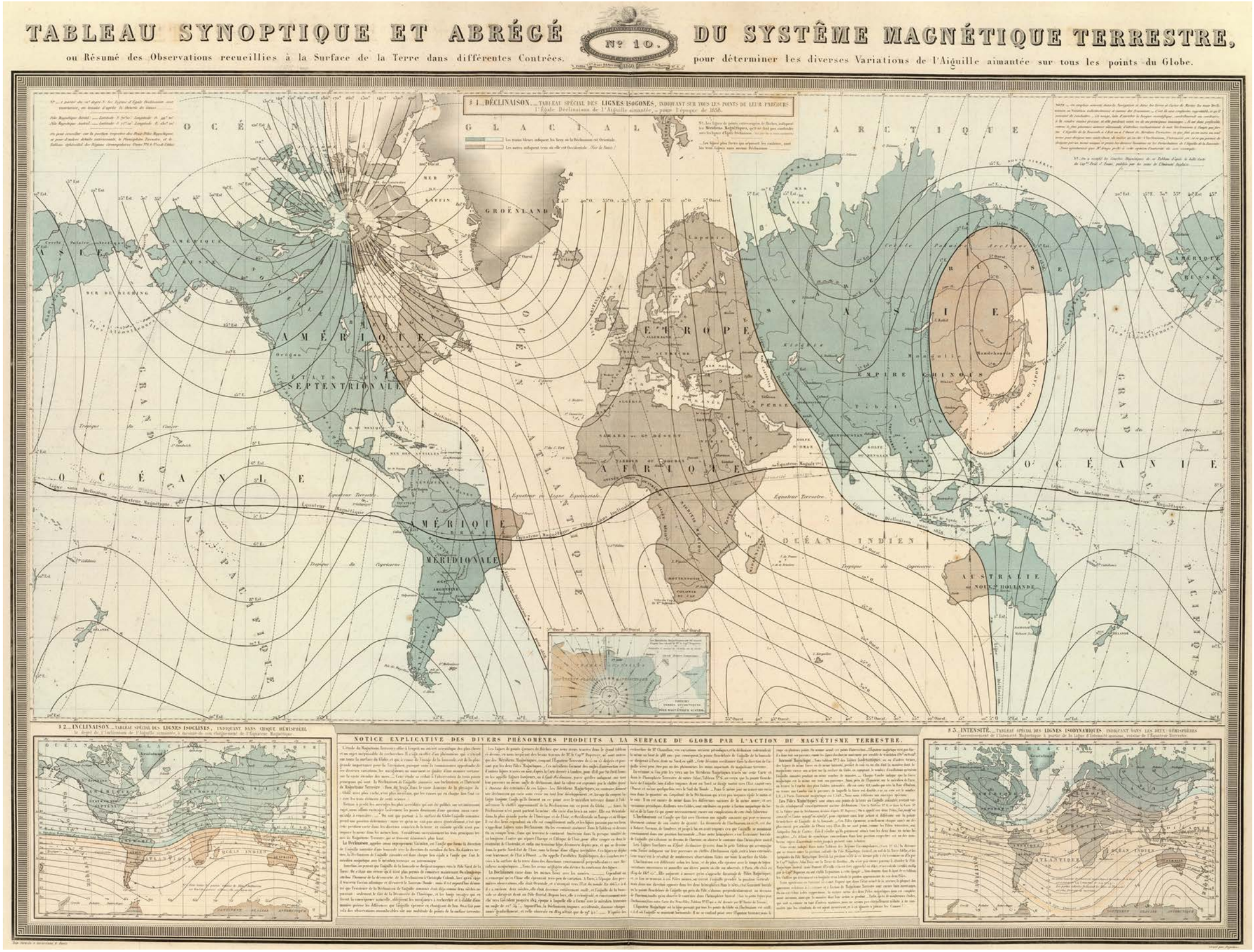
TABLEAU SYNOPTIQUE ET ABRÉGÉ DU SYSTÊME MAGNÉTIQUE TERRESTRE,
ou Résumé des Observations recueillies à la Surface de la Terre dans différentes Contrées.
N° 10.
pour déterminer les diverses Variations de l'Aiguille aimantée sur tous les points du Globe.
§ 1. DÉCLINAISON. — TABLEAU SPÉCIAL DES LIGNES ISOGONES, INDIQUANT SUR TOUS LES POINTS DE LEUR PARCOURS
l'égale Déclinaison de l'Aiguille aimantée, — pour l'époque de 1858.
§ 2. INCLINAISON. — TABLEAU SPÉCIAL DES LIGNES ISOCLINES, INDIQUANT DANS CHAQUE HÉMISPHÈRE
le degré de l'inclinaison de l'Aiguille aimantée, à mesure du son éloignement de l'Équateur Magnétique.
NOTICE EXPLICATIVE DES DIVERS PHÉNOMÈNES PRODUITS À LA SURFACE DU GLOBE PAR L'ACTION DU MAGNÉTISME TERRESTRE.
§ 3. INTENSITÉ. — TABLEAU SPÉCIAL DES LIGNES ISODYNAMIQUES INDIQUANT DANS LES DEUX HÉMISPHÈRES
l'accroissement de l'intensité Magnétique à partir de la ligne d'intensité minime, voisine de l'Équateur Terrestre.
OCÉAN ARCTIQUE
GLACIAL
GROËNLAND
AMÉRIQUE SEPTENTRIONALE
EUROPE
ASIE
EMPIRE CHINOIS
AFRIQUE
AMÉRIQUE MÉRIDIONALE
OCÉANIE
OCÉAN INDIEN
AUSTRALIE ou NOUVELLE HOLLANDE
Équateur Magnétique
Équateur Terrestre
Ligne sans Déclinaison
Ligne sans Inclinaison
Tropique du Cancer
Tropique du Capricorne

Annex 3. Auxiliary Maps

MAGNETIC OBSERVATORIES OF INTERMAGNET NETWORK

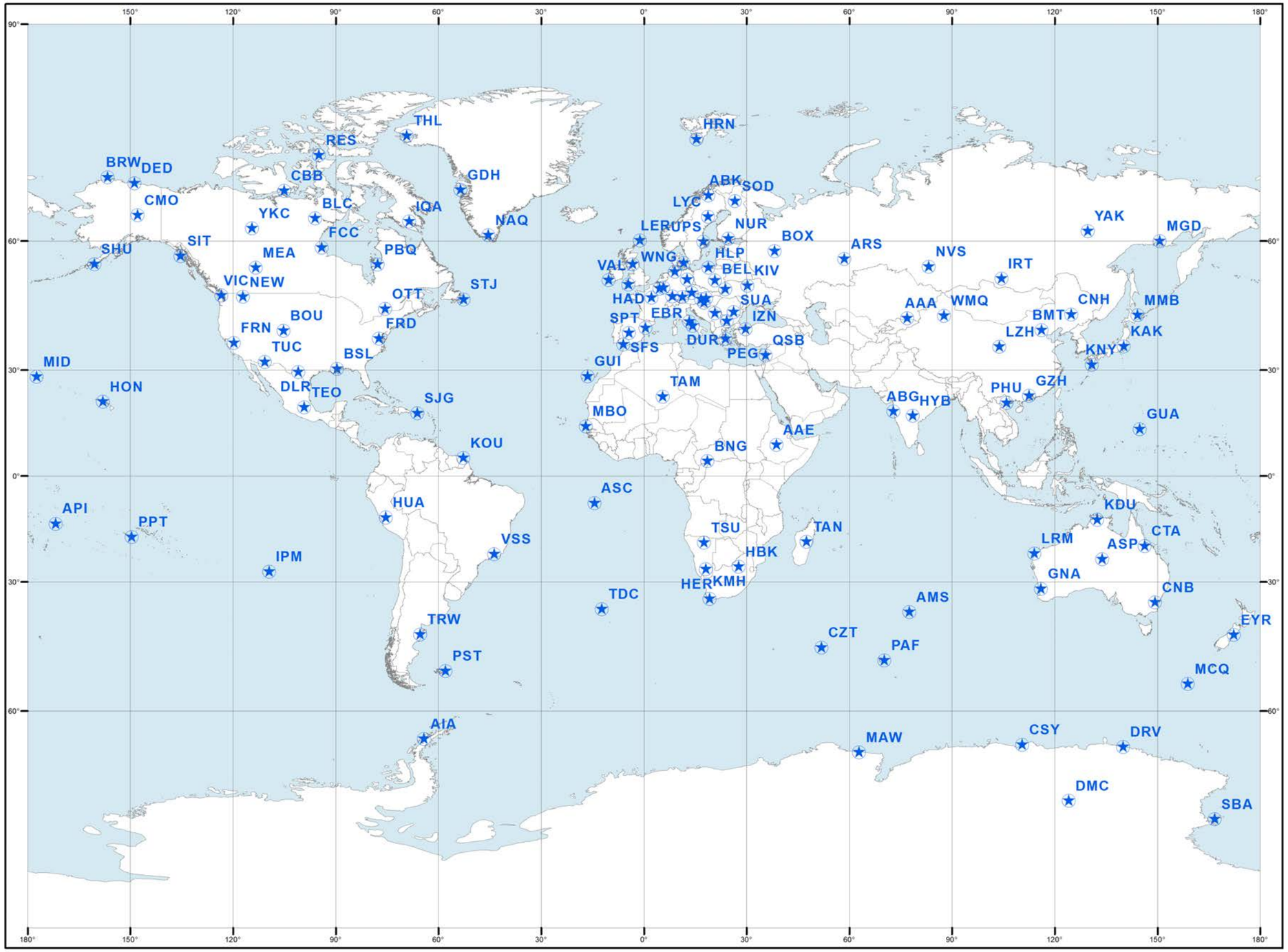

As of 2013

INTERMAGNET observatories with their codes

State borders and coastline

Hydrography

Scale 1: 120 000 000

Projection: Miller cylindrical

MAGNETIC STATIONS AND OBSERVATORIES OPERATING DURING IGY FROM 1957 TO 1959 (209)

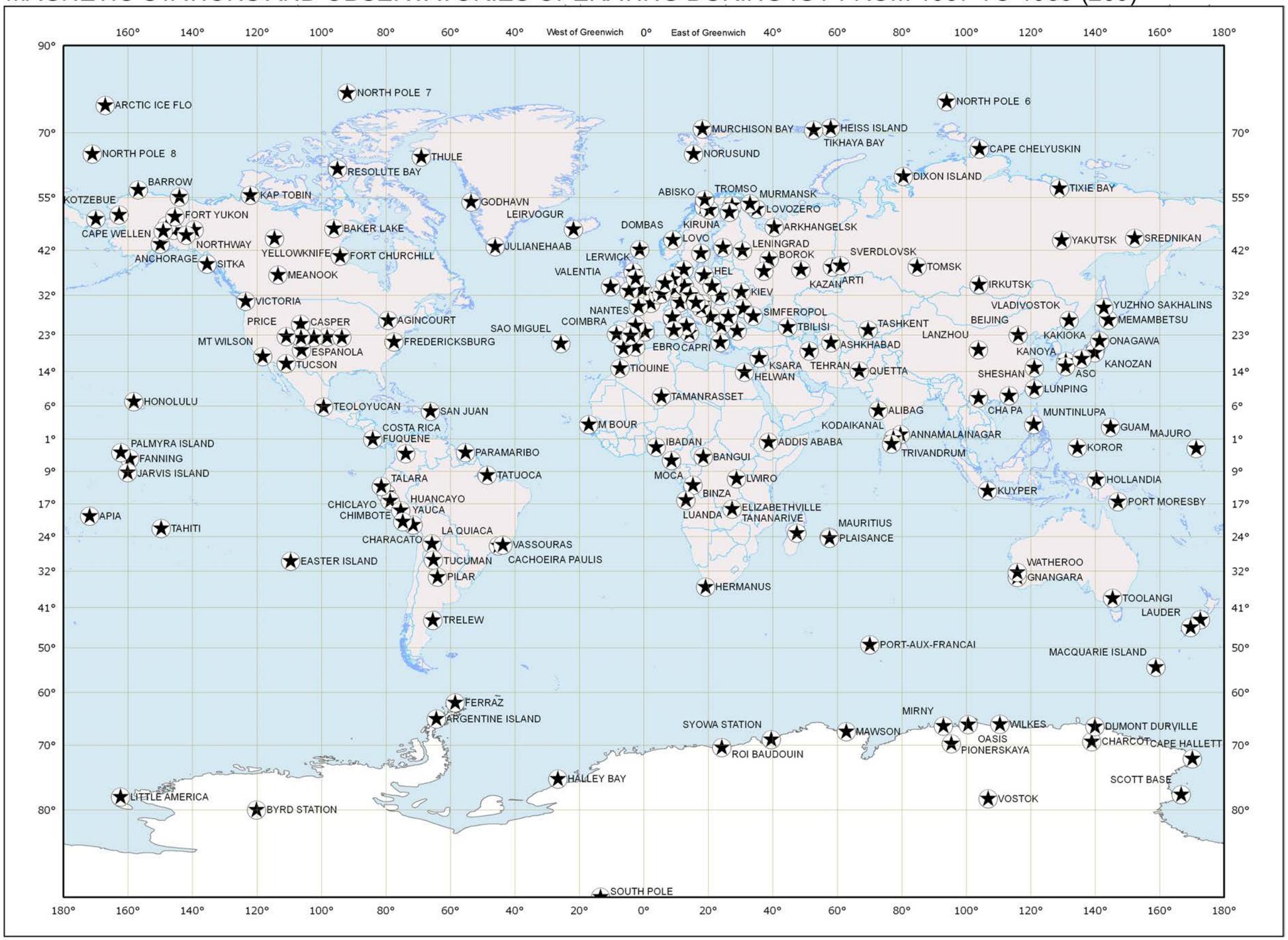

Scale 1: 120 000 000

Projection: Miller cylindrical

MAGNETIC STATIONS AND OBSERVATORIES OPERATING IN 1813-1837 (6)

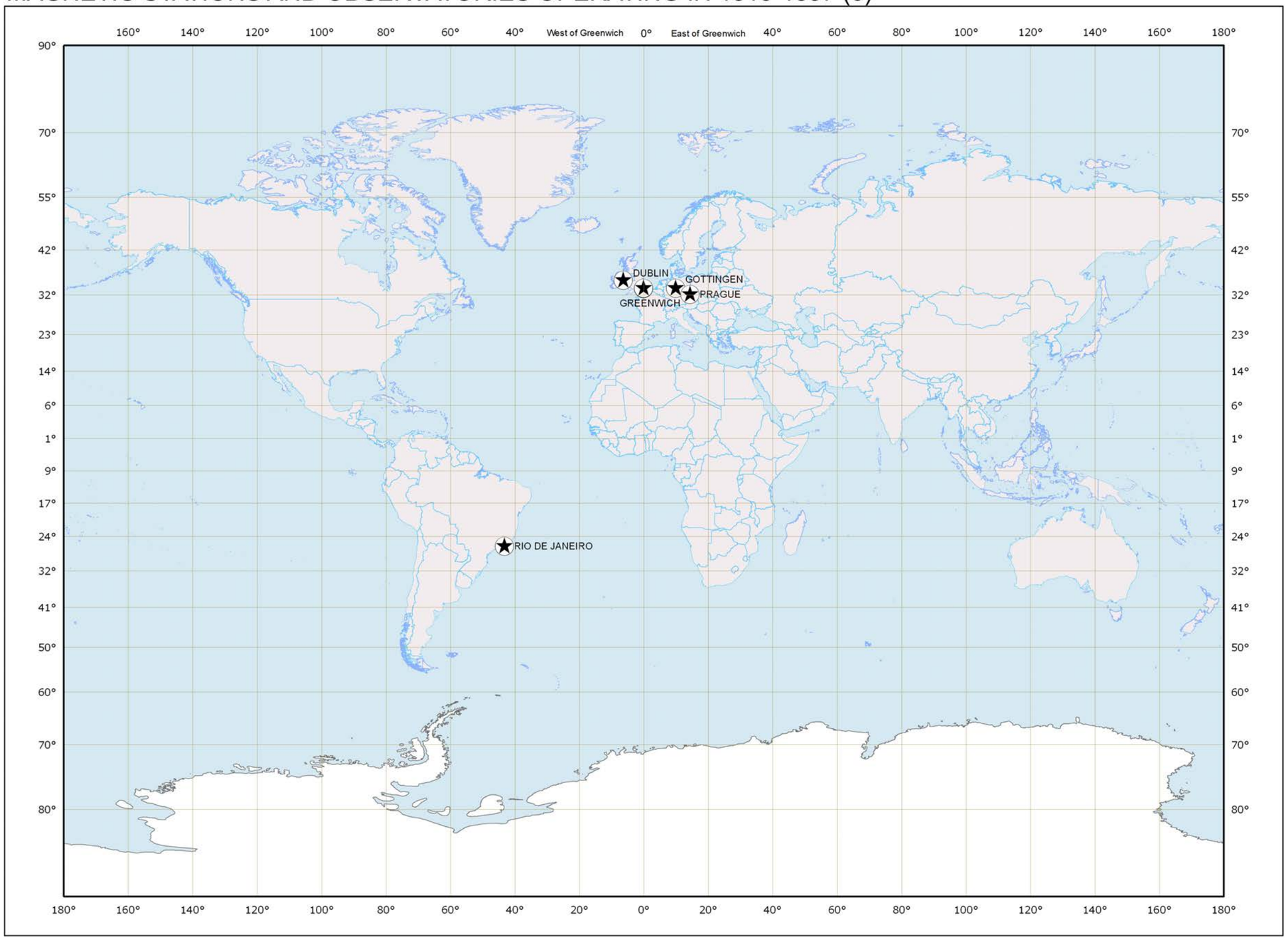

Scale 1: 120 000 000

Projection: Miller cylindrical

MAGNETIC STATIONS AND OBSERVATORIES OPERATING IN 1843-1872 (31)

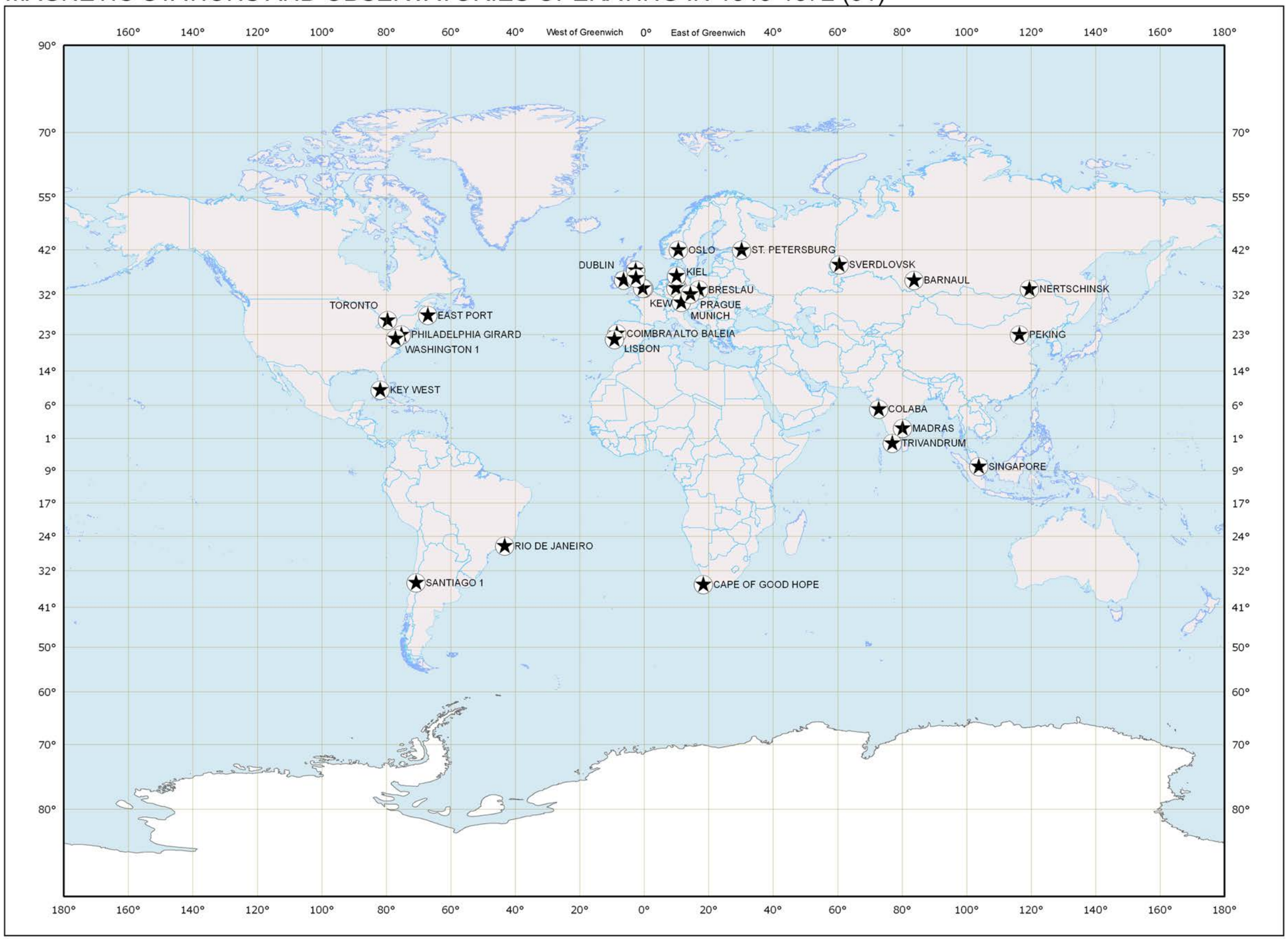

Scale 1: 120 000 000

Projection: Miller cylindrical

MAGNETIC STATIONS AND OBSERVATORIES OPERATING IN 1877-1901 (85)

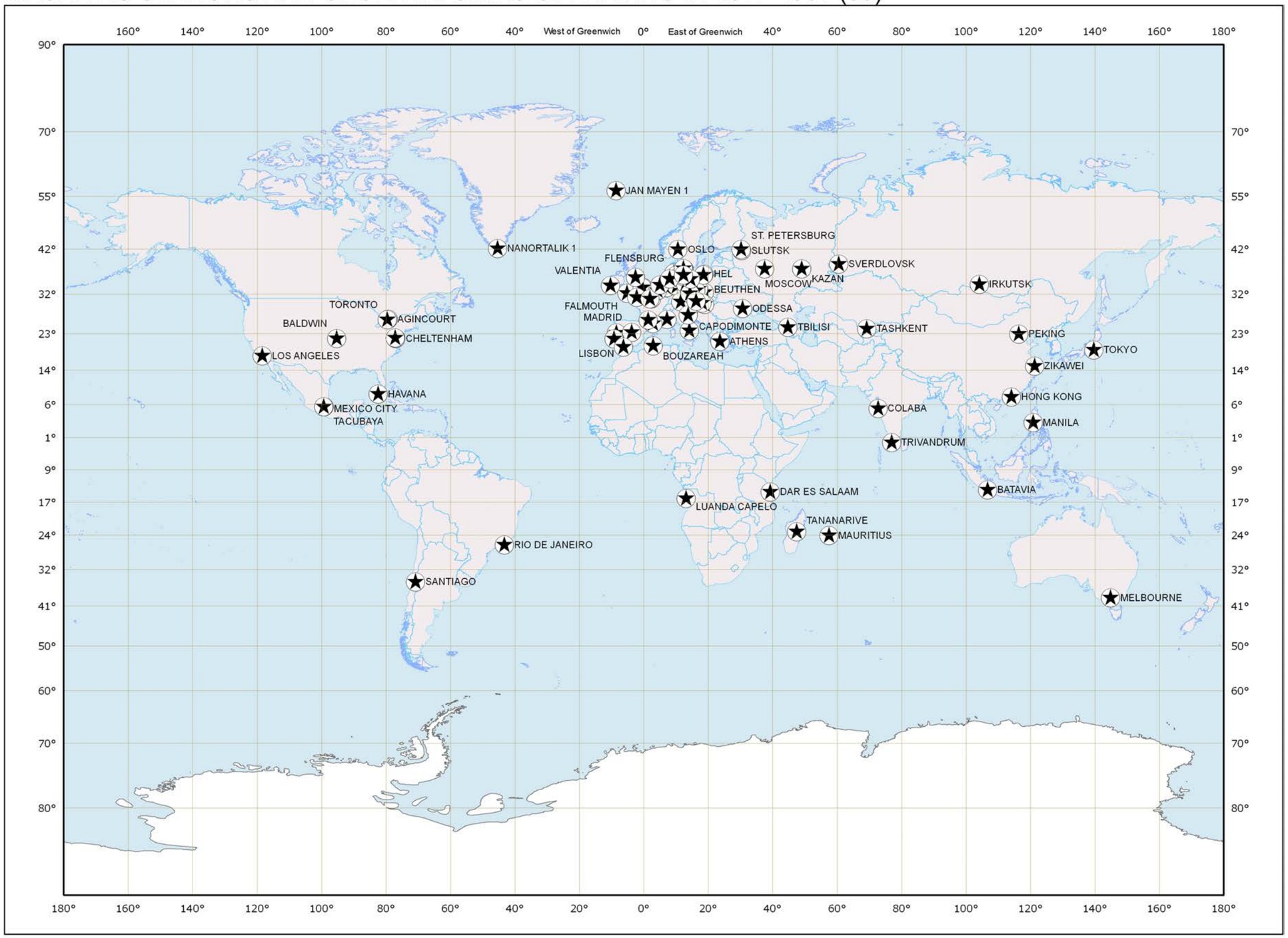

Scale 1: 120 000 000

Projection: Miller cylindrical

MAGNETIC STATIONS AND OBSERVATORIES OPERATING IN 1903-1922 (107)

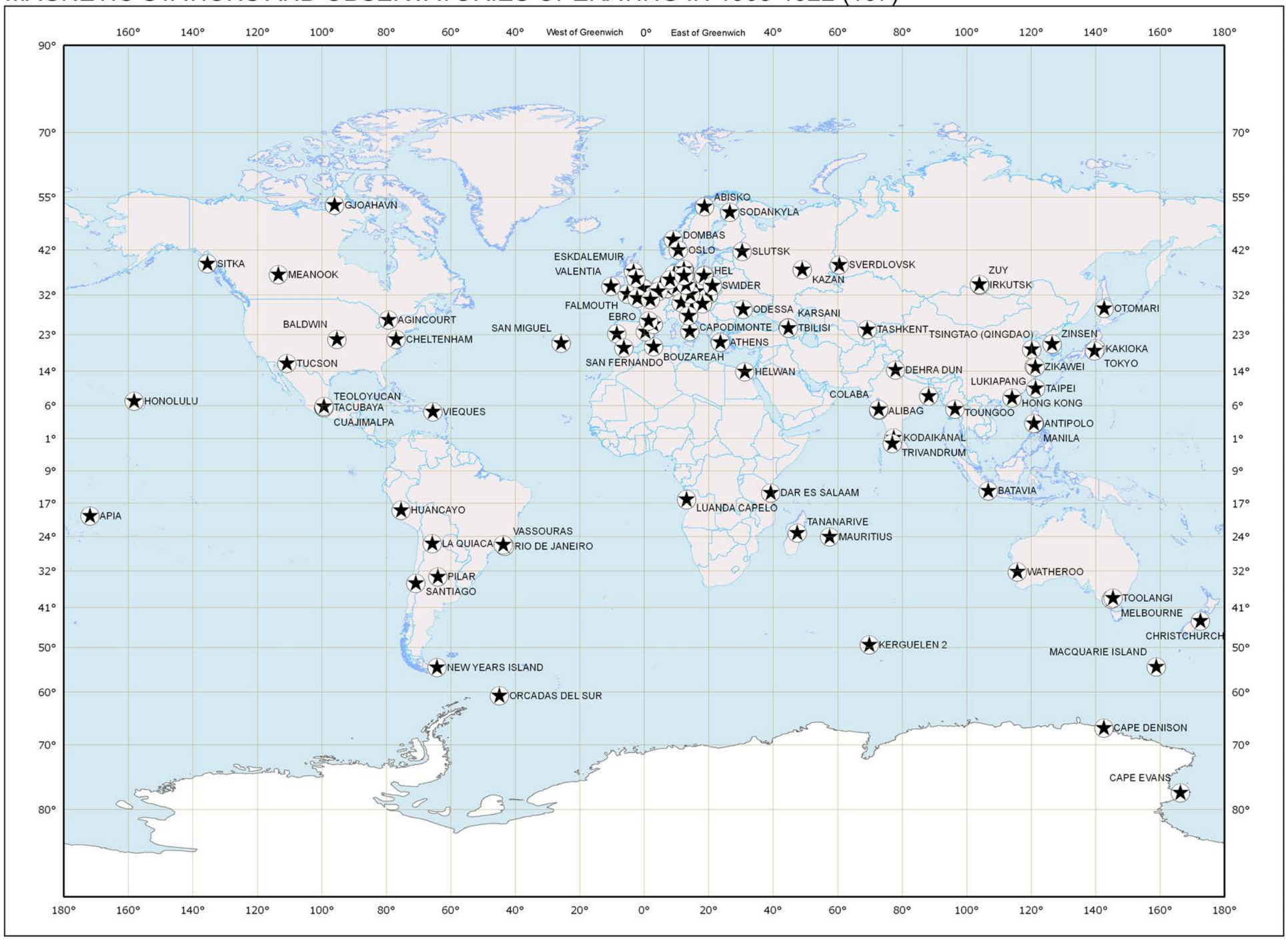

Scale 1: 120 000 000

Projection: Miller cylindrical

MAGNETIC STATIONS AND OBSERVATORIES OPERATING IN 1923-1947 (142)

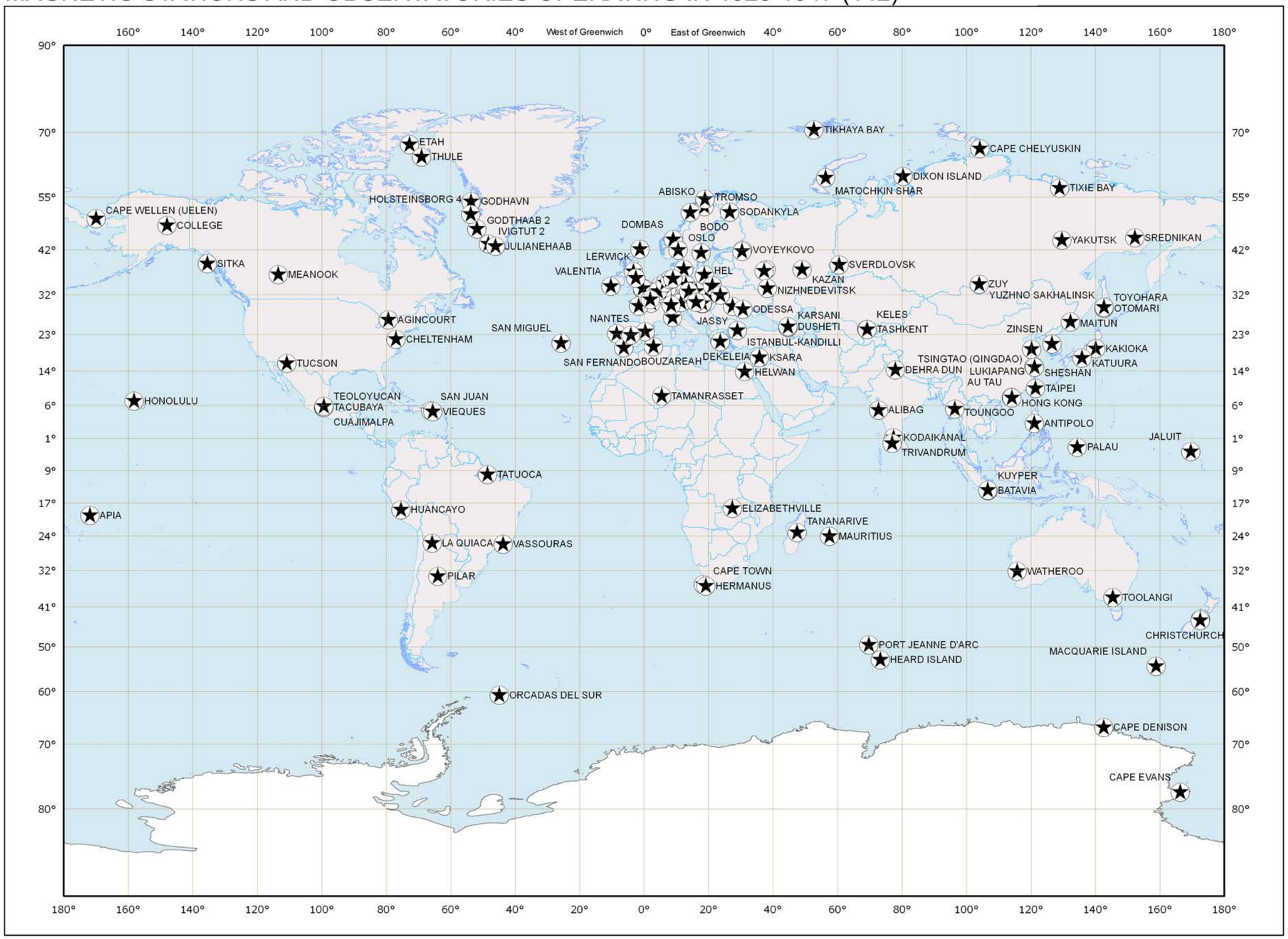

Scale 1: 120 000 000

Projection: Miller cylindrical

MAGNETIC STATIONS AND OBSERVATORIES OPERATING IN 1948-1957 (166)

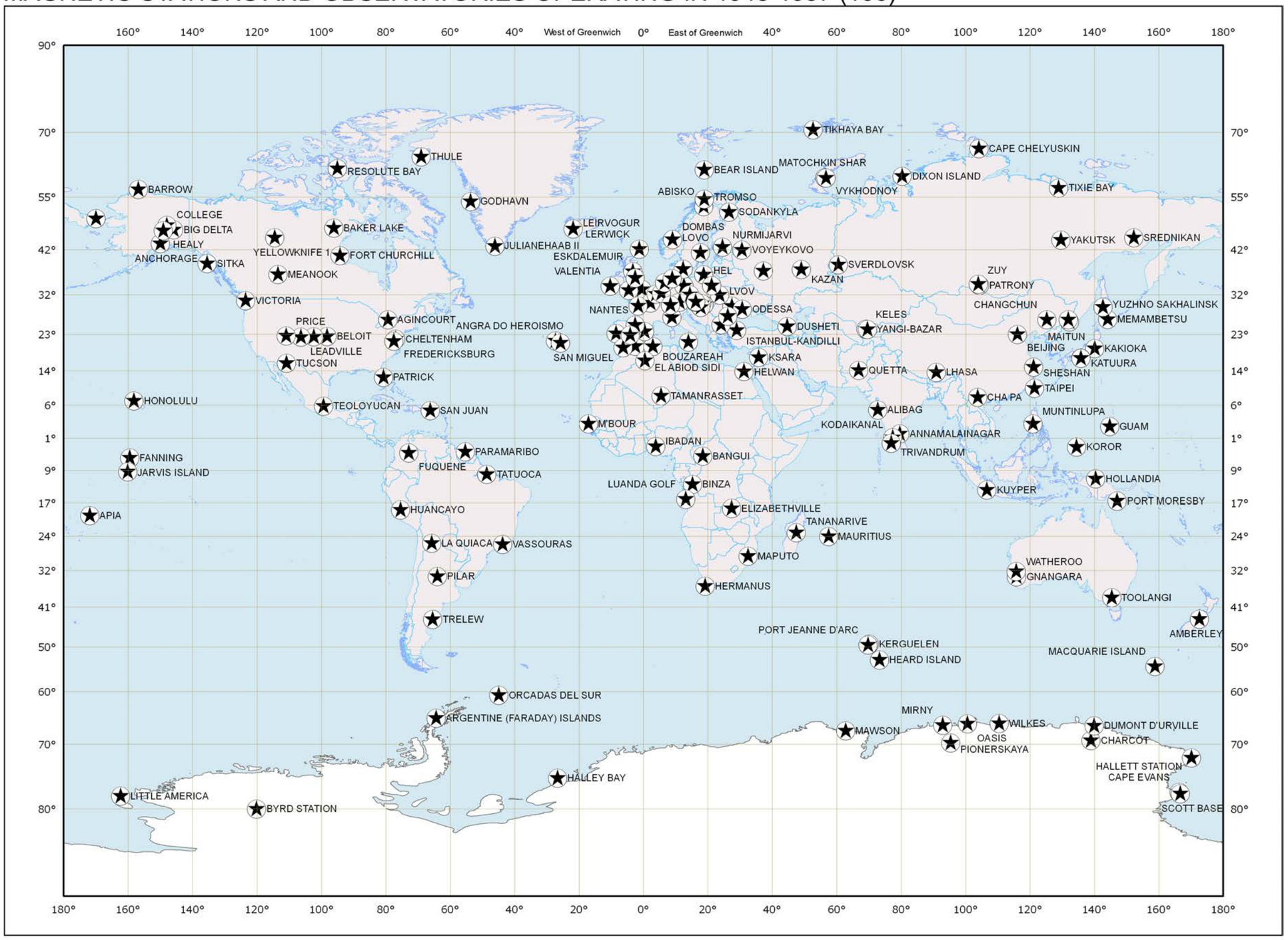

Scale 1: 120 000 000

Projection: Miller cylindrical

MAGNETIC STATIONS AND OBSERVATORIES OPERATING IN 1959-1968 (216)

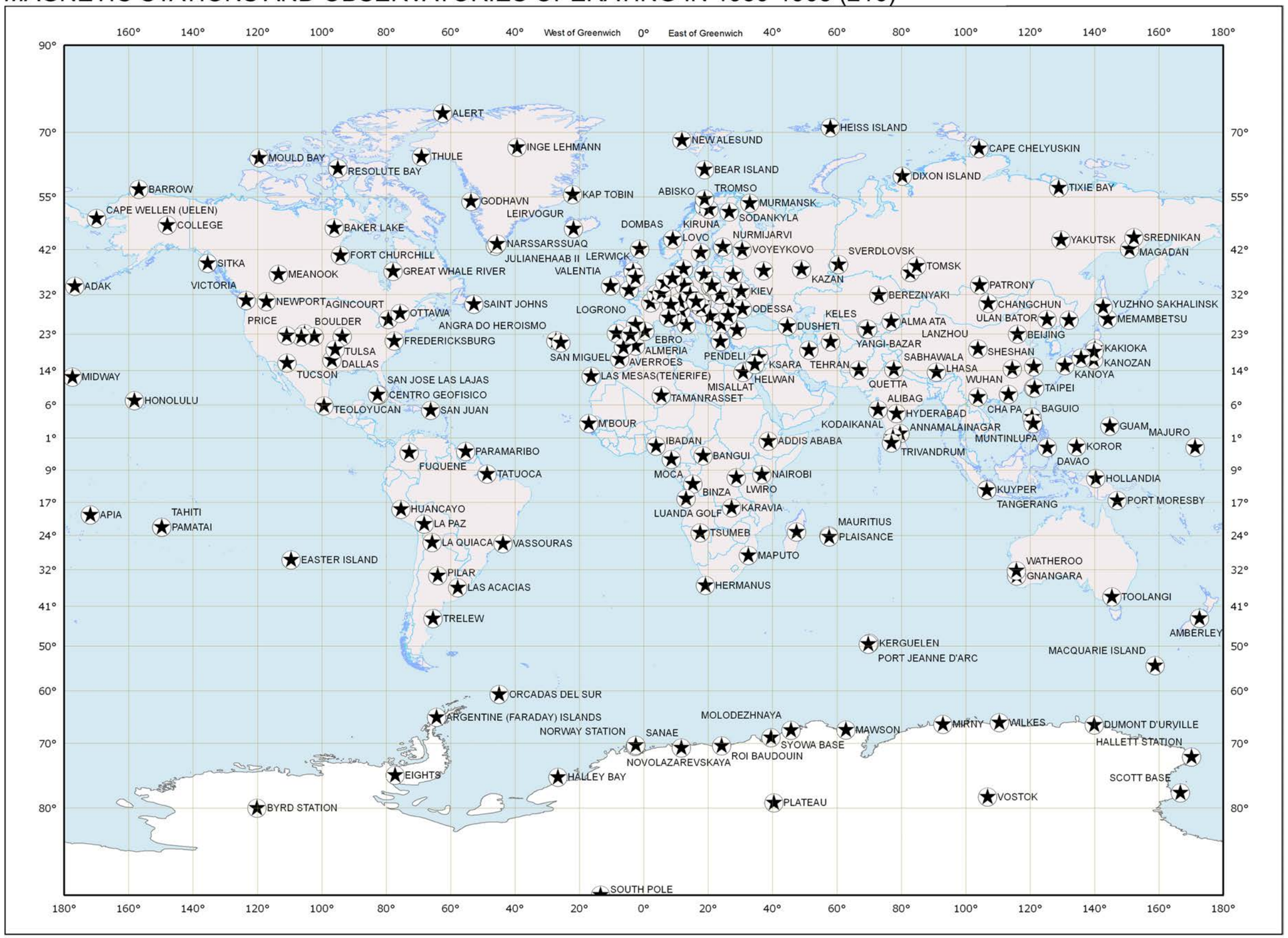

Scale 1: 120 000 000

Projection: Miller cylindrical

MAGNETIC STATIONS AND OBSERVATORIES OPERATING IN 1969-1988 (244)

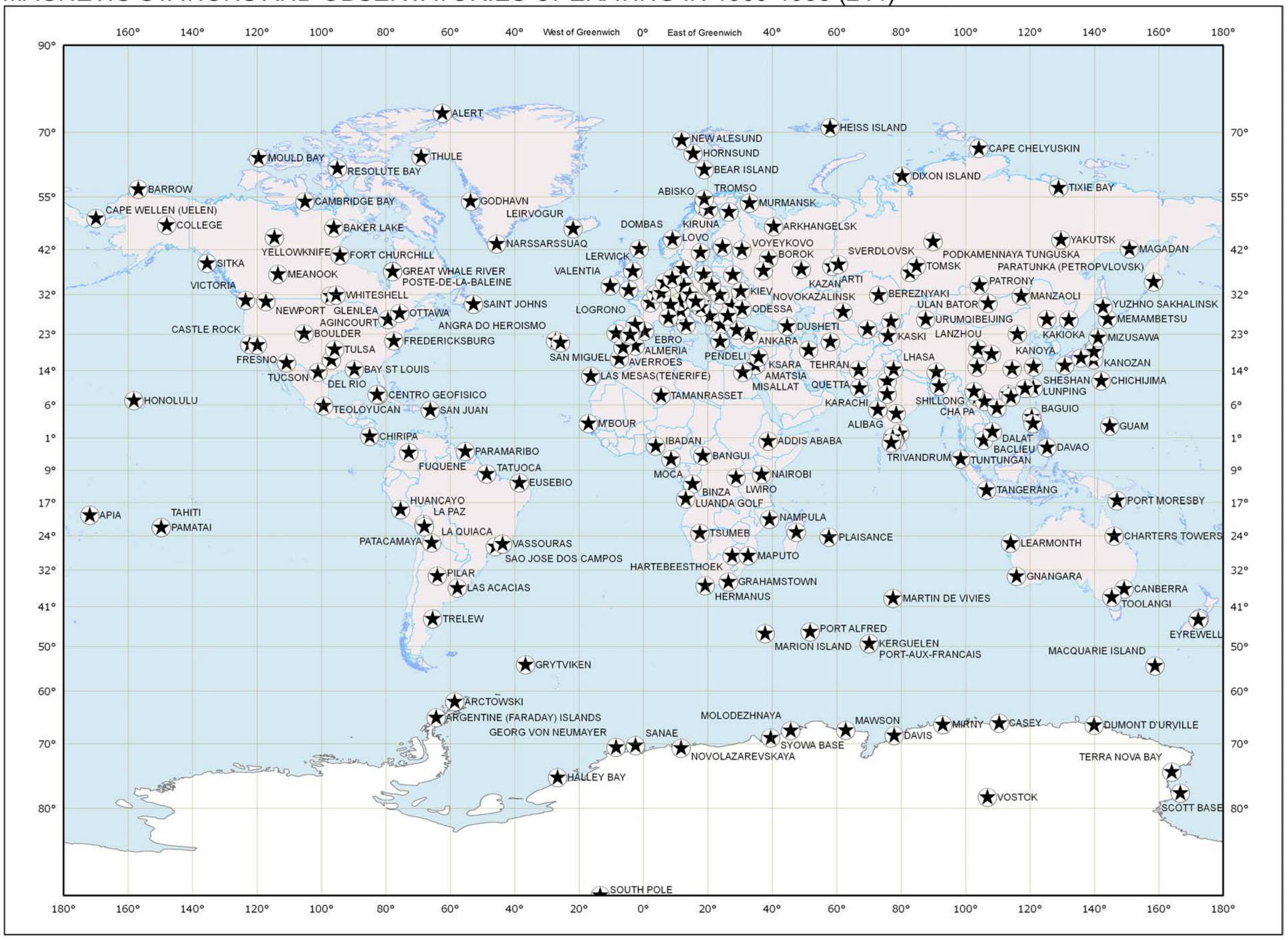

Scale 1: 120 000 000

Projection: Miller cylindrical

MAGNETIC STATIONS AND OBSERVATORIES OPERATING IN 1989-1999 (209)

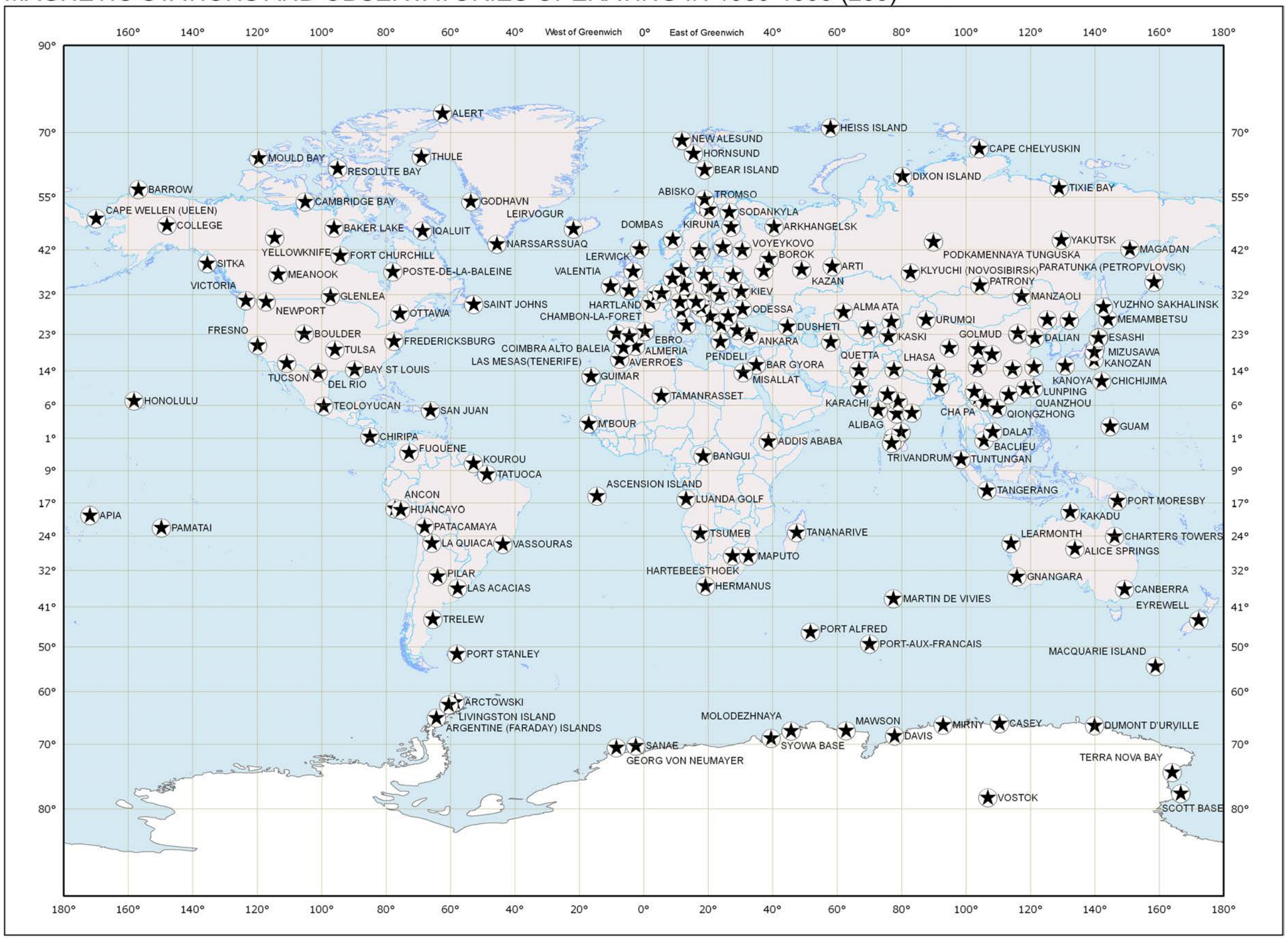

Scale 1: 120 000 000

Projection: Miller cylindrical

MAGNETIC STATIONS AND OBSERVATORIES OPERATING IN 2000-2005 (158)

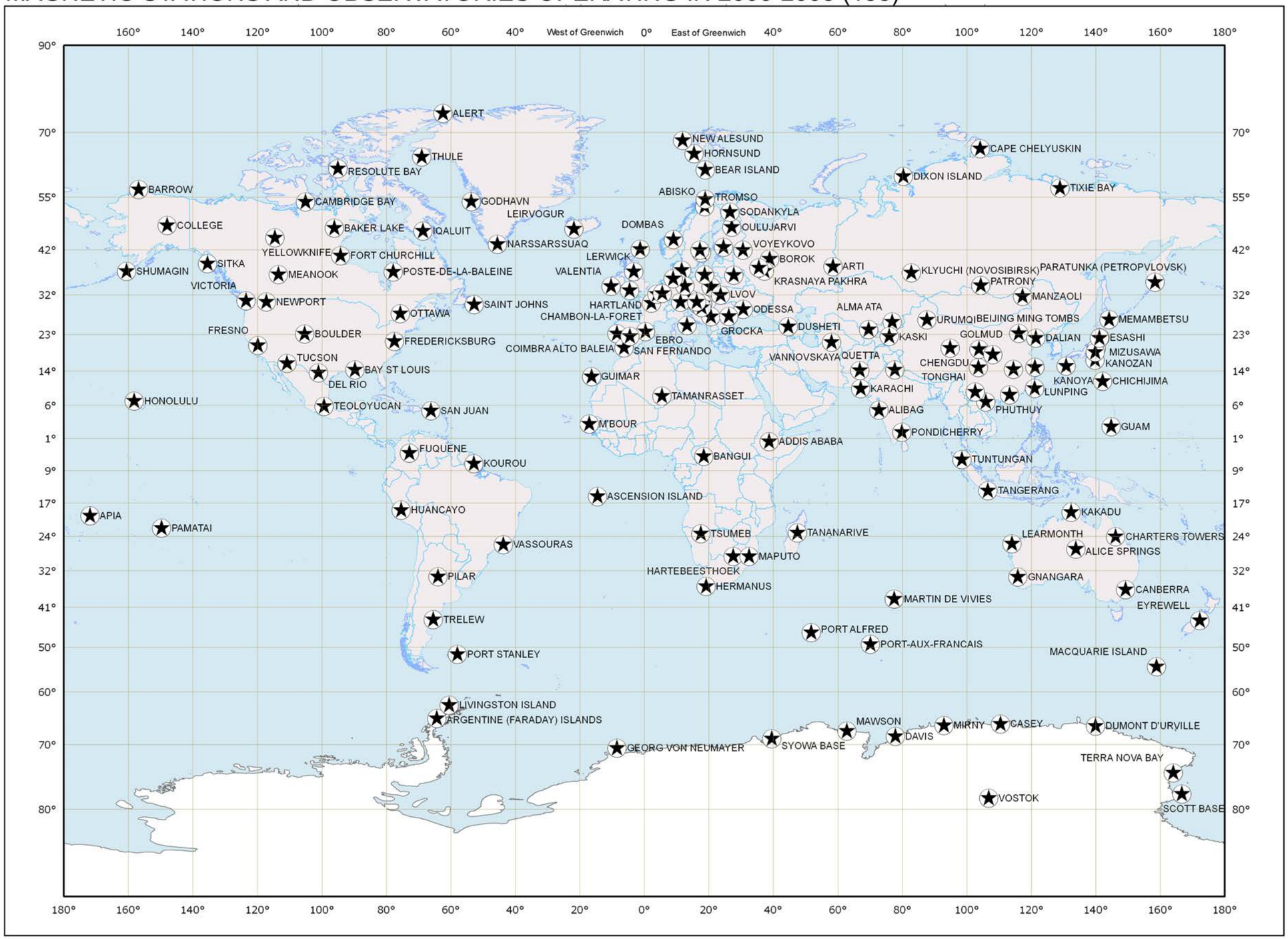

Scale 1: 120 000 000

Projection: Miller cylindrical